

Original

MAGNASTOR System

Docket No. 72-1031

TAC #L23764

NAC INTERNATIONAL

RESPONSE TO THE

UNITED STATES
NUCLEAR REGULATORY COMMISSION

REQUEST FOR ADDITIONAL INFORMATION

(MAY 23, 2005)

MAGNASTOR SYSTEM

(TAC. NO. L23764, DOCKET NO. 72-1031)

SEPTEMBER 2005

TABLE OF CONTENTS
MAGNASTOR SYSTEM RAI RESPONSES

	<u>Page</u>
Chapter 1 GENERAL DESCRIPTION	3
Chapter 2 PRINCIPAL DESIGN CRITERIA	10
Chapter 3 STRUCTURAL EVALUATION	13
Chapter 4 THERMAL EVALUATION	31
Chapter 5 SHIELDING EVALUATION	40
Chapter 6 CRITICALITY EVALUATION	51
Chapter 7 CONFINEMENT EVALUATION	84
Chapter 8 MATERIALS EVALUATION	89
Chapter 9 OPERATING PROCEDURES	108
Chapter 11 RADIATION PROTECTION	111
Chapter 12 ACCIDENT ANALYSIS	113
Chapter 13 OPERATING CONTROLS AND LIMITS	115
Chapter 13 Appendix A (Technical Specifications)	116
Chapter 13 Appendix B (Technical Specifications)	119
Chapter 15 DECOMMISSIONING	122

**NAC INTERNATIONAL RESPONSE
TO
REQUEST FOR ADDITIONAL INFORMATION**

CHAPTER 1 GENERAL DESCRIPTION

The following information is needed to determine compliance with 10 CFR 72.2(a)(1), 72.11, and 72.236(a), unless otherwise stated. It should be noted that other regulatory requirements may be applicable.

Section 1.3 General Description of MAGNASTOR

1-1 Clarify the inconsistency in the SAR listing for the fuel basket assembly diameter of 69.8 inches in Table 1.3.1 and 70.76 inches in Table 1.3.2.

NAC International Response

Table 1.3-1 is revised to show the correct fuel basket assembly diameter of 70.76 inches, consistent with the value shown in Table 1.3-2.

**NAC INTERNATIONAL RESPONSE
TO
REQUEST FOR ADDITIONAL INFORMATION**

CHAPTER 1 GENERAL DESCRIPTION

- 1-2 Revise Drawings 71160-551 and 71160-591 for the PWR and BWR fuel tubes, respectively, by adding the following:
- a. tube corner pin-to-socket connection details for both the pin and the socket sides, including dimensions, edge finishing, and tolerance, as appropriate, which are needed to secure the load paths for all loading conditions analyzed.
 - b. boss/bolt assembly details, including bolt torque, bolt thread, and boss-to-tube welds, to ensure proper development of the load paths assumed for all loading conditions analyzed.

NAC International Response

Drawings 71160-551 and 71160-591 have been revised to add the tube corner pin-to-socket connection details and boss details. Drawings 71160-575 and 71160-599 have been revised to add the boss/bolt assembly details. An additional drawing, 71160-600, has been issued for the 82-assembly BWR configuration with similar details (RAI 6-3).

**NAC INTERNATIONAL RESPONSE
TO
REQUEST FOR ADDITIONAL INFORMATION**

CHAPTER 1 GENERAL DESCRIPTION

1-3 On Drawing 71160-561, specify the size of the S-beams.

NAC International Response

Drawing 71160-561 has been revised to specify the size of the S-beams, as requested.

**NAC INTERNATIONAL RESPONSE
TO
REQUEST FOR ADDITIONAL INFORMATION**

CHAPTER 1 GENERAL DESCRIPTION

1-4 On Drawing 71160-561, add the eye diameter and location for the concrete cask lift lug and lift anchor.

NAC International Response

Drawing 71160-561 has been revised to add the lift lug eye diameter and location, as requested.

**NAC INTERNATIONAL RESPONSE
TO
REQUEST FOR ADDITIONAL INFORMATION**

CHAPTER 1 GENERAL DESCRIPTION

- 1-5 On Drawings 71160-574 and 71160-598, specify the hole diameter to ensure that the basket support weldments and fuel tubes can engage properly at the bosses welded to the fuel tubes.

NAC International Response

Drawings 71160-574 and 71160-598 have been revised to specify the boss hole diameters and locations, as requested.

**NAC INTERNATIONAL RESPONSE
TO
REQUEST FOR ADDITIONAL INFORMATION**

CHAPTER 1 GENERAL DESCRIPTION

- 1-6 On Drawing 71160-590, add design details for the alternative segmented concrete cask as stated in Note 2, "...concrete cask, may be constructed in segments using an upper section that can be removed to meet site specific requirements."

NAC International Response

Drawing 71160-590 has been revised to add the design details for the segmented alternate concrete cask configuration, as requested (RAI 5-1).

Separately, in addition, several other NAC drawings have also been revised in response to RAI 7-3 and RAI 8-12, as follows.

NAC drawings 71160-581, 71160-584 and 71160-585 have also been revised to incorporate RAI 7-3.

NAC drawings 71160-551, 71160-571, 71160-572 and 71160-591 have also been revised in response to RAI 8-12.

**NAC INTERNATIONAL RESPONSE
TO
REQUEST FOR ADDITIONAL INFORMATION**

CHAPTER 1 GENERAL DESCRIPTION

- 1-7 Delete references to MAGNASTOR transportation cask because it has not been submitted or approved.

For example, Page 1.1 states "MAGNASTOR transport cask will be licensed," Page 1.3-1 states "The loaded TSC may be placed into the MAGNASTOR transport cask for offsite transport" and further claims "The TSC is designed for transport per 10 CFR 71." These claims should be removed because they are premature and unverified. This information is needed to determine compliance with 10 CFR 72.230(b).

NAC International Response

A word search of the SAR text has identified references to the MAGNASTOR transportation cask, or transportation cask, in Chapters 1, 6, 8, 9 and 13A. Each of these items has been reviewed and all specific references to the MAGNASTOR transportation cask have been deleted. References to a generic transportation cask have been retained where appropriate.

**NAC INTERNATIONAL RESPONSE
TO
REQUEST FOR ADDITIONAL INFORMATION**

CHAPTER 2 PRINCIPAL DESIGN CRITERIA

Section 2.1 MAGNASTOR System Design Criteria

2-1 Add NUREG-0612 to SAR Table 2.1-1 as transfer cask design criteria.

Fuel loading with the transfer cask in the reactor or fuel building is also subject to the guidance provided in NUREG-0612, "Control of Heavy Loads at Nuclear Power Plants." This information is needed to determine compliance with 10 CFR 72.2(a)(1), 72.11, and 72.236.

NAC International Response

NUREG-0612 is added in Table 2.1-1 on Page 2.1-2 as a transfer cask design criteria reference.

**NAC INTERNATIONAL RESPONSE
TO
REQUEST FOR ADDITIONAL INFORMATION**

CHAPTER 2 PRINCIPAL DESIGN CRITERIA

Section 2.2 Spent Fuel to Be Stored

- 2-2 Identify the design basis fuel for both PWR and BWR fuel by manufacturer and array size.

This section has a generic list of fuel types, but does not identify the manufacturer nor the design basis fuel for shielding or criticality assessments.

This information is needed to determine compliance with 10 CFR 72.104, 72.106, 72.122, and 72.126.

NAC International Response

Sections 2.2.1 and 2.2.2 are revised to describe the bounding PWR and BWR fuel that are the bases for the criticality, thermal, shielding and structural evaluations and to provide references to the applicable SAR sections, figures and tables. Identification of a specific PWR or BWR fuel assembly by manufacturer and array size is not generally as appropriate as defining the bounding case for the evaluation.

Other minor editorial changes have been incorporated into Section 2.2 for clarification purposes.

**NAC INTERNATIONAL RESPONSE
TO
REQUEST FOR ADDITIONAL INFORMATION**

CHAPTER 2 PRINCIPAL DESIGN CRITERIA

- 2-3 Revise the entire application where burnup is indicated, including technical specifications to indicate peak average burnup. This should be limited to no more than 62.5GWd/MTU. Further, throughout the application where burnup is referenced, specify whether it is the peak rod burnup, average rod burnup, peak assembly burnup, etc. (Note: peak average rod burnup is determined by averaging the burnup in any rod over the length of the rod, then using the highest burnup calculated as the peak average for the assembly.)

As stated in Interim Staff Guidance (ISG-11), Revision 3, "Cladding Considerations for the Transportation and Storage of Spent Fuels," approval for storage and transport will be granted only for burnups up to that approved by the Office of Nuclear Reactor Regulation (NRR) for reactor operation. For example, the value is currently 62.5GWd/MTU peak average for PWR fuel. This information is needed to determine compliance with 10 CFR 72.122(h)(1).

NAC International Response

The application has been revised to limit the peak average rod burnup to 62.5 GWd/MTU. This limit has been inserted into Sections 2.2, Tables 2.2-1 and 2.2-2 and Chapter 13 Appendix B. The definitions "peak average rod burnup" and "assembly average burnup" have been added to SAR Sections 1.1 – Terminology and 1.1 – Definitions of Chapter 13, Appendix A.

The maximum assembly average burnup for the PWR system has been revised from 70 GWd/MTU to 60 GWd/MTU to provide a match to the specified peak average rod burnup limit. The SAR has been revised throughout to clearly indicate that assembly average burnup is employed in the shielding related analysis sections and that peak average rod burnup limits are set for fuel performance related analysis sections.

**NAC INTERNATIONAL RESPONSE
TO
REQUEST FOR ADDITIONAL INFORMATION**

CHAPTER 3 STRUCTURAL EVALUATION

The following information is needed to determine compliance with 10 CFR 72.2(a)(1), 72.11, and 72.236(a), unless otherwise stated. It should be noted that other regulatory requirements may be applicable.

Section 3.5.1 TSC Evaluation for Normal Operating Conditions

- 3-1 SAR Tables 3.5-1, -2, -3, and -4 - Revise stress summary tables to include stresses, as a minimum, at section cut locations 2, 3, 8, and 9 on the TSC shell body and location 1 at the closure-to-shell weld joint. (Note: This request also applies to stress summary tables for all other TSC loading conditions.)

The stress values and margins, reported mostly for locations in the closure and the bottom plates, are not sufficiently indicative of the TSC structural performance under various loading conditions. Stresses at other critical shell body locations and at the closure weld should also be listed for a comprehensive TSC evaluation.

NAC International Response

Tables 3.10.3-1 through 3.10.3-17 have been added in Section 3.10.3 to provide additional structural evaluation detail of the TSC finite element model analyses results for normal, off-normal, and accident conditions of storage.

**NAC INTERNATIONAL RESPONSE
TO
REQUEST FOR ADDITIONAL INFORMATION**

CHAPTER 3 STRUCTURAL EVALUATION

Section 3.5.2 Fuel Basket Evaluation for Normal Operating Conditions

- 3-2 On SAR Pages 3.5-6 and 3.5-16, describe how the bearing areas of 0.21 in² and 0.34 in² at the fuel tube and connector pin interfaces are established for the PWR and BWR baskets, respectively. The SAR sketches lack sufficient details for staff review. Also, it's unclear why the bearing area considered for the PWR basket tube, with a 5/16-inch thick wall, is smaller than that for the BWR basket tube with a relatively thinner wall thickness of 1/4 inch.

NAC International Response

The description and the sketches in the SAR have been enhanced to clarify the presentation of the bearing area for the PWR and BWR fuel tubes. The diameter of the connector pin assembly for the BWR fuel tubes, 1.0 inch, is larger than that for the PWR fuel tubes, 0.75 inch. Therefore, the corresponding bearing area is larger for the BWR configuration.

**NAC INTERNATIONAL RESPONSE
TO
REQUEST FOR ADDITIONAL INFORMATION**

CHAPTER 3 STRUCTURAL EVALUATION

- 3-3 Thermal Stress Evaluations - For the axial fuel power distribution of SAR Figures 4.4-4 and 4.4-5 for the PWR and BWR fuel assemblies, respectively, evaluate temperature effects on fuel basket deformations and thermal stresses resulting from the tube end constraints accorded by the connector/drive pin assemblies between fuel tubes.

For the design basis axial power distributions, the connector/drive pin assemblies at the basket top and bottom ends tend to restrain radial thermal growth of the basket, thereby resulting potentially in large thermal stresses in the fuel tubes. This information is needed for a comprehensive evaluation of the thermal performance of the baskets.

NAC International Response

Two new ANSYS three-dimensional models have been generated for the thermal stress evaluation for the PWR and BWR fuel baskets (Sections 3.10.1.2.2 and 3.10.2.2.2). The models represent approximately 47 inches of the top and bottom portions of the fuel baskets. The restraints due to the connector pin assemblies at the basket top and bottom are considered in the models by coupling the nodes of the pins from the adjacent fuel tubes. Bounding thermal gradients in the basket radial and axial directions are applied to the models to generate the worst case thermal stresses for the normal and off-normal conditions of storage and the transfer conditions.

The thermal stress evaluation results in Sections 3.5.2.1 (PWR) and 3.5.2.2 (BWR) have been updated. The stress analysis results indicate that combined P+Q (Primary + Secondary) stresses are well below the allowable stresses. The constraints at the top and bottom of the basket do not have a significant effect on the thermal stresses in the basket.

**NAC INTERNATIONAL RESPONSE
TO
REQUEST FOR ADDITIONAL INFORMATION**

CHAPTER 3 STRUCTURAL EVALUATION

Section 3.7.1 TSC Evaluations for Storage Accident Conditions

- 3-4 With respect to SAR Tables 3.7.1 and 3.7.2 and Figure 3.C-2, discuss why section cut location 1, in lieu of location 2, was determined to be the most critical for reporting membrane and membrane-plus-bending stresses during the tip-over accident.

Figure 3.C-2 shows that location one cuts right into the 2¾-inches thick TSC bottom plate while location two establishes the interface between the 1/2-inch thick shell body with the bottom plate. By inspection, internal forces developed at section cuts one and two should essentially be in equilibrium. Contrary to those reported in the tables, it appears that the TSC shell is much thinner than the bottom plate, stresses at cut location two should be much more critical than those at location one.

NAC International Response

The tip-over accident structural evaluation for the TSC has been updated. The finite element model has been revised to include the closure ring at the top of the TSC. The model boundary condition at the TSC shell surface is modified to reflect the actual locations of the concrete cask support rails. A tapered inertial load (40g at top of TSC closure lid and 1g at the base of the concrete cask) is considered as a side impact load of the TSC. The critical stress location for tip-over is in the TSC shell at the level of the termination of the concrete cask support rails (Section 5).

Tables 3.10.3-1 through 3.10.3-17 have been added in Section 3.10.3 of the SAR to provide additional structural evaluation detail of the TSC finite element analysis results for all conditions of storage.

**NAC INTERNATIONAL RESPONSE
TO
REQUEST FOR ADDITIONAL INFORMATION**

CHAPTER 3 STRUCTURAL EVALUATION

Section 3.7.2 Fuel Baskets Evaluation for Storage Accident Events

- 3-5 PWR Fuel Tube Evaluation - With respect to SAR Figures 3.7-2 and 3.A-8, explain the apparent discrepancy in element discretization scheme for the two-dimensional plane strain plastic finite element model for the basket fuel tube. (Note: This request also applies to the BWR fuel tube evaluation.)

NAC International Response

SAR Figures 3.7-2 and 3.A-8 correspond to two different models. The fuel tube cross-section of the finite element model shown in Figure 3.7-2 corresponds to the three-dimensional periodic model. The finite element discretization shown in Figure 3.A-8 corresponds to the two-dimensional plane strain plastic model.

Sections 3.A and 3.B have been renumbered to be Sections 3.10.1 and 3.10.2, respectively. Sections 3.10.1.2 (PWR) and 3.10.2.2 (BWR) have been revised to reflect the updated models used for the evaluation of the basket. Each model corresponds to a specific loading condition:

1. 3-D half-symmetry periodic model for stress evaluation for off-normal conditions.
2. 3-D quarter-symmetry model for thermal stress evaluation
3. 3-D half-symmetry periodic plastic model for stress evaluation for the cask tip-over accident condition.

Figures 3.A-8 (PWR) and 3.B-8 (BWR) are deleted from the SAR, since the 2-D plane strain plastic models have been replaced by the 3-D half-symmetry periodic plastic model.

**NAC INTERNATIONAL RESPONSE
TO
REQUEST FOR ADDITIONAL INFORMATION**

CHAPTER 3 STRUCTURAL EVALUATION

- 3-6 PWR Fuel Tube Evaluation - Revise SAR Figures 3.7-2 and 3.7-4 to provide sufficient description of finite element modeling details for the pin-to-socket connection by also recognizing, as appropriate, physical attributes of the pin and socket recess for force distribution consideration at the connection interface. (Note: This request also applies to the BWR fuel tube evaluation.)

NAC International Response

Figures 3.10.1-10 and 3.10.2-10 have been added to the SAR to show the modeling details of the pin-to-socket connections for the PWR and BWR fuel baskets, respectively. The interface between the pin and the fuel tube socket is represented by the ANSYS CONTAC52 gap elements. For the periodic models, BEAM4 elements with minimal properties (Area = 0.001 inch²) are defined at pin-to-socket weld locations. The purpose of the BEAM4 elements is to prevent numerical instability during the ANSYS solution of the finite element models. The BEAM4 elements have an insignificant effect on the structural behavior of the fuel baskets.

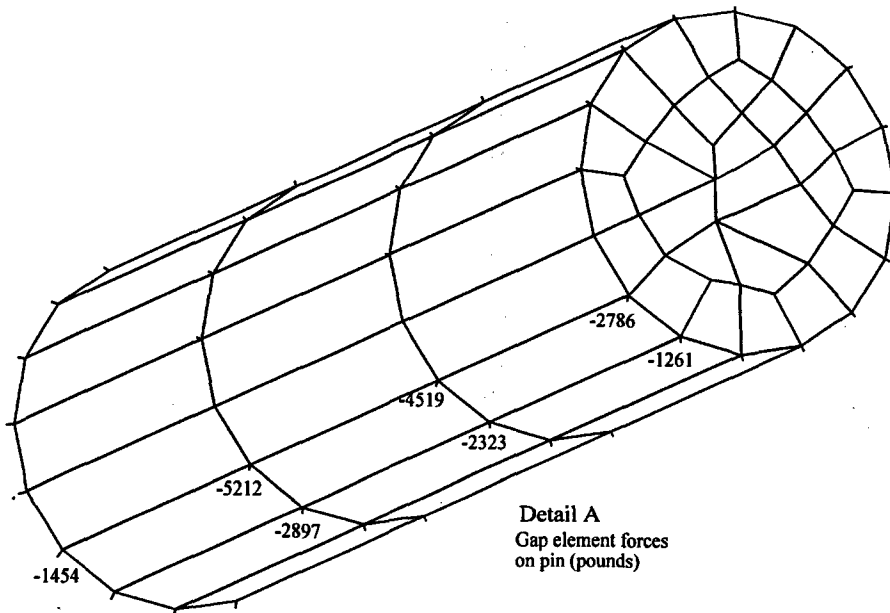
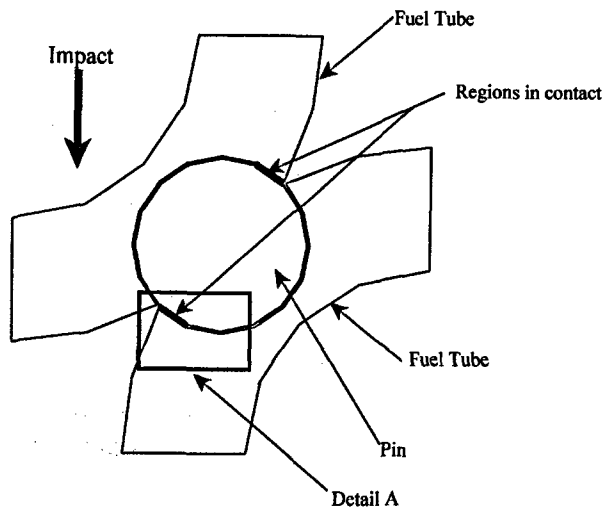
A typical pin-to-socket interface in the finite element model for a side impact loading condition is shown in the following sketch. At the region where the pin and the fuel tube socket are in contact, the gap is closed and a compression force normal to the contacting surfaces is calculated at each CONTAC52 element, as shown in Detail A of the sketch.

**NAC INTERNATIONAL RESPONSE
TO
REQUEST FOR ADDITIONAL INFORMATION**

RAI 3-6

NAC International Response (continued)

Contact Between Pin and Fuel Tube Socket



**NAC INTERNATIONAL RESPONSE
TO
REQUEST FOR ADDITIONAL INFORMATION**

CHAPTER 3 STRUCTURAL EVALUATION

- 3-7 PWR Fuel Tube Evaluation - On SAR Page 3.7-9, (1) clarify the statement, "The 45° basket orientation does not produce shear loads in the pins, the load between adjacent fuel tubes is reacting out directly in bearing in the corner flats;....," and (2) discuss how the bounding maximum shear load of 10,000 lbs. is established for the pins.

SAR Figure 3.7-4 appears to suggest that, for the 45° basket orientation, the pin at section cut location four is subject to shear, in lieu of bearing force, during a cask tip-over accident.

NAC International Response

SAR Section 3.7.2.1.2 has been revised to clarify the discussion and evaluation of shear loads in the pins for the PWR basket. The statement "The 45° basket orientation does not produce shear loads in the pins..." has been deleted. The shear load in the pins is obtained from the finite element models. The maximum shear load in the pins occurs in the 0-degree basket orientation for the cask tip-over accident and a bounding shear load of 18,000 pounds is used for the evaluation of pin shear load for the PWR fuel tube configuration. Note that the pin length is increased from 2.0 inches to 3.25 inches for the PWR fuel tubes to provide an adequate factor of safety. Similar changes have been incorporated in Section 3.7.2.2.2 for the BWR fuel tube configuration. The pin length is increased from 2.0 inches to 3.0 inches for the BWR fuel tubes. A bounding load of 15,000 pounds is used for the evaluation of pin shear load for the BWR fuel tubes.

**NAC INTERNATIONAL RESPONSE
TO
REQUEST FOR ADDITIONAL INFORMATION**

CHAPTER 3 STRUCTURAL EVALUATION

- 3-8 On the basis of the quasi-static analysis of the fuel baskets subject to a side-drop loading of 40 g, provide sketches, as appropriate, to depict the deformed basket configurations resulting from potential plastic deformations of the basket components. (Note: This request also applies to the BWR fuel tube evaluation.)

Information on permanent basket tube deformations due to material yielding, if any, is needed for criticality control evaluation of the stored fuel subject to the cask tip-over accident.

NAC International Response

The g-load used in the PWR and BWR fuel basket analyses has been revised from 40g to 35g, which remains conservative and bounding for a tip-over impact. The calculated maximum g-load, including the dynamic load factor, is 32.2g at the top of the PWR fuel basket for the concrete cask tip-over accident, as shown in Table 3.7-14 in the SAR.

A discussion on the basket displacements based on the quasi-static analysis for the side impact loading for the cask tip-over accident has been added to SAR Section 3.7.2.1.2 and Section 3.7.2.2.2 for the PWR and BWR baskets, respectively. To evaluate any possible permanent deformation of the basket fuel tubes after the tip-over impact, LS-DYNA analyses have been performed using two-dimensional half-symmetry models for the PWR and BWR fuel tubes to calculate the fuel tube displacement as a function of time, as presented in SAR Section 3.10.7. The analysis results indicate that any permanent displacements of the fuel tubes after the impact are insignificant and less than the fabrication tolerance of the fuel tubes, as shown in Figures 3.7-1 and 3.7-2 for the PWR and BWR configurations, respectively.

**NAC INTERNATIONAL RESPONSE
TO
REQUEST FOR ADDITIONAL INFORMATION**

CHAPTER 3 STRUCTURAL EVALUATION

- 3-9 PWR Corner Support Weldment Evaluation - For the stress evaluation on SAR Page 3.7-15, provide a free-body diagram to illustrate the forces and section cuts for which the weld stress is evaluated. (Note: This request also applies to the BWR support weldment evaluation.)

NAC International Response

Free-body diagrams have been added to the SAR to illustrate the forces and moments for which the weld stress is evaluated for the corner support weldments in Section 3.7.2.1.2 and 3.7.2.2.2 for the PWR and BWR fuel baskets, respectively.

**NAC INTERNATIONAL RESPONSE
TO
REQUEST FOR ADDITIONAL INFORMATION**

CHAPTER 3 STRUCTURAL EVALUATION

3-10 PWR Side Support Weldment Evaluation - On SAR Page 3.7-15, clarify the statement, "The minimum factors of safety for the corner support weldment mounting plates are 3.42 for membrane stresses and 1.43 for membrane plus bending stresses."

It is not clear why the stress results calculated for side support weldment is reported for the corner support weldment.

NAC International Response

This typographical error has been corrected to reflect that the minimum factors of safety in this section correspond to the side support weldments.

**NAC INTERNATIONAL RESPONSE
TO
REQUEST FOR ADDITIONAL INFORMATION**

CHAPTER 3 STRUCTURAL EVALUATION

3-11 PWR Fuel Basket Buckling Evaluation - Considering the unique features of the pin-to-socket connections between fuel tubes, perform time-history impact and rebound response sensitivity analysis, including the most adverse combination of fabrication tolerances, to demonstrate that the load path assumptions are conservative for the quasi-static evaluation of fuel basket buckling strengths. In performing impact response analyses for different azimuthal orientations (0°, 20°, 45°, etc.) about the cask axis, compute also time-history responses of the interface by recognizing potential relative motion between the pin and socket surfaces to demonstrate that pins and sockets will not become disengaged during the cask tip-over accident. The analysis should include drop orientations in addition to 0° and 45°. (Note: This request also applies to the BWR fuel basket evaluation.)

SAR Figures 3.7-23 and -24 indicate large, sharp impact response peaks and reversals. Because the pin-to-socket connections are not positively joined together, there exists a possibility for the out-of-phase motion among the fuel tubes to cause pins to jump out of corresponding sockets. This may result in disengagement of a pin from its notch recess during the cask tip-over accident. This type of basket instability has not been addressed in the SAR.

NAC International Response

LS-DYNA models were generated for the BWR fuel basket. Only the BWR fuel basket was considered since the 45 tubes in the basket exhibit a greater degree of response to dimensional variations than the 21 tubes in the PWR fuel basket. The larger number of tubes in the BWR fuel basket represents the bounding conditions that could challenge the geometric stability of the basket.

Three fuel basket orientations were considered in the evaluation: 0°, 22.5° and 45° orientations. The models used for the 0° and 45° orientations correspond to one-half of the basket cross-section. The model for the 22.5° orientation employed the entire cross-section of the basket. The length of each model was 10 inches, which corresponds to one-half of the distance between two consecutive pins located 20 inches apart. The initial velocity and the acceleration time history applied to the fuel basket correspond to the tip-over condition described in Section 3.7.3.7. Section 3.10.6 describes the finite element

**NAC INTERNATIONAL RESPONSE
TO
REQUEST FOR ADDITIONAL INFORMATION**

RAI-3-11

NAC International Response (continued)

models and the other conditions that were evaluated in the analysis of the BWR fuel basket. To establish the bounding conditions to assess the stability of the basket, the outer dimensional width of the fuel tubes, which are not attached to the support weldments, was reduced. Two cases of tube size reduction are considered: 0.030 inch and 0.069 inch. Note that the 0.069-inch case in the model is conservative since the largest allowable fabrication assembly gap is 0.031 inch (1/32) according to the fabrication process. While the size of the fuel tube was reduced, the pin diameter and the tube spacing were unchanged. This modeling consideration permitted the tubes to be suspended without initial contact with the pins at the start of the transient evaluation. Since the inner widths of the fabricated tube and the developed tubes are different, this modeling method also allows the impact of the fuel assemblies and the tubes to occur at slightly different times to accentuate any out-of-phase loading. The results indicate that the overall basket cross-section compresses in phase, even though the tubes and pins were not in contact initially and the gaps between adjacent tubes closed at different times. It was noted that after the basket had come to rest, the fuel tubes tended to remain at the displaced position due to the fact that the initial gaps between tubes are closed during the impact, while the weldments rebound to the original configuration. Throughout the time history evaluation, no tubes were seen to dislodge from the initial configuration, nor pins to assume any configuration other than the initial configuration. The results of the use of a uniform 0.069-inch gap show that the basket is stable, which indicates that the factor of safety for instability is larger than 2 (the largest fabrication assembly gap is 0.031 inch). These evaluations confirm the stability of the pin socket configuration for both the BWR and PWR fuel baskets.

**NAC INTERNATIONAL RESPONSE
TO
REQUEST FOR ADDITIONAL INFORMATION**

CHAPTER 3 STRUCTURAL EVALUATION

3-12 Fuel Rods - Demonstrate that fuel rods with high burnup properties will maintain cladding integrity during drop impacts. Section 3.8 does not address high burnup fuel cladding integrity under drop impact conditions.

NAC International Response

Section 3.8 has been expanded to include a structural evaluation of fuel rods subject to a bounding 60 g load. High burnup fuel rod cladding material properties used in these analyses are values presented in publications developed by PNNL. Results presented in these analyses show that structural integrity is maintained for high burnup fuel subject to a 60 g load.

**NAC INTERNATIONAL RESPONSE
TO
REQUEST FOR ADDITIONAL INFORMATION**

CHAPTER 3 STRUCTURAL EVALUATION

Appendix 3.A PWR Fuel Basket Finite Element Models

- 3-13 Related to the load path description on SAR Page 3.A-1, justify that friction can be relied upon for transmitting forces between tube corners (consider tube alignment details and dimension tolerances). Also, identify the element model capable of simulating friction force magnitude and direction at tube corners. (This request also applies to the BWR fuel basket of Appendix 3.B.)

The staff notes that, for the 0° basket drop orientation, development of tube corner friction will depend on the curvature of the tube flats and the friction realized between two convex surfaces is inherently unstable. For the 45° basket orientation, there exists generally no normal force between tube corners to call into action friction forces. Therefore, the pin-to-socket connections appear to be the only credible load paths for the cask tip-over accident. The bearing reaction across tube flats, F_B , per Figure 3.A-3, should not be counted on for load paths development. (This request also applies to the BWR fuel basket of Appendix 3.B.)

NAC International Response

For the PWR and BWR fuel baskets, the fabrication assembly methods will ensure that the tube corners will have minimal gaps. During a side impact, these gaps close. Therefore, frictional forces between adjacent fuel tubes do exist. However, the friction forces are conservatively not included in the finite element evaluations of the PWR and BWR fuel baskets. The interface between adjacent fuel tube corners is modeled with CONTAC52 gap elements. The friction option of the CONTAC52 elements is not used in any of the finite element models for the fuel basket evaluations. Sections 3.A and 3.B have been renumbered to be 3.10.1 and 3.10.2, respectively. Sections 3.10.1 and 3.10.2 have been revised to clarify that friction is not used in any of the finite element models.

**NAC INTERNATIONAL RESPONSE
TO
REQUEST FOR ADDITIONAL INFORMATION**

CHAPTER 3 STRUCTURAL EVALUATION

3-14 Provide relevant sketches to depict implementation of the BEAM4 element for the weld between the fuel tube and the pin, as described on SAR Page 3.A-2. (This request also applies to the BWR fuel basket of Appendix 3.B)

NAC International Response

Sections 3.A and 3.B have been renumbered to be 3.10.1 and 3.10.2, respectively. Figures 3.10.1-10 and 3.10.2-10 have been added to the SAR to show the modeling details of the pin-to-socket connections for the PWR and BWR fuel baskets, respectively. For additional details, see the NAC Response to RAI 3-6.

**NAC INTERNATIONAL RESPONSE
TO
REQUEST FOR ADDITIONAL INFORMATION**

CHAPTER 3 STRUCTURAL EVALUATION

Appendix 3.B BWR Fuel Basket Finite Element Models

- 3-15 For the middle fuel tube shown in SAR Figure 3.B-4, discuss how its rigid body rotation about the Z-axis can be averted during the cask tip-over accident over the full range of impact and rebound.

Figure 3.B-4 shows that only two out of four corners of the subject tube are constrained from diametrical displacement, which is statically unstable in the X-Y plane. Clarify the design provisions that are accorded to this inherently unstable tube array configuration to alleviate potential fuel basket collapse during the cask tip-over accident.

NAC International Response

Sections 3.A and 3.B have been renumbered to be 3.10.1 and 3.10.2, respectively. As shown in Figure 3.10.1-4 (previously Figure 3.B-4), the middle tube is actually constrained at three (3) corners of the tube (the two corners with T_R and the upper left corner with P_B). Therefore, the stability of the middle tube is assured. This middle tube has also been shown to be stable in the finite element analysis of the fuel basket for the tip-over accident event.

**NAC INTERNATIONAL RESPONSE
TO
REQUEST FOR ADDITIONAL INFORMATION**

CHAPTER 3 STRUCTURAL EVALUATION

3-16 Demonstrate that all quasi-static and time history impact analysis have been performed for the highest g loading that is expected to occur for either storage or transportation accidents.

SAR Page 1-1 states that, "The TSC is designed and fabricated to meet the requirements for storage in the concrete cask, for transport in the transport cask, and be compatible with the U. S. Department of Energy planning for permanent disposal in a Mined Geological Disposal System." As such the TSC, fuel basket, and fuel assemblies will be subjected to both storage and transportation accident events. Therefore, these components must be designed to resist the highest g loads that occur in either storage or transportation.

This information is needed to determine compliance with 10 CFR 72.236(m).

NAC International Response

As described in the response to Question 1-7, all specific references to the MAGNASTOR transportation cask throughout the SAR have been deleted.

Quasi-static analyses have been performed for the PWR and BWR fuel baskets for a governing loading condition of a 30-foot side drop of a transport cask. The analyses considered a 60g inertia load. The analyses results indicate that the fuel baskets are structurally adequate and meet all required acceptance criteria.

In addition, a time history impact analysis is performed for the BWR fuel basket using the LS-DYNA program to evaluate the stability of the basket during a 30-foot side drop transport accident condition. Only the BWR fuel basket is considered since the 45 tubes in the basket exhibit a greater degree of response to dimensional variations than the 21 tubes in the PWR fuel basket. The larger number of tubes in the BWR fuel basket represents the bounding conditions that could challenge the geometric stability of the basket. The model used in this evaluation is similar to those described in Section 3.10.6 for the evaluation of the cask tip-over condition for storage. The analysis results indicate that BWR fuel basket maintains its structural integrity and stability during and after the impact loading.

**NAC INTERNATIONAL RESPONSE
TO
REQUEST FOR ADDITIONAL INFORMATION**

CHAPTER 4 THERMAL EVALUATION

The following information is needed to determine compliance with 10 CFR 72.236(f).

- 4-1 Justify the assumption of applying the same porous media flow resistance parameters for the radial and axial components of the flow.

These parameters were calculated for the cross-sectional view of the storage cell(direction of flow) and should not be applied to the radial direction. Because the bounding walls of the basket storage cells do not allow transverse flow, one acceptable approach to represent the flow resistance in the radial direction (which is basically infinite) could be to use values that are at least two orders of magnitude larger than the calculated parameters of the main direction of flow.

NAC International Response

The CFD analysis for the flow of the helium gas in the canister has been revised to include a radial porosity factor for the active fuel region. This was performed for both the PWR and the BWR fuel assemblies. The effect of the radial porosity is confirmed by observing the radial velocity component to be sufficiently negligible. As a result of this model alteration as well as other modeling enhancements, the temperatures presented in Chapter 4 have been revised.

**NAC INTERNATIONAL RESPONSE
TO
REQUEST FOR ADDITIONAL INFORMATION**

CHAPTER 4 THERMAL EVALUATION

- 4-2 Justify why an emissivity value was specified for the bounding walls of the porous media in the FLUENT model of the storage cask.

Emissivity of the basket walls enclosing the porous media regions of the FLUENT 2-D model should be equal to zero or a very small value. Radiation heat transfer is used to calculate the effective thermal conductivity of the basket in the ANSYS models. Therefore, the radiation heat transfer through the porous media regions should be removed from the FLUENT model because it is already taken into consideration in the ANSYS model.

NAC International Response

The wall bounding the porous media model has two surfaces. One surface faces the interior, or the porous media. The emissivity on the surface facing the porous media should be set to zero, since it is taken into account in the effective properties for the basket. The surface of the bounding wall which faces the inner surface of the canister shell does radiate to the inner surface of the canister. The emissivity of this surface that faces the canister shell corresponds to electroless nickel. The CFD analysis for the flow of the helium gas in the canister has been revised to employ a zero emissivity on the inside of the wall of the porous media and the emissivity for electroless nickel on the outside of the wall. As a result of this model alteration, as well as other changes, the temperatures presented in Chapter 4 have been revised.

**NAC INTERNATIONAL RESPONSE
TO
REQUEST FOR ADDITIONAL INFORMATION**

CHAPTER 4 THERMAL EVALUATION

- 4-3 Provide a thermal calculation package of the BWR fuel configurations similar to the calculation package of the PWR fuel configurations provided in the SAR.

The staff needs to review the calculation package to ensure that it is acceptable.

NAC International Response

The calculation for the thermal analysis of the BWR canistered fuel in the concrete cask is being provided as proprietary information with this response.

**NAC INTERNATIONAL RESPONSE
TO
REQUEST FOR ADDITIONAL INFORMATION**

CHAPTER 4 THERMAL EVALUATION

- 4-4 Provide the flow resistance calculation for PWR and BWR fuel assembly configurations.

One possible approach to determine the porous media flow resistance parameters would be to perform a computational fluid dynamics (CFD) analysis for each type of fuel assembly for the expected operating conditions (pressure and average gas temperature) when it is inside the dry storage cask.

NAC International Response

The resistance to flow of the helium or water up through the fuel assemblies is represented by a pressure drop which is expressed as $(\mu/\alpha) V$. The quantities μ , α and V are viscosity, permeability and velocity respectively. In this expression the $1/\alpha$ is considered to be dependent on the geometry only. The flow inside the porous media region is considered to be laminar flow only which simplifies the modeling of the flow along the fuel rods and through the fuel assembly grids. The value for $1/\alpha$ is determined for the bounding PWR and bounding BWR fuel assemblies, which requires the use of two three-dimensional Fluent models. For the determination of the $1/\alpha$ for the PWR, a 17×17 fuel assembly is used, and for the BWR, a 10×10 fuel assembly is used. The dimensions used for these models correspond to the bounding dimensions which minimizes the cross sectional area for the flow. This is considered to be conservative, since the dimension of the largest fuel assembly is being combined with the largest fuel rods of the fuel assembly inventories. The additional flow resistance due to the fuel assembly grid is computed in a similar fashion using a three-dimensional model of a PWR fuel assembly grid. The revised porous media constants have been incorporated into BWR and PWR canister calculations to provide revised temperatures for all conditions of the canister in the transfer cask and the concrete cask. A description of the calculation for the porous media constants has been incorporated into the SAR in Section 4.8.3. Additionally, the details of the porous media constants are being provided in a separate proprietary calculation with this response.

**NAC INTERNATIONAL RESPONSE
TO
REQUEST FOR ADDITIONAL INFORMATION**

CHAPTER 4 THERMAL EVALUATION

- 4-5 Justify the assumed turbulent flow conditions for the air annular gap of the storage cask.

The staff believes that in order to justify the assumption of conditions of fully developed turbulent flow in the air annular gap, it would be necessary to validate the assumption by comparing it with experimental data obtained from a geometry that closely resembles the system geometry. Also, the applicable turbulent flow option (k-epsilon, k-omega, etc.) should be fully justified. The staff's analysis of the VSC-17 Ventilated Concrete Cask has indicated that the use of FLUENT's k-omega turbulent flow model (which includes transitional flow) may produce the best fit to experimental data.

NOTE: Additional information prepared by the staff on the use of FLUENT and other CFD codes can be found in the letter to Holtec International dated March 23, 2005 (Agencywide Documents Access and Management System (ADAMS) Accession Number ML050830056).

NAC International Response

A series of analyses have been performed for the thermal test of the VSC-17 as documented in EPRI TR-100305. The vertical concrete cask with canistered fuel used in this thermal test provides an accurate test model for the MAGNASTOR design. The heights are comparable since both designs store PWR fuel. The diametric thickness of the annular gap for the VSC-17 and MAGNASTOR are 3 inches and 3.75 inches respectively, which reinforces the acceptability of the VSC-17 thermal tests as a benchmark. While the thermal tests involved multiple conditions of the canister and vents, the primary focus of the thermal test was the use of the vacuum test since it minimized the uncertainty of the temperatures of the canister surface. Two-dimensional axisymmetric models were constructed for both the k- ω turbulent model and the k- ϵ turbulent models. The results for these models indicate that both turbulent models provided conservative canister surface and concrete liner temperatures. It was observed that the k- ϵ model provided closer agreement for the peak canister surface and concrete cask liner surface temperatures. Additionally, the k- ϵ turbulent model provided closer agreement for the temperature profile along the surface in the axial direction for both

**NAC INTERNATIONAL RESPONSE
TO
REQUEST FOR ADDITIONAL INFORMATION**

RAI 4-5

NAC International Response (continued)

the canister surface temperatures and the concrete cask liner surface temperatures. A description of the two models and the results are contained in SAR section 4.8.3. In addition to the two cases for the turbulent models, two cases are presented in Section 4.8.3 to confirm the use of the operating density at the inlet and the effect of the size of the heat generation region for the active fuel region. Additionally, the details of the thermal benchmark analyses are being provided in a separate proprietary calculation with this response.

**NAC INTERNATIONAL RESPONSE
TO
REQUEST FOR ADDITIONAL INFORMATION**

CHAPTER 4 THERMAL EVALUATION

- 4-6 Justify the use of a continuous annulus cooling system so allowable maximum temperatures are not exceeded during transfer operations.

This may not meet the 10 CFR Part 72 regulations for heat removal. An exemption and additional specific technical specifications may be required for this cooling system.

NAC International Response

Based on additional thermal transient analyses of the canister transfer and closure operations, transfer cask annulus cooling is not mandatory to the safe operation of MAGNASTOR. As detailed in the Operating procedures in Chapter 9, the TSC Annulus Cooling System may be used at facilities during the canister closure, draining, drying and testing operations to provide greater time to complete the specific sequence of canister preparation activities prior to storage operation.

In facilities where the canister and transfer cask are not removed from the spent fuel pool, an in-pool shelf or an equivalent immersion device, the spent fuel pool water inventory, or equivalent, will provide the necessary cooling for the canister during the canister preparation evolution. In these cases where the canister is then moved within a short time period to complete the canister to concrete cask transfer, auxiliary cooling of the canister is not required.

In order to increase the allowable times available to complete certain operational sequences, i.e, canister closure welding with the canister cavity essentially full of water; vacuum drying of the canister cavity following water draining; and during final canister preparations following canister drying, an auxiliary TSC Annulus Cooling Water System may be utilized. The operation and use of the TSC Annulus Cooling System increases allowable operating times, but does not eliminate the need to evaluate the appropriate times for completing the identified operational evolutions. However, the evolution times identified in Chapter 9 for canister loading with or without the auxiliary canister cooling system are sufficient to allow the canister closure and preparation sequence to be successfully completed without the need to take the defined corrective actions.

**NAC INTERNATIONAL RESPONSE
TO
REQUEST FOR ADDITIONAL INFORMATION**

RAI 4-6

NAC International Response (continued)

The details of the canister closure and preparation for storage are provided in the Chapter 9 operating procedures. These procedures provide directions for completing the operational sequence with, or without, the auxiliary canister cooling system, and the appropriate time and temperature limitations applicable to each phase of the canister closure, preparation and transfer operation.

In general, if an auxiliary cooling system is to be utilized as an operating tool during the loading sequence, the system will normally circulate clean water through the transfer cask-canister annulus, thereby removing heat from the canister exterior surfaces, and discharging the outlet flow to the spent fuel pool, plant drain system(s) or through a heat exchanger for return to the system inlet. The auxiliary cooling system will be identified by the user's QA program, and appropriately procured and operated.

**NAC INTERNATIONAL RESPONSE
TO
REQUEST FOR ADDITIONAL INFORMATION**

CHAPTER 4 THERMAL EVALUATION

- 4-7 Provide thermal analyses for off-normal and accident conditions for transfer operations with continuous annulus cooling, limiting conditions for operation, and design features.

Design features of the annulus cooling may need to be included in the technical specifications. It may also be necessary to include a requirement in the CoC for first time use of the cooling system. The SAR should include a description of the cooling system and the acceptance criteria for the first time use of the system.

NAC International Response

The off-normal condition for use of the continuous cooling system corresponds to loss of cooling by the annulus cooling system. This can occur during the water phase or the drying phase of transfer operations. If loss of cooling occurs during the water phase, a conservative energy balance shows that the cask can be maintained for 7 hours without exceeding 212°F. If the water phase is to exceed this time limit, the cask is to be returned to the spent fuel pool. In the event the loss of cooling occurs during the drying phase using vacuum drying, the canister is backfilled with helium, and a time of 11 hours is permitted to return the annulus cooling to service or return the canister to the pool. These procedures have been included in Chapter 9 for operations.

**NAC INTERNATIONAL RESPONSE
TO
REQUEST FOR ADDITIONAL INFORMATION**

CHAPTER 5 SHIELDING EVALUATION

The following information is needed to determine compliance with 10 CFR 72.104, 72.106, 72.122, and 72.126.

- 5-1 Provide a diagram of the concrete cask that includes dimensions and materials. This diagram should also include dimensions of the inlets and outlets.

Detailed drawings are provided of the canister, fuel baskets and transfer cask. No drawings could be found in the SAR that clearly identify the dimensions and locations of the inlets and outlets of the concrete canister. Drawings with dimensions of the inlets and outlets are needed to perform confirmatory calculations.

NAC International Response

Diagrams for the concrete cask are shown in Figures 5.5-1 through 5.5-3. Figure 5.5-1 contains a legend for the materials employed (limited to concrete and carbon steel for the concrete storage cask). Figure 5.5-2 contains a detailed side view of the inlets.

Additional dimensions are added to the diagrams shown in Figures 5.5-1 and 5.5-2 to minimize the need for consulting the licensing drawing in relation to the shielding analysis. A top view of the inlets, showing the inlet width, is added to the model sketch in Figure 5.5-2. Also added is Figure 5.5-3 describing the model for the upper concrete cask section. The upper model section shown in Figure 5.5-3 reflects the primary shielding model on which the revised licensing dose rates are based. This configuration bounds both the full length and segmented concrete casks reflected in the licensing drawings.

Key dimensions and materials for the concrete cask construction are provided in Table 5.5-2.

Detailed information on the concrete cask, including dimensions and locations for the air inlet and outlets, is provided in Drawing 790-561 "Structure, Weldment, Concrete Cask, MAGNASTOR." Drawing 790-590 is revised to include side and top views of the segmented concrete cask.

**NAC INTERNATIONAL RESPONSE
TO
REQUEST FOR ADDITIONAL INFORMATION**

CHAPTER 5 SHIELDING EVALUATION

- 5-2 Identify the PWR and BWR fuel used to determine the dose rates reported in Section 5.1 and Table 5.1-1 of the SAR.

This section and table list dose rates for the transfer cask and concrete cask, but does not specify the design basis fuel or if the dose rates are for PWR or BWR fuel.

NAC International Response

Design basis fuel types for the MAGNASTOR system are the generic fuel types listed in Tables 5.2-1 and 5.2-2, with further detail provided in Tables 5.8.1-1 and 5.8.1-2 (formerly Tables 5.A-1 and 5.A-2) and Tables 5.8.1-4 and 5.8.1-5 (formerly Tables 5.A-4 and 5.A-5).

The PWR intact fuel (no fuel insert) definitions for each cask surface producing maximum dose rates are included in Section 5.8.3.3 (formerly Section 5.C.3) for the transfer cask and Table 5.8.3-6 (formerly Table 5.C-6) for the concrete cask. Similar BWR intact fuel definitions for each cask surface producing maximum dose rates are listed in Section 5.8.4.3 and Table 5.8.4-7 (formerly Section 5.D.3 and Table 5.D-7). Increased dose rates associated with PWR hardware, per assembly type, are listed for BPRA and thimble plugs in Section 5.8.5.2.3 (formerly Section 5.E.2.3) and for CEAs in Section 5.8.6 (formerly Section 5.F). Maximum CEA dose rates calculated for a Westinghouse CEA payload.

To clarify bounding dose rate fuel types in Section 5.1, a table is added. The new table, Table 5.1-3, contains the reactor type (PWR/BWR), burnup/enrichment/cool time at which maximum dose rates occurred, and for PWR dose rates, what non-fuel hardware produced the bounding dose rate.

**NAC INTERNATIONAL RESPONSE
TO
REQUEST FOR ADDITIONAL INFORMATION**

CHAPTER 5 SHIELDING EVALUATION

- 5-3 Explain why the dose effect from the cask top for the design basis accident is enveloped by the concrete cask side dose.

In Table 5.1-2, a summary of the concrete cask maximum dose rates is given. For the cask top for the design basis accident, there is a footnote that indicates that the dose effect is enveloped by the concrete cask side dose, but there is no supporting evaluation provided in the SAR.

NAC International Response

The top of the concrete cask is covered by an 88-inch diameter steel and concrete lid (Dwg. 71160-561). The 0.75-inch thick steel plate component of the lid is of sufficient thickness to accept the missile impact loadings without perforation per Section 3.7.3.2 (no credit is taken in the impact analysis for the concrete backing the lid plate). This plate, in combination with the two anchor cavity covers in the segmented cask, protects the high dose rate areas on top of the concrete cask from being radiologically affected by the missile loadings. The outer region of the concrete cask top surface has lower normal condition dose rates than those on the cask side. Therefore, the dose rates in this outer region are bounded by the cask side dose rates for the accident shielding condition analysis, which removed 6 inches of concrete from the entire cask radial surface, an extremely conservative assumption as the penetrating tornado missile impact evaluated is limited to an 8-inch diameter projectile.

Accident analysis text in Section 12.2.11.5 is augmented to reflect the bounding nature of the radial analysis.

**NAC INTERNATIONAL RESPONSE
TO
REQUEST FOR ADDITIONAL INFORMATION**

CHAPTER 5 SHIELDING EVALUATION

- 5-4 Provide information on the verification and validation of the NAC-CASC code. Also, provide information on how the code was modified.

Section 5.1.3 indicates that the NAC-CASC is a modified version of SKYSHINE-III, but no information is provided as to how the code was modified, by whom, or the process used to validate the code after modification.

NAC International Response

A description of NAC-CASC is included in Section 5.6.1.2. NAC-CASC refers to the same code as previously employed in NAC-UMS and NAC-MPC evaluations as "NAC Version X.X of the SKYSHINE-III Code". Section 5.6.1.2 is revised to clearly indicate the code revisions and benchmarks employed in the validation and that all verification and validation is fully compliant with the applicable NAC Quality Assurance Program.

As additional information attached to this RAI response is a paper comparing various computer codes for skyshine analysis including NAC-CASC (referred to as the NAC International version of SKYSHINE-III). The evaluation documented in this paper employed the cask-specific analysis options added by NAC to the SKYSHINE-III code. The paper is attached as proprietary information as it has not been released as of this date (accepted to be published in "Radiation Protection Dosimetry," Nov. 2005).

**NAC INTERNATIONAL RESPONSE
TO
REQUEST FOR ADDITIONAL INFORMATION**

CHAPTER 5 SHIELDING EVALUATION

- 5-5 Provide additional information on how the source term for the PWR and BWR fuel with high burnup was determined.

The SAR indicated that the SAS2H module of SCALE4.4 was used to develop source terms for a range of average burnups and initial enrichments. However, as noted in NUREG-1536, many libraries used in the codes are not appropriate for burnups greater than 33,000 MWd/MTU.

NAC International Response

Source terms for the MAGNASTOR system were created using the 44-group SCALE LWR library labeled 44GROUPNDF5. This library is composed primarily of ENDF/B-V cross sections with ENDF/B-VI data for a limited number of isotopes (in particular ^{154}Eu and ^{155}Eu). The cross-section sets are collapsed using an LWR spectrum. The references 5-5.1 thru 5-5.5 identified in this response contain extensive SAS2H validation for PWR burnup up to 47 GWd/MTU and BWR burnup up to 57 GWd/MTU. As indicated in the reference documentation, the combination of the SCALE 4.4 SAS2H sequence and the 44 GROUPNDF5 cross-section library is applicable to LWR fuel assembly source term generation in excess of 33,000 MWd/MTU.

Open literature validations of the SCALE SAS2H/44 group library versus experimental data do not extend to the MAGNASTOR system allowable burnup of 62.5 GWd/MTU peak average rod (burnup limit modified per RAI 2-2 response). Studies performed in Reference 5-5.6, NUREG/CR-6701 (Appendix B), indicate no analysis trends in systems sensitivity for LWR SAS2H/44GROUPNDF5 evaluations up to a burnup of 75 GWd/MTU. The SAS2H/44GROUPNDF5 sequence is, therefore, applicable to the high burnup fuel evaluated.

SAR section 5.2 is modified to incorporate this response.

**NAC INTERNATIONAL RESPONSE
TO
REQUEST FOR ADDITIONAL INFORMATION**

RAI 5-5

NAC International Response (continued)

References for RAI 5-5

5-5.1. ORNL/TM-12667, "Validation of the SCALE System for PWR Spent Fuel Isotopic Composition Analyses," Oak Ridge National Laboratory, March 1995.

5-5.2. ORNL/TM-13317, "An Extension of the Validation of SCALE (SAS2H) Isotopic Prediction for PWR Spent Fuel," Oak Ridge National Laboratory, September 1996.

5-5.3. NUREG/CR-6798, "Isotopic Analysis of High Burnup PWR Spent Fuel Samples from the Takahama-3 Reactor," US Nuclear Regulatory Commission, January 2003.

5-5.4. ORNL/TM-13315, "Validation of SCALE (SAS2H) Isotopic Predictions for BWR Spent Fuel," Oak Ridge National Laboratory, September, 1998.

5-5.5. ORNL/TM-13687, "Prediction of the Isotopic Composition of UO₂ Fuel from a BWR: Analysis of the DU1 Sample from the Dodewaard Reactor," Oak Ridge National Laboratory, October 1998.

5-5.6. NUREG/CR-6701, "Review of Technical Issues Related to Predicting Composition and Source Terms for High-Burnup LWR Fuel," U.S. Nuclear Regulatory Commission, January 2001.

**NAC INTERNATIONAL RESPONSE
TO
REQUEST FOR ADDITIONAL INFORMATION**

CHAPTER 5 SHIELDING EVALUATION

- 5-6 Explain why the MCBEND neutron spectrum was used or revise the SAR to indicate the MCNP neutron spectrum.

SAR Section 5.2.2 indicates that the neutron energy spectrum was rebinned into the MCBEND default neutron structure. However, the SAR also indicates that the MCNP code was used to determine doses, not the MCBEND code.

NAC International Response

All shielding evaluations for the MAGNASTOR application were performed with MCNP using ORIGEN-S generated source terms in the default energy bins of the MCBEND shielding code. As a continuous energy library neutron transport code, MCNP has no distinct input requirement, or preference, for the source distribution (grouping). One of the capabilities of ORIGEN-S is to rebin the neutron spectrum into the requested 28-group format without loss of information. Rather than employing the 27-group neutron energy spectrum employed in ORIGEN-S, NAC chose to use the 28-group default neutron energy spectrum of MCBEND. The MCBEND neutron energy spectrum is an arbitrary choice for the source term output binning, but was used for consistency with the MCBEND gamma spectrum (employed due to its grouping around cobalt energy lines). MCBEND, with its group spectrum, is a validated and broadly employed code. NAC has used this binning in the licensing of NAC-UMS, NAC-MPC, NAC-STC, and NAC-LWT systems. There would be no increase in the MAGNASTOR calculation result accuracy for a revised input spectrum.

SAR Section 5.2.2 was revised to clarify the specification of shielding code and source energy spectrum.

**NAC INTERNATIONAL RESPONSE
TO
REQUEST FOR ADDITIONAL INFORMATION**

CHAPTER 5 SHIELDING EVALUATION

- 5-7 Provide information on the SKYSHINE component of annual doses for a single filled cask and for a 2×10 cask array, for both PWR and BWR fuel. Include the assumptions used to calculate the SKYSHINE component.

SAR Section 5.6.4, NAC-CASC Dose Evaluation, indicates that detailed PWR and BWR evaluations are presented in the calculation appendices. However, Section 5.C.5 of the Chapter 5 Appendices only contains a summary of the doses, not a description of how the doses were determined.

NAC International Response

A breakdown of the relative contributions of the neutron and gamma radiation emitted from the radial and axial cask surfaces for a single cask is shown in Section 5.8.3.5 (formerly Section 5.C.3.5) below Figure 5.8.3-14 (formerly Figure 5.C.3-14) for the PWR system. A breakdown for the BWR single cask radiation is shown in Section 5.8.4.5 (formerly Section 5.D.3.5) below Figure 5.8.4-14 (formerly Figure 5.D.3-14). The 2×10 PWR and BWR array figures contain a tabulation limited to gamma, neutron, and air scatter n-γ divisions. As part of this RAI response the 2×10 cask array data sets are augmented to match the single cask data presented. Note that all axially (cask top) emitted radiation is the result of air scatter since detectors are located below the cask top (at personnel, ground level, elevations). Breakdowns of the bounding PWR payload radial sources into collided (air scattered) and uncollided dose portions are included in this RAI response as Tables 5-7.1 and 5-7.2. The calculation provided in conjunction with the Chapter 11 RAI provides a detailed breakdown of the scattered and direct dose contributions for PWR and BWR systems at the various detector locations.

The SKYSHINE component of the dose rate evaluation required no distinct assumptions not already inherent in the ORIGEN-S source term and MCNP shielding evaluations. The surface currents produced in the MCNP analysis for the maximum dose rate MAGNASTOR payloads are directly applied to the NAC-CASC model. Inputs into the skyshine evaluations, beyond the MCNP method, are air density (0.001225 g/cm³) and detector elevation (3 ft for the MAGNASTOR analysis). All casks are loaded with maximum surface current payloads (no decay of casks on the pad and the combination of maximum radial and axial dose rate sources).

**NAC INTERNATIONAL RESPONSE
TO
REQUEST FOR ADDITIONAL INFORMATION**

RAI 5-7NAC International Response (continued)

The SAR text in Sections 5.5.3 (NAC-CASC model), 5.8.3.5 (PWR site boundary evaluation), and 5.8.4.5 (BWR site boundary evaluation) is augmented to include additional discussions and a sample NAC-CASC input files.

SAR site boundary exposures are based on a PWR canister maximum heat load of 40 kW and a BWR canister maximum heat load of 38 kW. Cask surface dose rate tables were revised to the thermally limited 37 kW PWR and 35 kW BWR heat loads. The conservative, higher, heat load based result tables are retained in the SAR for the skyshine evaluation. SAR sections 5.8.3.5 and 5.8.4.5 are revised to indicate the conservatism of the results presented.

Table 5-7.1 PWR Single Cask NAC-CASC Results – Radial Source

Distance (m)	Dose Rate (mrem/year)			Dose Rate (mrem/year)		
	Gamma			Neutron		
	Total	Uncollided	Collided	Total	Uncollided	Collided
10	2.44E+04	2.27E+04	1.70E+03	2.85E+02	2.38E+02	4.71E+01
25	4.66E+03	3.96E+03	7.02E+02	5.92E+01	4.00E+01	1.92E+01
50	1.11E+03	8.35E+02	2.76E+02	1.65E+01	7.96E+00	8.50E+00
100	2.34E+02	1.39E+02	9.46E+01	4.16E+00	1.20E+00	2.97E+00
125	1.36E+02	7.27E+01	6.30E+01	2.56E+00	5.98E-01	1.96E+00
150	8.48E+01	4.14E+01	4.34E+01	1.68E+00	3.26E-01	1.35E+00
175	5.57E+01	2.50E+01	3.07E+01	1.14E+00	1.89E-01	9.54E-01
200	3.80E+01	1.58E+01	2.22E+01	8.04E-01	1.15E-01	6.89E-01
225	2.67E+01	1.04E+01	1.63E+01	5.80E-01	7.24E-02	5.08E-01
250	1.91E+01	6.97E+00	1.22E+01	4.27E-01	4.69E-02	3.80E-01
275	1.40E+01	4.81E+00	9.17E+00	3.19E-01	3.11E-02	2.88E-01
300	1.04E+01	3.38E+00	6.99E+00	2.42E-01	2.11E-02	2.21E-01

**NAC INTERNATIONAL RESPONSE
TO
REQUEST FOR ADDITIONAL INFORMATION**

RAI 5-7

NAC International Response (continued)

Table 5-7.2 PWR 2x10 Cask Array NAC-CASC Results – Radial Source

Distance (m)	Dose Rate (mrem/year)					
	Gamma			Neutron		
	Total	Uncollided	Collided	Total	Uncollided	Collided
50	1.47E+04	1.12E+04	3.48E+03	2.05E+02	1.07E+02	9.86E+01
100	2.75E+03	1.61E+03	1.14E+03	4.82E+01	1.40E+01	3.42E+01
150	9.80E+02	4.60E+02	5.20E+02	1.92E+01	3.67E+00	1.55E+01
200	4.38E+02	1.72E+02	2.65E+02	9.16E+00	1.27E+00	7.90E+00
250	2.21E+02	7.51E+01	1.46E+02	4.87E+00	5.10E-01	4.35E+00
300	1.20E+02	3.61E+01	8.41E+01	2.77E+00	2.28E-01	2.54E+00
350	6.85E+01	1.86E+01	4.99E+01	1.65E+00	1.08E-01	1.54E+00
400	4.07E+01	1.01E+01	3.05E+01	1.02E+00	5.45E-02	9.66E-01
450	2.48E+01	5.73E+00	1.91E+01	6.51E-01	2.85E-02	6.23E-01
500	1.55E+01	3.36E+00	1.22E+01	4.26E-01	1.54E-02	4.11E-01
550	9.96E+00	2.03E+00	7.93E+00	2.84E-01	8.52E-03	2.76E-01
600	6.53E+00	1.25E+00	5.27E+00	1.93E-01	4.82E-03	1.88E-01

**NAC INTERNATIONAL RESPONSE
TO
REQUEST FOR ADDITIONAL INFORMATION**

CHAPTER 5 SHIELDING EVALUATION

5-8 In Figure 5.6-8, Site Boundary Dose Rates vs. Distance, include that this is for PWR fuel, the burnup, initial enrichment, and cooling time for the fuel.

Figure 5.6-8 does not indicate the parameters of the fuel used to develop the figure or whether it was design basis fuel.

NAC International Response

The title to Figure 5.6-8 "Site Boundary Dose Rates vs. Distance" is modified to "Bounding Site Boundary Dose Rates vs. Distance." This change clarifies that the data shown represents the bounding payload. Per Section 5.6.4, the bounding payload is defined to be the PWR TSC. Section 5.6.4 is modified to reference Section 5.8.3.5 (formerly 5.C.5) for the bounding payload description in terms of burnup, initial enrichment, and cooling time. Table 5.8.3-7 (formerly Table 5.C-7), which is referenced from Section 5.8.3.5, provides the fuel type, burnup, and initial enrichment for the bounding (maximum) surface currents input into NAC-CASC for the listed site boundary dose rates. Both PWR and BWR SAR skyshine analysis descriptions in Section 5.8 are modified to clearly state that the indicated currents are the bounding values for any allowed design basis assembly type, initial enrichment, burnup, and cool combination.

**NAC INTERNATIONAL RESPONSE
TO
REQUEST FOR ADDITIONAL INFORMATION**

CHAPTER 6 CRITICALITY EVALUATION

The following information is needed to determine compliance with 10 CFR 72.124.

- 6-1 Provide the method for calculating the isotopic content in the full density water with boron concentration of 2500 ppm that is given in Table 6.3-1.

These isotopic number densities do not appear to be consistent with the values used in the criticality analysis as indicated in the input file in Figure 6.A-3.

NAC International Response

Data in Table 6.3-1 did not contain the correct isotopic atom densities for borated water at 2500 ppm (by weight). The calculation method and input into the soluble boron calculation are shown below. Mass fractions are entered into the MCNP input as shown in Figure 6.7.1-1 (formerly 6.A-1). The densities in atoms/barn-cm are extracted from the MCNP output by multiplying the MCNP calculated atom density and isotope atom fractions. Note that the correct boron content (ppm) in the input can be verified by summing the ^{10}B and ^{11}B mass fraction. Attached to this response are relevant sections of the MCNP output containing the borated water isotope fraction and overall atom density and the calculation of the Table 6.3-1 listed atom densities.

$$\frac{1}{\rho_{\text{BoratedWater}}} = \frac{\chi_{\text{BoricAcid}}}{\rho_{\text{BoricAcid}}^{\text{Theoretical}}} + \frac{(1 - \chi_{\text{BoricAcid}})}{\rho_{\text{UnboratedWater}}^{\text{Theoretical}}} \quad \text{Where: } \chi_{\text{BoricAcid}} = \text{Weight Fraction of Boric Acid}$$

**NAC INTERNATIONAL RESPONSE
TO
REQUEST FOR ADDITIONAL INFORMATION**

RAI 6-1NAC International Response (continued)

Water Density	0.9982	g/cm ³
Boric Acid (H ₃ BO ₃) s.g.	1.435	
Boric Acid Density	1.432417	g/cm ³
Boron Weight	10.819	amu/mole
Boric Acid Molecular Weight	61.827	amu/mole
Parts per million B	2500	weight
Fraction of Boric Acid	0.014286672	weight
Mixture Density	1.00254	g/cm ³

MCNP Output (2500 ppm case; full density water)

Material 3 is borated water

material number	component nuclide, atom fraction		
3	1001, 6.60130E-01	8016, 3.30114E-01	1001,
4.18102E-03	8016, 4.18204E-03		
	5010, 2.66196E-04	5011, 1.12752E-03	

Cell 4 contains borated water

cell	atom density	gram density
4	1.00091E-01	1.00250E+00

Atom densities are calculated for borated water based on the MCNP output (verified conversion by EXCEL calculation). Note that the hydrogen and oxygen components of water and boric acid are summed in the SAR table.

Isotope ID	Atom Fraction	Atom Fraction (Summed)	Fraction multiplied by
1001	6.60E-01		0.100091 atm/b-cm
1001	4.18E-03	6.64E-01	6.65E-02
8016	3.30E-01		
8016	4.18E-03	3.34E-01	3.35E-02
5010	2.66E-04	2.66E-04	2.66E-05
5011	1.13E-03	1.13E-03	1.13E-04

**NAC INTERNATIONAL RESPONSE
TO
REQUEST FOR ADDITIONAL INFORMATION**

CHAPTER 6 CRITICALITY EVALUATION

- 6-2 Clarify the term “interface width” as used in Section 6.4.3.1 and elsewhere in the SAR.

This term is not commonly used, but appears to be applied to a specific aspect of the basket design.

NAC International Response

The “interface width” is the dimension diagonally across the tube. This dimension controls the size of the tube stack and the opening size of the developed cell. The tube sketch in Figure 6.3-1 is modified to show the “interface width.”

The text in Sections 6.4.2.1, 6.7.3.1 (formerly 6.C.1), and 6.7.6.1 (formerly 6.F.1) is also modified to clearly define the “interface width.”

**NAC INTERNATIONAL RESPONSE
TO
REQUEST FOR ADDITIONAL INFORMATION**

CHAPTER 6 CRITICALITY EVALUATION

- 6-3 Describe the controls used to prevent misloading of BWR fuel assemblies into the five cell locations which may not contain fuel assemblies in the 82-BWR maximum capacity configuration.

The analysis shows that fuel assemblies are not allowed in five of the center basket cell positions when the initial peak planar-average enrichment in the BWR fuel assemblies exceeds the specified value for that fuel assembly type. The operating procedures should include appropriate steps to ensure that effective controls are implemented and that a confirmatory check is made before the cask lid is put into place. Distinguishing features should be discussed and employed which would make it easy to visually determine that fuel assemblies have not been inserted into the designated non-fuel locations.

NAC International Response

The designated locations are physically blocked in the 82-assembly basket configuration. Licensing drawing 71160-600 is added to the SAR which indicates the blocking features. It is not physically possible to load an assembly into the 82-assembly basket blocked locations.

Operating procedures listed in Section 9.1.1 require a minimum of two independent checks to assure that: (1) the assembly to be loaded was verified for acceptability against the allowable payload per Technical Specifications; and (2) the assembly that was checked against the Technical Specification is the assembly being loaded. Verification of the assembly characteristics against the Technical Specifications for the allowed payload includes, but is not restricted to, a check on preferential heat load loading and minimum soluble boron content for PWR system limits and the 82-assembly or 87-assembly basket configuration for BWR systems.

**NAC INTERNATIONAL RESPONSE
TO
REQUEST FOR ADDITIONAL INFORMATION**

CHAPTER 6 CRITICALITY EVALUATION

- 6-4 Show that the neutron absorber sheets continue to cover the active fuel region of the fuel assemblies during off-normal and accident conditions.

Consider the maximum possible axial shifting of the absorber sheets and the fuel assemblies in opposite directions such that the active fuel may project past the ends of the absorber plates during off-normal and accident conditions. Revise the criticality safety analysis as necessary to show that criticality safety is maintained. This type of shifting could affect the safety of any unloading operations. The neutron absorber sheets have oblong slots that allow some axial movement and the sheets are different lengths in the PWR and BWR baskets. The response should consider all fuel types to be loaded into the PWR and BWR basket configurations.

It should be kept in mind that the hypothetical accident conditions (HAC) for transport may be more challenging to the design than the storage conditions, particularly, the potential for axial shifting may be greater. Thus, if there is a desire to gain approval to transport the canisters without repackaging, any necessary measures such as inserts needed to assure continued positioning of the fuel assemblies during the HAC should be incorporated into the current design and implemented before loading begins.

NAC International Response

This response is separated into storage and transfer cask related neutron absorber coverage concerns and those concerns related to transport hypothetical accident conditions.

Storage and Transfer Conditions

No design basis condition will place a wet, loaded, canister into a non-vertical or "upside down" condition. There are also no design basis conditions that will result in a wet canister being subjected to acceleration forces sufficient to produce significant fuel damage and/or axial re-location of fuel material within the assembly. Under normal vertical conditions of operations (transfer cask upright) a limited amount (< 0.2 inches) of fuel material may be exposed below the lower edge of the neutron absorber sheet for the

**NAC INTERNATIONAL RESPONSE
TO
REQUEST FOR ADDITIONAL INFORMATION**

RAI 6-4NAC International Response (continued)

PWR WE17H1 hybrid with no fuel exposure expected in the BWR or remaining PWR configurations. There is no fuel exposure for any fuel type above the neutron absorber sheet. The minimal bottom end exposure for the vertical transfer system is accounted for in the Chapter 6 evaluations.

The neutron absorber sheets contain oblong slots to allow for potential thermal growth of the sheet as the system is dried and backfilled with helium. The neutron absorber lower weld post hole is not oblong (slotted) and, thus, will retain the lower end of the neutron absorber in a fixed axial position through all normal and accident conditions, including unloading operations. Criticality evaluations of the system with an assembly partially inserted into the basket structure have shown that loading or unloading configuration do not increase system reactivity. The results of these evaluations of partially loaded assemblies are listed in Table 6-4.1 for the PWR system and Table 6-4.2 for the BWR system, which follow.

After the storage system is placed into an inert state, by backfilling with helium, axial shifting of the components has minimal impact on system reactivity. The neutron absorber sheets are boron based and, therefore, do not serve as the primary criticality control method under dry storage conditions. No hypothetical shift in axial location of the fuel with respect to the absorber will result in the dry storage system approaching criticality limits.

Table 6-4.1 PWR Assembly Loading/Unloading Results

Exposure (Inch)	k_{eff}	σ	$k_{eff}+2\sigma$	Δk	$\Delta k/\sigma$
N/A	0.93691	0.00076	0.93843	--	--
5	0.93765	0.00075	0.93915	0.00074	1.0
10	0.93663	0.00076	0.93815	-0.00028	-0.4
15	0.93656	0.00073	0.93802	-0.00035	-0.5
20	0.93612	0.00077	0.93766	-0.00079	-1.0
25	0.93808	0.00074	0.93956	0.00117	1.6
30	0.93621	0.00071	0.93763	-0.00070	-1.0

**NAC INTERNATIONAL RESPONSE
TO
REQUEST FOR ADDITIONAL INFORMATION**

RAI 6-4NAC International Response (continued)

Table 6-4.2 BWR Assembly Loading/Unloading Results

Exposure (inch)	k_{eff}	σ	$k_{eff}+2\sigma$	Δk	$\Delta k/\sigma$
N/A	0.95668	0.00071	0.95810	--	--
5	0.95745	0.00073	0.95891	0.00077	1.1
10	0.95711	0.00071	0.95853	0.00043	0.6
15	0.95671	0.00076	0.95823	0.00003	0.0
20	0.95751	0.00074	0.95899	0.00083	1.1
25	0.95625	0.00074	0.95773	-0.00043	-0.6
30	0.95776	0.00076	0.95928	0.00108	1.5

Effect of Transport Cask Hypothetical Accident Loading on Neutron Absorber Coverage

To address potential beyond design basis transfer condition concerns and to assure that the TSC and fuel basket assembly will be suitable for transport, calculations for transport cask hypothetical accident condition loadings were performed.

Fuel assembly neutron absorber coverage is evaluated by independently investigating top and bottom transport cask end drop effects on system reactivity. For each scenario the basket is shifted in the opposite direction of the fuel. For example in the top end drop, the fuel is shifted to the lid while the basket remains at the bottom the TSC cavity. In this context the fuel assembly is shifted to the lid, fuel rods are shifted to the upper end fitting tie plate, and fuel pellets are shifted into the top plenum (distance into the plenum is based on structural evaluations of the fuel rods). For the cask bottom end drop scenario, fuel rods are shifted to the bottom tie plate and active fuel material is shifted into contact with the lower fuel rod end-cap. The basket is shifted to the canister top for the bottom drop evaluations to maximize fuel exposure. For B&W fuel, the lower plenum height is reduced to zero to maximize potential reactivity changes.

PWR Fuel Assembly Neutron Absorber Coverage

PWR fuel results for the transport cask top end drop, with the fuel shifted towards the lid and the basket conservatively remaining at the TSC bottom, are shown in Table 6-4.3.

**NAC INTERNATIONAL RESPONSE
TO
REQUEST FOR ADDITIONAL INFORMATION**

RAI 6-4NAC International Response (continued)

Also shown in the table is the resulting height of exposed fuel, which is negative for each assembly. As expected no significant reactivity change is observed for these configurations as there is no exposed fuel.

PWR fuel results for the transport cask bottom end drop are shown in Table 6-4.4. The B&W fuel assemblies have the potential for the most exposed height, ~2 inches, and the evaluations are limited to these assemblies. No significant reactivity changes are observed for any of those fuel types.

Table 6-4.3 PWR Fuel Top End Drop Fuel Exposure Results

Assembly	No Axial Shift		Top End Drop Scenario		Δk	$\Delta k/\sigma$	Exposed Height	
	k_{eff}	σ	k_{eff}	σ			(cm)	(inch)
BW15H1	0.92987	0.00071	0.93000	0.00074	0.00013	0.2	-22.78	-8.97
BW15H2	0.93574	0.00076	0.93562	0.00073	-0.00012	-0.2	-24.05	-9.47
BW15H3	0.93761	0.00073	0.93834	0.00075	0.00073	1.0	-24.05	-9.47
BW15H4	0.92108	0.00075	0.92060	0.00073	-0.00048	-0.6	-24.05	-9.47
BW17H1	0.93495	0.00080	0.93441	0.00074	-0.00054	-0.7	-22.69	-8.93
CE14H1	0.87406	0.00073	0.87581	0.00077	0.00175	2.3	-16.33	-6.43
CE16H1	0.88307	0.00075	0.88396	0.00075	0.00089	1.2	-30.42	-11.98
WE14H1	0.86436	0.00075	0.86579	0.00074	0.00143	1.9	-12.68	-4.99
WE15H1	0.92197	0.00075	0.92132	0.00075	-0.00065	-0.9	-11.23	-4.42
WE15H2	0.90838	0.00074	0.90937	0.00075	0.00099	1.3	-11.06	-4.35
WE17H1	0.93090	0.00076	0.93014	0.00077	-0.00076	-1.0	-11.19	-4.41
WE17H2	0.90755	0.00076	0.90803	0.00073	0.00048	0.6	-11.00	-4.33

Table 6-4.4 PWR Fuel Bottom End Drop Fuel Exposure Results

Assembly	No Axial Shift		Top End Drop Scenario		Δk	$\Delta k/\sigma$	Exposed Height	
	k_{eff}	σ	k_{eff}	σ			(cm)	(inch)
BW15H1	0.92987	0.00071	0.93078	0.00074	0.00091	1.3	4.90	1.9
BW15H2	0.93574	0.00076	0.93621	0.00078	0.00047	0.6	4.90	1.9
BW15H3	0.93761	0.00073	0.93961	0.00075	0.00200	2.7	4.90	1.9
BW15H4	0.92108	0.00075	0.92239	0.00077	0.00131	1.7	4.90	1.9
BW17H1	0.93495	0.00080	0.93420	0.00077	-0.00075	-1.0	4.90	1.9

**NAC INTERNATIONAL RESPONSE
TO
REQUEST FOR ADDITIONAL INFORMATION**

RAI 6-4NAC International Response (continued)BWR Fuel Assembly Neutron Absorber Coverage

BWR fuel results for the transport cask top end drop, with the fuel shifted towards the lid and the basket conservatively remaining at the TSC bottom, are shown in Table 6.4-5. Analysis results include the effect of a damaged end-fitting (bale) as a result of the end-drop. No significant reactivity changes are observed for any of the evaluated fuel types as a result of the transport cask top end drop.

There is no fuel exposed for BWR fuel assemblies after the postulated bottom end drop. Therefore, no criticality evaluations are added for this scenario.

Table 6-4.5 BWR Fuel Top End Drop Fuel Exposure Results

Assembly	No Axial Shift		Top End Drop Scenario		Δk	$\Delta k/\sigma$	Exposed Height	
	k_{eff}	σ	k_{eff}	σ			(cm)	(inch)
B7_48A	0.93146	0.00073	0.93032	0.00074	-0.00114	-1.6	5.06	1.99
B7_49A	0.94139	0.00073	0.93940	0.00076	-0.00199	-2.7	8.30	3.27
B7_49B	0.93978	0.00077	0.93746	0.00078	-0.00232	-3.0	7.94	3.13
B8_59A	0.93354	0.00073	0.93391	0.00071	0.00037	0.5	8.31	3.27
B8_60A	0.93932	0.00071	0.94044	0.00076	0.00112	1.5	8.96	3.53
B8_60B	0.93981	0.00076	0.94182	0.00076	0.00201	2.6	8.96	3.53
B8_61B	0.94021	0.00074	0.94122	0.00074	0.00101	1.4	8.31	3.27
B8_62A	0.94468	0.00078	0.94318	0.00070	-0.00150	-2.0	8.67	3.41
B8_63A	0.94427	0.00078	0.94529	0.00073	0.00102	1.4	8.52	3.35
B8_64A	0.94133	0.00076	0.94149	0.00076	0.00016	0.2	8.31	3.27
B8_64B	0.95409	0.00072	0.95433	0.00075	0.00024	0.3	8.31	3.27
B9_72A	0.94508	0.00067	0.94396	0.00076	-0.00112	-1.6	8.31	3.27
B9_74A	0.95198	0.00081	0.95066	0.00078	-0.00132	-1.7	8.30	3.27
B9_76A	0.95816	0.00076	0.95804	0.00075	-0.00012	-0.2	8.31	3.27
B9_79A	0.95125	0.00076	0.95136	0.00075	0.00011	0.1	9.09	3.58
B9_80A	0.93990	0.00079	0.94067	0.00075	0.00077	1.0	8.31	3.27
B10_91A	0.94279	0.00073	0.94197	0.00075	-0.00082	-1.1	8.31	3.27
B10_92A	0.93784	0.00073	0.93815	0.00075	0.00031	0.4	8.31	3.27
B10_96A	0.95060	0.00078	0.95078	0.00074	0.00018	0.2	8.31	3.27
B10_100A	0.95219	0.00075	0.95063	0.00074	-0.00156	-2.1	8.31	3.27

**NAC INTERNATIONAL RESPONSE
TO
REQUEST FOR ADDITIONAL INFORMATION**

CHAPTER 6 CRITICALITY EVALUATION

- 6-5 Justify or delete the statement that removal of some absorber sheets on the basket periphery does not impact system reactivity.

This statement appears in Sections 6.A and 6.D, "The analyzed basket configuration includes absorber sheets on all four sides of the fuel tubes and no analysis has been provided to justify the removal of some of the sheets." The optional notes on Drawing No. 575, sheet 3, and Drawing No. 599, sheet 3, should be removed unless they are appropriately justified.

NAC International Response

Sections 6.7.1 and 6.7.4 (formerly 6.A and 6.D) are modified to state that the primary basket criticality evaluations are performed with a model containing neutron absorber sheets on all four fuel tube sides and that confirmatory PWR and BWR evaluations demonstrate that no reactivity effect is associated with the neutron absorber sheet removal or replacement by aluminum.

Sections 6.7.3 and 6.7.6 (formerly 6.C and 6.F) are revised to include the results of the absorber sheet removal and replacement calculations.

**NAC INTERNATIONAL RESPONSE
TO
REQUEST FOR ADDITIONAL INFORMATION**

CHAPTER 6 CRITICALITY EVALUATION

- 6-6 Provide a justification for not including specifications for the fuel pellet outer diameter, fuel rod pitch, and clad thickness in the TS.

The applicant has concluded that the fuel assemblies are under-moderated. Thus, there is a sensitivity to the moderator-to-fuel ratio in the fuel rod lattice. The analyses performed to create Tables 6.B-3 and 6.E-3 modeled the pellet-to-clad gap as dry. This assumption reduced the sensitivity to pellet outer diameter, fuel rod pitch, and clad thickness and also led to a decision to put only an upper limit on the pellet diameter. Data showing the sensitivity to variations of these three fuel parameters needs to be developed for the case where the pellet-to-clad gap is flooded with unborated water (gap flooding is most likely to result from conditions near the end of the irradiation cycle when the boron concentration is approaching zero). For some of the key fuel parameters such as pellet diameter, it may be necessary to establish a maximum and minimum limit.

The data reported in NUREG/CR-6716 show that sensitivity to these three parameters can be significant for some fuel types. The degree of sensitivity can depend on the specific basket design and conditions, and needs to be assessed on a case-by-case basis.

When a cask design is intended to be a dual purpose design, it should be kept in mind that the degree of sensitivity in the PWR basket may decrease as the boron concentration in the moderator increases. Thus, parameters which may be of low significance under the analysis for storage operations may be important when a canister is evaluated for transport. Care should be taken to assure that fuel assemblies are not loaded under parameter limits that may be acceptable for storage but are not able to meet the parameter limits necessary to qualify for transport.

- a. Provide the upper subcritical limits (USL) that apply to the sensitivity study results.

Tables 6.B-3 and 6.E-3 do not give the USL values. The margin in k_{eff} with respect to the USL, as well as the range of parameter variation considered, are important factors when assessing the significance of the

**NAC INTERNATIONAL RESPONSE
TO
REQUEST FOR ADDITIONAL INFORMATION**

RAI 6-6 (continued)

parameter sensitivity. Consider using the range of values given in Tables 6.2-1 and 6.2-2 when specifying the three fuel parameters discussed above.

- b. Add fuel assembly type BW15H3 to the sensitivity analysis.

The BW15H3 fuel type appears to be the most reactive case of the BW15 class.

NAC International Response

NAC prepared the Approved Contents section of the MAGNASTOR Technical Specifications as a modification of the standard technical specification format in Section 2.0 of NUREG-1745. In accordance with that format, SAR Chapter 13 – Appendix A, Section 2.1, is revised to define the contents approved for storage to be those included in Chapter 13 - Appendix B of the Technical Specifications and, by reference, those in SAR Chapter 6, Tables 6.4-1 and 6.4-2 (i.e., “controlled tables”). SAR Chapter 13 – Appendix A, Section 2.2 defines the procedure for obtaining NRC approval of proposed alternatives to those contents specifications contained in the “controlled tables.” Based upon further review of the MAGNASTOR approved contents specifications in response to this RAI, references to SAR Chapter 6 Tables 6.4-1 and 6.4-2 (i.e., “controlled tables”), which include the additional fuel characteristics requested, are added in SAR Chapter 13 – Appendix A, Sections 2.1 and 2.2.

To support the application of the standard technical specification format NAC has performed fuel parameter variation calculations for PWR assembly dry pellet-to-clad gap, wet unborated gap, and wet borated gap for sample fuel types of each core type (NSSS) evaluated (CE, WE, and B&W). The conclusions drawn from these studies all confirm the choice of critical fuel parameters. Calculations were done for three enrichment/soluble boron concentrations (1100 ppm / 3 wt% ²³⁵U, 1800 ppm / 4 wt% ²³⁵U, and 2500 ppm / 5 wt% ²³⁵U), with consistently the same conclusion set. To address the RAI concern, the result data set shown in the SAR is replaced by one containing

**NAC INTERNATIONAL RESPONSE
TO
REQUEST FOR ADDITIONAL INFORMATION**

RAI 6-6

NAC International Response (continued)

reactivities from the wet-unborated pellet-to-clad gap evaluations. The dry and wet-borated water gap evaluation results for the expanded set of fuel characteristics (applying an increased variance) are attached in RAI Tables 6-6.1 and 6-6.2. Result sets shown are obtained from a combination of 2500 ppm soluble boron and 5 wt% ^{235}U enriched fuel.

For each fuel type the range of parameters in Table 6.2-1 was applied in the fuel characteristics studies (as indicated by max and min in the result tables). Since the dimensional range in Table 6.2-1 was not sufficient for a Monte Carlo solution to arrive at statistically significant conclusions across all fuel types and parameters of interest an increased range was studied by applying tolerances to the fuel design parameters. For reviewer information Table 6-6.3 is added to the RAI response. Table 6-6.3 contains the results of a wet-unborated gap study based on the characteristics shown in Table 6.2-1 without applying the increased variance.

Since the analysis trends are constant over widely varying fuel types and configuration, the analysis presented in the SAR did not consider it necessary to include the BW15H3 hybrid. The BW15H3 hybrid contains significantly higher fuel mass than actual fuel assemblies for the particular core type and was not included in the initial data set. As a response to the RAI the BW15H3 hybrid is added to the analysis and SAR data. As shown in Section 6.7.2 (formerly Section 6.B) the addition of this data set did not invalidate the conclusions drawn from the previously listed assembly types.

The lattice parameter studies are meant to locate significant fuel variables and determine bounding characteristics. The addition of the USL to the tables was not considered to be relevant. To address the RAI the USL (fixed lower bound) is included in the section text discussing the results of the analysis.

To provide additional justification for the bounding fuel dimensional characteristics set (i.e., pitch, clad OD, clad thickness, pellet OD, and active fuel length) specified in the MAGNASTOR application and to apply the "Standard Technical Specification" fuel definition suggested in NUREG/CR-6716, NAC repeated a portion of the NUREG study with the fuel assemblies placed into the MAGNASTOR system. Results for criticality evaluations placing the NUREG defined PWR 17x17 and BWR 8x8 fuel types into the

**NAC INTERNATIONAL RESPONSE
TO
REQUEST FOR ADDITIONAL INFORMATION**

RAI 6-6NAC International Response (continued)

MAGNASTOR system (at a representative enrichment and soluble boron level) are shown in Tables 6-6.4 and 6-6.5. The study demonstrates that the response of the MAGNASTOR system is similar to the system evaluated in the NUREG and that the conclusions drawn in the NUREG, in particular those relating to criticality control parameters required in the Technical Specification section of the SAR, are applicable to the MAGNASTOR system.

Table 6-6.1 PWR Lattice Parameter Study – Dry Gap (Increased Variance)

	2	6	1	4	3	5	7	8
Fuel Pin Cell H/U	Max	Min	Max	Max	Max	Min	Min	Min
Pellet Dia.	Max	Max	Max	Min	Min	Max	Min	Min
GT/IT Thick & Dia.	Min	Min	Max	Min	Max	Max	Max	Min
CE14H1	0.86660	0.85741	0.86660	0.85176	0.85287	0.85779	0.84522	0.84431
CE16H1	0.87184	0.86089	0.87369	0.87278	0.87261	0.86151	0.86215	0.86186
BW15H3	0.93027	0.92423	0.93069	0.92438	0.92512	0.92408	0.92070	0.91839
BW15H4	0.91651	0.91032	0.91651	0.91394	0.91482	0.91110	0.91083	0.90928
BW17H1	0.92895	0.92268	0.93009	0.92501	0.92333	0.92001	0.91532	0.91647
WE14H1	0.85400	0.84084	0.85504	0.82412	0.82293	0.84169	0.81209	0.81275
WE15H1	0.91374	0.90718	0.91472	0.89935	0.89967	0.90962	0.89375	0.89557
WE17H1	0.92359	0.91592	0.92324	0.91923	0.92068	0.91674	0.91182	0.91289
		Case 2 To Case 6	Case 2 To Case 1	Case 2 to Case 4	Case 2 to Case 3	Case 2 to Case 5	Case 2 to Case 7	Case 2 To Case 8
		$\Delta k_{eff}/\sigma$						
CE14H1		-8.3	--	-13.6	-12.9	-8.2	-19.8	-20.5
CE16H1		-10.3	1.7	0.9	0.7	-9.6	-9.0	-9.4
BW15H3		-8.3	0.6	-8.1	-7.0	-8.7	-13.4	-16.5
BW15H4		-6.0	--	-2.5	-1.6	-5.2	-5.5	-7.0
BW17H1		-5.8	1.1	-3.7	-5.0	-8.3	-12.8	-11.5
WE14H1		-12.3	1.0	-28.0	-30.7	-11.4	-40.6	-38.1
WE15H1		-6.1	0.9	-13.2	-13.0	-3.8	-18.2	-16.8
WE17H1		-7.4	-0.3	-4.1	-2.8	-6.5	-10.7	-10.5

**NAC INTERNATIONAL RESPONSE
TO
REQUEST FOR ADDITIONAL INFORMATION**

RAI 6-6NAC International Response (continued)

Table 6-6.2 PWR Lattice Parameter Study – Wet Borated Gap (Increased Variance)

	2	6	1	4	3	5	7	8
Fuel Pin Cell H/U	Max	Min	Max	Max	Max	Min	Min	Min
Pellet Dia.	Max	Max	Max	Min	Min	Max	Min	Min
GT/IT Thick & Dia.	Min	Min	Max	Min	Max	Max	Max	Min
CE14H1	0.86478	0.85814	0.86799	0.85050	0.85181	0.85860	0.84430	0.84425
CE16H1	0.87235	0.86491	0.87351	0.87318	0.87204	0.86278	0.86163	0.86159
BW15H3	0.92918	0.92373	0.92880	0.92390	0.92388	0.92359	0.91901	0.92029
BW15H4	0.91479	0.91050	0.91362	0.91349	0.91426	0.91206	0.91089	0.91014
BW17H1	0.92613	0.92150	0.92886	0.92240	0.92419	0.92050	0.91783	0.91710
WE14H1	0.85452	0.84180	0.85235	0.82321	0.82245	0.84020	0.81151	0.81262
WE15H1	0.91257	0.90776	0.91541	0.89804	0.89974	0.90932	0.89395	0.89364
WE17H1	0.92402	0.91360	0.92209	0.91986	0.92322	0.91411	0.91182	0.91364
		Case 2 To Case 6	Case 2 To Case 1	Case 2 to Case 4	Case 2 to Case 3	Case 2 to Case 5	Case 2 to Case 7	Case 2 To Case 8
		$\Delta k_{eff}/\sigma$						
CE14H1		-6.1	3.1	-13.3	-12.6	-5.9	-19.7	-19.8
CE16H1		-6.8	1.1	0.7	-0.3	-8.8	-9.8	-9.8
BW15H3		-7.5	-0.5	-7.1	-6.9	-7.3	-13.7	-12.0
BW15H4		-4.0	-1.1	-1.2	-0.5	-2.6	-3.7	-4.4
BW17H1		-4.3	2.6	-3.5	-1.8	-5.3	-7.8	-8.7
WE14H1		-11.2	-2.0	-28.4	-29.2	-13.0	-39.2	-38.2
WE15H1		-4.5	2.7	-14.2	-11.9	-3.0	-17.6	-17.7
WE17H1		-10.1	-1.8	-4.1	-0.8	-9.5	-12.1	-10.0

**NAC INTERNATIONAL RESPONSE
TO
REQUEST FOR ADDITIONAL INFORMATION**

RAI 6-6NAC International Response (continued)

Table 6-6.3 PWR Lattice Parameter Study – Wet Unborated Gap (Table 6.2-1 Range)

Fuel Pin Cell H/U Pellet Dia. GT/IT Thick & Dia.	2	6	1	4	3	5	7	8
	Max	Min	Max	Max	Max	Min	Min	Min
	Max	Max	Max	Min	Min	Max	Min	Min
	Min	Min	Max	Min	Max	Max	Max	Min
CE14H1	0.86644	0.85969	0.86552	0.85659	0.85639	0.86224	0.85371	0.85317
CE16H1	0.87280	0.86997	0.87123	0.87280	0.87123	0.87175	0.87175	0.86997
BW15H3	N/A	N/A	N/A	N/A	N/A	N/A	N/A	N/A
BW15H4	0.91601	0.91601	0.91601	0.91601	0.91601	0.91601	0.91601	0.91601
BW17H1	0.93079	0.92583	0.92959	0.92653	0.92726	0.92657	0.92465	0.92466
WE14H1	0.84949	0.84509	0.84913	0.82532	0.82505	0.84671	0.82494	0.82607
WE15H1	0.91513	0.90991	0.91597	0.90415	0.90621	0.91233	0.89973	0.89921
WE17H1	0.92366	0.92182	0.92396	0.92251	0.92127	0.91981	0.91901	0.91943
		Case 2 To Case 6	Case 2 To Case 1	Case 2 to Case 4	Case 2 to Case 3	Case 2 to Case 5	Case 2 to Case 7	Case 2 To Case 8
		$\Delta k_{eff}/\sigma$						
CE14H1		-6.4	-0.9	-9.3	-9.7	-4.0	-12.4	-12.7
CE16H1		-2.6	-1.4	--	-1.4	-1.0	-1.0	-2.6
BW15H3		N/A						
BW15H4		--	--	--	--	--	--	--
BW17H1		-4.8	-1.2	-4.1	-3.4	-4.0	-5.9	-5.9
WE14H1		-4.1	-0.3	-22.5	-22.9	-2.6	-22.7	-21.4
WE15H1		-4.9	0.8	-10.3	-8.3	-2.6	-14.1	-14.9
WE17H1		-1.7	0.3	-1.0	-2.2	-3.6	-4.3	-3.9

Note: Data for BW15H3 hybrid was only generated for increased variable range.

**NAC INTERNATIONAL RESPONSE
TO
REQUEST FOR ADDITIONAL INFORMATION**

RAI 6-6NAC International Response (continued)

Table 6-6.4 Westinghouse 17×17 Lattice Parameter Study

Gap	Parameter	Minimum	Nominal	Maximum	% Δk_{eff}
Wet-Borated	Pitch	0.92732	0.92836	0.93114	0.4%
	Pellet OD	0.91237	0.92836	0.94116	2.9%
	Clad Thickness	0.92974	0.92836	0.92767	-0.2%
	Clad OD	0.93185	0.92836	0.92960	-0.2%
Wet-UnBorated	Pitch	0.93130	0.93383	0.93537	0.4%
	Pellet OD	0.92086	0.93383	0.94072	2.0%
	Clad Thickness	0.93553	0.93383	0.92948	-0.6%
	Clad OD	0.92886	0.93383	0.93534	0.6%
Dry	Pitch	0.92587	0.92839	0.92987	0.4%
	Pellet OD	0.91272	0.92839	0.94006	2.7%
	Clad Thickness	0.92895	0.92839	0.92686	-0.2%
	Clad OD	0.93191	0.92839	0.92667	-0.5%

Table 6-6.5 GE 8×8 Lattice Parameter Study

Gap	Parameter	Minimum	Nominal	Maximum	% Δk_{eff}
Wet-UnBorated	Pitch	0.92834	0.93414	0.93435	0.6%
	Pellet OD	0.93352	0.93414	0.93230	-0.1%
	Clad Thickness	0.93990	0.93414	0.92784	-1.2%
	Clad OD	0.93462	0.93414	0.93115	-0.3%
Dry	Pitch	0.92281	0.92858	0.92992	0.7%
	Pellet OD	0.92317	0.92858	0.93058	0.7%
	Clad Thickness	0.92825	0.92858	0.92834	0.0%
	Clad OD	0.93517	0.92858	0.92021	-1.5%

**NAC INTERNATIONAL RESPONSE
TO
REQUEST FOR ADDITIONAL INFORMATION**

CHAPTER 6 CRITICALITY EVALUATION

- 6-7 Include a specification for guide tube thickness in Tables 6.4-1 and 6.4-2 and a maximum limit on the assembly channel thickness of 120 mils in Table 6.4-2.

The presence of guide tubes has been included in the criticality analysis. As recommended in NUREG/CR-6716, it may be appropriate to eliminate guide tube thickness from the fuel parameter specification when these tubes are not included in the analysis. Alternatively, Section 6.B of the SAR states that the absence of guide tubes may increase reactivity significantly. This last statement implies that a minimum thickness is necessary in the guide tubes. A channel thickness of 120 mils maximized k_{eff} and forms an upper limit.

NAC International Response

Maximum nominal channel thickness of 120 mils is added to Table 6.4-2.

Criticality evaluations of the MAGNASTOR systems indicate that through all evaluated soluble boron and enrichment combinations, the guide tube thickness has no significant impact on the reactivity of the system and should, therefore, not be included in the characteristics table containing the significant criticality control fuel assembly parameters. As shown in Table 6.7.2-3 (formerly 6.B-3) no statistically significant change in reactivity occurred for any of the PWR fuel types as a result of guide tube diameter and thickness variations (including guide tube diameter in the study augments the potential change in reactivity associated with moderator addition or removal in the guide tube lattice cells). As a response to RAI 6-6 additional tables, containing lattice reactivity study results for various soluble boron content and pellet to clad gap conditions, are included in the RAI response and SAR. All tables confirm that guide tube thickness does not significantly impact system reactivity. As indicated in Section 6.7.2 (formerly Section 6.B), removal of guide tubes may impact system reactivity at low soluble boron contents. Table 6.4-1, therefore, specifies the number of guide tubes required for the assembly to be loaded. Since intact fuel assemblies are addressed by this evaluation, the number listed represents the nominal, intact, fuel assembly number of guide tubes.

**NAC INTERNATIONAL RESPONSE
TO
REQUEST FOR ADDITIONAL INFORMATION**

CHAPTER 6 CRITICALITY EVALUATION

- 6-8 Clarify whether the pellet-to-clad gap in the analysis used to generate the curves in Figure 6.C-1 was modeled as dry, wet with borated water, or wet with fresh water.

The data presented in Table 6.B-1 suggest that some of the assembly types have reached a condition of being over-moderated with high boron concentrations in full density water. The condition assumed in the gap could influence the results plotted in the Figure 6.C-1.

NAC International Response

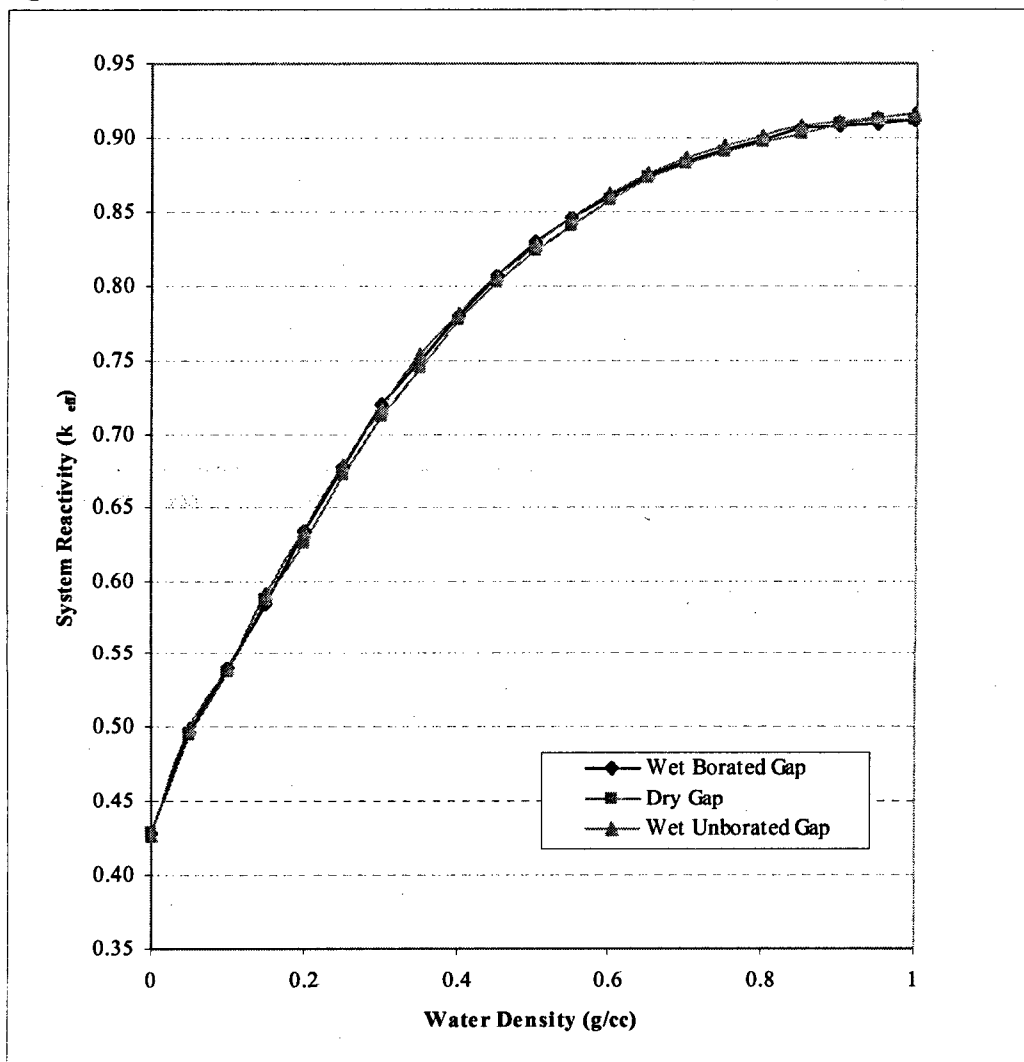
Data presented in Figure 6.C-1 included dry pellet to clad gap data for a soluble boron level of 2500 ppm. The figure is replaced by a data set containing results for an unborated water pellet to clad gap. The gap condition is added to the text description of Figure 6.7.3-1 in Section 6.7.3.1 (formerly Figure 6.C-1 in Section 6.C.1). Also added to the SAR is a figure containing results of moderator density studies for systems with a dry, borated wet, and unborated wet pellet to clad gap (no significant reactivity impacts are associated with canister exterior conditions for a flooded, or near full density water, canister). All three gap conditions provide similar results in that reactivity levels off in the 90-100% water density range (system is at, or near optimum moderation). NAC generated similar moderator density curves at 1800ppm and 1100ppm as shown in RAI response Figures 6-8.1 and 6-8-2. These plots indicate that at lower soluble boron content the MAGNASTOR system becomes increasingly undermoderated. Note that the data shown for the lower soluble boron levels also adjusts initial fuel enrichments to retain reactivities below the USL.

**NAC INTERNATIONAL RESPONSE
TO
REQUEST FOR ADDITIONAL INFORMATION**

RAI 6-8

NAC International Response (continued)

Figure 6-8.1 Canister Interior Moderator Density Study (1800 ppm Boron)

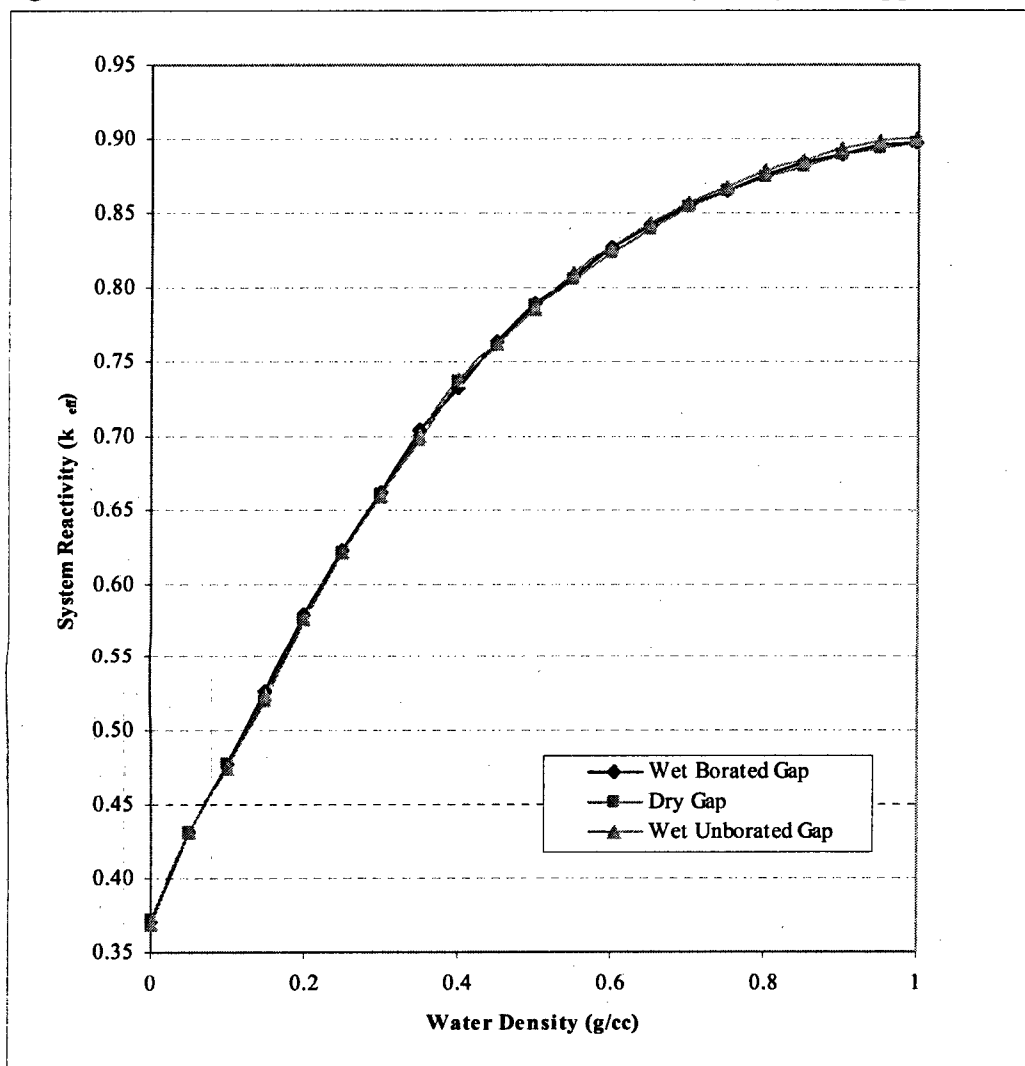


**NAC INTERNATIONAL RESPONSE
TO
REQUEST FOR ADDITIONAL INFORMATION**

RAI 6-8

NAC International Response (continued)

Figure 6-8.2 Canister Interior Moderator Density Study (1100 ppm Boron)



**NAC INTERNATIONAL RESPONSE
TO
REQUEST FOR ADDITIONAL INFORMATION**

CHAPTER 6 CRITICALITY EVALUATION

- 6-9 Clarify the configuration conditions assumed for the Normal case in the summary tables on pages 6.C-3 and 6.F-3.

It is not clear what modeling assumptions were changed for the Accident/Off-Normal case versus the Normal case in the two tables.

NAC International Response

Tables and text in Section 6.7.3.2(formerly 6.C.2) and Section 6.7.6.2 (formerly 6.F.2) are revised to clarify the conditions shown.

For the transfer cask the maximum reactivities listed represent a normal condition dry pellet-to-clad gap and an accident condition wet (unborated) pellet to-clad-gap. Maximum reactivity basket and fuel configurations and optimum moderation are applied in both normal and accident condition models. While flooding of the pellet-to-clad gap with unborated water may be considered under normal operating conditions it is not likely that a significant fraction of the fuel would be in this condition. As there is no transfer cask design basis accident condition that would impact system reactivity significantly, the unborated water-flooded gap was listed under accident conditions. The tables were revised in response to this RAI to indicate the pellet-to-clad gap condition. Both transfer cask dry and unborated wet gap results are now listed under normal conditions with an "N/A" and a text explanation for accident conditions. Concrete cask data represents a dry canister cavity with identical geometry for normal and accident conditions. Normal to accident condition model differences are limited to flooding of the canister to cask annulus under accident conditions.

**NAC INTERNATIONAL RESPONSE
TO
REQUEST FOR ADDITIONAL INFORMATION**

CHAPTER 6 CRITICALITY EVALUATION

- 6-10 State whether the boron areal density in the neutron absorber sheets was held constant (i.e., atom number density was changed as the sheet thickness was varied) for the analysis reported in Tables 6.C-2 and 6.C-3.

Proper interpretation of the results of the parameter variation depends on how the variation was carried out.

NAC International Response

The neutron absorber sheet ^{10}B areal density was held constant for the evaluations shown in Tables 6.7.3-2 (formerly 6.C-2) and 6.7.3-3 (formerly 6.C-3). Neutron absorber composition is adjusted to provide the same minimum ^{10}B areal density in all neutron absorber thickness tolerance study cases. As indicated in the general evaluation description, the minimum effective areal density allowed by the fabrication specification is employed in the analysis. Therefore, while material thickness and material composition are varied in the cases reported, the total neutron absorber content is not changed.

The neutron absorber sheet fabrication tolerance descriptions for PWR and BWR cases are adjusted to reflect this response.

**NAC INTERNATIONAL RESPONSE
TO
REQUEST FOR ADDITIONAL INFORMATION**

CHAPTER 6 CRITICALITY EVALUATION

6-11 Provide the number of fuel assemblies assumed in the basket to produce the results shown in Table 6.E-1.

Some values exceed the applicable USL.

NAC International Response

SAR Sections 6.7.5 (formerly 6.E) and 6.7.6.1 (formerly 6.F.1) are revised to state that, unless specifically noted, the 87-assembly basket configuration at an initial enrichment of 4 wt% ^{235}U is analyzed in the studies. For this 87-assembly basket configuration and initial enrichment level, some of the fuel types exceed the USL. Thus, in Section 6.7.6 (formerly 6.F), the enrichment of the fuel types that exceed the USL are limited to initial enrichments lower than 4 wt% ^{235}U , or the use of the 82-assembly basket configuration is mandated for those fuel types.

**NAC INTERNATIONAL RESPONSE
TO
REQUEST FOR ADDITIONAL INFORMATION**

CHAPTER 6 CRITICALITY EVALUATION

- 6-12 Provide a description and the results for the analysis that show that partial length rods are acceptable in the fuel assembly types as designated in Table 6.F-5.

In the description specify the number and location of partial length fuel rods that are to be allowed in the designated fuel assemblies.

NAC International Response

The MAGNASTOR SAR is revised in Section 6.2 and Table 6.4-2 to include the number of partial length rods. Figure 6.2-1 is added to Section 6.2 and includes sketches for the location of the partial length rods evaluated. Technical Specification Table 13B, 2-10, "BWR Fuel Assembly Loading Criteria," is also footnoted to reference the partial length fuel rod location sketches in Section 6.2.

Criticality results for the partial and full length rod assemblies are provided in Table 6.7.6-5. Table 6.7.6-5 was added as a response to RAI 6-13. The table contains reactivities at the limiting enrichments for assemblies containing both a complete set of full length fuel rods and for assemblies containing partial length fuel rods (modeled as open lattice locations).

**NAC INTERNATIONAL RESPONSE
TO
REQUEST FOR ADDITIONAL INFORMATION**

CHAPTER 6 CRITICALITY EVALUATION

6-13 In the BWR basket analysis, provide a table with the k_{eff} and USL values such as presented in Tables 6.C-4 and 6.C-5.

Table 6.F-5 does not provide sufficient information to compare the results of the criticality analysis with its applicable limits.

NAC International Response

A table, Table 6.7.6-5, containing the requested data is inserted into Section 6.7.6 (formerly 6.F-5). The new table contains maximum initial enrichments, maximum reactivities, and the USL for each of the BWR fuel types proposed as contents in the MAGNASTOR system.

**NAC INTERNATIONAL RESPONSE
TO
REQUEST FOR ADDITIONAL INFORMATION**

CHAPTER 6 CRITICALITY EVALUATION

- 6-14 Describe and justify any differences in the modeling approaches and code options that exist between the benchmark and design computations.

Section 6.G states that, where available, MCNP models were extracted from the references when performing the analysis to determine the appropriate USL. It is preferable that benchmark calculations are modeled and run by the analyst making the design calculations to provide as much commonality as possible. At a minimum, the modeling approaches and code options should be the same as those used for the design calculations. Any differences between the two calculations need to be identified and evaluated to show that the final value of the USL is appropriate.

NAC International Response

MCNP benchmark cases presented in the MAGNASTOR SAR represent a collection of files composed of inputs obtained directly from references (with cross-section sets adjusted to those used in the cask analysis), NAC modified input files representing unique geometries based on reference input files, and input files constructed from the experimental material and geometry information. All cases were reviewed on a "preparer/checker" principle for modeling consistency with the MAGNASTOR cask models and the choice of code options. Due to large variations in the benchmark complexities not all options employed in the cask models are reflected in each of the benchmarks (e.g., UNIVERSE structure). A review of the criticality results did not indicate any result trend due to particular modeling choices (e.g., using the UNIVERSE structure versus a single universe, or employing KSRC versus SDEF sampling).

Section 6.7.7 (formerly 6.G) is revised to include the information presented in this RAI response.

**NAC INTERNATIONAL RESPONSE
TO
REQUEST FOR ADDITIONAL INFORMATION**

CHAPTER 6 CRITICALITY EVALUATION

6-15 In the second sentence in Section 6.C.2, correct the word “coater.”

There appears to be a typographical error in this sentence.

NAC International Response

SAR text was corrected to refer to “water” in Section 6.7.3-2 (formerly Section 6.C.2).

**NAC INTERNATIONAL RESPONSE
TO
REQUEST FOR ADDITIONAL INFORMATION**

CHAPTER 6 CRITICALITY EVALUATION

- 6-16 Provide an analysis similar to that in Figure 6.F-1 for the case when only 82 BWR assemblies are allowed in the basket.

This analysis is needed to assure that the optimum moderation in the canister interior continues to be full density water.

NAC International Response

An evaluation of optimum moderator density for the 82-assembly BWR basket is added to the SAR in Section 6.7.6 (formerly 6.F). As demonstrated in the added figure, full density water continues to be the maximum reactivity configuration.

SAR text is modified to clarify that the data shown for 82-assembly and 87-assembly baskets represents a flooded pellet to clad gap. Also added to the SAR text are the fuel type and initial enrichment of the evaluated fuel assemblies.

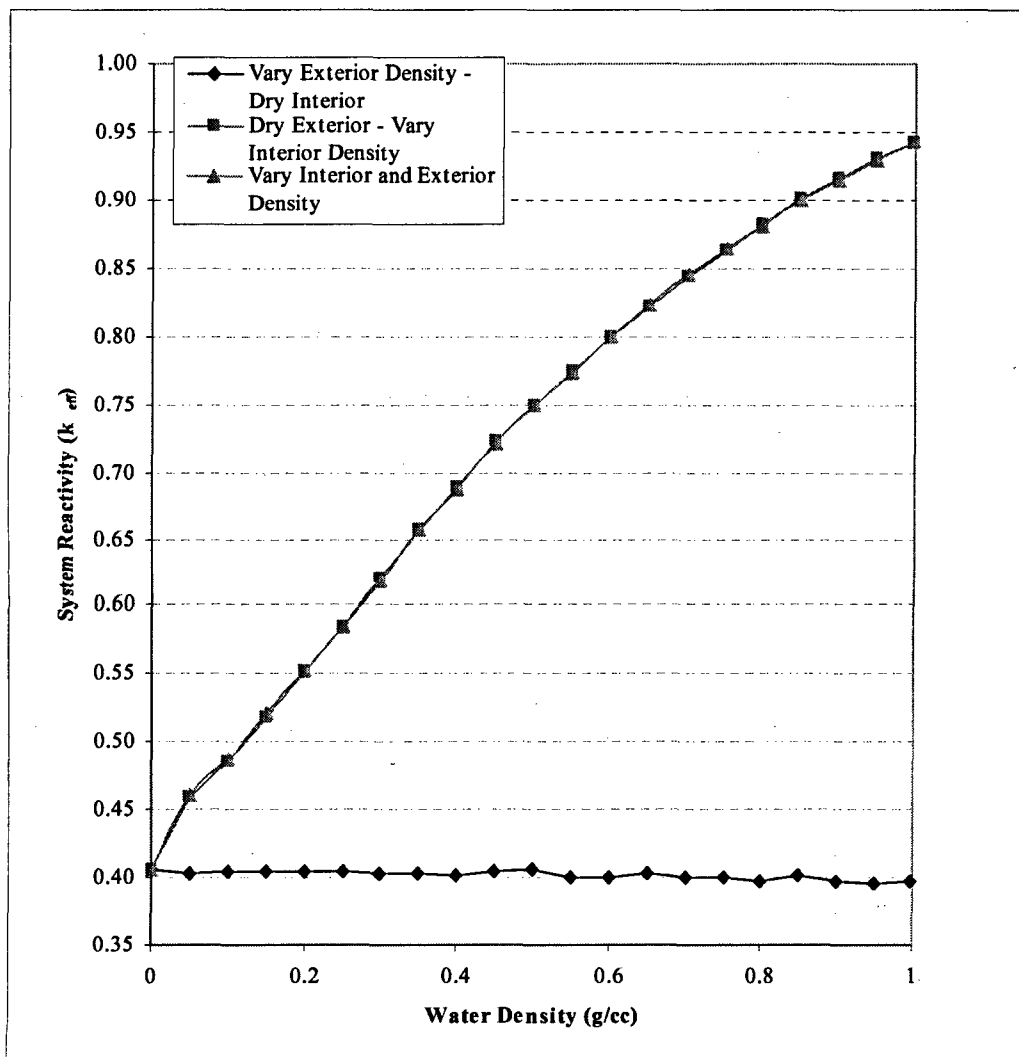
Dry pellet to clad gap moderator density study curves are included in this RAI response for both 87-assembly and 82-assembly configurations.

**NAC INTERNATIONAL RESPONSE
TO
REQUEST FOR ADDITIONAL INFORMATION**

RAI 6-16

NAC International Response (continued)

Figure 6-16.1 87-Assembly Basket Moderator Density Variation Study
Dry Pellet to Clad Gap (B9_79A, 4.0 wt% ²³⁵U)

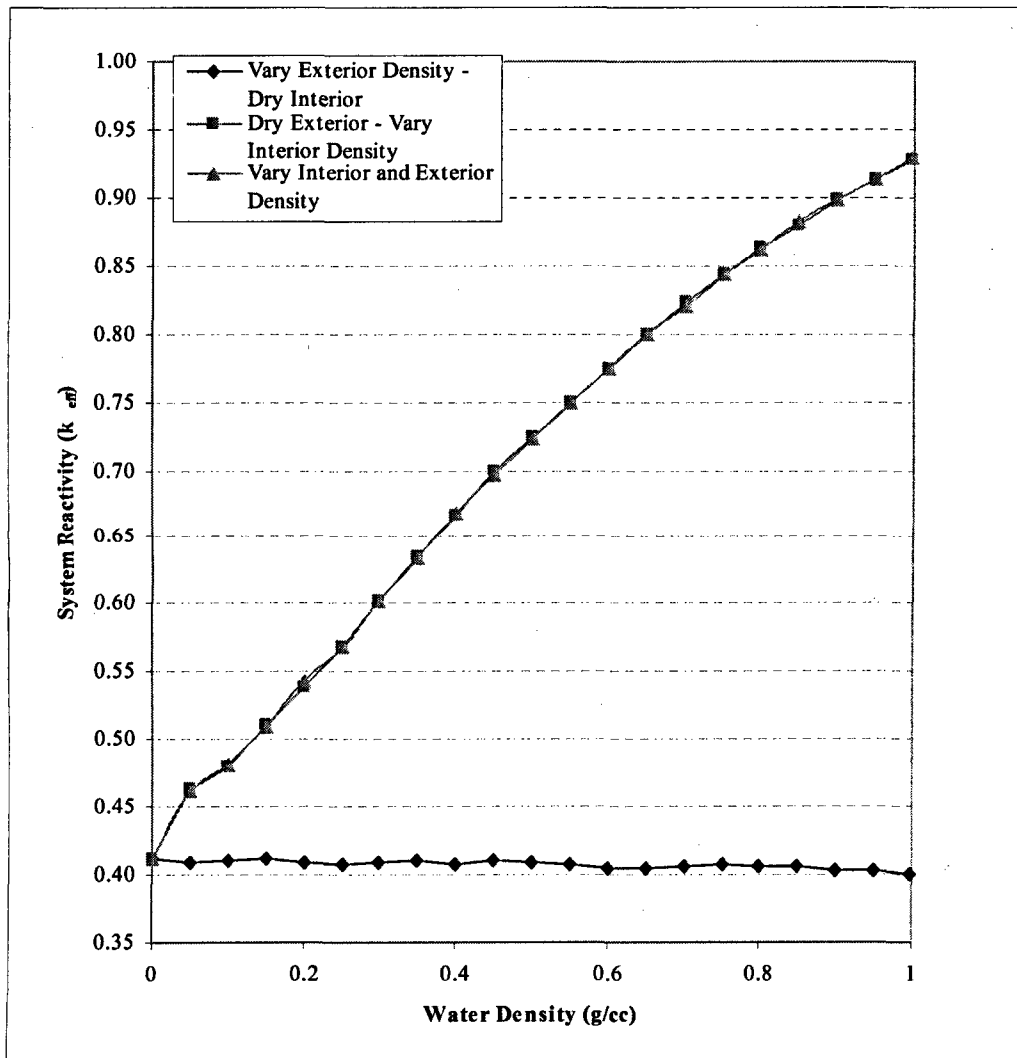


**NAC INTERNATIONAL RESPONSE
TO
REQUEST FOR ADDITIONAL INFORMATION**

RAI 6-16

NAC International Response (continued)

Figure 6-16.2 82-Assembly Basket Moderator Density Variation Study
Dry Pellet to Clad Gap (B9_79A, 4.5 wt% ²³⁵U)



**NAC INTERNATIONAL RESPONSE
TO
REQUEST FOR ADDITIONAL INFORMATION**

CHAPTER 6 CRITICALITY EVALUATION

6-17 Include BWR assembly type B9 76A in Tables 6.F-2, 6.F-3, and 6.F-4.

This fuel assembly type appears to be most limiting.

NAC International Response

Tables 6.7.6-2, -3 and -4 (formerly 6.F-2, -3, and -4) are revised to include the B9_76A fuel type. The maximum reactivity configuration conclusions drawn from the previously presented tables were not affected by the addition of the B9_76A data.

**NAC INTERNATIONAL RESPONSE
TO
REQUEST FOR ADDITIONAL INFORMATION**

CHAPTER 6 CRITICALITY EVALUATION

6-18 Correct the dimensions in Tables 6.1-2, 6.4-2 and 6.F-5.

The columns are incorrectly labeled. Verify that all values are the same as used in the applicant's analysis.

NAC International Response

The titles of the incorrectly labeled columns are corrected. The dimensions and the values in the columns were/are correct and were/are correctly implemented in the calculations.

**NAC INTERNATIONAL RESPONSE
TO
REQUEST FOR ADDITIONAL INFORMATION**

CHAPTER 7 CONFINEMENT EVALUATION

- 7-1 Delete reference to 'calculations' provided in Chapter 4 and substitute 'explanation' or 'information', or provide the specific reference and the calculations.

The last paragraph on Page 7.1.1 makes reference to calculations provided in Chapter 4 for determining the molar amount of helium in the canister. However, no such calculations are readily apparent in Chapter 4.

This information is needed to determine compliance with 10 CFR 72.146(b).

NAC International Response

The reference to 'calculations' provided in Chapter 4 is deleted. The section is revised to clearly indicate the origin of the molar amount of helium in the canister.

**NAC INTERNATIONAL RESPONSE
TO
REQUEST FOR ADDITIONAL INFORMATION**

Chapter 7 CONFINEMENT EVALUATION

- 7-2 Provide the specific calculations in the SAR for determining the TSC design pressure including the justification of the helium bulk average temperature associated with the final helium fill.

During an initial fill, the lower the bulk average temperature of helium, the more moles of helium are added. As a result, the canister pressure increases once it reaches thermal equilibrium. For example, if a helium bulk average temperature for the initial fill is assumed to be 245°F, the maximum normal canister pressure appears to be 130 psig (20 psig above the current design pressure) coinciding with a maximum helium equilibrium temperature of 467°F.

This information is needed to determine compliance with 10 CFR 72.122(h).

NAC International Response

There are two methods that may be used for drying, backfilling and pressurizing the TSC cavity. The first method is utilizing vacuum drying of the TSC and contents, dryness verification by pressure rise verification, additional cavity evacuation to < 3 torr, and backfilling the cavity free volume with a specified mass of high purity helium. The helium mass and resultant pressure is based on the free volume of the TSC as determined during the TSC draining operation, and corresponds to the required pressure and density of helium for TSC design basis heat transfer conditions.

The second method requires TSC cavity water blow down using high purity helium, drying of the cavity and contents by pressurized helium recirculation, and final adjustment of the high purity helium in the TSC cavity based on the TSC gas exit temperature and content decay heat load.

Both methods will assure that the final internal pressure of the TSC does not exceed the design pressure of the TSC at the normal operating conditions for a design basis content heat load of 37 kW.

The procedures in Chapter 9, Section 9.1.1 have been revised to require the measurement of the TSC free volume during draining, and the backfilling of the TSC to a specified mass of high purity helium based on the TSC free volume. The new helium mass

**NAC INTERNATIONAL RESPONSE
TO
REQUEST FOR ADDITIONAL INFORMATION**

RAI 7-2

NAC International Response (continued)

requirements have also been incorporated into the Surveillance Requirements (SR 3.1.1.2) of Limiting Condition of Operation (LCO) 3.1.1. of Chapter 13, appendix A, and in the Bases of LCO 3.1.1 in Appendix C.

The specific calculation of the required helium mass per liter of free volume, and the resultant pressure at operating temperatures are provided in Chapter 4.

**NAC INTERNATIONAL RESPONSE
TO
REQUEST FOR ADDITIONAL INFORMATION**

CHAPTER 7 CONFINEMENT EVALUATION

- 7-3 Provide redundant sealing of the confinement boundary as required by 10 CFR72.236(e).

ISG-4, "Cask Closure Weld Inspections," describes the weld examination method acceptable for the closure weld and provides relief from a hydrostatic pressure test providing the weld's margin of safety ≥ 1.5 was demonstrated by analysis against design pressure. This is relief from performing a hydrostatic pressure test that demonstrates the structural integrity of the weld's design and fabrication.

ISG-18, "The Design/Qualification of Final Closure Welds on Austenitic Stainless Steel Canisters as Confinement Boundary for Spent Fuel Storage and Containment Boundary for Spent Fuel Transportation" provides relief from performing a leakage test for austenitic stainless steels that are very ductile and don't lend themselves to crack propagation providing the final closure welds are executed in accordance with ISG-15, "Materials Evaluation."

In the 10 CFR Part 72 Statements of Consideration (SOC) for the TN-24 and VSC-24, dated April 30, 1993, it was recognized that volumetric examination as required by the ASME Code was not implemented because an additional margin of safety was provided by (1) a double weld, (2) weld joint has been analyzed for all load conditions, (3) pressure inside the canister is approximately one atmosphere resulting in low stress intensities, and (4) weld integrity is ensured by Code examination using liquid penetrate and a NRC required leak test. The aforementioned margin of safety has been further reduced in the MAGNASTOR application by pressurizing the canisters, not performing the hydrostatic pressure test, deletion of leak test, and the applicant's proposed single sealing of the MAGNASTOR canister.

Other factors influencing the double sealing requirement include the realization that the closure weld is performed in the field under conditions that could be an impedance to quality workmanship, examination and inspection. As a result, the requirement for double seal of the containment boundary is necessary.

**NAC INTERNATIONAL RESPONSE
TO
REQUEST FOR ADDITIONAL INFORMATION**

RAI 7-3 (continued)

NAC International Response

The MAGNASTOR transportable storage canister welded closure lid configuration has been redesigned as shown on Drawing No. 71160-585 to provide the double weld redundant sealing of the confinement boundary as required by 10 CFR 72.236(e).

In addition, the operating procedures in Chapter 9, Section 9.1.1 and the acceptance test program in Chapter 10 have been revised to specify that a hydrostatic pressure test of the closure-to-TSC shell weld shall be performed on each loaded TSC. The test's acceptance criteria are no loss of pressure or visible water leakage during the minimum 10-minute test duration. See the response to RAI 9-2.

**NAC INTERNATIONAL RESPONSE
TO
REQUEST FOR ADDITIONAL INFORMATION**

CHAPTER 8 MATERIALS EVALUATION

- 8-1 Clarify the definition of intact fuel in Chapter 1 and 13 and define damage fuel. Additionally, define cladding defects and quantify the size.

The definition of intact fuel on page 13A-1 uses the phrase "no fuel rod cladding defects." The rest of the definition implies that cladding defects do not refer to cladding breaches. The response to this question should also be included in the "Cladding Integrity" section of Chapter 8 and in the TS. It should be noted that the applicant's definition of damaged fuel can be broader than that specified in ISG-1, Revision 1, "Damaged Fuel." As a minimum, the definition should include items 1 through 3 from the ISG definition.

This information is needed to determine compliance with 10 CFR 72.122(h)(1).

NAC International Response

The definition of intact fuel is revised and clarified in SAR Sections 1.1 - Terminology, 8.11 - Cladding Integrity, and 1.1 of Chapter 13, Appendix A - Definitions. The revised definition incorporates the requirement that any missing fuel rods must be replaced by solid filler rods that displace a volume at least equal to that of the original rod. A definition of damaged fuel - a modified version of that provided in ISG-1 - is also incorporated in these SAR sections to complement the intact fuel definition.

**NAC INTERNATIONAL RESPONSE
TO
REQUEST FOR ADDITIONAL INFORMATION**

CHAPTER 8 MATERIALS EVALUATION

- 8-2 Revise Chapter 2 to define the term "Retrievability" and Chapter 8 to include a brief discussion that addresses retrievability of spent fuel from the MAGNASTOR using normal means of handling.

The spent fuel cladding must be protected during storage against degradation that leads to gross rupture of the fuel and must be otherwise confined such that degradation of the fuel during storage will not pose operational problems with respect to its removal from storage.

This information is needed to determine compliance with 10 CFR 72.122(h)(1), 72.122(l), and 72.236(m).

NAC International Response

Sections 2.4.1, 2.4.2, 2.5, 8.11 and 15.2 are revised to incorporate a definition of "retrievability" and to include a discussion addressing "retrievability" of spent fuel from the MAGNASTOR system using normal means of handling. These revisions clarify that the spent fuel cladding is protected against degradation during storage and that the fuel is confined such that there will be no operational problems with respect to its removal from storage for ultimate disposal by the Department of Energy.

**NAC INTERNATIONAL RESPONSE
TO
REQUEST FOR ADDITIONAL INFORMATION**

CHAPTER 8 MATERIALS EVALUATION

8-3 Provide a reflood analysis to show that the cladding will not be damaged and result in breaches and fracture. The analysis should support statements in Section 1.3.1.4, "alternatively the loaded TSC may be returned to the spent fuel pool for in-pool cooling" and in Section 8.11, where it is indicated that in the unlikely event that the TSC must be reopened that it will be filled with water.

ISG-15, Section X.5.4.3, Cask Reflooding, discusses the technical basis for performing a reflood analysis.

This information is needed to determine compliance with 10 CFR 72.122(l).

NAC International Response

Normal and accident condition thermal transients experienced by the MAGNASTOR canister, basket, and contained fuel are controlled and introduce insignificant thermal loading and material stress to fuel rod cladding. Normal condition cooldown transients during cask operations may be introduced during vacuum drying when the canister drying criteria are not met within the prescribed heat load dependent time limit. If the drying criteria is not met, the canister is filled with helium and may be returned to the pool as stated in referenced SAR Section 1.3.1.4. This backfill with helium may be performed when the temperature in the mid to upper regions of the fuel basket is in the range of 700°F and the fuel local to the bottom plate in the range of 250°F. Noting the significant difference in mass between helium and fuel, approximately five orders of magnitude, helium is heated with little temperature change to the fuel – the basket, canister bottom plate and shell mass add heat to the helium in combination with the fuel – reducing the thermal influence of the initial helium fill on the fuel cladding. Following the helium backfill the canister is returned to the pool. Water in contact with the canister wall provides more effective heat transfer than the air boundary when the transfer cask is sitting in a cask processing area outside the pool. Although this pool water boundary provides a more effective heat transfer path, the influence of the canister submergence in the pool does not produce a thermal shock or significant through wall gradient to the fuel rod cladding.

Investigation of the canister unloading sequence presented in SAR Section 9.3 leads to similar conclusions as those for the introduction of helium gas discussed above. When

**NAC INTERNATIONAL RESPONSE
TO
REQUEST FOR ADDITIONAL INFORMATION**

RAI 8-3

NAC International Response (continued)

the canister is first prepared for unloading and port covers removed, nitrogen gas is initially cycled through the canister for 10 minutes to flush the radioactive gases from the canister. This gas cycling is similar to the helium backfill – although nitrogen has a higher thermal capacitance than helium, about a factor of 10, when compared to the mass of the metal canister, basket and fuel, the influence of the nitrogen gas on the thermal gradient response in the fuel cladding remains insignificant. Following the nitrogen flush, water is introduced at a maximum 8 gpm. The maximum flow rate is based on reflood thermal hydraulic analyses of a bounding canister configuration. The bounding maximum flow rate has been added to step 14 of SAR Operating Procedures Section 9.3, “Wet Unloading a TSC.” The water initially introduced into the canister flashes to steam in the drain tube and on contact with the bottom plate. Steam in the cavity provides additional heat to be removed from the basket and fuel in a smooth transition without introducing thermal shock through wall stresses. Once water is permitted to form on the canister bottom plate the canister starts to fill at a maximum 8 gpm. Addition of water at 8 gpm permits the water to rise in the canister at a maximum rate of 0.8 inches per minute. Thermal hydraulic analyses results show thermal cladding temperature radial gradients are less than 1°F during the reflooding of the canister. Such a small increase is consistent with the gradual process of the initial steam condition followed by water. The axial temperature gradient along the fuel assembly is actually larger than the radial gradient. However, in the fuel axial direction, thermal stresses are not developed since the fuel clad is free to expand in the axial direction. The combination of initial nitrogen purge, followed by the cooling transition of the steam created in the canister cavity, provides a relatively smooth transition to water cooling and insignificant thermal stress in the fuel rod cladding.

**NAC INTERNATIONAL RESPONSE
TO
REQUEST FOR ADDITIONAL INFORMATION**

CHAPTER 8 MATERIALS EVALUATION

8-4 Specify what effects of the zirconium channel are evaluated (e.g., thermal, structural, shape effects, etc). Additionally, provide the supporting evaluation. On page 1.2.1, the SAR states: "effects of the zirconium channel are evaluated."

Information is needed to determine compliance with 10 CFR 72.122(h)(1).

NAC International Response

The statement in SAR Section 1.2, stating "The BWR fuel assembly groups are evaluated for the effects of the zirconium alloy channel that surrounds the fuel assembly in reactor operations" is intended to provide generic identification that the channel is included as appropriate in specific analyses details presented in subsequent Chapters. Details on the analytical model addressing the channel are found in Sections 4.4.1.3 and 4.4.1.4 and other discussions as appropriate for the thermal heat transfer analyses and Section 6.3 for the criticality analysis. Shielding analyses have conservatively ignored the presence of channel hardware and structural analyses have not included assembly hardware details.

SAR Section 1.2 text has been revised to clarify the specific analyses addressing channel considerations.

**NAC INTERNATIONAL RESPONSE
TO
REQUEST FOR ADDITIONAL INFORMATION**

CHAPTER 8 MATERIALS EVALUATION

8-5 Provide a copy of the document(s) used to obtain the fuel and cladding parameters in Tables 5.A-1, 5.A-4, 6.1-1, 6.1-2, 6.2-1, 6.2-2, 6.4-1, 6.4-2. Additionally, provide a diagram for the BWR 10 x 10 configuration, in Table 5.2-2, showing any sub-arrays, partial rods, extra grid spacers, etc.

The staff is unable to verify the fuel and cladding parameters in the tables for the varying structural configurations of the designs.

This information is needed to determine compliance with 10 CFR 72.122(h)(1).

NAC International Response

NAC calculations EA790-4003 "PWR and BWR Enveloping Fuel Assembly Physical Descriptions," and EA792-5001 "PWR and BWR Enveloping Fuel Assembly Descriptions for Nuclear Analysis" are provided as proprietary information documents. These calculations contain the references for the fuel data employed in the nuclear evaluations; including the list of references and/or copies of the reference information.

The majority of the documents are publicly available (such as DOE/RW-0184). A significant exception to the public information is Stoller Nuclear Fuel Report E00-19, which at the request of NAC, summarized commercial fuel characteristics employed at US nuclear plants. This report was requested by NAC in 2000 to verify data listed in previous NAC calculations and to generate models for newer fuel types (in particular BWR 9x9 and 10x10 lattices). A copy of the report is provided as a proprietary document.

Chapter 6 was modified to include sketches for the location of partial length rods in BWR fuel assemblies. A sketch of the sub-array and grid information for the SVEA-96 assembly type with sub-arrays is included as proprietary information, i.e., UMS[®] Additional Information, Enclosure 9, September 4, 1998, on pages 48 and 49. This information was previously provided as an RAI response for the UMS[®] system.

**NAC INTERNATIONAL RESPONSE
TO
REQUEST FOR ADDITIONAL INFORMATION**

CHAPTER 8 MATERIALS EVALUATION

8-6 In Table 8.3-26, indicate if emissivity is for oxidized cladding, crudded cladding, or bright cladding. If the emissivity is for bright cladding, provide emissivity values for oxidized cladding.

Radiant heat transfer will depend on the emissivity of the surface of the cladding.

This information is needed to determine compliance with 10 CFR 72.11.

NAC International Response

The emissivity value of 0.75 defined in Table 8.3-26 is representative of cladding with a minimum oxide layer. As oxide layers get thicker, values for emissivity get larger. An oxide layer in the 10 μ m range has an emissivity of 0.75; for an oxide layer of 28 μ m, emissivity increases to 0.82; for an oxide layer of 130 μ m, emissivity increases to 0.84; and a crud layer of 35 μ m has an emissivity of 0.88. It is noted that the reference for emissivity as shown in Table 8.3-26 is incorrect. The reference has been corrected to be Table 8.3-26, footnote "b" rather than footnote "c", as previously shown in the table.

**NAC INTERNATIONAL RESPONSE
TO
REQUEST FOR ADDITIONAL INFORMATION**

CHAPTER 8 MATERIALS EVALUATION

8-7 In Table 8.3-27, indicate the density of the fuel used to measure the conductivity and specific heat. Also, discuss briefly how the density compares to the density of the irradiated fuel. If they are not comparable, provide an estimate for conductivity and specific heat at the actual fuel density. The applicant should note that the conductivity of the fuel will depend on its density.

Staff is unable to verify and evaluate the physical properties of the fuel.

This information is needed to determine compliance with 10 CFR 72.11.

NAC International Response

Conductivity and specific heat values presented in Table 8.3-27, "Thermal Properties for Fuel (UO₂)", and used in the heat transfer analysis are from reference 19, "Matpro - Version 11, A Handbook of Material Properties for Use in the Analysis of Light Water Reactor Fuel Rod Behavior." Conductivity values represent 95% theoretical density. Specific heat values are defined from a plot of experimental and theoretical data that are in very good agreement over the temperature range that is applicable to spent fuel application.

It is noted that there is an irradiation influence on thermal conductivity, specific heat and density material properties for the fuel rod pellet. However, because the influence of the individual rod material property is relatively small with respect to the thermal performance of the package, variances introduced from pellet porosity, actinides and other burnup variables are of minor influence on peak cladding temperature. Thermal performance of the spent fuel dry storage system is controlled by the heat transfer path from the fuel rods to the outside ambient. The most significant influence on calculating fuel rod temperatures is the thermal boundary from the fuel rod surface consisting of radiation, conduction and convection. As discussed in response to RAI 8-6, emissivity for the fuel rod surface has been defined for a conservatively small oxide layer introducing higher heat transfer resistance for heat leaving the fuel rod. Effective heat transfer properties are calculated as a function of temperature for the fuel rod array by modeling conservatively low emissivity in combination with helium conduction properties between rods and the fuel rod cladding and pellet details. A second set of effective material properties are calculated without helium conduction for the canister

**NAC INTERNATIONAL RESPONSE
TO
REQUEST FOR ADDITIONAL INFORMATION**

RAI 8-7

NAC International Response (continued)

vacuum configuration. The effective thermal properties for the fuel rod array are used in the thermal model of the basket in combination with a porous media capturing convection heat transfer from the fuel rod array to naturally circulating helium. Evaluation of the heat transfer results define that 15% of the heat from the assembly is removed by radiation, 14 % is removed by conduction and 71% is removed by convection. The actual thermal gradient in the fuel rod is less than 1°F. It is concluded from these analyses and evaluation of the heat transfer material property influence that the actual differences that may be introduced from pellet burnup variables are an insignificant variable in thermal performance of the dry storage system and calculated peak cladding temperature.

**NAC INTERNATIONAL RESPONSE
TO
REQUEST FOR ADDITIONAL INFORMATION**

CHAPTER 8 MATERIALS EVALUATION

8-8 Revise Chapters 8 and 13 (Technical Specifications) in tabular form, to indicate for each neutron absorber material, the B-10 percent credit, the manufacturer's trade name, the minimum areal density required, actual areal density to be used, and the volume percent of B₄C used in metal matrix composites proposed for use in the MAGNASTOR system. Greater than 75% credit for BORAL is currently under review by the NRC and should not be considered by the applicant in the criticality analysis unless the applicant has the appropriate test data to support a greater credit. Furthermore, neutron attenuation testing should be done for materials taking greater than 75% credit in the criticality analysis. Note that an acceptance criterion for neutron attenuation would need to be presented by the applicant for any absorber in which a greater credit than 75 percent is taken. For tests methods other than neutron attenuation, the applicant should benchmark the results of the proposed acceptance test method against the results of neutron attenuation examination.

This information is needed to determine compliance with 10 CFR 72.11 and 72.236 (c).

NAC International Response

The NAC MAGNASTOR storage license application identifies the neutron absorber material as a metallic composite containing B₄C, i.e., Boral, a borated aluminum alloy, or a borated metal matrix composite (MMC). The application intentionally does not identify the specific neutron absorber, in order to provide fabrication flexibility to use an alternate material meeting the critical design characteristics necessary to ensure criticality safety in the fuel basket(s). Criticality safety in the fuel basket is dependent upon the neutron absorber material remaining fixed in position on the fuel tubes and containing the required amount of boron uniformly distributed throughout the sheet. The license application defines the critical design characteristics of the neutron absorber material to be the following:

- A minimum "effective" areal density of 0.036 g/cm² ¹⁰B for the PWR basket and 0.027 g/cm² ¹⁰B for the BWR basket; and
- A uniform distribution of boron carbide; and

**NAC INTERNATIONAL RESPONSE
TO
REQUEST FOR ADDITIONAL INFORMATION**

RAI 8-8

NAC International Response (continued)

- A strength at least equivalent to that of 1100 series aluminum at 700°F, which is sufficient to maintain its form; and
- An effective thermal conductivity greater than or equal to that used in the thermal analyses (Chapter 4).

The specification of the required minimum “effective” areal density of ^{10}B directly translates to the detailed qualification and acceptance testing required for the neutron absorber material. NAC has concluded that the specification of the neutron absorber material, as described in the NAC MAGNASTOR storage license application and summarized here, provides for alternative material selection and meets the control objectives of regulatory requirements.

SAR Sections 8.8 and 13A – 4.1.1 are revised to include a tabulation of the types of neutron absorbers, the required minimum “effective” areal density of ^{10}B for each type, the percent credit used in the criticality analyses for each type, and the required minimum as-fabricated areal density of ^{10}B .

SAR Sections 2.4.6.1, 8.8 and 10.1.6 are revised to clarify that 75 percent credit is used in the criticality analyses for Boral and that 90 percent credit is used in the criticality analyses for borated aluminum alloys and borated metal matrix composites.

SAR Sections 8.8 and 10.1.6 are revised to clarify acceptance testing for the effective areal density and homogenous distribution of the B10 in the neutron absorber materials. SAR Section 10.1.6 outlines the methods of acceptance testing based on the credit taken for the neutron absorber material. For MAGNASTOR neutron absorber materials where 90% credit is taken, neutron transmission testing will be used for both process qualification and acceptance testing. For MAGNASTOR neutron absorber materials where 75% credit is taken, neutron transmission testing will be used for process qualification and wet chemistry analysis will be used for acceptance testing.

Refer to RAI Responses 8-9, 8-10 and 8-11 for related information and SAR changes.

**NAC INTERNATIONAL RESPONSE
TO
REQUEST FOR ADDITIONAL INFORMATION**

CHAPTER 8 MATERIALS EVALUATION

8-9 Provide a detailed discussion of the sampling plan and acceptance criteria based on statistical analysis that includes how uncertainties are accounted for in the analysis. BORAL should not be considered at the 90% credit level unless the applicant supported the request with data.

- (a) Revise the application to state that neutron transmission testing will be used to verify the B-10 areal density for neutron absorbers at the 90% level. For neutron attenuation measurements, the applicant should specify a test area small enough that variations in neutron absorber content would not be masked by measurements of an average value over a large area. Alternatively, the applicant should demonstrate that chemical analysis is an acceptable alternative for verifying the minimum effective B-10 areal density for absorbers at the 90% level of credit.
- (b) Revise Chapter 8 to define the following terms: lot, physical sampling method, and statistical sampling plan. In particular, discuss: •how lot failure is handled (e.g., a rejection during reduced inspection will require a return to 100% inspection of the lot.) •the basis for reduced sampling, •locations of samples removed from the material (e.g., random, on the ends, etc.), •how the lower tolerance limit of neutron absorber content is determined, how the acceptability of the lot is determined, •the number of production runs or lots to be included in the data set used in the statistical analysis, and •how an estimation of the variances is done for greater than 75% credit.

Based upon recommendations in the applicable standard review plans, NUREGs - 1609, -1617, and -1537, it has been the staff practice to either (a) limit the credit for absorber materials to only 75% of the minimum amount of neutron poison shown to be present, or (b) consider giving credit up to 90% if comprehensive measures are implemented to establish the presence, uniformity, and neutronic effectiveness of an absorber material.

This information is needed to determine compliance with 10 CFR 72.11 and 72.236(c).

**NAC INTERNATIONAL RESPONSE
TO
REQUEST FOR ADDITIONAL INFORMATION**

RAI 8-9 (continued)

NAC International Response

SAR Sections 8.8 and 10.1.6 are revised to incorporate a detailed discussion of the sampling plan and acceptance criteria, including accounting for uncertainties in the analysis, for the neutron absorber materials used in the MAGNASTOR system. The sampling plan and acceptance criteria are provided to address the requirements of the draft ASTM C26.03, WK 936, "Standard Practice for Qualification and Acceptance of Boron Based Metallic Neutron Absorbers for Nuclear Criticality Control for Dry Cask Storage Systems and Transportation Packaging." As described in the Response to RAI 8-8, these SAR Sections are revised to clarify that Boral is credited with an effectiveness of 75%, that borated aluminum alloys and borated metal matrix composites are credited with an effectiveness of 90%, and to provide the appropriate acceptance criterion for neutron transmission testing.

SAR Sections 8.8 and 10.1.6 are revised to clarify acceptance testing for the effective areal density and homogenous distribution of the B10 in the neutron absorber materials. SAR Section 10.1.6 outlines the methods of acceptance testing based on the credit taken for the neutron absorber material. For MAGNASTOR neutron absorber materials where 90% credit is taken, neutron transmission testing will be used for both process qualification and acceptance testing. For MAGNASTOR neutron absorber materials where 75% credit is taken, neutron transmission testing will be used for process qualification and wet chemistry analysis will be used for acceptance testing.

SAR Section 8.8 is revised to provide terminology definitions. These definitions are then used in the discussion of the determination of – how a lot failure is handled, lot acceptability, the basis for reduced sampling, sampling locations, the lower tolerance limit of neutron absorber content, the number of production runs or lots required in the statistical analysis data set, and how an estimation of the variances is done for neutron absorbers for which an effectiveness of 90% is credited.

Refer to RAI Responses 8-8, 8-10 and 8-11 for related information and SAR changes.

**NAC INTERNATIONAL RESPONSE
TO
REQUEST FOR ADDITIONAL INFORMATION**

CHAPTER 8 MATERIALS EVALUATION

- 8-10 Revise the acceptance testing for the neutron absorbers to explain how an accurate determination of the B-10 areal density will be determined. The applicant should note that neutron attenuation should be done for greater than 75% credit or specify an alternate technique with a technical basis.

Wet chemical analysis of the boron in the absorber requires a knowledge of the fraction of B-10 in the boron in order to determine an accurate areal density. It is unclear how the applicant will determine the B-10 fraction from the information provided in the application.

This information is needed to determine compliance with 10 CFR 72.11 and 72.236(c).

NAC International Response

SAR Sections 8.8 and 10.1.6 are revised to clarify acceptance testing for the effective areal density and homogenous distribution of the B10 in the neutron absorber materials. SAR Section 10.1.6 outlines the methods of acceptance testing based on the credit taken for the neutron absorber material. For MAGNASTOR neutron absorber materials where 90% credit is taken, neutron transmission testing will be used for both process qualification and acceptance testing. For MAGNASTOR neutron absorber materials where 75% credit is taken, neutron transmission testing will be used for process qualification and wet chemistry analysis will be used for acceptance testing.

**NAC INTERNATIONAL RESPONSE
TO
REQUEST FOR ADDITIONAL INFORMATION**

CHAPTER 8 MATERIALS EVALUATION

8-11 Revise Chapters 8 and 10 to specify that standard industrial techniques for verifying other product acceptance characteristics will be conducted on all absorbers, (i.e., dimensions, including flatness, straightness, etc., chemical analysis, thermal conductivity, tensile properties, and surface quality and finish).

This information is needed to ensure that the acceptance tests done on the finished product are implemented in accordance with a recognized industry code, e.g., ASTM.

This information is needed to determine compliance with 10 CFR 72.11 and 72.236(c).

NAC International Response

In accordance with the draft ASTM C26.03, WK936, Standard Practice, SAR Sections 8.8 and 10.1.6 are revised to include standard industrial techniques to verify other characteristics of the MAGNASTOR neutron absorber materials, i.e., dimensions including flatness, straightness, etc., chemical analysis (as required), thermal conductivity, tensile properties – or where not appropriate for nonstructural components – other mechanical tests, and surface quality and finish. These product acceptance tests will be performed in accordance with applicable ASTM standards.

Refer to RAI Responses 8-8, 8-9 and 8-10 for related information and SAR changes.

**NAC INTERNATIONAL RESPONSE
TO
REQUEST FOR ADDITIONAL INFORMATION**

CHAPTER 8 MATERIALS EVALUATION

- 8-12 Justify the use of the mechanical properties for aluminum 1100 in the derivation of the mechanical properties of the neutron absorbers in Table 8.3-16, Mechanical Properties of Neutron Absorber.

Neutron absorbers proposed for this application could be fabricated from aluminum from the 6000 series. Further, these materials contain boron carbide in the matrix. The mechanical properties of a particular neutron absorber will be dependent on the volume percent of boron carbide in the matrix.

This information is needed to determine compliance with 10 CFR 72.11 and 72.236(c).

NAC International Response

Properties for the neutron absorber materials have been defined for analysis purposes to conservatively bound the properties for the family of potential aluminum-based neutron absorber materials that may be used in the fabrication of the MAGNASTOR fuel baskets. Neutron absorbers that may be used in the MAGNASTOR fuel baskets include BORAL, borated metal matrix composites and borated aluminum alloy materials. Type 1100 series aluminum alloy has significantly less structural capacity than other aluminum alloys, but all of these aluminum alloys demonstrate increases in strength with the addition of boron carbide. Depending on material type and boron carbide content, the room temperature ultimate strength for 1100 series aluminum alloy increases from the 13 ksi range to approximately 15.2 ksi, and for the 6000 series aluminum alloy it increases from the 45 ksi range to approximately 60 ksi for materials with 30% boron carbide. Similar strength increases are observed for material yield strength and modulus of elasticity properties for these aluminum alloys.

Required structural performance of the neutron absorbers in the MAGNASTOR fuel baskets is limited to maintaining neutron absorber sheet continuity, while sandwiched between a fuel tube wall and a stainless steel cover sheet. In addition to using material properties that represent minimum structural performance, the analytical model for the neutron absorber sheet is limited to the consideration of the BORAL composite core structure between sheets of aluminum. The analytical model uses the 1100 series aluminum alloy material properties for the aluminum sheets and defines the composite

**NAC INTERNATIONAL RESPONSE
TO
REQUEST FOR ADDITIONAL INFORMATION**

RAI 8-12

NAC International Response (continued)

core elastic modulus to be 1,000 psi with a material yield strength of 10 psi. Using these conservatively minimal values for the material properties of the core region eliminates any contribution of structural capacity to the performance of the basket.

Therefore, it is concluded that defining the material properties for the neutron absorber material as the temperature dependent properties for Type 1100 series aluminum alloy provides a conservative envelope for the family of aluminum-based neutron absorber materials that may be used in the fabrication of the MAGNASTOR fuel baskets.

The material presented in Table 8.3-16 is revised in order to provide a more descriptive presentation of the material properties and their respective use in analytical models. Information in Table 8.3-16 is revised as follows.

- 1) The heading for the temperatures is revised to be "Values at Temperature (°F)";
- 2) Removed e) from "Property" column heading;
- 3) Revised the Property column to Ultimate Tensile Strength and added footnote e);
- 4) Revised the Property column to Yield Strength, deleted footnote a, and added footnote e);
- 5) Added footnote f) to Modulus of Elasticity; Coefficient of Thermal Expansion; Poisson's Ratio; and Density; deleted footnote e from Modulus of Elasticity
- 6) Added footnote f) to the listing of foot notes as: f) ASME Boiler and Pressure Vessel Code, Section II, Part D [5]
- 7) Added two additional lines of information to the Table:
 - a. Modulus of Elasticity, E, for BORAL core (psi) = 1,000 for all temperatures;
 - b. Yield Strength, S_y , for BORAL core (psi) = 10 for all temperatures.

Editorial corrections are also made to Table 8.3-14 as follows.

- 1) The heading for the temperatures is revised to be "Values at Temperature (°F)";
- 2) The units for Density in the table are revised to be (lb/ft³);
- 3) The footnote for the Modulus of Elasticity value at 70 deg-F, 3.72, is revised to "b".

**NAC INTERNATIONAL RESPONSE
TO
REQUEST FOR ADDITIONAL INFORMATION**

CHAPTER 8 MATERIALS EVALUATION

8-13 Provide the mechanical properties for SA-182 steel.

The applicant has stated that SA182 stainless steel may be substituted for SA240 Type304/304L stainless steel provided that the SA182 material yield and ultimate strengths are equal to or greater than those of the SA240 material. However, the SA182 contains more than fifty grades, types, and classes. In some case, depending on the class and grade, the materials may have a lower yield and ultimate than SA 240.

This information is needed to determine compliance with 10 CFR 72.11 and 72.246.

NAC International Response

The note on Table 8.3-1, Mechanical Properties of SA240, Type 304, Stainless Steel, is revised to specifically identify that SA182, Type F304 stainless steel may be substituted for SA240, Type 304 stainless steel provided that the SA182, Type F304 material yield and ultimate strengths are equal to, or greater than, those of the SA240, Type 304 material. This material substitution provides flexibility in the form of material that may be acquired for fabrication of the applicable component(s). Section 8.1 is similarly revised.

**NAC INTERNATIONAL RESPONSE
TO
REQUEST FOR ADDITIONAL INFORMATION**

CHAPTER 8 MATERIALS EVALUATION

8-14 Specify the weld filler metal(s) for the confinement boundary welds.

As stated in ISG-15, the weld filler metals should be specified by ASME Section II, Part C, and an associated American Welding Society (AWS) classification.

This information is needed to determine compliance with 10 CFR 72.11 and 72.246.

NAC International Response

SAR Section 8.4, Weld Design and Specification, is revised to specify the weld filler materials for the TSC confinement boundary welds as AWS ER308L and AWS E308LTX-X in accordance with ASME Code Section II-C requirements for SFA 5.9 and SFA 5.22, respectively.

**NAC INTERNATIONAL RESPONSE
TO
REQUEST FOR ADDITIONAL INFORMATION**

CHAPTER 9 OPERATING PROCEDURES

9-1 State in Section 9.1.1, Step 57(c) and LCO 3.1.1 that the vacuum pump is not running during the 10 minute period when the pressure in the canister is being observed to be equal to or less than 10 mm Hg.

These sections of the SAR do not explicitly state that the vacuum pump is to be turned off when performing the canister vacuum pressure rise check. A leaking isolation valve could cause the canister vacuum conditions to be inappropriately maintained, resulting in an accurate reading of a pressure rise in the canister.

This information is needed to determine compliance with 10 CFR 72.162.

NAC International Response

The TSC loading procedures in Section 9.1.1 have been revised to require that during dryness verification of the cavity following vacuum drying, the vacuum pump will be turned off and isolated from the TSC cavity. These actions will ensure that any leakage of the vacuum drying system isolation valve(s) will not inappropriately affect the pressure rise results and resulting dryness verification results. LCO 3.1.1 in Chapter 13, Appendix A and Bases 3.1.1 in Chapter 13, Appendix C were also revised to incorporate instructions to turn the vacuum pump off during the TSC dryness verification.

**NAC INTERNATIONAL RESPONSE
TO
REQUEST FOR ADDITIONAL INFORMATION**

CHAPTER 9 OPERATING PROCEDURES

- 9-2 Perform a hydrostatic pressure test of the closure weld to 1.25 times the design pressure in accordance with ASME Code requirements, prior to drying operations.

Because the canister is pressurized to over 8 atm with a compressible gas during normal operations, a hydrostatic pressure test will insure weld integrity (both from a design and fabrication perspective) prior to adding the helium. In addition, the only approved spent fuel storage pressurized canister design requires performing a hydrostatic pressure test of the closure weld prior to drying operations. ISG-4, which excludes the hydrostatic pressure test, was written considering canisters containing approximately 1 atm of helium.

This information is needed to determine compliance with 10 CFR 72.122(h).

NAC International Response

The TSC loading procedures in Section 9.1.1 have been revised to incorporate the requirement to perform a hydrostatic pressure test of the TSC following completion of the closure lid-to-TSC shell weld, and prior to installing and welding the closure ring. The TSC will be refilled with clean water complying with the boron concentration requirements of LCO 3.2.1, if applicable, and pressurized to 125% of the maximum normal operating pressure of 104 psig. The hydrostatic test pressure of 130, +5,-0 psig shall be applied, isolated and held for a minimum of 10 minutes. The acceptance criteria for the test is no observable pressure drop during the hold period and no observable water leakage from the closure lid-to-TSC shell weld.

Chapters 10 and 13 have also been revised to incorporate a description and the acceptance criteria for the test, as appropriate.

Table 2.1-2 listing of ASME Code Alternatives for MAGNASTOR has also been revised to incorporate the alternative of the TSC pressure test to the pressure testing requirements of the ASME Code, Section III, Subsection NB, NB-6111.

**NAC INTERNATIONAL RESPONSE
TO
REQUEST FOR ADDITIONAL INFORMATION**

CHAPTER 9 OPERATING PROCEDURES

- 9-3 Add a step in the loading procedures to verify that the fuel assemblies being loaded meet the specifications, as applicable for the boron concentration and basket configuration of the canister being loaded.

The operating procedures only call for a check of the boron concentration in the pool or cask water prior to loading. A check that the proper fuel assemblies have been selected for loading is also needed.

This information is needed to assure that use of the package will comply with 10 CFR 72.124(a) and 72.150.

NAC International Response

The loading procedure in Section 9.1.1 has been revised to clarify the step for verifying that the fuel assemblies to be loaded meet the Technical Specifications for approved contents, authorized fuel assembly location and TSC cavity water boron concentration. Verification of fuel assembly identification and correct placement in the basket per the Technical Specifications has also been revised. The revised step is provided below:

- “15. Load the previously selected fuel assemblies into the TSC basket.

Note: The fuel assemblies shall be selected in compliance with the requirements of the approved contents and boron concentration limits of the Technical Specifications including limitations on fuel assembly positions within the basket. Assembly selection and placement within the basket shall be independently verified.”

Step 15 incorporates the specific requirement to perform an independent check of the assembly selection.

**NAC INTERNATIONAL RESPONSE
TO
REQUEST FOR ADDITIONAL INFORMATION**

CHAPTER 11 RADIATION PROTECTION

- 11-1 Provide the evaluation used to determine the estimated onsite collection dose summarized in Section 11.3 of the SAR.

The doses used to determine the person-rem exposure in Tables 11.3-1, 11.3-2, 11.3-3, and 11.3-4 seem to be much lower than they should be considering the surface dose rates determined in Chapter 5.

This information is needed to determine compliance with 10 CFR 72.104, 72.126, and 10CFR Part 20.

NAC International Response

The listed values for loading the system are based on NAC experience at several ISFSI sites loading similar systems. In particular the configuration of the MAGNASTOR seal design is expected to reduce personnel exposure significantly over those of the NAC-UMS and NAC-MPC systems. A significant portion of system loading exposure is associated with the sealing of the canister lid. The MAGNASTOR design requires sealing of a single 9 inch thick canister lid versus a thinner shield lid and a structural lid for the NAC-UMS and MPC systems. Note that the calculation results are revised to include the additional steps of hydrostatic testing the TSC and welding and inspecting the closure ring and secondary port covers. Offsetting the increase in exposure from the additional operational steps is the reduction in dose rates associated with the reduced PWR and BWR TSC heat loads.

The calculation packages supporting the bounding loading and site occupational exposure evaluations are provided as an attachment to the RAI response. The calculations provide details on the number of personnel, location of personnel, and dose field for each of the operational steps.

**NAC INTERNATIONAL RESPONSE
TO
REQUEST FOR ADDITIONAL INFORMATION**

CHAPTER 11 RADIATION PROTECTION

11-2 Provide the evaluations that demonstrate the exposure to the public.

SAR Section 11.4, Exposures to the Public, indicates that a detailed controlled area boundary is contained in Chapter 5. However, Section 5.1.3 contains only two paragraphs, which briefly summarize the methodology and Section 5.6, which provides a brief summary of results.

This information is needed to determine compliance with 10 CFR 72.106, 72.126, and 10CFR Part 20.

NAC International Response

As a response to RAI 5-7 additional information is provided on the site boundary dose evaluation (including a sample input).

The calculation packages supporting the skyshine (NAC-CASC) evaluations are provided as an attachment to the RAI response.

**NAC INTERNATIONAL RESPONSE
TO
REQUEST FOR ADDITIONAL INFORMATION**

CHAPTER 12 ACCIDENT ANALYSIS

12-1 Provide the evaluation for the radiological impact from a tornado-driven missile.

Section 12.2.11.5 provides only a brief summary of the results, but no supporting evaluation.

This information is needed to determine compliance with 10 CFR 72.106.

NAC International Response

The requested evaluation is identical to that performed for the normal condition concrete cask presented in Chapter 5, but with 6 inches of concrete removed from the entire radial surface of the cask body. Section 12.2.11.5 is revised to identify the base model for the accident analysis and to specify the model changes. The calculated dose rates for the tornado-driven missile accident condition are presented in Table 5.1-2.

**NAC INTERNATIONAL RESPONSE
TO
REQUEST FOR ADDITIONAL INFORMATION**

CHAPTER 12 ACCIDENT ANALYSIS

12-2 Provide the evaluation for the radiological impact from a cask tip-over on the concrete pad.

Section 12.2.12.6 provides only a brief summary of the results, but no supporting evaluation.

This information is needed to determine compliance with 10 CFR 72.106.

NAC International Response

Structural evaluations have demonstrated that no design basis condition will result in a tip-over of the concrete cask on the pad. No dose specific evaluations were therefore run for the MAGNASTOR system. Conclusions presented on the adverse radiological consequences of the hypothetical tip-over event are obtained from NAC-UMS system licensing evaluations. For the NAC-UMS system dose rates were estimated using 1-D analysis to be 34 rem/hr at 1 meter and 4 rem/hr at 4 meters from the bottom end of the tipped over concrete cask. The NAC-UMS concrete cask bottom end shielding consists of 4.75 inches of steel (1.75-inch canister bottom plate, a 2-inch concrete cask bottom weldment base plate with a 1-inch bottom plate). The MAGNASTOR concrete cask bottom end shielding consists of 5.75 inches of steel (2.75-inch canister bottom plate, a 2-inch concrete cask bottom weldment base plate with a 1-inch bottom plate). While the total source allowed for loading in the MAGNASTOR system is greater than that of the NAC-UMS system, dose rates at the site boundary (≥ 100 meters distance) are certainly sufficiently low to not exceed an accumulated exposure of 5 rem, as stated in the MAGNASTOR SAR.

**NAC INTERNATIONAL RESPONSE
TO
REQUEST FOR ADDITIONAL INFORMATION**

CHAPTER 13 OPERATING CONTROLS AND LIMITS

- 13-1 Explain how Table 3-1 is utilized to determine helium backfill pressure if vacuum drying is employed in accordance with Surveillance Requirement (SR) 3.1.1.1.

The subject table identifies the required helium backfill pressure in terms of decay heat load and temperature from the TSC outlet of the pressurized helium drying (PHD) system used per SR 3.1.1.1. No guidance is provided if the alternate means of vacuum drying the canister from SR 3.1.1.1 is utilized.

This information is needed to determine compliance with 10 CFR 72.146.

NAC International Response

SR 3.1.1.2 has been revised to incorporate the specific requirements for helium backfilling with a specified mass of helium corresponding to the TSC free volume following vacuum drying. Specifically, SR 3.1.1.2 has been revised to add the following:

“Following vacuum drying and evacuation to < 3 torr, backfill the cavity with high purity helium until a mass, M_{helium} , corresponding to the free volume of the TSC measured during draining (V_{TSC}), multiplied by the helium density (L_{helium}) required for the design basis heat load and specified in Table 3-1, is reached.

OR

Following pressurized helium drying of the cavity, backfill the TSC with high purity helium to the density required for the design basis heat load pressure as specified in Table 3-1.”

New Table 3-1 in Appendix A, identifies the required density of helium for a TSC containing design basis heat load contents.

Additionally, the LCO 3.1.1 Bases in Chapter 13, Appendix C, have been revised to incorporate the changes to SR 3.1.1.1 and SR 3.1.1.2.

**NAC INTERNATIONAL RESPONSE
TO
REQUEST FOR ADDITIONAL INFORMATION**

CHAPTER 13 OPERATING CONTROLS AND LIMITS

Chapter 13 Appendix A (Technical Specifications)

- 13-2 Revise the definition of INTACT FUEL ASSEMBLY (ROD) to state that any missing fuel rods must be replaced by solid filler rods that displace a volume at least equal to that of the original rod. Also, remove the last sentence of the definition.

The criticality analysis assumes that all fuel rods are present.

This information is needed to determine compliance with 10CFR 72.124(a).

NAC International Response

The definition of intact fuel is revised and clarified in SAR Sections 1.1 - Terminology, 8.11 - Cladding Integrity, and 1.1 of Chapter 13, Appendix A - Definitions. The revised definition incorporates the requirement that any missing fuel rods must be replaced by solid filler rods that displace a volume at least equal to that of the original fuel rod. A definition of damaged fuel - a modified version of that provided in ISG-1 - is also incorporated in these SAR sections to complement the intact fuel definition.

**NAC INTERNATIONAL RESPONSE
TO
REQUEST FOR ADDITIONAL INFORMATION**

CHAPTER 13 OPERATING CONTROLS AND LIMITS

Chapter 13 Appendix A (Technical Specifications)

- 13-3 Revise the frequency for SR 3.2.1.1 to be conducted within 4 hours prior to commencing loading or unloading operations and every 24 hours thereafter.

Recent information indicates that boron dilution events at some reactors may proceed fairly rapidly. Because of the small margin in setting the minimum boron concentrations and the fact that these specifications must be appropriate for all potential users, the surveillance times proposed do not provide an appropriate level of control for a general license certificate. Also, revise the bases accordingly.

This information is needed to assure compliance with 10 CFR 72.124(a).

NAC International Response

The frequency for Surveillance SR 3.2.1.1 in Appendix 13A is revised to be conducted within 4 hours prior to commencing loading or unloading operations and every 24 hours thereafter to provide the appropriate level of control of potential boron dilution in a reactor spent fuel pool. The Bases for SR 3.2.1.1 in Appendix 13C are similarly revised.

**NAC INTERNATIONAL RESPONSE
TO
REQUEST FOR ADDITIONAL INFORMATION**

CHAPTER 13 OPERATING CONTROLS AND LIMITS

Chapter 13 Appendix A (Technical Specifications)

13-4 Add a specification for the inner cross section dimensions of the fuel tubes to Section 4.1.1.

The parameters most important to safety should be included in the TS.

This information is needed to assure compliance with 10 CFR 72.124(a).

NAC International Response

In accordance with the requirements of 10 CFR 72.124(a), NAC has evaluated the MAGNASTOR system parameters associated with nuclear criticality safety, including the inner cross section dimensions of the fuel tubes. The evaluations of the fuel basket fabrication tolerances are described in SAR Section 6.4.2.1 and the results of those evaluations are discussed in Sections 6.4.3.1 and 6.4.3.2 for the PWR and BWR fuel baskets, respectively. Although a combination of basket fabrication tolerances minimizing the tube internal free volume showed a minor positive reactivity effect, no single component fabrication tolerance has a statistically significant effect on system reactivity. Therefore, it is concluded that inclusion of fuel tube dimensions in the Technical Specifications is not warranted by safety considerations.

**NAC INTERNATIONAL RESPONSE
TO
REQUEST FOR ADDITIONAL INFORMATION**

CHAPTER 13 OPERATING CONTROLS AND LIMITS

Chapter 13 Appendix B (Technical Specifications)

- 13-5 Provide footnotes in Tables 2-3 and 2-10 stating those detailed fuel dimensions by assembly type are specified in the SAR.

A link to the specifications in the SAR is needed to assure that they are followed and not overlooked by the user. The final limits on the fuel parameters should be consolidated into a single reference in part of the SAR like Tables 6.4-1 and 6.4-2.

This information is needed to assure compliance with 10 CFR 72.124(a).

NAC International Response

As requested, a footnote has been inserted in Table 2-3 to link the specific fuel characteristics to FSAR Table 6.4-1 for PWR fuel. A similar footnote has been inserted in Table 2-10 to provide a link to FSAR Table 6.4-2 for BWR fuel. Also, for clarification 13B - Section 2.0 on Page13B-1 has been revised to state, "INTACT FUEL ASSEMBLIES meeting the limits specified in Tables 2-1 through 2-17 and in Tables 6.4-1 and 6.4-2 of the FSAR may be stored in the MAGNASTOR SYSTEM."

**NAC INTERNATIONAL RESPONSE
TO
REQUEST FOR ADDITIONAL INFORMATION**

CHAPTER 13 OPERATING CONTROLS AND LIMITS

Chapter 13 Appendix B (Technical Specifications)

13-6 Revise item I.A.1 in Table 2-1 to read, "Uranium PWR INTACT FUEL ASSEMBLIES listed in Tables 2-2 and 2-3 and meeting the following specifications":

Important specifications are listed in each of the two tables.

This information is needed to assure compliance with 10 CFR 72.124(a).

NAC International Response

Table 2-1 for PWR fuel is revised as requested for clarity and completeness. Also, Table 2-8 for BWR fuel is similarly revised for consistency of presentation.

**NAC INTERNATIONAL RESPONSE
TO
REQUEST FOR ADDITIONAL INFORMATION**

CHAPTER 13 OPERATING CONTROLS AND LIMITS

Chapter 13 Appendix B (Technical Specifications)

13-7 Revise item B in Table 2-1 to state that filler rods must displace a volume at least equal to the original rod.

Also, see item 13-2 above.

This information is needed to assure compliance with 10 CFR 72.124(a).

NAC International Response

It appears that this comment was intended to refer to item C in 13B - Table 2-1.

Item I.C in 13B - Table 2-1, second sentence, has been revised to read, "Assemblies may contain solid filler rods that displace a volume equal to, or greater than, that of the original fuel rod." This is consistent with the intact fuel definition provided in response to RAI 13-2.

**NAC INTERNATIONAL RESPONSE
TO
REQUEST FOR ADDITIONAL INFORMATION**

CHAPTER 15 DECOMMISSIONING

- 15-1 Provide a discussion of the TSC decontamination efforts for fuel particulate release as a result of an off-normal event.

Section 15.2 states the following: "some effort may be required to remove surface contamination prior to disposal but absolute decontamination of the TSC internals is not necessary." Staff believes that this may be true for CRUD, but not if some fuel particulate is released from the rods during off-normal events (cask tip-over).

This information is needed to determine compliance with 10 CFR 72.11.

NAC International Response

Chapter 15, Section 15.2 has been revised to incorporate additional requirements to survey the internals of TSCs exposed to off-normal and accident conditions for fuel particulate materials that may have been released to the TSC internals from damaged fuel assemblies. The new instructions include direction to remove fuel particulate materials prior to final disposition of the empty TSC and its baskets and lid components. The process of removing fuel particulate from the TSC and basket is essentially identical to routine practices for deconning and disposing of spent fuel rack assemblies removed from a facilities spent fuel pool.

September 2005

Revision 05A

MAGNASTOR

(Modular Advanced Generation
Nuclear All-purpose STORage)

SAFETY ANALYSIS REPORT

Docket No. 72-1031



Atlanta Corporate Headquarters: 3930 East Jones Bridge Road, Norcross, Georgia 30092 USA
Phone 770-447-1144, Fax 770-447-1797, www.nacintl.com

Master Table of Contents

Chapter 1	General Description	1-i
Chapter 2	Principal Design Criteria.....	2-i
Chapter 3	Structural Evaluation	3-i
Chapter 4	Thermal Evaluation.....	4-i
Chapter 5	Shielding Evaluation.....	5-i
Chapter 6	Criticality Evaluation.....	6-i
Chapter 7	Confinement.....	7-i
Chapter 8	Materials Evaluation	8-i
Chapter 9	Operating Procedures.....	9-i
Chapter 10	Acceptance Criteria and Maintenance Program	10-i
Chapter 11	Radiation Protection.....	11-i
Chapter 12	Accident Analyses	12-i
Chapter 13	Operating Controls and Limits.....	13-i
Chapter 14	Quality Assurance.....	14-i
Chapter 15	Decommissioning	15-i

Chapter 1 General Description

Table of Contents

1	GENERAL DESCRIPTION.....	1-1
1.1	Terminology.....	1.1-1
1.2	Introduction.....	1.2-1
1.3	General Description of MAGNASTOR.....	1.3-1
1.3.1	MAGNASTOR Components.....	1.3-1
1.3.2	Operational Features.....	1.3-6
1.4	MAGNASTOR Contents.....	1.4-1
1.5	Identification of Agents and Contractors.....	1.5-1
1.6	Generic Concrete Cask Arrays.....	1.6-1
1.7	References.....	1.7-1
1.8	License Drawings.....	1.8-1

List of Figures

Figure 1.3-1	Major Component Configuration for Loading the Concrete Cask.....	1.3-9
Figure 1.3-2	TSC and Basket.....	1.3-10
Figure 1.3-3	Concrete Cask.....	1.3-11
Figure 1.6-1	Typical ISFSI Storage Pad Layout.....	1.6-2

List of Tables

Table 1.3-1	Design Characteristics.....	1.3-12
Table 1.3-2	Physical Design Parameters of the TSC and Fuel Baskets.....	1.3-13
Table 1.3-3	TSC Fabrication Specification Summary.....	1.3-14
Table 1.3-4	Concrete Cask Fabrication Specification Summary.....	1.3-15

1 **GENERAL DESCRIPTION**

This Safety Analysis Report (SAR) describes the NAC International Inc. (NAC) MAGNASTOR System for the storage of spent fuel. It demonstrates that MAGNASTOR satisfies the requirements of the U.S. Nuclear Regulatory Commission (NRC) for spent nuclear fuel storage as prescribed in Title 10 of the Code of Federal Regulations, Part 72 (10 CFR 72) [1] and NUREG-1536 [2]. MAGNASTOR is a canister-based system that accommodates both the storage and transport of Pressurized Water Reactor (PWR) and Boiling Water Reactor (BWR) spent fuel.

The principal components of MAGNASTOR are:

- transportable storage canister (TSC)
- concrete cask
- transfer cask

The TSC is designed and fabricated to meet the requirements for storage in the concrete cask, for transport in a transport cask and to be compatible with the U.S. Department of Energy planning for permanent disposal in a Mined Geological Disposal System. The TSC incorporates a welded closure to preclude the loss of contents and to preserve the general health and safety of the public during long-term storage of spent fuel.

In long-term storage, the TSC is installed in a concrete cask, which provides structural protection and radiation shielding, as well as natural convection cooling. The concrete cask also provides protection during storage for the TSC under adverse environmental conditions.

The transfer cask is used to move the TSC between the workstations during TSC loading and preparation activities. It is also used to transfer the TSC to or from the concrete cask and to a transport cask.

This SAR is formatted in accordance with NRC Regulatory Guide 3.61 [4], except that Chapter 8, Materials Evaluation, is added in accordance with the requirement of Interim Staff Guidance (ISG)-15 [5], with the subsequent renumbering of the remaining chapters. The terminology used in this report is presented in Section 1.1. The term TSC refers to both the PWR and BWR TSCs where the discussion is common to both configurations. Discussion of features unique to the PWR and BWR configurations is addressed in subsections, as appropriate, within each chapter.

1.1 Terminology

This section lists and defines the terms used in this SAR.

Adapter Plate

A carbon steel plate assembly positioned on the top of the concrete cask and used to align the transfer cask. It supports the operating mechanism for opening and closing the transfer cask shield doors.

Burnup

Amount of energy generated during irradiation – measured in MWd/MTU.

Assembly Average Burnup

Value calculated by averaging the burnup over the entire fuel region (UO₂) of an individual fuel assembly.

Peak Average Rod Burnup

Value calculated by averaging the burnup in any rod over the length of the rod, then using the highest burnup calculated as the peak average rod burnup.

Concrete Cask

A concrete cylinder that holds the TSC during storage. The concrete cask is formed around a steel inner liner and base and is closed by a lid.

Base

A carbon steel weldment incorporating the air inlets and the pedestal that supports the TSC inside of the concrete cask.

Lid

A thick concrete and carbon steel closure for the concrete cask. The lid precludes access to the TSC and provides radiation shielding.

Liner

A carbon steel shell that forms the inside diameter of the concrete cask. The liner serves as the inner form during concrete pouring and provides radiation shielding and structural protection for the TSC.

Standoffs (Channels)

Carbon steel weldments attached to the liner that assist in centering the TSC in the concrete cask and supporting the TSC and its contents in a nonmechanistic tip-over event.

Confinement System

The components of the TSC assembly that retain the spent fuel during storage.

Contents

Up to 37 PWR fuel assemblies or up to 87 BWR fuel assemblies. The fuel assemblies are confined in a TSC. Non-fuel hardware may be inserted into PWR fuel assemblies and BWR fuel assemblies may include channels.

Damaged Fuel

Spent nuclear fuel that includes any of the following conditions that result in either compromise of cladding confinement integrity or reconfiguration of fuel assembly geometry:

- 1) The fuel contains known or suspected cladding defects greater than a pinhole leak or a hairline crack that have the potential for release of significant amounts of fuel particles.
- 2) The fuel assembly:
 - a. is damaged in such a manner as to impair its structural integrity;
 - b. has missing or displaced structural components such as grid spacers;
 - c. is missing fuel pins that have not been replaced by filler rods which displace a volume equal to, or greater than, that of the original fuel rod;
 - d. cannot be handled using normal handling methods.
- 3) The fuel is no longer in the form of an intact fuel assembly and consists of, or contains, debris such as loose pellets, rod segments, etc.

Factor of Safety

An analytically determined value defined as the allowable stress or displacement of a material divided by its calculated stress or displacement.

Fuel Basket (Basket)

The structure inside the TSC that provides structural support, criticality control, and heat transfer paths for the fuel assemblies.

Developed Cell

A basket opening formed by either four fuel tubes or fuel tubes and basket weldments. Fuel assemblies are loaded into the developed cells.

Fuel Tube

A carbon steel tube with a square cross-section. Fuel assemblies are loaded into the fuel tubes. A fuel tube may have neutron absorber material attached on its interior faces.

Neutron Absorber

A borated aluminum metal matrix or composite with neutron absorption capability.

Intact Fuel (Assembly or Rod)

Spent nuclear fuel that is not Damaged Fuel, as defined herein. To be classified as intact, fuel must meet the criteria for both intact cladding and structural integrity. An intact fuel assembly can be handled using normal handling methods and any missing fuel rods have been replaced by solid filler rods that displace a volume equal to, or greater than, that of the original fuel rod.

MAGNASTOR (Modular Advanced Generation, Nuclear, All-purpose STORAGE)

The high-capacity system designed for safe, long-term spent fuel storage at a power reactor site or at an independent spent fuel storage installation.

Spent Nuclear Fuel (or Spent Fuel)

Irradiated fuel assemblies with the same configuration as when originally fabricated, consisting generally of the end fittings, fuel rods, guide tubes, and integral hardware. For PWR fuel, a thimble plug, an in-core instrument thimble, a burnable poison rod insert, or a control element assembly (CEA) is considered to be a component of standard fuel. For BWR fuel, the channel is considered to be integral hardware. Solid filler rods, burnable poison rods, burnable poison rod assemblies, thimble plugs, control element assemblies and stainless steel rod inserts may be inserted in PWR fuel assemblies.

Transfer Cask

A shielded device used to lift and handle the TSC during fuel loading and closure operations, as well as to transfer the TSC in/out of the concrete cask during storage or in/out of a transport cask. The transfer cask includes two lifting trunnions and two shield doors that can be opened to permit the vertical transfer of the TSC.

Trunnions

Two low-alloy steel components used to lift the transfer cask in a vertical orientation via a lifting assembly.

TSC (Transportable Storage Canister)

The stainless steel cylindrical shell, bottom-end plate, closure lid, closure ring, and redundant port covers that contain the fuel basket structure and the spent fuel contents.

Closure Lid

A thick, stainless steel disk installed directly above the fuel basket following fuel loading. The closure lid provides the confinement boundary for storage and operational shielding during TSC closure.

Drain and Vent Ports

Penetrations located in the closure lid to permit draining, drying, and helium backfilling of the TSC.

Port Cover

The stainless steel plates covering the vent and drain ports that are welded in place following draining, drying, and backfilling operations.

Closure Ring

A stainless steel ring welded to the closure lid and TSC shell to provide a double weld redundant sealing closure of the TSC satisfying 10 CFR 72.236(e) requirements.

1.2 Introduction

MAGNASTOR is a spent fuel dry storage system consisting of a concrete cask and a welded stainless steel TSC with a welded closure to safely store spent fuel. The TSC is stored in the central cavity of the concrete cask. The concrete cask provides structural protection, radiation shielding, and internal airflow paths that remove the decay heat from the TSC contents by natural air circulation. MAGNASTOR is designed and analyzed for a 50-year service life.

The loaded TSC is moved to and from the concrete cask using the transfer cask. The transfer cask provides radiation shielding during TSC closure and preparation activities. The TSC is transferred into the concrete cask by positioning the transfer cask with the loaded TSC on top of the concrete cask, opening the shield doors, and lowering the TSC into the concrete cask. Figure 1.3-1 depicts the major components of MAGNASTOR in such a configuration.

MAGNASTOR is designed to safely store up to 37 PWR or up to 87 BWR spent fuel assemblies in separate fuel basket assemblies. These capacities, combined with enhanced operational features, assure that MAGNASTOR reduces the time required and the personnel dose received on a per-assembly basis when placing spent fuel into dry storage. The fuel specifications and parameters that establish the design basis for the PWR and BWR fuel assemblies are presented in Chapter 2. The spent fuel considered in the design includes fuel assemblies that have different overall lengths. The PWR and BWR fuel assembly populations are divided into two groups based on fuel assembly length, and are accommodated by two different lengths of TSCs. The concrete cask and transfer cask are a fixed height and can accommodate both lengths of TSC. The designations and corresponding lengths of the TSCs are shown on the License Drawings.

For PWR fuel, the inclusion of nonfuel assembly hardware can increase an assembly's overall length, resulting in the need to use the longer TSC. Spacers may be used in a given TSC to allow loading of fuel that is significantly shorter than the TSC length. The BWR fuel assembly groups are evaluated for the effects of the zirconium alloy channel that surrounds the fuel assembly in reactor operations. Fuel assembly channel effects are addressed in both the thermal heat transfer and criticality analyses. BWR assembly channels are included in the assembly weight assigned to each basket opening in the structural analysis. The mass associated with the channel is conservatively neglected from the material homogenization in the shielding analysis.

The system design and analyses are in accordance with 10 CFR 72, ANSI/ANS 57.9 [6], the applicable sections of the ASME Boiler and Pressure Vessel Code (ASME Code), and the American Concrete Institute (ACI) code [7]. The analyses demonstrate that MAGNASTOR meets the regulatory requirements of 10 CFR 72 and the guidance of NUREG-1536 [2].

1.3 General Description of MAGNASTOR

MAGNASTOR provides for the long-term storage of PWR and BWR fuel assemblies as listed in Chapter 2. During long-term storage, the system provides an inert environment, passive structural shielding, cooling and criticality control, and a welded confinement boundary. The structural integrity of the system precludes the release of contents in any of the design basis normal conditions and off-normal or accident events, thereby assuring public health and safety during use of the system.

1.3.1 MAGNASTOR Components

The design and operation of the principal components of MAGNASTOR and the associated auxiliary equipment are described in this section. The design characteristics of the principal components of the system are presented in Table 1.3-1.

This list shows the auxiliary equipment generally needed to use MAGNASTOR.

- automated, remote, and /or manual welding equipment to perform TSC field closure welding operations
- an engine-driven or towed frame or a heavy-haul trailer to move the concrete cask to and from the storage pad and to position the concrete cask on the storage pad
- draining, drying, helium backfill, and water cooling systems for preparing the TSC and contents for storage
- hydrogen monitoring equipment to confirm the absence of explosive or combustible gases during TSC closure welding
- an adapter plate and a hydraulic supply system
- a lifting yoke for lifting and handling the transfer cask and rigging equipment for lifting and handling system components

In addition to these items, the system requires utility services (electric, helium, air, clean borated water, nitrogen gas supply, etc.), standard torque wrenches, tools and fittings, and miscellaneous hardware.

1.3.1.1 Transportable Storage Canister (TSC)

Two lengths of TSCs accommodate all evaluated PWR and BWR fuel assemblies. The TSC is designed for transport per 10 CFR 71 [3]. The load conditions in transport produce higher stresses in the TSC than are produced during storage conditions, except for TSC lifting.

Consequently, transport load conditions establish the design basis for the TSC and, therefore, the TSC design is conservative with respect to storage conditions.

The stainless steel TSC assembly holds the fuel basket structure and confines the contents (see Figure 1.3-2). The TSC is defined as the confinement boundary during storage. The welded closure lid, closure ring, and redundant port covers prevent the release of contents under normal conditions and off-normal or accident events. The fuel basket assembly provides the structural support and a heat transfer path for the fuel assemblies, while maintaining a subcritical configuration for all of the evaluated normal conditions and off-normal or accident events.

The major components of the TSC assembly are the shell, base plate, closure lid, closure ring, and redundant port covers for the vent and drain ports, which provide the confinement boundary during storage. The TSC component dimensions and materials of fabrication are provided in Table 1.3-1. The TSC overall dimensions and design parameters for the two lengths of TSCs are provided in Table 1.3-2.

The TSC consists of a cylindrical stainless steel shell with a welded stainless steel bottom plate at its closed end and a 9-in thick stainless steel closure lid at its open end. The stainless steel shell and bottom plate are dual-certified Type 304/304L. The closure lid and closure ring are Type 304 stainless steel. A fuel basket assembly is placed inside the TSC. The closure lid is positioned inside the TSC on the lifting lugs above the basket assembly following fuel loading. After the closure lid is placed on the TSC, the TSC is moved to a workstation, and the closure lid is welded to the TSC. After nondestructive examination and pressure testing of the closure lid weld, the closure ring is welded to the closure lid and TSC shell. The vent and drain ports are penetrations through the lid, which provide access for auxiliary systems to drain, dry, and backfill the TSC. The drain port has a threaded fitting for installing the drain tube. The drain tube extends the full length of the TSC and ends in a sump in the bottom plate. The vent port also provides access to the TSC cavity for draining, drying, and backfilling operations.

Following completion of backfilling, the redundant port covers at each of the ports are installed and welded in place. Each of the port cover welds in nondestructively examined.

The TSC is designed, fabricated, and inspected to the requirements of the ASME Boiler and Pressure Vessel Code (ASME Code), Section III, Division 1, Subsection NB [8], except as noted in the Alternatives to the ASME Code as provided in Table 2.1-2.

Refer to Table 1.3-3 for a summary of the TSC fabrication requirements.

1.3.1.2 Fuel Baskets

Each TSC contains either a PWR or BWR fuel basket, which positions and supports the stored fuel. As described in the following sections, the design of the basket is similar for the PWR and BWR configurations. The fuel basket for each fuel type is designed, fabricated, and inspected to the requirements of the ASME Code, Section III, Division 1, Subsection NG [9], except as noted in Table 2.1-2.

The structural components of both the PWR and BWR baskets are fabricated from ASME SA537, Class 1, carbon steel. To minimize corrosion and preclude significant generation of combustible gases during fuel loading, the assembled basket is coated with electroless nickel plating using an immersion process. Following coating, the neutron absorber panels and the stainless steel retainers are installed on the basket structure as shown on the License Drawings. The principal dimensions and materials of fabrication of the fuel basket are provided in Table 1.3-1.

Both fuel basket designs minimize horizontal surfaces that could entrain water and provide an open path for water flow to the drain tube and sump in the bottom of the TSC. The fuel baskets are supported from the baseplate by 3-in high spacers at the corner of the fuel tubes enabling the TSC to fill and drain evenly.

Spacers may be used to limit the movement of the spent fuel assemblies during storage or in subsequent transport operations.

PWR Fuel Basket

The PWR fuel basket design is an arrangement of square fuel tubes held in a right-circular cylinder configuration using support weldments that are bolted to the outer fuel tubes. The design parameters for the two lengths of PWR fuel baskets are provided in Table 1.3-2.

Fuel tubes support an enclosed neutron absorber sheet on up to four interior sides of the fuel tube. The neutron absorber panels, in conjunction with minimum TSC cavity water boron levels, provide criticality control in the basket. Each neutron absorber panel is covered by a sheet of stainless steel to protect the material during fuel loading and to keep it in position. The neutron absorber and stainless steel cover are secured to the fuel tube using weld posts located across the width and along the length of the fuel tube.

Each PWR fuel basket has a capacity of 37 fuel assemblies in an aligned configuration. Square tubes are assembled in an array where the tubes function as independent fuel positions and as sidewalls for the adjacent fuel positions in what is called a developed cell array. Consequently, the 37 fuel positions are developed using only 21 tubes. The array is surrounded by weldments

that serve both as sidewalls for some perimeter fuel positions and as the structural load path from the array to the TSC shell wall. Each PWR basket fuel tube has a nominal 8.86-in square opening. Each developed cell fuel position has a nominal 8.76-in square opening.

BWR Fuel Basket

The BWR fuel basket design is an arrangement of square fuel tubes held in a right-circular cylinder configuration using support weldments that are bolted to the outer fuel tubes. The design parameters for the two lengths of BWR fuel baskets are provided in Table 1.3-2.

Each fuel tube supports an enclosed neutron absorber sheet on up to four interior sides of the fuel tube, which provides criticality control in the basket. The neutron absorber is covered by a sheet of stainless steel to protect the material during fuel loading and to keep it in position. The neutron absorber and stainless steel cover are secured to the fuel tube using weld posts located across the width and along the length of the fuel tube.

Each BWR fuel basket has a capacity of 87 fuel assemblies in an aligned configuration. Square tubes are assembled in an array where the tubes function as independent fuel positions and as sidewalls for the adjacent fuel positions in what is called a developed cell array. Consequently, the 87 fuel positions are developed using only 45 tubes. The array is surrounded by weldments that serve both as sidewalls for some perimeter fuel positions and as the structural load path from the array to the TSC shell wall. Each BWR basket fuel tube has a nominal 5.86-in square opening. Each developed cell fuel position has a nominal 5.77-in square opening.

1.3.1.3 Concrete Cask

The concrete cask is the storage overpack for the TSC and it is designed to hold both lengths of TSCs. The concrete cask provides structural support, shielding, protection from environmental conditions, and natural convection cooling of the TSC during long-term storage. The principal dimensions and materials of fabrication of the concrete cask are shown in Table 1.3-1.

The concrete cask is a reinforced concrete structure with a structural steel inner liner and base. The reinforced concrete wall and steel liner provide the neutron and gamma radiation shielding for the stored spent fuel. Inner and outer reinforcing steel (rebar) assemblies are encased within the concrete. The reinforced concrete wall provides the structural strength to protect the TSC and its contents in natural phenomena events such as tornado wind loading and wind-driven missiles and during nonmechanistic tip-over events (refer to Figure 1.3-3). The concrete surfaces remain accessible for inspection and maintenance over the life of the cask, so that any necessary restoration actions may be taken to maintain shielding and structural conditions.

The concrete cask provides an annular air passage to allow the natural circulation of air around the TSC to remove the decay heat from the contents. The lower air inlets and upper air outlets are steel-lined penetrations in the concrete cask body. Each air inlet/outlet is covered with a screen. The weldment baffle directs the air upward and around the pedestal that supports the TSC. Decay heat is transferred from the fuel assemblies to the TSC wall by conduction, convection, and radiation. Heat is removed by convection and radiation from the TSC shell to the air flowing upward through the annular air passage and to the concrete cask inner liner, respectively. Heat radiated to the liner can be transferred to the air annulus and by conduction through the concrete cask wall. The heated air in the annulus exhausts through the air outlets. The passive cooling system is designed to maintain the peak fuel cladding temperature below acceptable limits during long-term storage [10]. The concrete cask thermal design also maintains the bulk concrete temperature and surface temperatures below the American Concrete Institute (ACI) limits under normal operating conditions. The inner liner of the concrete cask incorporates standoffs that provide lateral support to the TSC in side impact accident events.

A carbon steel and concrete lid is bolted to the top of the concrete cask. The lid reduces skyshine radiation and provides a cover to protect the TSC from the environment and postulated tornado missiles.

Fabrication of the concrete cask requires no unique or unusual forming, concrete placement, or reinforcement operations. The concrete portion of the cask is constructed by placing concrete between a reusable, exterior form and the steel liner. Reinforcing bars are used near the inner and outer concrete surfaces to provide structural integrity. The structural steel liner and base are shop fabricated. Refer to Table 1.3-4 for the fabrication specifications for the concrete cask.

Daily visual inspection of the air inlet and outlet screens for blockage assures that airflow through the cask meets licensed requirements. A description of the visual inspection is included in the Technical Specifications, Chapter 13. As an alternative to daily visual inspections, the loaded concrete cask in storage may include the capability to measure air temperature at the four outlets. Each air outlet may be equipped with a remote temperature detector mounted in the outlet air plenum. The air temperature-monitoring system, designed to provide verification of heat dissipation capabilities, can be designed for remote or local read-out capabilities at the option of the licensee. The temperature-monitoring system can be installed on all or some of the concrete casks at the Independent Spent Fuel Storage Installation (ISFSI) facility.

1.3.1.4 Transfer Cask

The transfer cask is designed, fabricated, and tested to meet the requirements of ANSI N14.6 [11] as a special lifting device. The transfer cask provides biological shielding and structural

protection for a loaded TSC, and is used to lift and move the TSC between workstations. The transfer cask is also used to shield the vertical transfer of a TSC into a concrete cask or a transport cask.

The transfer cask design incorporates three retaining blocks, pin-locked in place, to prevent a loaded TSC from being inadvertently lifted through its top opening. The transfer cask has retractable bottom shield doors. During TSC loading and handling operations, the shield doors are closed and secured. After placement of the transfer cask on the concrete cask, the doors are retracted using hydraulic cylinders and a hydraulic supply. The TSC is then lowered into a concrete cask for storage. Refer to Figure 1.3-1 for the general arrangement of the transfer cask, TSC, and concrete cask during loading and Table 1.3-1 for the principal dimensions and materials of fabrication of the transfer cask.

Sixteen penetrations, eight at the top and eight at the bottom, are available to provide a water supply to the transfer cask annulus. Penetrations not used for water supply or draining are capped. The transfer cask annulus is isolated using inflatable seals located between the transfer cask inner shell and the TSC near the upper and lower ends of the transfer cask.

During TSC closure, clean or demineralized spent fuel pool water may be circulated through these penetrations into the annulus region to minimize component temperatures and improve canister preparation time limits. The auxiliary cooling water circulation can be utilized through completion of TSC activities. The auxiliary cooling water is turned off prior to movement of the transfer cask for TSC transfer operations.

A similar process of clean or demineralized spent fuel pool water circulation in the annulus is used during in-pool fuel loading to minimize the potential for contamination of the TSC exterior surfaces.

The transfer cask penetrations can also be used for the introduction of auxiliary forced air or gas to cool the exterior of the TSC. Alternately, if auxiliary cooling is required to lower fuel cladding or TSC component temperatures, the loaded TSC may be returned to the spent fuel pool or shelf for cooling.

1.3.2 Operational Features

In storage, MAGNASTOR does not require any active operational systems. The principal MAGNASTOR operational activities are loading, welding, and preparing the TSC for storage and transferring the TSC to the concrete cask. The transfer cask is designed to meet the requirements of these operations. The transfer cask holds the TSC during fuel loading

operations, provides biological shielding during TSC closure and preparation, and positions the TSC for transfer into the concrete cask. The lid design of the TSC assures structural integrity, while reducing the time and dose involved in TSC closure.

The detailed generic step-by-step operating procedures for the loading and transferring of MAGNASTOR are presented in Chapter 9. The following is a list of the major loading activities. This list assumes that the empty TSC is installed in the transfer cask.

- Fill the TSC with water or borated water if required.
- Lift the transfer cask over the pool and start the flow of water to the transfer cask annulus and lower the cask to the bottom of the pool.
- Load the selected spent fuel assemblies into the TSC.
- Install the closure lid.
- Remove the transfer cask from the pool and place it in the cask preparation workstation.
- Decontaminate the transfer cask.
- Lower the TSC water level and weld the closure lid to the TSC shell. Examine the weld.
- Hydrostatically test the TSC.
- Install and weld the closure ring. Examine the weld.
- Drain the remaining pool water from the TSC.
- Dry the TSC cavity. Verify cavity dryness.
- Establish a helium backfill.
- Install the redundant vent and drain port covers and weld them to the closure lid. Examine the welds.
- Install the TSC lifting system.
- Install the adapter plate on the concrete cask.
- Lift and place the transfer cask on the transfer adapter.
- Attach the TSC lifting system to the crane hook and raise the TSC off of the shield doors.
- Open the shield doors.
- Lower the TSC into the concrete cask (see Figure 1.3-1).
- Remove the transfer cask, transfer adapter, and TSC lifting systems.
- Install the lid on the concrete cask.
- Move the loaded concrete cask to the storage pad.
- Move the concrete cask to its designated location on the storage pad.

The TSC unloading and spent fuel removal from the TSC are essentially the reverse of these steps, except that weld removal and cooldown of the contents is required. This typical sequence of operations, and individual steps, may be modified by the approved site procedure to

accommodate specific site requirements, as long as the requirements of the Technical Specifications and the CoC are met.

Figure 1.3-1 Major Component Configuration for Loading the Concrete Cask

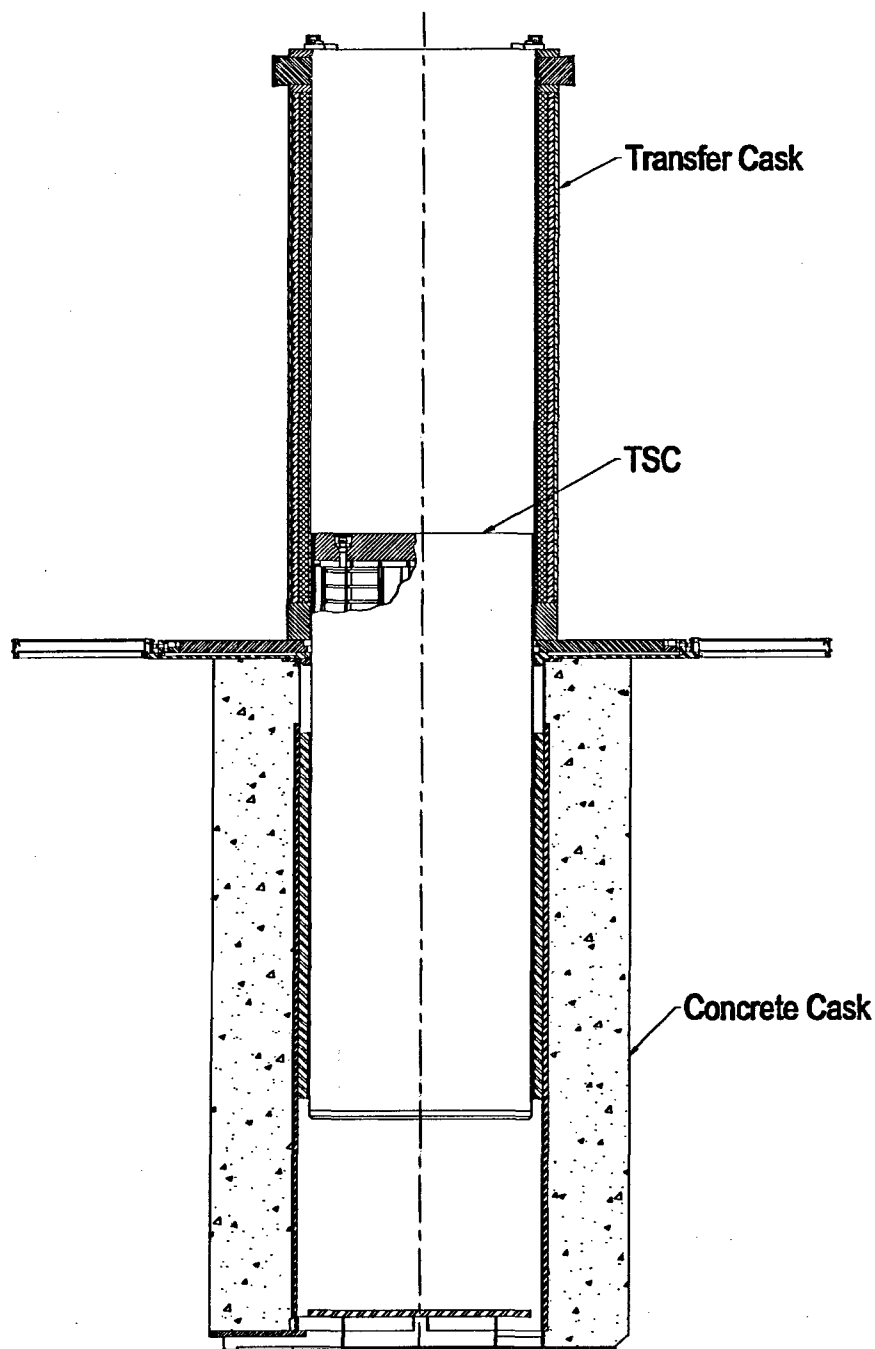


Figure 1.3-2 TSC and Basket

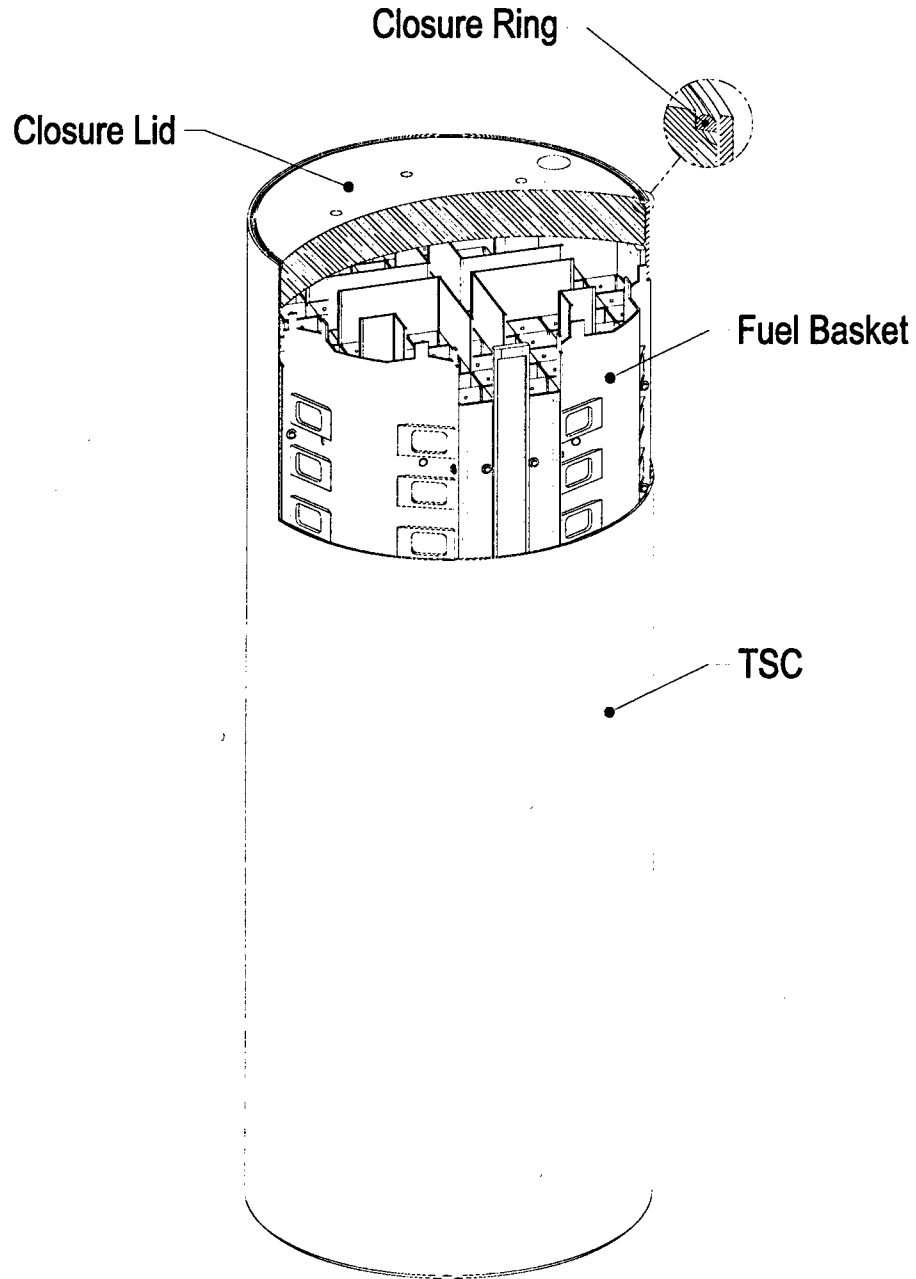


Figure 1.3-3 Concrete Cask

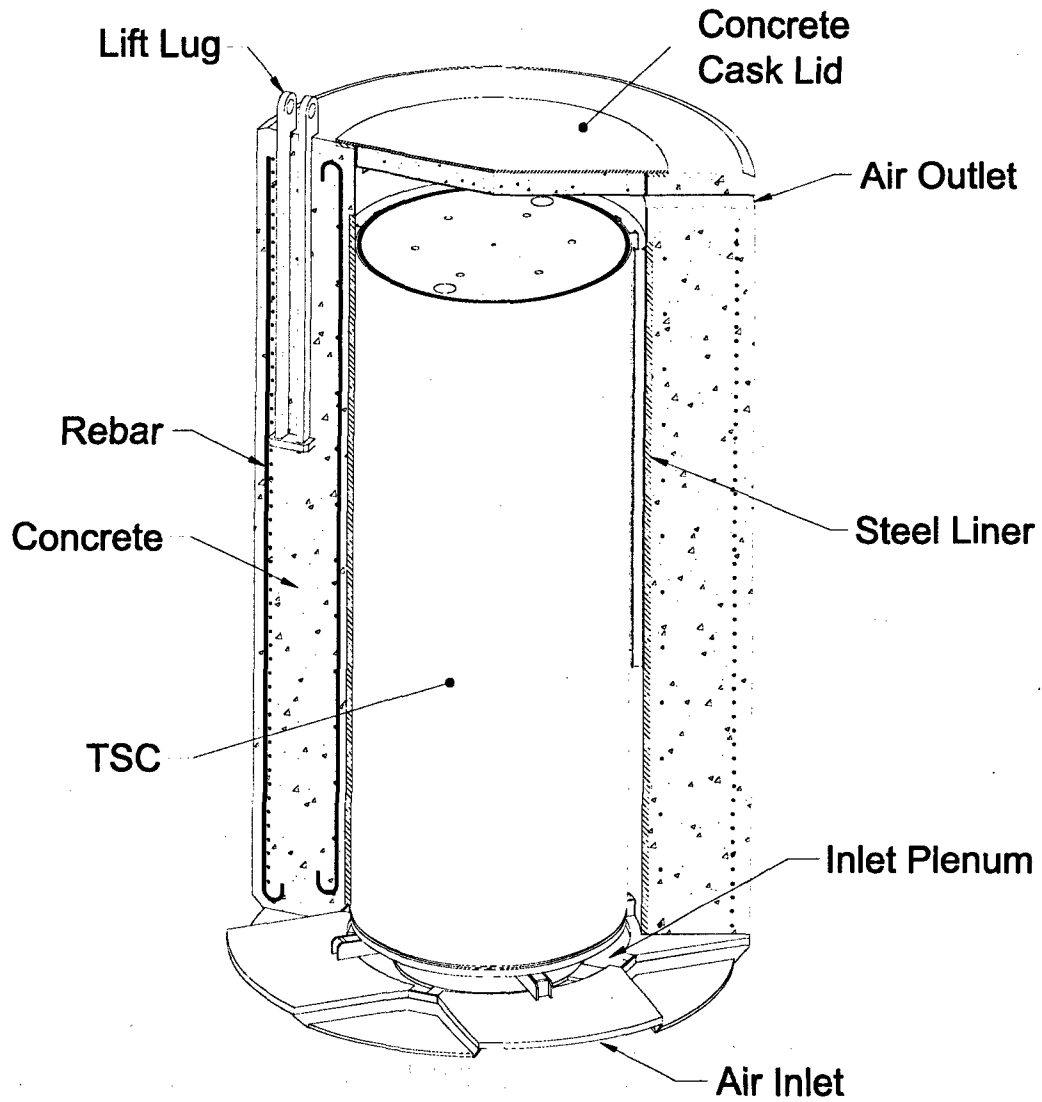


Table 1.3-1 Design Characteristics

	Design Characteristic	Nominal Value (in) ^a	Material	
TSC	Shell	0.5 × 72 dia.	Stainless Steel	
	Bottom	2.75	Stainless Steel	
	Closure Lid	9	Stainless Steel	
	Closure Ring	0.75 square	Stainless Steel	
	Length			
	Group 1 & 3	184.8		
	Group 2 & 4	191.8		
Fuel Basket	PWR Fuel Tube Wall	0.31	Carbon Steel	
	BWR Fuel Tube Wall	0.25	Carbon Steel	
	Neutron Absorber	0.125 (PWR), 0.1 (BWR)	Metallic Composite/Matrix	
	Neutron Absorber Retainer	0.015	Stainless Steel	
	Support Plates & Gussets	0.5 to 0.75	Carbon Steel	
	Support Bars (PWR)	0.875	Carbon Steel	
	Support Plate (BWR)	0.75	Carbon Steel	
	Length			
		Group 1 & 3	172.5	
		Group 2 & 4	179.5	
		Assembly dia.	70.76	
		# of Fuel Tubes/Fuel Loading Positions		
		PWR	21/37	
	BWR	45/87		
Transfer Cask	Outer Shell	1.25 × 88 dia.	Low Alloy Steel	
	Inner Shell	0.75 × 74.5 dia.	Low Alloy Steel	
	Retaining Block	8 × 8.75 × 1.50	Stainless Steel	
	Trunnions	9.5 dia.	Low Alloy Steel	
	Bottom Forging	12 × 88 dia.	Low Alloy Steel	
	Top Forging	14 × 88 dia.	Low Alloy Steel	
	Shield Doors	5.0	Low Alloy Steel	
	Door Rails	5.25 × 7.5 × 52.0	Low Alloy Steel	
	Gamma Shield	3.2	Lead	
	Neutron Shield	2.25	NS-4-FR, Solid Synthetic Polymer	
Transfer Adapter	Base Plate	2.0	Carbon Steel	
	Guide Ring	2.5 × 79 dia.	Carbon Steel	
Concrete Cask	Weldment Structures			
	Liner	1.75 × 83 dia	Carbon Steel	
	Top Flange	1 × 91 dia.	Carbon Steel	
	Standoffs (Channels)	3 × 7.5 (s-beam)	Carbon Steel	
	Pedestal Plate	2 × 72 dia.	Carbon Steel	
	Bottom Weldment	1 × 128 in	Carbon Steel	
	Inlet Top	2 × 136 dia.	Carbon Steel	
	Concrete Cask			
	Concrete Shell	26.5 × 136 dia.	Type II Portland Cement	
	Lid	6.75 × 88 dia.	Carbon Steel	
			Type II Portland Cement	
Rebar	various lengths	Carbon Steel		

^a Thickness unless otherwise indicated.

Table 1.3-2 Physical Design Parameters of the TSC and Fuel Baskets

Component	Characteristic	Parameter	Nominal Value
TSC	Canister Weldment	Shell Outside Diameter (in)	72
		Shell Thickness (in)	0.5
		Bottom Thickness (in)	2.75
	Length	Group 1 & 3 (in)	184.8
		Group 2 & 4 (in)	191.8
Capacity (# of fuel assemblies)	PWR	37	
	BWR	87	
Fuel Basket	Length (in)	Group 1 & 3 (in)	172.5
		Group 2 & 4 (in)	179.5
	Diameter	Assembly Diameter (in)	70.76
	Number of Fuel Tubes/Fuel Loading Positions	PWR	21/37
BWR		45/87	

Table 1.3-3 TSC Fabrication Specification Summary

Materials

- All materials shall be governed by the referenced drawings and meet the applicable ASME Code sections.

Welding

- Welds shall be in accordance with the referenced drawings.
- Filler metals shall be appropriate ASME Code materials.
- Welders and welding operators shall be qualified in accordance with ASME Code Section IX [12].
- Welding procedures shall be written and qualified in accordance with ASME Code Section IX.
- Personnel performing weld examinations shall be qualified in accordance with the NAC International Quality Assurance Program and SNT-TC-1A [13].
- Weld inspection and examination requirements and acceptance criteria are specified in Chapter 10.

Fabrication

- Cutting, welding, and forming shall be in accordance with ASME Code, Section III, NB-4000 [8] unless otherwise specified. Code stamping is not required.
- Surfaces shall be cleaned to a surface cleanliness classification C, or better, as defined in ANSI N45.2.1 [14], Section 2.
- Fabrication tolerances shall meet the requirements of the referenced drawings after fabrication.

Packaging

- Packaging and shipping shall be in accordance with ANSI N45.2.2 [15].

Quality Assurance

- The TSC shall be fabricated under a quality assurance program that meets 10 CFR 72, Subpart G, and 10 CFR 71, Subpart H.

Table 1.3-4 Concrete Cask Fabrication Specification Summary

Materials

- Concrete mix shall be in accordance with the requirements of ACI 318 and ASTM C94 [16].
- Type II Portland Cement, ASTM C150 [17].
- Fine aggregate ASTM C33 [18] or C637 [19].
- Coarse aggregate ASTM C33.

- Admixtures
 - Water Reducing and Superplasticizing ASTM C494 [20].
 - Pozzolanic Admixture (loss on ignition 6% or less) ASTM C618 [21].
- Compressive strength 4000 psi minimum at 28 days.
- Specified air entrainment per ACI 318.
- All steel components shall be of the material as specified in the referenced drawings.

Construction

- A minimum of two samples for each concrete cask shall be taken in accordance with ASTM C172 [22] and ASTM C31 [23] for the purpose of obtaining concrete slump, density, air entrainment, and 28-day compressive strength values. The two samples shall not be taken from the same batch or truck load.
- Test specimens shall be tested in accordance with ASTM C39 [24].
- Formwork shall be in accordance with ACI 318.
- All sidewall formwork shall remain in place in accordance with the requirements of ACI 318.
- Grade, type, and details of all reinforcing steel shall be in accordance with the referenced drawings.
- Embedded items shall conform to ACI 318 and the referenced drawings.
- The placement of concrete shall be in accordance with ACI 318.
- Surface finish shall be in accordance with ACI 318.
- Welding and inspection requirements and acceptance criteria are specified in Chapter 10.

Quality Assurance

- The concrete cask shall be constructed under a quality assurance program that meets 10 CFR 72, Subpart G.

1.4 MAGNASTOR Contents

MAGNASTOR is designed to store up to 37 PWR fuel assemblies or up to 87 BWR fuel assemblies in a pressurized helium atmosphere. PWR fuel assemblies may be stored with inserted burnable poison rod assemblies, thimble plugs or control element assemblies. Stainless steel rod inserts for guide tube dashpots may also be inserted. BWR fuel assemblies may be stored with or without channels. Assemblies may contain solid filler rods or burnable absorber rods replacing fuel rods in the assembly lattice. Steel filler rods must be unirradiated. The design content conditions are specified in the CoC for MAGNASTOR. Unenriched fuel assemblies are not evaluated and are not included as allowable contents. Assemblies may contain unenriched axial end blankets.

1.5 Identification of Agents and Contractors

The prime contractor for the MAGNASTOR design is NAC. All design, analysis, licensing, and procurement activities are performed by NAC in accordance with its approved Quality Assurance Program, as described in Chapter 14. Fabrication of the steel components will be by qualified vendors. A qualified concrete contractor will perform construction of the concrete cask. All vendors and contractors will be selected and their performance monitored in accordance with the NAC Quality Assurance Program. All MAGNASTOR fabrication and assembly activities will be performed in accordance with quality assurance programs that meet the requirements of 10 CFR 72, Subpart G.

NAC as a contractor, or the licensee, may perform construction of the ISFSI and MAGNASTOR loading operations on site in accordance with the NAC or licensee quality assurance program, as appropriate. The licensee will perform decommissioning of the ISFSI in accordance with the licensee quality assurance program.

NAC was founded as a private corporation in 1968, with the primary focus of tracking, inspecting, handling, storing, and transporting spent nuclear fuel. NAC is a wholly owned subsidiary of USEC, Inc., since completion of its acquisition in November 2004. NAC is recognized in the industry as an expert in all aspects of the design, licensing, and operation of spent fuel handling, inspection, storage, and transport equipment, as well as in the management of spent fuel inventories.

Within the past 15 years, NAC has completed fabrication or has under construction the following transportation and/or storage systems.

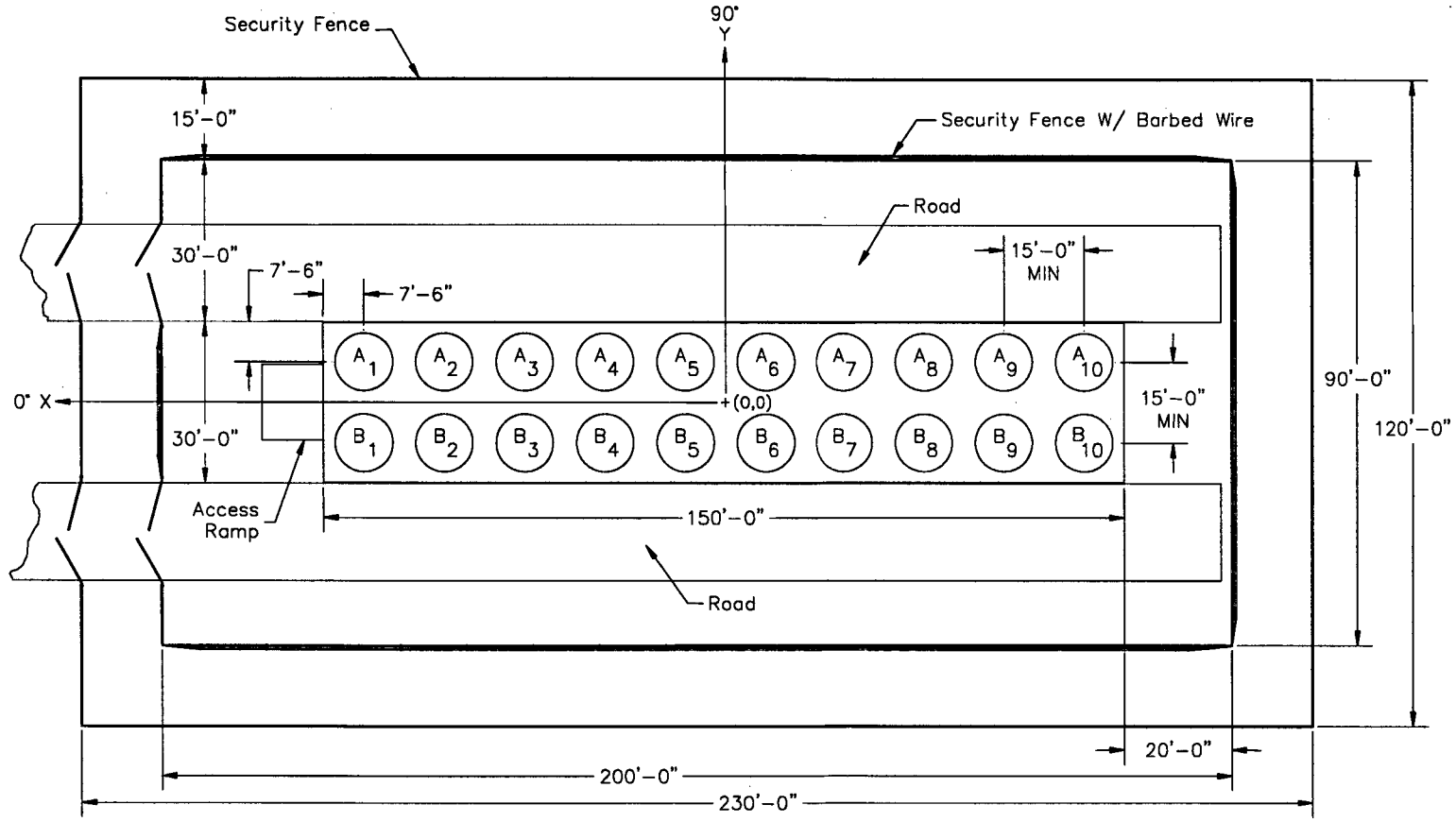
Part 71 (Transport Casks)	Part 72 (Storage System Casks and Components)
8 NAC-LWT	7 UMS®/MPC transfer casks
16 TRUPACT-II	2 NAC-I28 S/T metal casks
6 RH-TRU 72B	1 NAC-I26 S/T metal cask
2 NAC-STC	> 210 UMS®/MPC TSCs
	> 212 UMS®/MPC concrete casks

1.6 Generic Concrete Cask Arrays

A typical ISFSI storage pad layout for 20 MAGNASTOR systems is provided in Figure 1.6-1. As shown in this figure, roads parallel the sides of the pad to facilitate transfer of the concrete cask from the transporter to the designated storage position on the pad. Alternately, a ramp or low-profile concrete pad may be used to allow access for a motorized or towed frame for concrete cask transfer and placement. Loaded concrete casks are placed in the vertical orientation on the pad in a linear array. Array sizes could accommodate from 1 to more than 200 casks. Figure 1.6-1 shows the minimum concrete cask spacing and representative site dimensions. Actual spacing and facility dimensions are dependent on the general site layout, access roads, site boundaries, and transfer equipment selection, but must conform to the spacing specified in the Technical Specifications.

The reinforced concrete storage pad is capable of sustaining the transient loads from the cask transporter and the general loads of the stored casks. If necessary, the pad can be constructed in phases to specifically meet utility-required expansions.

Figure 1.6-1 Typical ISFSI Storage Pad Layout



1.7 References

1. 10 CFR 72, "Licensing Requirements for the Independent Storage of Spent Nuclear Fuel and High-Level Radioactive Waste and Reactor-Related Greater Than Class C Waste," Code of Federal Regulations, US Nuclear Regulatory Commission, Washington, DC.
2. NUREG-1536, "Standard Review Plan for Dry Cask Storage Systems," US Nuclear Regulatory Commission, Washington, DC, January 1997.
3. 10 CFR 71, "Packaging and Transportation of Radioactive Materials," Code of Federal Regulations, US Nuclear Regulatory Commission, Washington, DC.
4. Regulatory Guide 3.61, "Standard Format and Content for a Topical Safety Analysis Report for a Spent Fuel Dry Concrete Cask," US Nuclear Regulatory Commission, Washington, DC, February 1989.
5. ISG-15, "Materials Evaluation," US Nuclear Regulatory Commission, Washington, DC, Revision 0, January 10, 2001.
6. ANSI/ANS 57.9-1992, "Design Criteria for an Independent Spent Fuel Storage Installation (Dry Type)," American Nuclear Society, La Grange Park, IL, May 1992.
7. ACI 318-95, "Building Code Requirements for Structural Concrete," American Concrete Institute, Farmington Hills, MI.
8. ASME Boiler and Pressure Vessel Code, Section III, Subsection NB, "Class I Components," American Society of Mechanical Engineers, New York, NY, 2001 Edition with 2003 Addenda.
9. ASME Boiler and Pressure Vessel Code, Section III, Subsection NG, "Core Support Structures," American Society of Mechanical Engineers, New York, NY, 2001 Edition with 2003 Addenda.
10. ISG-11, "Cladding Considerations for the Transport and Storage of Spent Fuel," US Nuclear Regulatory Commission, Washington, DC, Revision 3, November 17, 2003.
11. ANSI N14.6-1993, "American National Standard for Radioactive Materials – Special Lifting Devices for Shipping Containers Weighing 10,000 Pounds (4,500 kg) or More," American National Standards Institute, Inc., Washington, DC, June 1993.
12. ASME Boiler and Pressure Vessel Code, Section IX, "Qualification Standards for Welding and Brazing Procedures, Welders, Brazers, and Welding and Brazing Operators," American Society of Mechanical Engineers, New York, NY, 2001 Edition with 2003 Addenda.
13. Recommended Practice No. SNT-TC-1A, "Personnel Qualification and Certification in Nondestructive Testing," The American Society for Nondestructive Testing, Inc., Columbus OH, edition as invoked by the applicable ASME Code.

14. ANSI N45.2.1, "Cleaning of Fluid Systems and Associated Components During Construction Phase of Nuclear Power Plants," American National Standards Institute, Inc., Washington, DC.
15. ANSI N45.2.2-1978, "Packaging, Shipping, Receiving, Storage, and Handling of Items for Nuclear Power Plants," American National Standards Institute, Inc., Washington, DC.
16. ASTM C94^a, "Standard Specification for Ready-Mixed Concrete," American Society for Testing and Materials, West Conshohocken, PA.
17. ASTM C150^a, "Standard Specification for Portland Cement," American Society for Testing and Materials, West Conshohocken, PA.
18. ASTM C33^a, "Standard Specification for Concrete Aggregates," American Society for Testing and Materials, West Conshohocken, PA.
19. ASTM C637^a, "Specification for Aggregates for Radiation-Shielding Concrete," American Society for Testing and Materials, West Conshohocken, PA.
20. ASTM C494^a, "Standard Specification for Chemical Admixtures for Concrete," American Society for Testing and Materials, West Conshohocken, PA.
21. ASTM C618^a, "Specification for Fly Ash and Raw or Calcined Natural Pozzolan for Use as a Mineral Admixture in Portland Cement Concrete," American Society for Testing and Materials, West Conshohocken, PA.
22. ASTM C172^a, "Standard Practice for Sampling Freshly Mixed Concrete," American Society for Testing and Materials, West Conshohocken, PA.
23. ASTM C31^a, "Method of Making and Curing Concrete Test Specimens in the Field," American Society for Testing and Materials, West Conshohocken, PA.
24. ASTM C39^a, "Standard Test Method for Compressive Strength of Cylindrical Concrete Specimens," American Society for Testing and Materials, West Conshohocken, PA.

^a Current edition of testing standards at time of fabrication/construction is to be used.

1.8 License Drawings

This section presents the list of License Drawings for MAGNASTOR.

Drawing Number	Title	Revision No.
71160-551	Fuel Tube Assembly, MAGNASTOR – 37 PWR	2
71160-560	Assembly, Standard Transfer Cask, MAGNASTOR	1
71160-561	Structure, Weldment, Concrete Cask, MAGNASTOR	3
71160-562	Reinforcing Bar and Concrete Placement, Concrete Cask, MAGNASTOR	2
71160-571	Details, Neutron Absorber, Retainer, MAGNASTOR – 37 PWR	2
71160-572	Details, Neutron Absorber, Retainer, MAGNASTOR – 87 BWR	2
71160-574	Basket Support Weldments, MAGNASTOR – 37 PWR	2
71160-575	Basket Assembly, MAGNASTOR – 37 PWR	3
71160-581	Shell Weldment, Canister, MAGNASTOR	2
71160-584	Details, Canister, MAGNASTOR	2
71160-585	TSC Assembly, MAGNASTOR	2
71160-590	Loaded Concrete Cask, MAGNASTOR	3
71160-591	Fuel Tube Assembly, MAGNASTOR – 87 BWR	2
71160-598	Basket Support Weldments, MAGNASTOR – 87 BWR	3
71160-599	Basket Assembly, MAGNASTOR – 87 BWR	2
71160-600	Basket Assembly, MAGNASTOR – 82 BWR	0

Figure Withheld Under 10 CFR 2.390

71160-371-4	
Drawing No. Description	
NAC INTERNATIONAL	
FUEL TUBE ASSEMBLY, MAGNASTOR - 37 PWR	
PROJECT 71160	DATE 551
REV 1 OF 2	BY

Figure Withheld Under 10 CFR 2.390

 NAC INTERNATIONAL	
FUEL TUBE ASSEMBLY, MAGNASTOR - 37 PWR	
PROJECT 71160	DESIGN 551
	REV 2

A

1

Figure Withheld Under 10 CFR 2.390

PLATE	
Drawing No.	of Revision
 NAC INTERNATIONAL	
ASSEMBLY, STANDARD TRANSFER CASK, MAGNASTOR	
71160	560
1	

Figure Withheld Under 10 CFR 2.390

 NAC INTERNATIONAL		
ASSEMBLY, STANDARD TRANSFER CASK, MAGNASTOR		
PROJECT	71160	REV
		560 1
		2 of 4

Figure Withheld Under 10 CFR 2.390

 NAC INTERNATIONAL	
ASSEMBLY, STANDARD TRANSFER CASK, MAGNASTOR	
PROJECT 71160	REV 560
	10 3 81

Figure Withheld Under 10 CFR 2.390

 NAC INTERNATIONAL		
ASSEMBLY, STANDARD TRANSFER CASK, MAGNASTOR		
PROJECT	71160	NUMBER 560
		1

Figure Withheld Under 10 CFR 2.390

DRAWING NO.		DESCRIPTION	
NAC INTERNATIONAL		STRUCTURE, WELDMENT, CONCRETE CASK, MAGNASTOR	
PROJECT	71160	DRAWING	561
DATE		BY	
1971		J. J. [unclear]	

Figure Withheld Under 10 CFR 2.390

NAC INTERNATIONAL	
STRUCTURE, WELDMENT, CONCRETE CASK, MAGNASTOR	
PROJECT 71160	DRAWING 561
	REV 2 OF 4

1

1

Figure Withheld Under 10 CFR 2.390

 NAC INTERNATIONAL	
STRUCTURE, WELDMENT, CONCRETE CASK, MAGNASTOR	
PROJECT 71160	DRAWING 561 3
	ON 3 OF 4

11
12
13
14
15
16
17
18
19
20
21
22
23
24
25
26
27
28
29
30
31
32
33
34
35
36
37
38
39
40
41
42
43
44
45
46
47
48
49
50
51
52
53
54
55
56
57
58
59
60
61
62
63
64
65
66
67
68
69
70
71
72
73
74
75
76
77
78
79
80
81
82
83
84
85
86
87
88
89
90
91
92
93
94
95
96
97
98
99
100

101
102
103
104
105
106
107
108
109
110
111
112
113
114
115
116
117
118
119
120
121
122
123
124
125
126
127
128
129
130
131
132
133
134
135
136
137
138
139
140
141
142
143
144
145
146
147
148
149
150
151
152
153
154
155
156
157
158
159
160
161
162
163
164
165
166
167
168
169
170
171
172
173
174
175
176
177
178
179
180
181
182
183
184
185
186
187
188
189
190
191
192
193
194
195
196
197
198
199
200

Figure Withheld Under 10 CFR 2.390

201
202
203
204
205
206
207
208
209
210
211
212
213
214
215
216
217
218
219
220
221
222
223
224
225
226
227
228
229
230
231
232
233
234
235
236
237
238
239
240
241
242
243
244
245
246
247
248
249
250

	
STRUCTURE, WELDMENT, CONCRETE CASK, MAGNASTOR	
PROJECT 71160	DWG NO. 561 / 3
1	

Figure Withheld Under 10 CFR 2.390

DRAWING No.		DESCRIPTION	
 NAC INTERNATIONAL		REINFORCING BAR AND CONCRETE PLACEMENT, CONCRETE CASK, MAGNASTOR	
		PROJECT 71160	562
		1	2

1

Figure Withheld Under 10 CFR 2.390

DRAWING NO.		SHEET/STRIP	
DESCRIPTION			
 NAC INTERNATIONAL			
DETAILS, NEUTRON ABSORBER, RETAINER, MAGNASTOR - 37 PWR			
PROJECT	71160	DRAWING	571
		OF 1	OF 1

Figure Withheld Under 10 CFR 2.390

NAC INTERNATIONAL	
DETAILS, NEUTRON ABSORBER, RETAINER, MAGNASTOR - 87 BWR	
PROJECT 71160	BLANK 572
1	1

Figure Withheld Under 10 CFR 2.390

SECTION FOR	
NAC INTERNATIONAL	
BASKET SUPPORT WELDMENTS, MAGNASTOR - 37 PWR	
71160	574
1	2

Figure Withheld Under 10 CFR 2.390

 NAC INTERNATIONAL	
BASKET SUPPORT WELDMENTS, MAGNASTOR - 37 PWR	
PROJECT 71160	ISSUE 574
	2 of 2

A

1

Figure Withheld Under 10 CFR 2.390

 NAC INTERNATIONAL	
BASKET ASSEMBLY, MAGNASTOR - 37 PWR	
PROJECT 71160	REVISED 575 3
	2 3

Faint, illegible text or a small table located in the top-left corner of the page.

Figure Withheld Under 10 CFR 2.390

 NAC INTERNATIONAL	
BASKET ASSEMBLY, MAGNASTOR - 37 PWR	
<small>PROJECT</small> 71160	<small>REV</small> 575 3
<small>3 3</small>	

A

Figure Withheld Under 10 CFR 2.390

PLATE	DESCRIPTION
	 NAC INTERNATIONAL
	SHELL WELDMENT, CANISTER, MAGNASTOR
PROJECT	71160
REV	581
	2
	1

Figure Withheld Under 10 CFR 2.390

 NAC INTERNATIONAL	
SHELL WELDMENT, CANISTER, MAGNASTOR	
PROJECT 71160	FORM 581
	REV 2

A

Figure Withheld Under 10 CFR 2.390

SEARCHED		SERIALIZED	
INDEXED		FILED	
 NAC INTERNATIONAL			
TSC ASSEMBLY, MAGNASTOR			
DATE	PROJECT	NUMBER	PAGE
1/10/05	71160	585	2
		1	2

Figure Withheld Under 10 CFR 2.390

 NAC INTERNATIONAL	
TSC ASSEMBLY, MAGNASTOR	
PROJECT 71160	REVISED 585
	IN 2 OF 2

A

1

11/15/05
11/16/05
11/17/05
11/18/05
11/19/05
11/20/05
11/21/05
11/22/05
11/23/05
11/24/05
11/25/05
11/26/05
11/27/05
11/28/05
11/29/05
11/30/05
12/01/05
12/02/05
12/03/05
12/04/05
12/05/05
12/06/05
12/07/05
12/08/05
12/09/05
12/10/05
12/11/05
12/12/05
12/13/05
12/14/05
12/15/05
12/16/05
12/17/05
12/18/05
12/19/05
12/20/05
12/21/05
12/22/05
12/23/05
12/24/05
12/25/05
12/26/05
12/27/05
12/28/05
12/29/05
12/30/05
12/31/05

Figure Withheld Under 10 CFR 2.390

NAC INTERNATIONAL	
LOADED CONCRETE CASK, MAGNASTOR	
DATE	590 13
11/05	
12/05	
1/06	
2/06	
3/06	
4/06	
5/06	
6/06	
7/06	
8/06	
9/06	
10/06	
11/06	
12/06	
1/07	
2/07	
3/07	
4/07	
5/07	
6/07	
7/07	
8/07	
9/07	
10/07	
11/07	
12/07	
1/08	
2/08	
3/08	
4/08	
5/08	
6/08	
7/08	
8/08	
9/08	
10/08	
11/08	
12/08	
1/09	
2/09	
3/09	
4/09	
5/09	
6/09	
7/09	
8/09	
9/09	
10/09	
11/09	
12/09	
1/10	
2/10	
3/10	
4/10	
5/10	
6/10	
7/10	
8/10	
9/10	
10/10	
11/10	
12/10	
1/11	
2/11	
3/11	
4/11	
5/11	
6/11	
7/11	
8/11	
9/11	
10/11	
11/11	
12/11	
1/12	
2/12	
3/12	
4/12	
5/12	
6/12	
7/12	
8/12	
9/12	
10/12	
11/12	
12/12	
1/13	
2/13	
3/13	
4/13	
5/13	
6/13	
7/13	
8/13	
9/13	
10/13	
11/13	
12/13	
1/14	
2/14	
3/14	
4/14	
5/14	
6/14	
7/14	
8/14	
9/14	
10/14	
11/14	
12/14	
1/15	
2/15	
3/15	
4/15	
5/15	
6/15	
7/15	
8/15	
9/15	
10/15	
11/15	
12/15	
1/16	
2/16	
3/16	
4/16	
5/16	
6/16	
7/16	
8/16	
9/16	
10/16	
11/16	
12/16	
1/17	
2/17	
3/17	
4/17	
5/17	
6/17	
7/17	
8/17	
9/17	
10/17	
11/17	
12/17	
1/18	
2/18	
3/18	
4/18	
5/18	
6/18	
7/18	
8/18	
9/18	
10/18	
11/18	
12/18	
1/19	
2/19	
3/19	
4/19	
5/19	
6/19	
7/19	
8/19	
9/19	
10/19	
11/19	
12/19	
1/20	
2/20	
3/20	
4/20	
5/20	
6/20	
7/20	
8/20	
9/20	
10/20	
11/20	
12/20	
1/21	
2/21	
3/21	
4/21	
5/21	
6/21	
7/21	
8/21	
9/21	
10/21	
11/21	
12/21	
1/22	
2/22	
3/22	
4/22	
5/22	
6/22	
7/22	
8/22	
9/22	
10/22	
11/22	
12/22	
1/23	
2/23	
3/23	
4/23	
5/23	
6/23	
7/23	
8/23	
9/23	
10/23	
11/23	
12/23	
1/24	
2/24	
3/24	
4/24	
5/24	
6/24	
7/24	
8/24	
9/24	
10/24	
11/24	
12/24	
1/25	
2/25	
3/25	
4/25	
5/25	
6/25	
7/25	
8/25	
9/25	
10/25	
11/25	
12/25	
1/26	
2/26	
3/26	
4/26	
5/26	
6/26	
7/26	
8/26	
9/26	
10/26	
11/26	
12/26	
1/27	
2/27	
3/27	
4/27	
5/27	
6/27	
7/27	
8/27	
9/27	
10/27	
11/27	
12/27	
1/28	
2/28	
3/28	
4/28	
5/28	
6/28	
7/28	
8/28	
9/28	
10/28	
11/28	
12/28	
1/29	
2/29	
3/29	
4/29	
5/29	
6/29	
7/29	
8/29	
9/29	
10/29	
11/29	
12/29	
1/30	
2/30	
3/30	
4/30	
5/30	
6/30	
7/30	
8/30	
9/30	
10/30	
11/30	
12/30	
1/31	
2/31	
3/31	
4/31	
5/31	
6/31	
7/31	
8/31	
9/31	
10/31	
11/31	
12/31	

Figure Withheld Under 10 CFR 2.390

 NAC INTERNATIONAL	
LOADED CONCRETE CASK, MAGNASTOR	
PROJECT 71160	REV 590 3
	DR 2 OF 2

1

Figure Withheld Under 10 CFR 2.390

 NAC INTERNATIONAL	
FUEL TUBE ASSEMBLY, MAGNASTOR - 87 BWR	
<small>PROJECT</small> 71160	<small>DESIGN</small> 591
<small>REV</small> 2	<small>REV</small> 2

Figure Withheld Under 10 CFR 2.390

 NAC INTERNATIONAL	
BASKET SUPPORT WELDMENTS, MAGNASTOR - 87 BWR	
PROJECT 71160	REVISION 598 3
	OF 2 OF 3

1

Figure Withheld Under 10 CFR 2.390

 NAC INTERNATIONAL	
BASKET SUPPORT WELDMENTS, MAGNASTOR - 87 BWR	
PROJECT 71160	DESIGN 598
	REV 3

Figure Withheld Under 10 CFR 2.390

QUANTITY	DESCRIPTION
	 NAC INTERNATIONAL
	BASKET ASSEMBLY, MAGNASTOR - 87 BWR
PRODUCT	71160
QUANTITY	599
DATE	01 03 1988

Figure Withheld Under 10 CFR 2.390

 NAC INTERNATIONAL		
BASKET ASSEMBLY, MAGNASTOR - 87 BWR		
PROJECT	71160	599
		2 3

1

Figure Withheld Under 10 CFR 2.390

 NAC INTERNATIONAL	
BASKET ASSEMBLY, MAGNASTOR - 87 BWR	
PROJECT 71160	ISSUED 599 2
	OF 3 OF 3

Figure Withheld Under 10 CFR 2.390

11710-091-99	
DRAWING NO.	
DESCRIPTION	
NAC INTERNATIONAL	
BASKET ASSEMBLY, MAGNASTOR - 82 BWR	
PROJECT	71160
QUANTITY	600
NO. 1 OF 5	1

Figure Withheld Under 10 CFR 2.390

 NAC INTERNATIONAL	
BASKET ASSEMBLY, MAGNASTOR - 82 BWR	
PART 71160	REV 600 8
	2 of 5

1

Figure Withheld Under 10 CFR 2.390

 NAC INTERNATIONAL	
BASKET ASSEMBLY, MAGNASTOR - 82 BWR	
PROJECT 71160	QUANTITY 600
	REV. 3 OF 5

Figure Withheld Under 10 CFR 2.390

 NAC INTERNATIONAL	
BASKET ASSEMBLY, MAGNASTOR - 82 BWR	
PROJECT 71160	DRAWING 600 8
SI 4	OF 5

1

Faint, illegible text or a small diagram located in the upper left corner of the page.

Figure Withheld Under 10 CFR 2.390

 NAC INTERNATIONAL	
BASKET ASSEMBLY, MAGNASTOR - 82 BWR	
PROJECT 71160	DATE 600 8
	BY 5 5

Chapter 2 Principal Design Criteria

Table of Contents

2	PRINCIPAL DESIGN CRITERIA	2-1
2.1	MAGNASTOR System Design Criteria	2.1-1
2.2	Spent Fuel To Be Stored	2.2-1
2.2.1	PWR Fuel Evaluation	2.2-1
2.2.2	BWR Fuel Evaluation	2.2-2
2.3	Design Criteria for Environmental Conditions and Natural Phenomena	2.3-1
2.3.1	Tornado Missiles and Wind Loadings	2.3-1
2.3.2	Water Level (Flood) Design	2.3-2
2.3.3	Seismic Design.....	2.3-3
2.3.4	Snow and Ice Loadings.....	2.3-4
2.3.5	Combined Load Criteria	2.3-5
2.3.6	Environmental Temperatures.....	2.3-6
2.4	Safety Protection Systems	2.4-1
2.4.1	General.....	2.4-1
2.4.2	Confinement Barriers and Systems.....	2.4-2
2.4.3	Concrete Cask Cooling	2.4-3
2.4.4	Protection by Equipment	2.4-3
2.4.5	Protection by Instrumentation.....	2.4-3
2.4.6	Nuclear Criticality Safety	2.4-4
2.4.7	Radiological Protection.....	2.4-5
2.4.8	Fire Protection.....	2.4-6
2.4.9	Explosion Protection.....	2.4-6
2.4.10	Auxiliary Structures	2.4-6
2.5	Decommissioning Considerations	2.5-1
2.6	References.....	2.6-1

List of Figures

Figure 2.2-1 PWR Fuel Preferential Loading Zones 2.2-4
Figure 2.2-2 82-Assembly-BWR Basket Pattern..... 2.2-5

List of Tables

Table 2.1-1 MAGNASTOR System Design Criteria 2.1-2
Table 2.1-2 ASME Code Alternatives for MAGNASTOR Components 2.1-3
Table 2.2-1 PWR Fuel Assembly Characteristics 2.2-6
Table 2.2-2 BWR Fuel Assembly Characteristics..... 2.2-7
Table 2.3-1 Load Combinations for the Concrete Cask..... 2.3-8
Table 2.3-2 Load Combinations for the TSC 2.3-8
Table 2.3-3 Structural Design Criteria for Components Used in the TSC..... 2.3-9
Table 2.4-1 Safety Classification of MAGNASTOR Components 2.4-8

2 PRINCIPAL DESIGN CRITERIA

MAGNASTOR is a canister-based spent fuel dry storage cask system designed in accordance with the requirements of 10 CFR 72 [10], Subpart L, Approval of Spent Fuel Storage Casks. It is designed to store a variety of intact PWR and BWR spent fuel assemblies. This chapter presents the principal design criteria for MAGNASTOR components.

2.1 MAGNASTOR System Design Criteria

The design of MAGNASTOR ensures that the stored spent fuel is maintained subcritical in an inert environment, within allowable temperature limits, and is retrievable. The acceptance testing and maintenance program specified in Chapter 10 ensures that the system is, and remains, suitable for the intended purpose. The MAGNASTOR design criteria appear in Table 2.1-1.

Approved alternatives to the ASME Code for the design procurement, fabrication, inspection, and testing of MAGNASTOR TSCs and spent fuel baskets are listed in Table 2.1-2.

Proposed alternatives to ASME Code, Section III, 2001 Edition with Addenda through 2003, including alternatives listed in Table 2.1-2, may be used when authorized by the Director of the Office of Nuclear Material Safety and Safeguards or designee. The request for such alternatives should demonstrate the following.

- The proposed alternatives would provide an acceptable level of quality and safety, or Compliance with the specified requirements of ASME Code, Section III, Subsections NB and NG, 2001 Edition with Addenda through 2003, would result in hardship or unusual difficulty without a compensating increase in the level of quality and safety.
- Requests for alternatives shall be submitted in accordance with 10 CFR 72.

Table 2.1-1 MAGNASTOR System Design Criteria

Parameter	Criteria
Design Life	50 years
Design Code – Confinement	
TSC	ASME Code, Section III, Subsection NB [1] for confinement boundary
TSC Cavity Atmosphere	Helium
Gas Pressure	7.0 atmospheres gauge (103 psig)
Design Code - Nonconfinement	
Fuel Basket	ASME Code, Section III, Subsection NG [2] and NUREG/CR-6322 [3]
Concrete Cask	ACI-349 [4], ACI-318 [5]
Transfer Cask	ANSI N14.6 [6], NUREG-0612 [15]
Thermal	
Maximum Fuel Cladding Temperature	752°F (400°C) for Normal, Off-Normal, and Transfer [7] 1058°F (570°C) for Accident [8]
Ambient Temperature	
Normal (average annual ambient)	100°F
Off-Normal (extreme cold; extreme hot)	-40°F; 106°F
Accident	133°F
Concrete Temperature	
Normal Conditions	≤150°F (bulk) [4]; ≤ 200°F (local) [9]
Off-Normal/Accident Conditions	≤ 350°F local/ surface [4]
Radiation Protection/Shielding	
Owner-Controlled Area Boundary Dose [10]	
Normal/Off-Normal Conditions	25 mrem (Annual Whole Body) [10]
Accident Whole Body Dose	5 rem (Whole Body) [10]

Table 2.1-2 ASME Code Alternatives for MAGNASTOR Components

Component	Reference ASME Code Section/Article	Code Requirement	Exception, Justification and Compensatory Measures
TSC and Fuel Basket	NCA-1000, NCA-2000, NCA-3000, NCA-4000, NCA-5000, NCA-8000, NB-1110, and NG-1110	Requirements for Code stamping of NB components and preparation of Code Design Specifications, Design Reports, Overpressure Protection Report (TSC only), and Data Reports, and Quality Assurance requirements in accordance with Code requirements.	Code stamping is not required for the TSC or fuel baskets. Code Design Specifications, Design Reports, Overpressure Protection Report, and Data Reports are not required. The TSC and Fuel Basket are designed, procured, fabricated, inspected and tested in accordance with a QA Program meeting 10 CFR 72, Subpart G. Authorized Nuclear Inspection Agency Services are not required.
TSC Pressure-Retaining Materials	NB-2000	Pressure-retaining material to be provided by ASME-approved Material Organization.	Materials will be supplied with Certified Material Test Reports by NAC approved suppliers.
TSC Closure Lid-to-Shell Weld	NB-4243	Full penetration welds required for Category C joints.	The closure lid-to-shell weld is not a full penetration weld. The design and analysis of the closure lid weld utilizes a 0.8 stress reduction factor in accordance with ASME Code Case N-595-4 [23].
Port Cover-to-Closure Lid Weld	NB-5230	Radiographic (RT) examination required.	Final surface liquid penetrant examination to be performed per ASME Code Section V, Article 6. PT acceptance criteria is to be in accordance with NB-5350.
TSC Closure Lid-to-Shell Weld	NB-5230	Radiographic (RT) examination required.	In accordance with ASME Code Case N-595-4, the TSC closure lid-to-shell weld is to be inspected by progressive surface liquid penetrant (PT) examination of the root, midplane and final surface layers. The progressive PT examination of the weld will be performed in accordance with ASME Code, Section V, Article 6, and acceptance criteria per NB-5350.

Table 2.1-2 ASME Code Alternatives for MAGNASTOR Components

Component	Reference ASME Code Section/Article	Code Requirement	Exception, Justification and Compensatory Measures
TSC Closure Ring-to-TSC Shell & TSC Closure Ring-to-Closure Lid	NB-5230	Radiographic (RT) examination required.	Final surface liquid penetrant examination to be performed per ASME Code Section V, Article 6. PT acceptance criteria is to be in accordance with NB-5350.
TSC	NB-6111	All completed pressure retaining systems shall be pressure tested.	Following closure lid to TSC shell welding, each TSC shall be hydrostatically pressure tested to 125% of MNOP. No observable pressure drop or water leakage from the closure lid to TSC shell weld is allowed.
TSC	NB-7000	Pressure vessels shall be protected from the consequences of pressure conditions exceeding design pressure.	No overpressure protection is provided. The function of the TSC is to confine radioactive contents without release under normal conditions, or off-normal and accident events of storage. The TSC is designed to withstand the maximum internal pressure considering 100% fuel rod failure and maximum accident condition temperatures.
TSC	NB-8000	States requirements for nameplates, stamping and reports per NCA-8000.	The TSC is marked and identified to ensure proper identification of the contents. Code stamping is not required.
TSC Basket Assembly Structural Materials	NG-2000	Core support structural materials are to be provided by an ASME approved Material Organization.	Fuel basket structural materials with Certified Material Test Reports to be supplied by NAC approved suppliers.
TSC Basket Assembly Structural Components	NG-8000	Requirements for nameplates, stamping and reports per NCA-8000.	The TSC basket structural assembly is marked and identified to ensure component traceability in accordance with NAC's QA Program.

2.2 Spent Fuel To Be Stored

MAGNASTOR is designed to safely store up to 37 PWR or up to 87 BWR spent fuel assemblies, contained within a TSC. The fuel assemblies are assigned to two groups of PWR and two groups of BWR fuel assemblies on the basis of fuel assembly length. Refer to Chapter 1 for the fuel assembly length groupings. For TSC spent fuel content loads less than a full basket, empty fuel positions shall include an empty fuel cell insert.

Intact PWR and BWR fuel assemblies having parameters as shown in Table 2.2-1 and Table 2.2-2, respectively, may be stored in MAGNASTOR.

The minimum initial enrichment limits are shown in Table 2.2-1 and Table 2.2-2 for PWR and BWR fuel, respectively, and exclude the loading of fuel assemblies enriched to less than 1.3 wt% ^{235}U , including unenriched fuel assemblies. Fuel assemblies with unenriched axial end-blankets may be loaded into MAGNASTOR.

2.2.1 PWR Fuel Evaluation

MAGNASTOR evaluations are based on bounding PWR fuel assembly parameters that maximize the source terms for the shielding evaluations, the reactivity for criticality evaluations, the decay heat load for the thermal evaluations, and the fuel weight for the structural evaluations. These bounding parameters are selected from the various spent fuel assemblies that are candidates for storage in MAGNASTOR. The bounding fuel assembly values are established based primarily on how the principal parameters are combined, and on the loading conditions (or restrictions) established for a group of fuel assemblies based on its parameters. Each TSC may contain up to 37 intact PWR fuel assemblies.

The limiting parameters of the PWR fuel assemblies authorized for loading in MAGNASTOR are shown in Table 2.2-1. The maximum initial enrichments listed are based on a minimum soluble boron concentration of 2,500 ppm in the spent fuel pool water. Lower soluble boron concentrations are allowed in the spent fuel pool water for fuel assemblies with lower maximum enrichments. The maximum initial enrichment authorized represents the peak fuel rod enrichment for variably enriched PWR fuel assemblies. The PWR fuel assembly allowable loading characteristics are summarized by fuel assembly type in Table 6.4-1. The maximum TSC decay heat load for the storage of PWR fuel assemblies is 37 kW. Uniform and preferential loading patterns are allowed in the PWR basket. The uniform loading pattern permits assemblies with a maximum heat load of 1 kW/assembly. The preferential loading pattern permits peak heat loads of 1.30 kW, as indicated in the zone description in Figure 2.2-1. The bounding thermal

evaluations are based on the Westinghouse 17×17 fuel assembly. The minimum cool times are determined based on the maximum decay heat load of the contents. The fuel assemblies and source terms that produce the maximum storage and transfer cask dose rates are summarized in Table 5.1-3. A bounding weight of 1,680 pounds, as shown in Table 2.2-1, based on a B&W 15×15 fuel assembly with control components inserted, has been structurally evaluated in each location of the PWR fuel basket.

As noted in Table 2.2-1, the evaluation of PWR fuel assemblies includes thimble plugs (flow mixers), burnable poison rod assemblies (BPRAs), control element assemblies (CEAs), and/or solid filler rods. Empty fuel rod positions are filled with a solid filler rod or a solid neutron absorber rod that displaces a volume not less than that of the original fuel rod.

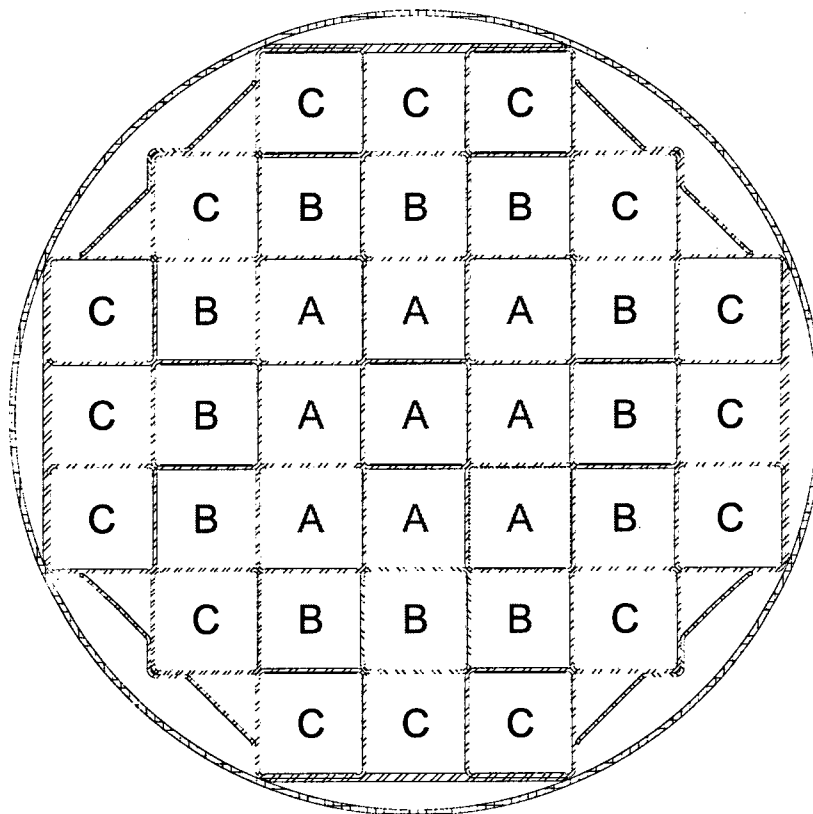
2.2.2 BWR Fuel Evaluation

MAGNASTOR evaluations are based on bounding BWR fuel assembly parameters that maximize the source terms for the shielding evaluations, the reactivity for the criticality evaluations, the decay heat load for the thermal evaluations, and the fuel weight for the structural evaluations. These bounding parameters are selected from the various spent fuel assemblies that are candidates for storage in MAGNASTOR. The bounding fuel assembly values are established based primarily on how the principal parameters are combined, and on the loading conditions or restrictions established for a group of fuel assemblies based on its parameters. Each TSC may contain up to 87 intact BWR fuel assemblies. To increase allowed assembly enrichments over those determined for the 87-assembly basket configuration, an optional 82-assembly loading pattern may be used. The required fuel assembly locations in the 82-assembly pattern are shown in Figure 2.2-2.

The limiting parameters of the BWR fuel assemblies authorized for loading in MAGNASTOR are shown in Table 2.2-2. The minimum initial enrichment represents the peak planar-average enrichment. The BWR fuel assembly allowable loading characteristics are summarized by fuel type in Table 6.4-2. The maximum decay heat load per TSC for the storage of BWR fuel assemblies is 35.0 kW (average of 0.402 kW/assembly). Only uniform loading is permitted for BWR fuel assemblies. The bounding thermal evaluations are based on the GE 10×10 fuel assembly. The minimum cooling times are determined based on the maximum decay heat load of the contents. The fuel assemblies and source terms that produce the maximum storage and transfer cask dose rates are summarized in Table 5.1-3. A bounding weight of 704 pounds, as shown in Table 2.2-2, is based on the maximum weight of GE 7×7 and 8×8 assemblies with channels; this weight has been structurally evaluated in each storage location of the BWR basket.

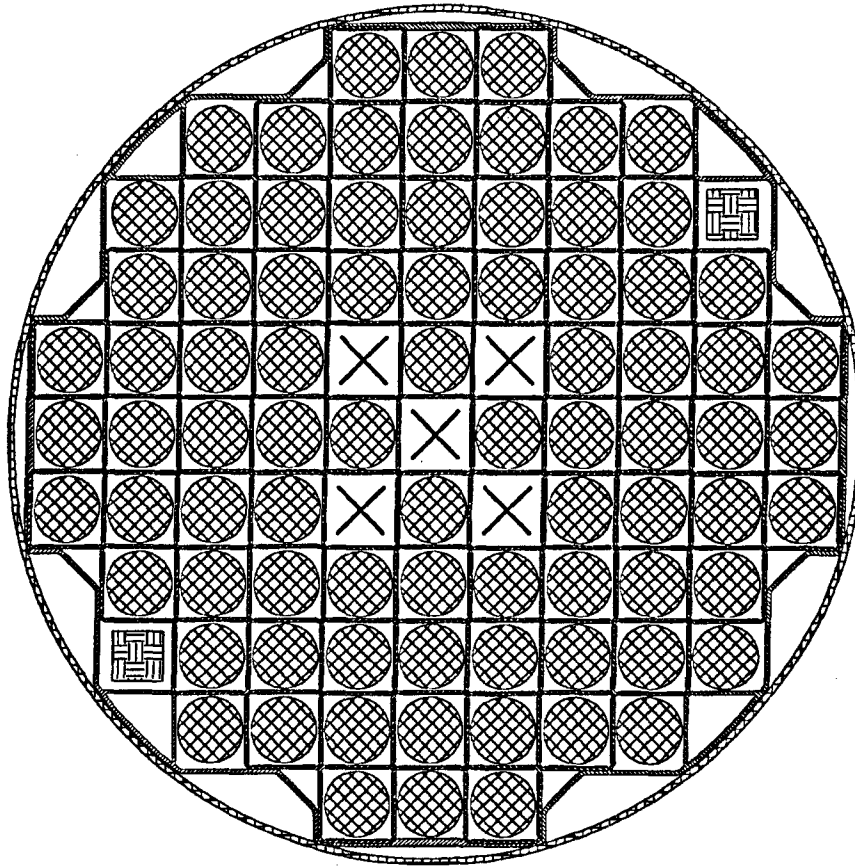
As noted in Table 2.2-2, the evaluation of BWR fuel envelopes unchanneled assemblies and assemblies with channels up to 120 mils thick. Empty fuel rod positions are filled with a solid filler rod or a solid neutron absorber rod that displaces a volume not less than that of the original fuel rod.

Figure 2.2-1 PWR Fuel Preferential Loading Zones



Zone Description	Designator	Heat Load (W/assy)	# Assemblies
Inner Ring	A	960	9
Middle Ring	B	1,300	12
Outer Ring	C	800	16

Figure 2.2-2 82-Assembly-BWR Basket Pattern



-  = Fuel Assembly Locations
-  = Vent/Drain Port Locations
-  = Designated Nonfuel Locations

Table 2.2-1 PWR Fuel Assembly Characteristics

Characteristic	Fuel Class					
	14x14	14x14	15x15	15x15	16x16	17x17
Max Initial Enrichment (wt% ²³⁵ U)	5.0	5.0	5.0	5.0	5.0	5.0
Min Initial Enrichment (wt% ²³⁵ U)	1.3	1.3	1.3	1.3	1.3	1.3
Number of Fuel Rods	176	179	204	208	236	264
Max Assembly Average Burnup (MWd/MTU)	60,000	60,000	60,000	60,000	60,000	60,000
Peak Average Rod Burnup (MWd/MTU)	62,500	62,500	62,500	62,500	62,500	62,500
Min Cool Time (years)	4	4	4	4	4	4
Max Weight (lb) per Storage Location	1,680	1,680	1,680	1,680	1,680	1,680
Max Decay Heat (Watts) per Storage Location	1,300	1,300	1,300	1,300	1,300	1,300

- Fuel cladding is a zirconium-based alloy.
- All reported enrichment values are nominal preirradiation fabrication values.
- Weight includes the weight of nonfuel-bearing components.
- Assemblies may contain a flow mixer (thimble plug), a burnable poison rod assembly, a control element assembly, and/or solid stainless steel or zirconium-based alloy filler rods.
- Maximum initial enrichment is based on a minimum soluble boron concentration in the spent fuel pool water. Required soluble boron content is fuel type and enrichment specific. Minimum soluble boron content varies between 1,500 and 2,500 ppm. Maximum initial enrichment represents the peak fuel rod enrichment for variably-enriched fuel assemblies.
- Spacers may be used to axially position fuel assemblies to facilitate handling.

Table 2.2-2 BWR Fuel Assembly Characteristics

Characteristic	Fuel Class			
	7×7	8×8	9×9	10×10
Max Initial Enrichment (wt% ²³⁵ U)	4.5	4.5	4.5	4.5
Number of Fuel Rods	48	59	72	91 ^a
	49	60	74 ^a	92 ^a
		61	76	96 ^a
		62	79	100
		63	80	
		64		
Max Assembly Average Burnup (MWd/MTU)	60,000	60,000	60,000	60,000
Peak Average Rod Burnup (MWd/MTU)	62,500	62,500	62,500	62,500
Min Cool Time (years)	4	4	4	4
Min Average Enrichment (wt% ²³⁵ U)	1.3	1.3	1.3	1.3
Max Weight (lb) per Storage Location	704	704	704	704
Max Decay Heat (Watts) per Storage Location	402	402	402	402

- Each BWR fuel assembly may have a zirconium-based alloy channel up to 120 mil thick.
- Assembly weight includes the weight of the channel.
- Maximum initial enrichment is the peak planar-average enrichment.
- Water rods may occupy more than one fuel lattice location. Fuel assembly to contain nominal number of water rods for the specific assembly design.
- All enrichment values are nominal preirradiation fabrication values.
- Spacers may be used to axially position fuel assemblies to facilitate handling.

^a Assemblies may contain partial-length fuel rods.

2.3 Design Criteria for Environmental Conditions and Natural Phenomena

This section presents the design criteria for site environmental conditions and natural phenomena applied in the design basis analyses of MAGNASTOR. Analyses to demonstrate that the design basis system meets the design criteria defined in this section are presented in the appropriate chapters.

The use of MAGNASTOR at a specific site requires that the site either meet the design criteria of this section or be separately evaluated against the site-specific conditions to ensure the acceptable performance of the system.

2.3.1 Tornado Missiles and Wind Loadings

The concrete casks are typically placed outdoors on an unsheltered reinforced concrete storage pad at an ISFSI site. This storage condition exposes the casks to tornado and wind loading.

2.3.1.1 Applicable Design Parameters

The design basis tornado and wind loading is defined based on Regulatory Guide 1.76 [11], Region 1, and NUREG-0800 [12]. The tornado and wind loading criteria are as follows.

<u>Tornado and Wind Condition</u>	<u>Limit</u>
Rotational Wind Speed, mph	290
Translational Wind Speed, mph	70
Maximum Wind Speed, mph	360
Radius of Maximum Wind Speed, ft	150
Pressure Drop, psi	3.0
Rate of Pressure Drop, psi/sec	2.0

2.3.1.2 Determination of Forces on Structures

Tornado wind forces on the concrete cask are calculated by multiplying the dynamic wind pressure by the frontal area of the cask normal to the wind direction. Wind forces are applied to the cask in the wind direction. No streamlining is assumed. The cask is demonstrated to remain stable under design basis tornado wind loading in conjunction with impact from a high-energy tornado missile.

2.3.1.3 Tornado Missiles

The design basis tornado missile impacts are defined in Paragraph 4, Subsection III, Section 3.5.1.4 of NUREG-0800 [12]. The design basis tornado is considered to generate three types of missiles that impact the cask at normal incidence.

Massive Missile – (deformable w/high kinetic energy)	Weight = 4,000 lb Frontal Area = 20 sq ft
Penetration Missile – (rigid hardened steel)	Weight = 280 lb Diameter = 8.0 in
Protective Barrier Missile – (solid steel sphere)	Weight = 0.15 lb Diameter = 1.0 in

Each missile is assumed to impact the concrete cask at a velocity of 126 miles per hour, horizontal to the ground, which is 35% of the maximum wind speed of 360 miles per hour. For missile impacts in the vertical direction, the assumed missile velocity is $(0.7)(126) = 88.2$ miles per hour.

The analysis of the loaded concrete cask for missile impacts applies the laws of conservation of momentum and conservation of energy to determine the rigid body response of the concrete cask. Each missile impact is evaluated, and all missiles are assumed to impact in a manner that produces the maximum damage to the cask.

2.3.2 Water Level (Flood) Design

The loaded concrete cask may be exposed to a flood during storage on an unsheltered concrete storage pad at an ISFSI site. The source and magnitude of the probable maximum flood depend on specific site characteristics.

2.3.2.1 Flood Elevations

The concrete cask design basis is a maximum floodwater depth of 50 feet above the base of the cask and a floodwater velocity of 15 ft per second. Under design basis flood conditions, the cask does not move or tip on the storage pad and the confinement function is maintained.

2.3.2.2 Phenomena Considered in Design Load Calculations

The occurrence of flooding at an ISFSI site is dependent upon the specific site location and the surrounding natural and man-made geographical features. Some possible sources of a flood at an ISFSI site are: overflow from a river or stream due to unusually heavy rain, snow-melt runoff, or a dam or major water supply line break caused by a seismic event (earthquake); high tides

produced by a hurricane; and a tsunami (tidal wave) caused by an underwater earthquake or volcanic eruption.

Flooding at an ISFSI site is highly improbable because of the extensive environmental impact studies that are performed during the selection of a site for a nuclear facility.

2.3.2.3 Flood Force Application

The evaluation of the concrete cask for a flood condition determines a maximum permissible floodwater current velocity and a maximum permissible floodwater depth. The criteria employed in the determination of the maximum permissible values are that a cask tip-over will not occur, and that the TSC material yield strength is not exceeded.

The force of the floodwater current on the concrete cask is calculated as a function of the velocity, which is a factor comprised of the dynamic water pressure, the frontal area of the cask that is normal to the direction of the current, and a drag coefficient dependent on the Reynold's number. The maximum permissible force of the floodwater current is determined such that the overturning moment on the cask will be less than that required to tip the cask over.

During a flood condition, the force of the floodwater exerts a hydrostatic pressure on the canister shell. This pressure is based on the design basis flood: floodwater depth of 50 ft and floodwater velocity of 15 ft per second. Therefore, the force exerted on the canister shell is 22 psi. The analysis of the canister shell will demonstrate that there is no containment malfunction or impairment of the ability to retrieve fuel from the canister.

2.3.2.4 Flood Protection

The inherent strength of the reinforced concrete cask provides a substantial margin of safety against any permanent deformation of the cask for a credible flood event at an ISFSI site. Therefore, no special flood protection measures for the cask are necessary. For the design basis flood, the allowable stresses in the TSC are not exceeded.

2.3.3 Seismic Design

An ISFSI site may be subject to seismic events (earthquakes) during its lifetime. The seismic response spectra experienced by the concrete cask depends upon the geographical location of the specific site and the distance from the epicenter of the earthquake. The possible significant effect of a beyond-design-basis seismic event on the concrete cask would be a tip-over; however, the loaded concrete cask does not tip over during the design-basis seismic event. Although it is a

nonmechanistic event, the loaded concrete cask design basis includes consideration of the consequences of a hypothetical cask tip-over event.

The TSC is analyzed for loads induced by the application of a 0.37g seismic acceleration to the concrete cask at the top surface of the ISFSI pad.

2.3.4 Snow and Ice Loadings

The criterion for determining design snow loads is based on ANSI/ASCE 7-93 [13], Section 7.0. Flat roof snow loads apply and the design basis snow and ice load are calculated from the following formula.

$$\begin{aligned} p_f &= 0.7C_eC_tIp_g \\ &= 100.8 \text{ psf} \end{aligned}$$

where:

p_f = flat roof snow load (psf)

C_e = exposure factor = 1.0

C_t = thermal factor = 1.2

I = importance factor = 1.2

p_g = ground snow load, (psf) = 100

The numerical values of C_e , C_t , I , and p_g are obtained from Tables 1, 18, 19, and 20 and Figure 7, respectively, of ANSI/ASCE 7-93.

The exposure factor, C_e , accounts for wind effects. The exposure factor of the concrete cask is assumed to be Category C, which is defined to be "locations in which snow removal by wind cannot be relied on to reduce roof loads because of terrain, higher structures, or several trees nearby." The thermal factor, C_t , accounts for the importance of buildings and structures in relation to public health and safety. The concrete cask is conservatively classified as a Category III building or other structure. Ground snow loads for the contiguous United States are given in Figures 5, 6, and 7 of ANSI/ASCE 7-93. A worst-case value of 100 lb per square ft is assumed.

The design basis snow and ice load is bounded by the weight of the loaded transfer cask on the top of the concrete cask shell and by the tornado missile loading on the concrete cask lid. The snow load is considered in the load combinations evaluations of the concrete cask.

2.3.5 Combined Load Criteria

Each normal condition and off-normal and accident event has a combination of load cases that defines the total combined loading for that condition/event. The individual load cases considered include thermal, seismic, external and internal pressure, missile impacts, drops, snow and ice loads, and/or flood water forces. The load conditions to be evaluated for storage casks are identified in 10 CFR 72 [10] and ANSI/ANS-57.9 [14].

2.3.5.1 Load Combinations and Design Strength - Concrete Cask

Refer to Table 2.3-1 for the load combinations for the concrete cask. The live loads are considered to vary from 0% to 100% to ensure that the worst-case condition is evaluated. In each case, use of 100% of the live load produces the maximum load condition. The steel liner of the concrete cask is a stay-in-place form that also provides radiation shielding. The concrete cask is designed to the requirements of ACI 349 [4].

In calculating the design strength of concrete in the concrete cask body, nominal strength values are multiplied by a strength reduction factor in accordance with Section 9.3 of ACI 349.

2.3.5.2 Load Combinations and Design Strength – TSC and Fuel Basket

The TSC is designed in accordance with the ASME Code, Section III, Subsection NB [1]. The basket is designed in accordance with the ASME Code, Section III, Subsection NG [2]. Structural buckling of the basket is evaluated in accordance with NUREG/CR-6322 [3].

Refer to Table 2.3-2 for the load combinations for all normal conditions and off-normal or accident events and the corresponding ASME service levels. Levels A and D service limits represent normal conditions and accident events, respectively. Levels B and C service limits are used for off-normal events. The analysis criteria of the ASME Code, Section III, Subsection NB are employed. Stress intensities produced by pressure, temperature, and mechanical loads are combined before comparison to the ASME Code allowable criteria. For components used in the TSC, refer to the allowable criteria in Table 2.3-3.

The load combinations considered for the fuel basket for normal conditions and off-normal or accident events are the same as those identified for the TSC in Table 2.3-2, except that there are

no internal pressure loads. The analysis criteria of the ASME Code, Section III, Subsection NG are employed. For the fuel basket components, refer to the allowable criteria in Table 2.3-3.

2.3.5.3 Design Strength - Transfer Cask

The transfer cask is a special lifting device. It is designed, fabricated, and load tested to meet the requirements of ANSI N14.6 [6] for the handling of vertical loads defined in NUREG 0612 [15]. The design criteria are as follows.

- The combined shear stress or maximum tensile stress during the lift (with 10% dynamic load factor) shall be $\leq S_y/6$ and $S_w/10$.
- For off-normal (Level C) conditions, membrane stresses shall be less than $1.2S_m$ and membrane plus bending stresses shall be the lesser of $1.8S_m$ and $1.5S_y$.
- The ferritic steel material used for the load-bearing members of the transfer cask shall satisfy the material toughness requirements of ANSI N14.6, paragraph 4.2.6.

Refer to Chapter 10 for information on load testing of the transfer cask.

2.3.6 Environmental Temperatures

A temperature of 100°F is selected to establish a conservative boundary for the annual average temperature for MAGNASTOR in storage. This temperature conservatively bounds the maximum average annual temperature in the 48 contiguous United States, specifically, Miami, FL, at 75.6°F [16], and is, therefore, used so as to bound existing and potential ISFSI sites. Refer to Chapter 4 for the evaluation of this environmental condition along with the thermal analysis models. Refer to Chapter 3 for the thermal stress evaluation for the normal operating conditions. Normal temperature fluctuations are bounded by the severe ambient temperature cases that are evaluated as off-normal and accident events.

Off-normal, severe environmental events are defined as -40°F with no solar loads and 106°F with solar loads. An extreme environmental condition of 133°F with maximum solar loads is evaluated as an accident case to show compliance with the maximum heat load case required by ANSI/ANS-57.9. Thermal performance is also evaluated assuming both the half blockage of the concrete cask air inlets and the complete blockage of the air inlets.

The design basis temperatures used in the concrete cask analysis follow. Solar insolation is as specified in 10 CFR 71.71 [17] and Regulatory Guide 7.8 [18].

Condition	Ambient Temperature	Solar Insolation
Normal	100°F	yes
Off-Normal - Severe Heat	106°F	yes
Off-Normal - Severe Cold	-40°F	no
Accident - Extreme Heat	133°F	yes

Table 2.3-1 Load Combinations for the Concrete Cask

Load Combination	Condition	Dead	Live	Wind	Thermal	Seismic	Tornado/ Missile	Drop/ Impact	Flood
1	Normal	1.4D	1.7L						
2	Normal	1.05D	1.275L		1.275T _o				
3	Normal	1.05D	1.275L	1.275W	1.275T _o				
4	Off-Normal and Accident	D	L		T _a				
5	Accident	D	L		T _o	E _{ss}			
6	Accident	D	L		T _o			A	
7	Accident	D	L		T _o				F
8	Accident	D	L		T _o		W _t		

Load Combinations are from ANSI/ANS-57.9 [14] and ACI 349 [4]. Where:

- | | |
|-------------------------------------|---|
| D = Dead Load | T _a = Off-Normal or Accident Temperature |
| L = Live Load | E _{ss} = Design Basis Earthquake |
| W = Wind | W _t = Tornado/Tornado Missile |
| T _o = Normal Temperature | A = Drop/Impact |
| F = Flood | |

Table 2.3-2 Load Combinations for the TSC

LOAD		NORMAL			OFF-NORMAL			ACCIDENT							
		A			B			D							
		1	2	3	1	2	3	4	5	1	2	3	4	5	6
ASME Service Level Load Combinations															
Dead Weight	TSC w/ fuel	X	X	X	X	X	X	X	X	X	X	X	X	X	X
Thermal	Inside concrete cask: 100°F ambient	X		X				X		X	X	X	X	X	
	Inside transfer cask: 100°F ambient		X		X		X								X
	Inside concrete cask: -40°F or 106°F ambient					X			X						
Internal Pressure	Normal	X	X	X			X	X	X	X	X	X	X		
	Off-Normal				X	X									
	Accident (fire)													X	X
Handling Load	Normal (1.1g)		X	X	X										
	Off-Normal						X	X	X						
Drop/Impact	24-in drop, < 60g									X					
Seismic	Tip-over and complete burial										X				
Flood	50-ft water head											X			
Tornado	Pressure drop of 3.0 psi												X		

Table 2.3-3 Structural Design Criteria for Components Used in the TSC

Component	Criteria
1. Normal Operations: Service Level A TSC: ASME Section III, Subsection NB [1] Basket: ASME Section III, Subsection NG [2]	$P_m \leq S_m$ $P_L + P_b \leq 1.5 S_m$ $P_L + P_b + Q \leq 3S_m$ $P_s < 0.6 S_m$
2. Off-Normal Operations: Service Level B TSC: ASME Section III, Subsection NB	$P_m < 1.1 S_m$ $P_L + P_b < 1.65 S_m$ $P_s < 0.6 S_m$
3. Off-Normal Operations: Service Level C TSC: ASME Section III, Subsection NB Basket: ASME Section III, Subsection NG	Subsection NB Criteria: $P_m < 1.2 S_m$ or S_y (whichever is greater) $P_L + P_b < 1.8 S_m$ or $1.5 S_y$ (whichever is lesser) $P_s < 0.6 S_m$ Subsection NG Criteria: $P_m < 1.5S_m$ $P_L + P_b < 2.25S_m$ $P_s < 0.6 S_m$
4. Accident Conditions, Service Level D TSC: ASME Section III, Subsection NB Basket: ASME Section III, Appendix F Basket: ASME Section III, Subsection NG	$P_m \leq 2.4 S_m$ or $0.7 S_u$ (whichever is lesser) $P_L + P_b \leq 3.6 S_m$ or $1.0 S_u$ (whichever is lesser) $P_s < 0.42 S_u$ Plastic Analysis (Basket): $P_m \leq 0.7S_u$ $P_{int} \leq 0.9S_u$ $P_s < 0.42 S_u$
5. Basket Structural Buckling	NUREG/CR-6322 [3]

Symbols:

S_m = material design stress intensity
 S_u = material ultimate strength
 S_y = material yield strength

P_L = primary local membrane stress
 P_m = primary general membrane stress
 P_b = primary bending stress
 P_{int} = primary stress intensity
 P_s = average primary shear across a section loaded in pure shear

2.4 Safety Protection Systems

MAGNASTOR relies upon passive systems to ensure the protection of public health and safety, except in the case of fire or explosion. As previously discussed, fire and explosion events are effectively precluded by site administrative controls that prevent the introduction of flammable and explosive materials. The use of passive systems provides protection from mechanical or equipment failure.

2.4.1 General

MAGNASTOR is designed for safe, long-term storage of spent fuel. The system will withstand all of the evaluated normal conditions and off-normal and postulated accident events without release of radioactive material or excessive radiation exposure to workers or the general public. The major design considerations to assure safe, long-term fuel storage and retrievability for ultimate disposal by the Department of Energy in accordance with the requirements of 10 CFR 72 and ISG-2 [24] are as follows.

- Continued radioactive material confinement in postulated accidents.
- Thick steel and concrete biological shield.
- Passive systems that ensure reliability.
- Pressurized inert helium atmosphere to provide corrosion protection for fuel cladding and enhanced heat transfer for the stored fuel.

Retrievability is defined as: "maintaining spent fuel in substantially the same physical condition as it was when originally loaded into the storage cask, which enables any future transportation, unloading and ultimate disposal activities to be performed using the same general type of equipment and procedures as were used for the initial loading."

Each major component of the system is classified with respect to its function and corresponding potential effect on public safety. In accordance with Regulatory Guide 7.10 [19], each major system component is assigned a safety classification (see Table 2.4-1). The safety classification is based on review of the component's function and the assessment of the consequences of its failure following the guidelines of NUREG/CR-6407 [20]. The safety classification categories are defined in the following list.

Category A - Components critical to safe operations whose failure or malfunction could directly result in conditions adverse to safe operations, integrity of spent fuel, or public health and safety.

Category B - Components with major impact on safe operations whose failure or malfunction could indirectly result in conditions adverse to safe operations, integrity of spent fuel, or public health and safety.

Category C - Components whose failure would not significantly reduce the packaging effectiveness and would not likely result in conditions adverse to safe operations, integrity of spent fuel, or public health and safety.

As discussed in the following sections, the MAGNASTOR design incorporates features addressing the design considerations described previously to assure safe operation during loading, handling, and storage of spent nuclear fuel.

2.4.2 Confinement Barriers and Systems

The radioactive materials that MAGNASTOR must confine during storage originate from the stored fuel assemblies and residual contamination inside the TSC. The system is designed to safely confine this radioactive material under all storage conditions.

The stainless steel TSC is assembled and closed by welding. All of the field-installed welds are liquid penetrant examined as detailed in Chapter 10 and on the License Drawings. The longitudinal and girth shop welds of the TSC shell are full penetration welds that are radiographically and liquid penetrant examined during fabrication. The TSC bottom-plate-to-shell shop weld joint is ultrasonically and liquid penetrant examined during fabrication.

The TSC vessel provides a leaktight boundary precluding the release of solid, volatile, and gaseous radioactive material. There are no evaluated normal conditions or off-normal or accident events that result in damage to the TSC producing a breach in the confinement boundary. Neither normal conditions of operation or off-normal events preclude retrieval of the TSC for transport and ultimate disposal. The TSC is designed to withstand accident conditions, including a 24-inch end drop in the concrete cask and a tip-over of the concrete cask, without precluding the subsequent removal of the fuel (i.e., the fuel tubes do not deform such that they bind the fuel assemblies).

Operator radiation exposure during handling and closure of the TSC is minimized by the following.

- Minimizing the number of operations required to complete the TSC loading and sealing process.
- Placing the closure lid on the TSC while the transfer cask and TSC are under water in the fuel pool.
- Using temporary shielding, including a weld shield plate as the mounting component of the weld machine.

- Using retaining blocks on the transfer cask to ensure that the TSC is not raised out of the transfer cask.

2.4.3 Concrete Cask Cooling

The loaded concrete cask is passively cooled. Ambient air enters at the bottom of the concrete cask through four air inlets and heated air exits through the four air outlets at the top of the cask due to natural convection heat transfer. Radiant heat transfer also occurs from the TSC to the concrete cask liner. Consequently, the liner also heats the convective airflow. This natural circulation of air inside the concrete cask, in conjunction with radiation from the TSC surface, maintains the fuel cladding and concrete cask component temperatures below their design limits. Conduction does not play a substantial role in heat removal from the TSC surface. Refer to Chapter 4 for details on the concrete cask thermal analyses.

2.4.4 Protection by Equipment

There is no important-to-safety equipment required for the safe storage operation of MAGNASTOR. The important-to-safety equipment employed in the handling of MAGNASTOR is the lifting yoke used to lift the transfer cask. The lifting yoke is designed, fabricated, and tested in accordance with ANSI N14.6 as a special lifting device as defined in NUREG-0612. The lifting yoke is proof load tested to 300% of its design load when fabricated. Following the load test, the bolted connections are disassembled, and the components are inspected for deformation. Permanent deformation of components is not acceptable. Engagement pins are examined by dye penetrant examination. The transfer cask and lifting yoke are inspected for visible defects prior to each use. Transfer cask annual maintenance requirements are defined in Chapter 10.

2.4.5 Protection by Instrumentation

No instrumentation is required for the safe storage operations of MAGNASTOR.

A remote temperature-monitoring system may be used to measure the outlet air temperature of the concrete casks in long-term storage. The outlet temperature can be monitored daily as a check of the continuing thermal performance of the concrete cask. Alternately, a daily visual inspection for blockage of the air inlet and air outlet screens of all concrete casks may be performed. Following any natural phenomena event, such as an earthquake or tornado, the concrete casks shall be inspected for damage and air inlet and air outlet blockage.

2.4.6 Nuclear Criticality Safety

MAGNASTOR design includes features to ensure that nuclear criticality safety is maintained (i.e., the cask remains subcritical under normal conditions and off-normal and accident events). The design of the TSC and fuel basket is such that, under all conditions, the highest neutron multiplication factor (k_{eff}) is less than 0.95.

2.4.6.1 Control Methods for Prevention of Criticality

The principal design criterion is that k_{eff} remain less than 0.95 for all conditions. Criticality control for PWR spent fuel is achieved using neutron absorber material fixed in the basket and by maintaining a minimum boron concentration in the TSC during fuel loading. The fixed neutron absorber attracts thermal neutrons that are moderated in the water surrounding the fuel. Fast, high-energy neutrons escape the system. The minimum effective loading for neutron absorber sheets is 0.036 and 0.027 g $^{10}\text{B}/\text{cm}^2$ for PWR and BWR fuel baskets, respectively. The required minimum boron loading in a neutron absorber sheet is determined based on the assumed boron effectiveness used in the criticality analysis, i.e., 75% for Boral (registered trademark of AAR Advanced Structures) and 90% for borated aluminum alloys and for borated metal matrix composites (MMCs). Neutron absorber sheets are mechanically attached to the fuel tube structure to ensure that the neutron absorber remains in place during the design basis normal conditions and off-normal and accident events.

The basket designs ensure that there is sufficient absorption of moderated neutrons by the neutron absorber (and by boron in the cavity water in some cases) to maintain criticality control in the basket ($k_{\text{eff}} < 0.95$). See Chapter 6 for the detailed criticality analyses.

2.4.6.2 Error Contingency Criteria

The standards and regulations of criticality safety require that k_{eff} , including uncertainties, be less than 0.95. The bias and 95/95 uncertainty are applied to the calculation using an upper safety limit (USL) approach [22]. The $k_{\text{eff}} + 2\sigma$ value must be less than the USL. Based on MCNP critical benchmarks, the USL as a function of fission neutron lethargy (eV) is shown as:

$$\text{USL} = 0.9364 + 8.4409 \times 10^{-3} \times x$$

where:

$$x = \text{energy of average neutron lethargy causing fission}$$

2.4.6.3 Verification Analyses

The MCNP criticality analysis code is benchmarked through a series of calculations based on critical experiments. These experiments span a range of fuel enrichments, fuel rod pitches, poison sheet characteristics, shielding materials, and geometries that are typical of light water reactor fuel in a cask. To achieve accurate results, three-dimensional models, as close to the actual experiment as possible, are used to evaluate the experiments.

2.4.7 Radiological Protection

MAGNASTOR is designed to minimize operator radiological exposure in keeping with the As Low As Reasonably Achievable (ALARA) philosophy.

2.4.7.1 Access Control

Access to MAGNASTOR at an ISFSI site will be controlled by a fence with lockable truck and personnel access gates to meet the requirements of 10 CFR 72, 10 CFR 73, and 10 CFR 20 [21]. Access to the storage area, and its designation as to the level of radiation protection required, will be established by site procedures by the licensee.

2.4.7.2 Shielding

MAGNASTOR is designed to limit the dose rates in accordance with 10 CFR 72.104 and 72.106, which set whole body dose limits for an individual located beyond the controlled area at ≤ 25 mrem per year (whole body) during normal operations and ≤ 5 rem (5,000 mrem) from any design basis accident.

2.4.7.3 Ventilation Off-Gas

MAGNASTOR is passively cooled by radiation and natural convection heat transfer at the outer surface of the concrete cask and in the TSC-concrete cask annulus. In the TSC-concrete cask annulus, air enters the air inlets, flows up between the TSC and concrete cask liner in the annulus, and exits the air outlets. If the exterior surface of the TSC is excessively contaminated, the possibility exists that contamination could be carried aloft by the airflow. Therefore, during fuel loading, the spent fuel pool water is minimized in the transfer cask/TSC annulus by supplying the annulus with clean or demineralized spent fuel pool water. Water is supplied into the annulus while the transfer cask is submerged. The use of the annulus system minimizes the potential for contamination of the exterior surfaces of the TSC.

After the transfer cask is removed from the pool, removable contamination levels on the TSC exterior are determined. If TSC decontamination is required, clean water can be used to flush the annulus. To facilitate decontamination, the TSC exterior surfaces are smooth.

MAGNASTOR has no radioactive releases during normal conditions or off-normal or accident events of storage. Hence, there are no off-gas system requirements for MAGNASTOR.

2.4.7.4 Radiological Alarm Systems

No radiological alarms are required on MAGNASTOR. Typically, total radiation exposure due to the ISFSI installation is monitored by the use of the licensee's boundary dose monitoring program.

2.4.8 Fire Protection

A major ISFSI fire is not considered credible, since there is very little material near the concrete casks that could contribute to a fire. The concrete cask is largely impervious to incidental thermal events. Administrative controls will be established by the licensee to ensure that the presence of combustibles at the ISFSI is minimized. A hypothetical 1,475°F fire occurring at the base of the cask for eight minutes is evaluated as an accident condition.

2.4.9 Explosion Protection

MAGNASTOR is analyzed to ensure its proper function under an over-pressure event. The TSC is protected from direct over-pressure conditions by the concrete cask. For the same reasons as for the fire condition, a severe explosion on an ISFSI site is not considered credible. The evaluated 20 psig over-pressure condition is considered to bound any explosive over-pressure resulting from an industrial explosion at the boundary of the owner-controlled area.

2.4.10 Auxiliary Structures

The loading, welding, drying, transfer, and transport of MAGNASTOR require the use of auxiliary equipment as described in Chapter 9. External transfer of a TSC may require the use of a structure, referred to as a "TSC Handling and Transfer Facility." The TSC Handling and Transfer Facility is a specially designed and engineered structure independent of the 10 CFR 50 facilities at the site.

The design of the TSC Handling and Transfer Facility would meet the requirements for MAGNASTOR described in the Design Features presented in Appendix A of the Technical Specifications, in addition to those requirements established by the licensee.

The design, analysis, fabrication, operation, and maintenance of the TSC Handling and Transfer Facility would be performed in accordance with the quality assurance program requirements of the licensee. The components of the TSC Handling and Transfer Facility would be classified as Important-to-Safety or Not-Important-to-Safety in accordance with the guidelines of NUREG-6407.

Table 2.4-1 Safety Classification of MAGNASTOR Components

Component Description	Reference Drawings	Safety Function	Safety Classification
TSC Assembly Shell and Base Plate Closure Lid Closure Ring Port Covers	71160-581 71160-584 71160-584 71160-585	Structural and Confinement	A
Fuel Basket Assembly Basket Support Weldments Fuel Tube Assemblies Neutron Absorbers	71160-551 71160-571 71160-572 71160-574 71160-575 71160-591 71160-598 71160-599	Criticality, Structural, and Thermal	A
Transfer Cask Assembly Trunnions Inner and Outer Shells Shield Doors and Rails Lead Gamma Shield Neutron Shield	71160-560	Structural, Shielding and Operations	B
Adapter Plate Assembly Base Plate Door Rails Hydraulic Operating System Side Shields	None	Operations and Shielding	NQ
Concrete Cask Assembly Structural Weldments and Base Plate Lid Weldment Lifting Lugs Reinforcing Bars Concrete	71160-561 71160-562 71160-590	Structural, Shielding, Operations, and Thermal	B

2.5 Decommissioning Considerations

The principal components of MAGNASTOR are the concrete cask and the TSC. Refer to Chapter 15 for information on decommissioning MAGNASTOR.

Decommissioning of MAGNASTOR involves removing the TSC by offsite transport and disassembling the concrete cask. It is expected that the concrete will be broken up and the steel components segmented to reduce volume. The concrete and carbon steel are not expected to be surface-contaminated and no significant activation is expected.

The TSC is designed and fabricated to ensure its retrievability for use as a component of the waste package for permanent disposal at the Mined Geological Disposal System in accordance with the guidance of ISG-2 [24] and the requirements of 10 CFR 72. Consequently, decommissioning may not be required. If necessary, the TSC could be decommissioned following unloading by decontaminating the inside and segmenting the shell and closure plates. Since the neutron flux rate from the stored fuel is low, only minimal activation of the TSC is expected. The resulting stainless steel could be disposed of, or recycled, in accordance with the appropriate regulatory requirements.

The storage pad, fence, and supporting utility fixtures are not expected to require decontamination as a result of use of MAGNASTOR. Consequently, these items may be reused or disposed of as locally generated clean waste.

2.6 References

1. ASME Boiler and Pressure Vessel Code, Section III, Subsection NB, "Class 1 Components," American Society of Mechanical Engineers, New York, NY, 2001 Edition with 2003 Addenda.
2. ASME Boiler and Pressure Vessel Code, Section III, Subsection NG, "Core Support Structures," American Society of Mechanical Engineers, New York, NY, 2001 Edition with 2003 Addenda.
3. NUREG/CR-6322, "Buckling Analysis of Spent Fuel Basket," US Nuclear Regulatory Commission, Washington, DC, May 1995.
4. "Code Requirements for Nuclear Safety Related Concrete Structures (ACI 349) and Commentary (ACI 349R)," American Concrete Institute, Farmington Hills, MI.
5. "Building Code Requirements for Structural Concrete (ACI 318) and Commentary (ACI 318R)," American Concrete Institute, Farmington Hills, MI.
6. ANSI N14.6-1993, "American National Standard for Radioactive Materials - Special Lifting Devices for Shipping Containers Weighing 10,000 Pounds (4,500 kg) or More," American National Standards Institute, Inc., Washington, DC, June 1993.
7. ISG-11, "Cladding Considerations for the Transport and Storage of Spent Fuel," US Nuclear Regulatory Commission, Washington, DC, Revision 3, November 17, 2003.
8. PNL-4835, "Technical Basis for Storage of Zircaloy-Clad Spent Fuel in Inert Gases," Johnson, A.B., and Gilbert, E.R., Pacific Northwest Laboratory, Richland, WA, September, 1983.
9. NUREG-1567, "Standard Review Plan for Spent Fuel Dry Storage Facilities," US Nuclear Regulatory Commission, Washington, DC, March 2000.
10. 10 CFR 72, Code of Federal Regulations, "Licensing Requirements for the Independent Storage of Spent Nuclear Fuel, High-Level Radioactive Waste and Reactor-Related Greater Than Class C Waste," US Government, Washington, DC.
11. Regulatory Guide 1.76, "Design Basis Tornado for Nuclear Power Plants," US Nuclear Regulatory Commission, Washington, DC, April 1974.
12. NUREG-0800, "Standard Review Plan," US Nuclear Regulatory Commission, Washington, DC, April 1996.
13. ANSI/ASCE 7-93 (formerly ANSI A58.1), "Minimum Design Loads for Buildings and Other Structures," American Society of Civil Engineers, New York, NY, May 1994.
14. ANSI/ANS-57.9-1992, "Design Criteria for an Independent Spent Fuel Storage Installation (Dry Type)," American Nuclear Society, La Grange Park, IL, May 1992.

15. NUREG-0612, "Control of Heavy Loads at Nuclear Power Plants," US Nuclear Regulatory Commission, Washington, DC, July 1980.
16. ASHRAE Handbook, "Fundamentals," American Society of Heating, Refrigeration, and Air Conditioning Engineers, Atlanta, GA, 1993.
17. 10 CFR 71, "Packaging and Transportation of Radioactive Materials," Code of Federal Regulations, US Government, Washington, DC.
18. Regulatory Guide 7.8, "Load Combinations for the Structural Analysis of Shipping Casks for Radioactive Material," US Nuclear Regulatory Commission, Washington, DC, March 1989.
19. Regulatory Guide 7.10, "Establishing Quality Assurance Programs for Packaging Used in the Transport of Radioactive Material," US Nuclear Regulatory Commission, Washington, DC.
20. NUREG/CR-6407, "Classification of Transportation Packaging and Dry Spent Fuel Storage System Components According to Importance to Safety," US Nuclear Regulatory Commission, Washington, DC, February 1996.
21. 10 CFR 20, "Standards for Protection Against Radiation," Code of Federal Regulations, US Government, Washington, DC.
22. NUREG/CR-6361, "Criticality Benchmark Guide for Light-Water-Reactor Fuel in Transportation and Storage Packages," US Nuclear Regulatory Commission, Washington, DC, December 1997.
23. ASME Boiler and Pressure Vessel Code Case 595-4, "Requirements for Spent Fuel Storage Canisters, Section III."
24. ISG-2, "Fuel Retrievability," US Nuclear Regulatory Commission, Washington, DC, October 1998.

Chapter 3 Structural Evaluation

Table of Contents

3	STRUCTURAL EVALUATION	3-1
3.1	MAGNASTOR Structural Design	3.1-1
3.1.1	Major Components	3.1-1
3.1.2	Discussion of MAGNASTOR	3.1-1
3.1.3	Design Criteria Summary	3.1-4
3.2	Weights and Centers of Gravity	3.2-1
3.3	Materials	3.3-1
3.4	General Standards for Casks	3.4-1
3.4.1	Chemical and Galvanic Reactions	3.4-1
3.4.2	Positive Closure	3.4-1
3.4.3	Lifting Devices	3.4-2
3.5	Normal Operating Conditions	3.5-1
3.5.1	TSC Evaluation for Normal Operating Conditions	3.5-1
3.5.2	Fuel Basket Evaluation for Normal Operating Conditions	3.5-5
3.5.3	Concrete Cask Evaluations for Normal Operating Conditions	3.5-23
3.6	Off-Normal Operating Events	3.6-1
3.6.1	TSC Evaluations for Off-Normal Operating Events	3.6-1
3.6.2	Fuel Basket Evaluation for Off-Normal Operating Events	3.6-2
3.6.3	Concrete Cask Evaluation for Off-Normal Operating Events	3.6-11
3.7	Storage Accident Events	3.7-1
3.7.1	TSC Evaluations for Storage Accident Conditions	3.7-1
3.7.2	Fuel Baskets Evaluation for Storage Accident Events	3.7-4
3.7.3	Concrete Cask Evaluation for Storage Accident Events	3.7-38
3.8	Fuel Rods	3.8-1
3.8.1	PWR Fuel Rod Evaluation	3.8-1
3.8.2	BWR Fuel Rod Evaluation	3.8-4
3.8.3	Thermal Evaluation of Fuel Rods	3.8-5
3.9	References	3.9-1
3.10	Structural Evaluation Detail	3.10-1
3.10.1	PWR Fuel Basket Finite Element Models	3.10.1-1
3.10.2	BWR Fuel Basket Finite Element Models	3.10.2-1
3.10.3	TSC Finite Element Model	3.10.3-1
3.10.4	Concrete Cask Finite Element Models	3.10.4-1
3.10.5	Transfer Cask Finite Element Model	3.10.5-1

3.10.6	Basket Stability Evaluation for Concrete Cask Tip-Over Accident Condition.....	3.10.6-1
3.10.7	Fuel Tube Plastic Analysis for Concrete Cask Tip-Over Accident Condition.....	3.10.7-1

List of Figures

Figure 3.1-1	Principal Components of MAGNASTOR	3.1-5
Figure 3.4-1	Top Ring Section Cuts	3.4-26
Figure 3.7-1	PWR Basket Fuel Tube Displacement for Tip-Over Accident.....	3.7-58
Figure 3.7-2	BWR Basket Fuel Tube Displacement for Tip-Over Accident	3.7-59
Figure 3.7-3	PWR Neutron Absorber and Retainer Finite Element Model	3.7-60
Figure 3.7-4	Acceleration Time History of the Upper-Bound Weight TSC – 24- Inch Concrete Cask Drop.....	3.7-61
Figure 3.7-5	Acceleration Time History of the Lower-Bound Weight TSC – 24- Inch Concrete Cask Drop.....	3.7-62
Figure 3.7-6	Acceleration Time History for Concrete Cask Tip-Over Condition - Standard Pad	3.7-63
Figure 3.7-7	Acceleration Time History of Oversized Pad	3.7-64
Figure 3.8-1	Two-Dimensional Beam Finite Element Model for MAGNASTOR Fuel Rod.....	3.8-6
Figure 3.8-2	Mode Shape and First Buckling Shape for the MAGNASTOR Fuel Rod.....	3.8-7
Figure 3.10.1-1	Expanded View of PWR Basket.....	3.10.1-8
Figure 3.10.1-2	Bolted Attachment Details.....	3.10.1-9
Figure 3.10.1-3	Free-Body Diagram of PWR Basket Fuel Tube Detail	3.10.1-10
Figure 3.10.1-4	Free-Body Diagram of Basket Support Structure.....	3.10.1-11
Figure 3.10.1-5	PWR Basket Periodic Model – 0° Basket Orientation	3.10.1-12
Figure 3.10.1-6	PWR Basket Periodic Model – 45° Basket Orientation	3.10.1-13
Figure 3.10.1-7	Thermal Stress Evaluation Model.....	3.10.1-14
Figure 3.10.1-8	PWR Basket Plastic Model - 0° Basket Orientation.....	3.10.1-15
Figure 3.10.1-9	PWR Basket Plastic Model - 45° Basket Orientation.....	3.10.1-16
Figure 3.10.1-10	Typical PWR Fuel Tube Pin Finite Element Model Details	3.10.1-17
Figure 3.10.1-11	PWR Basket Model Boundary Conditions for a Transverse Loading – 0° Basket Orientation.....	3.10.1-18
Figure 3.10.1-12	PWR Basket Model Boundary Conditions for a Transverse Loading – 45° Basket Orientation.....	3.10.1-19
Figure 3.10.1-13	PWR Fuel Tube Array – 0° Basket Orientation	3.10.1-20
Figure 3.10.1-14	PWR Fuel Tube Section Cuts – 0° Basket Orientation	3.10.1-21
Figure 3.10.1-15	PWR Fuel Tube Array – 45° Basket Orientation	3.10.1-22
Figure 3.10.1-16	PWR Fuel Tube Section Cuts – 45° Basket Orientation	3.10.1-23
Figure 3.10.1-17	PWR Corner Support Weldment Section Cuts – 0° Basket Orientation	3.10.1-24
Figure 3.10.1-18	PWR Corner Support Weldment Section Cuts – 45° Basket Orientation	3.10.1-25
Figure 3.10.1-19	PWR Side Support Weldment Section Cuts – 0° Basket Orientation ...	3.10.1-26
Figure 3.10.1-20	PWR Side Support Weldment Section Cuts – 45° Basket Orientation .	3.10.1-27
Figure 3.10.2-1	Expanded View of BWR Basket.....	3.10.2-7

Figure 3.10.2-2	Bolted Attachment Details.....	3.10.2-8
Figure 3.10.2-3	Free-Body Diagram of BWR Basket Fuel Tube Detail.....	3.10.2-9
Figure 3.10.2-4	Free-Body Diagram of Basket Support Structure.....	3.10.2-10
Figure 3.10.2-5	BWR Basket Periodic Model – 0° Basket Orientation.....	3.10.2-11
Figure 3.10.2-6	BWR Basket Periodic Model – 45° Basket Orientation.....	3.10.2-12
Figure 3.10.2-7	Thermal Stress Evaluation Model.....	3.10.2-13
Figure 3.10.2-8	BWR Basket Plastic Model - 0° Basket Orientation.....	3.10.2-14
Figure 3.10.2-9	BWR Basket Plastic Model - 45° Basket Orientation.....	3.10.2-15
Figure 3.10.2-10	Typical BWR Fuel Tube Pin Finite Element Model Details.....	3.10.2-16
Figure 3.10.2-11	BWR Basket Model Boundary Conditions for a Transverse Loading – 0° Basket Orientation.....	3.10.2-17
Figure 3.10.2-12	BWR Basket Model Boundary Conditions for a Transverse Loading – 45° Basket Orientation.....	3.10.2-18
Figure 3.10.2-13	BWR Fuel Tube Array – 0° Basket Orientation.....	3.10.2-19
Figure 3.10.2-14	BWR Fuel Tube Section Cuts – 0° Basket Orientation.....	3.10.2-20
Figure 3.10.2-15	BWR Fuel Tube Array – 45° Basket Orientation.....	3.10.2-21
Figure 3.10.2-16	BWR Fuel Tube Section Cuts – 45° Basket Orientation.....	3.10.2-22
Figure 3.10.2-17	BWR Corner Support Weldment Section Cuts – 0° Basket Orientation.....	3.10.2-23
Figure 3.10.2-18	BWR Corner Support Weldment Section Cuts – 45° Basket Orientation.....	3.10.2-24
Figure 3.10.2-19	BWR Side Support Weldment Section Cuts – 0° Basket Orientation...	3.10.2-25
Figure 3.10.2-20	BWR Side Support Weldment Section Cuts – 45° Basket Orientation.	3.10.2-26
Figure 3.10.3-1	MAGNASTOR TSC Finite Element Model.....	3.10.3-5
Figure 3.10.3-2	Identification of Sections for Evaluating Linearized Stresses in TSC ..	3.10.3-6
Figure 3.10.4-1	Concrete Cask Pedestal Finite Element Model for Lift Evaluation.....	3.10.4-8
Figure 3.10.4-2	Concrete Cask Finite Element Model for Thermal Stress Evaluation.....	3.10.4-9
Figure 3.10.4-3	Concrete Cask Model – Elements for Rebar.....	3.10.4-10
Figure 3.10.4-4	Concrete Cask Model Boundary Conditions.....	3.10.4-11
Figure 3.10.4-5	Concrete Cask Pedestal Finite Element Model for 24-inch Drop Evaluation.....	3.10.4-12
Figure 3.10.4-6	Stress-Strain Curve for A36 Carbon Steel.....	3.10.4-13
Figure 3.10.4-7	Finite Element Models for Tip-Over Evaluation.....	3.10.4-14
Figure 3.10.5-1	Finite Element Model for the Transfer Cask.....	3.10.5-2
Figure 3.10.6-1	Finite Element Model for the 0° Fuel Basket Orientation for a Concrete Cask Tip-Over Accident.....	3.10.6-8
Figure 3.10.6-2	Finite Element Model for the 45° Fuel Basket Orientation for a Concrete Cask Tip-Over Accident.....	3.10.6-9
Figure 3.10.6-3	Finite Element Model for the 22.5° Fuel Basket Orientation for a Concrete Cask Tip-Over Accident.....	3.10.6-10
Figure 3.10.6-4	Definition of Tube Reduction for Fuel Basket Stability Evaluation	3.10.6-11
Figure 3.10.6-5	Motion of Fuel Tubes for the 0° Fuel Basket Orientation (Case 2).....	3.10.6-12
Figure 3.10.6-6	Motion of Fuel Tubes for the 22.5° Fuel Basket Orientation (Case 3)..	3.10.6-13

Figure 3.10.6-7 Motion of Fuel Tubes for the 45° Fuel Basket Orientation (Case 4/Case 5) 3.10.6-14

Figure 3.10.6-8 Motion of Fuel Tubes for the 45° Fuel Basket Orientation (Case 6/Case 7) 3.10.6-15

Figure 3.10.7-1 Typical Finite Element Model for the Basket Fuel Tube Displacement . 3.10.7-3

List of Tables

Table 3.2-1	MAGNASTOR Storage Weight and Center of Gravity Summary.....	3.2-2
Table 3.4-1	Stresses for Trunnions and Top Ring	3.4-27
Table 3.4-2	Stresses for Transfer Cask Shells and Bottom Ring	3.4-27
Table 3.5-1	TSC Thermal Stress, Q	3.5-26
Table 3.5-2	TSC Normal Conditions, P_m Stresses	3.5-26
Table 3.5-3	TSC Normal Conditions, $P_m + P_b$ Stresses	3.5-26
Table 3.5-4	TSC Normal Conditions, $P + Q$ Stresses	3.5-26
Table 3.5-5	Concrete Cask Vertical Stress Summary – Outer Surface, psi	3.5-26
Table 3.5-6	Concrete Cask Vertical Stress Summary – Inner Surface, psi.....	3.5-27
Table 3.5-7	Concrete Cask Circumferential Stress Summary – Inner Surface, psi	3.5-27
Table 3.6-1	TSC Off-Normal Events, P_m Stresses	3.6-12
Table 3.6-2	TSC Off-Normal Events, $P_m + P_b$ Stresses	3.6-12
Table 3.6-3	TSC Off-Normal Events, $P + Q$ Stresses	3.6-12
Table 3.7-1	TSC Accident Events, P_m Stresses.....	3.7-65
Table 3.7-2	TSC Accident Events, $P_m + P_b$ Stresses.....	3.7-65
Table 3.7-3	PWR Fuel Tube Nodal Stress Intensities – Concrete Cask Tip-over Accident.....	3.7-65
Table 3.7-4	PWR Corner Support Mounting Plate Nodal Stress Intensities – Concrete Cask Tip-over Accident	3.7-66
Table 3.7-5	PWR Corner Support Bar Nodal Stress Intensities – Concrete Cask Tip-over Accident.....	3.7-66
Table 3.7-6	PWR Side Weldment Nodal Stress Intensities – Concrete Cask Tip- over Accident.....	3.7-66
Table 3.7-7	BWR Fuel Tube Nodal Stress Intensities – Concrete Cask Tip-over Accident.....	3.7-67
Table 3.7-8	BWR Corner Support Mounting Plate Nodal Stress Intensities – Concrete Cask Tip-over Accident	3.7-67
Table 3.7-9	BWR Corner Support Plate Nodal Stress Intensities – Concrete Cask Tip-over Accident.....	3.7-67
Table 3.7-10	BWR Side Weldment Nodal Stress Intensities – Concrete Cask Tip- over Accident.....	3.7-68
Table 3.7-11	Concrete Cask Vertical Stress Summary – Inner Surface, psi.....	3.7-68
Table 3.7-12	Concrete Cask Circumferential Stress Summary – Inner Surface, psi	3.7-68
Table 3.7-13	Basket Modal Frequency for Concrete Cask Tip-over	3.7-69
Table 3.7-14	DLF and Amplified Accelerations for Concrete Cask Tip-over.....	3.7-69
Table 3.10.3-1	TSC Normal Pressure plus Handling, P_m , ksi	3.10.3-7
Table 3.10.3-2	TSC Normal Pressure plus Handling, $P_m + P_b$, ksi	3.10.3-8
Table 3.10.3-3	TSC Normal Pressure plus Handling, $P + Q$, ksi.....	3.10.3-9
Table 3.10.3-4	TSC Normal Pressure, P_m , ksi	3.10.3-10
Table 3.10.3-5	TSC Normal Pressure, $P_m + P_b$, ksi.....	3.10.3-11
Table 3.10.3-6	TSC Thermal Stresses, Q, ksi	3.10.3-12

Table 3.10.3-7	TSC Off-Normal Pressure plus Handling, P_m , ksi	3.10.3-13
Table 3.10.3-8	TSC Off-Normal Pressure plus Handling, $P_m + P_b$, ksi	3.10.3-14
Table 3.10.3-9	TSC Off-Normal Pressure plus Handling, $P + Q$, ksi	3.10.3-15
Table 3.10.3-10	TSC Normal Pressure plus Off-Normal Handling, P_m , ksi	3.10.3-16
Table 3.10.3-11	TSC Normal Pressure plus Off-Normal Handling, $P_m + P_b$, ksi	3.10.3-17
Table 3.10.3-12	TSC Normal Pressure plus 24-inch Drop, P_m , ksi	3.10.3-18
Table 3.10.3-13	TSC Normal Pressure plus 24-inch Drop, $P_m + P_b$, ksi	3.10.3-19
Table 3.10.3-14	TSC Accident Pressure plus Dead Weight, P_m , ksi	3.10.3-20
Table 3.10.3-15	TSC Accident Pressure plus Dead Weight, $P_m + P_b$, ksi	3.10.3-21
Table 3.10.3-16	TSC Tip-Over plus Normal Pressure, P_m , ksi	3.10.3-22
Table 3.10.3-17	TSC Tip-Over plus Normal Pressure, $P_m + P_b$, ksi	3.10.3-23
Table 3.10.6-1	Load Cases Evaluated for Fuel Basket Stability	3.10.6-16

3 STRUCTURAL EVALUATION

This chapter describes the design and analysis of the principal structural components of MAGNASTOR. It demonstrates that MAGNASTOR meets the structural requirements for confinement of contents, criticality control, heat dissipation, radiological shielding, and contents retrievability required by 10 CFR 72 [1] for the design basis normal conditions, and off-normal and accident events.

3.1 MAGNASTOR Structural Design

3.1.1 Major Components

The three principal components of MAGNASTOR are the concrete cask, the TSC, and the transfer cask (refer to Figure 3.1-1). The following table shows the principal structural components of the three major MAGNASTOR components.

Concrete Cask	TSC	Transfer Cask
Reinforced concrete shell	Closure lid and closure ring	Trunnions
Liner weldment	Shell	Inner and outer steel shells
Bottom weldment	Bottom plate	Shield doors
Lid assembly	Fuel basket assembly (PWR or BWR)	Door support rails
		Lead and NS-4-FR shielding

3.1.2 Discussion of MAGNASTOR

MAGNASTOR has four basic configurations to accommodate all PWR and BWR fuel assemblies. The type (PWR or BWR) and overall length of the fuel assembly determine the basic storage configuration, or group. The allocation of a fuel design to the MAGNASTOR grouping is shown in Table 1.3-2. The TSC is designed in two different lengths to accommodate the four groupings of PWR (2) and BWR (2) fuel assemblies. The concrete cask and transfer cask are one length that accommodates the two TSC lengths. The bounding weights and center of gravity of a loaded concrete cask are presented in Table 3.2-1.

The evaluations presented in this chapter are based on the bounding, or limiting, configuration of the components for the condition being evaluated. In most cases, the bounding condition evaluates the heaviest configuration, with either a total weight or bounding weight used as specified in the analysis. Factors of safety greater than ten are generally stated in the analyses as "Large." Numerical values are shown for factors of safety that are less than ten.

Concrete Cask

The concrete cask is a reinforced concrete cylinder with an outside diameter of 136 inches and an overall height of approximately 225 inches. The internal cavity of the concrete cask is lined by a 1.75-inch thick carbon steel shell with an inside diameter of 79.5 inches. There are 24 standoffs (3 × 7½ S-Beam) welded to the inner diameter of the liner. The overall cavity opening in the concrete cask is 73.5 inches. The liner thickness is designed primarily on radiation shielding requirements, but is also related to the need to establish a practical limit for the diameter of the concrete shell. The concrete shell, constructed using Type II Portland Cement,

has a nominal density of 145 lb/ft³ and a nominal compressive strength of 4,000 psi. Vertical hook bars and horizontal hoop bars form the inner and outer rebar assemblies.

A ventilation airflow path is formed by inlets at the bottom of the concrete cask, the annular space between the concrete cask inner shell and the TSC, and outlets in the concrete cask lid assembly. The passive ventilation system operates by natural convection as cool air enters the bottom inlets, is heated by the TSC, and exits from the outlets. Both the air inlets and air outlets are formed with carbon steel in the concrete cask body.

The lid assembly is composed of carbon steel and concrete and forms the concrete cask closure. The lid assembly is 6.75-inches thick and 88 inches in diameter.

TSC

The TSC consists of a cylindrical shell closed at its top end by a closure lid. The bottom of the TSC is a 2.75-inch thick stainless steel plate that is welded to the TSC shell. The TSC forms the confinement boundary for the PWR or BWR spent fuel that is contained in the fuel basket assembly. The TSC is designed to accommodate both PWR and BWR classes of spent fuel assemblies. The TSC is fabricated from dual-certified SA240 Type 304/304L stainless steel. SA182 Type 304 stainless steel may be substituted for the SA240 Type 304 stainless steel used in the closure lid assembly provided that the SA182 material yield and ultimate strengths are equal to, or greater than, those of the SA240 material. The TSC shell is a 0.5-inch thick plate formed into a 72-inch outer diameter cylinder. The TSC closure lid consists of a 9-inch thick stainless steel plate. The closure lid is welded to the TSC shell to seal the TSC with a partial penetration groove weld. Prior to welding, the closure lid assembly is supported by four lift lugs attached to the inside diameter of the TSC at equally spaced angular intervals. A closure ring is welded to the closure lid and canister shell and redundant port covers are welded to the closure lid at both the vent and the drain ports to provide the redundant sealed closure of the TSC. Handling of the TSC is accomplished by the use of six hoist rings threaded into the closure lid, providing redundancy for heavy lifts.

The fuel basket assembly is provided in two configurations – one for up to 37 PWR fuel assemblies and one for up to 87 BWR fuel assemblies. The baskets are manufactured from SA537 Class 1 Carbon Steel. For both the PWR basket and BWR basket, the basic components are the same. The baskets are assembled from three major components – fuel tube assemblies, corner support weldments, and side support weldments. The fuel tube assemblies are equipped with neutron absorbers and stainless steel covers on up to four interior surfaces of the fuel tubes. The geometric integrity of the fuel tube array (21 fuel tubes – PWR, 45 fuel tubes – BWR) is maintained by the corner and side support weldments, which are bolted to the fuel tube array.

The nominal inner dimension of the PWR fuel tubes is 8.86-inches square. The nominal inner dimension of the BWR fuel tubes is 5.86-inches square.

Transfer Cask

The transfer cask, with its lifting yoke, is primarily a shielded lifting device used to handle the TSC. It provides biological shielding for a loaded TSC. The transfer cask is used for the vertical transfer of the TSC between workstations and the concrete cask, or transport cask. The shielding of the cask incorporates a multiwall (steel/lead/NS-4-FR/steel) design. The transfer cask is provided in one configuration capable of handling both the PWR and BWR configurations. The transfer cask can handle a loaded TSC weighing up to 118,000 pounds. The transfer cask is a heavy lifting device that is designed, fabricated, and load-tested to the requirements of ANSI-N14.6 [2] and NUREG-0612 [3]. The transfer cask design incorporates three retainer assemblies attached to the top of the transfer cask to prevent a loaded TSC from being inadvertently lifted through the top of the transfer cask. The transfer cask has retractable bottom shield doors. During loading operations, the doors are closed and secured by bolts/pins so they cannot inadvertently open. During unloading, the doors are retracted using hydraulic cylinders to allow the TSC to be lowered into the concrete cask or transport cask.

Component Evaluation

The following components are evaluated in this chapter.

- TSC lifting devices
- TSC shell, bottom plate, and closure lid
- Fuel basket assembly
- Transfer cask trunnions, shells, retainer assemblies, shield doors, and support rails
- Concrete cask body
- Concrete cask steel components (reinforcement, inner shell, lid assembly, bottom weldment, etc.)

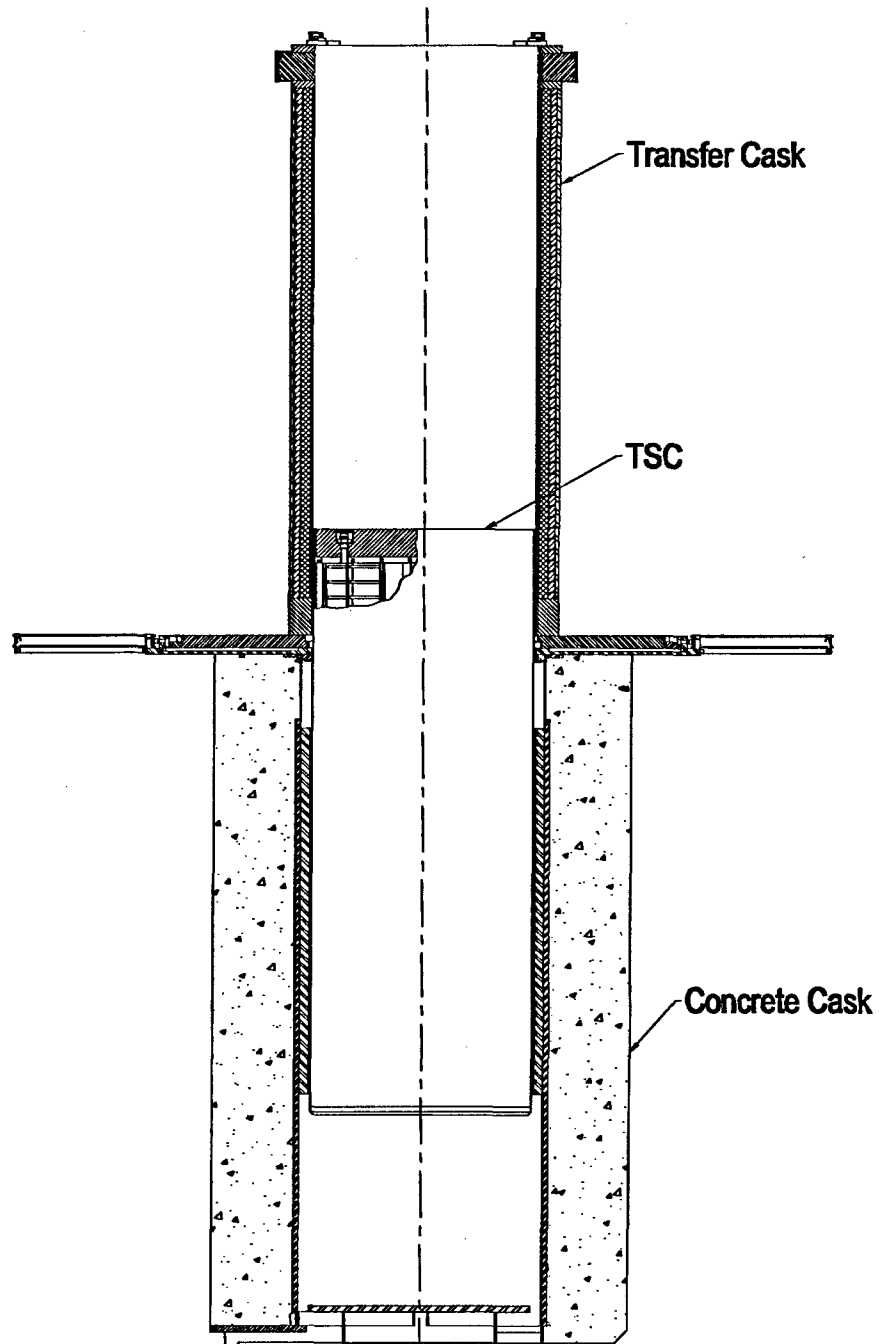
Other MAGNASTOR components shown on the license drawings in Chapter 1 are included as loads in these component evaluations.

The structural evaluations in this chapter demonstrate that MAGNASTOR components meet their respective structural design criteria and are capable of safely storing the design basis PWR or BWR spent fuel assemblies.

3.1.3 Design Criteria Summary

MAGNASTOR structural design criteria are described in Chapter 2. Load combinations for normal, off-normal, and accident loads are evaluated in accordance with ANSI/ANS-57.9 [4] and ACI 349 [5]. The TSC is evaluated in accordance with ASME Code, Section III, Subsection NB for Class 1 components [6]. The basket is evaluated in accordance with ASME Code, Section III Subsection NG [7] and ASME Code, Section III, Appendix F [8]. The buckling evaluation of the fuel basket is performed in accordance with NUREG/CR-6322 [9]. The transfer cask and lifting yoke are lifting devices that are designed to NUREG-0612 [3] and ANSI N14.6 [2].

Figure 3.1-1 Principal Components of MAGNASTOR



3.2 Weights and Centers of Gravity

The maximum calculated weights and centers of gravity (CGs) for MAGNASTOR PWR and BWR configurations are presented in Table 3.2-1. The weights and CGs presented in this section are calculated based on nominal design dimensions.

Table 3.2-1 MAGNASTOR Storage Weight and Center of Gravity Summary

Description	PWR		BWR	
	Weight (lb)	CG (in)	Weight (lb)	CG (in)
Fuel (rod insert weight included for PWR fuel)	62,500	-	61,500	-
Basket	20,000	-	22,000	-
TSC w/o lid	9,500	-	9,500	-
Closure Lid	10,500	-	10,500	-
Water in TSC	17,000	-	16,000	-
Transfer Cask (does not include lifting yoke or transfer adapter)	108,500	-	108,500	-
Concrete Cask (does not include Lid)	214,000	-	214,000	-
Lifting Yoke (not included in transfer cask weight)	3,000	-	3,000	-
Concrete Cask Lid	5,000	-	5,000	-
Loaded TSC (TSC, lid, basket, and fuel)	101,500	96	102,500	98
Storage Cask Loaded (concrete cask, TSC, basket, fuel, concrete cask lid)	320,000	103	321,000	104
Transfer Cask, TSC, Basket, Lifting yoke - Empty	151,000	-	152,500	-
Under Hook Wet Weight (Transfer Cask, TSC, Basket, Lifting Yoke, Closure Lid, Fuel, and Water)	229,500	-	229,500	-
Under Hook Dry Weight (Transfer Cask, TSC, Basket, Transfer Yoke, Closure Lid, Fuel)	212,000		213,000	

- Weights and CGs are maximum calculated values based on nominal component dimensions.
- All weights rounded to the nearest 500 pounds. Component weights are rounded individually, so total assembly weights may not equal the sum of the component weights.
- CG is measured from the bottom of each component.
- Average concrete density is considered to be 148 pcf.
- Transfer cask lifting yoke weight for specific sites may vary from listed weight. The site-specific yoke weight should be used for site-specific applications.
- Concrete cask weight bounds alternate segmented body.

3.3 Materials

Refer to Chapter 8 for the information on Materials.

3.4 General Standards for Casks

MAGNASTOR is designed for safe, long-term storage of spent fuel. The system will withstand all of the evaluated normal conditions, and off-normal and postulated accident events without release of radioactive material or excessive radiation exposure to workers or to the general public.

3.4.1 Chemical and Galvanic Reactions

The materials used in the fabrication and operation of MAGNASTOR are evaluated in Section 8.10.

3.4.2 Positive Closure

A stainless steel closure lid closes the top end of the TSC. Prior to being welded to the TSC shell, the closure lid is supported by lugs welded on the inside surface of the TSC shell at an elevation that allows for thermal expansion of the canister and fuel basket without contact with the closure lid. The lugs also serve as the handling points for the empty TSC shipping/receiving and placement in the transfer cask. The closure lid includes locations for installing load-tested hoist rings or lifting points that are used to lift and lower the loaded TSC after the closure lid is welded to the TSC shell. The closure lid and its weld to the TSC shell can support the weight of the TSC with a load factor of six on material yield strength and ten on material ultimate strength (ANSI N14.6/NUREG-0612). The TSC has a single 0.5-inch J-groove weld attaching the closure lid to the TSC shell. A closure ring, which provides the double weld redundant sealing of the confinement boundary, is installed in the TSC-to-closure lid groove and welded to both the closure lid and the TSC shell. Two port penetrations through the closure lid are used for water removal/TSC drying/helium backfill. Both have single welded, redundant port covers over them to provide the double weld confinement boundary. The port cover welds and the closure ring welds are field welds, and the final weld surfaces are liquid penetrant (PT) examined. The TSC closure lid weld is a field weld and the root, midplane, and final weld surfaces are liquid penetrant (PT) examined. The critical flaw evaluation defines the progressive inspection requirements for the closure lid weld and considers the following criteria.

- Weld is a partial penetration groove weld with an effective throat of 0.5 inch
- Weld filler material is E308L
- Weld process is Gas Tungsten Arc Welding (GTAW)
- Inner diameter of the TSC is 71.0 inches

3.4.3 Lifting Devices

To provide more efficient handling of MAGNASTOR, different methods of lifting are designed for each of the components. The transfer cask, the TSC, and the concrete cask, are handled using trunnions, hoist rings, and lift lugs, respectively.

The design of the MAGNASTOR addresses the concerns identified in NRC Bulletin 96-02, "Movement of Heavy Loads Over Spent Fuel, Over Fuel in the Reactor Core, or Over Safety-Related Equipment" (April 11, 1996) listed as follows.

- The MAGNASTOR lifting and handling components satisfy the requirements of NUREG-0612 and ANSI N14.6 for safety factors on redundant and nonredundant load paths as described in this chapter.
- Transfer cask lifting in the spent fuel pool or cask loading pit, or transfer cask lifting and movement above the spent fuel pool operating floor will be addressed on a plant-specific basis.

3.4.3.1 Concrete Cask Lift

The concrete cask is lifted by means of embedded lug assemblies located in the top of the concrete cask body or by air pads beneath the cask. The concrete cask lift is analyzed in accordance with ANSI N14.6 and ACI 349. The concrete cask lid assembly is evaluated for lift conditions related to installation on the concrete cask body.

Lift Lug

A weight of 322,000 lb is conservatively used for the evaluation of the lift lugs, which bounds the maximum weight of a loaded concrete cask. Assuming a 10% dynamic load factor, the design load (P) on each lug is as follows.

$$P = \frac{322,000 \times 1.1}{4} = 88,550 \text{ lb}$$

The lugs are evaluated for adequate strength using this bounding load. The bearing stresses and loads for lug failure involving bearing, shear-tear-out, or hoop tension are determined using an allowable load coefficient (K). Actual lug failures may involve more than one failure mode, but such interaction effects are accounted for in the values of K [10].

The allowable ultimate bearing load (P_{brUL}) for lug failure in bearing, shear-tear-out, or hoop tension is determined to be as follows.

$$P_{brUL} = 445.8 \text{ kip}$$

where the lug materials are:

$$F_{tu} = 80.0 \text{ ksi} \text{ ----- Ultimate strength, A537 CL2, at } 100^{\circ}\text{F}$$
$$F_{ty} = 60.0 \text{ ksi} \text{ ----- Yield strength, A537 CL2, at } 100^{\circ}\text{F}$$

The allowable yield bearing load (P_{bryL}) is calculated as follows.

$$P_{bryL} = 341.9 \text{ kip}$$

Using the criteria of minimum factors of safety of 5 on ultimate strength and 3 on yield strength, the factors of safety (FS) for the lugs are shown as follows.

Ultimate Bearing:

$$FS = \frac{P_{bruL}}{P} = \frac{445.8}{88.55} = 5.03 > 5$$

Yield Bearing:

$$FS = \frac{P_{bryL}}{P} = \frac{341.9}{88.55} = 3.86 > 3$$

The tensile stress (σ) in the net cross-sectional area of the lug is calculated to be as follows.

$$\sigma = \frac{P}{A} = \frac{88.55}{7.08} = 12.5 \text{ ksi}$$

The factors of safety (FS) are listed as follows.

Ultimate:

$$FS = \frac{80.0}{12.5} = 6.4 > 5$$

Yield:

$$FS = \frac{60.0}{12.5} = 4.8 > 3$$

Lift Anchor

From the previous lug analysis, the maximum load on each embedment plate is 88.55 kip. The ultimate strength (σ) in the plate is calculated as follows.

$$\sigma = \frac{P}{A} = \frac{88.55}{15.2} = 5.8 \text{ ksi}$$

The factors of safety (FS) are as follows.

Ultimate Tensile:

$$FS = \frac{80.0}{5.8} = 13.8 > 5$$

Yield Tensile:

$$FS = \frac{53.0}{5.8} = 9.1 > 3$$

Where the embedment plate material strengths are listed as follows.

$$F_{tu} = 80.0 \text{ ksi} \text{ ----- Ultimate strength, A537 CL2, at } 200^{\circ}\text{F}$$
$$F_{ty} = 53.0 \text{ ksi} \text{ ----- Yield strength, A537 CL2, at } 200^{\circ}\text{F}$$

Concrete Anchor

The concrete shear area is conservatively assumed to be the perimeter of the bottom plate of the lift anchor. The shear cone in the concrete is ignored. The required anchor depth, D, is determined to be as follows.

$$D = \frac{W}{\phi 2P\sqrt{f'_c}} = \frac{177,100}{0.85 \times 2 \times 39.6 \times \sqrt{3800}} = 42.7 \text{ inch} \quad [5]$$

where:

$$W = 2 \times 88.55 \text{ kip} = 177,100 \text{ lb} \text{ ----- Anchor load}$$
$$\phi = 0.85 \text{ ----- Shear factor}$$
$$f'_c = 3800 \text{ psi} \text{ ----- Concrete strength, } 300^{\circ}\text{F}$$
$$P = 39.6 \text{ inch} \text{ ----- Perimeter of bottom plate}$$

Excluding the bottom anchor plate, the length of the anchor is 65.5 inches; therefore, the factor of safety (FS) is as follows.

$$FS = \frac{65.5}{42.7} = 1.53$$

Lift Pin

The lift pin allowable ultimate shear load (P_{usp}) for the symmetrical joint is the double shear strength of the pin.

$$P_{usp} = 1.571D_p^2 F_{sup} = 678.6 \text{ kip} \quad [10]$$

where:

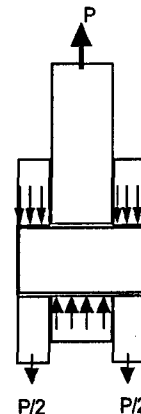
$$D_p = 4.0 \text{ inch} \text{----- Pin diameter}$$

$$F_{sup} = 0.6S_m = 0.6 \times 45.0 \text{ ksi} = 27 \text{ ksi}$$

$$S_m = 45.0 \text{ ksi} \text{----- 17-4PH stainless steel, at 200°F}$$

The load on the pin is twice the lift lug load (P); therefore, the factor of safety (FS) for the pin is as follows.

$$FS = \frac{P_{usp}}{2 \times P} = \frac{678.6}{2 \times 88.55} = 3.83 > 3.0$$



Lift Lug Bolt

The eight bolts that attach each set of the lift lugs to the embedded anchor are in tension. The tensile load is the combination of axial loads and the prying action of the lug fitting. The load per bolt (P_t) is as follows.

$$P_t = \frac{W_1}{8} = \frac{177.1}{8} = 22.1 \text{ kip}$$

where:

$$W_1 = 2 \times 88.55 = 177.1 \text{ kip} \text{----- Anchor load}$$

The tensile load (Q) on the bolt due to prying is calculated to be 2.4 kip [11].

The total load on the bolt (T) is as follows.

$$T = P_t + Q = 22.1 + 2.4 = 24.5 \text{ kip}$$

The allowable bolt tensile load is as follows.

$$T_{all} = \frac{\pi D^2 F_y}{4} = \frac{\pi \times 1.25^2 \times 144.0}{4} = 176.7 \text{ kip}$$

where:

$$F_y = 144.0 \text{ ksi} \text{----- Yield strength, SB637 Grade N07718 nickel alloy steel, at 200°F}$$

The factor of safety (FS) is as follows.

$$FS = \frac{176.7}{24.5} = 7.2$$

The bolts are threaded into the top plate of the lift anchor. The plate material is A537 Class 2 carbon steel. The bolt material is SB637 Grade N07718 nickel alloy steel. Bolt threads are 1-1/4-7 UNC 2A. For mating internal and external threads of materials having equal tensile strength, the length of engagement (L_e) is calculated as shown in the following.

$$L_e = \frac{2A_t}{3.1416(K_{n,max}) \left[\frac{1}{2} + 0.57735(n)(E_{s,min} - K_{n,max}) \right]} = 0.90 \text{ inch [12]}$$

where:

$$A_t = \pi \left(\frac{E_{s,min}}{2} - \frac{0.16238}{n} \right)^2 = 0.952 \text{ inch}^2 \text{ -- Tensile area of 1-1/4-7 UNC 2A}$$

Since the bolt and plate materials are different, the required length of engagement (Q) is calculated to be as follows.

$$Q = L_e J = 0.9 \times 1.59 = 1.43$$

where:

$$J = \frac{A_s \times S_{u \text{ bolt}}}{A_n \times S_{u \text{ plate}}} = 1.59 > 1.0$$

$$S_{u \text{ bolt}} = 177.6 \text{ ksi} \text{ ----- Ultimate strength, SB-637 Grade N07718 nickel alloy steel, at 200°F}$$

$$S_{u \text{ plate}} = 80.0 \text{ ksi} \text{ ----- Ultimate strength, A-537 Class 2 carbon steel, at 200°F}$$

The bolt thread length is 2.0 inches; therefore, the factor of safety (FS) is as follows.

$$FS = \frac{2.0}{1.43} = 1.40$$

Concrete Cask Lid Assembly Lift

The lid assembly of the concrete cask is lifted using three 3/4-10 UNC 2A threaded bolts with a 3/4-inch thread engagement in the A36 carbon steel lid. A weight of 5,000 lb is conservatively used for the evaluation of the cask lid assembly lift, which bounds the maximum weight of the lid assembly. The load per bolt (P), including dynamic load factor of 10%, is as follows.

$$P = \frac{5,000 \times 1.1}{3} = 1,834 \text{ lb}$$

The required length of engagement is calculated to be as shown in the following.

$$L_e = \frac{2A_t}{3.1416(K_{n\max}) \left[\frac{1}{2} + 0.57735(n)(E_{s\min} - K_{n\max}) \right]} = 0.54 \text{ inch [12]}$$

The factor of safety (FS) is as follows.

$$FS = \frac{0.75}{0.54} = 1.39$$

Pedestal Structural Evaluation

This section presents the structural evaluation of the pedestal during a concrete cask top-end lift. The ANSYS finite element model, presented in Section 3.1.1, is used to evaluate the concrete cask pedestal. The critical loading is during the concrete cask lift operations using the concrete cask lift anchors mounted on top of the concrete cask body.

Component Stresses

From the finite element model, the maximum stresses in the pedestal stand occur in the support rails. The critical section is the unsupported region between the pedestal stand and the inlet top. The maximum membrane stress is 16.7 ksi. The maximum membrane plus bending stress is 25.3 ksi. The factors of safety (FS) are shown as follows.

Membrane

$$FS = \frac{S_m}{\sigma_m} = \frac{19.3}{16.7} = 1.16$$

Membrane plus bending

$$FS = \frac{1.5S_m}{\sigma_{m+b}} = \frac{28.95}{25.3} = 1.14$$

where:

$$S_m = 19.3 \text{ ksi} \text{ ----- Design stress intensity, A-36 carbon steel, at } 300^\circ\text{F}$$

Pedestal Welds

The pedestal is a welded assembly. The structural welds in the pedestal are evaluated using an allowable stress of $0.6S_m$. The weld forces (F_x , F_y , and F_z) are obtained from the pedestal finite element analysis results. The total weld load (F_w) is obtained by using the square root of the sum of the squares method of the weld forces.

Support Rail to Inlet Top Weld

The support rails are welded to the inlet top with a $\frac{3}{8}$ -inch fillet weld. The stress in the weld (σ) is as follows.

$$\sigma = \frac{F_w}{A} = 9.1 \text{ ksi}$$

where:

- $F_w = 36,077 \text{ lb}$ ----- Total weld load
- $F_x = 3,248 \text{ lb}$ ----- Weld force, X-direction
- $F_y = 32,351 \text{ lb}$ ----- Weld force, Y-direction
- $F_z = -15,633 \text{ lb}$ ----- Weld force, Z-direction
- $A = 3.95 \text{ inch}^2$ ----- Area
- $l_w = 8.95 \text{ inches}$ ----- Weld length
- $t_w = \frac{3}{8}\text{-inch}$ ----- Weld size

The factor of Safety (FS) is as follows.

$$FS = \frac{0.6S_m}{\sigma} = 1.27$$

where:

- $S_m = 19.3 \text{ ksi}$ ----- Design stress intensity, A-36 carbon steel, 300°F

Inlet Top to Inlet Side Weld

The inlet top is welded to the inlet side with a $\frac{1}{8}$ -inch fillet weld plus a $\frac{1}{4}$ -inch groove weld. The stress in the weld is as follows.

$$\sigma = \frac{F_w}{A} = \frac{34,099}{8.03} = 4.2 \text{ ksi}$$

where:

$$\begin{aligned}
 F_w &= 34,099 \text{ lb} \text{ ----- Total weld load} \\
 F_x &= 10,437 \text{ lb} \text{ ----- Weld force, X-direction} \\
 F_y &= -32,351 \text{ lb} \text{ ----- Weld force, Y-direction} \\
 F_z &= -2,685 \text{ lb} \text{ ----- Weld force, Z-direction} \\
 A &= l_w \times t_w = 8.03 \text{ inch}^2 \text{ ----- Area} \\
 l_w &= 30.9 \text{ inches} \text{ ----- Weld length} \\
 t_w &= ((0.125 + 0.25) \times .707) = 0.26 \text{ inch} \text{ ---- Weld size}
 \end{aligned}$$

The factor of Safety (FS) is as follows.

$$FS = \frac{0.6S_m}{\sigma} = \frac{0.6 \times 19.3}{4.2} = 2.76$$

where:

$$S_m = 19.3 \text{ ksi} \text{ ----- Design stress intensity, A-36 carbon steel, at } 300^\circ\text{F}$$

Inlet Side to Base Plate Weld

The critical section of the inlet side to base plate weld is the 8.25-inch segment at the inner end of the inlet. The weld is a ¼-inch groove weld. The stress in the weld is as follows.

$$\sigma = \frac{F_w}{A} = 9.9 \text{ ksi}$$

where:

$$\begin{aligned}
 F_w &= \sqrt{F_x^2 + F_y^2 + F_z^2} = 20,484 \text{ lb} \\
 F_x &= 270 \text{ lb} \text{ ----- Weld force, X-direction} \\
 F_y &= 20,459 \text{ lb} \text{ ----- Weld force, Y-direction} \\
 F_z &= -971 \text{ lb} \text{ ----- Weld force, Z-direction} \\
 A &= l_w \times t_w = 2.06 \text{ inch}^2 \\
 l_w &= 8.25 \text{ inches} \text{ ----- Weld length} \\
 t_w &= 0.25 \text{ inch} \text{ ----- Weld size}
 \end{aligned}$$

The factor of safety (FS) is as follows.

$$FS = \frac{0.6S_m}{\sigma} = \frac{0.6 \times 19.3}{9.9} = 1.17$$

where:

$$S_m = 19.3 \text{ ksi} \text{----- Design stress intensity, A-36 carbon steel, at } 300^\circ\text{F}$$

Support Rail Gusset to Support Rail Weld

The rail gusset weld is a 5/8-inch fillet weld. The stress in the weld is as follows.

$$\sigma = \frac{F_w}{A} = 2.5 \text{ ksi}$$

where:

$$F_w = \sqrt{F_x^2 + F_y^2 + F_z^2} = 4,915 \text{ lb}$$

$$F_x = 2,224 \text{ lb} \text{----- Weld force, X-direction}$$

$$F_y = -1,636 \text{ lb} \text{----- Weld force, Y-direction}$$

$$F_z = -4,066 \text{ lb} \text{----- Weld force, Z-direction}$$

$$A = l_w \times (t_w \times 0.707) = 1.97 \text{ inch}^2$$

$$l_w = 4.45 \text{ inches} \text{----- Weld length}$$

$$t_w = 5/8\text{-inch} \text{----- Weld size}$$

The factor of safety (FS) is as follows.

$$FS = \frac{0.6S_m}{\sigma} = 4.63$$

where:

$$S_m = 19.3 \text{ ksi} \text{----- Design stress intensity, A-36 carbon steel, at } 300^\circ\text{F}$$

Nelson Studs

During a top-end concrete cask lift, the Nelson studs transmit the weight of a loaded TSC to the concrete cask. The liner is not directly attached to the pedestal. The ability of the Nelson studs to transfer load to the concrete cask is based upon the compressive strength of the concrete.

Using ACI 349-85 [5], the maximum pullout strength of the concrete is defined by the equation

$$P_d = 4 \times \phi \times \sqrt{f'_c} \times A_{cd}$$

where:

$$\begin{aligned}\phi &= 0.85 \text{ ----- Strength reduction factor} \\ f_c &= 3,800 \text{ psi ----- Concrete compression strength, } 300^\circ\text{F} \\ A_{cd} &= \text{Projected cone area of Nelson stud less head area}\end{aligned}$$

The projected area of a single Nelson stud is calculated by creating a cone that projects 45° from the head of the Nelson stud and omits the projected area of the Nelson stud head.

For a 0.75-inch diameter, 6.0-inch long Nelson stud, the projected area is as follows.

$$A_{cd} = \pi(l_c(l_c + d_h)) = 116.6 \text{ inch}^2$$

where:

$$\begin{aligned}l_c &= 5.5 \text{ inches ----- Bolt length} \\ d_h &= 1.25 \text{ inches ----- Head diameter}\end{aligned}$$

For a single Nelson stud, the allowable concrete pullout strength is as follows.

$$P_d = 4 \times 0.85 \times \sqrt{3800} \times 116.6 = 24,438 \text{ lb}$$

The maximum load on a Nelson stud is 17,145 lb; therefore, the factor of safety (FS) is as follows.

$$FS = \frac{P_d}{F} = \frac{24,438}{17,145} = 1.43$$

The geometry of the four Nelson studs on the inlet top plate is such that the projected cones intersect each other. The combined projected area (A_{cd}) is 332 inches². The total load on the four Nelson studs is 18,817 pounds. The allowable concrete pullout strength (P_{cd}) is as follows.

$$P_{cd} = 4 \times 0.85 \times \sqrt{3800} \times 332.0 = 69,584 \text{ lb}$$

The factor of safety (FS) is as follows.

$$FS = \frac{P_{cd}}{F} = \frac{69,584}{18,817} = 3.70$$

The maximum stress in a Nelson stud is as follows.

$$\sigma = \frac{F}{A_s} = 39.0 \text{ ksi}$$

where:

$$A_s = \frac{\pi}{4} D^2 = 0.44 \text{ inch}^2$$

The factor of safety (FS) is as follows.

$$FS = \frac{S_u}{\sigma} = \frac{58.0}{39.0} = 1.49$$

where:

$$S_u = 58.0 \text{ ksi} \text{ ----- Ultimate strength, A-36 carbon steel, at } 300^\circ\text{F}$$

3.4.3.2 TSC Lift

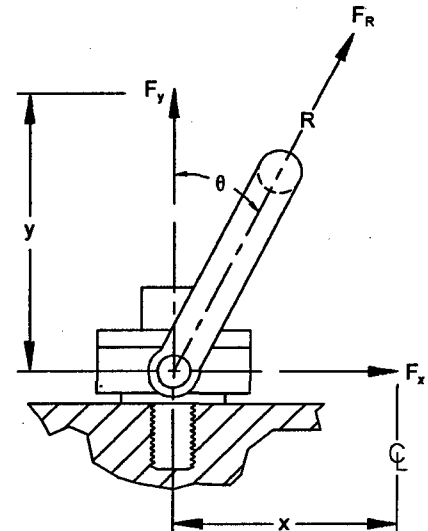
The adequacy of the TSC lifting components is demonstrated by evaluating the hoist rings, the TSC closure lid, and the weld that joins the closure lid to the TSC shell against the criteria in NUREG-0612 [3] and ANSI N14.6 [2]. The lifting configuration for the TSC consists of six hoist rings threaded into the closure lid assembly at equally spaced angular intervals. The hoist rings are analyzed as a redundant system with two three-legged lifting slings. For redundant lifting systems, ANSI N14.6 requires that load-bearing members be capable of lifting three times the load without exceeding the yield strength of the material and five times the load without exceeding the ultimate strength of the material. The closure lid is evaluated for lift conditions as a redundant system that demonstrates a factor of safety greater than three based on yield strength and a factor of safety greater than five based on ultimate strength. The TSC lift analysis is based on a load of 120,000 lb, which bounds the weight of the heaviest loaded TSC configuration. A dynamic load factor of 10% is considered in the analysis.

Hoist Ring and Sling Evaluation

The TSC lift configuration is shown in the accompanying sketch. The vertical component force on the hoist ring, assuming a 10% dynamic load factor, is as follows.

$$F_y = \frac{120,000 \text{ lb} \times 1.1}{3 \text{ lift points}} = 44,000 \text{ lb}$$

As shown in the sketch, x is the distance from the TSC centerline to the hoist ring centerline (20.5 inch); F_x is the



horizontal component of force on the hoist ring; R is the sling length; F_R is the maximum allowable force on the hoist ring; and the angle θ is the angle from vertical to the sling.

The hoist rings are rated at 50,000 lb with a safety factor of five on ultimate strength. Calculating the maximum angle (θ) that will limit F_R to 50,000 pounds is as follows.

$$\theta = \cos^{-1}\left(\frac{F_y}{F_R}\right) = \cos^{-1}\left(\frac{44,000}{50,000}\right) = 28.4^\circ$$

The minimum sling length, R, is as follows.

$$R = \frac{x}{\sin \theta} = \frac{20.5}{\sin 28.4} = 43.1 \text{ inches}$$

A 50-inch sling places the lift hook about 44 inches above the top of the TSC ($y = R \cos \theta = 50 \cos 28.4^\circ = 44$ inches).

Bolt Shear

From the Machinery's Handbook [12], the shear stress (τ) in the hoist ring hole threads (2½-4-UNC) in the closure lid is calculated as follows.

$$\tau = \frac{F_y}{A_n} = \frac{44,000 \text{ lb}}{12.148 \text{ in}^2} = 3,622 \text{ psi}$$

where:

$$A_n = 12.148 \text{ inch}^2 \text{ ----- Shear area of the closure lid assembly threads based on a length of engagement of 2.0 inches.}$$

The TSC closure lid is constructed of SA240, Type 304 stainless steel. Using shear allowables of 0.6 S_y and 0.5 S_u at a temperature of 300°F, the shear stress factors of safety are as follows.

Yield:

$$FS_y = \frac{0.6 \times 22,400 \text{ psi}}{3,622 \text{ psi}} = 3.7 > 3$$

Ultimate:

$$FS_u = \frac{0.5 \times 66,200 \text{ psi}}{3,622 \text{ psi}} = 9.1 > 5$$

The criteria of NUREG-0612 and ANSI N14.6 for redundant systems are met and the minimum thread engagement length of 2.0 inches is adequate.

The weight of the heaviest loaded transfer cask is less than 230,000 pounds. Three times the bounding weight of the loaded TSC is $(3 \times 120,000)$ 360,000 lb, which is greater than the weight of the heaviest transfer cask plus the weight of the loaded TSC (108,500 + 102,500 lb).

Consequently, the preceding analysis bounds the inadvertent lift of the transfer cask during the handling of the TSC.

TSC Lift Evaluation

The structural adequacy of the TSC closure lid assembly and weld is evaluated using a finite element model described in Section 3.10.3. During a TSC lift, the acceleration due to gravity, with a dynamic load factor of 10%, is applied to the fully loaded TSC in the vertical direction. The maximum nodal stress intensity experienced by the various TSC components during a three-point lift is as follows.

Component Description	Nodal Stress (psi)
TSC Shell (below Closure Lid Weld)	1,516
Closure Lid Weld	1,481

The TSC shell and closure lid are constructed of SA240, Type 304 stainless steel. The yield strength is 18,000 psi and the ultimate strength is 63,400 psi. These are conservatively evaluated at a temperature of 650°F. The strength of the weld joint is taken as the same as the strength of the base material. Thus, when compared to the yield and ultimate strengths, the maximum nodal stress intensity of 1,516 psi produces the following factors of safety for a three-point lift.

Yield:

$$FS_y = \frac{\text{yield strength}}{\text{maximum nodal stress intensity}} = \frac{18,000 \text{ psi}}{1,516 \text{ psi}} = 12 > 3$$

Ultimate:

$$FS_u = \frac{\text{ultimate strength}}{\text{maximum nodal stress intensity}} = \frac{63,400 \text{ psi}}{1,516 \text{ psi}} = 42 > 5$$

The criteria of NUREG-0612 and ANSI N14.6 for nonredundant systems are met. Thus, the TSC shell and closure lid are adequate.

3.4.3.3 Transfer Cask Lift

The MAGNASTOR transfer cask is analyzed for loads associated with the heavy lift requirements specified in ANSI N14.6 [2] and NUREG-0612 [3]. All load path components of the cask are evaluated for structural adequacy. The transfer cask is analyzed for loads associated with the vertical lift of the transfer cask. The transfer cask is not designed for redundant lifting; therefore, factors of safety of six on material yield strength and ten on material ultimate strength are required for the lifting trunnions.

The analysis of the fully loaded transfer cask consists of a finite element analysis using the ANSYS program to calculate the stress in the transfer cask forgings, shells, and the trunnion region for the operational vertical lift condition. Details of the ANSYS finite element model are presented in Section 3.10.5. The structural evaluations of the rail, the shield door, and the rail welds are performed using standard engineering equations. The design weight of the transfer cask is 230,000 pounds. A bounding weight of the transfer cask of 240,000 lb is considered in the evaluation. A conservative load of 264,000 lb ($240,000 \times 1.1$ dynamic load factor) is used in the finite element analysis.

Transfer Cask Body

Table 3.4-1 provides the summaries of the stress intensities for the seven cross-sectional locations of the trunnion and top ring. Table 3.4-2 provides the stress summaries for the inner and outer shells and bottom ring. The maximum primary membrane, P_m , and the maximum primary membrane plus bending stress, $P_m + P_b$, is compared with the allowable stress criteria.

The cross-section of the trunnion is circular. Two cross-sectional areas are examined as shown in Figure 3.4-1. The maximum bending stress occurs at the cross-section ($x = 43.9$ inches) at the intersection of the trunnions with the outer diameter of the top forging ring. The maximum stress occurs at the trunnion surface. The maximum stress in the trunnion is 3.8 ksi. Comparing the stress to the material (A350 Grade LF 2) allowable yield and ultimate strength, the factors of safety are 8.1 (>6) for material yield strength and 18.5 (>10) for material ultimate strength.

For the top ring, the five cross-sectional areas selected for stress examination are shown in Figure 3.4-1. The maximum bending plus membrane stress occurs at the radial cross-section (topring-A1) above the trunnion. The bending stress through this cross-sectional area is 4.9 ksi. Comparing the stress to the material (A516 Gr 70) allowable yield and ultimate strength, the factors of safety are 6.6 (>6) and 14.2 (>10) for yield and ultimate material strengths, respectively.

For the inner shell, the maximum stress intensity occurs at the location of " $\theta = 10^\circ$, $z = -7.0$ inches", which is outside the intersection just below the trunnion. The maximum bending plus membrane stress through the shell is 2.3 ksi. Comparing the stress to the material (A588) allowable yield and ultimate strengths, the factors of safety are 18.6 (>6) and 30.2 (>10), respectively.

For the outer shell, the maximum stress intensity occurs at the location of " $\theta = 10^\circ$, $z = -7.0$ inches", which is outside the intersection just below the trunnion. The maximum bending plus membrane stress in the shell thickness is 3.5 ksi. Comparing the stress to the material (A588) allowable yield and ultimate strengths, the factors of safety are 12.3 (>6) and 20 (>10), respectively.

For the bottom ring the maximum stress intensity occurs at the nodal location of " $\theta = 90^\circ$, $z = -173.5$ inches", which is just below the inner and outer shells. The maximum bending plus membrane stress in the ring thickness is 0.7 ksi. Comparing the stress to the material (A588) allowable yield and ultimate strengths, the factors of safety are 58 (>6) and 94 (>10) for yield and ultimate strength, respectively.

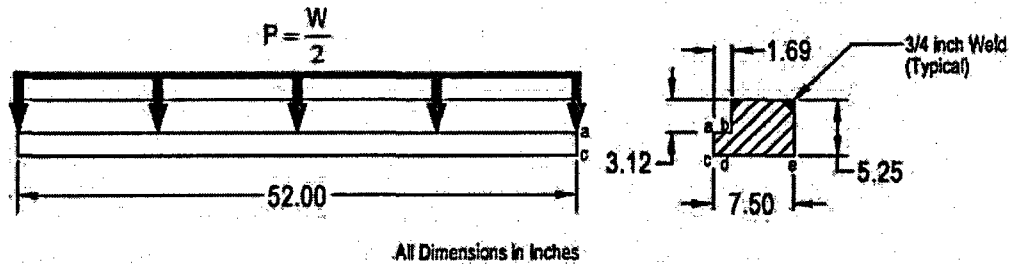
Transfer Cask Shield Door Rails and Welds

This section demonstrates the adequacy of the transfer cask shield doors, door rails, and welds in accordance with NUREG-0612 and ANSI N14.6, which require safety factors of six and ten on material yield strength and ultimate strength, respectively, for nonredundant lift systems. The transfer cask shield doors and door rails are designed to retain and support the maximum loaded TSC weight of 118,000 lb, which includes the weight of basket, fuel, and water. The shield doors are 5-inch thick plates that slide on the door rails. The rails are 7.50-inches wide \times 52-inches long and are welded to the bottom ring of the transfer cask. The doors and the rails are constructed of A-588 and SA-350 Grade LF 2 low alloy steel, respectively.

A weight of 143,000 lb ($>118,000 \times 1.1$) is conservatively used for the evaluation of the rails. This weight bounds the weight of the heaviest loaded TSC, the weight of the water in the TSC, and the weight of the shield doors and rails. The 10% dynamic load factor is included to ensure that the evaluation bounds all normal operating conditions. Allowable stresses for the component materials are taken at 400°F, which bounds the maximum temperature at the bottom of the transfer cask under normal conditions.

Stress Evaluation for Door Rail

Each rail is assumed to carry one-half of the load.



The shear stress (τ) in each door rail bottom plate (section b-d) due to the applied load is as follows.

$$\tau = \frac{P}{A} = \frac{143.0/2}{110.8} = 0.65 \text{ ksi}$$

where:

$$A = (5.25 - 3.12) \times 52 = 110.8 \text{ inch}^2 \text{----- Shear area}$$

The bending stress (σ_b) in each rail bottom section b-d due to the applied load, P, is as follows.

$$\sigma_b = \frac{6M}{Lt_{a-c}} = 3.1 \text{ ksi}$$

where:

- $M = P \times L_{a-b} = 120.8 \text{ inch-kip}$
- $L_{a-b} = 1.69 \text{ inches}$ ----- Applied load moment arm
- $L = 52 \text{ inches}$ ----- Length of the rail
- $t_{a-c} = 2.13 \text{ inches}$ ----- Thickness of the rail

The maximum stress (σ) intensity in the bottom section of the rail is as follows.

$$\sigma = \sqrt{(\sigma_b)^2 + 4\tau^2} = 3.4 \text{ ksi}$$

The factor of safety (FS) based on the material yield strength is as follows.

$$FS = \frac{S_y}{\sigma} = \frac{30.8 \text{ ksi}}{3.4 \text{ ksi}} = 9.1 > 6$$

where:

$$S_y = 30.8 \text{ ksi} \text{----- Yield strength for A350 Grade LF 2, at } 400^\circ\text{F}$$

The factor of safety (FS) based on the material ultimate strength is as follows.

$$FS = \frac{S_u}{\sigma} = \frac{70 \text{ ksi}}{3.4 \text{ ksi}} = 20.6 > 10$$

where:

$$S_u = 70.0 \text{ ksi} \text{----- Ultimate strength A-350 Grade LF 2, at } 400^\circ\text{F}$$

Stress Evaluation for the Shield Doors

The shield doors are 5-inches thick at the center and step down to 2.94-inches thick at the edges, where they rest on the rails. The stepped edges of the two door leaves are designed to interlock at the center. Therefore, the doors are analyzed as single simply supported plates. The engagement length of the door with the rail is 52 inches. The shear stress (τ) at the edge of the shield door where the door contacts the rail is as follows.

$$\tau = \frac{P}{A_s} = 0.94 \text{ ksi}$$

where:

$$A_s = t_d \times L = 152.9 \text{ inch}^2 \text{----- Total shear area}$$

$$t_d = 5.0 - 2.06 = 2.94 \text{ inches} \text{----- Thickness of the door at edge}$$

$$L = 52 \text{ inches} \text{----- Length of door and rail engagement}$$

The maximum bending stress (σ_b) at the center of the doors is as follows.

$$\sigma_b = \frac{Mc}{I} = 4.0 \text{ ksi}$$

where:

$$M = \frac{WL}{8} = 1.36 \times 10^6 \text{ inch-lb}$$

$$W = 143,000 \text{ lb} \text{----- Total weight}$$

$$c = \frac{h}{2} = 2.5 \text{ inches} \text{----- Distance to surface}$$

$$I = \frac{bh^3}{12} = 855 \text{ inch}^4 \text{----- Cross-sectional moment of inertia}$$

$$L = 76 \text{ inches} \text{----- Span length}$$

The maximum stress intensity (σ) in the door is as follows.

$$\sigma = \sqrt{(\sigma_b)^2 + 4\tau^2} = 4.1 \text{ ksi}$$

The factor of safety (FS) based on the yield strength is as follows.

$$FS = \frac{S_y}{\sigma} = \frac{43 \text{ ksi}}{4.1 \text{ ksi}} = 10.5 > 6$$

where:

$$S_y = 43 \text{ ksi} \text{ ----- Yield strength for A-588, at } 400^\circ\text{F}$$

The factor of safety (FS) based on the ultimate strength is as follows.

$$FS = \frac{S_u}{\sigma} = \frac{70 \text{ ksi}}{4.1 \text{ ksi}} = 17.1 > 10$$

where:

$$S_u = 70.0 \text{ ksi} \text{ ----- Ultimate strength for A-588, at } 400^\circ\text{F}$$

Door Rail Weld Evaluation

The door rails are attached to the bottom forging of the transfer cask by 0.75-inch partial penetration bevel groove welds that extend the full length of the inside and outside of each rail. The loaded TSC weight is conservatively assumed to act at a point on the inside edge of the rail. Since the base metal is the limiting strength of the welded section, the ultimate strength on the inner weld is evaluated. Summing moments about the edge of outer weld are as follows.

$$\Sigma M = 0 = P \times L_{c-e} - F_w \times \left(L_{d-e} - \frac{L_w}{2} \right) \Rightarrow F_w = 91 \text{ kip}$$

where:

$$P = \frac{W}{2} = 71.5 \text{ kip} \text{ ----- Load on a single rail}$$

$$L_w = 0.75 \text{ inch} \text{ ----- Weld length}$$

$$L_{d-e} = 7.5 - 1.69 = 5.81 \text{ ----- Distance from edge of inner weld to edge of outer weld}$$

$$L_{c-e} = 7.5 \text{ inches} \text{ ----- Width of the rail}$$

The maximum stress (σ) in the base metal attached by the inner weld is as follows.

$$\sigma = \frac{F_w}{A_w} = 2.3 \text{ ksi}$$

where:

$$A_w = 0.75 \times 52 = 39 \text{ inch}^2 \text{ ----- Area on the base metal supporting inner weld}$$

The factor of safety (FS) based on the yield strength is as follows.

$$FS = \frac{43 \text{ ksi}}{2.3 \text{ ksi}} = 18.7 > 6$$

The factor of safety (FS) based on the ultimate strength is as follows.

$$FS = \frac{70 \text{ ksi}}{2.3 \text{ ksi}} = 30.4 > 10$$

Trunnion Bearing Stress Evaluation

During a vertical lifting load case, the transfer cask is being lifted by the trunnions.

The load on each trunnion is 132 kips ($240 \times 1.1/2$). The minimum trunnion bearing engagement depth is 7.5-inches, but only 50% of this is used in the evaluation. The diameter of the trunnion is 9 inches. The bearing stress on the trunnion (σ_b) is as follows.

$$\sigma_{brg} = \frac{W_{VL}}{A_{brg}} = \frac{132}{33.75} = 3.92 \text{ ksi}$$

The factor of safety (FS) is as follows.

$$FS = \frac{S_y}{\sigma} = \frac{30.8}{3.92} = 7.85$$

where:

$$S_y = 30.8 \text{ ksi} \text{ ----- Yield strength, SA-350 LF2, at } 400^\circ\text{F}$$

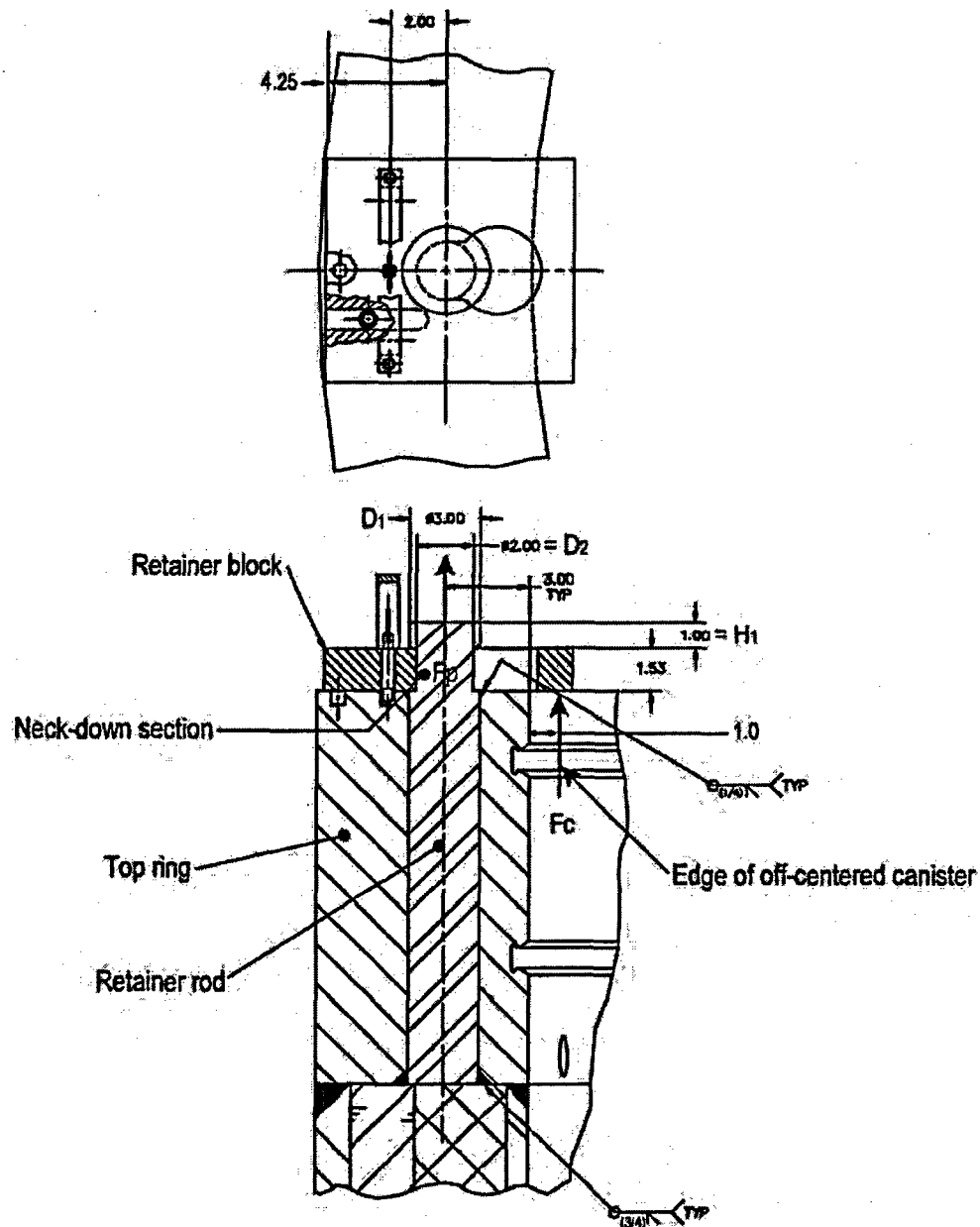
Inadvertent Lift of Transfer Cask by TSC

The inadvertent lift of the transfer cask by the TSC is considered an off-normal event. The stresses associated with this condition are required to satisfy allowable stress limits for ASME Boiler and Pressure Vessel Code, Service Level C condition. The temperature of the cask at the top is assumed to be 300°F.

In the event the transfer cask is lifted by the TSC during handling operations, instead of by the transfer cask trunnions, the weight of the transfer cask is supported by the three retaining blocks mounted on top of the transfer cask top ring. In this case, the retaining blocks must have sufficient strength to support the weight of the transfer cask. The three retaining blocks on the top-forging ring are spaced 120° apart.

Retainer Rod Evaluation

During an inadvertent lift of the transfer cask, the retainer rod is subjected to a tensile load, F_p , due to the prying action of the retaining block. The top view and the side view of the retaining block are shown in the following sketches.



A conservative weight of 110,000 lb is used for this evaluation. This weight bounds the maximum weight of the transfer cask. The dynamic load factor, DLF, is 1.1. The maximum uplifting force applied by the TSC to the retainer block, F_c , is 110 kip $(1.1)/3 = 40.3$ kip. When the TSC is off-center, the maximum distance between the TSC outer edge and the inner edge of the transfer cask is one inch. The prying force applied to the retainer rod (F_p) is as follows.

$$F_p = \frac{40.3 \times (1 + 3 + 4.25)}{4.25} = 78.2 \text{ kip}$$

Effective Stress Areas of Retainer Rod

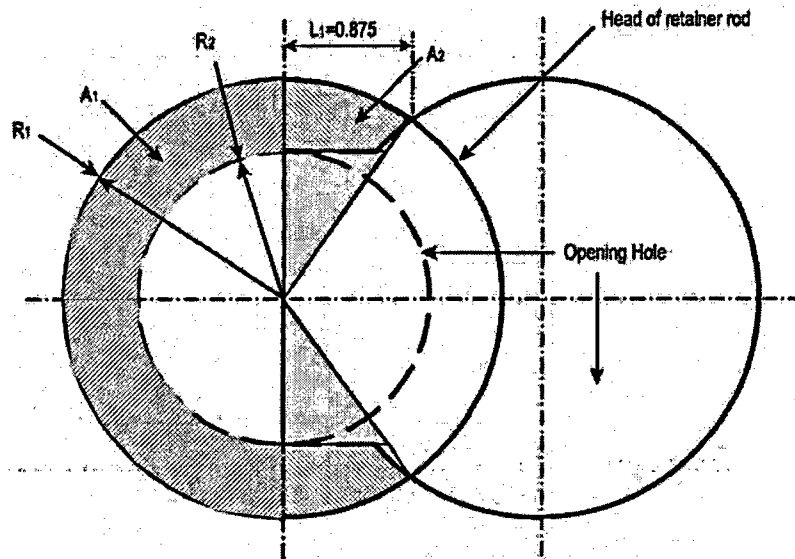
Referring to the previous sketch, the cross-sectional areas for the retainer rod evaluation are as follows.

$$A_t = \frac{\pi}{4} D_2^2 = 3.14 \text{ inch}^2 \text{----- Tensile area (neck down area)}$$

$$A_{ws} = \pi D_1 H_w = 7.07 \text{ inch}^2 \text{----- Weld shear area}$$

$$A_{sh} = \pi D_2 H_1 = 6.28 \text{ inch}^2 \text{----- Head shear area (through head thickness)}$$

The bearing area in the retainer rod just above the neck-down area is the hatched area as shown in the following sketch.



The total bearing area (A_{brg}) is as follows.

$$A_{brg} = 2(A_1 + A_2) = 2(0.982 + 0.342) = 2.648 \text{ inch}^2$$

Retainer Rod Load Capacity:

The load capabilities of the retainer rod are calculated in the following.

$$F_{tensile} = (A_t)(S_M) = (3.14)(26.9) = 84.4 \text{ kip} \text{----- Load capability at D2}$$

$$F_{ws} = (A_{ws})(S_S) = (7.07)(13.4) = 94.7 \text{ kip} \text{----- Shear capability of weld}$$

$$F_{brg} = (A_{brg})(S_{brg}) = (2.648)(33.6) = 88.9 \text{ kip} \text{----- Bearing capability of rod head}$$

$$F_{sh} = (A_{sh})(S_S) = (6.28)(13.4) = 84.2 \text{ kip} \text{----- Shear capability under rod head}$$

where:

$$S_M = 1.2 S_m = 1.2 (22.4) = 26.9 \text{ ksi}$$

$$S_S = 0.6 S_m = 0.6 (22.4) = 13.4 \text{ ksi}$$

$$S_{brg} = S_y = 33.6 \text{ ksi}$$

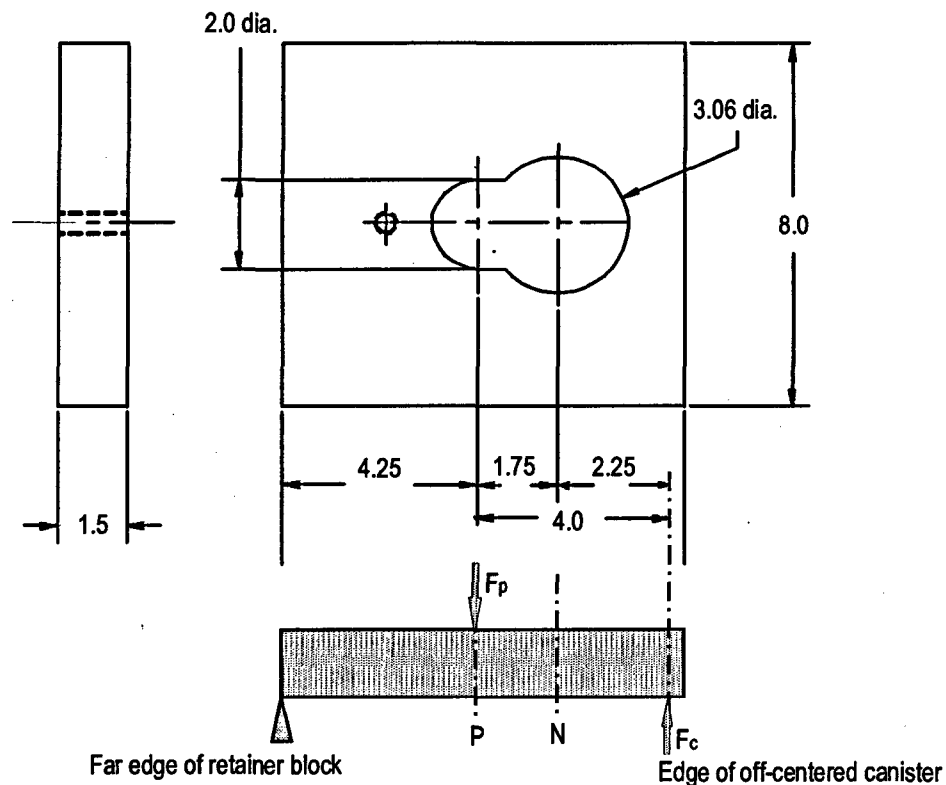
$S_y = 33.6$ ksi ----- Yield strength, SA-516 Grade 70 at 300°F
 $S_m = 22.4$ ksi ----- Design stress intensity, SA-516 Grade 70 at 300°F

The minimum factor of safety (FS) is as follows.

$$FS = \frac{F_{sh}}{F_p} = \frac{84.2}{78.2} = 1.08$$

Retainer Block Evaluation

The retainer block and the force-loading diagram are shown in the following sketch.



Point P is where the headed retainer rod is loaded under prying force F_p . The maximum bending stress (σ_b) in the retainer block is as follows.

$$\sigma_b = \frac{Mc}{I} = 71.6 \text{ ksi}$$

where:

$$M = F_c(4) = 161.2 \text{ kip-inch}$$

$$F_c = 40.3 \text{ kip}$$

$$I = \frac{bh^3}{12} = 1.688 \text{ inch}^4$$

$$C = 0.75 \text{ inch}$$

The factor of safety (FS) is as follows.

$$FS = \frac{1.8S_m}{\sigma_b} = 1.13$$

where:

$$S_m = 45.0 \text{ ksi} \text{ ----- Yield strength, 17-4 PH at } 300^\circ\text{F}$$

Figure 3.4-1 Top Ring Section Cuts

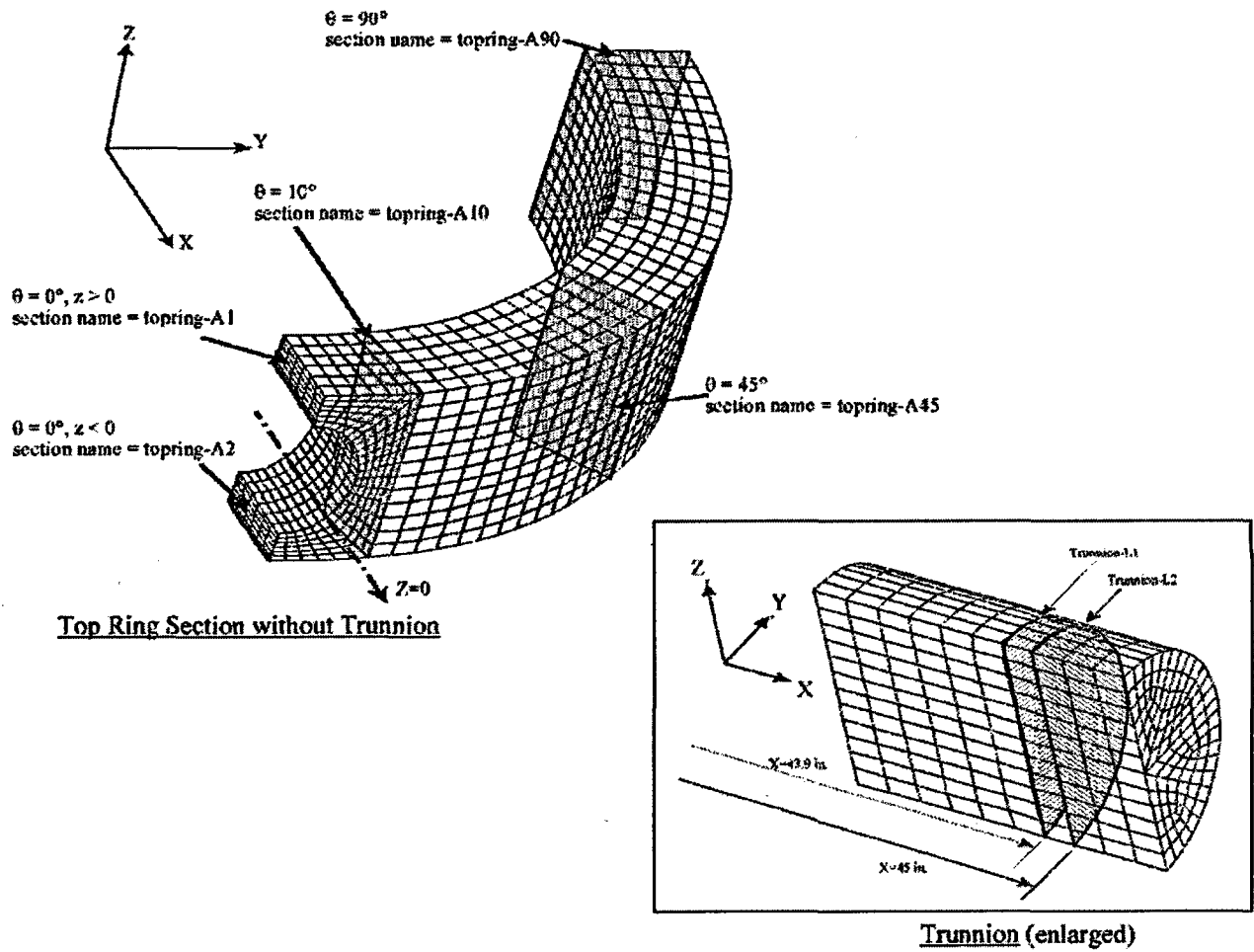


Table 3.4-1 Stresses for Trunnions and Top Ring

Location ^a	Position ^a	P _m ^b ksi	P _b ^b ksi	P _m + P _b ^b ksi	Material	S _{yield} ksi	S _{ultimate} ksi	FS _{Yield}	FS _{Ultimate}
Trunnion-L1	x = 43.9 inch	0.04	3.75	3.79	SA350	30.8	70.0	8.1	Large
Trunnion-L2	x = 45 inch	0.00	2.05	2.05	SA350	30.8	70.0	Large	Large
TopRing-A1	θ = 0°, z > 0	2.37	2.57	4.93	SA516	32.5	70.0	6.6	Large
TopRing-A2	θ = 0°, z < 0	0.33	1.29	1.63	SA516	32.5	70.0	Large	Large
TopRing-A10	θ = 10°	0.07	1.02	1.09	SA516	32.5	70.0	Large	Large
TopRing-A45	θ = 45°	0.11	0.84	0.95	SA516	32.5	70.0	Large	Large
TopRing-A90	θ = 90°	0.11	0.75	0.86	SA516	32.5	70.0	Large	Large

Table 3.4-2 Stresses for Transfer Cask Shells and Bottom Ring

Location ^c	Position ^c	P _m + P _b ^d ksi	Material	S _{yield} ksi	S _{ultimate} ksi	FS _{Yield}	FS _{Ultimate}
Inner Shell	θ = 10°, z=-7 inch	2.32	A588	43.0	70.0	Large	Large
Outer Shell	θ = 10°, z=-7 inch	3.50	A588	43.0	70.0	Large	Large
Bottom Ring	θ = 90°, z=-173.5	0.74	A588	43.0	70.0	Large	Large

^a The locations and positions are defined in Figure 3.4-1.

^b P_m = primary membrane stress; P_b = primary bending stress; P_m + P_b = primary membrane + bending stress

^c The locations and positions correspond to the axis shown in Figure 3.10.5-1, Section 3.10.5.

^d P_m + P_b = primary membrane + bending stress

3.5 Normal Operating Conditions

This section presents the analyses of the major structural components of MAGNASTOR for normal conditions of storage. The TSC, fuel baskets, and concrete cask are evaluated using finite element models and classical hand calculations.

3.5.1 TSC Evaluation for Normal Operating Conditions

For normal conditions of storage, the TSC is evaluated using ASME Code, Section III, Subsection NB 'Service Level A' allowable stresses. For detailed analysis results for normal conditions, see Table 3.10.3-1 through Table 3.10.3-6.

3.5.1.1 TSC Thermal Stress Analysis

The thermal stresses in the TSC during normal conditions of storage are evaluated using a finite element model described in Section 3.10.3. The thermal gradient applied to the TSC model bounds all conditions of storage; therefore, the results presented are conservative. The resulting maximum (secondary) thermal stresses in the TSC are shown in Table 3.5-1. The locations of the stress sections are shown in Figure 3.10.3-2 in Section 3.10.3.

3.5.1.2 TSC Dead Load

The TSC is analyzed for a dead load using the finite element model described in Section 3.10.3. The normal handling plus normal pressure conditions presented in Section 3.5.1.5 bound the resulting maximum TSC dead load stresses; therefore, results for the dead load analysis are not presented separately.

3.5.1.3 TSC Maximum Internal Pressure

The TSC is analyzed for a maximum internal pressure load using the finite element model described in Section 3.10.3. A maximum internal pressure of 110 psig is applied as a surface load to the elements along the internal surface of the TSC shell, bottom plate, and closure lid. This pressure bounds the maximum calculated pressure for PWR and BWR fuel under normal conditions.

The resulting maximum internal pressure load stresses for the TSC are summarized in Table 3.5-2 and Table 3.5-3 for primary membrane and primary membrane plus primary bending stress categories, respectively. The locations for the stress sections are shown in Figure 3.10.3-2 in Section 3.10.3.

3.5.1.4 TSC Handling Loads

The TSC is analyzed for handling loads using the finite element model described in Section 3.10.3. Normal handling is simulated by constraining the model at nodes on the closure lid simulating three lift points. A 1.1g acceleration load, which corresponds to the dead weight with a 10% dynamic load factor, is applied to the model in the axial direction. Pressure is applied to the TSC bottom plate to simulate the weight of the basket and fuel with an acceleration of 1.1g.

The resulting maximum stresses in the TSC due to handling loads are bounded by the maximum stresses for the normal handling loads plus normal pressure condition presented in Section 3.5.1.5; therefore, the stress results for the handling condition are not presented separately.

The lift lugs are evaluated for dead weight using classical methods. The TSC lift lugs are welded to the inner surface of the TSC shell to accommodate handling of the empty TSC and to support the closure lid prior to completion of the weld to the shell. The total weight, W, imposed on the lift lugs conservatively considers the weight of the closure lid and supplemental support equipment. A 10% load factor is also applied to ensure all normal operating loads are bounded. The stresses evaluated for the lift lugs are bearing stress and shear stress through the weld. The bearing stress is as follows.

$$\sigma_{\text{bearing}} = \frac{W}{4A} = \frac{22,550 \text{ lb}}{21.6 \text{ in}^2} = 1,044 \text{ psi}$$

where:

$$W = (10,500 \text{ lb} + 10,000 \text{ lb}) \times 1.1 = 22,550 \text{ lb}$$
$$A = 5.4 \text{ inch}^2 \text{----- Area of lifting lug}$$

Using a conservative temperature of 650°F, the factor of safety (FS) is as follows.

$$FS = \frac{1.0 S_y}{\sigma_{\text{bearing}}} = \frac{19,400 \text{ psi}}{1,044 \text{ psi}} = \text{Large}$$

where:

$$S_y = 19,400 \text{ psi} \text{----- Yield strength of SA-240, Type 304 stainless steel}$$

The attachment weld for the lift lugs is a 1/8-inch double-bevel weld. The shear stress (τ_w) is as follows.

$$\tau_w = \frac{W}{4A_{\text{eff}}} = \frac{22,550 \text{ lb}}{5.40 \text{ in}^2} = 4,176 \text{ psi}$$

where:

$$A_{\text{eff}} = L_{\text{eff}} \times t_{\text{eff}} = 1.35 \text{ inch}^2 \text{ ----- Area of lifting lug weld}$$

$$L_{\text{eff}} = 5.4 \times = 10.8 \text{ inches ----- Length of lifting lug weld}$$

$$t_{\text{eff}} = 0.125 \text{ inch ----- Thickness of lifting lug weld}$$

Conservatively using the temperature of 650°F and material allowables of the base metal, the factor of safety (FS) is as follows.

$$FS = \frac{S_{\text{allow}}}{\tau_w} = \frac{0.6 S_m}{\tau_w} = \frac{9,720 \text{ psi}}{4,176 \text{ psi}} = 2.3$$

where:

$$S_{\text{allow}} = 0.6 S_m \text{ ----- Weld allowable}$$

$$S_m = 16,200 \text{ psi ----- Design stress intensity of SA-240, Type 304 stainless steel}$$

3.5.1.5 TSC Load Combinations

The TSC is structurally analyzed for combined thermal, dead, maximum internal pressure, and handling loads using the finite element model described in Section 3.10.3.

The resulting maximum stresses in the TSC for combined loads are summarized in Table 3.5-2, Table 3.5-3, and Table 3.5-4 for primary membrane, primary membrane plus primary bending, and primary plus secondary stresses, respectively. The sectional stresses at 15 locations are evaluated for each angular division of the model. The locations for the stress sections are shown in Figure 3.10.3-2, Section 3.10.3.

As shown in Table 3.5-2 through Table 3.5-4, the TSC maintains factors of safety greater than one for the combined load conditions. The minimum factor of safety of 1.23 occurs at Section 3 for the P_m+P_b stresses.

3.5.1.6 TSC Fatigue Evaluation

The purpose of this section is to evaluate whether an analysis for cyclic service is required for the TSC. For the TSC, the requirements for cyclic operation are presented in ASME Code, Section III, Subsection NB, Article NB-3222.4 [6]. The criteria for determining whether cyclic

loading analysis is required are comprised of six conditions, which, if met, preclude the requirement for further analysis.

1. Atmospheric to Service Pressure Cycle
2. Normal Service Pressure Fluctuation
3. Temperature Difference — Startup and Shutdown
4. Temperature Difference — Normal and Off-Normal Service
5. Temperature Difference — Dissimilar Materials
6. Mechanical Loads

The evaluation of these conditions is as follows.

Condition 1 — Atmospheric to Service Pressure Cycle

This condition is not applicable. The ASME Code defines a cycle as an excursion from atmospheric pressure to service pressure and back to atmospheric pressure. Once sealed, the TSC remains closed throughout its operational life, and no atmospheric to service pressure cycles occur.

Condition 2 — Normal Service Pressure Fluctuation

This condition is not applicable. The condition establishes a maximum pressure fluctuation as a function of the number of significant pressure fluctuation cycles specified for the component, the design pressure, and the allowable stress intensity of the component material. Operation of the TSC is not cyclic, and no significant cyclic pressure fluctuations are anticipated.

Condition 3 — Temperature Difference — Startup and Shutdown

This condition is not applicable. MAGNASTOR is a passive, long-term storage system that does not experience cyclic startups and shutdowns.

Condition 4 — Temperature Difference — Normal and Off-Normal Service

The ASME Code specifies that temperature excursions are not significant if the change in ΔT between two adjacent points does not experience a cyclic change of more than the quantity:

$$\Delta T = \frac{S_a}{2E\alpha} = 57^\circ\text{F}$$

where: for Type 304 stainless steel,

$$S_a = 28,200 \text{ psi} \text{ ----- Value obtained from the fatigue curve for service cycles } < 10^6$$

$$E = 25.1 \times 10^6 \text{ psi} \text{----- Modulus of elasticity at } 650 \text{ }^\circ\text{F}$$
$$\alpha = 9.9 \times 10^{-6} \text{ inch/inch-}^\circ\text{F} \text{----- Coefficient of thermal expansion at } 650^\circ\text{F}$$

Because of the large thermal mass of the TSC and the concrete cask and the relatively constant heat load produced by the TSC's contents, cyclic changes in ΔT greater than 57°F will not occur.

Condition 5 — Temperature Difference — Dissimilar Materials

The TSC and its internal components contain several materials. However, the design of all components considers thermal expansion, thus precluding the development of unanalyzed thermal stress concentrations.

Condition 6 — Mechanical Loads

This condition does not apply. Cyclic mechanical loads are not applied to the concrete cask and TSC during storage conditions. Therefore, no further cyclic loading evaluation is required.

The criteria of ASME Code, Section III, Subsections NB, Articles NB-3222.4 and NG-3222.4 are met; therefore, fatigue analysis is not required.

3.5.2 Fuel Basket Evaluation for Normal Operating Conditions

3.5.2.1 PWR Fuel Basket

This section evaluates the MAGNASTOR PWR fuel basket for normal operating conditions. Factors of safety for the PWR fuel basket are calculated based on the criteria for Service Level 'A' limits from ASME Code, Section III, Subsection NG [7].

Normal Handling Evaluation

The PWR fuel basket is analyzed using classical hand calculations for a 1.1g inertia loading in the basket axial direction to account for the dead load and the handling load. During normal conditions, the PWR fuel assemblies do not apply loads to the basket; they rest on the TSC bottom. Using a bounding basket weight of 22,500 lb, the maximum stress in the fuel tube is calculated. There are 21 fuel tubes in the PWR fuel basket. Conservatively assuming the entire basket weight is carried through the fuel tubes, the stress in the tube (σ_{tube}) is as follows.

$$\sigma_{\text{tube}} = \frac{P_{\text{tube}}}{A} = \frac{1178}{11.4} = 0.1 \text{ ksi}$$

where:

$$P_{\text{tube}} = \frac{W \times a}{n} = 1,178 \text{ lb} \text{ ----- Load per tube}$$

$$W = 22,500 \text{ lb} \text{ ----- Bounding basket weight}$$

$$a = 1.1g \text{ ----- Inertia g-load}$$

$$n = 21 \text{ ----- Number of fuel tubes}$$

$$A = 11.4 \text{ inch}^2 \text{ ----- Tube cross-sectional area}$$

The factor of safety (FS) is as follows.

$$FS = \frac{S_m}{\sigma_{\text{tube}}} = \frac{21.4}{0.1} = \text{Large}$$

where:

$$S_m = 21.4 \text{ ksi} \text{ ----- Design stress intensity, SA-537 Class 1, at } 700^\circ\text{F}$$

The weight of the fuel tubes, P_t , is supported on connector pins. Referring to Figure 3.10.1-13, the interior tubes (Tube #4) are supported by four connector pins; the side fuel tubes (Tube #1) are supported by two connector pins and the side and corner weldments; and the corner fuel tubes (Tube #3) are supported by three connector pins. The bearing area is the intersection of the connector pin assembly and the fuel tubes. The following sketch shows the cross-sectional area of adjacent fuel tubes that are loaded by the connector pin assembly supporting the basket. The diameter of the connector pin assembly is 0.75 inch. The bearing stress on the fuel tube (σ_{brg}) is as follows.

$$\sigma_{\text{brg}} = \frac{1.1 \times P_{\text{pin}}}{A_{\text{brg}}} = \frac{1.1 \times 394}{0.21} = 2.1 \text{ ksi}$$

where:

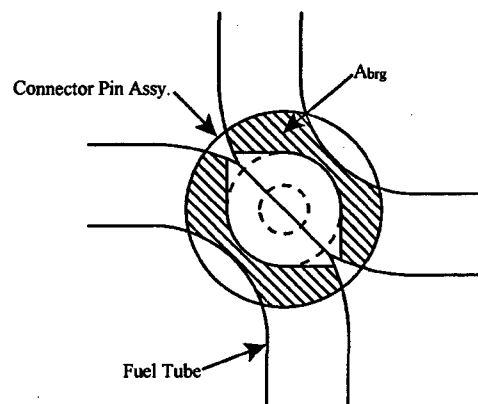
$$A_{\text{brg}} = 0.21 \text{ inch}^2$$

$$P_{\text{pin}} = \frac{1}{3}P_t + \frac{1}{4}P_t = 394 \text{ lb}$$

$$P_t = 675 \text{ lb}$$

The factor of safety (FS) for bearing is as follows.

$$FS = \frac{S_y}{\sigma_{\text{brg}}} = \frac{32.3}{2.1} = \text{Large}$$



where:

$$S_y = 32.3 \text{ ksi} \text{ ----- Yield strength, SA-537 Class 1, at } 700^\circ\text{F}$$

The bearing stress (σ_{brg}) in the connector pin at the TSC bottom plate, conservatively using P_{tube} , as previously determined is as follows.

$$\sigma_{brg} = \frac{P_{tube}}{A_{brg}} = \frac{1178}{0.41} = 2.9 \text{ ksi}$$

where:

$$A_{brg} = \frac{\pi}{4}(D_o^2 - D_i^2) = \frac{\pi}{4}(0.75^2 - 0.19^2) = 0.41 \text{ inch}^2$$

The factor of safety (FS) for bearing is as follows.

$$FS = \frac{S_y}{\sigma_{brg}} = \frac{24.7}{2.9} = 8.5$$

where:

$$S_y = 24.7 \text{ ksi} \text{ ----- Yield strength, SA-240 Type 304, at } 400^\circ\text{F}$$

The buckling evaluation of the connector pin is performed for the governing condition of the 24-inch concrete cask end-drop accident, as shown in Section 3.7.2.1. The accident condition buckling is bounding due to the 60g axial inertia loading.

The weight of the side and corner weldments is carried through to the TSC bottom plate by supports at the bottom of the basket. The bounding dimensions for the supports of the weldments are 5.0 inches in length and 0.3125-inch thickness (corner weldment). The maximum weight of one weldment is 800 lb (bounding side weldment). The weldment supports one-quarter of the weight of two fuel tubes (675 lb per tube, bounding). The bearing stress (σ_{brg}) is as follows.

$$\sigma_{brg} = \frac{1.1 \times W_{sup}}{A_{sup}} = \frac{1.1 \times 1138}{1.56} = 0.8 \text{ ksi}$$

where:

$$W_{sup} = 800 + 2 \times (0.25 \times 675) = 1138 \text{ lb}$$

$$A_{\text{sup}} = 5.0 \times 0.3125 = 1.56 \text{ inch}^2$$

The factor of safety (FS) for bearing is as follows.

$$FS = \frac{S_y}{\sigma_{\text{brg}}} = \frac{32.3}{0.8} = \text{Large}$$

where:

$$S_y = 32.3 \text{ ksi} \text{ ----- Yield strength, SA-537 Class 1, 700}^\circ\text{F}$$

The side and corner weldments are attached to the fuel tube array with bolts. The maximum torque on the 5/8-inch bolt is 50.0 inch-lb (40 inch-lb \pm 10 inch-lb). The preload on the bolt (P) is as follows.

$$P = \frac{T}{0.2D} = \frac{50}{0.2 \times 0.625} = 400 \text{ lb} \quad [12]$$

where:

$$T = 50 \text{ inch-lb} \text{ ----- Maximum bolt torque}$$

$$D = 0.625 \text{ inch} \text{ ----- Bolt diameter}$$

A bounding bolt load of 1,500 lb is used for the bolt evaluation. The bolt thread is a 5/8-11 UNC and the length of engagement is 0.50 inch. From Machinery's Handbook [12], the tensile stress (σ_t) in the bolt is as follows.

$$\sigma_t = \frac{P}{A_t} = \frac{1,500}{0.23} = 6.5 \text{ ksi}$$

where:

$$A_t = 0.7854 \left(D - \frac{0.9743}{n} \right)^2 = 0.23 \text{ inch}^2$$

$$D = 0.625 \text{ inch}$$

$$n = 11$$

The factor of safety (FS) is as follows.

$$FS = \frac{2(S_{\text{mBM}})}{\sigma_t} = \frac{2 \times 21.2}{6.5} = 6.5$$

where:

$$S_{mBM} = 21.2 \text{ ksi} \text{ ----- Design stress intensity for SA 193, Gr B6 at } 700^{\circ}\text{F}$$

The shear stress (τ_{bolt}) in the bolt thread is as follows.

$$\tau_{bolt} = \frac{P}{A_s} = \frac{1,500}{0.499} = 3.0 \text{ ksi}$$

where:

$$A_s = 3.1416nL_e K_{n \max} \left[\frac{1}{2n} + 0.57735(E_{s \min} - K_{n \max}) \right] = 0.499 \text{ inch}^2$$

The factor of safety (FS) is as follows.

$$FS = \frac{0.6S_m}{\tau_{bolt}} = \frac{0.6 \times 23.3}{3.0} = 4.66$$

where:

$$S_m = 23.3 \text{ ksi} \text{ ----- Design stress intensity, SA-193 Grade B6 at } 700^{\circ}\text{F}$$

The shear stress in the boss thread (τ_{boss}) is as follows.

$$\tau_{boss} = \frac{P}{A_n} = \frac{1,500}{0.713} = 2.1 \text{ ksi}$$

where:

$$A_n = 3.1416nL_e D_{s \min} \left[\frac{1}{2n} + 0.57735(D_{s \min} - E_{n \max}) \right] = 0.713 \text{ inch}^2$$

The factor of safety (FS) is as follows.

$$FS = \frac{0.6S_m}{\tau_{bolt}} = \frac{0.6 \times 19.2}{2.1} = 5.4$$

where:

$$S_m = 19.2 \text{ ksi} \text{ ----- Design stress intensity, SA-695 Type B, Gr } 40, \text{ at } 700^{\circ}\text{F}$$

The boss is welded into the fuel tube with a 1/4-inch groove weld. The shear stress in the boss weld (τ_{weld}), is as follows.

$$\tau_{\text{weld}} = \frac{P}{A_w} = \frac{1,500}{0.98} = 1.5 \text{ ksi}$$

where:

$$P = 1,500 \text{ lb}$$

$$A_w = \pi D t_{\text{weld}} = \pi \times 1.25 \times 0.25 = 0.98 \text{ inch}$$

$$D = 1.25 \text{ inches} \text{----- Boss diameter}$$

Using the lesser allowable, S_m , of SA537 Class 1 or SA695 Type B, Gr 40, the factor of safety (FS) is as follows.

$$FS = \frac{0.35 \times 0.6 S_m}{\tau_{\text{weld}}} = 2.7$$

where:

$$S_m = 19.2 \text{ ksi} \text{----- Design stress intensity, SA-695 Type B, Gr 40, at } 700^\circ\text{F}$$

The washers under the bolts are subjected to a bending load due to the bolt preload. Using Roark's [13], Table 24-1a, the maximum stress in the washer is calculated. The maximum stress (σ) in the washer is as follows.

$$\sigma = \frac{6M_t}{t^2} = \frac{6 \times 180}{0.3125^2} = 11.1 \text{ ksi}$$

where:

$$a = \frac{1.50}{2} = 0.75 \text{ inch} \text{----- Radius of the cut out in support weldments}$$

$$b = \frac{0.75}{2} = 0.375 \text{ inch} \text{----- Inner radius of the washer}$$

$$r_o = 0.55 \text{ inch} \text{----- Average radius of bolt head}$$

$$t = 5/16 \text{ inch} \text{----- Thickness of washer}$$

$$E = 27.0 \times 10^6 \text{ psi} \text{----- Modulus of elasticity (SA-240 Type 304)}$$

$$\nu = 0.3 \text{----- Poisson's ratio}$$

$$w = \frac{P}{\pi \times 2r_o} = \frac{1,500}{\pi \times 2 \times 0.55} = 434 \text{ lb/in}$$

$$G = \frac{E}{2(1+\nu)} = \frac{27.0 \times 10^6}{2(1+0.3)} = 10.38 \times 10^6 \text{ psi}$$

$$D = \frac{Et^3}{12(1-\nu^2)} = \frac{27.0 \times 10^6 (0.3125^3)}{12(1-0.3^2)} = 75,460 \text{ inch-lb}$$

$$M_t = 180 \text{ inch-lb} \text{----- Calculated using formulas in Roark's [13]}$$

The factor of safety (FS) is as follows.

$$FS = \frac{1.5S_m}{\sigma} = \frac{1.5 \times 16.0}{11.1} = 2.16$$

where:

$$S_m = 16.0 \text{ ksi} \text{----- Design stress intensity, SA-240 Type 304, at } 700^\circ\text{F}$$

The evaluation of the neutron absorber for normal handling conditions is bounded by the evaluation for the 24-inch concrete cask end-drop accident (60g) as shown in Section 3.7.2.1. Therefore, no evaluation for normal handling is presented in this section.

Thermal Stress Evaluation

The thermal stresses for the PWR fuel basket are calculated using a three-dimensional quarter-symmetry ANSYS finite element model (Section 3.10.1.2). The model represents the top or bottom 47 inches of the basket and calculates the stresses in the basket based upon bounding thermal gradients in basket axial and radial directions. The thermal stresses are combined with the maximum stresses for the normal handling condition. Factors of safety are calculated based on Service Level 'A' limits from ASME Code, Section III, Subsection NG [7]. The maximum handling stress in the basket is 0.1 ksi. The following presents the combined normal handling plus thermal stress (P+Q) for the PWR basket.

Component	S _{therm} , ksi	S _{total} , ksi	S _{allow} , ksi	FS
Fuel Tube	48.1	48.2	64.2	1.33
Support Weldments	17.4	17.5	64.2	3.67

The total stress is the sum of the component thermal stress and the normal handling stress. The allowable stress is 3S_m (3 × 21.4 = 64.2 ksi for SA537 Class 1 at 700°F).

The axial average temperature at the center of the basket is 475°F. The axial average temperature at the outer radius of the basket is 425°F. The relative thermal expansion of the basket in the axial direction between the center and outer edge of the basket is as follows.

$$\Delta x = \Delta x_{\text{inner}} - \Delta x_{\text{outer}} = 0.51 - 0.44 = 0.07 \text{ inch}$$

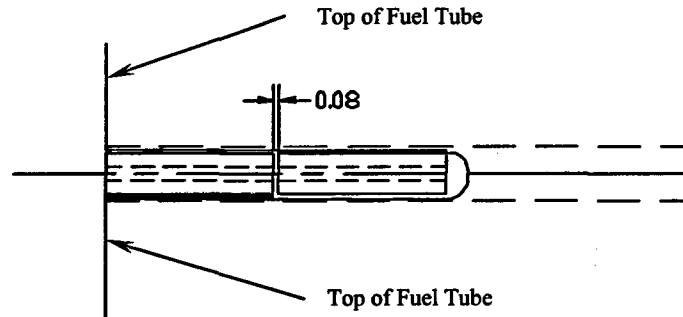
where:

$$\Delta x_{\text{inner}} = \Delta T \times L \times \alpha_1 = (475 - 70)(173.5)(7.25 \times 10^{-6}) = 0.51 \text{ inch}$$

$$\Delta x_{\text{outer}} = \Delta T \times L \times \alpha_2 = (425 - 70)(173.5)(7.15 \times 10^{-6}) = 0.44 \text{ inch}$$

$L = 173.5 \text{ inches}$ ----- Fuel tube length
 $\alpha_1 = 7.25 \times 10^{-6} \text{ inch/inch/}^\circ\text{F}$ ----- Coefficient of thermal expansion, SA537 CL1, at 475°F
 $\alpha_2 = 7.15 \times 10^{-6} \text{ inch/inch/}^\circ\text{F}$ ----- Coefficient of thermal expansion, SA537 CL1, at 425°F

Connector pins at the top and bottom of the basket are used to maintain the geometry of the fuel tube array during manufacturing. A pin is inserted into the connector pin to maintain geometry between adjacent fuel tubes. Adjacent fuel tube connector pins have a 0.08-inch gap between the connector pins; see the following sketch. Since the relative thermal expansion of the basket between the center and outer edge of the basket is less than the pin gap, no axial thermal stresses are produced by the axial expansion of the basket.



The maximum shear load calculated by ANSYS in the basket attachment bosses is 3.5 kip due to the radial thermal expansion of the basket. The shear stress in the boss (τ_{boss}) is as follows.

$$\tau_{\text{boss}} = \frac{P}{A} = \frac{3.5}{0.92} = 3.8 \text{ ksi}$$

where:

$$A = \frac{\pi}{4}(D_o^2 - D_i^2) = 0.92 \text{ inch}^2$$

$D_o = 1.25 \text{ inches}$
 $D_i = 0.63 \text{ inch}$

The factor of safety (FS) is as follows.

$$FS = \frac{0.6S_m}{\tau_{boss}} = \frac{0.6 \times 19.2}{3.8} = 3.03$$

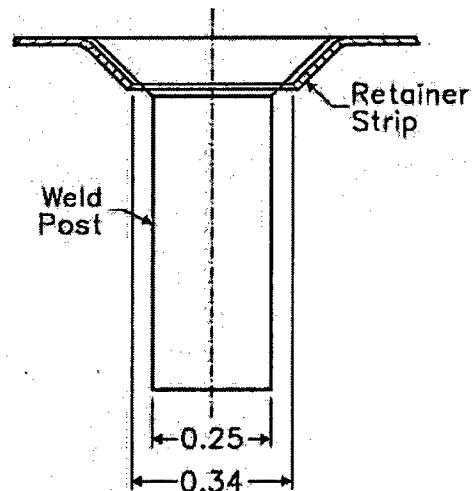
where:

$$S_m = 19.2 \text{ ksi} \text{ ----- Design stress intensity SA-695 Type B, Gr 40 at } 700^\circ\text{F}$$

Based on the analysis results from the thermal stress model, the thermal expansion of the basket does not result in additional tensile load in the attachment bolts. Therefore, no additional bolt analysis for thermal loads is required.

Neutron Absorber Retainer Thermal Stress Evaluation

The attachment of the retainer strip and neutron absorber to the fuel tube using weld posts allows each component to move independently during thermal growth. In the case of the stainless steel retainer strip, the expansion of the neutron shield material, which is composed primarily of aluminum, and the carbon steel fuel tube tends to tighten the joint created by the weld post. Thermal stresses may develop between the weld posts because the carbon steel fuel tube expands at a different rate than the retainer strip.



The equation used to calculate the difference in expansion between carbon and stainless steel, Δ , is as follows.

$$\Delta = (\alpha_{ss} \times \Delta T \times L) - (\alpha_{cs} \times \Delta T \times L) \quad (1)$$

The standard formula to calculate the deflection of a beam or plate is as follows.

$$\Delta = \frac{PL}{AE} = \frac{\sigma L}{E} \quad (2)$$

Substituting equation (1) into equation (2) and solving the retainer strip thermal stress, σ , is as follows.

$$\sigma = \frac{E\Delta}{L} = E(\alpha_{ss} - \alpha_{cs})(\Delta T) = 37,350 \text{ psi} \quad (3)$$

where:

$\alpha_{ss} = 10.0 \times 10^{-6}$ inch/inch/°F	-----	Coefficient of thermal expansion, SA-240 Type 304, at 700°F
$\alpha_{cs} = 7.6 \times 10^{-6}$ inch/inch/°F	-----	Coefficient of thermal expansion, SA-537 Class 1, at 700°F
$\Delta T = 700^\circ\text{F} - 70^\circ\text{F} = 630^\circ\text{F}$	-----	Difference between maximum PWR temperature and ambient conditions
$T_{\max} = 700^\circ\text{F}$	-----	Bounding basket temperature
$E = 24.7 \times 10^6$ psi	-----	Modulus of elasticity, SA-240 Type 304, at 700°F

The factor of safety (FS) is as follows.

$$FS = \frac{3S_m}{\sigma} = \frac{47,700}{37,350} = 1.28$$

where:

$S_m = 15,900$ psi	-----	Design stress intensity, SA-240 Type 304, at 667°F
--------------------	-------	--

3.5.2.2 BWR Fuel Basket

This section evaluates the MAGNASTOR BWR basket for normal operating conditions. Factors of safety for the BWR basket are calculated based on the criteria for Service Level 'A' limits from ASME Code, Section III, Subsection NG [7].

Normal Handling Evaluation

The BWR basket is analyzed using classical hand calculations for a 1.1g inertia loading in the basket axial direction to account for the dead load and the handling load. During normal conditions, the BWR fuel assemblies do not apply loads to the basket; they rest on the TSC bottom. Using a bounding weight of 24,000 lb, the maximum stress in the fuel tube is calculated. There are 45 fuel tubes in the BWR basket. Conservatively assuming the entire basket weight is carried through the fuel tubes, the stress in the tube (σ_{tube}) is as follows.

$$\sigma_{tube} = \frac{P_{tube}}{A} = \frac{587}{6.1} = 0.1 \text{ ksi}$$

where:

$$P_{tube} = \frac{W \times a}{n} = 587 \text{ lb} \text{ ----- Load per tube}$$

$$W = 24,000 \text{ lb} \text{ ----- Bounding basket weight}$$

$$a = 1.1g \text{ ----- Inertia g-load}$$

$$n = 45 \text{ ----- Number of fuel tubes}$$

$$A = 6.1 \text{ inch}^2 \text{ ----- Tube cross-sectional area}$$

The factor of safety (FS) is as follows.

$$FS = \frac{S_m}{\sigma_{tube}} = \frac{21.4}{0.1} = \text{Large}$$

where:

$$S_m = 21.4 \text{ ksi} \text{ ----- Design stress intensity, SA-537 Class 1, at } 700^\circ\text{F}$$

The weight of the fuel tubes, P_t , is supported on connector pins. For tube locations presented in Figure 3.10.2-13, the interior tubes (Tube #4) are supported by four connector pins; the side fuel tubes (Tube #1) are supported by two connector pins and the side and corner weldments; and the corner fuel tubes (Tube #5) are supported by three connector pins. The bearing area is the intersection of the connector pin assembly and the fuel tubes. The following sketch shows the

cross-sectional area of adjacent figure tubes that is loaded by the connector pin assembly. The diameter of the connector pin assembly is 1.0 inch. The bearing stress on the fuel tube (σ_{brg}) is as follows.

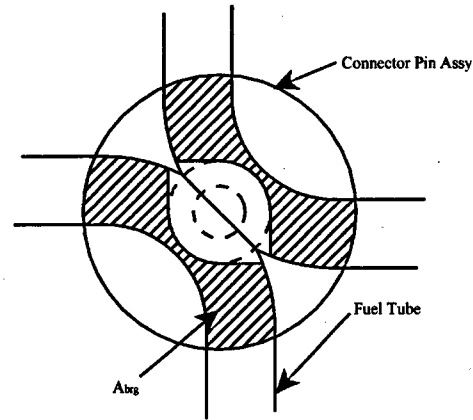
$$\sigma_{brg} = \frac{1.1 \times P_{pin}}{A_{brg}} = \frac{1.1 \times 233}{0.34} = 0.8 \text{ ksi}$$

where:

$$A_{brg} = 0.34 \text{ inch}^2$$

$$P_{pin} = \frac{1}{3}P_t + \frac{1}{4}P_t = 233 \text{ lb}$$

$$P_t = 400 \text{ lb}$$



The factor of safety (FS) for bearing is as follows.

$$FS = \frac{S_y}{\sigma_{brg}} = \frac{32.3}{0.8} = \text{Large}$$

where:

$$S_y = 32.3 \text{ ksi} \text{ ----- Yield strength, SA-537 Class 1, at } 700^\circ\text{F}$$

The bearing stress (σ_{brg}) in the connector pin at the TSC bottom plate, conservatively using P_{tube} as previously determined, is as follows.

$$\sigma_{brg} = \frac{P_{tube}}{A_{brg}} = \frac{587}{0.75} = 0.8 \text{ ksi}$$

where:

$$A_{brg} = \frac{\pi}{4}(D_o^2 - D_i^2) = \frac{\pi}{4}(1.0^2 - 0.19^2) = 0.75 \text{ inch}^2$$

The factor of safety (FS) for bearing is as follows.

$$FS = \frac{S_y}{\sigma_{brg}} = \frac{24.7}{0.8} = \text{Large}$$

where:

$$S_y = 24.7 \text{ ksi} \text{ ----- Yield strength, SA-240 Type 304, at } 700^\circ\text{F}$$

The buckling evaluation of the connector pin is performed for the governing condition of the 24-inch concrete cask end-drop accident, as prescribed in Section 3.7.2.2. The accident event buckling evaluation is bounding due to the 60g axial inertia loading.

The weight of the side and corner weldments is carried through to the TSC bottom plate by supports at the bottom of the basket. The corner weldment is bounding for the top and bottom supports. The dimensions for the corner support weldment are 8.0 inches in length and 0.375-inch thickness. The bounding weight of the corner weldment is 1,100 pounds. The corner weldment also supports one-quarter of the weight of four fuel tubes (400 lb per tube, bounding). The bearing stress (σ_{brg}) is as follows.

$$\sigma_{brg} = \frac{W_{sup}}{A_{sup}} = \frac{1650}{3.0} = 0.6 \text{ ksi}$$

where:

$$W_{sup} = 1.1 \times (1,100 + 4 \times (0.25 \times 400)) = 1650 \text{ lb}$$

$$A_{sup} = 8.0 \times 0.375 = 3.0 \text{ inch}^2$$

The factor of safety (FS) for bearing is as follows.

$$FS = \frac{S_y}{\sigma_{brg}} = \frac{32.3}{0.6} = \text{Large}$$

where:

$$S_y = 32.3 \text{ ksi} \text{ ----- Yield strength, SA-537 Class 1, } 700^\circ\text{F}$$

The side and corner weldments are attached to the fuel tube array with bolts. The maximum torque on the $\frac{3}{8}$ -inch bolt is 50 inch-lb (40 ±10 inch-lb). The preload on the bolt (P) is as follows.

$$P = \frac{T}{0.2D} = \frac{50}{0.2 \times 0.625} = 400 \text{ lb} \quad [12]$$

where:

$$T = 50 \text{ inch-lb} \text{ ----- Maximum bolt torque}$$

$$D = 0.625 \text{ inch} \text{ ----- Bolt diameter}$$

The bolt thread is a $\frac{3}{8}$ -11 UNC and the minimum length of engagement is 0.38 inch. A bolt load of 1,000 lb is conservatively used for the evaluation. From Machinery's Handbook [12], the tensile strength (σ_t) in the bolt is as follows.

$$\sigma_t = \frac{P}{A_t} = \frac{1,000}{0.23} = 4.3 \text{ ksi}$$

where:

$$A_t = 0.7854 \left(D - \frac{0.9743}{n} \right)^2 = 0.23 \text{ inch}^2$$

$$D = 0.625 \text{ inch}$$

$$n = 11$$

The factor of safety (FS) is as follows.

$$FS = \frac{2(S_{mBM})}{\sigma_t} = \frac{2 \times 21.2}{4.3} = 9.8$$

where:

$$S_{mBM} = 21.2 \text{ ksi} \text{ ----- Design stress intensity for SA-193, Gr B6, at } 700^\circ\text{F}$$

The shear stress in the bolt thread (τ_{bolt}) is as follows.

$$\tau_{bolt} = \frac{P}{A_s} = \frac{1,000}{0.379} = 2.6 \text{ ksi}$$

where:

$$A_s = 3.1416nL_e K_{n \max} \left[\frac{1}{2n} + 0.57735(E_{s \min} - K_{n \max}) \right] = 0.379 \text{ inch}^2$$

$$n = 11$$

The factor of safety (FS) is as follows.

$$FS = \frac{0.6S_m}{\tau_{bolt}} = \frac{0.6 \times 23.3}{2.6} = 5.37$$

where:

$$S_m = 23.3 \text{ ksi} \text{ ----- Design stress intensity, SA-193 Grade B6, at } 700^\circ\text{F}$$

The shear stress in the boss thread (τ_{boss}) is as follows.

$$\tau_{boss} = \frac{P}{A_n} = \frac{1,000}{0.542} = 1.8 \text{ ksi}$$

where:

$$A_n = 3.1416nL_c D_{s \min} \left[\frac{1}{2n} + 0.57735(D_{s \min} - E_{n \max}) \right] = 0.542 \text{ inch}^2$$

$$L_c = 0.38 \text{ inch}$$

$$E_{n \max} = 0.5732$$

$$D_{s \min} = 0.6113$$

$$n = 11$$

The factor of safety (FS) is as follows.

$$FS = \frac{0.6S_m}{\tau_{\text{bolt}}} = \frac{0.6 \times 19.2}{1.8} = 6.4$$

where:

$$S_m = 19.2 \text{ ksi} \text{ ----- Design stress intensity, SA-695, Type B, Gr 40, at } 700^\circ\text{F}$$

The boss is welded into the fuel tube with a 3/16-inch groove weld. The shear stress in the boss weld (τ_{weld}) is as follows.

$$\tau_{\text{weld}} = \frac{P}{A_w} = \frac{1,000}{0.59} = 1.7 \text{ ksi}$$

where:

$$P = 1000 \text{ lb}$$

$$A_w = \pi D t_{\text{weld}} = \pi \times 1.00 \times 0.1875 = 0.59 \text{ inch}$$

$$D = 1.00 \text{ inch} \text{ ----- Smallest boss diameter}$$

Using the lesser allowable, S_m , of SA-537 Class 1 or SA-695 Type B, Gr 40, the factor of safety (FS) is as follows.

$$FS = \frac{0.35 \times 0.6S_m}{\tau_{\text{weld}}} = 2.37$$

where:

$$S_m = 19.2 \text{ ksi} \text{ ----- Design stress intensity, SA-695 Type B Grade 40, at } 700^\circ\text{F}$$

The washers under the bolts are subjected to a bending load to the torque of the bolts. Using "Roark's Formulas for Stress and Strain" Table 24-1a [13], the maximum stress in the washer is calculated. The maximum stress (σ) in the washer is as follows.

$$\sigma = \frac{6M_t}{t^2} = \frac{6 \times 120}{0.19^2} = 20.0 \text{ ksi}$$

where:

$$a = \frac{1.50}{2} = 0.75 \text{ inch} \text{----- Radius of cut out in support weldments}$$

$$b = \frac{0.625}{2} = 0.31 \text{ inch} \text{----- Inner radius of the washer}$$

$$r_o = 0.55 \text{ inch} \text{----- Average radius of bolt head}$$

$$t = 3/16 \text{ inch} \text{----- Thickness of washer}$$

$$E = 27.0 \times 10^6 \text{ psi} \text{----- Modulus of elasticity (SA240 Type 304)}$$

$$\nu = 0.3 \text{----- Poisson's ratio}$$

$$w = \frac{P}{\pi \times 2r_o} = \frac{1,000}{\pi \times 2 \times 0.55} = 290 \text{ inch-lb}$$

$$G = \frac{E}{2(1+\nu)} = \frac{27.0 \times 10^6}{2(1+0.3)} = 10.38e6 \text{ psi}$$

$$D = \frac{Et^3}{12(1-\nu^2)} = \frac{27.0 \times 10^6 (0.3125^3)}{12(1-0.3^2)} = 16,300 \text{ inch-lb}$$

$$M_t = 120 \text{ inch-lb} \text{----- Calculated using the formula in Roark's [13]}$$

The factor of safety (FS) is as follows.

$$FS = \frac{1.5S_m}{\sigma} = \frac{1.5 \times 16.0}{20.0} = 1.20$$

where:

$$S_m = 16.0 \text{ ksi} \text{----- Design stress intensity, SA-240 Type 304, at 700°F}$$

The evaluation of the neutron absorber for normal handling conditions is bounded by the evaluation for the 24-inch concrete cask end-drop accident (60g) as shown in Section 3.7.2.2. Therefore, no evaluation for normal handling is presented in this section.

Thermal Stress Evaluation

The thermal stresses for the BWR fuel basket are calculated using a three-dimensional quarter-symmetry ANSYS finite element model (Section 3.10.2.2). The model represents the top or bottom 43 inches of the basket and calculates the stresses in the basket based upon bounding thermal gradients in basket axial and radial directions. The thermal stresses are combined with the maximum stresses for the normal handling condition. Factors of safety are calculated based on Service Level 'A' limits from ASME Code, Section III, Subsection NG [7]. The maximum handling stress in the basket is 0.1 ksi. The following presents the combined normal handling plus thermal stress (P+Q) for the BWR fuel basket.

Component	S _{therm} , ksi	S _{total} , ksi	S _{allow} , ksi	FS
Fuel Tube	28.5	28.6	64.2	2.24
Support Weldments	8.5	8.6	64.2	7.46

The total stress is the sum of the component thermal stress and the normal condition stress. The allowable stress is 3Sm (3 × 21.4 = 64.2 ksi for SA-537 Class 1 steel at 700°F).

The average temperature at the center of the basket is 465°F. The average temperature at the outer radius of the basket is 430°F. The relative thermal expansion of the basket in the axial direction between the center and outer edge of the basket is as follows.

$$\Delta x = \Delta x_{\text{inner}} - \Delta x_{\text{outer}} = 0.48 - 0.43 = 0.05 \text{ inch}$$

where:

$$\Delta x_{\text{inner}} = \Delta T \times L \times \alpha_1 = (465 - 70)(166.5)(7.3 \times 10^{-6}) = 0.48 \text{ inch}$$

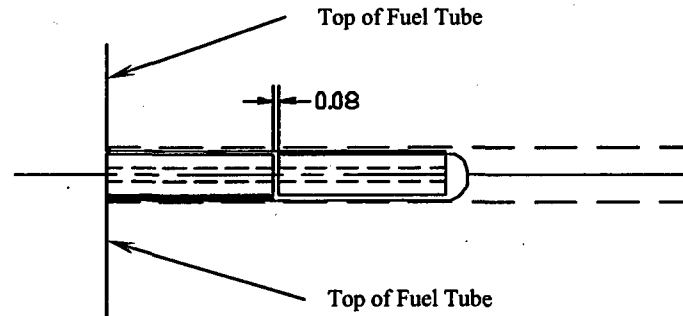
$$\Delta x_{\text{outer}} = \Delta T \times L \times \alpha_2 = (430 - 70)(166.5)(7.2 \times 10^{-6}) = 0.43 \text{ inch}$$

L = 166.5 inch ----- Fuel tube length

$\alpha_1 = 7.3 \times 10^{-6}$ inch/inch/°F ----- Coefficient of thermal expansion, SA537 CL1, at 500°F

$\alpha_2 = 7.2 \times 10^{-6}$ inch/inch/°F ----- Coefficient of thermal expansion, SA537 CL1, at 450°F

Connector pins at the top and bottom of the basket are used to maintain the geometry of the fuel tube array. A pin is inserted into the connector pin to maintain geometry between adjacent fuel tubes. Adjacent fuel tube connector pins have a 0.08-inch gap between the connector pins; see the following sketch. Since the relative thermal expansion of the basket between the center and outer edge of the basket is less than the pin gap, no axial thermal stresses are produced by the axial expansion of the basket.



The maximum shear load calculated by ANSYS in the basket attachment bosses is 4.2 kip due to the radial thermal expansion of the basket. The shear stress in the boss (τ_{boss}) is as follows.

$$\tau_{\text{boss}} = \frac{P}{A} = \frac{4.2}{0.47} = 8.9 \text{ ksi}$$

where:

$$A = \frac{\pi}{4}(D_o^2 - D_i^2) = 0.47 \text{ inch}^2$$

$$D_o = 1.00 \text{ inch}$$

$$D_i = 0.63 \text{ inch}$$

The factor of safety (FS) is as follows.

$$FS = \frac{0.6S_m}{\tau_{\text{boss}}} = \frac{0.6 \times 19.2}{8.9} = 1.29$$

where:

$$S_m = 19.2 \text{ ksi} \text{ ----- Design stress intensity, SA-695 Type B, Gr 40, at } 700^\circ\text{F}$$

The thermal expansion of the basket does not add significant additional tensile loads to the bolts; therefore, no additional bolt analysis for thermal loads is required.

Neutron Absorber Retainer Thermal Stress Evaluation

The stainless steel retainer strips are fastened to the carbon steel fuel tube using fixed weld posts spaced along the length of the tube. Because of the dissimilar material properties, differential thermal expansion of the components results in thermal stresses in some of the components.

Since the stress due to differential thermal expansion is not a function of length, the evaluation provided in Section 3.5.2.1 for retainer for the PWR is applicable to that for the BWR. No further analysis is required.

3.5.3 Concrete Cask Evaluations for Normal Operating Conditions

The structural evaluation of the concrete cask for normal conditions considers the combination of thermal stresses, dead and live loads, and wind loads (see Chapter 2 for load combinations). The analysis results are presented in Section 3.5.3.3. The conservative stress due to wind loads is obtained from Section 3.7.3.2.

3.5.3.1 Concrete Cask Thermal Stresses

Using the finite element model presented in Section 3.1.1, a structural evaluation of the concrete cask for normal conditions thermal loads was performed. The analysis conservatively considered a bounding temperature profile corresponding to the off-normal thermal event (106°F ambient). The following summarizes the critical thermal stresses for normal conditions.

Component	Stress (ksi)
Circumferential Rebar	15.6
Vertical Rebar	19.1
Concrete, Compression	1.0
Concrete, Tension	0.1

3.5.3.2 Dead and Live Loads

Dead Loads

The concrete cask dead load consists primarily of the weight of the concrete. Assuming all dead loads are reacted by the lower concrete surface only, stress levels can be determined. Under these conditions, the only stress component is the vertical axial compression stress. The maximum stress (σ_{cask}) at the base of the concrete cask in the concrete is as follows.

$$\sigma_{\text{cask}} = \frac{W_{\text{cask}}}{A} = \frac{210,000}{9,119} = 23.0 \text{ psi}$$

where:

$$\begin{aligned} W_{\text{cask}} &= 210,000 \text{ lb} \text{----- Bounding weight for empty concrete cask} \\ D_o &= 136.0 \text{ inch} \\ D_i &= 82.98 \text{ inch} \\ A &= \pi (D_o^2 - D_i^2) / 4 = 9,119 \text{ inch}^2 \end{aligned}$$

The concrete bearing strength (f_b) is much larger than the applied load.

$$f_b = \phi(0.85f'_cA) = 0.85(0.85 \times 3800 \times 9119) = 25.0 \times 10^6 \text{ lb} > 210,000 \text{ lb}$$

where:

$$f'_c = 3,800 \text{ psi} \text{----- Compressive strength, concrete, at } 300^\circ\text{F}$$

Live Loads

The live load calculation considers the loaded transfer cask positioned on top of the concrete cask for transfer of the TSC for development of the peak live load bounding condition.

Assuming live loads are reacted by concrete sections (no credit taken for steel liner), stress levels are conservatively determined. Under these conditions, the only stress component is the vertical axial compression stress ($\sigma_{\text{concrete cask}}$).

$$\sigma_{\text{concrete cask}} = \frac{W_{\text{TFR}}}{A} = \frac{230,000}{9,119} = 25.2 \text{ psi}$$

where:

$$W_{\text{TFR}} = 230,000 \text{ lb} \text{----- Loaded transfer cask}$$

$$D_o = 136.0 \text{ inch}$$

$$D_i = 82.98 \text{ inch}$$

$$A = \pi (D_o^2 - D_i^2) / 4 = 9,119 \text{ inch}^2$$

3.5.3.3 Concrete Cask Combined Stresses

The load combinations described in Chapter 2 are used to evaluate the concrete cask for normal conditions of storage (Load Conditions 1, 2, and 3). Concrete cask stresses are summarized in Table 3.5-5, Table 3.5-6, and Table 3.5-7 for the various loading conditions on the concrete cask.

The allowable compressive stress for concrete (S_{con}) is as follows.

$$S_{\text{con}} = \phi f'_c = 2,660 \text{ psi}$$

where:

$$\phi = 0.7 \text{----- Strength reduction factor [5]}$$

$$f'_c = 3800 \text{ psi} \text{----- Compressive strength, concrete, at } 300^\circ\text{F}$$

The concrete ultimate strength allowable is 8% to 15% of the compressive stress [14]; therefore, the allowable ultimate strength (S_{tc}) is as follows.

$$S_{\text{tc}} = 0.08 \times S_{\text{con}} = 0.08 \times 2660 = 213 \text{ psi or } 0.21 \text{ ksi}$$

The maximum concrete compressive stress is 1,332 psi (see Table 3.5-6); therefore, the minimum factor of safety (FS) for normal conditions is as follows.

$$FS = \frac{2,660}{1,332} = 2.00$$

From Section 3.5.3.1, the maximum concrete ultimate strength due to thermal load is 0.1 ksi. Multiplying the stress by a 1.275 factor for normal conditions thermal stresses (see Chapter 2), the factor of safety (FS) for concrete ultimate strengths is as follows.

$$FS = \frac{S_{tc}}{S_t \times 1.275} = \frac{0.21}{0.1 \times 1.275} = 1.62$$

The allowable stress for rebar (S_{rebar}) is as follows.

$$S_{rebar} = \phi F_r = 54.0 \text{ ksi}$$

where:

$$\phi = 0.9 \text{ ----- Strength reduction factor [5]}$$

$$F_r = 60.0 \text{ ksi ----- Yield strength, rebar}$$

From Section 3.5.3.1, the maximum rebar stress due to thermal load is 19.1 ksi. The stresses due to other loadings are negligible for normal conditions. Compressive loads are carried by the concrete. Multiplying the stress by a 1.275 factor for normal conditions thermal stresses (see Chapter 2), the factor of safety (FS) for the rebar is as follows.

$$FS = \frac{S_{rebar}}{S_t \times 1.275} = \frac{54.0}{19.1 \times 1.275} = 2.21$$

Table 3.5-1 TSC Thermal Stress, Q

Load Case	Service Level	Section ^a	Component Stresses (ksi) ^b						S _{int}
			S _x	S _y	S _z	S _{xy}	S _{yz}	S _{xz}	
Thermal	A	12	-16.87	-14.95	-4.20	-0.50	-1.60	-0.10	13.05

Table 3.5-2 TSC Normal Conditions, P_m Stresses

Load Case	Service Level	Section ^a	Component Stresses (ksi) ^b						S _{int}	S _{allow}	FS
			S _x	S _y	S _z	S _{xy}	S _{yz}	S _{xz}			
Pressure	A	3	-0.50	-6.93	3.91	0.13	0.02	0.85	11.01	N/A	N/A
Pressure + Handling	A	3	-0.58	-9.49	4.83	-0.19	-0.03	1.01	14.51	20.00	1.38

Table 3.5-3 TSC Normal Conditions, P_m + P_b Stresses

Load Case	Service Level	Section ^a	Component Stresses (ksi) ^b						S _{int}	S _{allow}	FS
			S _x	S _y	S _z	S _{xy}	S _{yz}	S _{xz}			
Pressure	A	2	2.37	-11.47	-16.71	0.00	0.00	-0.99	19.19	N/A	N/A
Pressure + Handling	A	3	-0.25	-4.94	19.45	-0.08	-0.04	1.27	24.48	30.00	1.23

Table 3.5-4 TSC Normal Conditions, P + Q Stresses

Load Case	Service Level	Section ^a	Component Stresses (ksi) ^b						S _{int}	S _{allow}	FS
			S _x	S _y	S _z	S _{xy}	S _{yz}	S _{xz}			
Pressure + Handling + Thermal	A	12	-41.04	-37.90	-8.45	-1.25	-0.15	-1.51	33.17	60.00	1.81

Table 3.5-5 Concrete Cask Vertical Stress Summary – Outer Surface, psi

Condition	Dead	Live	Wind	Thermal	Seismic	Flood	Tornado	Total
1	-32	-43	0	0	0	0	0	-75
2	-24	-32	0	0	0	0	0	-56
3	-24	-32	-24	0	0	0	0	-80

^a See Figure 3.10.3-2 for section locations.

^b The x,y,z component of stress are to be interpreted radial, circumferential, and axial directions, respectively.

Table 3.5-6 Concrete Cask Vertical Stress Summary – Inner Surface, psi

Condition	Dead	Live	Wind	Thermal	Seismic	Flood	Tornado	Total
1	-32	-43	0	0	0	0	0	-75
2	-24	-32	0	-1261	0	0	0	-1317
3	-24	-32	-15	-1261	0	0	0	-1332

Table 3.5-7 Concrete Cask Circumferential Stress Summary – Inner Surface, psi

Condition	Dead	Live	Wind	Thermal	Seismic	Flood	Tornado	Total
1	0	0	0	0	0	0	0	0
2	0	0	0	-566	0	0	0	-566
3	0	0	0	-566	0	0	0	-566

3.6 Off-Normal Operating Events

This section presents the analyses of the major structural components of MAGNASTOR for off-normal events of storage. MAGNASTOR is evaluated using finite element models and classical hand calculations for the fuel baskets and TSC. Off-normal environmental events are defined as -40°F with no solar load, 106°F with solar load, and half-blockage of the concrete cask air inlets.

3.6.1 TSC Evaluations for Off-Normal Operating Events

3.6.1.1 Thermal Stresses for Off-Normal Events

The thermal stresses of the TSC are calculated using the ANSYS finite element model described in Section 3.10.3. As discussed in Section 3.5.1.1, the temperature gradient applied to the TSC bounds the temperature gradient for all conditions of storage. Therefore, the maximum thermal stresses for the off-normal severe ambient temperature event are bounded by those presented in Table 3.5-1.

3.6.1.2 Off-Normal TSC Load Analyses

Based on the load combinations specified in Table 2.3-2, the following two off-normal load events are evaluated.

- Off-normal internal pressure + normal handling + thermal (ASME Code, Level B)
- Normal internal pressure + off-normal handling (ASME Code, Level C)

For detailed analyses results for off-normal conditions, see Table 3.10.3-7 through Table 3.10.3-11.

Off-Normal Internal Pressure with Normal Handling

The TSC is analyzed for off-normal pressurization and normal handling loads using the finite element model described in Section 3.10.3. Applying a 1.1g acceleration load in the axial direction to a loaded TSC simulates normal handling. To represent the off-normal pressure, an internal pressure of 130 psig is applied to all internal surfaces. A bounding temperature profile is considered for the thermal stress calculation, as discussed in Section 3.10.3.

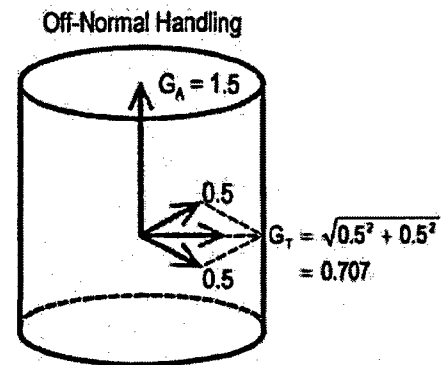
The resulting maximum stresses in the TSC for Service Level 'B' off-normal loads are summarized in Table 3.6-1 for primary membrane, Table 3.6-2 for primary membrane plus primary bending, and Table 3.6-3 for primary plus secondary stress categories. The minimum

factor of safety of 1.18 ($P_m + P_b$) occurs at Section 3. The locations for the stress sections are shown in Section 3.10.3.

Off-Normal Handling with Normal Internal Pressure

An evaluation is performed for the off-normal handling loads on the TSC during the installation of the TSC in the concrete cask, removal of the TSC from the concrete cask, and removal from the transfer cask. The TSC is handled vertically in both the concrete and transfer casks.

The TSC is analyzed for handling loads using the finite element model described in Section 3.10.3. The off-normal TSC handling loads are defined as 0.5g applied in all directions (i.e., in the global x, y, and z directions) in addition to a 1g lifting load applied in the finite element model. The resulting off-normal handling accelerations are 0.707g in the lateral direction and 1.5g (0.5g + 1.0g) in the vertical direction. To represent the normal pressure, an internal pressure of 110 psig is applied to all internal surfaces.



The resulting maximum stresses in the TSC for Service Level 'C' off-normal loads are summarized in Table 3.6-1 for primary membrane, Table 3.6-2 for primary membrane plus primary bending, and Table 3.6-3 for primary plus secondary stress categories. The minimum factor of safety of 1.27 ($P_m + P_b$) occurs at Section 3. The locations for the stress sections are shown in Section 3.10.3.

3.6.2 Fuel Basket Evaluation for Off-Normal Operating Events

3.6.2.1 PWR Fuel Basket

This section evaluates the MAGNASTOR PWR basket for off-normal events using both classical hand calculations and finite element analysis methods. Factors of safety for the PWR basket are calculated based on the criteria for Service Level 'C' limits from ASME Code, Section III, Subsection NG [7].

The inertia loading for off-normal handling events is a 1.5g vertical acceleration and a 0.707g (0.5g in each transverse direction) transverse acceleration. The basket stresses due to the transverse loading are calculated using the three-dimensional periodic finite element models described in Section 3.10.1. Both half-symmetry models for the 0° and 45° basket orientations are used. Using a bounding weight of 22,500 pounds for the PWR basket, the maximum stress in

the fuel tube in the axial direction is calculated. Conservatively assuming the entire basket weight is carried through the fuel tubes, the stress in the tube due to the axial acceleration is as follows.

$$\sigma_{\text{tube}} = \frac{P_{\text{tube}}}{A} = \frac{1607}{11.4} = 0.14 \text{ ksi}$$

where:

$$P_{\text{tube}} = \frac{W \times a}{n} = \frac{22500 \times 1.5}{21} = 1,607 \text{ lb}$$

W = 22,500 lb ----- Bounding basket weight

n = 21 ----- Number of fuel tubes

a = 1.5g ----- Inertia g-load

A = 11.4 inch² ----- Tube cross-sectional area

The maximum primary membrane and primary membrane plus bending due to transverse loading (S_{tran}) from the finite element analysis results are shown in the following table. See Figure 3.10.1-13 through Figure 3.10.1-20 for locations of critical sections where the stresses are reported. The combined maximum stress intensity (S_{tot}) is conservatively obtained by adding the maximum stresses due to axial load (σ_{tube}) to the maximum stresses due to transverse load (S_{tran}). The combined stresses and factors of safety are presented in the following table. The allowable stresses for the off-normal events (Level C) are $1.5S_m$ for membrane stresses and $2.25S_m$ for membrane plus bending stresses.

Component	S_{tran} , ksi	S_{tot} , ksi	S_{allow} , ksi	FS
Fuel Tube, P_m	5.8	5.9	32.10	5.44
Fuel Tube, $P_m + P_b$	18.9	19.0	48.15	2.53
Support Weldments, P_m	0.4	0.5	32.10	Large
Support Weldments, $P_m + P_b$	5.6	5.7	48.15	8.45

The weight of the fuel tubes is supported on connector pins. Referring to Figure 3.10.1-13, the interior tubes (Tube #4) are supported by four connector pins; the side fuel tubes (Tube #1) are supported by two connector pins and the side and corner weldments; and the corner fuel tubes (Tube #3) are supported by three connector pins. The bearing stress on the fuel tube (σ_{brg}) is as follows.

$$\sigma_{\text{brg}} = \frac{1.5 \times P_{\text{pin}}}{A_{\text{brg}}} = \frac{1.5 \times 394}{0.21} = 2.8 \text{ ksi}$$

where:

$$A_{\text{brg}} = 0.21 \text{ inch}^2 \text{ ----- Bearing area}$$

$$P_{\text{pin}} = \frac{1}{3}P_t + \frac{1}{4}P_t = 394 \text{ lb ----- Combined loading on one support pin}$$

$$P_t = 675 \text{ lb ----- Tube weight}$$

The factor of safety (FS) for bearing is as follows.

$$FS = \frac{S_y}{\sigma_{\text{brg}}} = \frac{32.3}{2.8} = \text{Large}$$

where:

$$S_y = 32.3 \text{ ksi ----- Yield strength, SA-537 Class 1, at } 700^\circ\text{F}$$

The bearing stress (σ_{brg}) in the connector pin at the TSC bottom plate, conservatively using P_{tube} as previously determined, is as follows.

$$\sigma_{\text{brg}} = \frac{P_{\text{tube}}}{A_{\text{brg}}} = \frac{1607}{0.41} = 3.9 \text{ ksi}$$

where:

$$A_{\text{brg}} = \frac{\pi}{4}(D_o^2 - D_i^2) = \frac{\pi}{4}(0.75^2 - 0.19^2) = 0.41 \text{ inch}^2$$

$$D_o = 0.75 \text{ inch}$$

$$D_i = 0.19 \text{ inch}$$

The factor of safety (FS) for bearing is as follows.

$$FS = \frac{S_y}{\sigma_{\text{brg}}} = \frac{24.7}{3.9} = 6.3$$

where:

$$S_y = 24.7 \text{ ksi ----- Yield strength, SA-240 Type 304, at } 700^\circ\text{F}$$

The weight of the side and corner weldments is carried through to the TSC bottom plate by supports at the bottom of the basket. The bounding dimensions for the supports of the weldments are 5.0 inches in length and 0.3125-inch thickness (corner weldment). The maximum weight of one weldment is 800 lb (bounding, side weldment). The weldment supports one-quarter of the weight of two fuel tubes (675 lb per tube, bounding). The bearing stress is as follows.

$$\sigma_{\text{brg}} = \frac{1.5 \times W_{\text{sup}}}{A_{\text{sup}}} = 1.1 \text{ ksi}$$

where:

$$W_{\text{sup}} = 800 + 2 \times (0.25 \times 675) = 1138 \text{ lb}$$
$$A_{\text{sup}} = 5.0 \times 0.3125 = 1.56 \text{ inch}^2$$

The factor of safety (FS) for bearing is as follows.

$$\text{FS} = \frac{S_y}{\sigma_{\text{brg}}} = \frac{32.3}{1.1} = \text{Large}$$

where:

$$S_y = 32.3 \text{ ksi} \text{ ----- Yield strength, SA-537 Class 1, at } 700^\circ\text{F}$$

The buckling evaluation of the connector pin is performed in Section 3.7.2.1. The accident condition buckling evaluation is bounding due to the conservative 60g axial inertia loading.

The maximum tensile load in the attachment bolts for the off-normal condition is 770 pounds. The bolts have been evaluated for the bounding load of 1,500 lb for the normal condition in Section 3.5.2.1. The maximum shear load on a boss for the off-normal condition is 842 pounds. The bosses were evaluated with a bounding shear load of 3,500 lb for the normal condition. Therefore, no further analysis is required for the bolts and bosses for off-normal conditions.

The analysis presented in Section 3.7.2.1 bounds the off-normal analysis of the neutron absorber and retainer strip; therefore, no additional analysis is required.

3.6.2.2 BWR Fuel Basket

The analysis of the BWR basket for off-normal events uses both classical hand calculations and finite element analysis methods. The ANSYS finite element model and boundary conditions are presented in Section 3.10.2 for the 0° and 45° basket orientations. Factors of safety for the BWR basket are calculated based on the criteria for Service Level 'C' limits from ASME Code, Section III, Subsection NG [7]. The inertia loading for off-normal events is a 1.5g vertical acceleration and a 0.707g (0.5g in each transverse direction) transverse acceleration

For off-normal events of storage, a 1.5g acceleration (a) is applied to the basket in the axial direction. Using a bounding weight of 24,000 lb for the BWR basket, the maximum stress in the

fuel tube in the axial direction is calculated. Conservatively assuming the entire basket weight is carried through the fuel tubes, the stress in the tube due to the axial acceleration is as follows.

$$\sigma_{\text{tube}} = \frac{P_{\text{tube}}}{A} = \frac{800}{6.1} = 0.13 \text{ ksi}$$

where:

$$P_{\text{tube}} = \frac{W \times a}{n} = \frac{24,000 \times 1.5}{45} = 800 \text{ lb}$$

W = 24,000 lb ----- Bounding basket weight

N = 45 ----- Number of fuel tubes

a = 1.5g ----- Inertia g-load

A = 6.1 inch² ----- Tube cross-sectional area

The maximum primary membrane and primary membrane plus bending stresses due to transverse loading (S_{tran}) from the finite element analysis results are as follows. See Figure 3.10.2-13 through Figure 3.10.2-20 for locations of critical sections where stresses are reported.

The combined maximum stress intensity (S_{tot}) is conservatively obtained by adding the maximum stresses due to axial load (σ_{tube}) to the maximum stresses due to transverse load (S_{tran}).

The combined stresses and factors of safety are presented in the following table. The allowable stresses for the off-normal events (Level C) are $1.5S_m$ for membrane stresses and $2.25S_m$ for membrane plus bending stresses.

Component	S_{tran} , ksi	S_{tot} , ksi	S_{allow} , ksi	FS
Fuel Tube, P_m	11.8	11.9	32.10	2.70
Fuel Tube, $P_m + P_b$	32.9	33.0	48.15	1.46
Support Weldments, P_m	0.5	0.6	32.10	Large
Support Weldments, $P_m + P_b$	5.3	5.4	48.15	8.92

The weight of the fuel tubes is supported on connector pins. Referring to Figure 3.10.2-13, the interior tubes (Tube #4, typical) are supported by four connector pins; the side fuel tubes (Tube #1, typical) are supported by two connector pins and the side and corner weldments; and the corner fuel tubes (Tube #5, typical) are supported by three connector pins. The bearing stress (σ_{brg}) on the fuel tube is as follows.

$$\sigma_{\text{brg}} = \frac{1.5 \times P_{\text{pin}}}{A_{\text{brg}}} = \frac{1.5 \times 233}{0.34} = 1.0 \text{ ksi}$$

where:

$$A_{\text{brg}} = 0.34 \text{ inch}^2 \text{ ----- Bearing area}$$

$$P_{\text{pin}} = \frac{1}{3}P_t + \frac{1}{4}P_t = 233 \text{ lb} \text{ ----- Combined loading on one pin}$$
$$P_t = 400 \text{ lb} \text{ ----- Fuel tube weight}$$

The factor of safety (FS) for bearing is as follows.

$$FS = \frac{S_y}{\sigma_{\text{brg}}} = \frac{32.3}{1.0} = \text{Large}$$

where:

$$S_y = 32.3 \text{ ksi} \text{ ----- Yield strength, SA-537 Class 1, at } 700^\circ\text{F}$$

The bearing stress (σ_{brg}) in the connector pin at the TSC bottom plate, conservatively using P_{tube} as previously determined, is as shown.

$$\sigma_{\text{brg}} = \frac{P_{\text{tube}}}{A_{\text{brg}}} = \frac{800}{0.75} = 1.1 \text{ ksi}$$

where:

$$A_{\text{brg}} = \frac{\pi}{4}(D_o^2 - D_i^2) = \frac{\pi}{4}(1.0^2 - 0.19^2) = 0.75 \text{ inch}^2$$

$$D_o = 1.00 \text{ inch}$$

$$D_i = 0.19 \text{ inch}$$

The factor of safety (FS) for bearing is as follows.

$$FS = \frac{S_y}{\sigma_{\text{brg}}} = \frac{24.7}{1.1} = \text{Large}$$

where:

$$S_y = 24.7 \text{ ksi} \text{ ----- Yield strength, SA-240 Type 304, at } 700^\circ\text{F}$$

The weight of the side and corner weldments is carried through to the TSC bottom plate by supports at the bottom of the basket. The corner weldment is bounding for the top and bottom supports. The dimensions for the corner support weldment are 8.0 inches in length and 0.375-inch thickness. The bounding weight of the corner weldment is 1,100 pounds. The corner weldment also supports one-quarter of the weight of four fuel tubes (conservatively 400 lb per tube). The bearing stress is as follows.

$$\sigma_{\text{brg}} = \frac{W_{\text{sup}}}{A_{\text{sup}}} = 0.8 \text{ ksi}$$

where:

$$W_{\text{sup}} = 1.5 \times (1,100 + 4 \times (0.25 \times 400)) = 2,250 \text{ lb}$$
$$A_{\text{sup}} = 8.0 \times 0.375 = 3.0 \text{ inch}^2$$

The factor of safety (FS) for bearing is as follows.

$$\text{FS} = \frac{S_y}{\sigma_{\text{brg}}} = \frac{32.3}{0.8} = \text{Large}$$

where:

$$S_y = 32.3 \text{ ksi} \text{ ----- Yield strength, SA-537 Class 1, at } 700^\circ\text{F}$$

The maximum bolt load due to off-normal load is 1,241 pounds. Combined with a bolt preload of 400 lb, the maximum bolt load is 1,641 pounds. A bolt load of 1,700 lb is used for the evaluation. From Machinery's Handbook [12], the tensile strength (σ_t) in the bolt is as follows.

$$\sigma_t = \frac{P}{A_t} = \frac{1,700}{0.23} = 7.4 \text{ ksi}$$

where:

$$A_t = 0.7854 \left(D - \frac{0.9743}{n} \right)^2 = 0.23 \text{ inch}^2$$

$$D = 0.625 \text{ inch}$$
$$n = 11$$

The factor of safety (FS) is as follows.

$$\text{FS} = \frac{S_m}{\sigma_t} = \frac{23.3}{7.4} = 3.15$$

where:

$$S_m = 23.3 \text{ ksi} \text{ ----- Design stress intensity for SA-193, Gr B6, at } 700^\circ\text{F}$$

The shear stress in the bolt thread (τ_{bolt}) is as follows.

$$\tau_{\text{bolt}} = \frac{P}{A_s} = \frac{1,700}{0.379} = 4.5 \text{ ksi}$$

where:

$$A_s = 3.1416nL_e K_{n \text{ max}} \left[\frac{1}{2n} + 0.57735(E_{s \text{ min}} - K_{n \text{ max}}) \right] = 0.379 \text{ inch}^2$$

$$n = 11$$

The factor of safety (FS) is as follows.

$$FS = \frac{0.6S_y}{\tau_{\text{bolt}}} = \frac{0.6 \times 70.0}{4.5} = 9.3$$

where:

$$S_y = 70.0 \text{ ksi} \text{ ----- Yield strength, SA-193 Grade B6, at } 700^\circ\text{F}$$

The shear stress in the boss thread (τ_{boss}) is as follows.

$$\tau_{\text{boss}} = \frac{P}{A_n} = \frac{1,700}{0.542} = 3.1 \text{ ksi}$$

where:

$$A_n = 3.1416nL_e D_{s \text{ min}} \left[\frac{1}{2n} + 0.57735(D_{s \text{ min}} - E_{n \text{ max}}) \right] = 0.542 \text{ inch}^2$$

$$L_e = 0.38 \text{ inch}$$

$$E_{n \text{ max}} = 0.5732$$

$$D_{s \text{ min}} = 0.6113$$

$$n = 11$$

The factor of safety (FS) is as follows.

$$FS = \frac{0.6S_y}{\tau_{\text{bolt}}} = \frac{0.6 \times 28.6}{3.1} = 5.54$$

where:

$$S_y = 28.6 \text{ ksi} \text{ ----- Yield strength, SA-695, Type B, Gr 40, at } 700^\circ\text{F}$$

The boss is welded into the fuel tube with a 3/16-inch groove weld. The shear stress in the boss weld (τ_{weld}) is as follows.

$$\tau_{\text{weld}} = \frac{P}{A_w} = \frac{1,700}{0.59} = 2.9 \text{ ksi}$$

where:

$$P = 1,700 \text{ lb}$$

$$A_w = \pi D t_{\text{weld}} = \pi \times 1.00 \times 0.1875 = 0.4959 \text{ inch}$$

$$D = 1.00 \text{ inch} \text{ ----- Smallest boss diameter}$$

Using the lesser allowable, S_m , of SA-537 Class 1 or SA-695 Type B, Gr 40, the factor of safety (FS) is as follows.

$$FS = \frac{0.35 \times 0.9 S_m}{\tau_{\text{weld}}} = 2.10$$

where:

$$S_m = 19.2 \text{ ksi} \text{ ----- Design Stress Intensity, SA-695 Type B Grade 40, at } 700^\circ\text{F}$$

The washers under the bolts are subjected to a bending load to the torque of the bolts. Using "Roark's Formulas for Stress and Strain" Table 24-1a [13], the maximum stress in the washer is calculated. The maximum stress (σ) in the washer is as follows.

$$\sigma = \frac{6M_t}{t^2} = \frac{6 \times 203}{0.19^2} = 33.7 \text{ ksi}$$

where:

$$w = \frac{P}{\pi \times 2r_o} = \frac{1,700}{\pi \times 2 \times 0.55} = 491 \text{ inch-lb}$$

$$M_t = 203 \text{ inch-lb} \text{ ----- Calculated using the formula in Roark [13]}$$

The factor of safety (FS) is as follows.

$$FS = \frac{2.25 S_m}{\sigma} = 1.07$$

where:

$$S_m = 16.0 \text{ ksi} \text{ ----- Design stress intensity, SA-240 Type 304, at } 700^\circ\text{F}$$

The buckling evaluation of the connector pin is performed in Section 3.7.2.1. The accident condition buckling evaluation is bounding due to the 60g axial inertia loading.

The maximum shear load on a boss for the off-normal condition is 821 pounds. The bosses were evaluated with a bounding shear load of 4,200 lb for the normal condition in Section 3.5.2.2. Therefore, no further analysis is required for the bosses for off-normal conditions.

The analysis presented in Section 3.7.2.2 bounds the off-normal analysis of the neutron absorber and retainer strip; therefore, no additional analysis is required.

3.6.3 Concrete Cask Evaluation for Off-Normal Operating Events

Section 3.5.3.1 presents the thermal stress evaluation for normal conditions for the concrete cask. The analysis used the 106°F ambient condition thermal gradient, which is the off-normal event; therefore, the analysis is conservative. The analysis bounds both the normal and off-normal events; therefore, no thermal stress evaluation is presented in this section. All analyses of the concrete cask are bounded by the analyses presented in the normal and accident sections

Table 3.6-1 TSC Off-Normal Events, P_m Stresses

Load Case	Service Level	Section ^a	Component Stresses (ksi) ^b						S_{int}	S_{allow}	FS
			S_x	S_y	S_z	S_{xy}	S_{yz}	S_{xz}			
Off-Normal Pressure + Normal Handling	B	3	-0.67	-10.75	5.54	-0.21	-0.03	1.16	16.51	22.00	1.33
Normal Pressure + Off-Normal Handling	C	3	-0.62	-10.75	5.15	-0.25	-0.02	1.07	16.10	24.50	1.52

Table 3.6-2 TSC Off-Normal Events, $P_m + P_b$ Stresses

Load Case	Service Level	Section ^a	Component Stresses (ksi) ^b						S_{int}	S_{allow}	FS
			S_x	S_y	S_z	S_{xy}	S_{yz}	S_{xz}			
Off-Normal Pressure + Handling	B	3	-0.28	-5.53	22.31	0.00	0.00	1.47	27.94	33.00	1.18
Normal Pressure + Off-Normal Handling	C	3	-0.23	-6.17	21.24	-0.14	0.05	1.35	27.49	34.80	1.27

Table 3.6-3 TSC Off-Normal Events, $P + Q$ Stresses

Load Case	Service Level	Section ^a	Component Stresses (ksi) ^b						S_{int}	S_{allow}	FS
			S_x	S_y	S_z	S_{xy}	S_{yz}	S_{xz}			
Off-Normal Pressure + Normal Handling + Thermal	B	12	-44.54	-41.22	-9.07	-1.36	0.06	-1.71	36.12	60.00	1.66

^a See Figure 3.10.3-2 for section cut locations.

^b The x,y,z component of stress are to be interpreted radial, circumferential, and axial directions, respectively.

3.7 Storage Accident Events

This section presents the analyses of the structural components of MAGNASTOR for storage accident events. MAGNASTOR is evaluated using finite element models and classical hand calculations for the TSC, fuel baskets, and concrete cask.

3.7.1 TSC Evaluations for Storage Accident Conditions

The TSC is analyzed for an accident pressurization of 250 psig, a 24-inch end drop of the concrete cask, and the hypothetical concrete cask tip-over accident. For detailed analyses results for accident conditions, see Table 3.10.3-12 through Table 3.10.3-17.

3.7.1.1 Accident Pressurization

Accident pressurization is a hypothetical event that assumes the failure of all of the fuel rods contained within the TSC. No postulated storage condition is expected to lead to the rupture of all fuel rods. The TSC is analyzed for accident pressurization and dead weight loads using the finite element model and conditions described in Section 3.10.3. Dead weight is simulated by applying a 1.0g acceleration load in the axial direction in conjunction with pressure being applied to the TSC bottom plate to simulate the weight of the basket and fuel. To represent the accident pressure, an internal pressure of 250 psig is applied to all inner surfaces of the TSC. The canister bottom plate, which is resting on the pedestal plate, is conservatively subjected to the 250 psig pressure and the dead weight of the fuel and basket.

The resulting TSC stresses for the accident pressurization condition are summarized in Table 3.7-1 and Table 3.7-2 for primary membrane and primary membrane plus primary bending stress categories, respectively. The minimum factor of safety of 1.59 occurs at Section 3 for the P_m+P_b stresses. The locations for the stress sections are shown in Section 3.10.3.

Results of analysis of this event demonstrate that the TSC is not significantly affected by the increase in internal pressure that results from the hypothetical rupture of all PWR or BWR fuel rods in the TSC.

3.7.1.2 Concrete Cask 24-inch End-Drop

This section addresses the TSC stresses and potential TSC shell buckling associated with the postulated 24-inch end-drop accident of the concrete cask. The evaluation of the TSC during the end impact is performed using an inertial load of 60g. This inertial load conservatively bounds the maximum calculated acceleration including dynamic load factor (DLF).

3.7.1.2.1 TSC End Impact Stress Evaluation

The TSC is analyzed for the concrete cask 24-inch drop accident condition using the finite element model described in Section 3.10.3. The 24-inch drop is simulated by applying a 60g acceleration load in the axial direction, with pressure applied to the TSC bottom plate to simulate the inertial load of the basket and fuel. To represent the normal pressure, an internal pressure of 110 psig is applied to all inner surfaces of the TSC. The canister bottom plate, which is resting on the pedestal plate, is conservatively subjected to the pressure due to the 60g inertia of the basket and fuel, as well as the 110 psig internal pressure.

The resulting maximum stresses in the TSC for the 24-inch drop accident events are summarized in Table 3.7-1 and Table 3.7-2 for primary membrane, and primary membrane plus primary bending stress categories, respectively. The minimum factor of safety of 3.71 occurs at section 4 (lower TSC shell) for the P_m stresses. The locations for the stress sections are shown in Section 3.10.3.

3.7.1.2.2 TSC Buckling Evaluation

During the 24-inch bottom-end drop of the concrete cask, the 60g inertial load conservatively applied to the closure lid assembly generates longitudinal compressive stresses in the TSC shell. The critical buckling stress (S_{CR}) in the TSC shell based on the TSC geometry and material properties is as follows.

$$S_{CR} = E \frac{0.605 - 10^{-7} m^2}{m(1 + 0.004\phi)} = 34.5 \text{ ksi} \quad [15]$$

where:

$E = 25.8 \times 10^3 \text{ ksi}$ ----- Modulus of elasticity of SA-240, Type 304, at 500°F

$\phi = \frac{E}{S_y} = 1,330$ ----- Inverse strain parameter

$S_y = 19.4 \text{ ksi}$ ----- Yield strength of SA-240, Type 304, at 500°F

$m = \frac{r_m}{t} = 71.5$ ----- Mean radius to thickness ratio

$r_m = 35.75 \text{ inch}$ ----- Mean radius TSC shell

$t = 0.5 \text{ inch}$ ----- Thickness of TSC shell

The results from the 24-inch end-drop analysis are screened for the maximum longitudinal compressive stress. The maximum longitudinal compressive stress, S_z , of 9.3 ksi occurs at the

intersection of the TSC shell and bottom plate (see Section 3.10.3). The factor of safety (FS) is as follows.

$$FS = \frac{S_{CR}}{S_z} = \frac{34.5 \text{ ksi}}{9.3 \text{ ksi}} = 3.7$$

Therefore, buckling of the TSC does not occur.

3.7.1.3 Concrete Cask Tip-Over

The TSC is analyzed for the concrete cask tip-over using the finite element model described in Section 3.10.3. A tapered inertial load (40g at top of TSC closure lid and 1g at the base of the concrete cask) is considered as a side impact load on the TSC. The 40g inertial load is conservatively used in the evaluation to bound the calculated maximum g-load for the TSC during the concrete cask tip-over event including the dynamic load factor (Section 3.7.3.7).

The resulting maximum stresses in the TSC for tip-over conditions are summarized in Table 3.7-1 and Table 3.7-2 for primary membrane and primary membrane plus primary bending stress categories, respectively. The minimum factor of safety is 1.20 at Section 11 for the P_m stresses and 1.08 at Section 5 for the P_m+P_b stresses. The factor of safety, P_m+P_b , for the structural lid closure weld, Section 11, is 1.39. The locations for the stress sections are shown in Section 3.10.3. Note that the maximum stresses occur at the section cut at the 0-degree location.

3.7.1.4 Flood

This evaluation considers design basis flood conditions of a 50-foot depth of water having a velocity of 15 feet per second. The hydrostatic pressure (P_h) exerted on the TSC during a 50-foot flood event is as follows.

$$P_h = \rho \times h = \left(62.4 \frac{\text{lb}}{\text{ft}^3} \right) \left(\frac{1 \text{ ft}^3}{1728 \text{ in}^2} \right) \times (50 \text{ ft}) \left(\frac{12 \text{ in}}{1 \text{ ft}} \right) = 22 \text{ psi}$$

where:

$$\begin{aligned} \rho &= 62.4 \text{ lb/ft}^3 \text{----- Density of water} \\ h &= 50 \text{ ft----- Immersion depth} \end{aligned}$$

During normal conditions, the TSC is evaluated for an internal pressure of 110 psig. Because the pressure differential is reduced during flood conditions ($110 - 22 = 88$ psig), stresses in the TSC shell are reduced. Therefore, the hydrostatic pressure exerted by the 50-foot depth of water

actually reduces the stress in the TSC. MAGNASTOR is, therefore, not adversely affected by the design basis flood.

3.7.1.5 Tornado and Tornado-Driven Missiles

The postulated tornado wind loading and tornado missile impacts are not capable of overturning the concrete cask, or penetrating the boundary established by the concrete cask. Consequently, there is no effect on the TSC. Stresses resulting from the decreased external pressure due to a tornado are bounded by the stresses due to the accident internal pressure condition evaluated in Section 3.7.1.1.

3.7.2 Fuel Baskets Evaluation for Storage Accident Events

3.7.2.1 PWR Basket

3.7.2.1.1 24-inch Concrete Cask End Drop

For the 24-inch concrete cask drop, a 60g acceleration (a) is conservatively applied to the PWR basket in the axial direction. The basket is evaluated using classical hand calculations. Using a bounding weight of 22,500 lb for the PWR basket, the maximum stress in the fuel tube is calculated. Factors of safety for the PWR basket are calculated based on the criteria for Service Level 'D' limits from ASME Code, Section III, Subsection NG [7] and Appendix F [8]. Conservatively assuming the entire basket weight is carried through the fuel tubes, the stress in the tube is as follows.

$$\sigma_{\text{tube}} = \frac{P_{\text{tube}}}{A} = \frac{64286}{11.4} = 5.6 \text{ ksi}$$

where:

$$P_{\text{tube}} = \frac{W \times a}{n} = \frac{22,500 \times 60}{21} = 64,286 \text{ lb}$$

W = 22,500 lb ----- Bounding basket weight
n = 21 ----- Number of fuel tubes
A = 11.4 inch² ----- Tube cross-sectional area

The factor of safety (FS) is as follows.

$$FS = \frac{0.7 \times S_u}{\sigma_{\text{tube}}} = \frac{0.7 \times 68.4}{5.6} = 8.6$$

where:

$$S_u = 68.4 \text{ ksi} \text{ ----- Ultimate strength, SA-537 Class 1, at } 700^\circ\text{F}$$

The weight of the fuel tubes is supported by connector pins. Referring to Figure 3.10.1-13, the interior tubes (Tube #4, typical) are supported by four connector pins; the side fuel tubes (Tube #1, typical) are supported by two connector pins and the side and corner weldments; and three connector pins support the corner fuel tubes (Tube #3, typical). The load is transferred by shear through the connector pin welds (four welds on two connector pins, which attaches them to the fuel tube at bottom of basket) and by axial compression through the area of the end of the fuel tube in contact with the connector pin assembly, which rests on the bottom canister plate.

The load capability (P_{joint}) of the weld and the common area is determined by the sum of the loads, which each load path can sustain. A conservative evaluation is performed in which the stresses are evaluated against allowables associated with an elastic evaluation, as opposed to the plastic evaluation permitted in Appendix F [8].

$$P_{\text{joint}} = A_m(0.7S_u) + A_w(wf \times 0.42S_u) = 25.3 \text{ kips}$$

where:

$$\begin{aligned} A_m &= 0.21 \text{ inch}^2 \text{ ----- Common area for compression} \\ A_w &= 4(l_w t_w) = 1.52 \text{ inch}^2 \text{ ----- Weld area for shear} \\ l_w &= 2.0 \text{ inch} \text{ ----- Connector pin length} \\ t_w &= 3/16 \text{ inch} \text{ ----- Weld size} \\ wf &= 0.35 \text{ ----- Weld quality factor visual inspection} \\ &\quad \text{(ASME Code Section III, Subsection NG, Article NG-3352)} \\ S_u &= 68.4 \text{ ksi} \text{ ----- Tensile strength, SA-537 Class 1, at } 700^\circ\text{F} \end{aligned}$$

The load in the tube joint (P) is as follows.

$$P = 60 \times P_{\text{pin}} = 60 \times 394 = 23.6 \text{ ksi}$$

where:

$$\begin{aligned} P_{\text{pin}} &= \frac{1}{3}P_t + \frac{1}{4}P_t = 394 \text{ lb} \\ P_t &= 675 \text{ lb} \text{ ----- Tube weight} \end{aligned}$$

The factor of safety (FS) is as follows.

$$FS = \frac{P_{\text{joint}}}{P} = \frac{25.3}{23.6} = 1.07$$

The weight of the side and corner weldments is carried through to the TSC base plate by supports at the bottom of the weldments. The bounding dimensions for the supports of the weldments are 5.0 inches in length and 0.3125-inch thickness (corner weldment). The maximum weight of one weldment is 800 lb (bounding, side weldment). The weldment supports one-quarter of the weight of two fuel tubes (675 lb per tube, bounding). The membrane stress (σ_m) is as follows.

$$\sigma_m = \frac{60 \times W_{sup}}{A_{sup}} = \frac{60 \times 1,138}{1.56} = 43.8 \text{ ksi}$$

where:

$$W_{sup} = 800 + 2 \times (0.25 \times 675) = 1138 \text{ lb}$$

$$A_{sup} = 5.0 \times 0.3125 = 1.56 \text{ inch}^2$$

The factor of safety (FS) is as follows.

$$FS = \frac{0.7S_u}{\sigma_m} = \frac{0.7 \times 68.4}{43.8} = 1.09$$

where:

$$S_u = 68.4 \text{ ksi} \text{ ----- Ultimate strength, SA-537 Class 1, at } 700^\circ\text{F}$$

The 32-basket connector pins support the PWR basket during a 60g bottom-end drop accident. The bounding temperature at the bottom of the basket is 500°F. The pins are subjected to compressive loads; therefore, a buckling evaluation of the pins is presented. The load on one connector pin (P_{pin}) is as follows.

$$P_{pin} = \frac{W \times 60}{n} = \frac{22500 \times 60}{32} = 42.2 \text{ kips}$$

where:

$$W = 22,500 \text{ lb} \text{ ----- Bounding basket weight}$$

$$n = 32 \text{ ----- Number of pins}$$

Using the Euler buckling theory, the critical buckling load (P_{cr}) is as follows.

$$P_{cr} = \frac{\pi^2 EI}{(KL)^2} = \frac{\pi^2 \times (25.8 \times 10^6) \times 0.015}{(2 \times 3.0)^2} = 106.0 \text{ kip [9]}$$

where:

$$A_{pin} = 0.44 \text{ inch}^2$$

$$D = 0.75 \text{ inch} \text{ ----- Pin diameter}$$

$$L = 3.0 \text{ inch} \text{ ----- Pin length}$$

$$I = \frac{\pi r^4}{4} = 0.015 \text{ inch}^4$$

$$K = 2.0 \text{ ----- Buckling constant, clamped-free}$$

$$E = 25.8 \times 10^6 \text{ psi} \text{ ----- SA-240 Type 304, at } 500^\circ\text{F}$$

The factor of safety (FS) for buckling of the connector pins is as follows.

$$FS = \frac{P_{cr}}{P_{pin}} = \frac{106.0 \text{ kip}}{42.2 \text{ kip}} = 2.51$$

PWR Neutron Absorber Evaluation

During the end impact condition, the PWR neutron absorber and the weld post are subject to shearing force in the longitudinal direction of the neutron absorber. The neutron absorber is considered to be supported by two weld posts located at the bottom end of the neutron absorber. The evaluation is conservatively performed for an acceleration of 60g at a bounding temperature of 350°F. The inertia load applied to the neutron absorber (F_{na}) at each weld post during the end impact is as follows.

$$F_{na} = L \times W \times t \times \rho \times a / 2 = 525 \text{ lb}$$

where:

$$\rho = 0.1 \text{ lb/in}^3 \text{ ----- Bounding density of the neutron absorber}$$

$$a = 60g \text{ ----- End drop acceleration}$$

$$t = 0.125 \text{ in} \text{ ----- Thickness of neutron absorber}$$

$$L = 173 \text{ in} \text{ ----- Length of neutron absorber}$$

$$W = 8.1 \text{ in} \text{ ----- Width of neutron absorber}$$

The shearing capacity of the neutron absorber is as follows.

$$F_{shear_na} = A_s \times \Phi_a = 0.44 \times 2260 = 994 \text{ lb}$$

where:

$$A_s = L_{NA} \times 1.414 \times 2 \times t = 0.44 \text{ in}^2 \text{----- Shear area at both sides of each weld-post (at the } 45^\circ \text{ shear planes)}$$
$$L_{NA} = 1.25 \text{ in ----- Min. edge distance of the neutron absorber}$$
$$\Phi_a = 0.42 S_u = 2.26 \text{ ksi----- Allowable shear stress}$$
$$S_u = 5.38 \text{ ksi ----- Tensile strength of neutron absorber at } 350^\circ\text{F}$$

The factor of safety (FS) is as follows.

$$FS = F_{\text{shear_na}} / F_{na} = 994 / 525 = 1.89$$

The strength of the weld posts is significantly higher than that of the neutron absorber. Therefore, no evaluation is required for the weld posts for the concrete cask 24-inch end-drop condition.

3.7.2.1.2 Concrete Cask Tip-Over

The analysis results for the PWR basket subjected to a hypothetical concrete cask tip-over accident are presented in this section. Factors of safety for the PWR basket are calculated based on the criteria for Service Level 'D' limits from ASME Code, Section III, Subsection NG [7] and Appendix F [8].

PWR Fuel Tube Evaluation

The PWR basket fuel tubes are analyzed for a tip-over accident using the three dimensional periodic plastic finite element models described in Section 3.10.1. The fuel tube is conservatively evaluated for 35g side impact load.

Plastic stress intensities are calculated for the PWR fuel tubes for the bounding basket orientations of 0° and 45° (see Figure 3.10.1-13 and Figure 3.10.1-15 for tube IDs). The maximum primary membrane and primary membrane plus bending nodal stress intensities for each fuel tube are reported in Table. Note that for plastic analysis, ANSYS reports stresses in the elastic region as the yield strength (31.7 ksi, at 500°F) for the stress-strain curve.

The ANSYS plastic finite element model follows the material stress-strain curve and allows for nonlinear behavior above the yield strength point. The stress allowables for plastic analysis are based on ASME Code, Section III, Appendix F [8]. The allowable primary membrane stress is $0.7S_u$. The allowable primary stress intensity is $0.9S_u$. The minimum factors of safety for the PWR fuel tubes are 1.48 for primary membrane stresses and 1.70 for primary membrane plus bending stress intensity (0° basket orientation). The critical stress locations occur in the fuel tube corners.

The PWR fuel tubes are constructed by welding two tube halves together using a full-penetration weld for the length of the fuel tube. A surface MT weld examination per ASME Code, Section III, Subsection NG, Article NG-5232 is used, which has a 0.65 weld quality factor (wf). From the plastic analysis of the PWR basket, the maximum membrane and membrane plus bending stress intensity at a tube weld is 10.3 ksi and 31.1 ksi, respectively (0° basket orientation). The factors of safety (FS) for the weld are as follows.

Membrane:

$$FS = \frac{0.7S_u \times wf}{\sigma} = 3.02$$

Membrane plus bending:

$$FS = \frac{0.9S_u \times wf}{\sigma} = 1.29$$

where:

$$S_u = 68.4 \text{ ksi} \text{ ----- Ultimate strength, SA-537 Class 1, at } 700^\circ\text{F}$$

The pins between adjacent tubes are subjected to shear load. From the finite element models, the maximum shear load (P) in the pin is 17,400 lb and 10,946 lb for 0° and 45° basket orientations, respectively. The shear load is determined by summing the nodal forces at the contact region between the pin and tube socket. Using a bounding load of 18,000 lb, the shear stress in the pin is

$$\tau_{pin} = \frac{P}{Dl_{pin}} = 25.2 \text{ ksi}$$

where:

$$D = 0.44 \text{ inch} \text{ ----- Pin diameter}$$
$$l_{pin} = 3.25/2 = 1.625 \text{ inch} \text{ ----- Length of pin in the model}$$

The factor of safety (FS) is as follows.

$$FS = \frac{0.42S_u}{\tau_{pin}} = 1.17$$

where:

$$S_u = 70.0 \text{ ksi} \text{ ----- Ultimate strength, SA-695 Type B Gr 40, at } 700^\circ\text{F}$$

The bearing stress (σ_{brg}) on the pin is evaluated using the bounding load of 18,000 lb. The bearing area is determined based on a 30° contact arc between the pin and the fuel tube socket.

$$\sigma_{\text{brg}} = \frac{P}{LS} = 100.7 \text{ ksi}$$

where:

$$P = 18,000 \text{ lb} \text{ ----- Maximum load on pin}$$

$$L = 1.625 \text{ inch} \text{ ----- Length of pin in ANSYS model}$$

$$S = \pi D \frac{30}{360} = 0.11 \text{ in} \text{ ----- Bearing arc length}$$

$$D = 0.44 \text{ inch} \text{ ----- Pin diameter}$$

Per ASME Appendix F-1336, the allowable bearing stress is $2.1S_u$. The factor of safety (FS) is as follows.

$$FS = \frac{2.1S_u}{\sigma_{\text{brg}}} = 1.43$$

where:

$$S_u = 70.0 \text{ ksi} \text{ ----- Ultimate strength, SA-695 Type B Gr 40, at } 700^\circ\text{F}$$

PWR Neutron Absorber and Retainer

The PWR neutron absorber and retainer are conservatively evaluated for a 60g side-impact load and for the concrete cask tip-over event. The retainer strip consists of 304 stainless steel and is restrained by an array of posts welded to the inside surface of the fuel tube. Two rows of posts are separated four inches apart and a spacing of ten inches exists between the posts along the axial direction of the fuel tube.

The pitches of the slotted holes in the neutron absorber are the same as the holes in the retainer strip through which the weld posts are connected to the fuel tube. The slotted holes are used to prevent interference during differential thermal expansion between the neutron absorber and the fuel tube. The head of the weld posts supporting the retainer strip are engaged in the recessed conical pockets of the retainer.

As shown in Figure 3.7-3, a quarter-symmetry finite element model is generated to represent one-half of the ten-inch periodic section for the PWR design. The model is comprised of the retainer strip with the conical slot, the neutron absorber, and the weld post. Inelastic properties are employed for the stainless steel retainer strip and the neutron absorber at 700°F to adequately represent the stiffness at the maximum temperature condition. The model for the neutron absorber plate is comprised of three layers of materials. The two outer layers employ the inelastic properties of aluminum 1100 series cladding at 700°F. The center layer represents the neutron absorber material, which is assigned a yield strength of 10 psi and an elastic modulus of elasticity of 1,000 psi. The low yield strength for the core material allows the neutron absorber core to provide only a minimal contribution of stiffness to the neutron absorber plate. The weld post was modeled as being rigid to maximize deformation of the conical-shaped section of the retainer by the weld post. Symmetry conditions were imposed along the planes of symmetry, which are present on all four sides of the model. The parts are modeled independently and the automatic contact surface option in LS-DYNA was used between the parts to transfer load between the neutron absorber, the retainer and the weld post. The evaluation of the side impact was performed using LS-DYNA and the impact was simulated by imposing the acceleration time history whose maximum acceleration was 60g. This conservatively envelops the maximum tip-over acceleration of 35g.

Since the function of the retainer is to maintain the neutron absorber in its position, the criteria for the retainer is to limit the motion of the neutron absorber during and after the impact. This is confirmed by considering the permanent strain and the permanent displacement of the retainer. The strain of 3.3%, which is minimal, is local to the conical-shaped hole. Since inelastic strains are not recovered, this indicates that maximum inelastic strain during the impact is also limited to 3.3 percent. Such a minimal strain level indicates that the conical pocket retains its configuration for the weld post to restrain the retainer. The final maximum displacement of the retainer strip at the axial midpoint between the weld posts is computed to be 0.06 inch, which is consistent with the minimal plastic strain in the retainer. This also confirms that the retainer remains engaged with the weld post during and after the impact.

The maximum stress intensity in the stainless steel retainer strip is determined to be 35.8 ksi, which is also local to conical-shaped hole at the weld post. The allowable stress for accident condition is $0.9S_u$ per ASME Section III Appendix F. The ultimate strength (S_u) of Type 304 stainless steel at 700°F is 63.2 ksi.

The factor of safety (FS) is as follows.

$$FS = \frac{0.9 \times 63.2}{35.8} = 1.59$$

The peak force on the weld post determined from the analysis is 74 pounds. The shear area governs the capacity of the weld. The depth of the weld (h) is 0.13 inch. The diameter of the weld post (D) is 0.25 inch. The governing stress is the shear stress in the base material. The allowable shear stress for the accident condition is $0.42S_u$. The ultimate strength (S_u) of the base material (SA240, Type 304) is 63,200 psi. The weld capacity, F_{cap} , is calculated as shown in the following.

$$\begin{aligned} F_{cap} &= 0.42 \times n \times S_u \times h \times BD \\ &= 0.42 \times 0.3 \times 63,200 \times 0.13 \times (3.1416 \times 0.25) \\ &= 813 \text{ lb} \end{aligned}$$

where:

$$n = 0.3 \text{----- The design factor per ASME Code, Section III, Subsection NG, Table NG-3352-1 for the intermittent plug weld employing a surface visual examination method per NG-5260.}$$

The factor of safety (FS) is as follows.

$$FS = \frac{813}{74} = 11$$

PWR Corner Support Weldment Evaluation

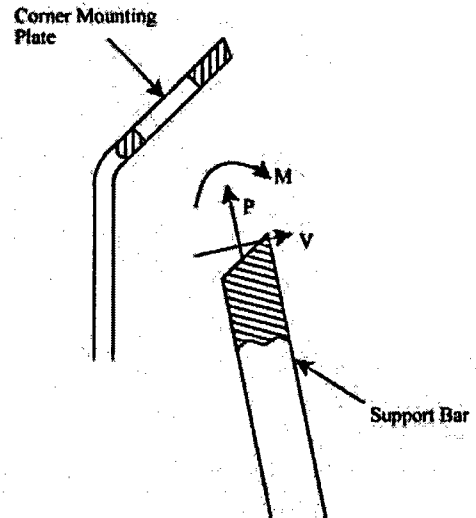
The PWR basket corner support weldment is analyzed for the tip-over accident using the three-dimensional plastic finite element model and boundary conditions described in Section 3.10.1. The corner support weldment is comprised of two major components: the mounting plate (vertical plate) and the side support bars, which are located on five-inch centers.

The analysis results for the corner support weldment are presented in Table 3.7-4 and Table 3.7-5. The maximum nodal stress intensity is conservatively compared to the primary membrane stress allowable of $0.7 S_u$ per ASME Code Section III Appendix F. The minimum factor of safety for the corner weldment mounting plates is 1.50. The minimum factor of safety for the corner weldment support bars is 1.51.

The support bar is a continuous bar that is bent at the ridge gusset. The support bars are welded to the corner mounting plate where cutouts in the corner mounting plate accept the end of the bars. The bars are welded to the wall on the backside with a minimum 5/16-inch groove weld on the sides of the bars and 3/16-inch groove welds on the top and bottom of the bar using the

visual inspection criteria per ASME Code, Section III, Subsection NG, Article NG-5260. A weld quality factor of 0.35 is applied based on visual inspection of the weld per ASME Code, Section III, Subsection NG, Article NG-3352.

The welded joint between the support bar and corner mounting plate is capable of carrying bending, axial, and shear loads. The maximum weld loads occur in the 0° basket orientation. The bending moment (M), axial load (P), and shear load (V) are 4,334 in-lb, 4,185 lb, and 629 lb, respectively. The weld stress intensity (σ_{weld}) is as follows.



$$\sigma_{\text{weld}} = \sqrt{\left(\frac{M}{S_w} + \frac{P}{A_w}\right)^2 + 4\left(\frac{V}{A_w}\right)^2} = 19.9 \text{ ksi}$$

where:

$$S_w = (0.875 \times 0.3125 \times 0.875) + \frac{(0.19 \times 0.875^2)}{3} = 0.288 \text{ in}^3$$

$$A_w = (0.875 \times 2 \times 0.3125) + (2 \times 0.19 \times 0.875) = 0.88 \text{ in}^2$$

The factor of safety (FS) for the weld is as follows.

$$FS = \frac{0.35(S_u)}{\sigma_{\text{weld}}} = 1.20$$

where:

$$S_u = 68.4 \text{ ksi} \text{ ----- Ultimate strength, SA-537 Class 1, at } 700^\circ\text{F}$$

The ridge gusset is welded to the corner mounting plate with 1/8-inch flair bevel welds on both sides of the plate. The weld uses the visual inspection criteria per ASME Code, Section III, Subsection NG, Article NG-5260 and quality factor of 0.35, as defined previously. From the finite element analysis, the governing weld loads consists of a bending moment of 130 in-lb and a shear force of 113 pounds. The stress in the weld (σ_{weld}) is as follows.

$$\sigma_{\text{weld}} = \sqrt{\left(\frac{130}{0.5}\right)^2 + 4\left(\frac{113}{1.0}\right)^2} = 0.4 \text{ ksi}$$

where:

$$S_w = t_{\text{plate}} \times t_{\text{weld}} \times l_{\text{weld}} = 0.5 \text{ in}^3$$

$$A_{\text{wg}} = t_{\text{weld}} \times l_{\text{weld}} = 0.125 \times 8.0 = 1.0 \text{ in}^2$$

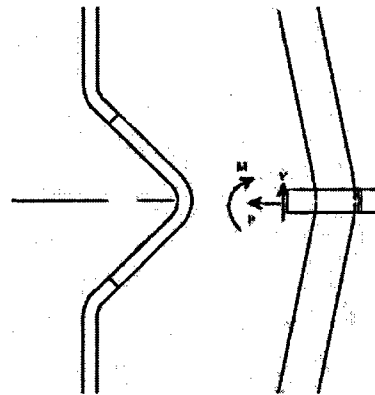
$$t_{\text{weld}} = \frac{1}{8}\text{-inch}$$

$$t_{\text{plate}} = 0.5 \text{ inch}$$

$$l_{\text{weld}} = 8.0 \text{ inch}$$

The factor of safety (FS) in the weld is as follows.

$$FS = \frac{0.35 \times S_u}{\sigma_{\text{weld}}} = \text{Large}$$



where:

$$S_u = 68.4 \text{ ksi} \text{ ----- Ultimate strength, SA-537 Class 1, at } 700^\circ\text{F}$$

PWR Side Support Weldment Evaluation

The PWR basket side support weldment is analyzed for the tip-over accident using the three-dimensional periodic plastic finite element model and boundary conditions described in Section 3.10.1. The analysis results for the side support weldment are presented in Table 3.7-6.

Conservatively, the maximum nodal stress intensity is compared to the primary membrane stress allowable, $0.7S_u$. The minimum factor of safety for the side support weldment is 1.50.

PWR Side and Corner Weldment / Fuel Tube Attachment Evaluation

The corner and side support weldments are the primary structure that maintains the geometry of the fuel tube array during a hypothetical tip-over accident. The support weldments are bolted to the fuel tubes at 16 circumferential locations. The boss and bolt connection is designed so that the bolts are only loaded in tension, including preload. Otherwise, the support weldments apply a bearing load on the fuel tube array. From the finite element results of the 0° and 45° basket orientations, the maximum bolt tensile load is 5,994 pounds. Combined with the bolt preload of 400 lb, the maximum bolt load is 6,394 pounds.

The tensile stress in the bolt is as follows.

$$\sigma_t = \frac{P}{A_t} = \frac{6.394}{0.23} = 27.8 \text{ ksi}$$

where:

$$A_t = 0.7854 \left(D - \frac{0.9743}{n} \right)^2 = 0.23 \text{ inch}^2$$

$$D = 0.625 \text{ inch}$$

$$n = 11$$

The factor of safety (FS) is as follows.

$$FS = \frac{S_y}{\sigma_t} = \frac{70.0}{27.8} = 2.52$$

where:

$$S_y = 70.0 \text{ ksi} \text{ ----- Yield strength for SA 193, Gr B6 at } 700^\circ\text{F}$$

The shear stress (τ_{bolt}) in the bolt thread is as follows.

$$\tau_{\text{bolt}} = \frac{P}{A_s} = \frac{6.394}{0.499} = 12.8 \text{ ksi}$$

where:

$$A_s = 3.1416nL_eK_{n \text{ max}} \left[\frac{1}{2n} + 0.57735(E_{s \text{ min}} - K_{n \text{ max}}) \right] = 0.499 \text{ inch}^2$$

The factor of safety (FS) is as follows.

$$FS = \frac{0.42S_u}{\tau_{\text{bolt}}} = \frac{0.42 \times 90.6}{12.8} = 2.97$$

where:

$$S_u = 90.6 \text{ ksi} \text{ ----- Ultimate strength, SA-193 Grade B6 at } 700^\circ\text{F}$$

The shear stress in the boss thread (τ_{boss}) is as follows.

$$\tau_{\text{boss}} = \frac{P}{A_n} = \frac{6.394}{0.713} = 9.0 \text{ ksi}$$

where:

$$A_n = 3.1416nL_c D_{s\min} \left[\frac{1}{2n} + 0.57735(D_{s\min} - E_{n\max}) \right] = 0.713 \text{ inch}^2$$

The factor of safety (FS) is as follows.

$$FS = \frac{0.42S_u}{\tau_{\text{boss}}} = \frac{0.42 \times 70.0}{9.0} = 3.27$$

where:

$$S_u = 70.0 \text{ ksi} \text{ ----- Ultimate strength, SA-695 Type B, Gr 40, at } 700^\circ\text{F}$$

The boss is welded into the fuel tube with a 1/4-inch groove weld. The weld uses the visual inspection criteria per ASME Code, Section III, Subsection NG, Article NG-5260 and a quality factor of 0.35. The shear stress in the boss weld (τ_{weld}), is as follows.

$$\tau_{\text{weld}} = \frac{P}{A_w} = \frac{6.394}{0.98} = 6.5 \text{ ksi}$$

where:

$$\begin{aligned} P &= 1,381 \text{ lb} \\ A_w &= \pi D t_{\text{weld}} = \pi \times 1.25 \times 0.25 = 0.98 \text{ inch} \\ D &= 1.25 \text{ inches} \text{ ----- Boss diameter} \end{aligned}$$

The factor of safety (FS) is

$$FS = \frac{0.42S_u}{\tau_{\text{weld}}} = \frac{0.42 \times 68.4 \times 0.35}{6.5} = 1.55$$

where:

$$S_u = 68.4 \text{ ksi} \text{ ----- Ultimate strength, SA-537 Class 1, at } 700^\circ\text{F}$$

The washers under the bolts are subjected to a bending load due to the bolt preload. Using Roark's, Table 24-1a, the maximum stress in the washer is calculated. The maximum stress (σ) in the washer is as follows.

For the corner and side support weldment, the maximum load, including pre-load, on the washer is 6,394 lb, 0° basket orientation.

$$\sigma = \frac{6M_t}{t^2} = \frac{6 \times 766}{0.3125^2} = 47.1 \text{ ksi}$$

where:

$$a = \frac{1.50}{2} = 0.75 \text{ inch} \text{----- Radius of the cutout in support weldments}$$

$$b = \frac{0.75}{2} = 0.375 \text{ inch} \text{----- Inner radius of the washer}$$

$$r_o = 0.55 \text{ inch} \text{----- Average radius of bolt head}$$

$$t = 5/16 \text{ inch} \text{----- Thickness of washer - thinnest}$$

$$E = 27.0 \times 10^6 \text{ psi} \text{----- Modulus of elasticity (SA-240 Type 304)}$$

$$\nu = 0.3 \text{----- Poisson's ratio}$$

$$w = \frac{P}{\pi \times 2r_o} = \frac{6,394}{\pi \times 2 \times 0.55} = 1,850 \text{ lb/in}$$

$$G = \frac{E}{2(1+\nu)} = \frac{27.0 \times 10^6}{2(1+0.3)} = 10.38 \times 10^6 \text{ psi}$$

$$D = \frac{Et^3}{12(1-\nu^2)} = \frac{27.0 \times 10^6 (0.3125^3)}{12(1-0.3^2)} = 75,460 \text{ inch-lb}$$

$$M_t = 766 \text{ inch-lb} \text{----- Calculated using formulas in Roark's [13]}$$

The factor of safety (FS) is as follows.

$$FS = \frac{S_u}{\sigma} = \frac{63.2}{47.1} = 1.34$$

where:

$$S_u = 63.2 \text{ ksi} \text{----- Ultimate strength, SA-240 Type 304, at } 700^\circ\text{F}$$

The bosses transfer shear loads between the support weldments and fuel tube array. The maximum shear load on a boss is 13.4 kip, 0° basket orientation. The outer diameter of the boss is 1.25 inches and the inner diameter is 0.625 inch. The corresponding cross-sectional area (A) is 0.92 in². The shear stress on the boss is as follows.

$$\tau_{\text{boss}} = \frac{P}{A} = \frac{13.4}{0.92} = 14.6 \text{ ksi}$$

The factor of safety (FS) is as follows.

$$FS = \frac{0.42S_u}{\tau_{\text{boss}}} = \frac{0.42 \times 70.0}{14.6} = 2.01$$

where:

$$S_u = 70.0 \text{ ksi} \text{----- Ultimate strength, SA-695, Type B, Gr 40, at } 700^\circ\text{F}$$

Loads between the fuel tube array and the corner and side weldments are reacted out in shear and bearing in the support weldments. Bearing stresses are not considered for accident events. Due to the geometry of the basket, the cutout in the corner support weldments has an edge distance less than two times the diameter of the cutout. The shear stress in the corner weldment mounting plate is as follows.

$$\tau = \frac{P}{A_{\text{shear}}} = \frac{13.4}{1.14} = 11.8 \text{ ksi}$$

where:

$$A_{\text{shear}} = 2 \left[\frac{L_{\text{ed}}}{\sin 45^\circ} t_{\text{plate}} \right] = 1.14 \text{ inch}^2$$

$$L_{\text{ed}} = 1.30 \text{ inch} \text{----- Boss cutout edge distance in corner weldment}$$

$$t_{\text{plate}} = 0.31 \text{ inch} \text{----- Mounting plate thickness}$$

The factor of safety (FS) is as follows.

$$FS = \frac{0.42 S_u}{\tau} = \frac{0.42 \times 68.4}{11.8} = 2.43$$

where:

$$S_u = 68.4 \text{ ksi} \text{----- Ultimate strength, SA-537 Class 1, at } 700^\circ\text{F}$$

PWR Fuel Basket Buckling Evaluation

For the hypothetical concrete cask tip-over accident, a buckling evaluation of the basket tube side wall is performed per NUREG/CR-6322 [9] is also performed. Based on the finite element analysis results, the governing buckling load of a fuel tube side wall (Axial Compression=12.4 kips, Bending Moment=6.4 inch-kip) occurs at Tube 11 (see Figure 3.10.1-13) for the 0° basket orientation. The factor of safety is calculated based on the interaction Equations 31 and 32 in NUREG/CR-6322. These two equations adopt the "Limit Analysis Design" approach for structural members subjected to stresses beyond the yield limit of the material. Methodology and equations for the buckling evaluation are summarized as follows.

Symbols and Units:

- P = Applied axial compressive loads, kips
 M = Applied bending moment, kips-inch
 P_a = Allowable axial compressive load, kips
 P_{cr} = Critical axial compression load, kips
 P_e = Euler buckling loads, kips
 P_y = Average yield load, equal to profile area times specified yield strength, kips
 C_c = Column slenderness ratio separating elastic and inelastic buckling
 C_m = Coefficient applied to bending term in interaction equation
 M_m = Critical moment that can be resisted in the absence of axial load, kip-inch
 M_p = Plastic moment, kip-inch.
 F_a = Axial compressive stress permitted in the absence of bending moment, ksi
 F_e = Euler stress for a prismatic member divided by factor of safety, ksi
 K = Ratio of effective column length to actual unsupported length
 l = Unsupported length of member, inch
 r = Radius of gyration, inch
 S_y = Yield strength, ksi
 A = Cross sectional area of member, inch²
 Z_x = Plastic section modulus, inch³
 λ = Allowable reduction factor, dimensionless.

From NUREG/CR-6322, the following interaction equations (Eqn. 31 and 32) are used for the evaluation of accident events.

$$\frac{P}{P_{cr}} + \frac{C_m M}{M_m \left[1 - \frac{P}{P_e} \right]} \leq 1.0$$

$$\frac{P}{P_y} + \frac{M}{1.18M_p} \leq 1.0$$

where:

$$P_{cr} = 1.7 \times A \times F_a$$

$$F_a = \frac{P_a}{A} \text{ for } P_a = P_y \left[\frac{1 - \frac{\lambda^2}{4}}{1.11 + 0.5\lambda + 0.17\lambda^2 - 0.28\lambda^3} \right]$$

and

$$\lambda = \frac{1}{\pi} \left(\frac{Kl}{r} \right) \sqrt{\frac{S_y}{E}}$$

$$F_e = \frac{\pi^2 E}{1.30 \left(\frac{kl}{r} \right)^2}$$

$$P_e = 1.92 \times A \times F_e$$

$$P_y = S_y \times A$$

$$C_m = 0.85 \text{ for members with joint translation (sideways)}$$

$$M_p = S_y \times Z_x$$

$$M_m = M_p \left(1.07 - \frac{\left(\frac{1}{r} \right) \sqrt{S_y}}{3160} \right) \leq M_p$$

From NUREG/CR-6322 the factors of safety are calculated using the following equations.

$$P_1 = \frac{P}{P_{cr}}$$

$$M_1 = \frac{C_m M}{\left(1 - \frac{P}{P_e} \right) M_m}$$

$$P_2 = \frac{P}{P_y}$$

$$M_2 = \frac{M}{1.18} M_p$$

$$FS_1 = \frac{1}{P_1 + M_1}$$

$$FS_2 = \frac{1}{P_2 + M_2}$$

For the PWR basket fuel tube the following parameters are used in the buckling evaluation.

- t = 0.31 inch ----- Tube thickness
- b = 10.00 inch ----- Model length
- l = 8.20 inch ----- Sidewall length
- K = 0.80 ----- Effective length factor
- E = 27.3 × 10⁶ psi ----- Modulus of elasticity, SA-537 Class 1, at 700°F
- Sy = 35.4 ksi ----- Yield strength, SA-537 Class 1, at 700°F

For P = 12.4 kip and M = 6.4 inch-kip (Tube 11, 0° basket orientation):

$$P_1 = \frac{P}{P_{cr}} = 0.07$$

$$M_1 = \frac{C_m M}{\left(1 - \frac{P}{P_c}\right) M_m} = 0.70$$

$$P_2 = \frac{P}{P_y} = 0.11$$

$$M_2 = \frac{M}{1.18} M_p = 0.63$$

The factors of safety are listed as follows.

$$FS_1 = \frac{1}{P_1 + M_1} = \frac{1}{0.07 + 0.66} = 1.29$$

$$FS_2 = \frac{1}{P_2 + M_2} = \frac{1}{0.11 + 0.59} = 1.35$$

PWR Basket Displacement

The nominal dimension of the fuel tube opening for the PWR basket is 8.86 in × 8.86 in for the manufactured fuel tubes and 8.76 in × 8.76 in for the developed fuel slot formed by 4 adjacent fuel tubes. The maximum width of a PWR fuel assembly is 8.54 inches. Based on the quasi-static analysis results using the three-dimensional periodic plastic models for the cask tip-over accident, the minimum clearance between the fuel assembly and the fuel tube is 0.23 inch for the

manufactured tubes and 0.18 inch for the developed tubes during the 35-g side impact loading. As presented in Section 3.10.7, a three-dimensional half-symmetry model for a PWR fuel tube is constructed using the LS-DYNA program to calculate the maximum displacement of a fuel tube as function of time due the side impact load for cask tip-over accident. The LS-DYNA analysis considers a displacement loading based on the maximum diagonal displacements of the fuel tubes during the impact (see Figure 3.7-1) obtained from the finite element analysis results using the three-dimensional periodic plastic model. The permanent displacement in the tube diagonal direction, after the impact, is calculated to be 0.008 inch, which is less than the fabrication tolerance of the fuel tubes and, therefore, not significant.

3.7.2.2 BWR Fuel Basket

3.7.2.2.1 24-inch Concrete Cask End-Drop

For the 24-inch concrete cask drop, a 60g acceleration (a) is conservatively applied to the BWR basket in the axial direction. The basket is evaluated using classical hand calculations. Factors of safety for the BWR basket are calculated based on the criteria for Service Level 'D' limits from ASME Code, Section III Subsection NG [7] and Appendix F [8]. Using a bounding weight of 24,000 pounds for the BWR basket, the maximum stress in the fuel tube is calculated. Conservatively assuming the entire basket weight is carried through the fuel tubes, the stress in the tube is as follows.

$$\sigma_{\text{tube}} = \frac{P_{\text{tube}}}{A} \approx 5.3 \text{ ksi}$$

where:

$$P_{\text{tube}} = \frac{W \times 60}{n} = \frac{24,000 \times 60}{45} = 32,000 \text{ lb}$$

$$W = 24,000 \text{ lb} \text{ ----- Bounding basket weight}$$

$$n = 45 \text{ ----- Number of fuel tubes}$$

$$A = 6.1 \text{ inch}^2 \text{ ----- Tube cross-sectional area}$$

The factor of safety (FS) is as follows.

$$FS = \frac{0.7 \times S_u}{\sigma_{\text{tube}}} = \frac{0.7 \times 68.4}{5.3} = 9.03$$

where:

$$S_u = 68.4 \text{ ksi} \text{ ----- Ultimate strength, SA-537 Class 1, at 700°F}$$

The weight of the fuel tubes is supported on connector pins. Referring to Figure 3.10.2-13, the interior tubes (Tube #4) are supported by four connector pins; the side fuel tubes (Tube #1) are supported by two connector pins and the side and corner weldments; and the corner fuel tubes (Tube #5) are supported by three connector pins. The stress (σ) on the fuel tube is as follows.

$$\sigma = \frac{60 \times P_{pin}}{A_m} = \frac{60 \times 233}{0.34} = 41.1 \text{ ksi}$$

where:

$$A_m = 0.34 \text{ inch}^2 \text{ ----- Common area}$$

$$P_{pin} = \frac{1}{3}P_i + \frac{1}{4}P_i = 233 \text{ lb}$$

$$P_i = 400 \text{ lb ----- Tube weight}$$

The factor of safety (FS) is as follows.

$$FS = \frac{0.7 \times S_u}{\sigma_{brg}} = \frac{0.7 \times 68.4}{41.1} = 1.17$$

where:

$$S_u = 68.4 \text{ ksi ----- Ultimate strength, SA-537 Class 1, at 700°F}$$

The weight of the side and corner weldments is carried through to the TSC base plate by supports at the bottom of the weldments. The corner weldment is bounding for the supports. The dimensions for the corner support weldment are 8.0 inches in length and 0.375-inch thickness. The bounding weight of the corner weldment is 1,100 pounds. The corner weldment also supports one-quarter of the weight of four fuel tubes (400 lb per tube, bounding). The membrane stress (σ_m) is as follows.

$$\sigma_m = \frac{W_{sup}}{A_{sup}} = \frac{90,000}{3.0} = 30.0 \text{ ksi}$$

where:

$$W_{sup} = 60 \times (1,100 + 4 \times (0.25 \times 400)) = 90,000 \text{ lb}$$

$$A_{sup} = 8.0 \times 0.375 = 3.0 \text{ inch}^2$$

The factor of safety (FS) is as follows.

$$FS = \frac{0.7S_u}{\sigma_m} = \frac{0.7 \times 68.4}{30.0} = 1.60$$

where:

$$S_u = 68.4 \text{ ksi} \text{ ----- Ultimate strength, SA-537 Class 1, at } 700^\circ\text{F}$$

The 76 basket connector pins support the BWR basket during a 60g bottom-end drop accident. The bounding temperature at the bottom of the basket is 500°F. The pins are subjected to compressive loads; therefore, a buckling evaluation of the pins is presented as follows. The load on one connector pin (P_{pin}) is as follows.

$$P_{pin} = \frac{W \times 60}{n} = \frac{24,000 \times 60}{76} = 18.9 \text{ kips}$$

where:

$$W = 24,000 \text{ lb} \text{ ----- Bounding basket weight}$$

$$n = 76 \text{ ----- Number of pins}$$

Using the Euler buckling theory, the critical buckling load (P_{cr})

$$P_{cr} = \frac{\pi^2 EI}{(KL)^2} = \frac{\pi^2 \times (25.8 \times 10^6) \times 0.049}{(2 \times 3.0)^2} = 346.6 \text{ kip} \quad [9]$$

where:

$$A_{pin} = \frac{\pi D^2}{4} = 0.78 \text{ inch}^2$$

$$D = 1.0 \text{ inch} \text{ ----- Pin Diameter}$$

$$L = 3.0 \text{ inches} \text{ ----- Pin Length}$$

$$I = \frac{\pi r^4}{4} = 0.049 \text{ inch}^4$$

$$K = 2.0 \text{ ----- Buckling constant, clamped-free}$$

$$E = 25.8 \times 10^6 \text{ psi} \text{ ----- Modulus of elasticity of SA-240 Type 304, at } 500^\circ\text{F}$$

The factor of safety (FS) for buckling of the hinge pins is as follows.

$$FS = \frac{P_{cr}}{P_{pin}} = \frac{346.6}{18.9} = \text{Large}$$

BWR Neutron Absorber Evaluation

During the end impact condition, the BWR neutron absorber and the weld post are subject to shearing force in the longitudinal direction of the neutron absorber. The neutron absorber is considered to be supported by two weld posts located at the bottom end of the neutron absorber. The evaluation is conservatively performed for an acceleration of 60g at a bounding temperature of 350°F. The inertia load applied to the neutron absorber (F_{na}) at each weld post during the end impact is as follows.

$$F_{na} = L \times W \times t \times \rho \times a / 2 = 272 \text{ lb}$$

where:

- $\rho = 0.1 \text{ lb/in}^3$ ----- Bounding density of the neutron absorber
- $a = 60g$ ----- End drop acceleration
- $t = 0.1 \text{ in}$ ----- Thickness of neutron absorber
- $L = 165 \text{ in}$ ----- Length of neutron absorber
- $W = 5.5 \text{ in}$ ----- Width of neutron absorber

The shearing capacity of the neutron absorber is as follows.

$$F_{\text{shear}_{na}} = A_s \times \Phi_a = 0.15 \times 2260 = 339 \text{ lb}$$

where:

- $A_s = L_{NA} \times 1.414 \times 2 \times t = 0.15 \text{ in}^2$ ----- Shear area at both sides of each weld-post
(at the 45° shear planes)
- $L_{NA} = 0.53 \text{ in}$ ----- Min. edge distance of the neutron absorber
- $\Phi_a = 0.42 S_u = 2.26 \text{ ksi}$ ----- Allowable shear stress
- $S_u = 5.38 \text{ ksi}$ ----- Tensile strength of neutron absorber at
350°F

The factor of safety (FS) is as follows.

$$FS = F_{\text{shear}_{na}} / F_{na} = 339 / 272 = 1.25$$

The strength of the weld posts is significantly higher than that of the neutron absorber. Therefore, no evaluation is required for the weld posts for the concrete cask 24-inch end-drop evaluation.

3.7.2.2.2 Concrete Cask Tip-over

The analysis results for the BWR basket subjected to a hypothetical concrete cask tip-over accident are presented in this section. Each basket component is evaluated in the following sections. Factors of safety for the BWR basket are calculated based on the criteria for Service Level 'D' limits from ASME Code, Section III, Subsection NG [7] and Appendix F [8].

BWR Fuel Tube Evaluation

The BWR basket fuel tubes are analyzed for a tip-over accident using the three-dimensional periodic plastic finite element models described in Section 3.10.2. The fuel tube is conservatively evaluated for a 35g side impact load.

Plastic stress intensities are calculated for the BWR fuel tubes for the 0° and 45° basket orientations (see Figure 3.10.2-13 and Figure 3.10.2-15 for tube IDs). The maximum primary membrane and primary membrane plus bending nodal stress intensities for each fuel tube are reported in Table 3.7-7. Note that for a plastic analysis, ANSYS reports stresses in the elastic region as the yield strength (31.7 ksi at 500°F).

The ANSYS plastic finite element model employs the material stress-strain curve and accounts for the inelastic behavior of the material. The stress allowables for plastic analysis are based on ASME Code, Section III, Appendix F [8]. The allowable primary membrane stress is $0.7S_u$. The allowable primary membrane plus bending stress intensity is $0.9S_u$. The minimum factors of safety for the fuel tubes are 1.46 (45° basket orientation) for membrane stresses and 1.77 (0° basket orientation) for primary stress intensities. The critical stress locations occur in the fuel tube corners.

The fuel tubes are constructed by welding two tube halves together using a full penetration weld the length of the fuel tube. A root and final MT weld examination per ASME Code, Section III, Subsection NG-5232 is used, which has a 0.75 weld quality factor (wf). From the plastic analysis of the BWR basket, the maximum membrane and primary stress intensity at the tube weld is 11.2 ksi and 31.7 ksi respectively. The factors of safety for the weld are as follows.

Membrane:

$$FS = \frac{0.7S_u \times wf}{\sigma} = \frac{0.7 \times 68.4 \times 0.75}{11.2} = 3.21$$

Membrane plus bending:

$$FS = \frac{0.9S_u \times wf}{\sigma} = \frac{0.9 \times 68.4 \times 0.75}{31.7} = 1.46$$

where:

$$S_u = 68.4 \text{ ksi} \text{ ----- Ultimate strength, SA-537 Class 1, at } 700^\circ\text{F}$$

The pins react shear loads between adjacent tubes. From the finite element models, the maximum shear load (P) in the pin is 13,157 lb for the 0° basket orientation and 11,399 lb for the 45° basket orientation. The shear load is calculated by summing the nodal forces of the nodes in the pin socket on the tube adjacent to the tube to which the pin is welded. The forces are calculated in a localized coordinate system aligned with the corner flat on the fuel tube. Using a bounding load of 15,000 lb, the shear stress in the pin is

$$\tau_{\text{pin}} = \frac{P}{Dl_{\text{pin}}} = 26.3 \text{ ksi}$$

where:

$$D = 0.38 \text{ inch} \text{ ----- Pin diameter}$$
$$l_{\text{pin}} = 1.5 \text{ inch} \text{ ----- Half length of pin}$$

The factor of safety (FS) is as follows.

$$FS = \frac{0.42S_u}{\tau_{\text{pin}}} = 1.12$$

where:

$$S_u = 70.0 \text{ ksi} \text{ ----- Ultimate strength, SA-695 Type B Gr 40, at } 700^\circ\text{F}$$

The bearing stress (σ_{brg}) on the pin is evaluated using the bounding load of 15,000 lb. The bearing area is determined based on a 30° contact arc between the pin and the fuel tube socket.

$$\sigma_{\text{brg}} = \frac{P}{LS} = 100.7 \text{ ksi}$$

where:

$$P = 15,000 \text{ lb} \text{ ----- Maximum load on pin}$$
$$L = 1.5 \text{ inch} \text{ ----- Length of pin in ANSYS model}$$
$$S = \pi D \frac{30}{360} = 0.10 \text{ in} \text{ ----- Bearing arc length}$$

$$D = 0.38 \text{ inch} \text{----- Pin diameter}$$

Per ASME Appendix F-1336, the allowable bearing stress is $2.1S_u$. The factor of safety (FS) is as follows.

$$FS = \frac{2.1S_u}{\sigma_{brg}} = 1.47$$

where:

$$S_u = 70.0 \text{ ksi} \text{----- Ultimate strength, SA-695 Type B Gr 40, at } 700^\circ\text{F}$$

BWR Neutron Absorber and Retainer

The BWR neutron absorber and retainer are conservatively evaluated for a 60g side-impact load and for the concrete cask tip-over event. The retainer strip assembly consists of 304 stainless steel and is restrained by an array of posts welded to the inside surface of the fuel tube. Two rows of post are separated 3.6 inches apart, and a spacing of 12 inches exists between the posts along the axial direction of the fuel tube.

The neutron absorber is supported by the retainer strip at the inside surface of the fuel tube. The pitches of the slotted holes in the neutron absorber are the same as the holes in the retainer strip through which the weld posts are connected to the fuel tube. The slotted holes are used to prevent interference during differential thermal expansion between the neutron absorber and the fuel tube. The head of the weld posts supporting the retainer strip are engaged in the recessed conical pockets of the retainer.

The finite element model for the BWR neutron absorber and retainer is similar to the model shown in Figure 3.7-3, with the exception of the spacing of the posts in the lateral direction and the axial direction. This resulted in minimal change to the finite element mesh used for the PWR model. Boundary conditions applied in the PWR model shown in Figure 3.7-3 were also applied to the BWR model. LS-DYNA was used to determine the dynamic response to a 60g loading, which was also used for the PWR design.

The results of the transient evaluations show that the maximum strain in the retainer for the BWR fuel is 2.5%, which is minimal, and is local to the conical-shaped hole. Since inelastic strains are not recovered, this indicates that maximum inelastic strain during the impact is also limited to 2.5 percent. Such a minimal strain level indicates that the conical pocket retains its configuration for the weld post to restrain the retainer. The final displacement of the retainer strip at the midpoint between the weld posts is computed to be 0.07 inch, which is consistent

with the minimal plastic strain in the retainer. This also confirms that the retainer remains engaged with the weld post during and after the impact.

The peak force on the weld post determined from the analysis is 50 pounds. The shear area governs the capacity of the weld. The depth of the weld (h) is 0.13 inch. The diameter of the weld post (D) is 0.25 inch. The governing stress is the shear stress in the base material. The allowable shear stress for the accident condition is $0.42S_u$. The ultimate strength (S_u) of the base material (SA240, Type 304) is 63,200 psi. The weld capacity, F_{cap} , is calculated as shown in the following.

$$\begin{aligned} F_{cap} &= 0.42 \times n \times S_u \times h \times BD \\ &= 0.42 \times 0.3 \times 63,200 \times 0.13 \times (3.1416 \times 0.25) \\ &= 813 \text{ lb} \end{aligned}$$

where:

$$n = 0.3 \text{----- The design factor per ASME Code, Section III, Subsection NG, Table NG-3352-1 for the intermittent plug weld employing a surface visual examination method per NG-5260.}$$

The factor of safety (FS) is as follows.

$$FS = \frac{813}{50} = 16$$

BWR Corner Support Weldment Evaluation

The BWR basket corner support weldment is analyzed for the tip-over accident using the three-dimensional periodic plastic finite element model and boundary conditions described in Section 3.10.2. The corner support weldment is comprised of two major components: the mounting plate, which is the vertical plate, and the side support plate, which are located on ten-inch centers.

The analysis results for the corner support weldment mounting plate are presented in Table 3.7-8 and Table 3.7-9. The maximum nodal stress intensity is compared to the primary membrane stress allowable. The minimum factor of safety for the corner support weldment is 1.49.

The center support plates are welded to the corner mounting plates with full-penetration welds. The welds have an inspection criteria per ASME Code, Section III, Subsection NG-5233, and a

weld quality factor of 0.65. The maximum nodal stress intensity in the weld is 31.7 ksi. The factor of safety (FS) for the weld is as follows.

$$FS = \frac{0.65(S_u)}{\sigma_{\text{weld}}} = \frac{0.65 \times 68.4}{31.7} = 1.40$$

where:

$$S_u = 68.4 \text{ ksi} \text{----- Tensile strength, SA-537 Class 1, at } 700^\circ\text{F}$$

The support plate is welded to the corner mounting plate. The plate is welded to the wall cutout with two $\frac{5}{16}$ -inch groove welds on the sides of the plate using the visual inspection criteria per ASME Code, Section III, Subsection NG-5260, and a weld quality factor of 0.35. The maximum loads in the plate weld consist of a bending moment of 7,809 in-lb, an axial force of 19,307 lb and a shear force of 700 lb. The weld stress intensity is

$$\sigma_{\text{weld}} = \sqrt{(S_b)^2 + 4\tau^2} = 11.1 \text{ ksi}$$

where:

$$S_b = \frac{7,809}{1.35} + \frac{19,307}{3.62} = 11.1 \text{ ksi}$$

$$\tau = \frac{900}{3.62} = 0.3 \text{ ksi}$$

$$S_w = h \times t_p \times t_w = 1.35 \text{ in}^2$$

$$A = 2 \times h \times t_w = 2 \times 5.8 \times 0.3125 = 3.62 \text{ in}^2$$

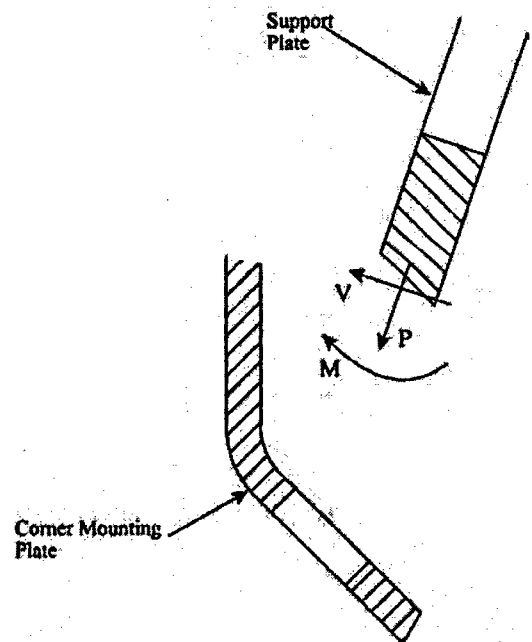
$$h = 5.8 \text{ inch} \text{----- Height of plate}$$

$$t_w = \frac{5}{16} \text{ inch} \text{----- Weld size}$$

$$t_p = 0.75 \text{ inch} \text{----- Plate thickness}$$

The factor of safety (FS) for the weld is as follows.

$$FS = \frac{0.35(S_u)}{\sigma_{\text{weld}}} = \frac{0.35 \times 68.4}{11.1} = 2.16$$



where:

$$S_u = 68.4 \text{ ksi} \text{ ----- Tensile strength, SA-537 Class 1, at } 700^\circ\text{F}$$

BWR Side Support Weldment Evaluation

The BWR basket side support weldment is analyzed for the tip-over accident using the three-dimensional periodic finite element model and boundary conditions described in Section 3.10.2. The analysis results for the side support weldment are presented in Table 3.7-10. The maximum nodal stress intensity is compared to the primary membrane stress allowable. The minimum factor of safety for the side support weldment is 1.49.

BWR Side and Corner Weldment / Fuel Tube Attachment Evaluation

The corner and side support weldments are the primary structure that maintains the geometry of the fuel tube array during a hypothetical tip-over accident. The support weldments are bolted to the fuel tubes at eight circumferential locations. The boss and bolt connection is designed so that the bolts are only loaded in tension, including preload. Otherwise, the support weldments apply a bearing load on the fuel tube array.

During a hypothetical concrete cask tip-over accident, the maximum tensile load on a bolt is 6,511 lb (0° basket model). Combining this load with the bolt preload (400 lb), the tensile load on the bolt is 6,911 pounds.

The bolt thread is a 5/8-11 UNC and the length of engagement is a minimum of 0.38 inch. The bolt material is SA-193 Grade B6 stainless steel. From Machinery's Handbook [12], the ultimate stress in the bolt (σ_t) is as follows.

$$\sigma_t = \frac{P}{A_t} = \frac{6.91}{0.23} = 30.0 \text{ ksi}$$

where:

$$A_t = 0.7854 \left(D - \frac{0.9743}{n} \right)^2 = 0.23 \text{ inch}^2 \quad [12]$$

$$D = 0.625 \text{ inch}$$

$$n = 11$$

The factor of safety (FS) is as follows.

$$FS = \frac{S_y}{\sigma_t} = 2.33$$

where:

$$S_y = 70.0 \text{ ksi} \text{ ----- Yield strength for SA 193, Gr B6, at } 700^\circ\text{F}$$

The shear stress in the bolt thread (τ_{bolt}) is as follows.

$$\tau_{\text{bolt}} = \frac{P}{A_s} = \frac{6.91}{0.370} = 18.7 \text{ ksi}$$

where:

$$A_s = 3.1416nL_eK_{n\text{max}} \left[\frac{1}{2n} + 0.57735(E_{s\text{min}} - K_{n\text{max}}) \right] = 0.379 \text{ inch}^2 [12]$$

$$L_e = 0.38 \text{ inch}$$

$$K_{n\text{max}} = 0.546$$

$$E_{s\text{min}} = 0.5589$$

$$n = 11$$

The factor of safety (FS) is as follows.

$$\text{FS} = \frac{0.42S_u}{\tau_{\text{bolt}}} = 2.03$$

where:

$$S_u = 90.6 \text{ ksi} \text{ ----- Ultimate strength for SA 193, Gr B6, at } 700^\circ\text{F}$$

The shear stress in the boss thread (τ_{boss}) is as follows.

$$\tau_{\text{boss}} = \frac{P}{A_n} = \frac{6.91}{0.541} = 12.8 \text{ ksi}$$

where:

$$A_n = 3.1416nL_eD_{s\text{min}} \left[\frac{1}{2n} + 0.57735(D_{s\text{min}} - E_{n\text{max}}) \right] = 0.541 \text{ inch}^2 [12]$$

$$L_e = 0.38 \text{ inch}$$

$$E_{n\text{max}} = 0.5732$$

$$D_{s\text{min}} = 0.6113$$

$$n = 11$$

The factor of safety (FS) is as follows.

$$FS = \frac{0.42S_u}{\tau_{bolt}} = 2.30$$

where:

$$S_u = 70.0 \text{ ksi} \text{ ----- Ultimate strength, SA-695 Type B, Gr 40, at } 700^\circ\text{F}$$

The boss is welded into the fuel tube with a 3/16-inch groove weld. The weld uses the visual inspection criteria per ASME Code, Section III, Subsection NG, Article NG-5260 and a quality factor of 0.35. For the corner weldment, the shear stress in the boss (τ_{weld}) is as follows.

$$\tau_{weld} = \frac{P}{A_w} = \frac{6.91}{0.81} = 8.5 \text{ ksi}$$

where:

$$\begin{aligned} P &= 6.9 \text{ kip} \\ A_w &= \pi D t_{weld} = \pi \times 1.38 \times 0.1875 = 0.81 \text{ in}^2 \\ D &= 1.38 \text{ inch} \text{ ----- Boss Diameter} \end{aligned}$$

For the side weldment ($P_{bolt} = 2,753 \text{ lb}$), the shear stress in the boss (τ_{weld}) is as follows.

$$\tau_{weld} = \frac{P}{A_w} = \frac{2.75}{0.59} = 4.7 \text{ ksi}$$

where:

$$\begin{aligned} P &= 2.75 \text{ kip} \\ A_w &= \pi D t_{weld} = \pi \times 1.00 \times 0.1875 = 0.59 \text{ in}^2 \\ D &= 1.00 \text{ inch} \text{ ----- Boss Diameter} \end{aligned}$$

Using the lesser of SA-537 Class 1 and SA-695 Type B, Gr 40 S_u allowable, the minimum factor of safety (FS) is as follows.

$$FS = \frac{0.35 \times 0.42 S_u}{\tau_{weld}} = 2.14$$

where:

$$S_u = 68.4 \text{ ksi} \text{ ----- Ultimate strength, SA-537 Class 1, at } 700^\circ\text{F}$$

The washers under the bolts are subjected to a bending load due to the preload. Using "Roark's Formulas for Stress and Strain" Table 24-1a [13], the maximum bending moment (M_t) is calculated for the washers under the bolt heads for the side and corner weldments.

For the side weldment, the bending moment in the washer is 330 in-lb for a 2,753 lb bolt load. The stress in the washer is as follows

$$\sigma = \frac{6M_t}{t^2} = \frac{6 \times 330}{0.19^2} = 54.9 \text{ ksi}$$

where:

$$t = 3/16 \text{ inch} \text{ ----- Thickness of washer}$$

The factor of safety (FS) is as follows.

$$FS = \frac{S_u}{\sigma} = \frac{63.2}{54.9} = 1.15$$

where:

$$S_u = 63.2 \text{ ksi} \text{ ----- Ultimate Strength, SA-240 Type 304, at } 700^\circ\text{F}$$

For the corner weldment, the bending moment in the washer is 829 in-lb for a 6,911 lb bolt load. The stress in the washer is as follows

$$\sigma = \frac{6M_t}{t^2} = \frac{6 \times 829}{0.3125^2} = 50.9 \text{ ksi}$$

where:

$$t = 0.3125 \text{ inch} \text{ ----- Thickness of washer}$$

The factor of safety (FS) is as follows.

$$FS = \frac{S_u}{\sigma} = \frac{63.2}{50.9} = 1.24$$

where:

$$S_u = 63.2 \text{ ksi} \text{ ----- Ultimate strength, SA-240 Type 304, at } 700^\circ\text{F}$$

The maximum shear load in the bosses for side support weldment attachment (P_1) is 6.95 kip (0° basket orientation). The maximum shear loads in the corner support weldments are 11.63 kip

(P₂) for the bosses with a mounting bolt and 7.66 kip (P₃) for the bosses without the attachment bolts (45° basket orientation). For the side weldment boss, the shear stress in the boss (τ_{boss}) is as follows.

$$\tau_{\text{boss}} = \frac{P_1}{A} = \frac{6.95}{0.47} = 14.8 \text{ ksi}$$

where:

$$A = \frac{\pi}{4}(D_o^2 - D_i^2) = 0.47 \text{ inch}^2$$

$$D_o = 1.00 \text{ inch}$$

$$D_i = 0.63 \text{ inch}$$

The factor of safety (FS) is as follows.

$$FS = \frac{0.42S_u}{\tau_{\text{boss}}} = 1.99$$

where:

$$S_u = 70.0 \text{ ksi} \text{ ----- Ultimate strength, SA-695 Type B, Gr 40, at } 700^\circ\text{F}$$

The corner weldments have two attachment joints. One joint can react both shear and tensile loads with the addition of a bolt. The other joint can only react shear loads parallel to the face of a fuel tube because the boss is solid. For the corner weldment boss with a bolt, the shear stress in the boss (τ_{boss}) is as follows.

$$\tau_{\text{boss}} = \frac{P_2}{A} = \frac{11.63}{1.17} = 9.9 \text{ ksi}$$

where:

$$A = \frac{\pi}{4}(D_o^2 - D_i^2) = 1.17 \text{ inch}^2$$

$$D_o = 1.375 \text{ inch}$$

$$D_i = 0.63 \text{ inch}$$

The factor of safety (FS) is as follows.

$$FS = \frac{0.42S_u}{\tau_{\text{boss}}} = 2.97$$

where:

$$S_u = 70.0 \text{ ksi} \text{----- Ultimate strength, SA-695 Type B, Gr 40, at } 700^\circ\text{F}$$

For the corner weldment boss without a bolt, the shear stress in the boss (τ_{boss}) is as follows.

$$\tau_{\text{boss}} = \frac{P_3}{A} = \frac{7.66}{1.48} = 5.2 \text{ ksi}$$

where:

$$A = \frac{\pi}{4}(D^2) = 1.48 \text{ inch}^2$$

$$D = 1.375 \text{ inch}$$

The factor of safety (FS) is as follows.

$$FS = \frac{0.42S_u}{\tau_{\text{boss}}} = 5.68$$

where:

$$S_u = 70.0 \text{ ksi} \text{----- Ultimate strength, SA-695 Type B, Gr 40, at } 700^\circ\text{F}$$

Loads between the fuel tube array and the corner and side weldments are reacted out in shear and bearing in the support weldments. Bearing stresses are not considered for accident events. Due to the geometry of the basket, the cutout in the corner support weldments has an edge distance less than two times the diameter of the cutout. The shear stress in the corner weldment mounting plate is as follows.

$$\tau = \frac{P}{A_{\text{shear}}} = \frac{11.63}{1.14} = 10.2 \text{ ksi}$$

where:

$$A_{\text{shear}} = 2 \left[\frac{L_{\text{ed}}}{\sin 45^\circ} t_{\text{plate}} \right] = 1.14 \text{ inch}^2$$

$$L_{\text{ed}} = 1.30 \text{ inch} \text{----- Boss edge distance}$$

$$t_{\text{plate}} = 0.31 \text{ inch} \text{----- Mounting plate thickness}$$

The factor of safety (FS) is as follows.

$$FS = \frac{0.42S_u}{\tau} = 2.82$$

where:

$$S_u = 68.4 \text{ ksi} \text{ ----- Ultimate strength, SA-537 Class 1, at } 700^\circ\text{F}$$

BWR Basket Buckling Evaluation

The buckling evaluation of the BWR basket is an evaluation of a side of the fuel tube per NUREG/CR-6322 [9]. Using the plastic finite element model, the critical buckling of a fuel tube occurs in the 0° basket orientation (Tube 24, Figure 3.10.2-13). The applied loads on a side of the fuel tube are 13.8 kip axial compression and 5.0 inch-kip bending moment.

The factor of safety is calculated based on the interaction Equations 31 and 32 in NUREG/CR-6322. These two equations adopt the “Limit Analysis Design” approach for structural members subjected to stresses beyond the yield limit of the material. Methodology and equations for the buckling evaluation are the same as those presented in Section 3.7.2.1.2 for the PWR basket.

For the BWR basket fuel tube, the following parameters are used in the buckling evaluation.

- t = 0.25 inch ----- Tube thickness
- b = 10.00 inches ----- Unit thickness
- l = 5.34 inches ----- Sidewall length
- K = 0.80 ----- Effective length factor
- E = 27.3 × 10⁶ psi ----- SA-537 Class 1, at 700°F
- S_y = 35.4 ksi ----- Yield strength, SA-537 Class 1, at 700°F

For P = 13.8 kip and M = 5,023 inch-lb (Tube 24, 0° basket orientation)

$$P_1 = \frac{P}{P_{cr}} = 0.10$$

$$M_1 = \frac{C_m M}{\left(1 - \frac{P}{P_c}\right) M_m} = 0.83$$

$$P_2 = \frac{P}{P_y} = 0.16$$

$$M_2 = \frac{M}{1.18} M_p = 0.77$$

The factors of safety are as follows.

$$FS_1 = \frac{1}{P_1 + M_1} = 1.07$$

$$FS_2 = \frac{1}{P_2 + M_2} = 1.08$$

BWR Basket Displacement

The nominal dimensions of the fuel tube opening for the BWR basket is 5.86 in × 5.86 in for the manufactured fuel tubes and 5.77 in × 5.77 in for the developed fuel slot formed by four adjacent fuel tubes. The maximum width of a BWR fuel assembly is 5.52 inches. Based on the quasi-static analysis results using the three-dimensional periodic plastic models for the cask tip-over accident, the minimum clearance between the fuel assembly and the fuel tube is 0.31 inch for the manufactured tubes and 0.30 inch for the developed tubes during the 35-g side impact loading. As presented in Section 3.10.7, a three-dimensional half-symmetry model for a BWR fuel tube is constructed using the LS-DYNA program to calculate the maximum displacement of the fuel tube as function of time due to the side impact loading for the cask tip-over accident. The LS-DYNA analysis consider a displacement loading based on the maximum diagonal displacement of the fuel tubes during the impact (see Figure 3.7-2) from the LS-DYNA analysis presented in Section 3.10.6. The permanent displacement in the tube diagonal direction, after the impact, is calculated to be 0.018 inch, which is less than the fabrication tolerance of the fuel tubes and, therefore, not significant.

3.7.3 Concrete Cask Evaluation for Storage Accident Events

Structural evaluation of the concrete is performed for accident events, including the extreme temperature events (133°F ambient), tornado and tornado-driven missiles, flood, earthquake, concrete cask 24-inch drop and the tip-over accident.

3.7.3.1 Concrete Cask Thermal Stresses

Using the finite element model presented in Section 3.1.1, a structural evaluation of the concrete cask for accident thermal loads was performed. The analysis considered a temperature profile corresponding to the accident thermal condition (133°F ambient). The following summarizes the critical thermal stresses for accident events.

<u>Component</u>	<u>Stress (ksi)</u>
Circumferential Rebar	16.6

Vertical Rebar	20.2
Concrete, Compression	1.0
Concrete, Tension	0.1

3.7.3.2 Tornado and Tornado-Driven Missiles

This section evaluates the strength and stability of the concrete cask for a maximum tornado wind loading and for the impacts of tornado-driven missiles. It also demonstrates that the concrete cask remains stable in tornado wind loading in conjunction with an impact from a high-energy tornado missile.

Concrete cask stability analysis for the maximum tornado wind loading is based on NUREG-0800, Section 3.3.1, "Wind Loadings," and Section 3.3.2, "Tornado Loadings," [16]. Loads due to tornado-driven missiles are based on NUREG-0800, Section 3.5.1.4, "Missiles Generated by Natural Phenomena."

The concrete cask stability in a maximum tornado wind is evaluated based on the design wind pressure calculated in accordance with ANSI/ASCE 7-93, [17] and using classical free body stability analysis methods.

Local damage to the concrete shell is assessed using a formula developed in NSS 5-940.1 [18]. This formula predicts the depth of missile penetration and minimum concrete thickness requirements to prevent scabbing of the concrete.

The local shear strength of the concrete shell is evaluated on the basis of ACI 349-85, Section 11.11.2.1 [5], without considering the reinforcing steel and the steel liner. The concrete shell shear capacity is also evaluated for missile loading using ACI 349-85, Section 11.7.

Tornado Wind Loading

The tornado wind velocity is transformed into an effective pressure applied to the concrete cask using procedures in ANSI/ASCE 7-93, "Building Code Requirements for Minimum Design Loads in Buildings and Other Structures" [17]. The maximum pressure (q) is determined from the maximum tornado wind velocity as follows:

$$q = (0.00256)(K \times I \times V)^2 \text{ lb/ft}^2 = (0.00256)(360)^2 \times 180 = 331.8 \text{ psf}$$

where:

- V = 360 mph ----- Maximum tornado wind speed
- K = 1.0 ----- Terrain effect
- I = 1.0 ----- Importance factor

Considering that the concrete cask is small with respect to the tornado radius, the velocity pressure is assumed uniform over the projected area of the concrete cask. Because the concrete cask is vented, the tornado-induced pressure drop is equalized from inside to outside and has no effect on the concrete cask structure. The total wind loading (F_w) on the projected area of the concrete cask is computed as follows.

$$F_w = q \times G \times C_f \times A_p = 36,003 \text{ lb} \cong 36,100 \text{ lb}$$

where:

- $q = 331.8 \text{ lb/ft}^2$ ----- Maximum pressure
- $C_f = 0.51$ ----- Force coefficient (ASCE 7-93)
- $A = H \times D_o = 30,637 \text{ inch}^2 = 212.7 \text{ ft}^2$ ----- Projected area
- $H = 225.27 \text{ inch}$ ----- Concrete cask height
- $D_o = 136.0 \text{ inch}$ ----- Concrete cask outer diameter
- $G = 1.0$ ----- Gust factor

The wind overturning moment (M_w) is as follows.

$$M_w = F_w \times \frac{H}{2} = 4,066,123 \text{ inch-lb} = 3.38 \times 10^5 \text{ ft-lb}$$

The stability moment (M_s) of the concrete cask (with the TSC, basket and no fuel load) about the edge of the base is as follows.

$$M_s = W_{cc} \times \frac{D_o}{2} = 14.72 \times 10^6 \text{ inch-lb} = 1.23 \times 10^6 \text{ ft-lb}$$

where:

- $D_o = 128.0 \text{ inch}$ ----- Concrete cask base plate diameter
- $W_{cc} = 230,000 \text{ lb}$ ----- Minimum concrete cask loaded weight

ASCE 7-93 requires that the overturning moment due to wind load shall not exceed two-thirds of the dead load stabilizing moment unless the structure is anchored. Therefore, the factor of safety (FS) against overturning is as follows.

$$FS = \frac{0.67M_s}{M_w} = 2.44$$

The stresses in the concrete due to the tornado wind load are conservatively calculated. The concrete cask is considered to be fixed at its base. The stresses in the concrete are as follows.

$$\sigma_{\text{outer}} = \frac{M_{\text{max}} c_{\text{outer}}}{I} = 19.1 \text{ psi (tension or compression)}$$

$$\sigma_{\text{inner}} = \frac{M_{\text{max}} c_{\text{inner}}}{I} = 11.7 \text{ psi (tension or compression)}$$

where:

$$D_o = 136.0 \text{ inches}$$

$$D_i = 82.98 \text{ inches}$$

$$H = 225.27 \text{ inches}$$

$$A = \frac{\pi(D_o^2 - D_i^2)}{4} = 9,119 \text{ inch}^2$$

$$I = \frac{\pi(D_o^4 - D_i^4)}{64} = 14.47 \times 10^6 \text{ inch}^4$$

$$M_{\text{max}} = \frac{F_w \times H}{2} = 4.07 \times 10^6 \text{ lb-inch}$$

$$c_{\text{outer}} = 136.0/2 = 68.0 \text{ inches}$$

$$c_{\text{inner}} = 82.98/2 = 41.49 \text{ inches}$$

Tornado Missiles

The concrete cask is designed to withstand the effects of impacts associated with postulated tornado-driven missiles identified in NUREG-0800 [16], Section 3.5.1.4.III.4, Spectrum I missiles. These missiles are listed as follows.

- A massive high kinetic-energy missile (4,000 lb automobile, with a frontal area of 20 square feet that deforms on impact).
- A 280 lb, 8.0-inch-diameter armor piercing artillery shell.
- A 1.0-inch-diameter solid steel sphere.

All of these missiles are assumed to impact in a manner that produces the maximum damage at a velocity of 126 mph (35% of the maximum tornado wind speed of 360 mph). The concrete cask is evaluated for impact effects associated with each of the previously listed missiles.

The concrete cask has no openings except for the four air outlets at the top and four air inlets at the bottom. The outlets are configured such that a one-inch diameter solid steel missile cannot directly enter the concrete cask interior. Additionally, the basket is protected by the TSC closure lid. The TSC is protected from small missiles entering the inlets by the pedestal plate; therefore, a detailed analysis of the impact of a one-inch diameter steel missile is not required.

Concrete Shell Local Damage (Penetration Missile)

Local damage to the concrete cask body is assessed by using the methodology presented by NSS 5-940.1 [18]. This method predicts the depth of penetration and minimum concrete thickness requirements to prevent scabbing. Penetration depths calculated by using this formula have been shown to provide reasonable correlation with test results. The penetration depth is as follows.

$$x = \left[4KNW(d^{-0.8}) \left(\frac{V}{1000} \right)^{1.8} \right]^{0.5} = 5.82 \text{ inch}$$

where:

- d = 8.0 inch ----- Missile diameter
- K = $180/(f'_c)^{1/2} = 2.92$ ----- Coeff. depending on concrete strength
- N = 1.14 ----- Shape factor for sharp nosed missiles
- W = 280 lb ----- Missile weight
- V = 126 mph = 185 ft/sec ----- Missile velocity
- f'_c = 3,800 psi ----- Concrete compressive strength

The minimum concrete shell thickness to prevent scabbing is three times the penetration depth (17.46 inch). The thickness of the concrete shell is 26.51 inches. The factor of safety (FS) is as follows.

$$FS = \frac{26.51}{17.46} = 1.52$$

Note that the steel liner and rebar of the concrete cask is conservatively ignored in the previously listed evaluation.

Closure Plate Local Damage (Penetration Missile)

The concrete cask is closed with a 6.75-inch deep lid assembly. The top plate is 3/4-inch carbon steel with a carbon steel clad disk of concrete 5.75-inches deep. In this evaluation, only the steel plate is considered to withstand the impact of the 280-lb armor-piercing missile, impacting at 126 mph. The perforation thickness (T) of the closure steel plate is calculated by using the methodology presented in BC-TOP-9A [19].

$$T = \frac{\left(\frac{m_m V_s^2}{2} \right)^{2/3}}{672D} = 0.52 \text{ inch}$$

where:

$$m_m = 280 \text{ lb}/32.174 \text{ ft}/\text{sec}^2 \text{ ----- } 8.70 \text{ slugs (lb}\cdot\text{sec}^2/\text{ft) missile mass}$$

$$V_s = 185 \text{ ft}/\text{sec} \text{ ----- Missile velocity}$$

$$D = 8 \text{ inch} \text{ ----- Missile diameter}$$

The report recommends that the plate thickness be 25% greater than the calculated perforation thickness (T) to prevent perforation. The recommended plate thickness is as follows.

$$T = 1.25 \times 0.52 = 0.65 \text{ inch}$$

The factor of safety (FS) is as follows.

$$FS = \frac{0.75}{0.65} = 1.15$$

High-Energy Missile Impact Damage Prediction

The concrete cask is a freestanding structure. Therefore, the principal consideration in overall damage response is the potential for overturning the concrete cask as a result of the high-energy missile impact. From the principle of conservation of momentum, the impulse of the force from the missile impact on the concrete cask must equal the change in angular momentum of the concrete cask. Also, the impulse force due to the impact of the missile must equal the change in linear momentum of the missile. These relationships may be expressed as follows:

Change in momentum of the missile, during the deformation phase

$$\int_{t_1}^{t_2} (F)(dt) = m_m (v_2 - v_1)$$

where:

$$F \text{ ----- Impact impulse force on missile}$$

$$m_m = 4,000 \text{ lb}/g = 124 \text{ slugs}/12 = 10.4 \text{ (lb sec}^2/\text{inch)}$$

$$\text{----- Missile mass}$$

$$t_1 \text{ ----- Time at missile impact}$$

$$t_2 \text{ ----- Time at conclusion of deformation phase}$$

$$v_1 = 126 \text{ mph} = 185 \text{ ft}/\text{sec} \text{ ----- Missile velocity at impact}$$

$$v_2 \text{ ----- Velocity of missile at time } t_2$$

The change in angular momentum of the concrete cask, about the bottom outside edge/rim, opposite the side of impact is as follows.

$$\int_{t_1}^{t_2} M_c (dt) = \int_{t_1}^{t_2} (H)(F)(dt) = I_m (\omega_1 - \omega_2)$$

Substituting,

$$\int(F)(dt) = m_m(v_2 - v_1) = \frac{I_m(\omega_1 - \omega_2)}{H}$$

where:

M_c	-----	Moment of the impact force on the concrete cask
I_m	-----	Concrete cask mass moment of inertia, about point of rotation on the bottom rim
ω_1	-----	Angular velocity at time t_1
ω_2	-----	Angular velocity at time t_2
$m_c = 230,000/32.174 = 7,149$	slugs/12 = 596 lb sec ² /inch	-----
	-----	Mass of concrete cask
$I_{mx} = 1/12(m_c)(3r^2 + H^2) = 3.21 \times 10^6$	lb-sec ² -inch	
$I_m = I_{mx} + (m_c)(d_{CG})^2 = 13.9 \times 10^6$	lb-sec ² -inch	
$r = 68.0$	inches	-----
	-----	Concrete cask radius
$H = 225.27$	inches	-----
	-----	Concrete cask height
$d_{CG} = \sqrt{118.0^2 + 64.0^2} = 134.2$	inches	-----
	-----	Distance from CG to rotation point

Based on conservation of momentum, the impulse of the impact force on the missile is equated to the impulse of the force on the concrete cask.

$$m_m(v_2 - v_1) = I_m(\omega_1 - \omega_2)/H$$

at time t_1 , $v_1 = 185$ ft/sec and $\omega_1 = 0$ rad/sec
at time t_2 , $v_2 = 0$ ft/sec

During the restitution phase, the final velocity of the missile depends upon the coefficient of restitution of the missile, the geometry of the missile and target, the angle of incidence, and on the amount of energy dissipated in deforming the missile and target. On the basis of tests conducted by EPRI, the final velocity (v_f) of the missile following the impact is assumed to be zero. This conservatively assumes that all of the missile energy is transferred to the concrete cask. Equating the impact force on the missile to the impulse force on the concrete cask yields the following.

$$(10.4)(v_2 - 185(12)) = 13.9 \times 10^6 (0 - \omega_2)/225.27$$

Setting $v_2 = 0$ and solving for ω_2

$$\omega_2 = 0.374 \text{ rad/sec}$$

The distance (Z) from the point of missile impact to the point of concrete cask rotation is as follows.

$$Z = \sqrt{132.0^2 + 225.27^2} = 261.1 \text{ inch}$$

And the impulse velocity is as follows.

$$v_2 = Z \times \omega_2 = (261.1)(0.374) = 97.7 \text{ inch/sec}$$

The line of missile impact is conservatively assumed normal to the concrete cask. Equating the force on the missile during restitution to the impulse of the force on the concrete cask yields the following.

$$-[m_m(v_f - v_2)] = I_m (\omega_f - \omega_2)/Z$$

$$-[10.4(0 - 97.7)] = 13.9 \times 10^6 (\omega_f - 0.374)/261.1$$

$$\omega_f = 0.393 \text{ rad/sec}$$

where:

$$v_f = 0$$

$$v_2 = 97.7 \text{ inch/sec}$$

$$\omega_2 = 0.374 \text{ rad/sec}$$

Thus, the final energy (E_k) of the concrete cask following the impact is as follows.

$$E_k = (I_m)(\omega_f)^2 / (2) = 10.73 \times 10^5 \text{ inch-lb}$$

The change in potential energy (E_p) of the concrete cask due to rotating it until its center of gravity is above the point of rotation is calculated. The height of the center of gravity has increased by the distance, $h_{PE} = d_{cg} - h_{cg}$.

$$E_p = (W_{cc})(h_{PE})$$

$$E_p = 230,000 \text{ lb} \times 16.2 \text{ inch}$$

$$E_p = 3.73 \times 10^6 \text{ inch-lb}$$

The massive high kinetic-energy tornado-driven missile imparts less kinetic energy to the concrete cask than the change in potential energy of the concrete cask to reach the tip-over point. Therefore, concrete cask overturning from missile impact will not occur. The factor of safety (FS) against overturning is as follows.

$$FS = \frac{3.73 \times 10^6}{10.73 \times 10^5} = 3.48$$

Combined Tornado Wind and Missile Loading (High-Energy Missile)

The concrete cask rotation due to the heavy missile impact is as follows.

$$h_{KE} = \frac{E_k}{W_{cc}} = \frac{10.73 \times 10^5}{230,000} = 4.67 \text{ inch}$$

The rotation after impact is as follows.

$$\theta = \alpha - \beta = 28.4 - 23.9 = 4.5^\circ$$

where:

$$\cos \beta = \frac{h_{cg} + h_{KE}}{d_{cg}} = \frac{118.0 + 4.67}{134.2} = 0.9141$$

$$\beta = 23.9^\circ$$

$$\cos \alpha = \frac{h_{cg}}{d_{cg}} = \frac{118.0}{134.2} = 0.8793$$

$$\alpha = 28.4^\circ$$

$$e = d_{cg} \sin \beta = 134.2 \times \sin(23.9^\circ) = 54.4 \text{ inch}$$

The available gravity restoration moment after missile impact is as follows.

$$M_{rst} = W_{cc}e = 230,000 \times 54.4 = 12.5 \times 10^6 \text{ inch-lb} = 1.04 \times 10^6 \text{ ft-lb}$$

The tornado wind moment is 3.38×10^5 ft-lb; therefore, the factor of safety (FS) is as follows.

$$FS = \frac{0.67(1.04 \times 10^6)}{3.38 \times 10^5} = 2.06$$

Therefore, the concrete cask will not overturn due to the combined effect of tornado wind loading and high-energy missile impact.

Local Shear Strength Capacity of Concrete Shell (High-Energy Missile)

This section evaluates the punching shear strength of the concrete shell when impacted by a high-energy missile. The high-energy missile is equivalent to a 20-ft² cross-sectional area object moving at 185 ft/sec, weighing 4,000 lb, having proportions of 2 horizontal to 1 vertical. The missile is assumed to impact flush with the top of the concrete shell. The concrete area required to resist the high-energy missile impact is as follows.

$$A = 2b \times b = 2(9.64)^2 = 185.9 \text{ inch}^2 = 1.3 \text{ ft}^2 < 20 \text{ ft}^2$$

where:

Setting the factored shear force, V_u , equal to the force of the high kinetic-energy missile, F_u , the leg dimension, b , of the equivalent impacting area is as follows.

$$V_u = F_u \Rightarrow \phi V_c = F_u \Rightarrow \phi 4\sqrt{f'_c} b_o d = F_u \Rightarrow \phi 4\sqrt{f'_c} (4b + 53)d \Rightarrow b = 9.64 \text{ inch}$$

and

$$V_c = \left(2 + \frac{4}{\beta_c} \right) \sqrt{f'_c} (b_o d) = 4\sqrt{f'_c} (b_o d) \text{ ----- Concrete punching shear strength capacity}$$

[5, Eq. 11-36]

$$\beta_c = 2/1 = 2 \text{ ----- Ratio of long side to short side}$$

$$d = 26.51 \text{ inch ----- Concrete thickness}$$

$$f'_c = 3,800 \text{ psi ----- Concrete strength, } 300^\circ\text{F}$$

$$b_o = (2b + 26.51) + 2(b + 13.26) = 4b + 53 \text{ Perimeter of punching shear area at approximately } d/2 \text{ from the missile contact area}$$

$$\phi = 0.85 \text{ ----- Strength reduction factor [5]}$$

$$F_u = LF \times F = 508.8 \text{ kip ----- Force of high kinetic energy missile with load factor [19]}$$

$$F = 0.625(v)(W_m) = 462.5 \text{ kip ----- Force of high-energy missile [19]}$$

$$v = 185 \text{ ft/sec ----- Velocity of the missile}$$

$$W_m = 4,000 \text{ lb ----- Weight of high-energy missile}$$

$$LF = 1.1 \text{ ----- 10\% load factor}$$

Therefore, the concrete shell alone has sufficient capacity to resist the high-energy missile impact force.

3.7.3.3 Flood

This section will verify the stability of the concrete cask against overturning during a design basis flood accident, and ensure that the design is adequate to withstand stresses induced by the flood.

Overturning of the concrete cask due to the drag force of the flood water flow is resisted by the weight of the loaded cask. Assuming a full submersion and steady-state flow conditions, the drag force (F_D) on the concrete cask is calculated using classical fluid mechanics for turbulent flow conditions. The resultant drag force acts horizontally through the CG of the cask. The effective weight of the concrete cask acts vertically downward through the CG. The tendency of the concrete cask to overturn is determined by comparing the moment of the drag force about a

point on the bottom edge of the concrete cask to the moment of effective concrete cask weight about the same point.

The effective weight of the fully submerged concrete cask is the actual weight minus the buoyancy force due to the displaced water. The bounding condition for buoyancy occurs for the concrete cask configuration with the greatest volume to weight ratio. Thus, for conservatism, the concrete cask is assumed to be empty.

The capacity of the concrete cask to react to the stresses induced by the flood water flow drag forces is evaluated using the methodology described in ACI 349-85 [5]. For conservatism, only the concrete shell is considered.

Assuming a hollow cylinder, the volume of the concrete cask (V_{cc}) is as follows.

$$V_{cc} = \frac{\pi}{4}(D_o^2 - D_i^2)h = \frac{\pi}{4}(136.0^2 - 79.48^2)225.27 = 2,154,777 \text{ inch}^3$$

where:

- $D_o = 136.0$ inches ----- Concrete cask outer diameter
- $D_i = 79.48$ inches ----- Concrete cask inner diameter
- $H = 225.27$ inches ----- Concrete cask height

The buoyancy force (F_b) is equal to the weight of water (62.4 lb/ft^3) displaced by the fully submerged concrete cask.

$$F_b = \frac{V_{cc}}{12^3} W_{h20} = \frac{2,154,777}{12^3} 62.4 \approx 77,800 \text{ lb}$$

Assuming complete submersion and steady-state flow for a rigid cylinder, the drag force (F_{D15}) of the water on the concrete cask is as follows.

$$F_{D15} = C_D \rho V^2 \left(\frac{A}{2} \right) = 0.7 \times 1.94 \times 15.0^2 \left(\frac{212.7}{2} \right) \approx 32,500 \text{ lb} \quad [20]$$

where:

- $C_D = 0.7$ ----- Drag coefficient [20]
- $\rho = 1.94$ slugs/ft³ ----- Density of water
- $V = 15$ ft/sec ----- Flow velocity
- $A = H \times D_o = 30,637 \text{ inch}^2 = 212.7 \text{ ft}^2$ ----- Projected area
- $H = 225.27$ inches ----- Concrete cask height
- $D_o = 136.0$ inches ----- Concrete cask outer diameter

The force (F_D) required to overturn the concrete cask is determined by summing the moments of the drag force and the submerged concrete cask about a point on the bottom of the concrete cask. Assuming an empty concrete cask, the minimum required overturning force is as follows.

$$F_D = \frac{(W_{cc} - F_b)D_r}{h} = \frac{(200,000 - 77,800)128}{225.27} = 69,435 \text{ lb}$$

where:

$$\begin{aligned} W_{cc} &= 200,000 \text{ lb} \text{----- Minimum empty concrete cask weight} \\ D_r &= 128.0 \text{ inches} \text{----- Concrete cask base diameter} \\ h &= 225.27 \text{ inches} \text{----- Concrete cask height} \end{aligned}$$

The water velocity (V) required to overturn the concrete cask is as follows.

$$V = \sqrt{\frac{2F_D}{C_D \rho A}} = \sqrt{\frac{2 \times 69,435}{0.7 \times 1.94 \times 212.7}} = 21.9 \text{ ft/sec}$$

Therefore, the factor of safety (FS) is as follows.

$$FS = \frac{21.9}{15.0} = 1.46$$

The stresses in the concrete due to the drag force (F_D) are conservatively calculated by considering the concrete cask to be fixed.

$$\sigma_{v \text{ outer}} = M / S_{\text{outer}} = 17.2 \text{ psi (tension or compression)}$$

$$\sigma_{v \text{ inner}} = M / S_{\text{inner}} = 10.5 \text{ psi (tension or compression)}$$

where:

$$\begin{aligned} D_o &= 136.0 \text{ inches} \\ D_i &= 82.98 \text{ inches} \\ h &= 225.27 \text{ inches} \\ A &= \pi (D_o^2 - D_i^2) / 4 = 9,119 \text{ inch}^2 \\ I &= \pi (D_o^4 - D_i^4) / 64 = 14.47 \times 10^6 \text{ inch}^4 \\ S_{\text{outer}} &= 2I / D_o = 212,794 \text{ inch}^3 \\ S_{\text{inner}} &= 2I / (D_i) = 348,759 \text{ inch}^3 \\ w &= F_{D15} / h = 144.3 \text{ lb/inch} \\ M &= w (h)2 / 2 = 3.66 \times 10^6 \text{ inch-lb} \end{aligned}$$

3.7.3.4 Earthquake

The maximum horizontal acceleration at the surface of the concrete storage pad due to an earthquake is evaluated. Per 10 CFR 72.102 [1], the required minimum earthquake ground acceleration is 0.25g. This evaluation will show that MAGNASTOR is stable during a 0.37g earthquake horizontal acceleration (including a 1.1 factor of safety). The vertical acceleration is defined as two-thirds of the horizontal acceleration in accordance with ASCE 4-86 [21].

This calculation determines the effects of ground accelerations (components a_x , a_y and a_z) on the concrete cask for tip-over. The peak ground acceleration is associated with a safe shutdown earthquake. For this evaluation, the maximum overturning moment is compared to the restoring moment required to keep the concrete cask in a stable upright position (i.e., a concrete cask will not tip over due to the earthquake). The maximum ground accelerations and overturning/restoring forces and moment are calculated for both empty and fully loaded concrete cask configurations.

In the event of earthquake, there exists a base shear force or overturning force due to the horizontal ground acceleration, and a restoring force due to the net force of vertical ground acceleration and gravity. This ground motion tends to rotate the concrete cask about its bottom corner at the point of rotation (at the chamfer). The horizontal moment arm is from the center of gravity (CG) toward the outer radius of the concrete cask. The vertical moment arm is from the CG to the bottom of the concrete cask. If the overturning moment is greater than the restoring moment, the concrete cask may tip over. Using the geometry of the concrete cask design, the maximum horizontal and vertical ground accelerations that the concrete cask can safely withstand without becoming unstable are identified.

The two orthogonal horizontal acceleration components (a_x and a_z) are combined for maximum horizontal acceleration magnitude. The result is applied simultaneously with the vertical component to statically evaluate the overturning force and moment. Upward ground acceleration reduces the vertical force that restores the cask to its undisturbed vertical position. Based upon the requirements presented in NUREG-0800 [16], the static analysis method is considered applicable if the natural frequency of the structure is greater than 33 cps. The natural frequency of the MAGNASTOR concrete cask is 138.3 Hz. During the design basis earthquake event, a factor of safety of 1.1 against tip-over of the concrete cask must be maintained.

Tip-Over Evaluation

To maintain the concrete cask in equilibrium, the restoring moment, M_R , must be greater than, or equal to, the overturning moment, M_o . The combination of horizontal and vertical acceleration

components is based on the 100-40-40 approach of ASCE 4-86 [21], which considers that when the maximum response from one component occurs, the responses from the other two components are 40% of the maximum. The vertical component of acceleration can be obtained by scaling the corresponding ordinates of the horizontal components by two-thirds. The vertical component is conservatively considered to be the same as the horizontal component.

Let:

- $a_x = a_z = a$ ----- Horizontal acceleration components
- $a_y = a$ ----- Vertical acceleration component
- G_h ----- Vector sum of two horizontal acceleration components
- G_v ----- Vertical acceleration component

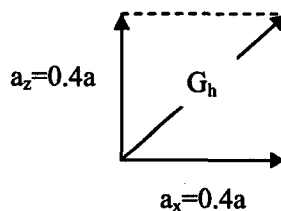
Two cases are analyzed:

Case 1) The vertical acceleration, a_y , is at its peak:

$$(a_y = 1.0a, a_x = 0.4a, \text{ and } a_z = 0.4a)$$

$$G_h = \sqrt{a_x^2 + a_z^2} = \sqrt{(0.4a)^2 + (0.4a)^2} = 0.566a$$

$$G_v = 1.0a_y = 1.0a$$

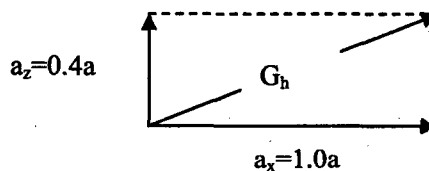


Case 2) One horizontal acceleration, a_x , is at its peak:

$$(a_y = 0.4 \times a, a_x = a, \text{ and } a_z = 0.4a)$$

$$G_h = \sqrt{a_x^2 + a_z^2} = \sqrt{(1.0a)^2 + (0.4a)^2} = 1.077a$$

$$G_v = 0.4a_y = 0.4a$$



For the cask to resist overturning, the restoring moment (M_R) about the point of rotation must be greater than the overturning moment (M_o).

$$M_R \geq M_o, \text{ or } F_r b \geq F_o d \Rightarrow (W \times 1 - W \times G_v) \times b \geq (W \times G_h) \times d$$

- d ----- Vertical distance measured from the base of the concrete cask to the center of gravity
- b ----- Horizontal distance measured from the point of rotation to the C.G.
- W ----- Weight of the concrete cask
- F_o ----- Overturning force
- F_r ----- Restoring force

Substituting for G_y and G_x gives:

Case 1

$$(1-a)\frac{b}{d} \geq 0.566a$$

$$a \leq \frac{\frac{b}{d}}{0.566 + \frac{b}{d}}$$

Case 2

$$(1-0.4a)\frac{b}{d} \geq 1.077a$$

$$a \leq \frac{\frac{b}{d}}{1.077 + 0.4\frac{b}{d}}$$

Empty concrete cask:

Case 1

$$a \leq \frac{\frac{64.0}{116.0}}{0.566 + \frac{64.0}{116.0}} = 0.49$$

Case 2

$$a \leq \frac{\frac{64.0}{116.0}}{1.077 + 0.4\frac{64.0}{116.0}} = 0.43$$

where:

$$b = 64.0 \text{ inch}$$

$$d = 116.0 \text{ inch}$$

Loaded concrete cask:

Case 1

$$a \leq \frac{\frac{63.77}{118.0}}{0.566 + \frac{63.77}{118.0}} = 0.488$$

Case 2

$$a \leq \frac{\frac{63.77}{118.0}}{1.077 + 0.4\frac{63.77}{118.0}} = 0.41$$

where:

$$d = 118.0 \text{ inch}$$

$$b = 64.0 - x = 64.0 - 0.23 = 63.77 \text{ inches}$$

$$e = \frac{73.44 - 72.0}{2} = 0.72 \text{ inch} \text{----- TSC CG shift}$$

$$x = \frac{W_{\text{can}} e}{W_{\text{cc}}} = \frac{103,000 \times 0.72}{322,000} = 0.23 \text{ inch -- Loaded concrete cask CG shift}$$

The minimum acceleration is 0.41g. A factor of safety of 1.1 is required for an earthquake evaluation; therefore, the maximum allowable horizontal acceleration (a_{max}) at the top of the concrete pad that will preclude a cask tip-over is as follows.

$$a_{\max} = \frac{0.41}{1.1} = 0.37g$$

Concrete Cask Stress

To demonstrate the ability of the concrete cask to withstand earthquake loading conditions, the fully loaded cask is conservatively evaluated for seismic loads of 0.5g in the horizontal and 0.5g in the vertical direction. These accelerations reflect a more rigorous seismic loading and, therefore, bound the design basis earthquake. No credit is taken for the concrete cask steel liner. The maximum compressive stresses at the concrete shell outer and inner surfaces are conservatively calculated by considering the cask as a cantilever beam with its bottom end fixed. The maximum compressive stresses are as follows.

$$\sigma_{v \text{ outer}} = \frac{M}{S_{\text{outer}}} + \frac{(1 + a_y)W_{\text{cc}}}{A} = 138 \text{ psi}$$

$$\sigma_{v \text{ inner}} = \frac{M}{S_{\text{inner}}} + \frac{(1 + a_y)W_{\text{cc}}}{A} = 105 \text{ psi}$$

where

- $a_x = 0.50g$ ----- Horizontal direction
- $a_y = 0.50g$ ----- Vertical direction
- $W_{\text{cc}} = 322,000 \text{ lb}$ ----- Bounding weight of concrete cask
- $D_o = 136.0 \text{ inches}$
- $D_i = 82.98 \text{ inches}$
- $A = \pi (D_o^2 - D_i^2) / 4 = 9,119 \text{ inch}^2$
- $I = \pi (D_o^4 - D_i^4) / 64 = 14.47 \times 10^6 \text{ inch}^4$
- $S_{\text{outer}} = 2I/D_o = 212,794 \text{ inch}^3$
- $S_{\text{inner}} = 2I/(D_i) = 348,759 \text{ inch}^3$
- $w = (a_x \times W_{\text{cc}}) / 225.27 = 715 \text{ lb-inch}$
- $M = (w \times 225.27^2) / 2 = 1.81 \times 10^7 \text{ lb-inch}$

3.7.3.5 Concrete Cask Combined Stresses

The load combinations described in Table 2.3-1 are used to evaluate the concrete cask for accident events of storage. Concrete stresses are summarized in Table 3.7-11 and Table 3.7-12 for the loading combination Nos. 4, 5, 7, and 8. Loading combination No. 6 corresponds to drop accidents, 24-inch end drop and tip-over, which are evaluated in Section 3.7.3.6 and Section 3.7.3.7, respectively.

As shown in Table, the maximum concrete compressive stress is 1,201 psi; therefore, the minimum compressive factor of safety (FS) for accident events is as follows.

$$FS = \frac{S_{con}}{S_c} = \frac{2,660}{1,201} = 2.21$$

where:

$$S_{con} = \phi F_c = 0.7 \times 3,800 = 2,660 \text{ psi} \text{----- Concrete compressive allowable}$$

From Section 3.7.3.1, the maximum concrete ultimate strength due to thermal load is 0.1 ksi. The factor of safety (FS) for concrete ultimate strengths is as follows.

$$FS = \frac{S_{tc}}{S_t} = \frac{0.21}{0.1} = 2.10$$

where:

$$S_{tc} = 0.08 \times S_{con} = 0.08 \times 2660 = 213 \text{ psi or } 0.21 \text{ ksi} \text{..... Concrete ultimate strength}$$

From Section 3.7.3.1, the maximum rebar stress (S_{rb}) is due to thermal load is 20.2 ksi. The factor of safety (FS) for the rebar is as follows.

$$FS = \frac{S_{rebar}}{S_{rb}} = \frac{54.0}{20.2} = 2.67$$

where:

$$S_{rebar} = \phi F_r = 0.9 \times 60.0 = 54.0 \text{ ksi} \text{----- Rebar stress allowable}$$

3.7.3.6 Concrete Cask 24-inch Drop

Evaluation of the Concrete Cask

During the 24-inch bottom-end drop of the concrete cask, the cylindrical portion of the concrete is in contact with the steel bottom plate that is a part of the base weldment. The plate is assumed to be part of an infinitely rigid storage pad. No credit is taken for the crush properties of the storage pad or the underlying soil layer. Therefore, energy absorbed by the crushing of the cylindrical concrete region of the concrete cask equals the product of the compressive strength of the concrete, the crush depth of the concrete, and the projected area of the concrete cylinder. Crushing of the concrete continues until the energy absorbed equals the potential energy of the

cask at the initial drop height. The TSC is not rigidly attached to the concrete cask, so it is not considered to contribute to the concrete crushing. The energy balance equation is as follows.

$$w(h + \delta) = P_o A \delta$$

where:

- h = 24.0 inches ----- Drop height
- δ ----- The crush depth of the concrete cask
- P_o = 3,800 psi ----- Compressive strength of the concrete, 300°F
- A = π(R₂² - R₁²) = 9,119 inch² ----- Area of the concrete shield wall
- R₁ = 41.49 inches ----- Inside radius of the concrete
- R₂ = 68 inches ----- Outside radius of the concrete
- w = 185,000 lb ----- Bounding weight of concrete, rebar, and lid assembly

It is assumed that the maximum force that can be exerted on the concrete cask is the compressive strength of the concrete multiplied by the area of the concrete being crushed. The concrete cask's steel shell will not experience any significant damage during a 24-inch drop. Therefore, its functionality will not be impaired due to the drop.

The crush distance computed from the energy balance equation is as follows.

$$\delta = \frac{hw}{P_o A - w} = \frac{(24)(185,000)}{(3800)(9,119) - (185,000)} = 0.13 \text{ inch}$$

Pedestal Crush Evaluation

Upon a bottom-end impact of the concrete cask, the TSC produces a force on the pedestal (base weldment) located near the bottom of the cask. The ring above the air inlets is expected to yield. To determine the resulting acceleration of the TSC and deformation of the pedestal, a LS-DYNA analysis is used. As described in Section 3.1.1, a quarter-symmetry finite element model of the pedestal is used for this evaluation. To ensure that maximum deformations and accelerations are determined, two analyses are performed. One analysis, which uses the upper-bound weight of 105 kips, envelops the maximum deformation of the pedestal. The second analysis employs the lower-bound weight of 60 kips to account for maximum acceleration.

The maximum accelerations of the TSC during the 24-inch bottom-end impact are calculated to be 14.5g and 25.2g for the upper-bound weight TSC and lower-bound weight TSC, respectively. The resulting acceleration time histories of the TSC, which correspond to a filter frequency of 200 Hz, are shown in Figure 3.7-4 for the analysis using the upper-bound weight model and Figure 3.7-5 for the lower-bound weight model. The dynamic load factor (DLF) for the TSC is calculated to be 1.35 for the upper-bound weight TSC and 0.95 (consider 1.0) for the lower-

bound weight TSC, based on the response of one-degree systems subjected to a triangular load pulse [22]. Therefore, the accelerations for the upper-bound weight and lower-bound weight TSC are 19.6g and 25.2g, respectively.

The maximum strain in the pedestal is 15.4%. Since the ultimate strain of A36 steel is greater than 25%, the pedestal is not subject to failure. The maximum vertical displacement of the air inlet is calculated to be 1.46 inches for the upper-bound and lower-bound weight TSC. The original opening is 4.4 inches. Since the maximum displacement is 1.46 inches, the minimum air inlet opening is 2.9 inches (4.4 – 1.46), which is approximately 66% of the original air inlet opening. This condition is bounded by the consequences of the loss of one-half of the air inlets off-normal event.

3.7.3.7 Concrete Cask Tip-Over

Tip-over of the concrete cask is a nonmechanistic, hypothetical accident condition that presents a bounding case for evaluation. Existing postulated design basis accidents do not result in the tip-over of the concrete cask. Functionally, the concrete cask does not suffer significant adverse consequences due to this event. The concrete cask, TSC, and basket maintain design basis shielding, geometry control of contents, and contents confinement performance requirements.

For a tip-over event to occur, the center of gravity of the concrete cask and loaded TSC must be displaced beyond its outer radius, i.e., the point of rotation. When the center of gravity passes beyond the point of rotation, the potential energy of the cask and TSC is converted to kinetic energy as the cask and TSC rotate toward a horizontal orientation on the ISFSI pad. The subsequent motion of the cask is governed by the structural characteristics of the cask, the ISFSI pad and the underlying soil.

The MAGNASTOR concrete cask tip-over analyses are performed using LS-DYNA. LS-DYNA is an explicit finite element program for the nonlinear dynamic analysis of structures in three dimensions. Details of the finite element model are presented in Section 3.1.1.

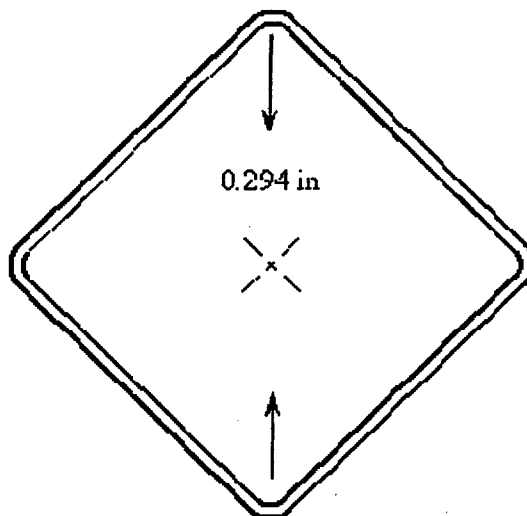
Two geometries are considered in this evaluation. The pad width of 30 ft in the models corresponds to the typical width of a concrete storage pad. One model considers a pad length of 30 ft, while the second model referred to as the “oversized pad,” employs a length of 60 feet. The second model allows the effect of the pad length used in the analysis to be assessed.

The acceleration time histories for the TSC and basket for the standard and oversized pad cases are shown in Figure 3.7-6 and Figure 3.7-7. A cut-off frequency of 200 Hz is applied to filter the analysis results and measure the peak accelerations. The following is a summary of the peak accelerations.

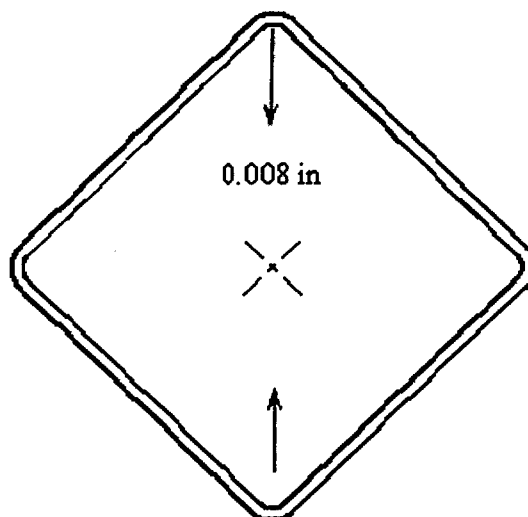
Location	Position from base of concrete cask (in)	Acceleration Standard Pad (g)	Acceleration Oversized Pad (g)
Top of basket	177.7	26.4	26.6
Top of TSC closure lid	197.6	29.5	29.6

Using two-dimensional models of the PWR and BWR basket (similar to the models described in Sections 3.10.1 and 3.10.2, meshing density modified for modal analysis), the modal frequencies for the basket are calculated. Table summarized the frequencies for the first mode shape for the PWR and BWR baskets in the 0° and 45° basket orientations. The dynamic load factors are determined using the response of one-degree systems subjected to a triangular load pulse [22]. The dynamic load factors and the maximum accelerations at the top of the TSC and top of the basket are summarized in Table 3.7-14. As the table and figures show, maximum accelerations are less than the specified design value of 40g. The acceleration results indicate that even with a 100% increase in the pad length, the resulting change in the maximum accelerations is less than 1 percent. This demonstrates that the effect of the pad size employed in the analysis has an insignificant effect on the maximum accelerations.

Figure 3.7-1 PWR Basket Fuel Tube Displacement for Tip-Over Accident

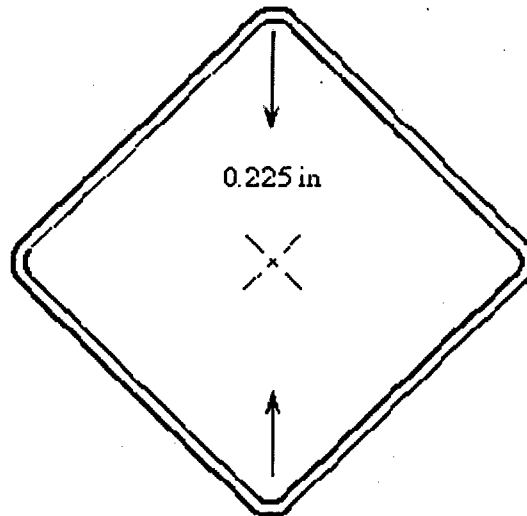


Maximum Diagonal Displacement During Impact

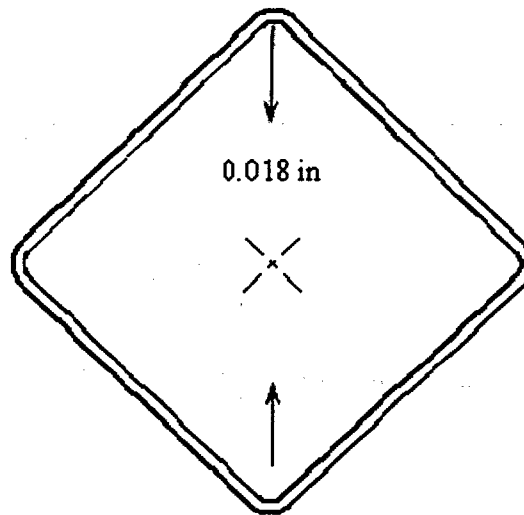


Maximum Diagonal Displacement After Impact

Figure 3.7-2 BWR Basket Fuel Tube Displacement for Tip-Over Accident



Maximum Diagonal Displacement During Impact



Maximum Diagonal Displacement After Impact

Figure 3.7-3 PWR Neutron Absorber and Retainer Finite Element Model

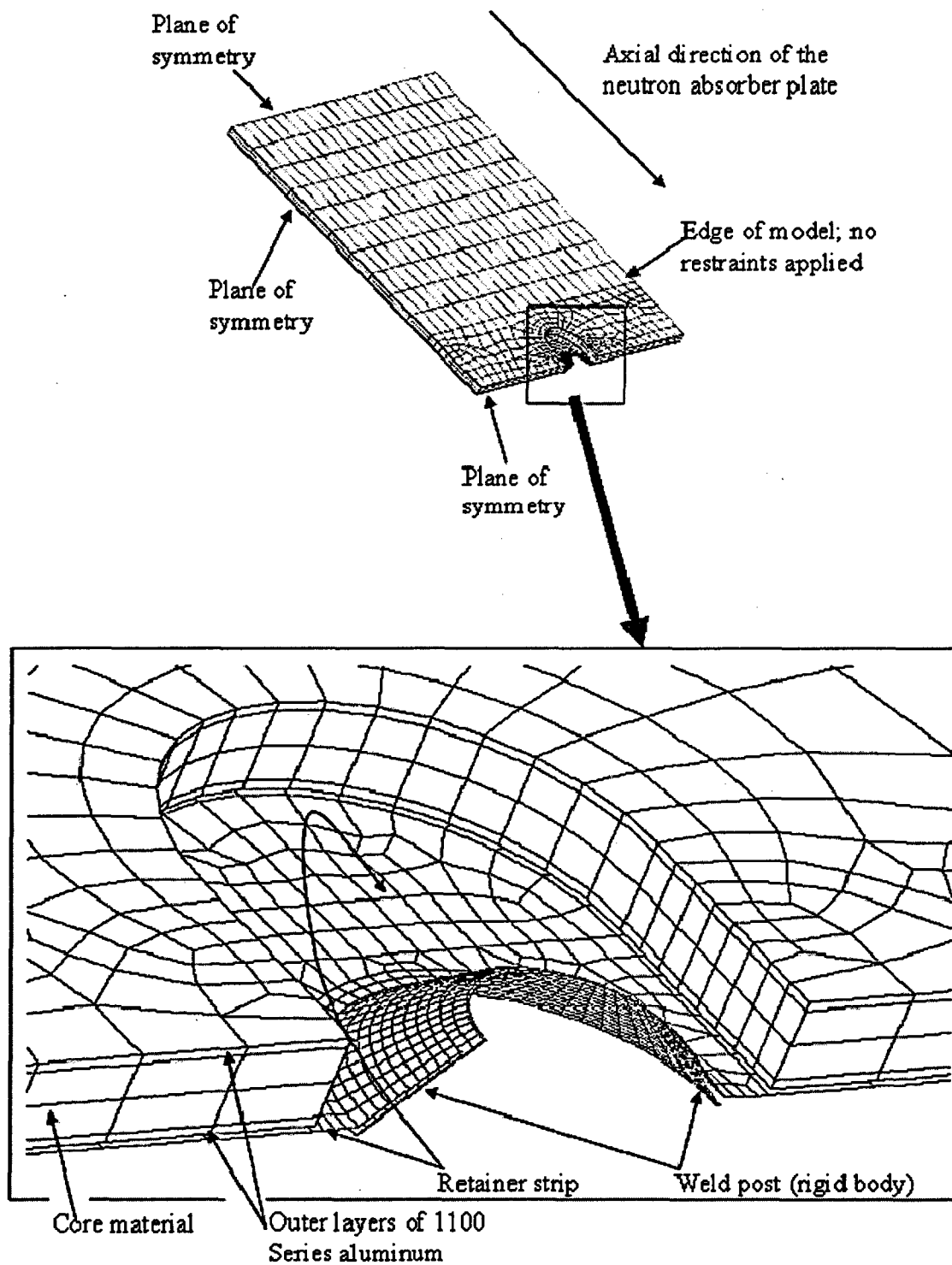


Figure 3.7-4 Acceleration Time History of the Upper-Bound Weight TSC – 24-Inch Concrete Cask Drop

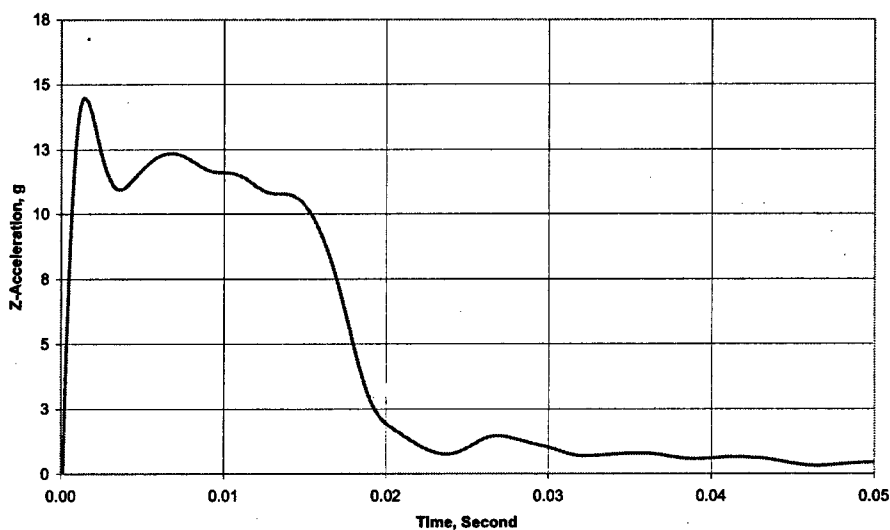


Figure 3.7-5 Acceleration Time History of the Lower-Bound Weight TSC – 24-Inch Concrete Cask Drop

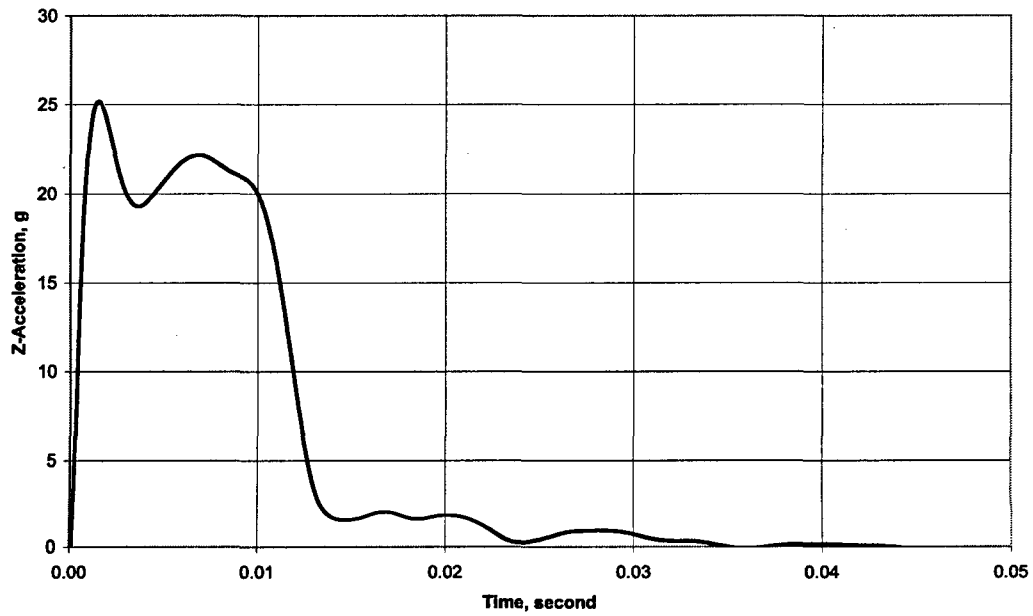


Figure 3.7-6 Acceleration Time History for Concrete Cask Tip-Over Condition - Standard Pad

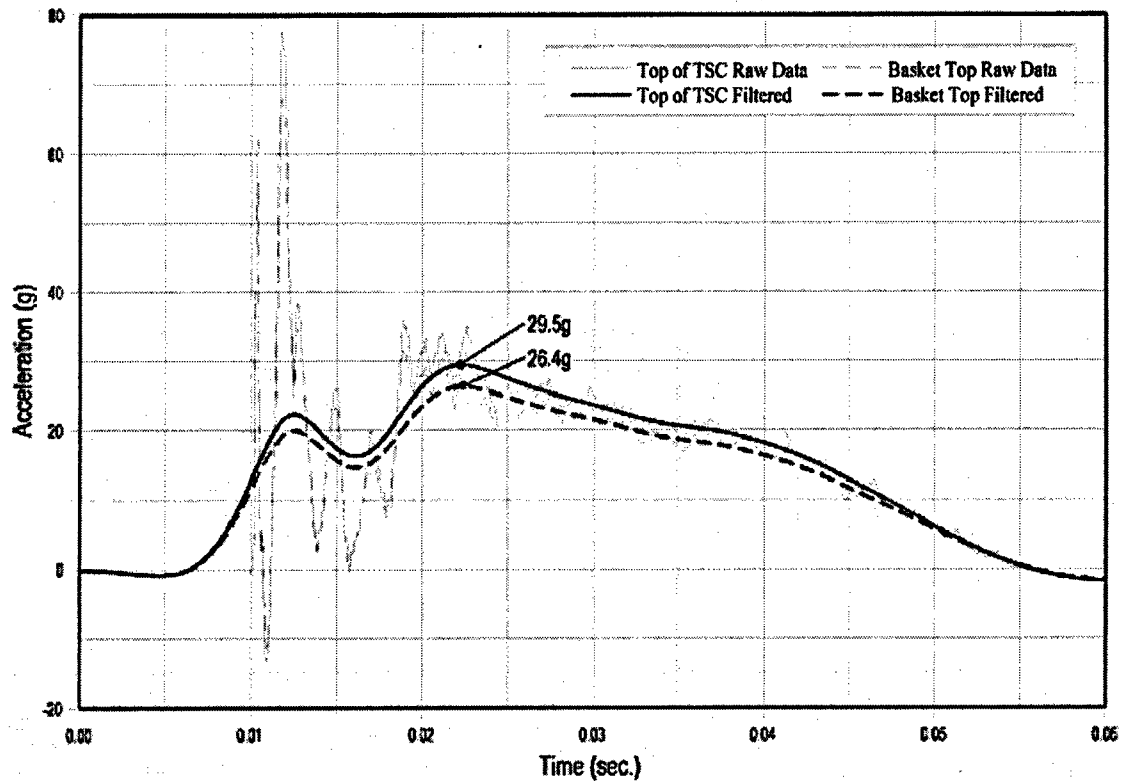


Figure 3.7-7 Acceleration Time History of Oversized Pad

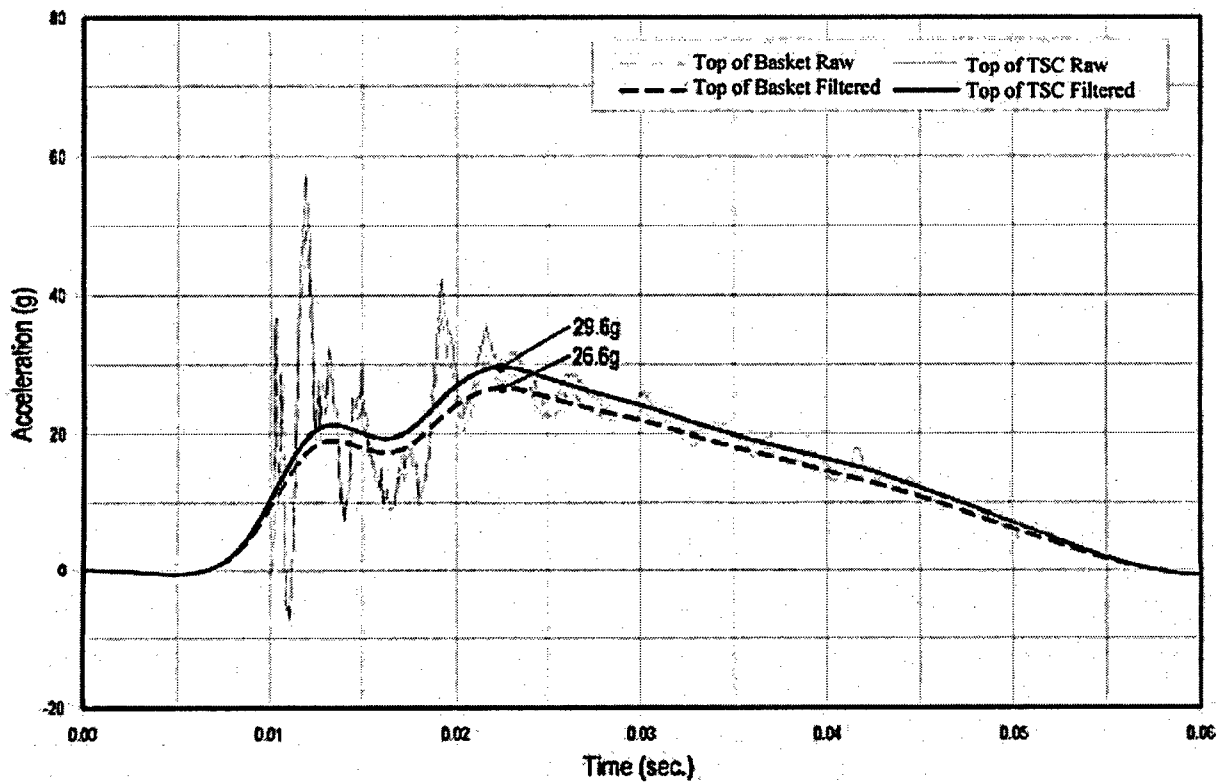


Table 3.7-1 TSC Accident Events, P_m Stresses

Load Case ^a	Service Level	Section ^b	Component Stresses ^a (ksi)						S_{int}	S_{allow}	FS
			S_x	S_y	S_z	S_{xy}	S_{yz}	S_{xz}			
Accident Pressure	D	3	-1.13	-15.79	8.74	0.29	0.06	1.93	24.90	47.15	1.89
Normal Pressure + 24-inch Drop	D	4	-0.03	7.81	-4.26	0.00	0.00	0.00	12.07	44.80	3.71
Normal Pressure + Tip-Over	D	11	-23.89	-17.09	-19.05	10.77	-1.77	-8.92	29.05	34.72	1.20

Table 3.7-2 TSC Accident Events, $P_m + P_b$ Stresses

Load Case ^c	Service Level	Section ^d	Component Stresses ^a (ksi)						S_{int}	S_{allow}	FS
			S_x	S_y	S_z	S_{xy}	S_{yz}	S_{xz}			
Accident Pressure	D	3	-0.46	-7.35	35.72	0.09	0.07	2.43	43.24	68.60	1.59
Normal Pressure + 24-inch Drop	D	12	17.98	18.23	1.64	0.67	0.76	-0.94	17.24	68.60	3.98
Normal Pressure + Tip-Over	D	5	0.68	59.72	41.78	0.02	0.81	0.28	59.06	63.75	1.08

Table 3.7-3 PWR Fuel Tube Nodal Stress Intensities – Concrete Cask Tip-over Accident

Tube	Basket (deg)	P_m (ksi)			Tube	Basket (deg)	$P_m + P_b$ (ksi)		
		S_{int}	S_{allow}	FS			S_{int}	S_{allow}	FS
8	0	32.4	47.88	1.48	8	0	36.3	61.56	1.70
11	0	32.2	47.88	1.49	1	0	35.8	61.56	1.72
6	45	32.1	47.88	1.49	11	0	32.9	61.56	1.87
3	45	32.0	47.88	1.50	12	0	32.9	61.56	1.87
7	45	32.0	47.88	1.50	3	45	32.9	61.56	1.87
10	0	32.0	47.88	1.50	10	45	32.9	61.56	1.87
12	0	31.9	47.88	1.50	5	0	32.7	61.56	1.88
9	45	31.8	47.88	1.51	7	45	32.7	61.56	1.88
8	45	31.8	47.88	1.51	4	45	32.5	61.56	1.89
10	45	31.8	47.88	1.51	9	45	32.3	61.56	1.91

^a The x,y,z component of stress are to be interpreted radial, circumferential, and axial directions, respectively.

^b See Figure 3.10.3-2 for section cut locations.

^c The x,y,z component of stress are to be interpreted radial, circumferential, and axial directions, respectively.

^d See Figure 3.10.3-2 for section cut locations.

Table 3.7-4 PWR Corner Weldment Mounting Plate Nodal Stress Intensities – Concrete Cask Tip-over Accident

Basket	S _{int} (ksi)	S _{allow} (ksi)	FS
0°	32.0 ^a	47.88	1.50
45°	31.9 ^b	47.88	1.50

Table 3.7-5 PWR Corner Support Bar Nodal Stress Intensities – Concrete Cask Tip-over Accident

Basket	S _{int} (ksi)	S _{allow} (ksi)	FS
0°	31.8 ^c	47.88	1.51
45°	31.7 ^d	47.88	1.51

Table 3.7-6 PWR Side Weldment Nodal Stress Intensities – Concrete Cask Tip-over Accident

Basket	S _{int} (ksi)	S _{allow} (ksi)	FS
0°	32.0 ^e	47.88	1.50
45°	31.8 ^f	47.88	1.50

^a Maximum stress occurs at location 24 of Figure 3.10.1-17.

^b Maximum stress occurs at location 25 of Figure 3.10.1-18.

^c Maximum stress occurs at location 19 of Figure 3.10.1-17.

^d Maximum stress occurs at location 14 of Figure 3.10.1-18.

^e Maximum stress occurs at location 12 of Figure 3.10.1-19.

^f Maximum stress occurs at location 12 of Figure 3.10.1-20.

Table 3.7-7 BWR Fuel Tube Nodal Stress Intensities – Concrete Cask Tip-over Accident

Tube	Basket (deg)	P _m (ksi)			Tube	Basket (deg)	P _m + P _b (ksi)		
		S _{int}	S _{allow}	FS			S _{int}	S _{allow}	FS
8	45	32.8	47.88	1.46	24	0	34.7	61.56	1.77
18	45	32.3	47.88	1.48	8	45	34.7	61.56	1.77
13	45	32.2	47.88	1.49	25	0	34.1	61.56	1.81
21	0	32.1	47.88	1.49	23	0	34.0	61.56	1.81
23	0	32.0	47.88	1.49	18	45	33.8	61.56	1.82
12	45	32.0	47.88	1.49	13	45	33.5	61.56	1.84
5	45	31.9	47.88	1.50	21	0	33.0	61.56	1.87
25	0	31.9	47.88	1.50	15	0	32.9	61.56	1.87
18	0	31.9	47.88	1.50	5	45	32.9	61.56	1.87
24	45	31.9	47.88	1.50	23	0	32.7	61.56	1.88

Table 3.7-8 BWR Corner Weldment Mounting Plate Nodal Stress Intensities – Concrete Cask Tip-over Accident

Basket	S _{int} (ksi)	S _{allow} (ksi)	FS
0°	31.9 ^a	47.88	1.50
45°	32.2 ^b	47.88	1.49

Table 3.7-9 BWR Corner Support Plate Nodal Stress Intensities – Concrete Cask Tip-over Accident

Basket	S _{int} (ksi)	S _{allow} (ksi)	FS
0°	32.0 ^c	47.88	1.50
45°	32.0 ^d	47.88	1.50

^a Maximum stress occurs at location 36 of Figure 3.10.2-17.

^b Maximum stress occurs at location 37 of Figure 3.10.2-18.

^c Maximum stress occurs at the plate cut-out near location 36 of Figure 3.10.2-17.

^d Maximum stress occurs at the plate cut-out near location 35 of Figure 3.10.2-18.

Table 3.7-10 BWR Side Weldment Nodal Stress Intensities – Concrete Cask Tip-over Accident

Basket	S _{int} (ksi)	S _{allow} (ksi)	FS
0°	31.7 ^a	47.88	1.51
45°	32.1 ^b	47.88	1.49

Table 3.7-11 Concrete Cask Vertical Stress Summary – Inner Surface, psi

Condition	Dead	Live	Wind	Thermal	Seismic	Flood	Tornado	Total
4	-23	-25	0	-1048	0	0	0	-1096
5	-23	-25	0	-989	-105	0	0	-1201
7	-23	-25	0	-989	0	-11	0	-1107
8	-23	-25	0	-989	0	0	-12	-1108

Table 3.7-12 Concrete Cask Circumferential Stress Summary – Inner Surface, psi

Condition	Dead	Live	Wind	Thermal	Seismic	Flood	Tornado	Total
4	0	0	0	-217	0	0	0	-217
5	0	0	0	-211	0	0	0	-211
7	0	0	0	-211	0	0	0	-211
8	0	0	0	-211	0	0	0	-211

^a Maximum stress occurs at location 9 of Figure 3.10.2-19.

^b Maximum stress occurs at location 6 of Figure 3.10.2-20.

Table 3.7-13 Basket Modal Frequency for Concrete Cask Tip-over

Fuel Type and Basket Angle	Frequency (F), Hz
PWR-0°	269
PWR-45°	33
BWR-0°	140
BWR-45°	39

Table 3.7-14 DLF and Amplified Accelerations for Concrete Cask Tip-over

Fuel Type and Basket Angle	Top of TSC Lid			Top of Fuel Basket		
	Base Acceleration, g	DLF	Amplified Acceleration, g	Base Acceleration, g	DLF	Amplified Acceleration, g
PWR-0°	29.6	1.0	29.6	26.6	1.01	26.9
PWR-45°	29.6	1.0	29.6	26.6	1.21	32.2
BWR-0°	29.6	1.0	29.6	26.6	1.02	27.1
BWR-45°	29.6	1.0	29.6	26.6	1.07	28.5

3.8 Fuel Rods

This section presents an evaluation of the PWR and BWR fuel rods for all conditions of storage of the MAGNASTOR system.

3.8.1 PWR Fuel Rod Evaluation

3.8.1.1 Buckling Evaluation of PWR Fuel Rods with High Burnup

This section presents the buckling evaluation for MAGNASTOR high burnup PWR fuel (burnup greater than 45,000 MWd/MTU) having cladding oxide layers that are 80 and 120 microns thick. These analyses show that the high burnup PWR fuel and the damaged high burnup PWR fuel do not buckle in the design basis accident events. An end drop orientation is considered with an acceleration of 60g, which subjects the fuel rod to axial loading. A reduced cladding thickness is assumed, due to the cladding oxide layer.

In the end drop orientation, the fuel rods are laterally restrained by the grids and come into contact with the fuel assembly base. The only vertical constraint for the fuel rod is the base of the assembly. The weight of the fuel pellets is included in this evaluation, as the pellets are considered to be vertically supported by the cladding. A two-dimensional model comprised of ANSYS BEAM3 elements, shown in Figure 3.8-1, is used for the evaluation. This evaluation is considered to be the bounding condition (as opposed to an evaluation, which considers the cladding only).

80 Micron Cladding Oxide Layer Thickness Evaluation

During the end drop, the fuel rod impacts the fuel assembly base. The fuel rod itself will respond as an elastic bar under a sudden compression load at its bottom end. The duration of this impact is bounded by the first extentional mode shape of the fuel rod. Contribution of higher frequency extentional modes of the fuel rod would tend to shorten the duration of impact of the fuel rod with the fuel assembly base. The fuel rod, upon initiation of impact, corresponds to an undeformed state. In the process of the impact, the compression of the fuel rod will increase to a maximum and then return to a near uncompressed state, at which point the time of impact has been completed. This impact process actually represents half of a cycle of the lowest frequency mode shape of the fuel rod. The shape of the time dependence of the deformation is sinusoidal. The single extentional mode shape can also be considered to be a single degree of freedom with a corresponding mass and stiffness. In viewing such an event as a spring mass system, the time variation of the deformation during the impact is expected to be sinusoidal.

The buckling mode for the fuel rod is governed by the boundary conditions. For this configuration, the grids provide a lateral support, but no vertical support. The only vertical restraint is considered to be at the point of contact of the fuel rod and the base of the fuel assembly. The weight of the fuel rod pellets and cladding is assumed to be uniformly distributed along the length of the fuel rod. In the end drop, this results in the maximum compressive load occurring at the base of the fuel rod. The first buckling mode shape corresponding to these conditions is computed as shown in Figure 3.8-2.

Typically eigenvalue buckling is applied for static environments. For dynamic loading, it is assumed that the duration of the loading is sufficiently long to allow the system to experience the complete load, even as the deformation associated with the buckling is commenced. For dynamic loading, the lateral motion, which would correspond to the buckled shape, will correspond to the lowest mode shape. This lowest frequency mode shape is shown in Figure 3.8-2 and corresponds to a frequency of 25.9 Hz. The similarity of the two shapes shown in Figure 3.8-2 is expected, since both have the same displacement boundary conditions, the same stiffness matrix, and the same governing finite element equations, i.e.,

$$[K] \{\phi_i\} = \lambda_i [A] \{\phi_i\}$$

where:

- [K] = structure stiffness matrix
- $\{\phi_i\}$ = eigenvector
- λ_i = eigenvalue
- [A] = mass matrix for the mode shape calculation or stress stiffening matrix for the buckling evaluation

Based on the time duration of the impact and the inherent inability of the fuel rod to rapidly displace in the lateral direction, the effect of the actual lateral motion of buckling can be computed with a dynamic load factor (DLF) [24]. The expression for the DLF for a half-sine loading for a single degree of freedom is given by

$$DLF = \frac{2\beta \cos\left(\frac{\pi}{2\beta}\right)}{1 - \beta^2}$$

where:

β = ratio of the first extentional mode frequency to the first lateral mode frequency

These values, computed in this section, are $\beta = 8.32$ and $DLF = 0.244$.

This DLF is applied to the end drop acceleration of 60g, which is the bounding load to potentially result in the buckling of the fuel rod. The product of $60g \times DLF (= 14.6g)$ is well below the vertical acceleration corresponding to the first buckling mode shape, 37.9g as computed in this section. This indicates that the time duration of the impact of the fuel onto the fuel assembly base is of sufficiently short nature that buckling of the fuel rod cannot occur.

An effective cross-sectional property is used in the model to consider the properties of the fuel pellet and the fuel cladding. The modulus of elasticity (EX) for the fuel pellet has a nominal value of 26.0×10^6 psi [25]. To be conservative, only 50 percent of this value is used in the evaluation. The EX for the fuel pellet was, therefore, taken to be 13.0×10^6 psi. The value of EX (10.47×10^6 psi) was used for the irradiated zirconium alloy cladding [26]. The analysis contained in Reference 27 used an elastic modulus of 10.98×10^6 psi, which is bounded by the above value. Reference 28 information shows that there is no additional reduction of the ductility of the cladding due to extended burnup in the 45,000 – 50,000 MWd/MTU range.

The bounding dimensions and physical data (minimum clad thickness, maximum rod length and minimum number of support grids) for the MAGNASTOR fuel rod used in the model are:

Outer diameter of cladding (inches)	0.434
Cladding thickness (inches)	0.023
Cladding density (lb/in ³)	0.237
Fuel pellet density (lb/in ³)	0.396

The cladding thickness is reduced from its nominal value of 0.026 inches by the assumed 80 micron oxidation layer (0.003 inches) to 0.023 inches. Similarly, the fuel rod outer diameter is reduced from the nominal value of 0.44 inches to 0.434 inches.

The elevation of the grids, measured from the bottom of the fuel assembly, are: 2.3, 33.0, 51.85, 70.7, 89.6, 108.4, 127.3 and 144.9 (inches).

The effective cross-sectional properties (EI_{eff}) for the beam are computed by adding the value of EI for the cladding and the pellet, where:

$$E = \text{modulus of elasticity (lb/in}^2\text{)}$$

$$I = \text{cross-sectional moment of inertia (in}^4\text{)}$$

The lowest frequency for the extentional mode shape was computed to be 219.0 Hz. The first mode shape corresponds to a frequency of 25.9 Hz. Using the expression for the DLF previously discussed, the DLF is computed to be 0.240 ($\beta = 8.44$).

120 Micron Cladding Oxide Layer Thickness Evaluation

The buckling calculation used the same model employed for the mode shape calculation: The load that would potentially buckle the fuel rod in the end drop is due to the deceleration of the

rod. This loading was implemented by applying a 1g acceleration in the direction that would result in compressive loading of the fuel rod. The acceleration required to buckle the fuel rod is computed to be 37.3g, which is much higher than the calculated effective g-load (14.3g) due to the 60g end drop. Therefore, the fuel rods with a 120 micron cladding oxide layer do not buckle in the 60g end drop event.

3.8.2 BWR Fuel Rod Evaluation

The evaluation of the BWR fuel rod is based on the following representative sample of BWR fuel rods:

Fuel Assembly	Cladding Diameter (in)	Cladding Thickness (in)	Cladding Material	Pellet Diameter (in)	Rod Length (in)
GE 7x7	0.563	0.032	Zirc-2	0.487	158.15
GE 7x7	0.563	0.032	Zirc-2	0.487	163.42
GE 8x8-2	0.483	0.032	Zirc-2	0.410	158.67
GE 8x8-2	0.483	0.032	Zirc-2	0.410	163.42
GE 8x8-4	0.484	0.032	Zirc-4	0.410	163.42
GE 8x8-4	0.484	0.032	Zirc-4	0.410	163.42
GE 9x9-2	0.441	0.028	Zirc-4	0.376	163.42
GE 10x10-2	0.378	0.024	Zirc-4	0.322	163.42

The location of the lateral constraints in the BWR fuel are: 0.00 in, 22.88 in, 43.03 in, 63.18 in, 83.33 in, 103.48 in, 122.3 in, 143.78 in, and 163.42 in.

For the PWR fuel rod the largest ratio of unsupported length (L) to radius of gyration of the cladding cross section (r) [13] is

$$L/r = \frac{30.7}{0.5 \times \sqrt{(.434/2)^2 + (.388/2)^2}} = 211$$

The ratio (L/r) for a BWR fuel rod is

$$L/r = \frac{22.88}{0.5 \times \sqrt{(.378/2)^2 + (.330/2)^2}} = 182$$

The analysis presented in Section 3.8.1 is bounding for both PWR and BWR fuel rods, because the (L/r) for the PWR fuel rod is larger than the (L/r) for the BWR fuel rod. Therefore, no further evaluation of the BWR fuel rod is required.

3.8.3 Thermal Evaluation of Fuel Rods

MAGNASTOR limits normal storage condition fuel cladding temperatures to be $\leq 400^{\circ}\text{C}$ (752°F) in accordance with ISG-11, Rev 3. Zirconium alloy or stainless steel cladding degradation is not expected to occur below this temperature in an inert gas environment.

The fuel cladding temperature limit for short-term off-normal and accident events is 570°C ($1,058^{\circ}\text{F}$). Refer to Chapter 4, which demonstrates that the maximum fuel cladding temperatures are well below the temperature limits for all design conditions of storage.

Figure 3.8-1 Two-Dimensional Beam Finite Element Model for MAGNASTOR Fuel Rod

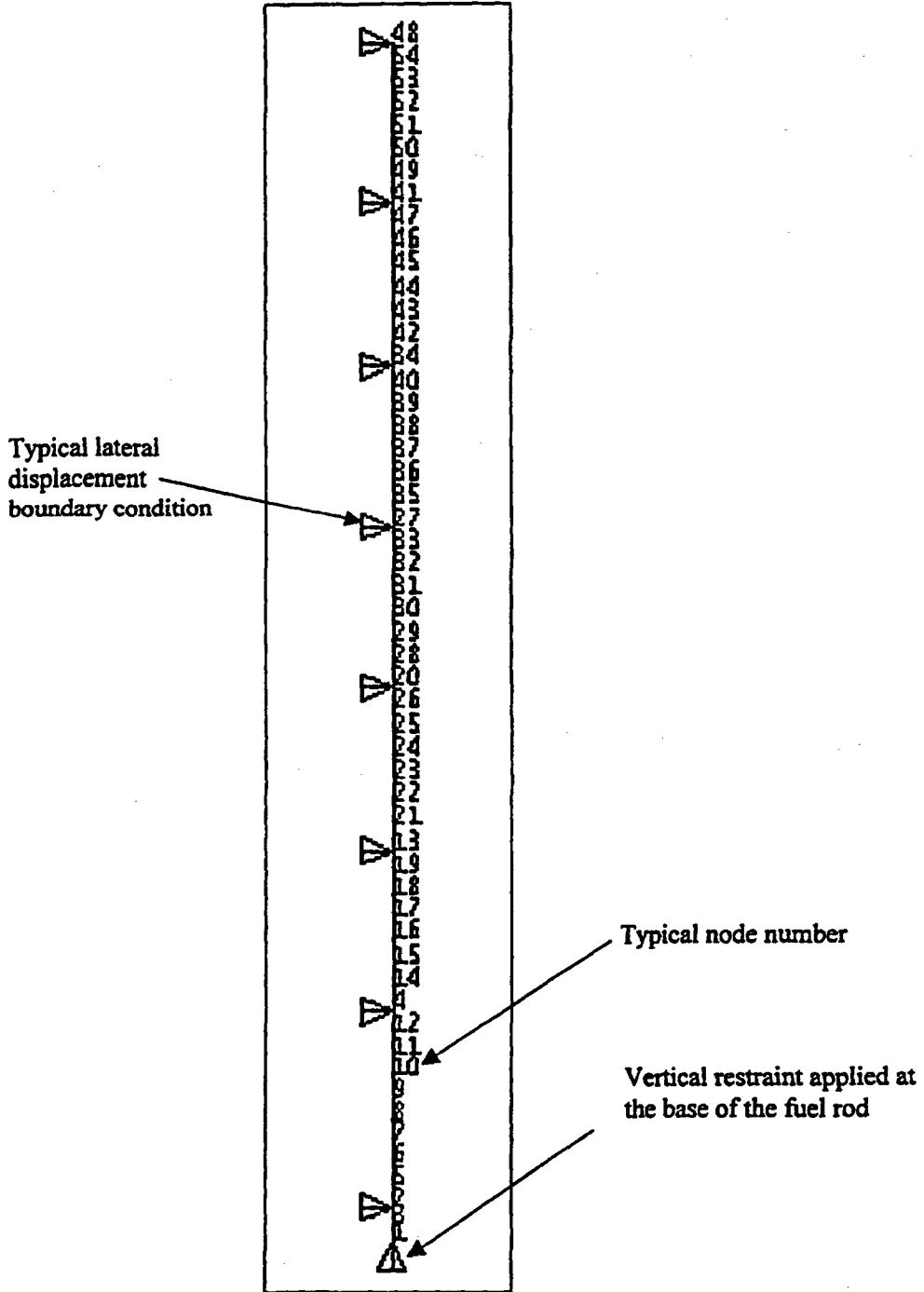
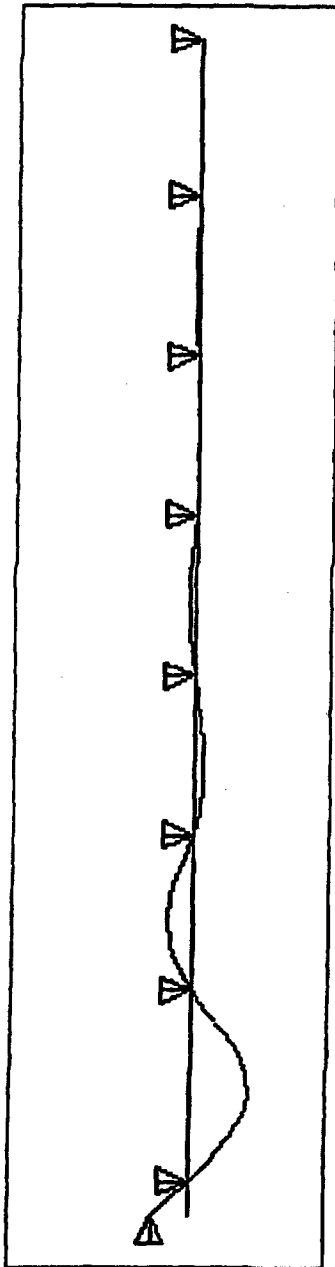
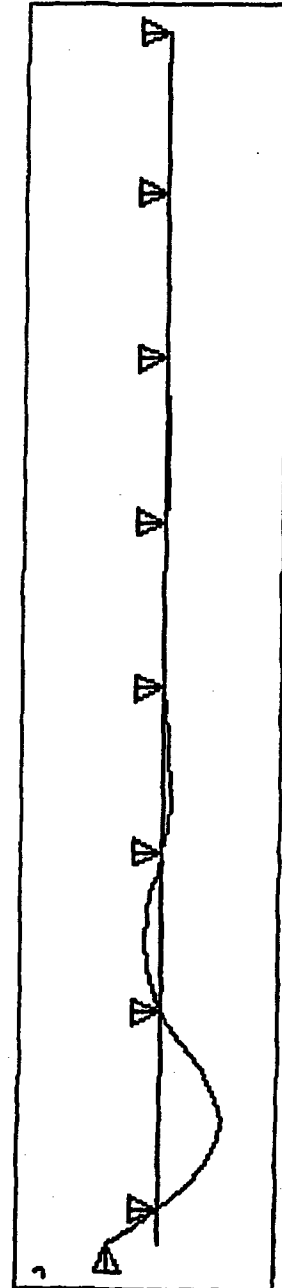


Figure 3.8-2 Mode Shape and First Buckling Shape for the MAGNASTOR Fuel Rod

First Lateral Dynamic
Mode Shape at 25.9 Hz



First Buckling
Shape at 37.9g



3.9 References

1. 10 CFR 72, Code of Federal Regulations, "Licensing Requirements for the Independent Storage of Spent Fuel, High Level Radioactive Waste and Reactor-Related Greater than Class C Waste," US Nuclear Regulatory Commission, Washington, DC.
2. American National Standard for Radioactive Materials N14.6-1993, "Special Lifting Devices for Shipping Containers Weighing 10,000 Pounds (4500 kg) or More," American National Standard Institute, Inc., Washington, DC, 1993.
3. NUREG-0612, "Control of Heavy Loads at Nuclear Power Plants," U. S. Nuclear Regulatory Commission, Washington, D.C., 1980.
4. ANSI/ANS-57.9-1992, American National Standard Design Criteria for an Independent Spent Fuel Storage Installation (Dry Type), American Nuclear Society, La Grange Park, IL, May 1992.
5. "Code Requirements for Nuclear Safety Related Concrete Structures (ACI 349-85) and Commentary (ACI 349R)," American Concrete Institute, Farmington Hills, MI.
6. ASME Boiler and Pressure Vessel Code, Section III, Subsection NB, "Class 1 Components," American Society of Mechanical Engineers, New York, NY, 2001 Edition with 2003 Addenda.
7. ASME Boiler and Pressure Vessel Code, Section III Subsection NG, "Core Support Structures", American Society of Mechanical Engineers, New York, NY, 2001, with 2003 Addenda.
8. ASME Boiler and Pressure Vessel Code, Appendix F, "Rules for Evaluation of Service Loadings with Level D Service Limits," The American Society of Mechanical Engineers, New York, NY, 2001, with 2003 Addenda.
9. NUREG/CR-6322, "Buckling Analysis of Spent Fuel Basket," Lawrence Livermore National Laboratory, Livermore, CA, 1995.
10. AFFDL-TR-69-42, "Stress Analysis Manual", Air Force Flight Dynamics Laboratory, Dayton, Ohio, 1969.
11. "Steel Structures Design and Behavior," C.G. Salmon and J.E. Johnson, Harper and Row Publishers, New York, NY, Second Edition, 1980.
12. "Machinery's Handbook," Industrial Press, New York, NY, 25th Edition, 1996.
13. "Roark's Formulas for Stress & Strain," Young, Warren C., McGraw Hill, New York, NY, Sixth Edition, 1989.
14. "Reinforced Concrete Design," Leet, Kenneth, McGraw-Hill, New York, NY, Second Edition, 1991.

15. "Practical Stress Analysis in Engineering Design," Alexander Blake, Marcel Dekker, Inc., New York, NY, Second Edition, 1990.
16. NUREG-0800, "Standard Review Plan," U.S. Nuclear Regulatory Commission Draft, Washington, DC, June 1987.
17. ASCE 7-93, "Minimum Design Loads for Buildings and Other Structures," American Society of Civil Engineers, New York, NY, March 12, 1994.
18. NSS 5-940.1, "A Review of Procedures for the Analysis and Design of Concrete Structures to Resist Missile Impact Effects," Nuclear and Systems Sciences Group, Holmes & Narver, Inc., Anaheim, CA, September 1975.
19. BC-TOP-9A, Revision 2, Topical Report, "Design of Structures for Missile Impact," Bechtel Power Corporation, San Francisco, CA, September 1974.
20. "Engineering Fluid Mechanics," Roberson, J.A. and Crowe, C.T. Houghton Mifflin Co., Boston, MA, 1975.
21. ASCE 4-86, "Seismic Analysis of Safety-related Nuclear Structures and Commentary on Standard for Seismic Analysis of Safety-related Nuclear Structures," American Society of Civil Engineers, New York, NY, 1986.
22. "Structural Dynamics," Biggs, John M., McGraw-Hill, New York, NY, 1964.
23. ISG-15, Revision 0, "Materials Evaluation," US Nuclear Regulatory Commission, Washington, DC, January 10, 2001.
24. "Dynamics of Structures," Clough, R.W., and Joseph Penzien, 2nd Edition, McGraw-Hill, Inc., New York, NY, 1993.
25. Nuclear Power Plant Engineering, Rust, J.H., Georgia Institute of Technology, 1979.
26. ISG-12, Revision 1, "Buckling of Irradiated Fuel Under Bottom End Drop Conditions," US Nuclear Regulatory Commission, Washington, DC, January 15, 2001.
27. "Spent Nuclear Fuel Structural Response when Subjected to an End Impact Accident," Adkins, H.E., *et. al.*, 2004 ASME Pressure Vessels and Piping Conference, San Diego, CA.
28. NUREG/CR-5009, "Assessment of the Use of Extended Burnup Fuel in Light Water Power Reactors," Battelle Pacific Northwest Labs, Richland, Washington, February 1998.

3.10 Structural Evaluation Detail

This section contains evaluation detail not found in the preceding sections.

3.10.1 PWR Fuel Basket Finite Element Models

3.10.1.1 Load Path Description

This section describes the load paths and interactions between basket components during storage conditions. The MAGNASTOR PWR fuel basket is designed to accommodate 37 PWR fuel assemblies. For the normal conditions of storage, the weight of the fuel assemblies is directly supported by the bottom plate of the TSC. The basket is subjected to its self-weight only. For the off-normal and accident events associated with loadings in the transverse direction of the basket (e.g., off-normal handling load, concrete cask tip-over accident), the weight of the fuel assemblies is supported by the 21 fuel tubes, side support weldments, and corner support weldments. Referring to Figure 3.10.1-1, load transfer between the fuel tubes, '1', is through contact at the tube corners. This contact consists of two types: the connector pins and the region between pins where the tube sections are in contact. The connector pin socket connections at 20-inch center-to-center distance prevent the fuel tubes from sliding past each other. The shear load transmitted across the pins is reacted out in bearing in the fuel tube pin sockets. The tube region between pins transmits bearing directly between fuel tubes. Shear loads between the tube corners can be transmitted by friction; however, friction is not considered in the finite element analyses of the basket. The detailed interaction between fuel tube corners, as well as a free-body diagram of a tube section, is shown in Figure 3.10.1-3. As the figure shows, the pin welded to one tube fits into the slots cut into the adjoining tube.

Connector pin assemblies are installed as redundant supports at the top and bottom of the fuel basket. The connector pin assemblies join adjacent fuel tubes to ensure each tube is properly aligned during the assembly process. The connector pin assembly provides an end weldment effect that allows for handling of the assembled basket outside of the TSC without special fixtures. The bottom connector pins also provide a standoff between the TSC bottom plate and basket tubes, and transmit bearing loads from the basket to the TSC bottom plate.

The corner and side support weldments provide rigidity to the basket. The weldments are attached to the fuel tube array by means of bolted boss connections. Bosses welded to the fuel tubes are slotted into the weldments. Connection is made with the use of a washer and bolt combination. Figure 3.10.1-1 and Figure 3.10.1-2 show the boss connection details, '2'. To ensure the connection is in tension, the bosses are designed not to penetrate completely through the weldment wall. Therefore, once installed and preloaded, the bolts are always in tension. Shear loads are reacted out by the interaction of the bosses, boss welds, and the support weldments. When the support weldments are in compression, bearing loads are transferred

through the support weldment to the fuel tube array, '3' (Figure 3.10.1-1 and Figure 3.10.1-2). Figure 3.10.1-4 shows a free-body diagram of the fuel tube interaction with the support structure.

3.10.1.2 Finite Element Model Descriptions

This section describes the finite element models used in the PWR basket structural evaluation. The following describes the finite element models and the applicable ASME Code section.

Finite Element Model	Analysis Usage	Loading Condition	ASME Code Section
3D Periodic Model	Off-normal TSC handling conditions (loads in basket in transverse direction)	Level C	III-NG
3D Thermal Stress Model	Thermal stress evaluation	Level A	III-NG
3D Periodic Plastic Model	Concrete cask tip-over accident evaluation	Level D	III-NG, App. F

3.10.1.2.1 PWR Basket Three-Dimensional Periodic Models

Two three-dimensional periodic half-symmetry models of the PWR basket are used to calculate the stresses in the basket due to the transverse loading during the off-normal TSC handling conditions. These models correspond to the critical basket orientations, 0° and 45°, as shown in Figure 3.10.1-5 and Figure 3.10.1-6. The fuel tube support pins and slot joints are spaced on 20.0-inch centers. Therefore, the periodic model extends from the axial center of a fuel tube support pin to the midpoint of the fuel tube between the pins (10.0-inch segment). The end effect of the basket on pinned connections is ignored.

The finite element models are constructed using ANSYS SOLID45, SHELL63, and BEAM4 elements. Fuel tube assemblies, pins, and side support weldments are modeled using SOLID45 elements. Corner weldment plates are modeled using SHELL63 elements. BEAM4 elements are used to model the support bars on the corner support weldments. The interaction between fuel tubes, corner support assemblies, and side support assemblies are modeled with CONTAC52 gap elements. These gap elements allow the transfer of loads between the basket structural components. Figure 3.10.1-10 shows the details of the modeling of the fuel tube/pin interaction with the CONTAC52 elements at the gap between the pin and the tube socket. BEAM4 elements with minimal properties (Area = 0.001 in²) are defined at pin-to-socket weld locations between the fuel tubes and pins to assist in obtaining convergence of the ANSYS solution. CONTAC52 gap elements are used to simulate the total gap between the PWR basket and the transfer cask. The effect of the TSC shell is conservatively not included in the model.

The corner support and side support weldment assemblies are bolted to the fuel tube array at eight locations in the half-symmetry basket models. The bolt/boss joints are modeled using LINK10 (tension only) elements for the bolts and COMBIN40 elements for the boss. The COMBIN40 elements represent the shear restraint generated by the bosses welded to the fuel tubes.

Loads and boundary conditions are discussed in Section 3.10.1.3. The weight of the neutron absorbers and the retainers, which are not included in the finite element model, are considered by adjusting the density of the carbon steel for the fuel tube sides.

3.10.1.2.2 PWR Basket Three-Dimensional Thermal Stress Model

The structural evaluation for thermal stresses is performed using a three-dimensional quarter-symmetry finite element model, as shown in Figure 3.10.1-7. The model represents the top or bottom 47 inches of the PWR basket to evaluate the bounding axial and radial thermal gradients considering the end restraint of the basket due to the connector pin assemblies. This model includes the connector pin assemblies at the end of the fuel tubes and two intermediate pin and bolt locations. The connector pin assemblies at the end of the basket are modeled with nodal constraints in the basket transverse directions at the interface of two adjacent connector pins. The modeling methodology of the model is the same as that of the three-dimensional periodic model as discussed in Section 3.10.1.2.1.

3.10.1.2.3 PWR Basket Three-Dimensional Periodic Plastic Model

The evaluation of the PWR basket of the cask tip-over event is performed using two three-dimensional plastic periodic models, as shown in Figure 3.10.1-8 and Figure 3.10.1-9 for 0° and 45° basket orientations, respectively. The model is a half-symmetry one based on the three-dimensional periodic model used for the off-normal handling evaluations presented in Section 3.10.1.2.1. In this model, the SHELL43 elements are used for the corner weldment mounting plates instead of SHELL63 elements. SHELL43 elements are also used for the corner weldment support bars instead of BEAM4 elements. The CONTAC52 elements are used to model the interface between basket components. CONTAC52 elements are also used to simulate the total gap between the PWR basket and the vertical concrete cask. The bolt/boss joints are modeled the same as in the 3-dimensional period model using LINK10 and COMBIN40 elements. Bilinear elastic-plastic material properties are used for all basket components in the model, except for the pins and elements in the fuel tube socket interfacing with the pins. The acceptance criteria using plastic system analysis in ASME Section III Appendix F (F-1340) [8] requires that a bearing stress be only evaluated for pinned joints for the accident condition. The requirements

for the bearing stress evaluation for pinned joints are defined in Appendix F-1336, which is associated with an elastic evaluation limiting the bearing stress to $2.1S_u$. The use of the elastic properties for the pin in the basket model is consistent with the requirements of Appendix F-1340 for the plastic system analysis.

Loads and boundary conditions are discussed in Section 3.10.1.3. The weight of the neutron absorbers and the retainers, which are not included in the finite element model, are considered by adjusting the density of the carbon steel for the fuel tube sides.

3.10.1.3 Finite Element Model Boundary Conditions

3.10.1.3.1 Off-Normal Handling Boundary Conditions

For off-normal handling events, the three-dimensional periodic models described in Section 3.10.1.2.1 are used to calculate the stresses due to loading in the transverse direction of the basket. The gap between the basket and the transfer cask is 0.62 inch (0.12-inch basket-TSC and 0.50-inch TSC-cask). To represent the loads from the fuel assemblies, a bounding pressure load of 1.2 psi is applied to the fuel tubes.

The boundary conditions for 0° and 45° basket orientations are shown in Figure 3.10.1-11 and Figure 3.10.1-12, respectively. For off-normal events, an inertia load of 0.707g (resultant of 0.5g loading in the two transverse directions) is applied in the transverse direction of the basket. Applied pressure loads for fuel assemblies are also multiplied by 0.707g.

The 0° and 45° basket orientations are critical for the PWR basket for loading in the transverse direction. The 0° basket orientation maximizes the stresses in the fuel tube sidewalls and the 45° basket orientation maximizes the bending stresses in the tube corners. Intermediate basket orientations are bounded by the 0° and 45° orientations. Therefore, the basket evaluation is performed using two half-symmetry models for the 0° and 45° basket orientations, respectively. Symmetry boundary conditions are applied at the plane of symmetry. Symmetry boundary conditions are also applied to both ends of the finite element model to represent a periodic section of the basket. Fixed nodes are used to represent the transfer cask. For off-normal events, material properties at 100°F are conservatively used (using the modulus of elasticity for carbon steel at lower temperature results in slightly higher stress results.)

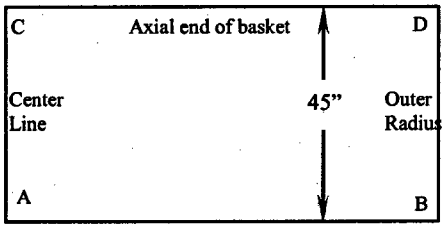
3.10.1.3.2 Thermal Stress Analysis Boundary Conditions

The three-dimensional quarter-symmetry model described in Section 3.10.1.2.1 is used to calculate the thermal stress due to the thermal expansion. As shown in the following table, a

total of five cases of temperature boundary conditions are considered to envelop the maximum temperature, as well as the maximum temperature gradients (ΔT), in the axial and radial directions of the basket for all conditions of storage and transfer. Prior to performing the thermal stress analysis, the steady-state temperature distribution in the model is determined by a thermal conduction analysis. The SOLID45, SHELL43 and BEAM4 structural elements were converted to SOLID70, SHELL57 and LINK33 thermal elements, respectively, for the thermal conduction solution.

Thermal Boundary Temperatures – PWR Basket (°F)

Case	A	B	C	D
1	600	440	360	300
2	680	500	580	440
3	640	520	700	590
4	430	380	210	260
5	700	500	550	400



Symmetry boundary conditions are applied at the planes of symmetry. In the basket axial direction, the model is restrained at one end.

3.10.1.3.3 Concrete Cask Tip-Over Accident Boundary Conditions

The concrete cask tip-over is evaluated as a side impact for the basket. During the concrete cask tip-over event, acceleration varies from 1g at the bottom of the concrete cask to a maximum acceleration at the top of the TSC. The three-dimensional plastic model is used for the evaluation of the basket (Section 3.10.1.2.3). A bounding acceleration of 35g is applied to the basket models in the transverse direction. The 35g acceleration bounds the maximum acceleration in the basket, including the dynamic load factor for the concrete cask tip-over accident.

The gap between the basket and the concrete cask is 0.84 inch (0.12-inch basket-TSC and 0.72-inch TSC-cask). Pressure loads are applied to the PWR basket models to represent the fuel assembly weight with a 35g acceleration.

For the tip-over accident (loading in the transverse direction), the 0° and 45° basket orientations are critical for the PWR basket as discussed in Section 3.10.1.3.2. Therefore, the basket is evaluated using models corresponding to the 0° and 45° basket orientations. Symmetry boundary conditions are applied at the plane of symmetry. Symmetry boundary conditions are also applied to both ends of the three-dimensional periodic finite element model. Fixed nodes are used to represent the concrete cask stand-offs. The boundary conditions for these models are

shown in Figure 3.10.1-11 and Figure 3.10.1-12. For accident conditions, material properties at 100°F are conservatively used.

3.10.1.4 Post-Processing Finite Element Analysis Results

3.10.1.4.1 Maximum Stresses for Off-Normal Handling Condition

The post-processing of the finite element analysis results from the periodic model for the off-normal event is performed by taking section cuts at various locations in the model.

The fuel tube section cuts are divided into two regions. Region 1 is the region between the pin supports. For the periodic model, this region is defined from the base of the model (mid-distance between pins) to the base of the pin. Region 2 is the pin region. This region starts at the base of the pin and extends to the top of the finite element model (mid-plane of pin). For both regions, the region just above and below the pin cutout (± 0.25 inch) is omitted from the section cuts to eliminate stress concentrations in the model. The membrane stresses are calculated by taking a section cut at the center of the tube thickness. The membrane plus bending stress is calculated by taking the maximum of the stresses calculated at the inner or outer surface of the fuel tube. Refer to Figure 3.10.1-13 through Figure 3.10.1-16 for the tube identification and the locations of the section cuts.

The maximum stresses for the corner support weldments are calculated by taking section cuts along the length of the weldment (ten inches for the periodic model). Since the corner weldment is modeled using SHELL63 elements, the membrane stresses are calculated at the mid plane of the element and the membrane plus bending stresses are calculated using the maximum stresses of either the inner or outer surface of the element. Refer to Figure 3.10.1-17 and Figure 3.10.1-18 for the locations of the section cuts.

The maximum stresses for the side weldments are calculated taking section cuts along the length of the weldment (ten inches for the periodic model). The membrane stresses are calculated by taking a section cut at the mid-thickness of the weldment. The membrane plus bending stress is calculated by taking the maximum of the stresses calculated at the inner or outer surface of the weldment. Refer to Figure 3.10.1-19 and Figure 3.10.1-20 for the locations of the section cuts.

The bolt tensile loads are obtained from the LINK10 element results. The boss shear loads are extracted from the COMBIN40 element results.

3.10.1.4.2 Maximum Thermal Stresses

The post-processing of the finite element analysis results for the thermal stress evaluation is performed by extracting the maximum nodal stress intensities from the model. The maximum nodal stress is obtained for two separate regions: (1) fuel tubes and (2) corner and side support weldments. The bolt tensile loads are extracted from the LINK10 elements, and the boss shear loads are extracted from the COMBIN40 elements.

3.10.1.4.3 Maximum Stresses for Concrete Cask Tip-Over Accident

The post-processing of finite element analysis results for the basket tip-over accident using the three-dimensional plastic model is performed by extracting stresses in the basket for the 0° and 45° basket orientations.

For the fuel tube stresses, the membrane stresses are calculated by extracting the nodal stress intensity at the mid-thickness of the tube thickness. The primary stresses are calculated by extracting the maximum nodal stress intensity of each fuel tube.

The stresses for the corner and side support weldments are calculated using the three-dimensional model. The maximum nodal stress intensities for the corner and side weldments are extracted from the model. The nodal stress intensity is conservatively compared to the membrane allowable to obtain the critical factors of safety.

Figure 3.10.1-1 Expanded View of PWR Basket

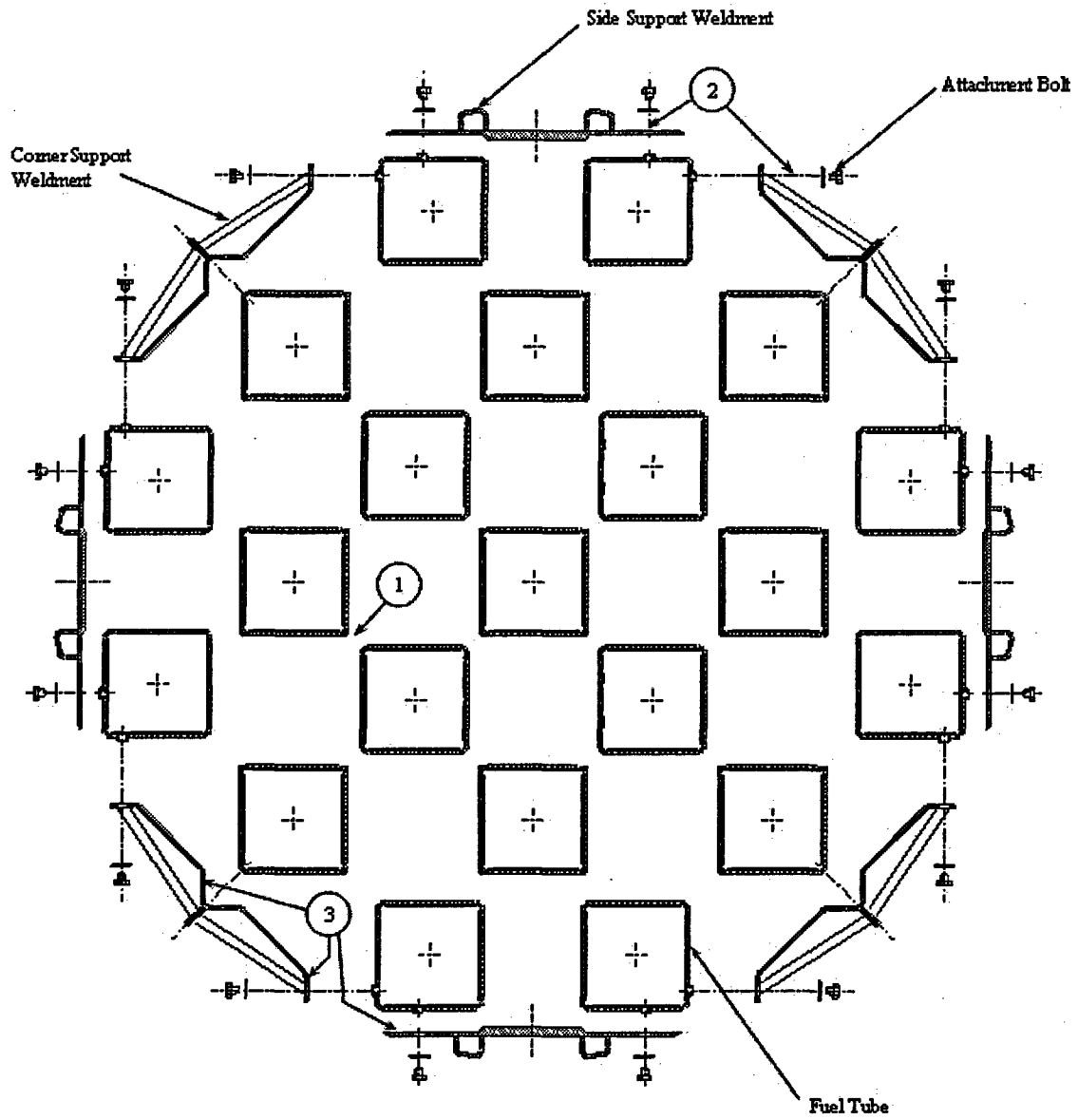


Figure 3.10.1-2 Bolted Attachment Details

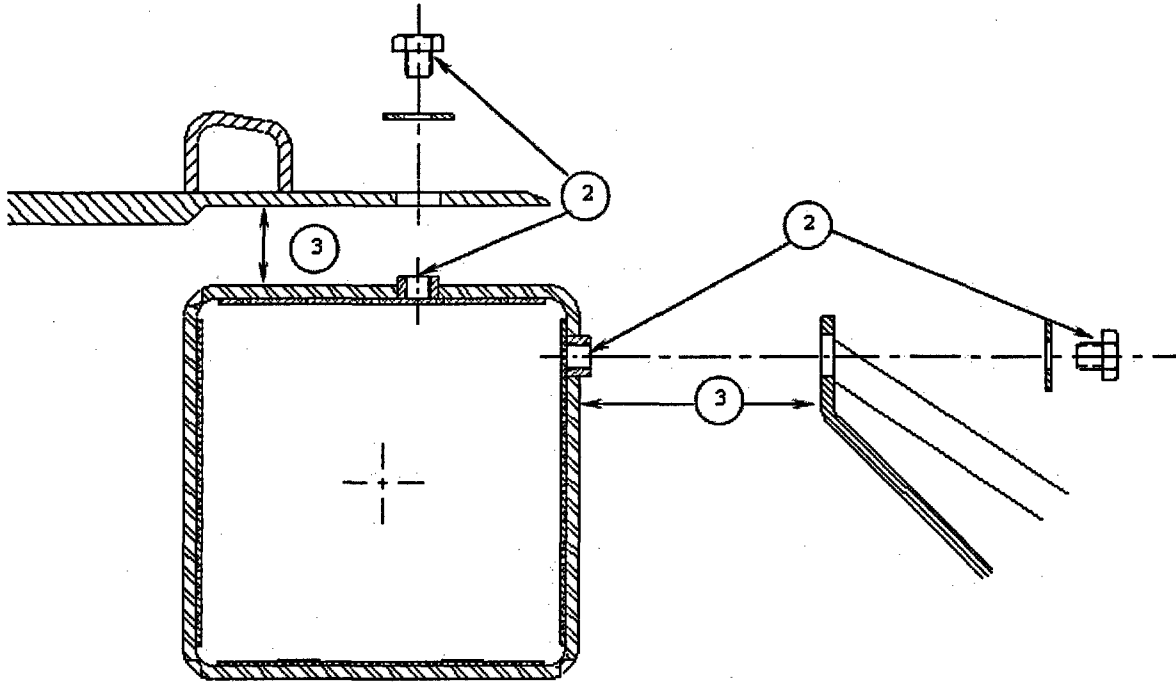
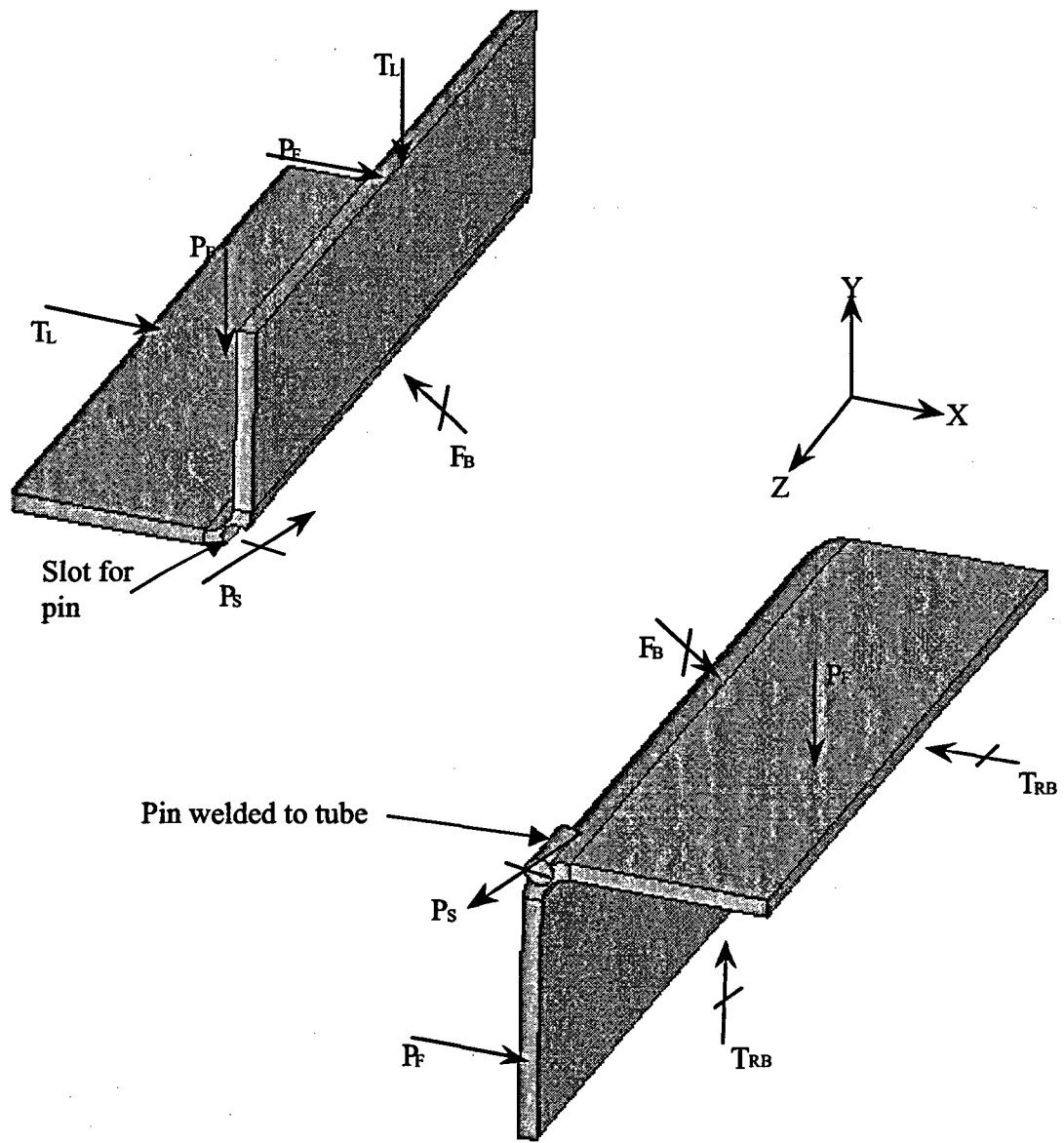
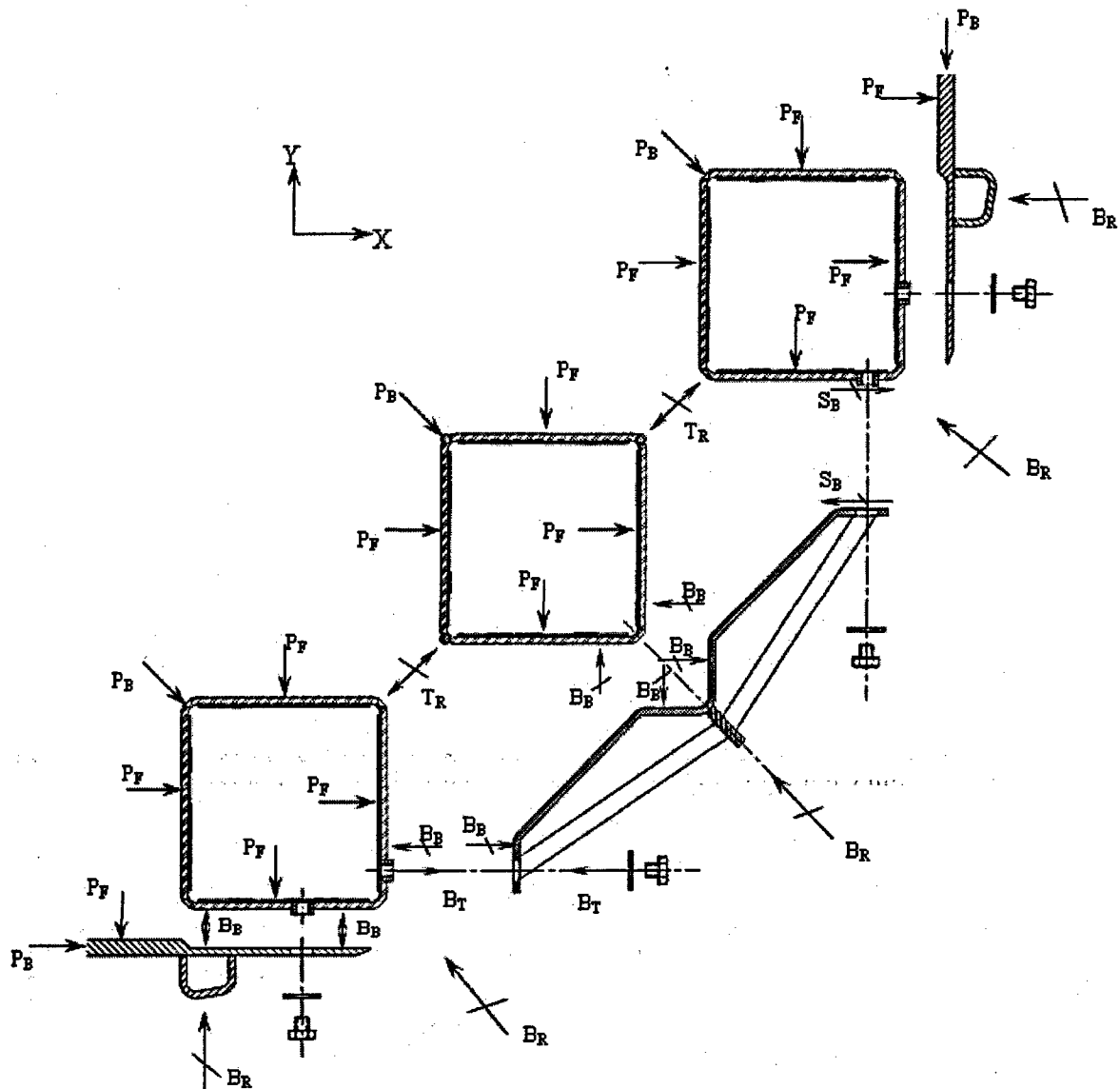


Figure 3.10.1-3 Free-Body Diagram of PWR Basket Fuel Tube Detail



- T_L Loads from adjacent tube or fuel assembly
- P_F Local load due to fuel assembly
- T_{RB} Reaction loads in tubes for equilibrium at symmetry planes of tubes
- P_S Shear Reaction thru pin joint (in the XY plane)
- F_B Bearing Reaction across tube flat

Figure 3.10.1-4 Free-Body Diagram of Basket Support Structure



- P_B Loads due to adjacent basket structure
- P_F Local load due to fuel assembly
- B_R Basket reaction with TSC shell locations
- B_T Tensile load at bolt and tube boss (typical)
- B_B Bearing reaction between tube sidewall and support structure (typical)
- S_B Shear reaction between support structure and tube boss (typical)
- T_R Reactions between tubes detailed in Figure 3.10.1-3

Figure 3.10.1-5 PWR Basket Periodic Model – 0° Basket Orientation

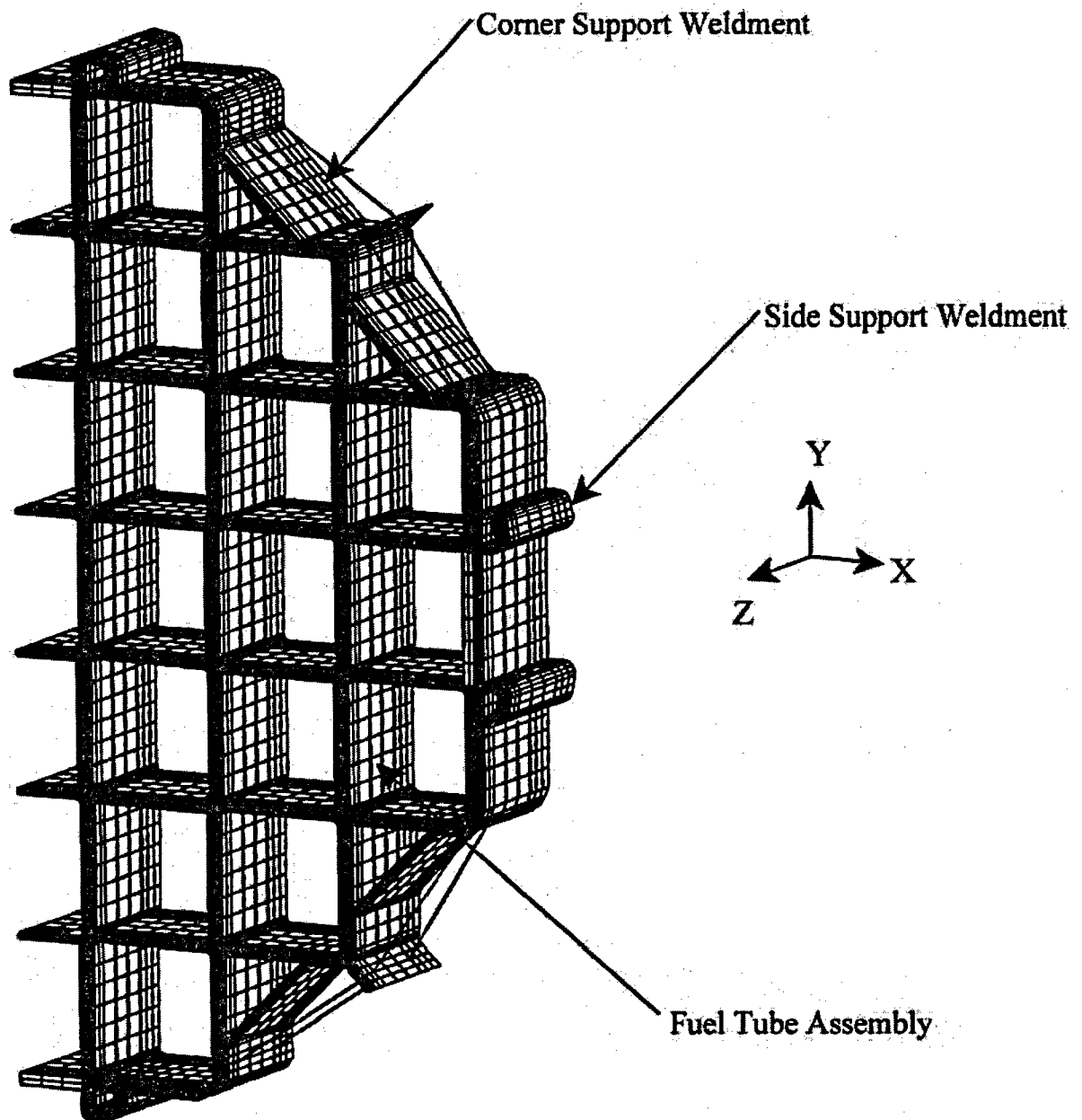


Figure 3.10.1-6 PWR Basket Periodic Model – 45° Basket Orientation

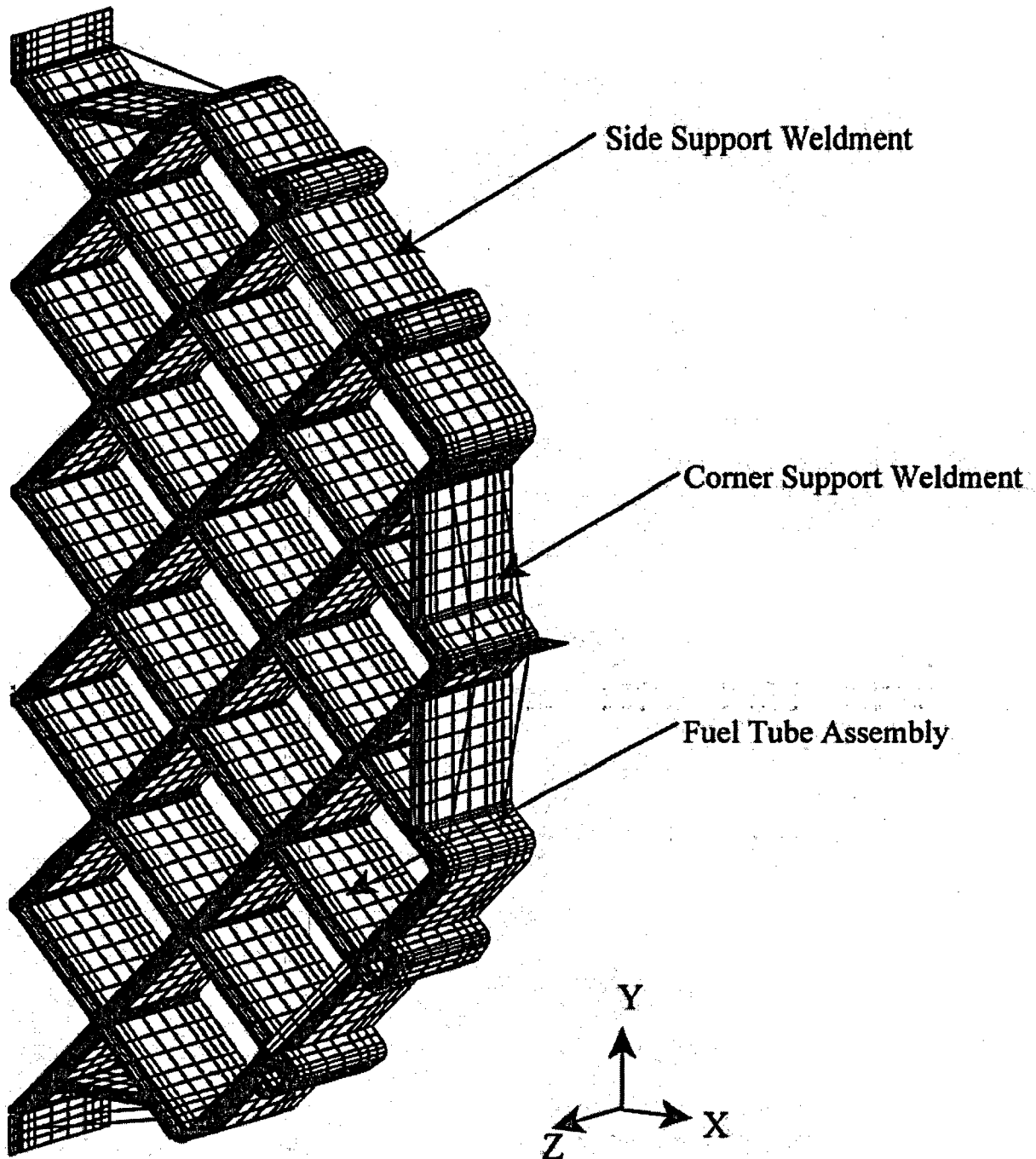


Figure 3.10.1-7 Thermal Stress Evaluation Model

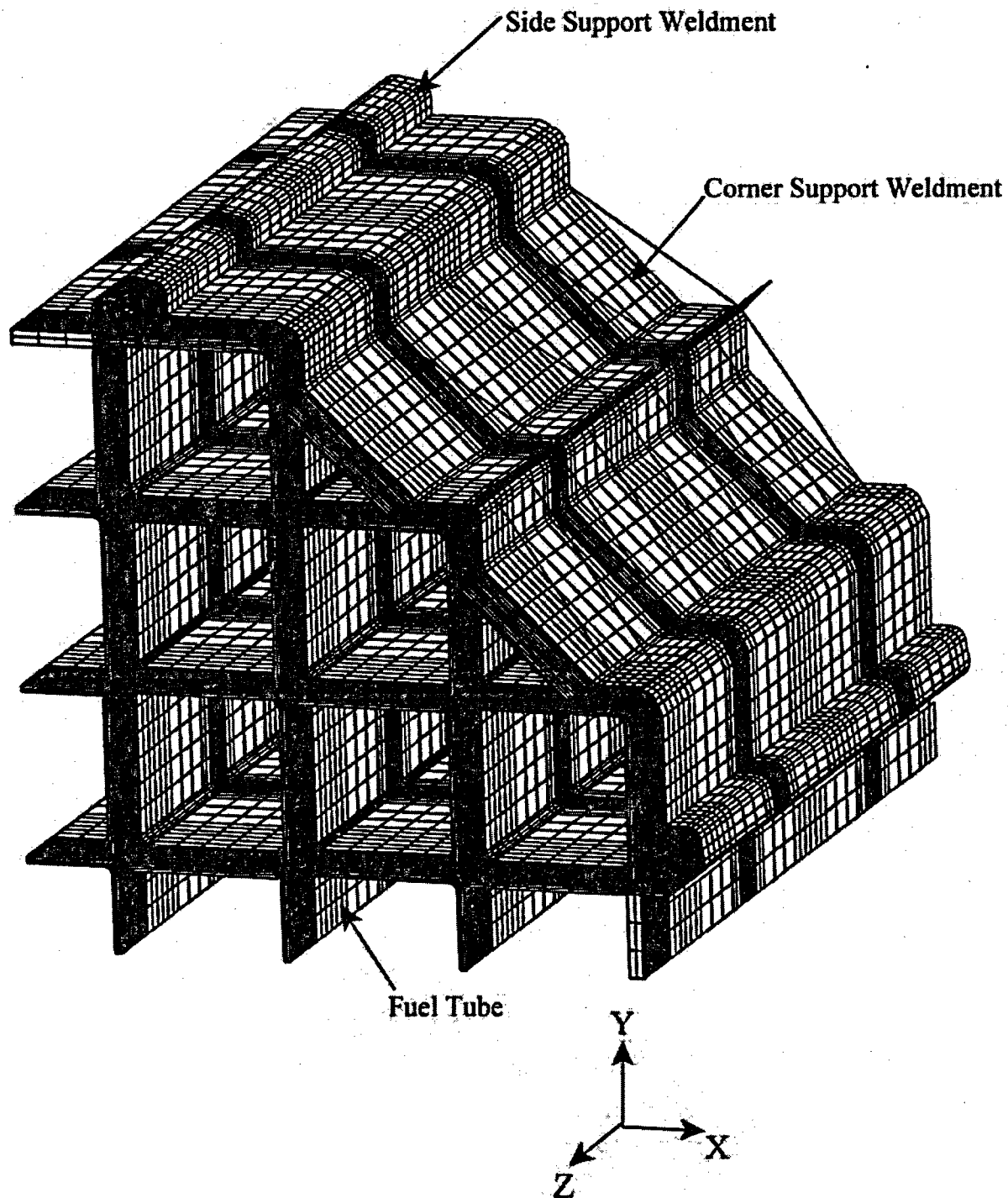


Figure 3.10.1-8 PWR Basket Plastic Model - 0° Basket Orientation

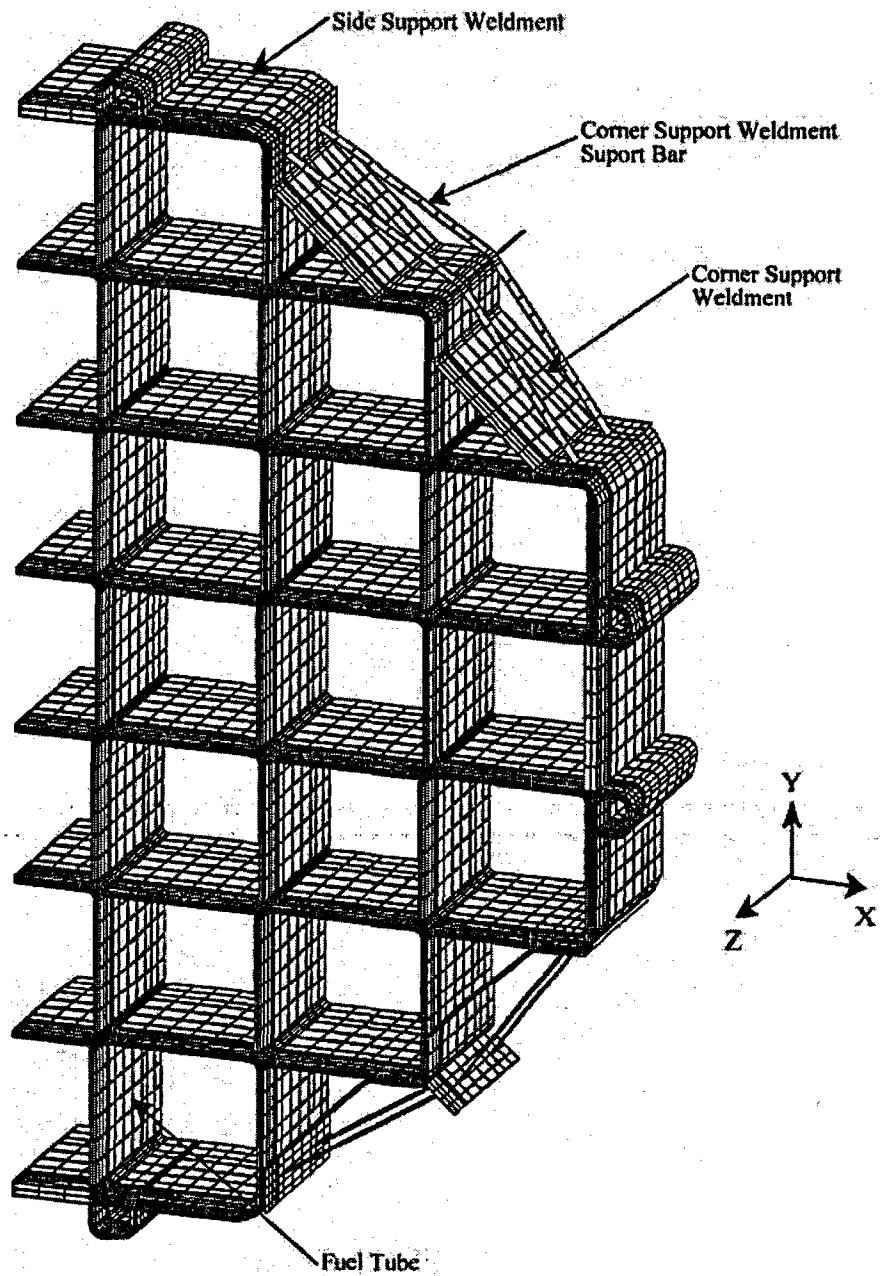


Figure 3.10.1-9 PWR Basket Plastic Model - 45° Basket Orientation

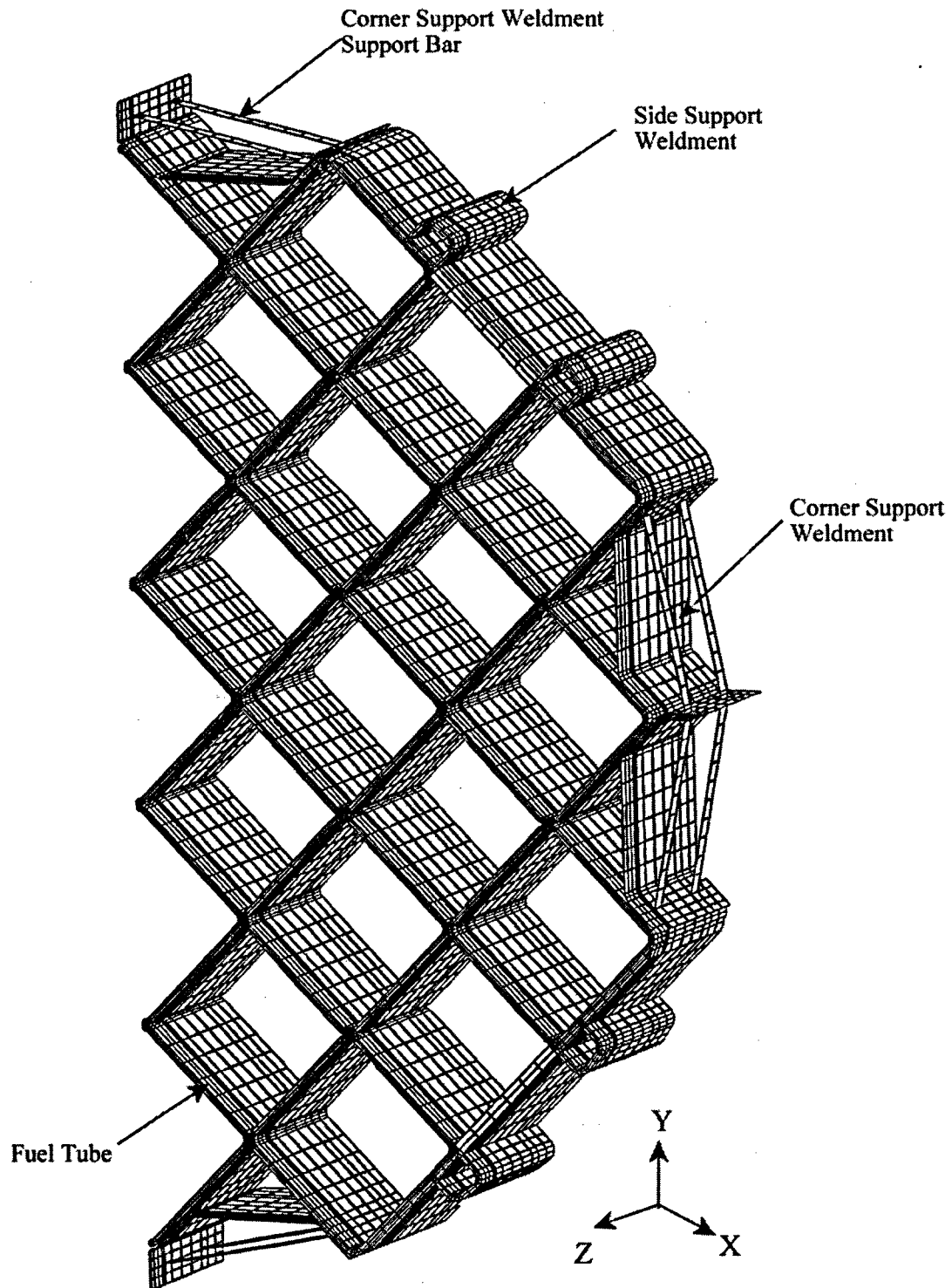


Figure 3.10.1-10 Typical PWR Fuel Tube Pin Finite Element Model Details

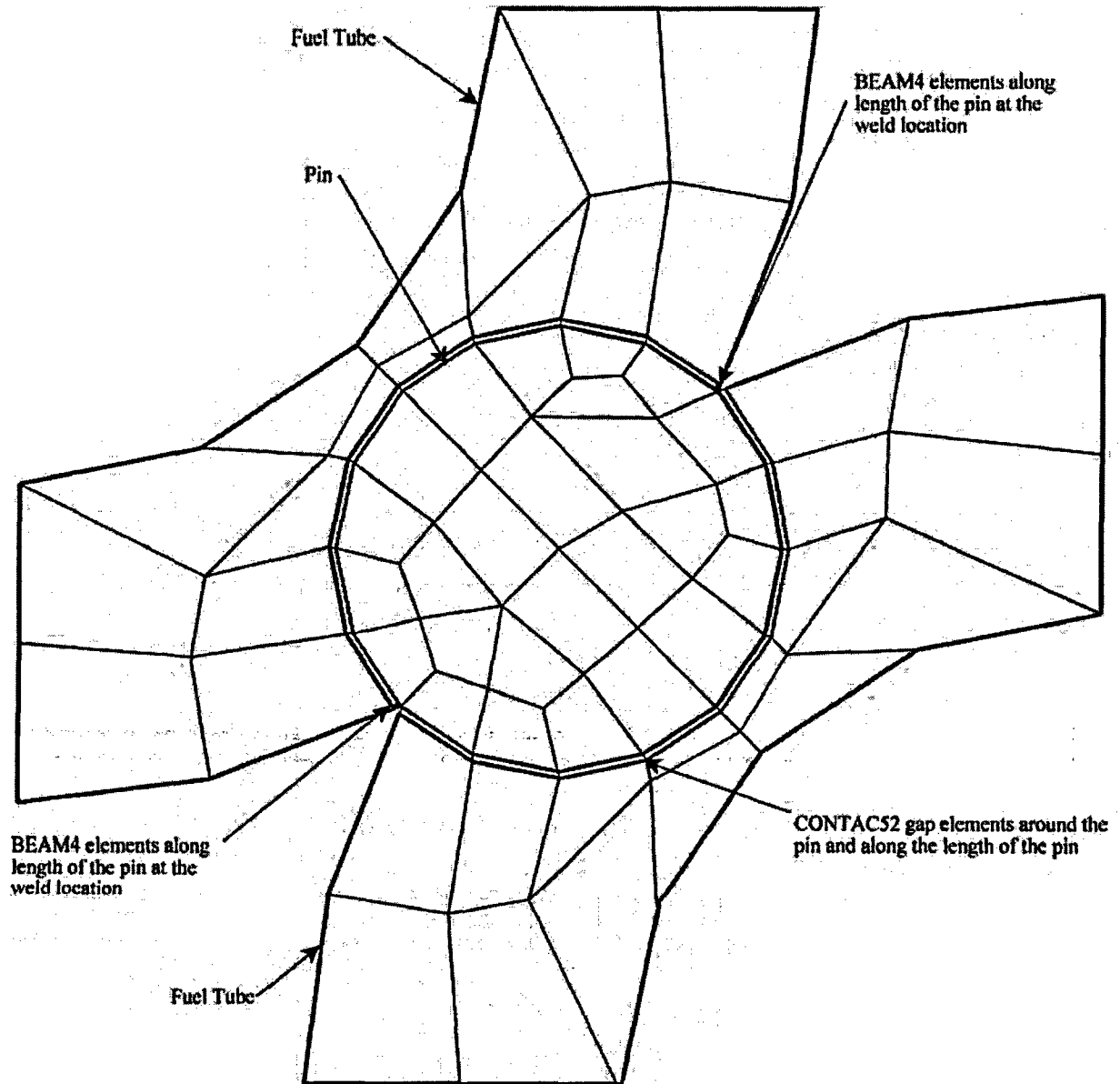


Figure 3.10.1-11 PWR Basket Model Boundary Conditions for a Transverse Loading –
0° Basket Orientation

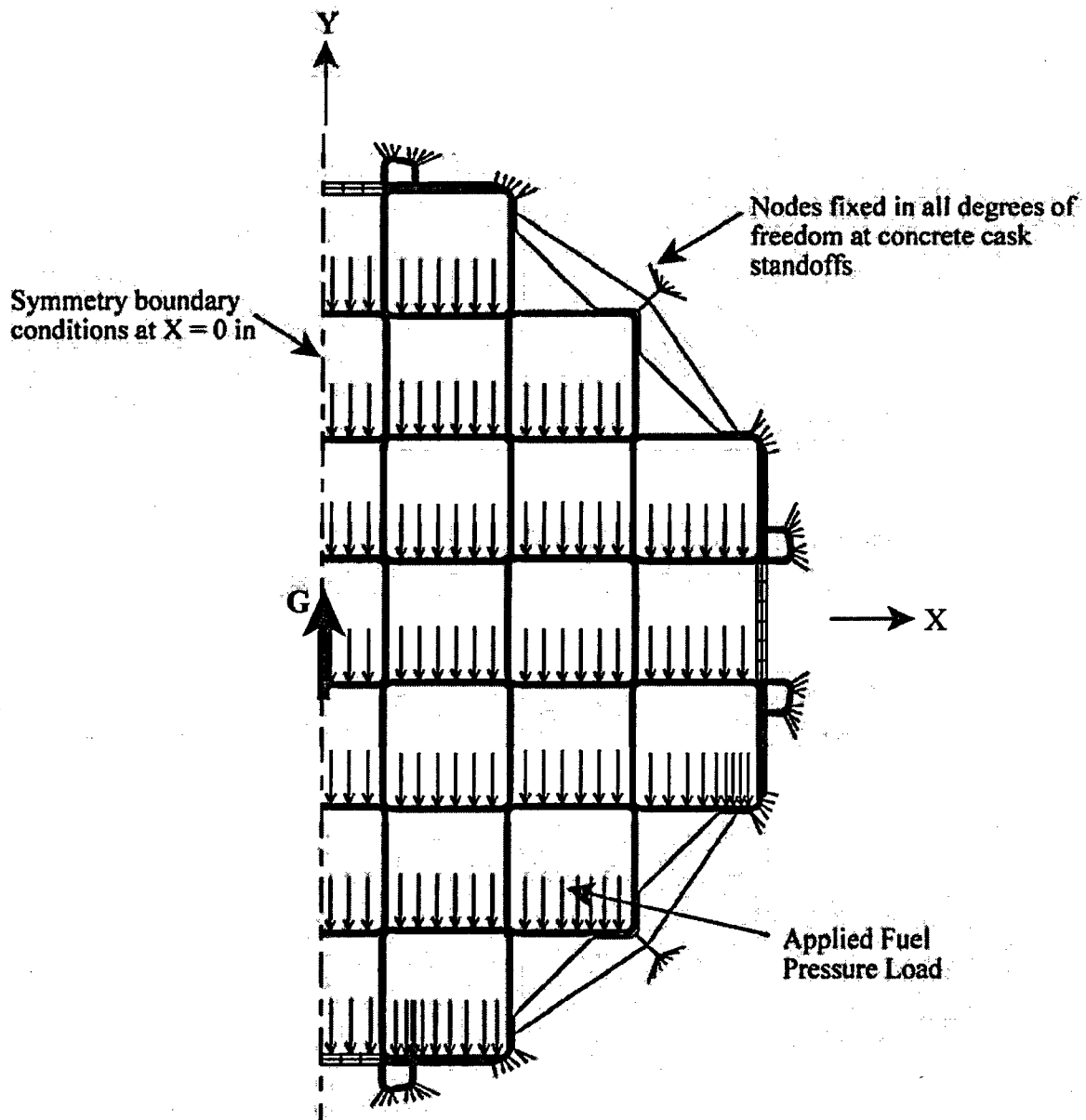


Figure 3.10.1-12 PWR Basket Model Boundary Conditions for a Transverse Loading – 45° Basket Orientation

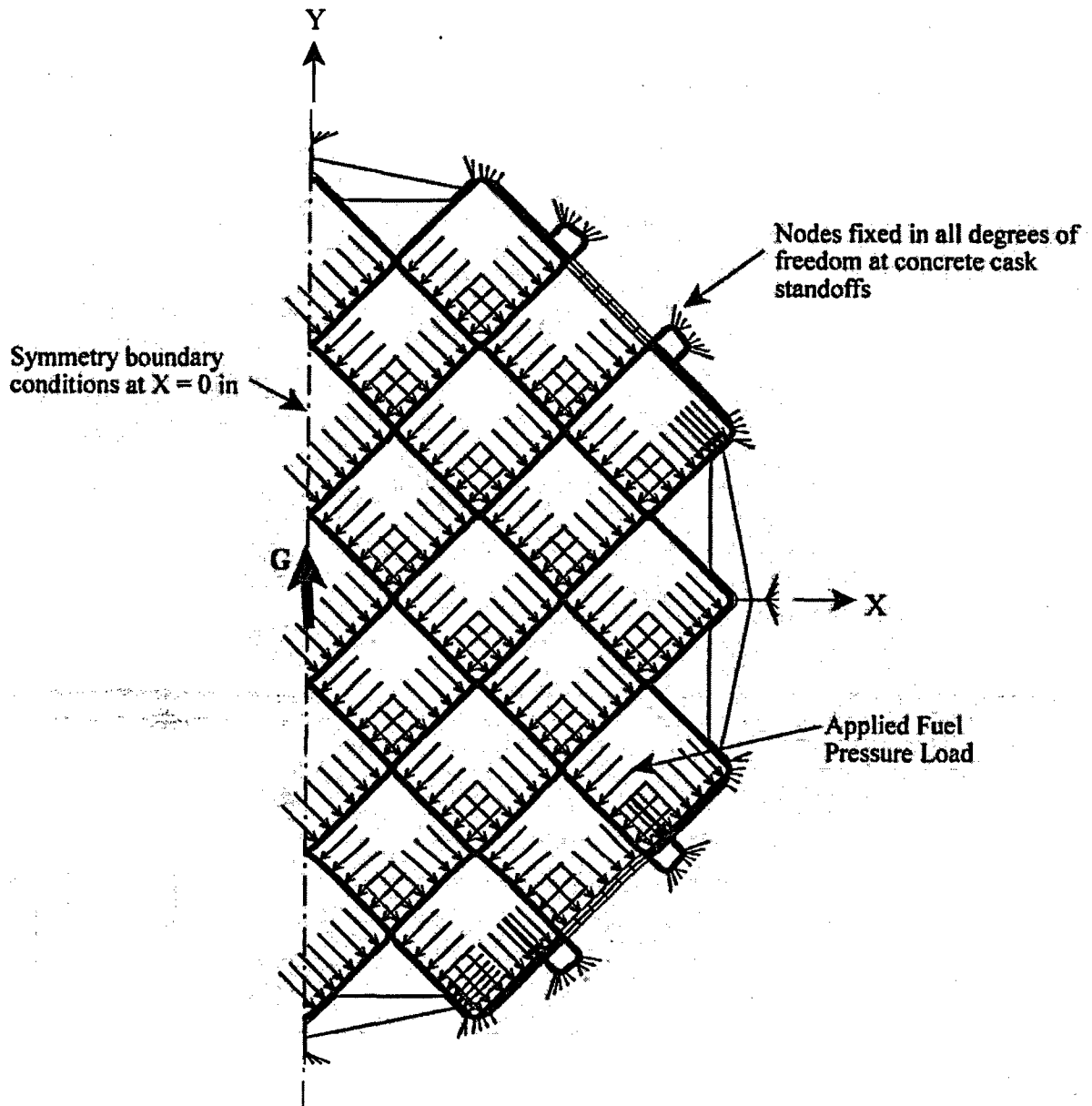


Figure 3.10.1-13 PWR Fuel Tube Array – 0° Basket Orientation

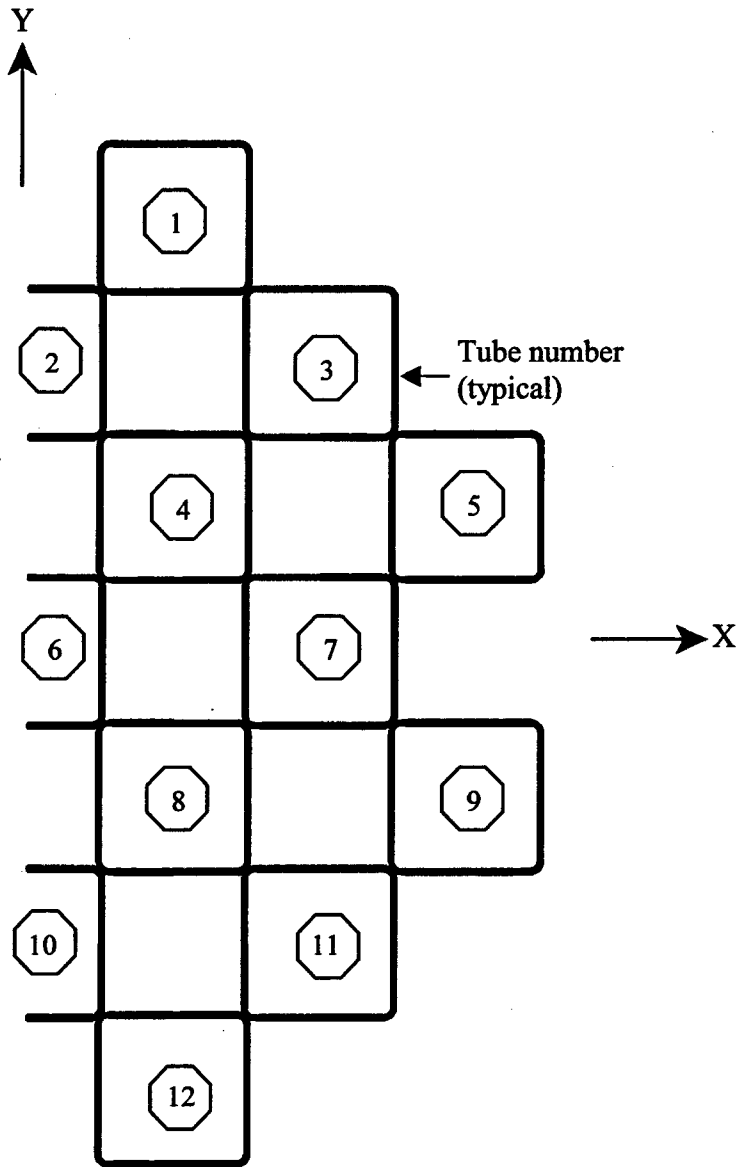


Figure 3.10.1-14 PWR Fuel Tube Section Cuts – 0° Basket Orientation

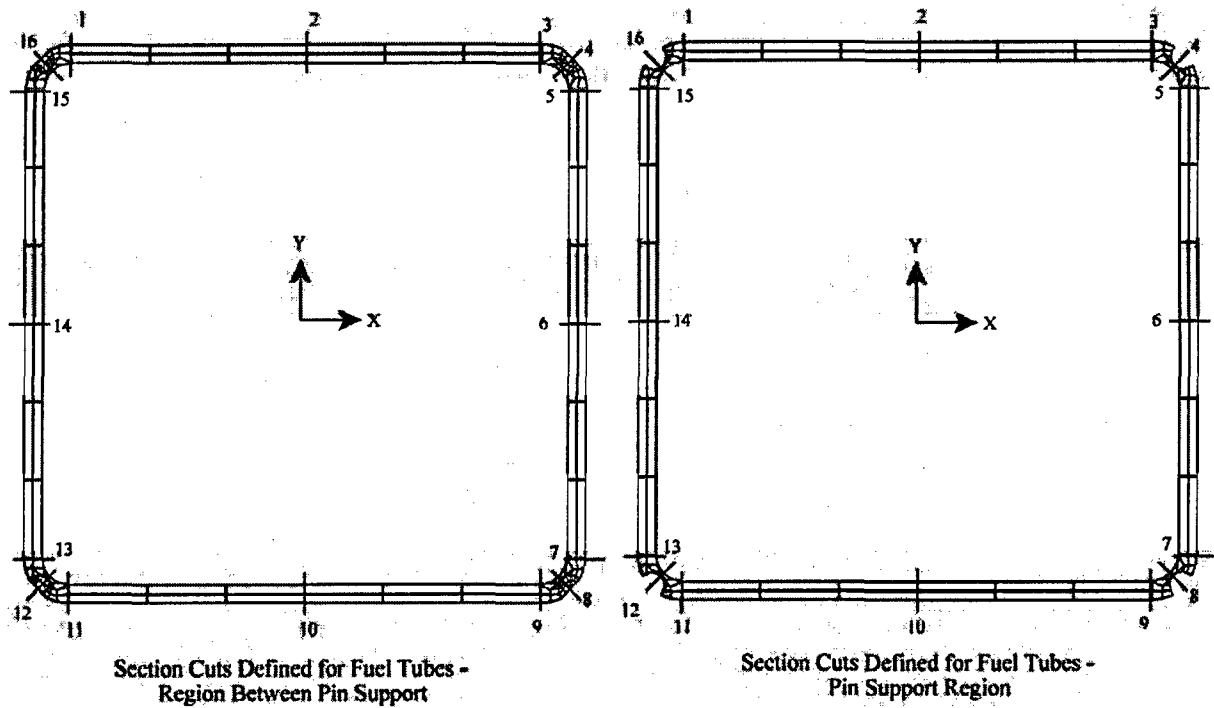


Figure 3.10.1-15 PWR Fuel Tube Array – 45° Basket Orientation

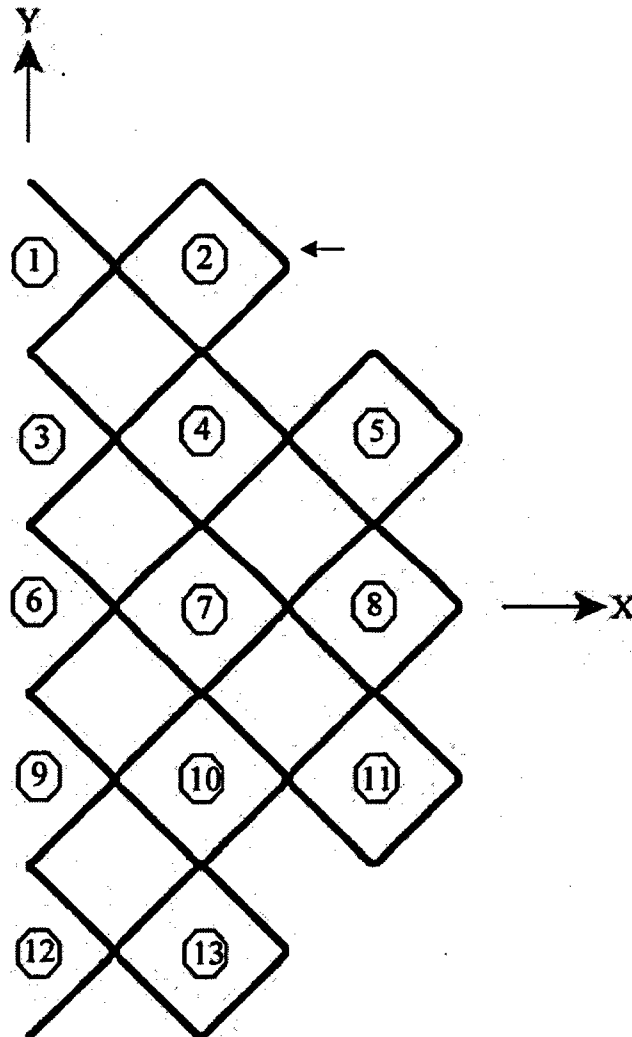
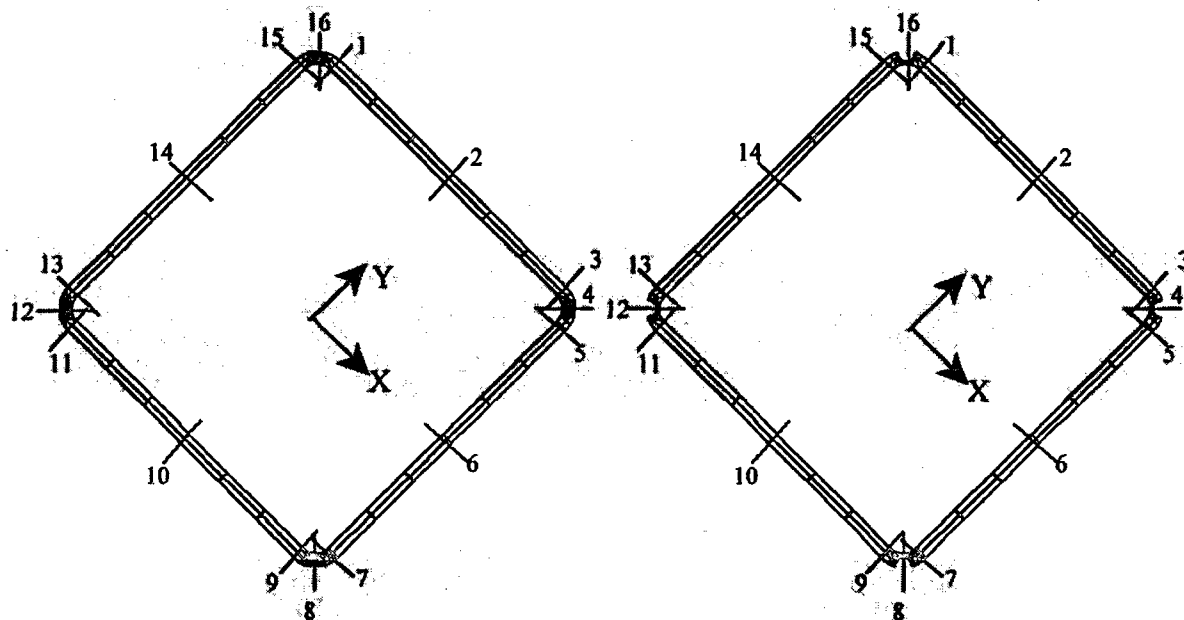


Figure 3.10.1-16 PWR Fuel Tube Section Cuts – 45° Basket Orientation



Section Cuts Defined for Fuel Tubes -
Region Between Pin Support

Section Cuts Defined for Fuel Tubes -
Pin Support Region

Figure 3.10.1-17 PWR Corner Support Weldment Section Cuts – 0° Basket Orientation

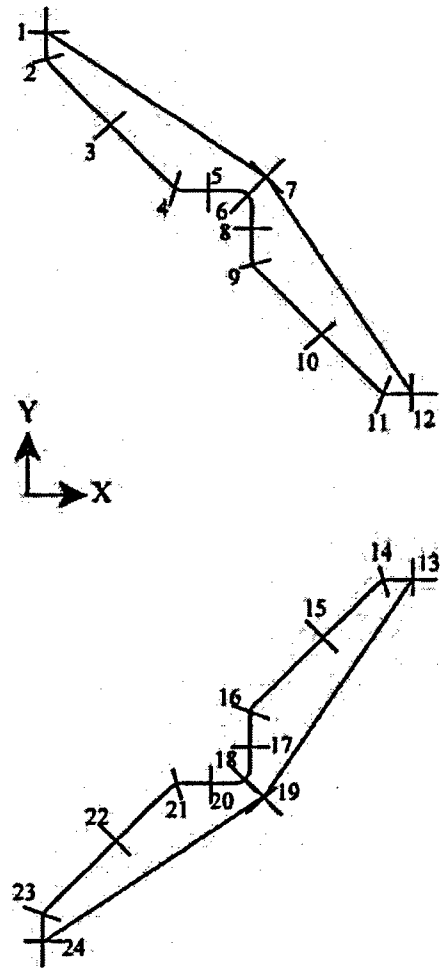


Figure 3.10.1-18 PWR Corner Support Weldment Section Cuts – 45° Basket Orientation

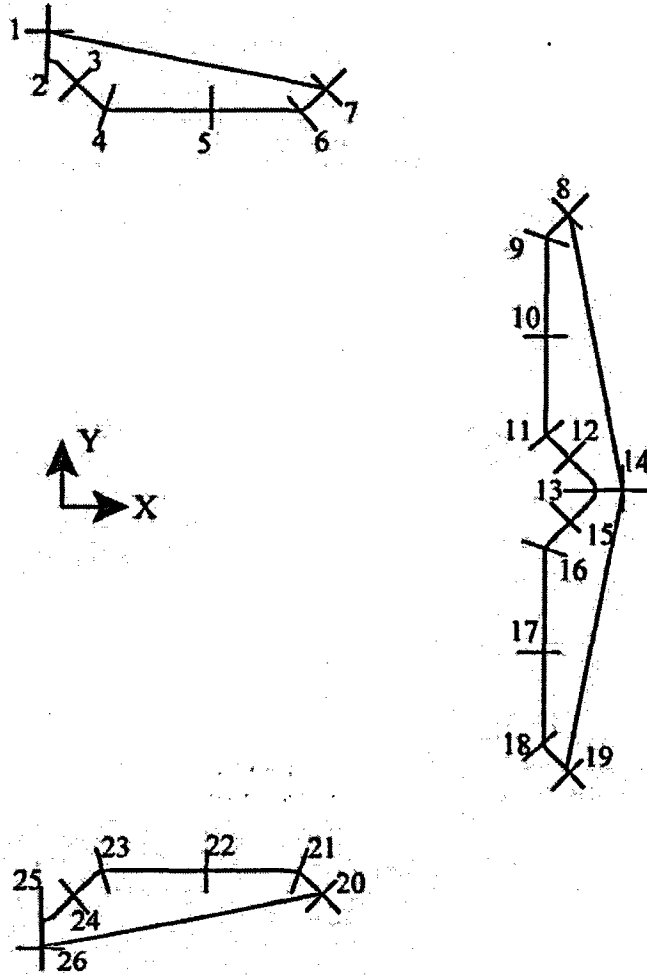


Figure 3.10.1-19 PWR Side Support Weldment Section Cuts – 0° Basket Orientation

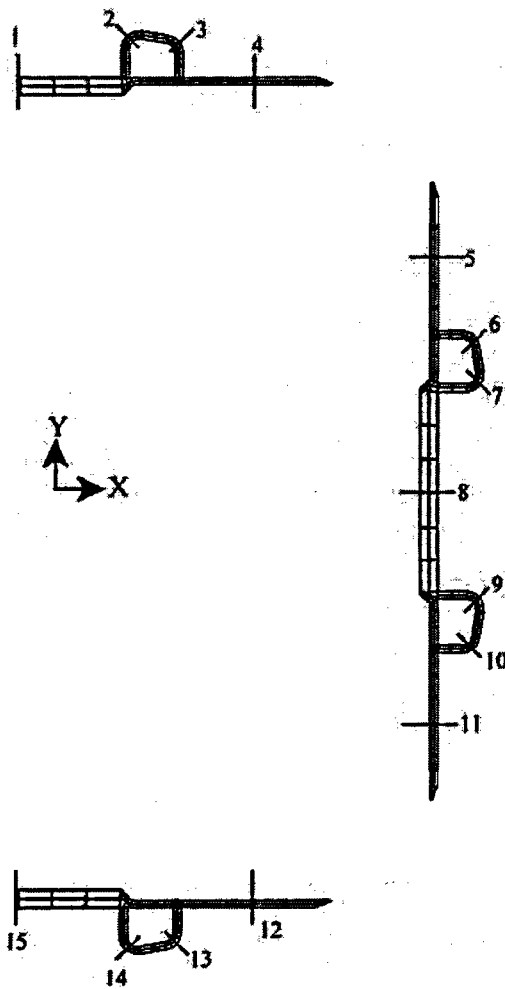
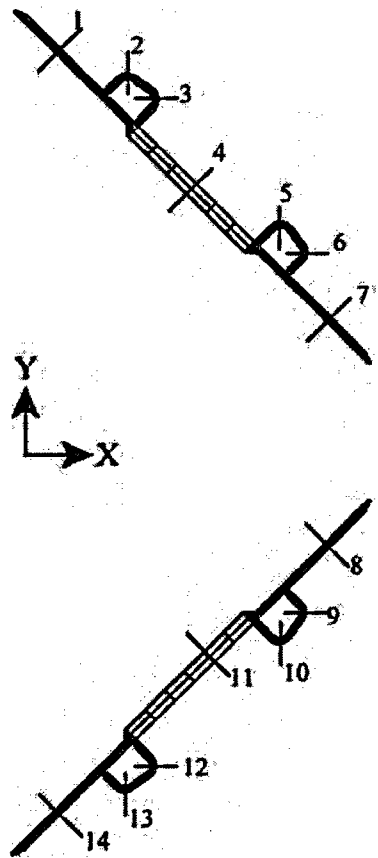


Figure 3.10.1-20 PWR Side Support Weldment Section Cuts – 45° Basket Orientation



3.10.2 BWR Fuel Basket Finite Element Models

3.10.2.1 Load Path Description

This section explains the load paths in the basket that ensure the structural integrity of the BWR MAGNASTOR during all conditions of storage. The MAGNASTOR BWR fuel basket is designed to accommodate 87 BWR fuel assemblies. For normal conditions of storage, the weight of the fuel assemblies is directly supported by the bottom plate of the TSC. The basket is subjected to its self-weight only. For the off-normal and accident conditions associated with loadings in the transverse direction of the basket (e.g. off-normal handling load, concrete cask tip-over accident), the weight of the fuel assemblies is supported by the 45 fuel tubes, side support weldments, and the corner support weldments. Referring to Figure 3.10.2-1, load transfer between the fuel tubes, '1', is through bearing contact at the corners. The bearing contact consists of two load paths: the connector pins transmit load directly between each fuel tube; and where the tubes are in contact, bearing loads are transmitted. The shear load transmitted across the pins is reacted out in bearing in the pin sockets. The detailed interaction between fuel tube corners is shown in Figure 3.10.2-1 and Figure 3.10.2-3. As the figures show, the pins welded to one tube mate to the slots cut into the adjoining tube. Figure 3.10.2-3 shows a free-body diagram of the fuel tube pin joint. Frictional forces are not considered in the finite element analysis of the basket.

At the top and bottom of the fuel basket, connector pin assemblies are used to add additional support to the basket. The end basket configurations do not affect the periodic model analysis of the basket because the connector pin assemblies do not transmit loads in the lateral direction. The connector pin assemblies are installed as a redundant support for the basket system to maintain the structural configuration of the basket. The bottom connector pin assemblies also provide a standoff between the TSC bottom plate and basket tubes, and transmit bearing loads from the basket to the TSC bottom plate.

The corner and side support weldments provide rigidity to the basket. The weldments are attached to the fuel tube array by means of bolted boss connections. Bosses welded to the fuel tubes are slotted in to the weldments. Connection is made with the use of a washer and bolt combination. Referring to Figure 3.10.2-1 and Figure 3.10.2-2, the bolted joints, '2', are designed to transmit tensile loads. Therefore, once installed and preloaded the bolts are always in tension. Shear loads are reacted out by interaction of the bosses, boss welds, and the support weldments. If the support weldments are bearing on the fuel tube array, the load is transferred through the bearing contact, '3', of the support weldments and fuel tube array (Figure 3.10.2-1

and Figure 3.10.2-2). Figure 3.10.2-4 shows a free-body diagram of the fuel tube interaction with the basket support structure.

3.10.2.2 Finite Element Model Descriptions

This section describes the finite element models used in the BWR basket structural evaluation. The following table describes the finite element models and the applicable ASME Code section.

Finite Element Model	Analysis Usage	Loading Condition	ASME Code Section
3D Periodic Model	Off-normal TSC handling conditions (loads in basket in transverse direction)	Level C	III-NG
3D Thermal Stress Model	Thermal stress evaluation	Level A	III-NG
3D Periodic Plastic Model	Concrete cask tip-over accident evaluation	Level D	III-NG, App. F

3.10.2.2.1 BWR Basket Three-Dimensional Periodic Model

Two three-dimensional periodic half-symmetry models of the BWR basket are used to calculate the stresses in the basket due to transverse loading during the off-normal TSC handling conditions. These models correspond to the critical basket orientations, 0° and 45°, as shown in Figure 3.10.2-5 and Figure 3.10.2-6. The fuel tube support pins are spaced on 20.0-inch centers; therefore, the periodic model extends from the axial center of a tube pin to the mid-point of the spacing between the pins, a 10.0-inch segment.

The finite element models are constructed using SOLID45, SHELL63, and BEAM4 elements. The fuel tube assemblies, pins, and side support weldments are modeled using SOLID45 elements. The weight of the poison plates is included in the finite element model by adjusting the density of the carbon steel for the fuel tube sides. The corner support weldment is modeled using SHELL63 elements for the vertical wall and support plates. Similar to the three-dimensional periodic model for PWR basket, the interaction between fuel tubes, corner support assemblies, and side support assemblies are modeled with CONTAC52 gap elements. These gap elements allow the transfer of loads between the basket structural components. Figure 3.10.2-10 shows the details of the modeling of the fuel tube/pin interaction with the CONTAC52 elements at the gap between the pin and the tube socket. For the basket structural evaluation, the TSC is not modeled. CONTAC52 gap elements are used to model the total gap between the BWR basket and the transfer cask.

The corner support and side support assemblies are bolted to the fuel tube array at eight locations in the half-symmetry basket model. The bolt/boss joints are modeled using LINK10 tension only

elements for the bolts and COMBIN40 elements for the boss. The COMBIN40 elements represent the shear restraint generated by the bosses welded to the fuel tubes.

Loads and boundary conditions are discussed in Section 3.10.2.3. The weight of the neutron absorbers and the retainers, which are not included in the finite element model, are considered by adjusting the density of the carbon steel for the fuel tube sides.

3.10.2.2 BWR Basket Three-Dimensional Thermal Stress Model

The structural evaluation for thermal stresses is performed using a three-dimensional quarter-symmetry finite element modeled, as shown in Figure 3.10.2-7. The three-dimensional model represents the top or bottom 43 inches of the BWR basket to evaluate the bounding axial and radial thermal gradients considering the end restraint of the basket due to the connector pin assemblies. This model includes the connector pin assemblies at the end of the fuel tubes and two intermediate pin and bolt locations. The connector pin assemblies at the end of the basket are modeled with nodal constraints in the basket transverse directions at the interface of two adjacent connector pins. The modeling methodology of the model is the same as that of the three-dimensional periodic model as discussed in Section 3.10.2.2.1.

3.10.2.3 BWR Basket Three-Dimensional Periodic Plastic Model

The evaluation of the BWR basket for the cask tip-over event is performed using two three-dimensional plastic periodic models, as shown in Figure 3.10.2-8 and Figure 3.10.2-9. The model is a half-symmetry model based on the periodic model presented in Section 3.10.2.2.1. SHELL43 elements are used for the corner support weldment. Other modeling details are identical to those described in Section 3.10.1.2.3 for the three-dimensional periodic plastic model for the PWR basket.

Loads and boundary conditions are discussed in Section 3.10.2.3. The weight of the neutron absorbers and the retainers, which are not included in the finite element model, are considered by adjusting the density of the carbon steel for the fuel tube sides.

3.10.2.3 Finite Element Model Boundary Conditions

3.10.2.3.1 Off-Normal Handling Boundary Conditions

The three-dimensional periodic models as described in Section 3.10.2.2.1 are used to calculate the stresses due to loading in the transverse direction of the basket for off-normal handling conditions. The gap between the basket and the transfer cask is 0.62 inch (0.12-inch basket-TSC

and 0.50-inch TSC-cask). To represent the loads from the fuel assemblies, a bounding pressure load is applied to the fuel tubes.

The boundary conditions are the models for 0° and 45° basket orientations, as shown in Figure 3.10.2-11 and Figure 3.10.2-12, respectively. For off-normal events, an inertia load of 0.707g (resultant of 0.5g acceleration applied in the two transverse directions) is applied in the transverse direction of the basket. Applied pressure loads for fuel assemblies are also multiplied by 0.707g.

The 0° and 45° basket orientations are critical for the BWR basket for loading in the transverse direction. The 0° basket orientation maximizes the stresses in the fuel tube sidewalls and the 45° basket orientation maximizes the bending stresses in the tube corners. Intermediate basket orientations are bounded by the 0° and 45° orientations. Therefore, the basket evaluation is performed using two half-symmetry models for the 0° and 45° basket orientations, respectively. Symmetry boundary conditions are applied at the plane of symmetry. Symmetry boundary conditions are also applied to both ends of the finite element model to represent a periodic section of the basket. Fixed nodes are used to represent the transfer cask. For off-normal events, material properties at 100°F are conservatively used (using the modulus of elasticity for carbon steel at lower temperature results in slightly higher stress results.)

3.10.2.3.2 Thermal Stress Boundary Conditions

The three-dimensional model described in Section 3.10.2.2.2 is used to calculate the thermal stress due to the thermal expansion. As shown in the following table, a total of five cases are considered to envelop the maximum temperature, as well as the maximum temperature gradients (ΔT), of the basket for all conditions of storage and transfer. The thermal stress analysis is performed based on the temperature distribution in the model determined by thermal conduction analyses using these boundary temperatures.

Thermal Boundary Temperatures – BWR Basket (°F)

C	Axial end of basket	D	Case	A	B	C	D
Center Line	43"	Outer Radius	1	530	410	680	500
A	↓	B	2	680	500	580	440
			3	650	475	700	570
			4	525	425	250	300
			5	700	500	550	400

Symmetry boundary conditions are applied at the planes of symmetry. In the basket axial direction, the model is restrained at one end.

3.10.2.3.3 Concrete Cask Tip-Over Accident Boundary Conditions

The concrete cask tip-over is evaluated as a side impact for the basket. During the concrete cask tip-over event, the acceleration varies from 1g at the bottom of the concrete cask to a maximum acceleration at the top of the TSC. The three-dimensional plastic model is used for the evaluation of the BWR basket (see Section 3.10.2.2.3). A bounding acceleration of 35g is applied to the BWR models. The 35g acceleration bounds the maximum acceleration in the basket, including dynamic load factor, for the concrete cask tip-over accident.

The total gap between the basket and the concrete cask is 0.84 inch. Pressure loads are applied to the BWR basket models to represent the fuel assembly weight with a 35g acceleration.

For the tip-over accident (loading in the transverse direction), the 0° and 45° basket orientations are critical for the BWR basket as discussed in Section 3.10.2.3.2. Therefore, the basket is evaluated using models corresponding to the 0° and 45° basket orientations. Symmetry boundary conditions are applied at the plane of symmetry. Symmetry boundary conditions are also applied to both ends of the three-dimensional periodic finite element model. Fixed nodes are used to represent the concrete cask stand-offs. The boundary conditions are shown in Figure 3.10.2-11 and Figure 3.10.2-12 for the tip-over basket evaluation. For accident conditions, material properties at 100°F are conservatively used.

3.10.2.4 Post-Processing Finite Element Analysis Results

3.10.2.4.1 Maximum Stresses for Off-Normal Handling Condition

The post-processing of the finite element analysis results from the periodic model for the off-normal handling event is performed by taking section cuts at various locations in the model.

The fuel tube section cuts are divided into two regions. Region 1 is the region between the pin supports. For the periodic model, this region is defined from the base of the model (mid-distance between pins) to the base of the pin. Region 2 is the pin region. This region starts at the base of the pin and extends to the top of the finite element model (mid-plane of pin). For both regions, the region just above and below the pin cutout (± 0.25 inch) is omitted from the section cuts to eliminate local stress concentrations in the model. The membrane stresses are calculated by taking a section cut at the center of the tube thickness. The membrane plus bending stress is calculated by taking the maximum of the stresses calculated at the inner or outer surface of the fuel tube. Refer to Figure 3.10.2-13 through Figure 3.10.2-16 for tube identification and the locations of the section cuts.

The maximum stresses for the corner support weldments are calculated by taking section cuts along the length of the weldment (ten inches for the periodic model). Since the corner weldment is modeled using SHELL63 elements; the membrane stresses are calculated at the mid-plane of the element, and the membrane plus bending stresses are calculated using the maximum stresses of either the inner or outer surface of the element. Refer to Figure 3.10.2-17 and Figure 3.10.2-18 for the locations of the section cuts.

The maximum stresses for the side weldments are calculated taking section cuts along the length of the weldment (ten inches for the periodic model). The membrane stresses are calculated by taking a section cut at the mid-thickness of the weldment. The membrane plus bending stress is calculated by taking the maximum of the stresses calculated at the inner or outer surface of the weldment. Refer to Figure 3.10.2-19 and Figure 3.10.2-20 for the locations of the section cuts.

The bolt tensile loads are obtained from the LINK10 element results. The boss shear loads are extracted from the COMBIN40 element results.

3.10.2.4.2 Maximum Thermal Stresses

The post-processing of the finite element analysis results for thermal stress evaluation is performed by extracting the maximum nodal stress intensities from the model. The maximum stress is obtained for two separate regions: (1) fuel tubes and (2) corner and side support weldments. The bolt tensile loads are extracted from the LINK10 elements, and the boss shear loads are extracted from the COMBIN40 elements.

3.10.2.4.3 Maximum Stresses for Concrete Cask Tip-over Accident

The post-processing of finite element analysis results for the basket tip-over accident using the three-dimensional periodic plastic model is performed by extracting stresses in the basket structure for 0° and 45° basket orientations.

For the fuel tubes, the membrane stresses are calculated by extracting the nodal stress intensity at the mid-thickness of the tube thickness. The primary stresses are calculated by extracting the maximum nodal stress intensity for each fuel tube.

The stresses for the corner and side support weldments are calculated using the three-dimensional plastic model. The maximum nodal stress intensities for the corner and side weldment are extracted from the models. The nodal stress intensity is conservatively compared to the membrane allowable to obtain critical factors of safety.

Figure 3.10.2-1 Expanded View of BWR Basket

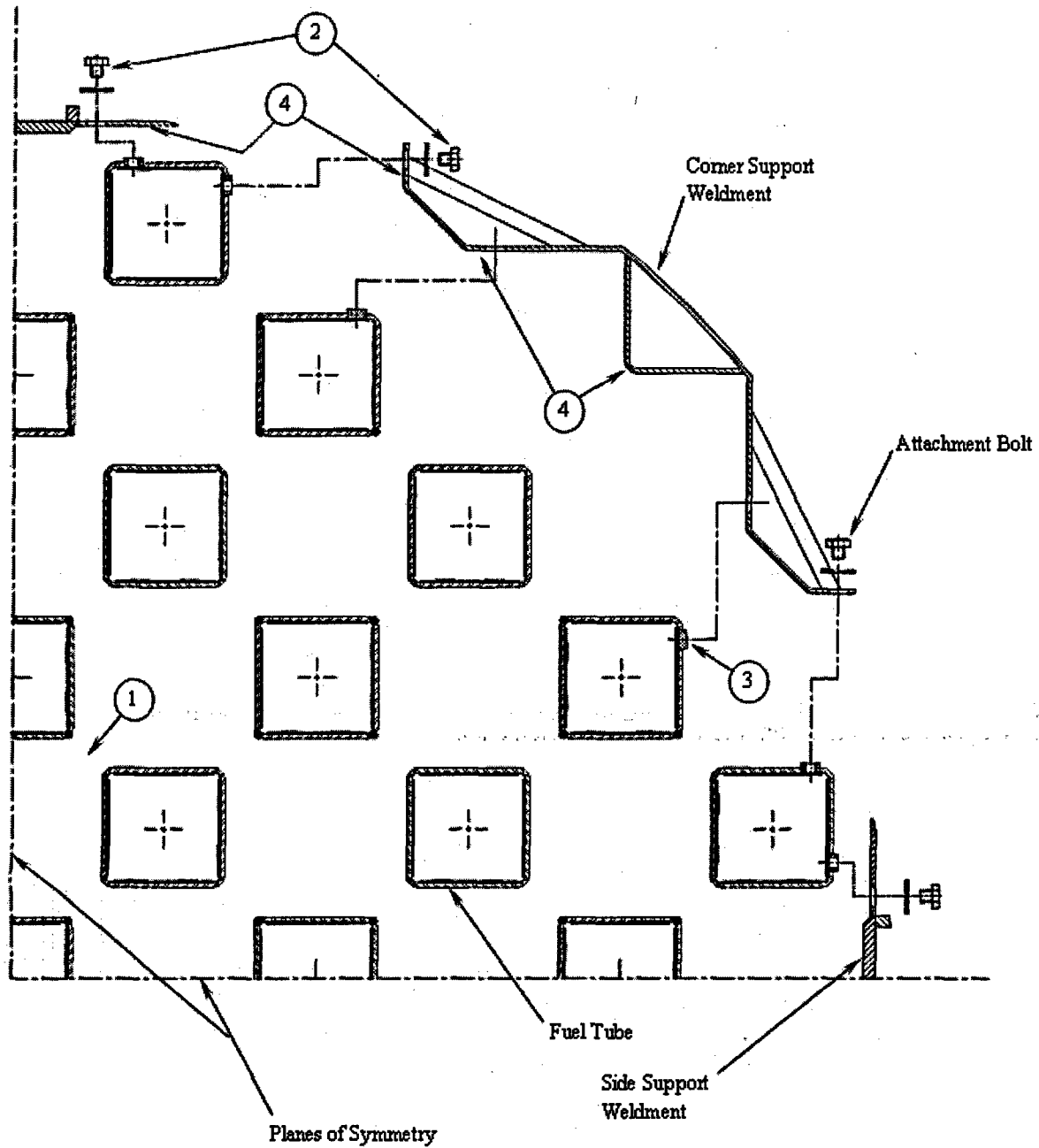


Figure 3.10.2-2 Bolted Attachment Details

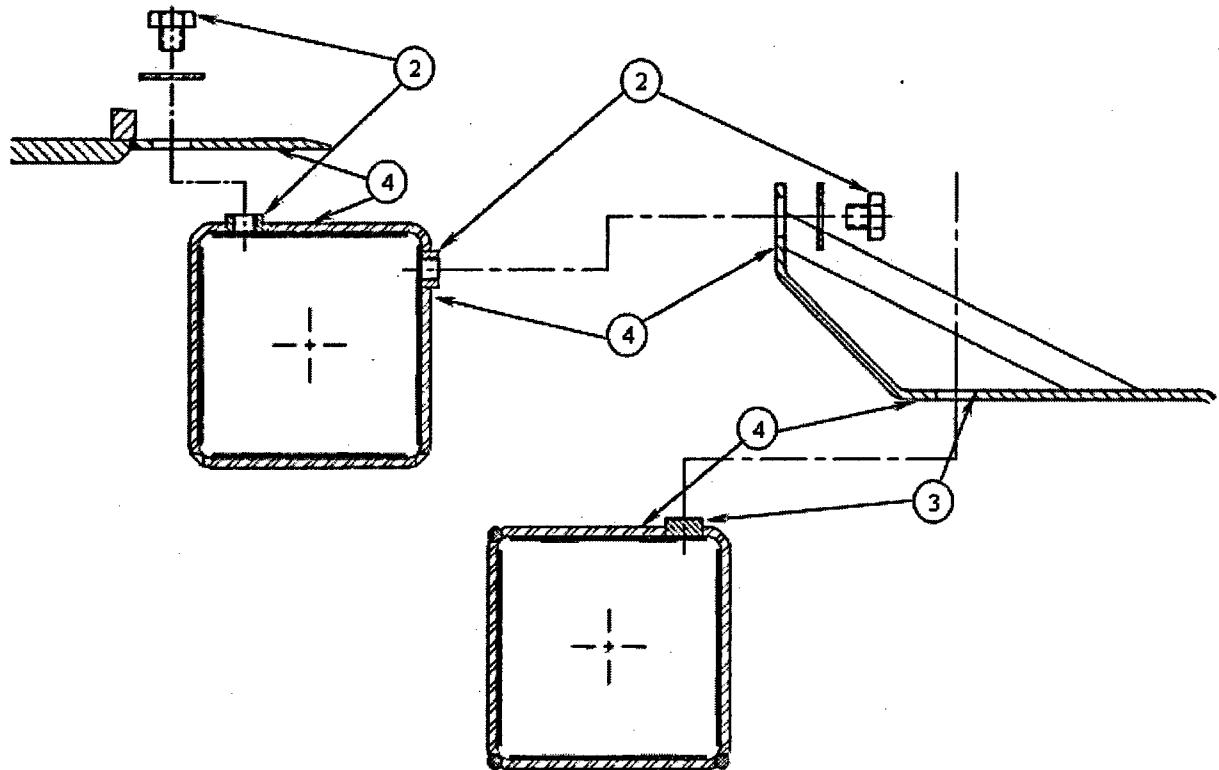
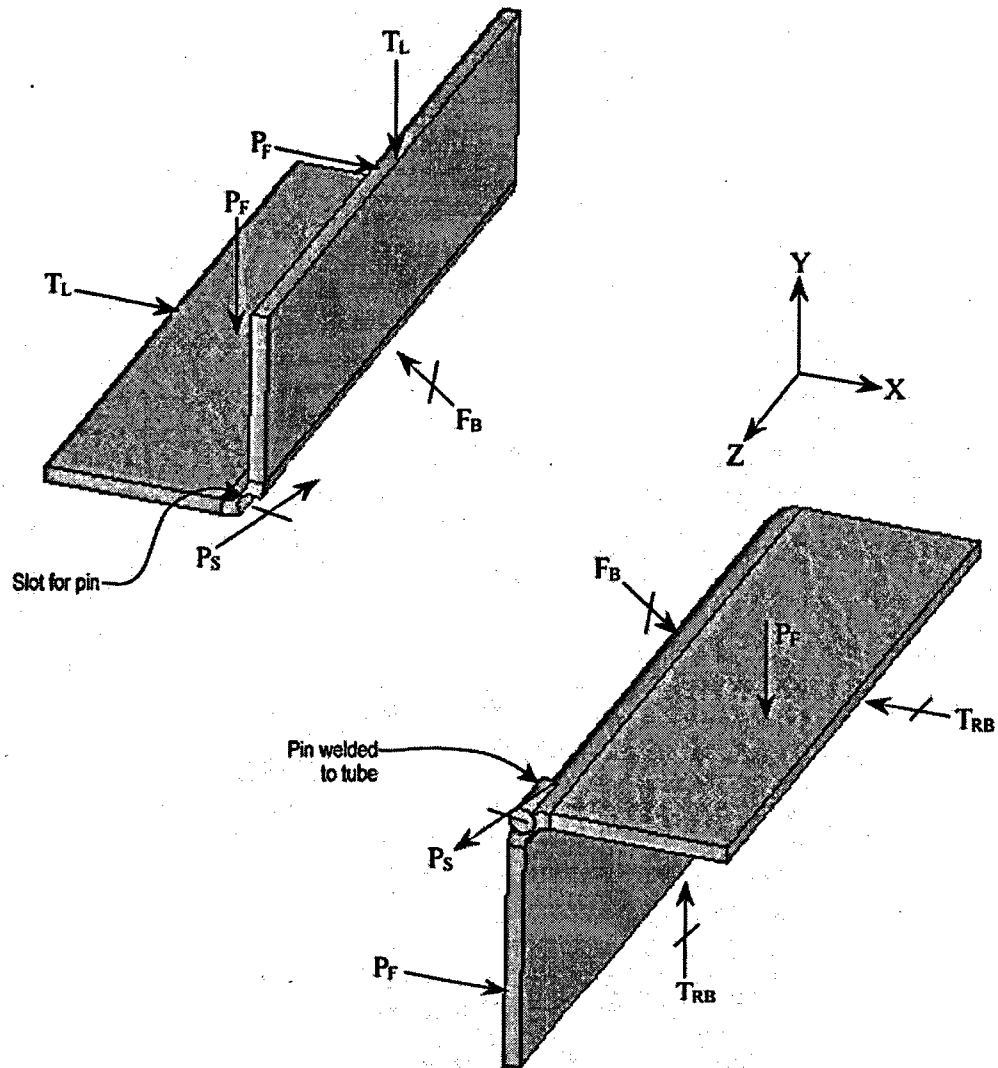
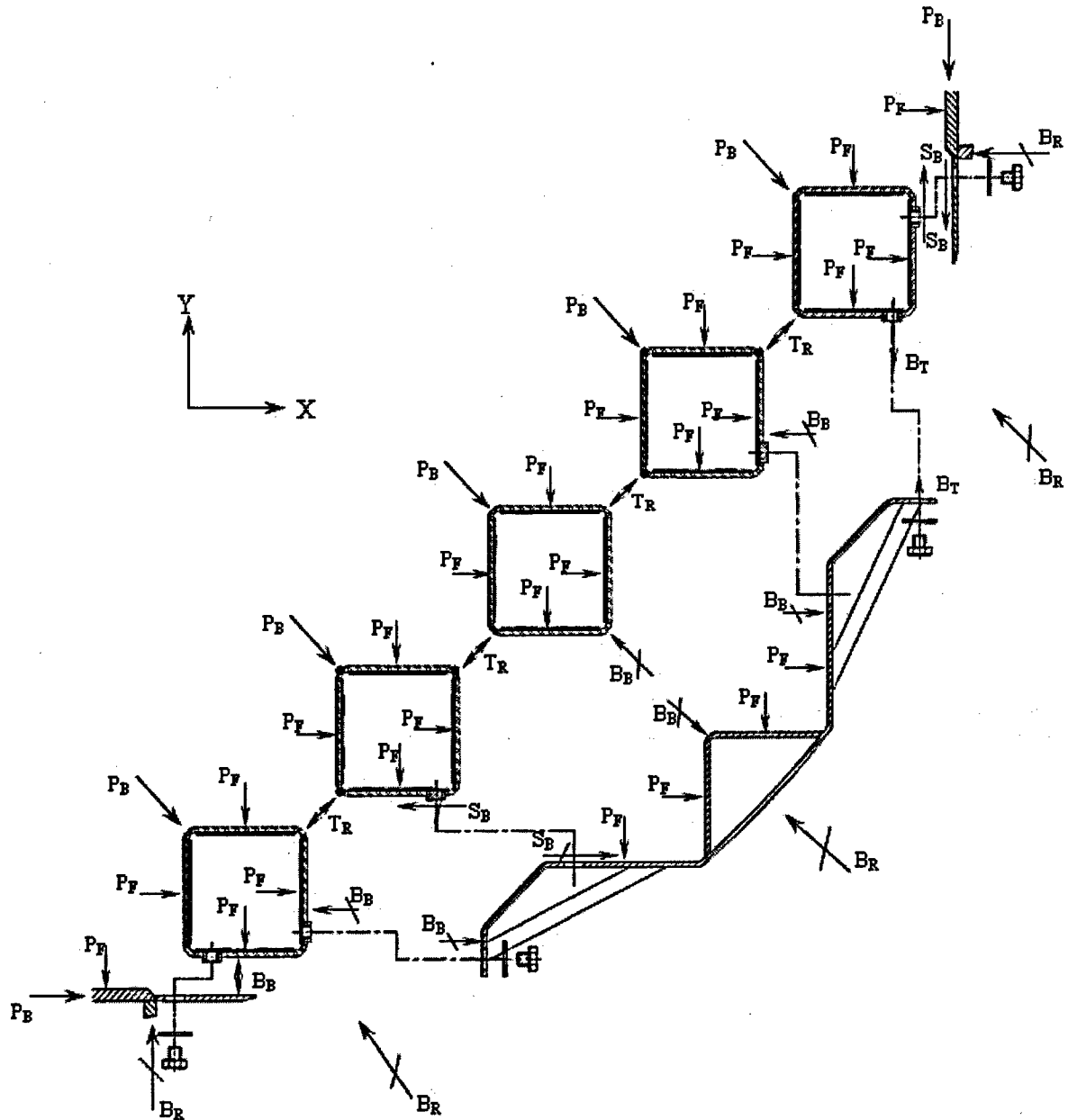


Figure 3.10.2-3 Free-Body Diagram of BWR Basket Fuel Tube Detail



- T_L Loads from adjacent tube or fuel assembly
- P_F Local load due to fuel assembly
- T_{RB} Reaction loads in tubes for equilibrium at symmetry planes of tubes
- P_S Shear Reaction thru pin joint (in the X-Y plane)
- F_B Bearing Reaction across tube flat

Figure 3.10.2-4 Free-Body Diagram of Basket Support Structure



- P_B Loads due to adjacent basket structure
- P_F Local load due to fuel assembly
- B_R Basket reaction with TSC shell locations
- B_T Tensile load at bolt and tube boss (typical)
- B_B Bearing reaction between tube sidewall and support structure (typical)
- S_B Shear reaction between support structure and tube boss (typical)
- T_R Reactions between tubes detailed in Figure 3.10.2-3

Figure 3.10.2-5 BWR Basket Periodic Model – 0° Basket Orientation

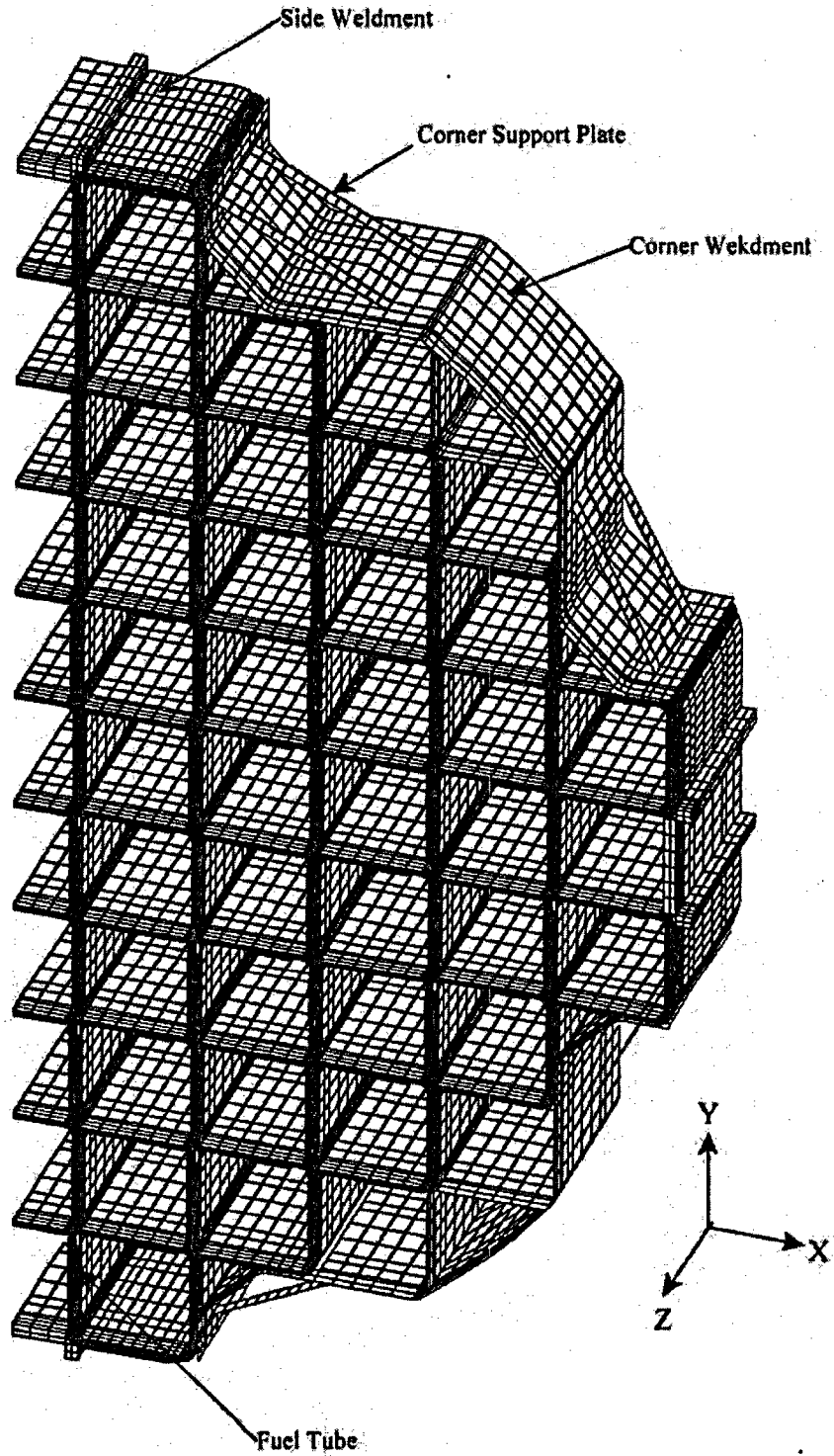


Figure 3.10.2-6 BWR Basket Periodic Model – 45° Basket Orientation

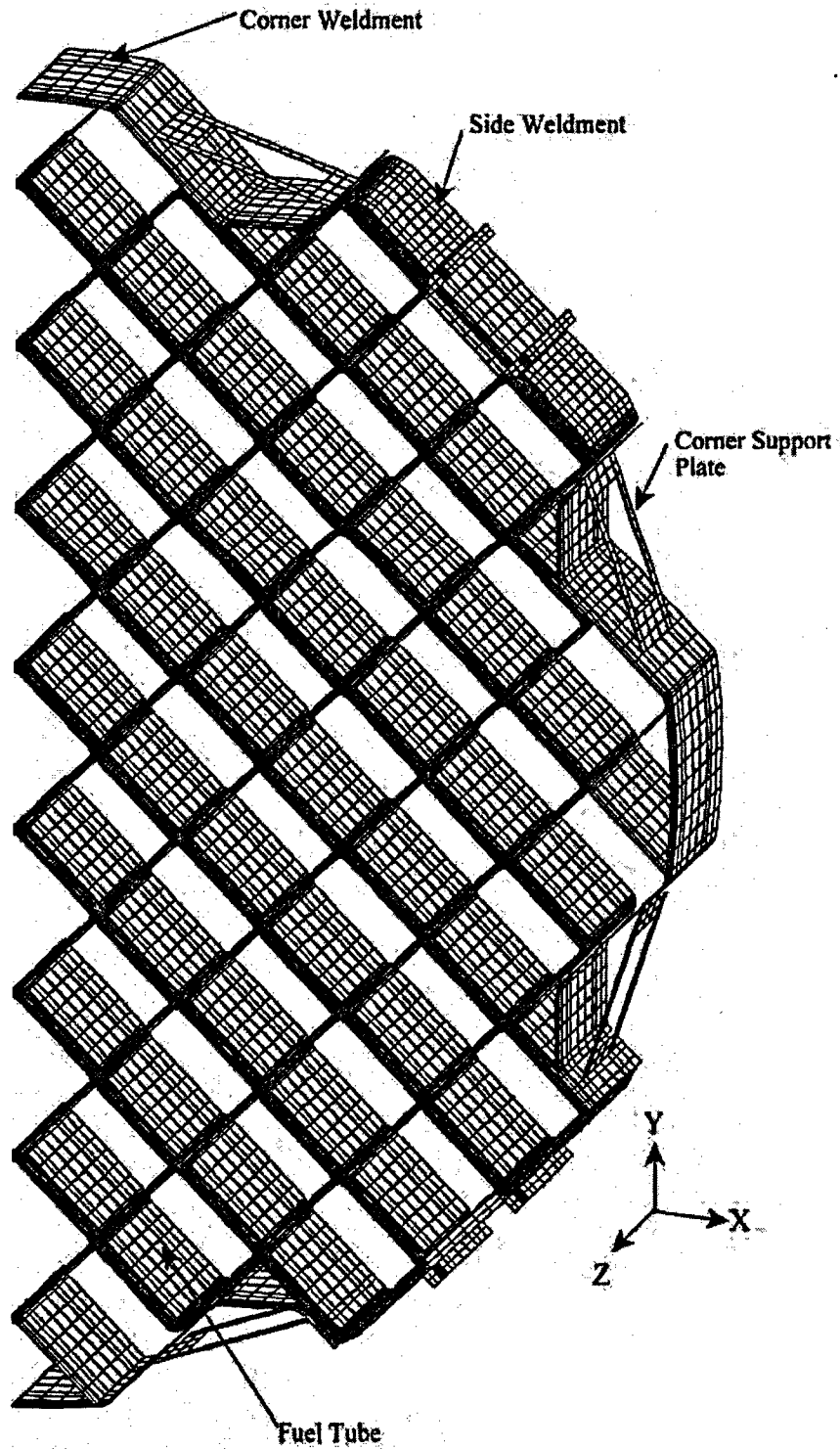


Figure 3.10.2-7 Thermal Stress Evaluation Model

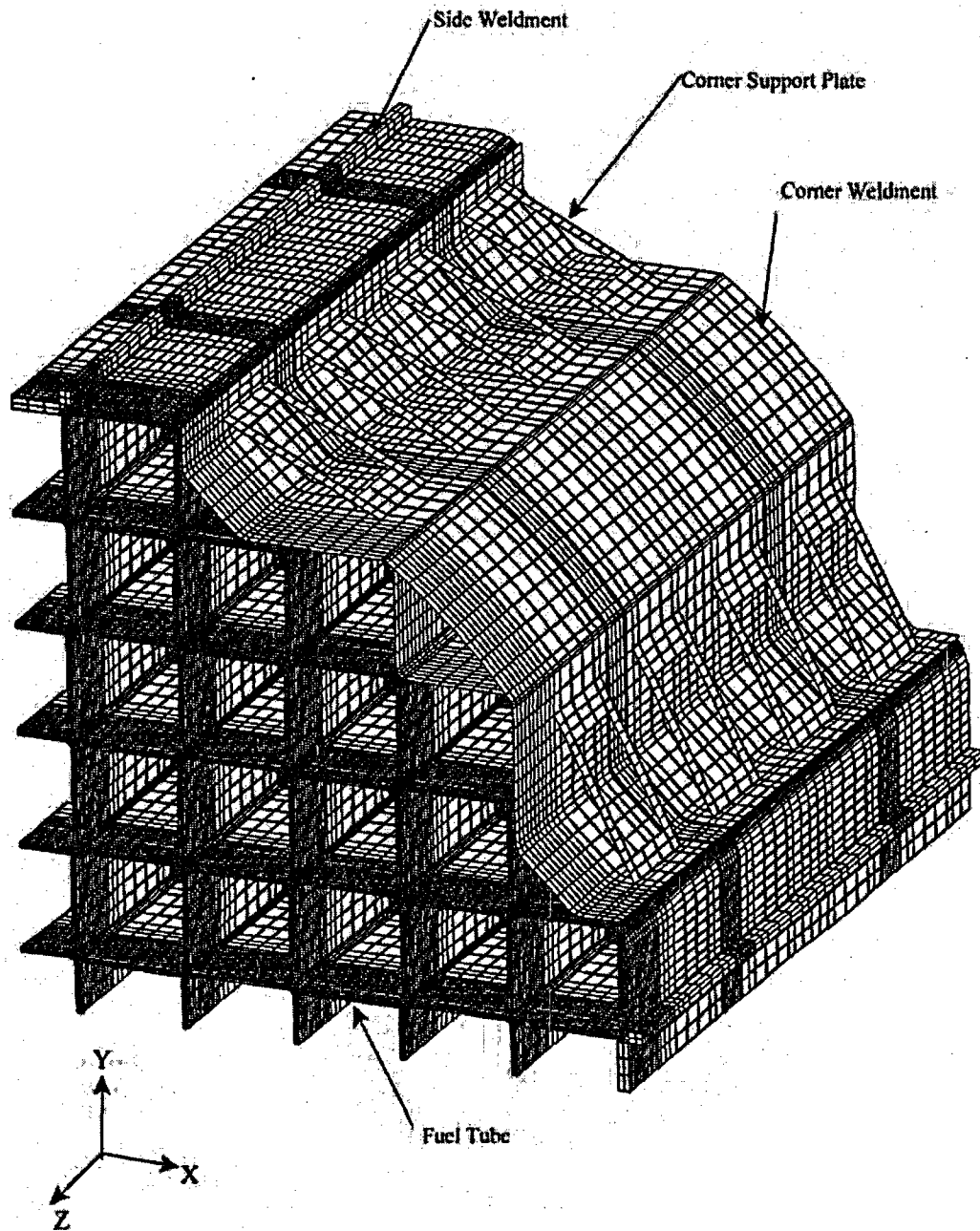


Figure 3.10.2-8 BWR Basket Plastic Model - 0° Basket Orientation

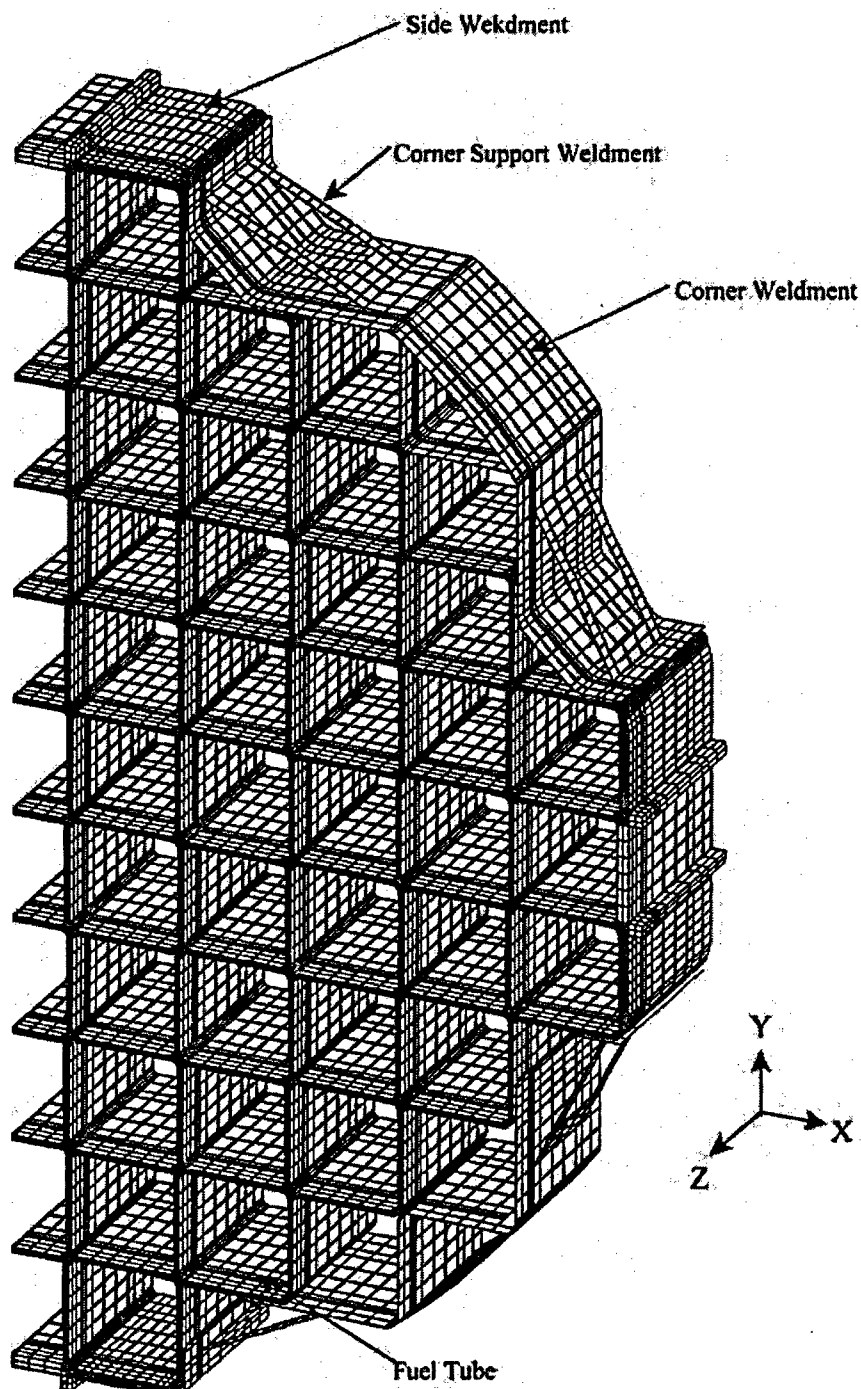


Figure 3.10.2-9 BWR Basket Plastic Model - 45° Basket Orientation

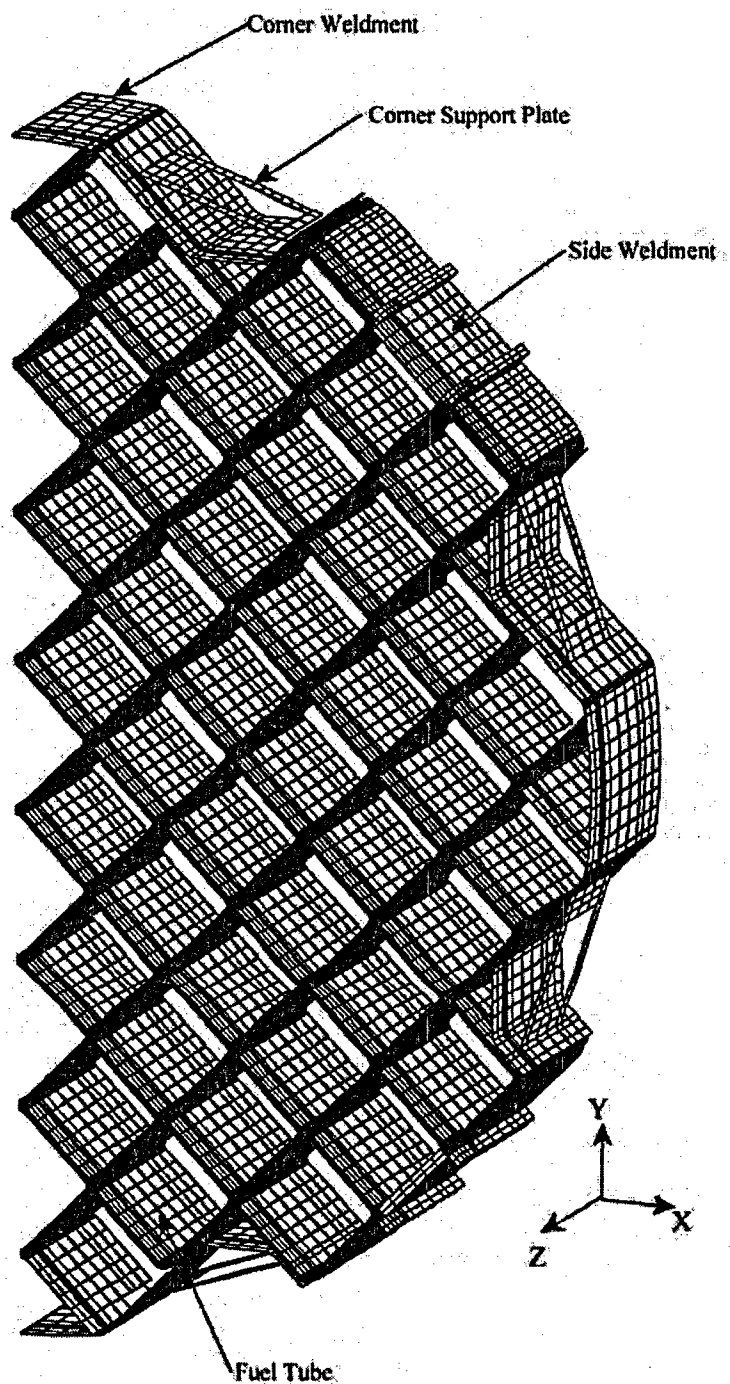


Figure 3.10.2-10 Typical BWR Fuel Tube Pin Finite Element Model Details

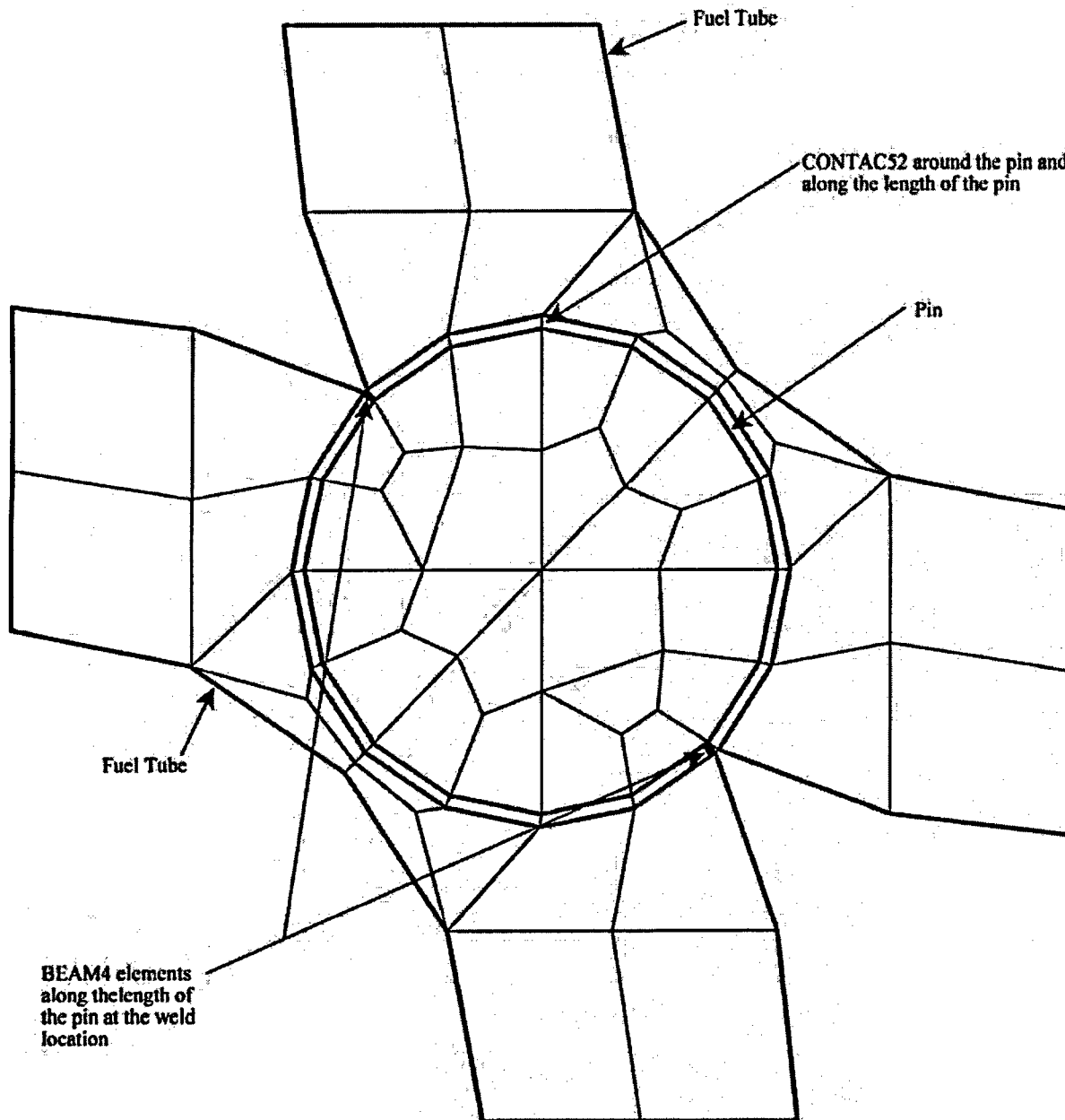


Figure 3.10.2-11 BWR Basket Model Boundary Conditions for a Transverse Loading –
0° Basket Orientation

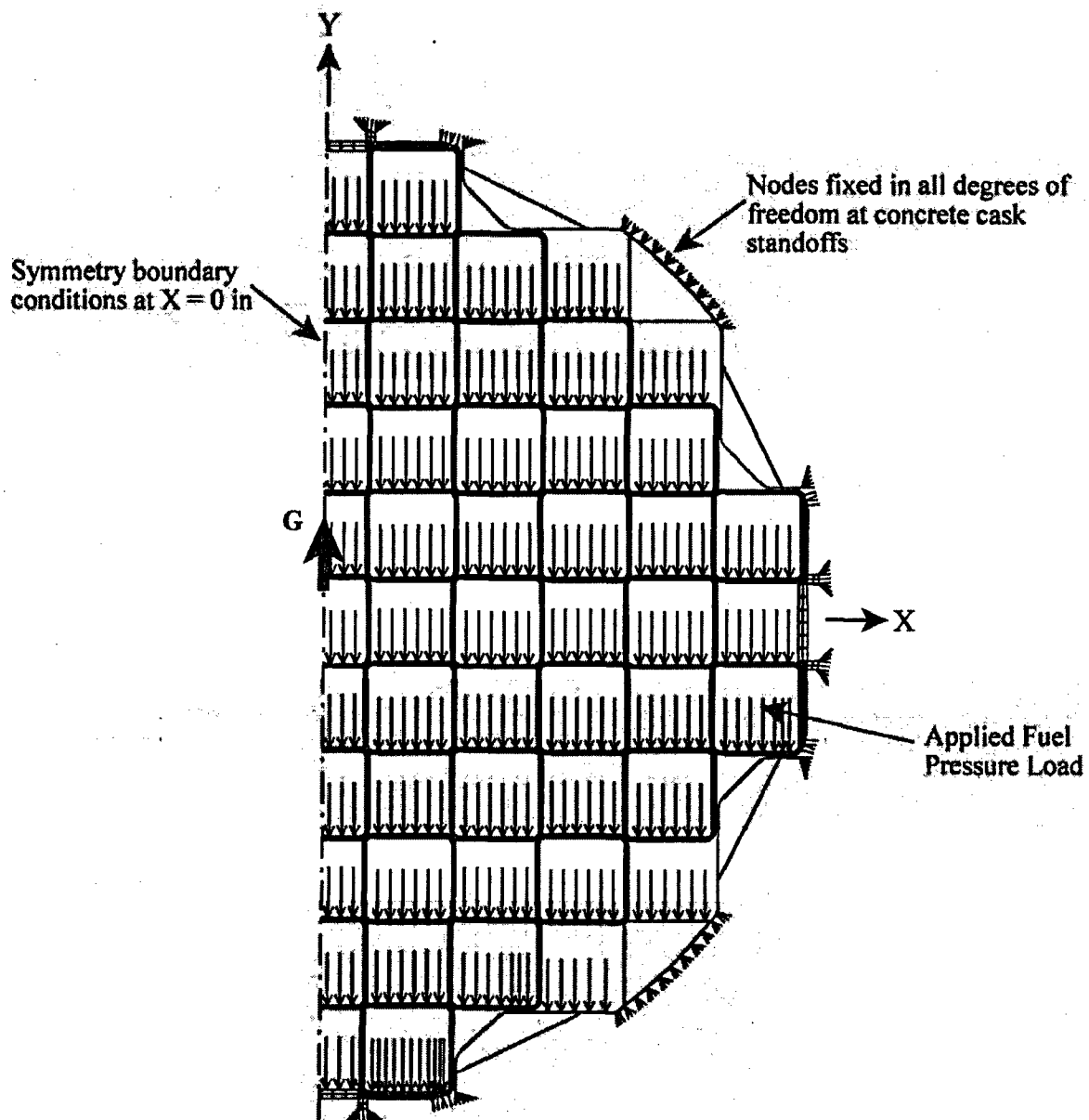


Figure 3.10.2-12 BWR Basket Model Boundary Conditions for a Transverse Loading –
45° Basket Orientation

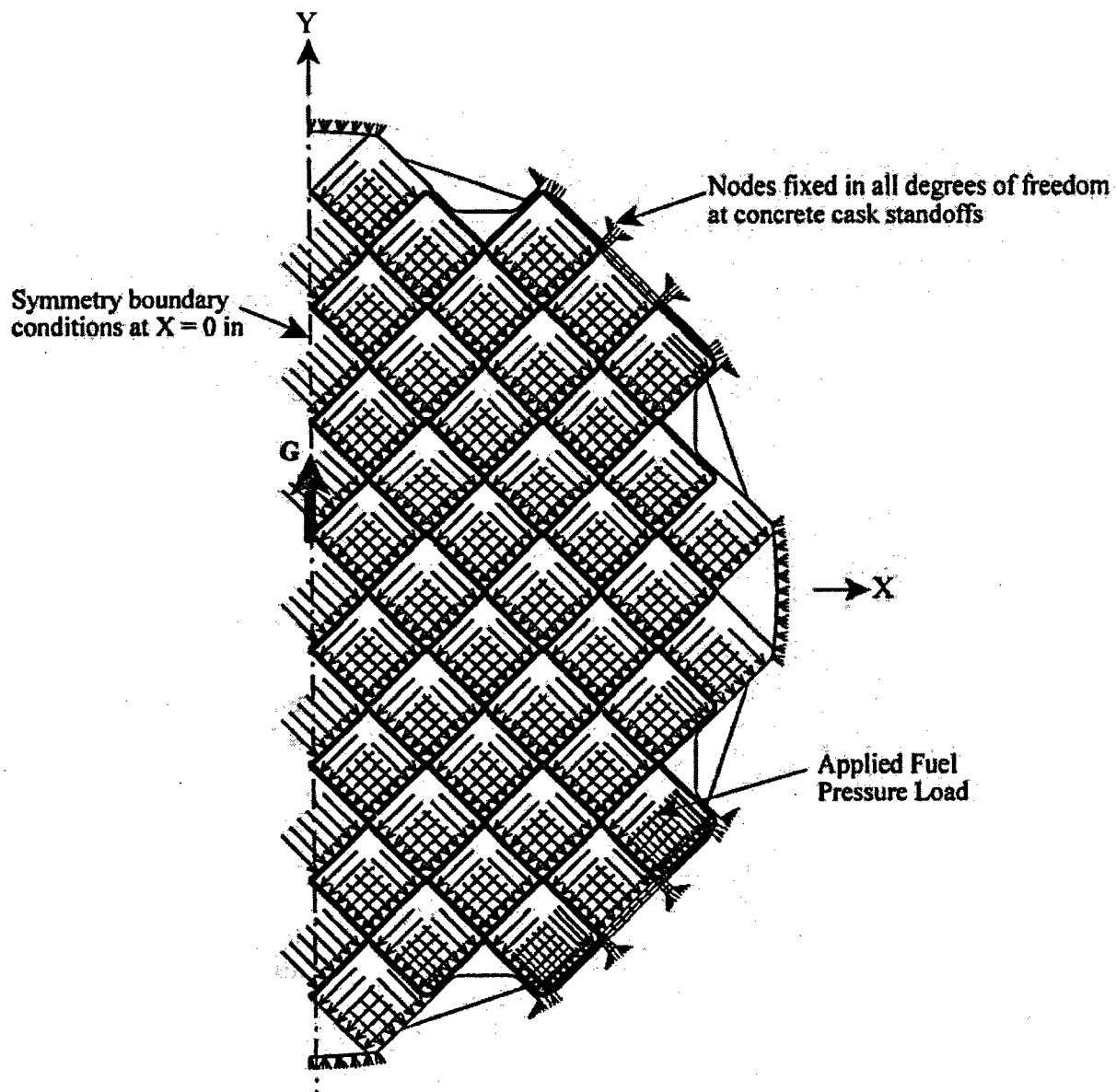


Figure 3.10.2-13 BWR Fuel Tube Array – 0° Basket Orientation

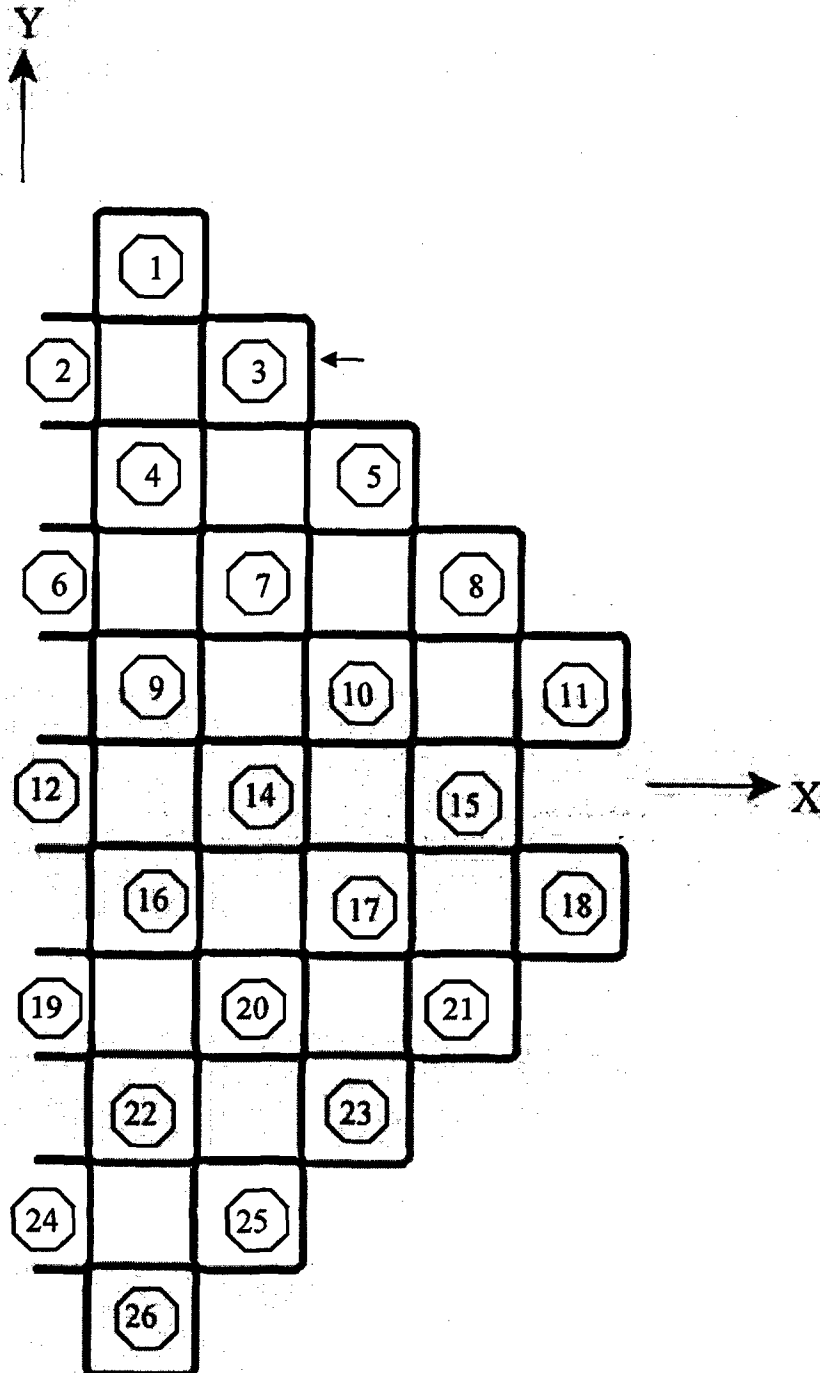


Figure 3.10.2-14 BWR Fuel Tube Section Cuts – 0° Basket Orientation

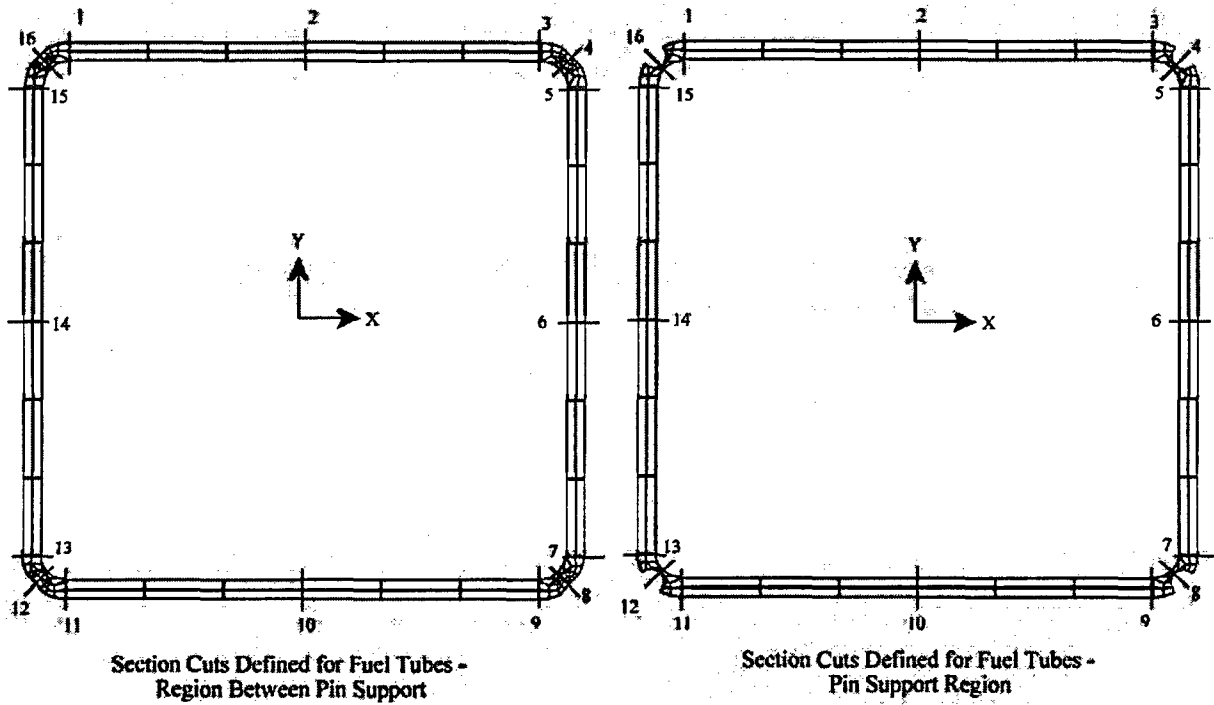


Figure 3.10.2-15 BWR Fuel Tube Array – 45° Basket Orientation

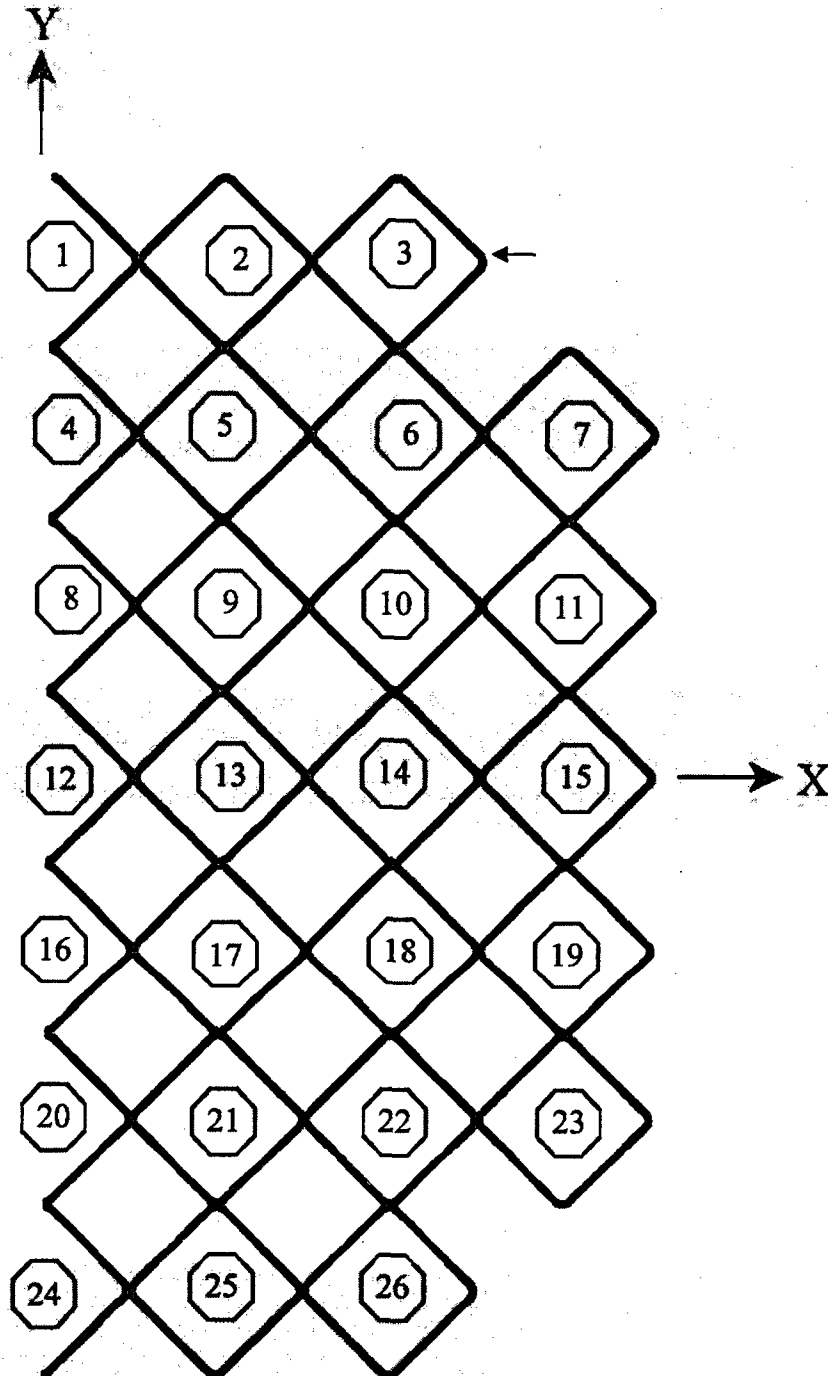
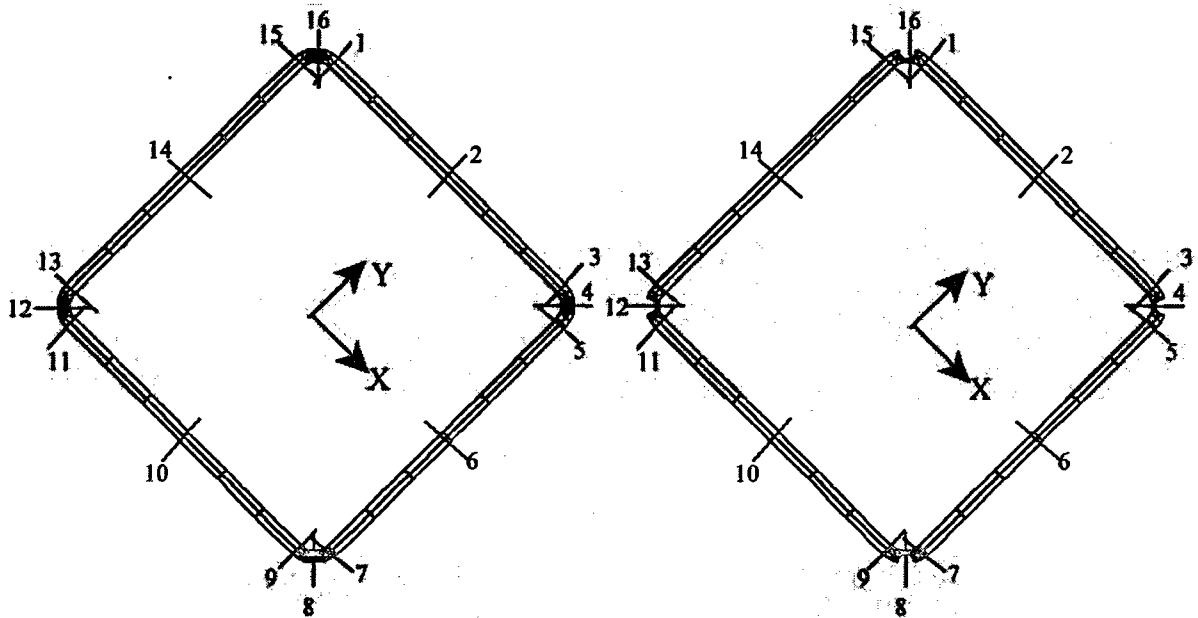


Figure 3.10.2-16 BWR Fuel Tube Section Cuts – 45° Basket Orientation



Section Cuts Defined for Fuel Tubes -
Region Between Pin Support

Section Cuts Defined for Fuel Tubes -
Pin Support Region

Figure 3.10.2-17 BWR Corner Support Weldment Section Cuts – 0° Basket Orientation

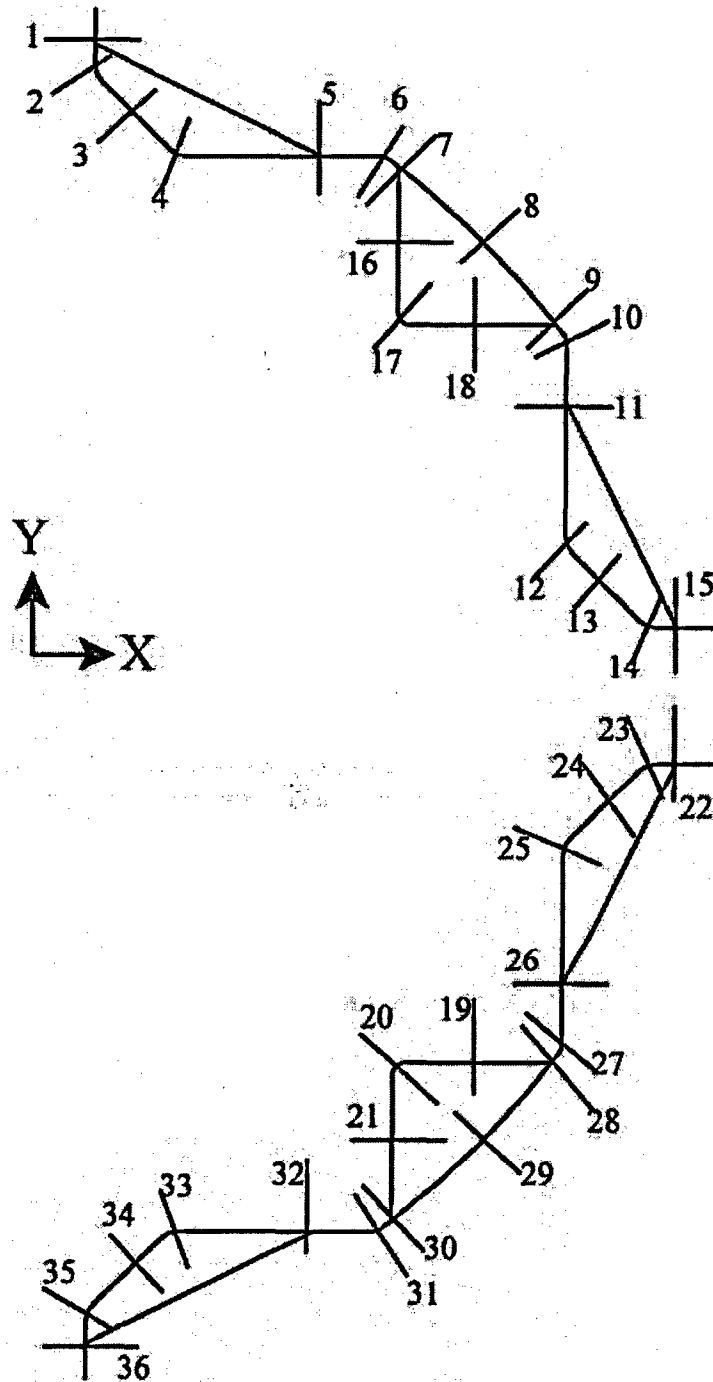


Figure 3.10.2-18 BWR Corner Support Weldment Section Cuts – 45° Basket Orientation

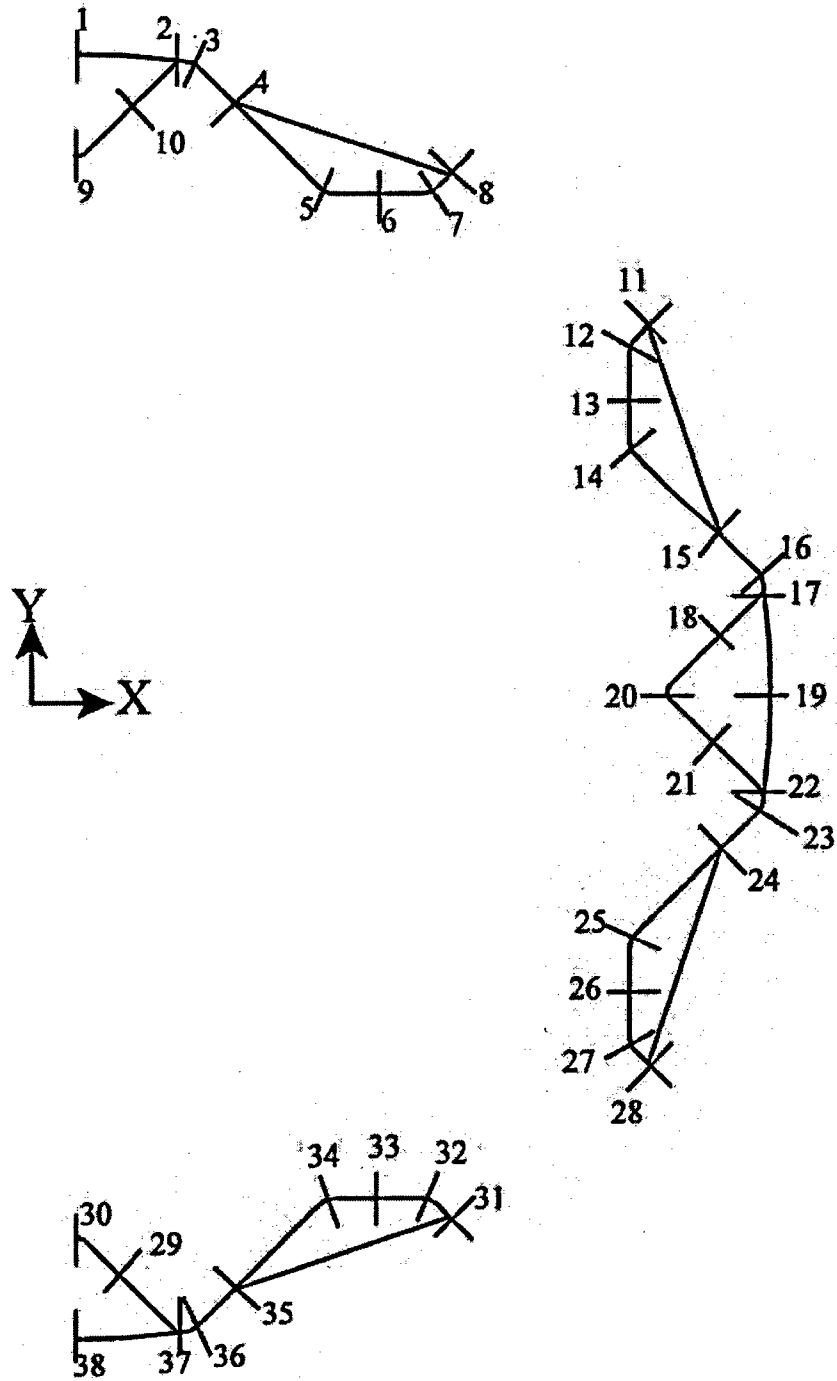


Figure 3.10.2-19 BWR Side Support Weldment Section Cuts – 0° Basket Orientation

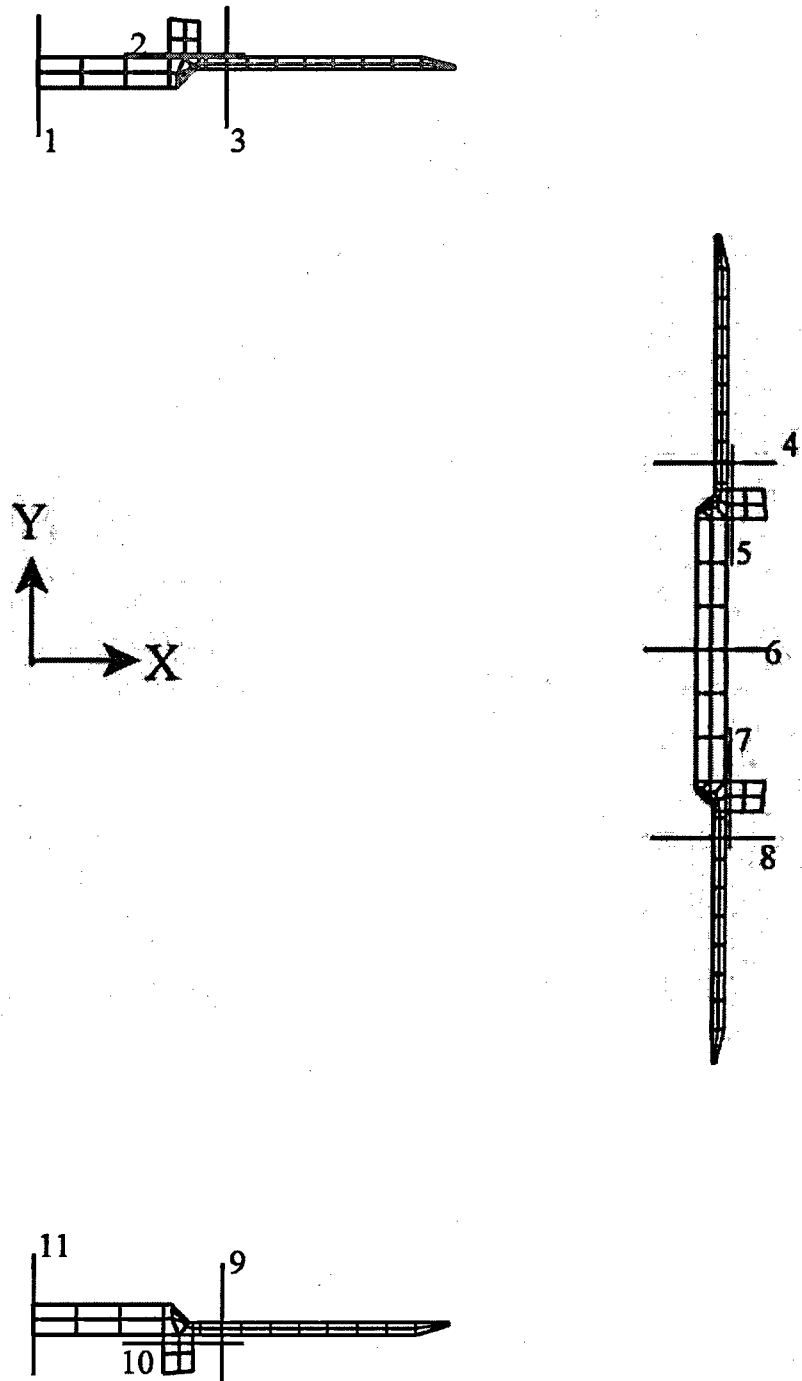
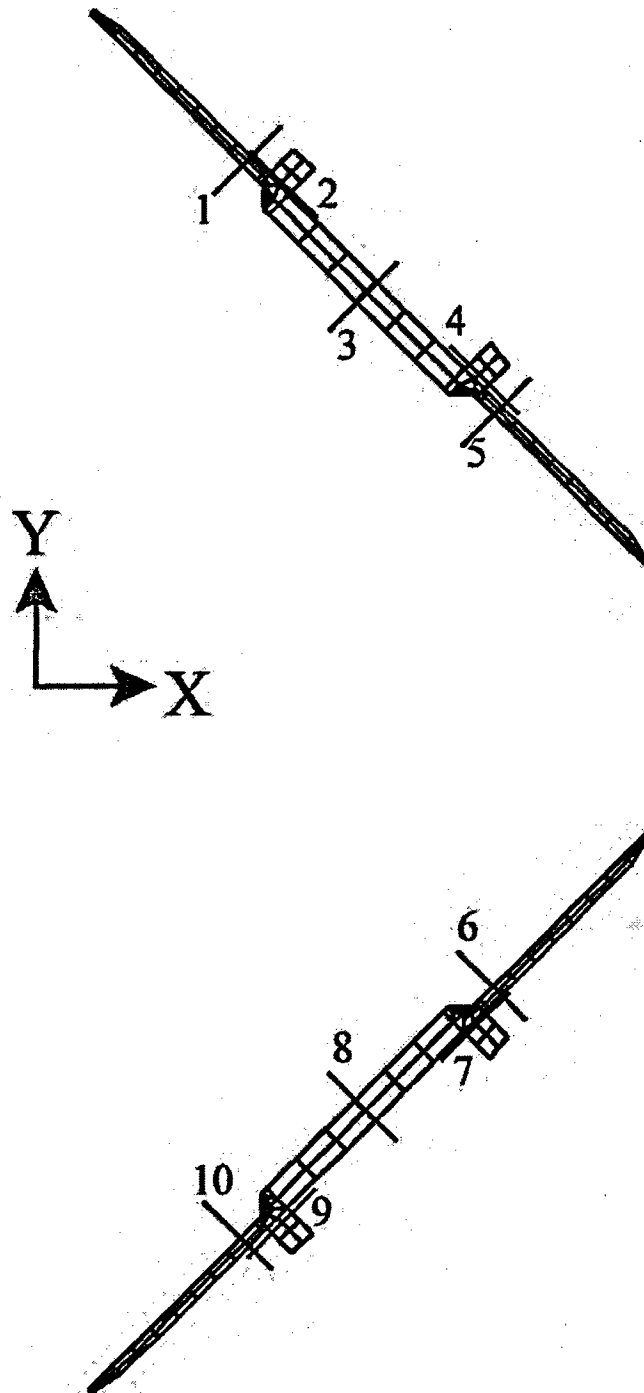


Figure 3.10.2-20 BWR Side Support Weldment Section Cuts – 45° Basket Orientation



3.10.3 TSC Finite Element Model

This section presents details on the TSC finite element model used in the structural evaluation of the TSC for lift, normal conditions and off-normal or accident events of storage.

TSC Finite Element Model Description

The three-dimensional finite element model of the TSC is constructed using ANSYS SOLID45 elements. By taking advantage of the symmetry of the TSC, the model represents one-half (180° section) of the TSC, including the TSC shell, bottom plate, and closure lid. The finite element model of the TSC is shown in Figure 3.10.3-1. ANSYS CONTAC52 elements are used to model the interaction between the closure lid and the TSC shell. Gap elements are also used to simulate the interaction with the concrete cask inner liner standoffs or transfer cask inner shell during a side impact and pedestal during an end impact. The size of the CONTAC52 gaps is determined from nominal dimensions of contacting components. Due to the relatively large gaps resulting from the nominal geometry, these gaps remain open during all loadings considered. All gap elements are assigned a stiffness of 1×10^8 lb/in.

This model represents a “bounding” combination of geometry and loading that envelops the MAGNASTOR PWR and BWR TSCs. Specifically, the longest TSC is modeled in conjunction with a conservative fuel and basket combination. By using the longest TSC with the conservative content weight, bending stresses are maximized at the junction of the shell and lid. Thus, the analysis yields conservative results relative to the expected performance of the actual TSC configurations.

Boundary Conditions for TSC Lift

The lifting configuration for the TSC consists of six hoist rings bolted to the closure lid at equally spaced angular intervals. To simulate the lifting of the TSC, nodes representing the hoist rings on the closure lid are constrained in the Y-direction. For heavy lift evaluation, only three of the hoist rings are considered. Due to the symmetry of the model, only the nodes at 60° and 180° are constrained. Symmetry boundary conditions are applied at the plane of symmetry of the model. Pressure representing the weight of the fuel and basket is applied to the TSC bottom. A 1.1g inertia load is applied in the axial direction.

Boundary Conditions for Normal Conditions and Off-normal or Accident Events

Model Constraints

The model is constrained in the global Z-direction for all nodes in the plane of symmetry. Other constraints for different loading conditions are summarized below. The directions of the coordinate system are shown in Figure 3.10.3-1.

Model Constraint Summary	
Condition	Constraint
Dead Weight	Y-direction at TSC bottom
Normal Handling	Y-direction – lift points in TSC lid
Off-normal Handling - axial	Y-direction – lift points in TSC lid
Off-normal Handling – lateral	Gap elements at TSC shell in radial direction
24-inch drop	Y-direction at TSC bottom
Tip-over	Gap elements at TSC shell in radial direction

Inertial Load

Inertial loads resulting from the weight of the TSC and contents are considered by applying an appropriate deceleration factor (g-load). Inertial loads are summarized below.

Inertial Load Summary	
Condition	Inertial Load
Dead Weight	1g – axial
Normal Handling	1.1g – axial
Off-normal Handling	1.5g – axial, 0.707g – lateral
24-inch drop	60g – axial
Tip-over	Tapered 40g – lateral (40g at top of TSC closure lid, 1g at base of concrete cask)

Pressure Load – Internal Pressure

A uniform pressure is applied to all internal surfaces of the TSC. The TSC pressures used for the normal condition (110 psig), off-normal (130 psig) and accident events (250 psig) bound all pressure conditions.

Pressure Load – Dead Load, Handling, and 24-inch Drop

For the dead load, handling, and 24-inch drop analyses, the inertial load produced by the contents weight is considered to be uniformly distributed on the inner surface of TSC bottom plate. Based on the contents weight of 90,000 lb and the TSC inside radius of 35.5 inches, the pressure corresponding to the contents weight is shown below.

$$p = \frac{90,000}{\pi(35.5^2)} = 22.7 \text{ psi}$$

The pressure load is multiplied by appropriate inertia loading (1g, 1.1g and 60g for dead load, handling, and 24-inch drop, respectively).

Pressure Load—Off-Normal Handling

For the off-normal handling analysis, the inertial load produced by the contents weight is considered to be uniformly distributed on the inner surface of TSC bottom plate multiplied by 1.5g for the axial component of off-normal handling. For the lateral component of the off-normal handling, the content weight is represented as an equivalent static pressure, with 0.707g, applied on the interior surface of the TSC shell. The pressure is uniformly applied to the canister shell along the TSC cavity length, and is applied in the circumferential direction as a cosine distribution over a 21° arc from the impact centerline in the half-symmetry model.

Pressure Load—Tip-Over

The inertial load produced by the 90,000 lb (45,000 lb for the half-symmetry model) content weight is represented as an equivalent static pressure applied on the interior surface of the TSC shell. The pressure is uniformly tapered along the cavity length based on a tapered inertia load of 40g at the top of the canister closure lid and 1g at the base of the concrete cask, and is applied in the circumferential direction as a cosine distribution over a 21° arc from the impact centerline.

Temperatures for Thermal Stress Analysis

The finite element thermal stress analysis is performed with TSC temperatures that envelop the TSC temperature gradients for normal (100°F ambient temperature) and off-normal storage (106°F and -40°F ambient temperatures), and transfer conditions for all TSC configurations. Prior to performing the thermal stress analysis, the steady-state temperature distribution is determined using bounding temperature data from the storage and transfer thermal analyses. This is accomplished by converting the SOLID45 structural elements of the TSC model to SOLID70 thermal elements to perform a thermal conduction analysis. Nodal temperatures are applied at key locations for the thermal analysis: top-center of the closure lid, top-outer diameter of the closure lid, bottom-center of the closure lid assembly, bottom-center of the bottom plate, bottom-outer diameter of the bottom plate, and the TSC shell where the maximum temperature occurs.

The temperature distribution used in the structural analyses envelops the temperature gradients experienced by all PWR and BWR TSC configurations under storage and transfer conditions. The temperatures at the key locations are listed below. Temperatures locations (A through F) are defined in Figure 3.10.3-2. The temperatures for all nodes in the TSC model are obtained by the solution of the steady-state thermal conduction analysis.

Top-center of the closure lid (C)	=	510°F
Top-outer diameter of the closure lid (F)	=	430°F
Bottom-center of the closure lid (B)	=	570°F
Bottom-center of the bottom plate (A)	=	350°F
Bottom-outer diameter of the bottom plate (D)	=	240°F
Canister shell at 166 inches from TSC bottom (E)	=	510°F

Post-Processing

The stress evaluation for the TSC is performed in accordance with the ASME Code, Section III, Subsection NB, by comparing the linearized sectional stresses against allowable stresses. The sectional stresses at 15 locations of the TSC model are obtained for each 3° angular division of the model. The locations for the stress sections are shown in Figure 3.10.3-2. The allowable stresses for normal conditions and off-normal or accident events are taken from Subsection NB.

Bounding temperatures that envelop the maximum temperatures experienced by TSC components during storage and transfer conditions are used to determine allowable stress values. Temperatures used at each stress section are given in Figure 3.10.3-2. Allowable stress values at temperatures are determined based on mechanical properties for SA-240 Type 304 stainless steel. All stress components are reported in the global cylindrical coordinate system (X = Radial, Y = Circumferential, Z = Axial). Additionally, in accordance with ISG 15, Revision 0, an 0.8 weld reduction factor is applied to the allowable stresses for the closure lid weld (Section 11 of Figure 3.10.3-2).

TSC Analysis Result Details

Table 3.10.3-1 through Table 3.10.3-17 present detailed analyses results for the TSC for normal conditions and off-normal and accident events of storage. Refer to Figure 3.10.3-2 for section cut locations.

Figure 3.10.3-1 MAGNASTOR TSC Finite Element Model

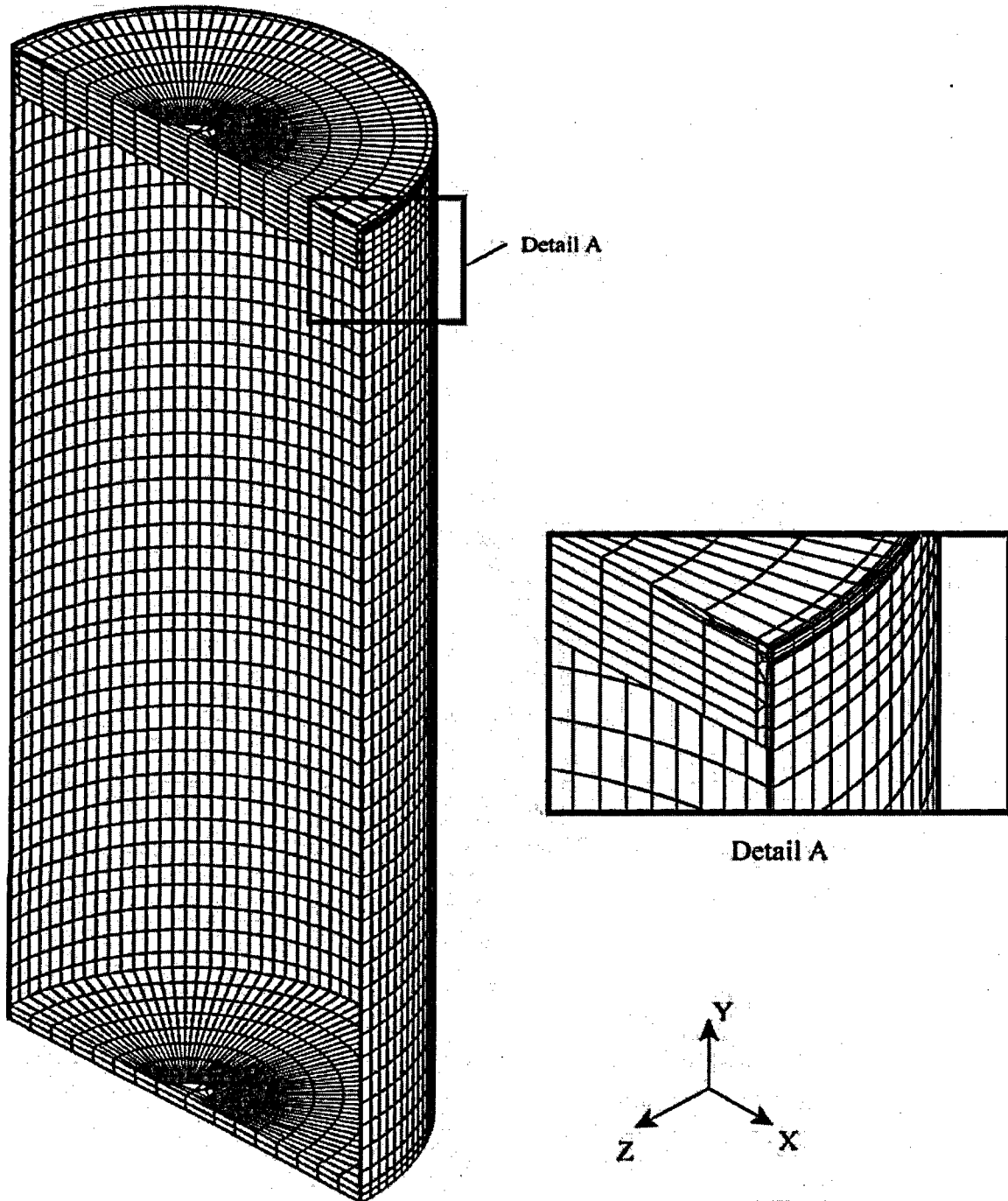


Figure 3.10.3-2 Identification of Sections for Evaluating Linearized Stresses in TSC

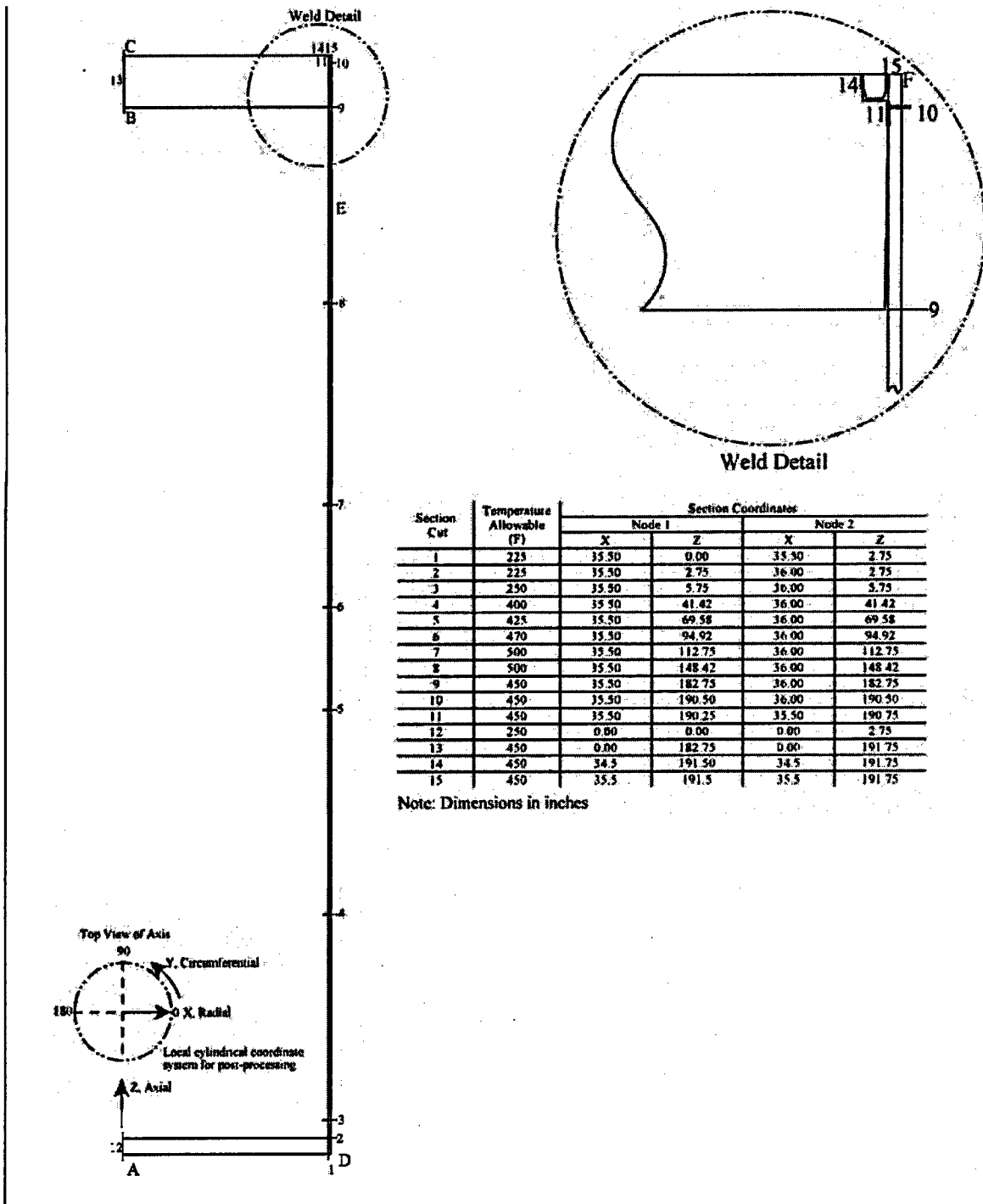


Table 3.10.3-1 TSC Normal Pressure plus Handling, P_m , ksi

Section ^a	Component Stresses						S_{int}	S_{allow}	FS
	S_x	S_y	S_z	S_{xy}	S_{yz}	S_{xz}			
1	-0.12	1.60	4.36	-0.04	0.05	-0.18	4.50	20.00	4.44
2	0.92	-9.06	-1.29	-0.22	0.01	-0.66	10.17	20.00	1.97
3	-0.58	-9.49	4.83	-0.19	-0.03	1.01	14.51	20.00	1.38
4	-0.02	7.81	4.78	-0.21	0.00	0.00	7.84	18.70	2.39
5	-0.04	7.81	4.78	-0.20	0.00	0.00	7.86	18.40	2.34
6	-0.04	7.81	4.77	-0.21	0.00	0.00	7.86	17.86	2.27
7	-0.05	7.81	4.76	-0.21	0.00	0.00	7.86	17.50	2.23
8	-0.05	7.80	4.74	-0.21	0.00	0.00	7.86	17.50	2.23
9	-0.07	7.70	4.72	-0.20	0.00	0.03	7.78	18.10	2.33
10	-0.35	1.26	1.08	0.00	0.00	0.07	1.62	18.10	large
11	-0.09	1.15	0.38	-0.01	0.00	-0.85	1.89	14.48 ^b	7.66
12	0.25	0.29	-0.65	0.00	1.26	-1.41	3.90	20.00	5.13
13	0.03	0.03	-0.06	0.00	-0.05	0.05	0.17	18.10	large
14	0.49	1.59	-0.04	0.02	-0.05	-0.13	1.67	18.10	large
15	0.18	1.51	0.08	0.00	0.00	-0.10	1.50	18.10	large

^a See Figure 3.10.3-2 for section locations.

^b Allowable stress includes a reduction factor of 0.8 for the closure lid weld.

Table 3.10.3-2 TSC Normal Pressure plus Handling, $P_m + P_b$, ksi

Section ^a	Component Stresses						S_{int}	S_{allow}	FS
	S_x	S_y	S_z	S_{xy}	S_{yz}	S_{xz}			
1	-0.96	-5.82	11.51	-0.09	-0.02	-0.25	17.33	30.00	1.73
2	2.84	-14.16	-1.29 ^b	0.00	0.00	-1.19	17.32	30.00	1.73
3	-0.25	-4.94	19.45	-0.08	-0.04	1.27	24.48	30.00	1.23
4	-0.05	7.92	4.82	-0.21	0.00	0.01	7.98	28.05	3.52
5	-0.06	7.94	4.81	-0.21	0.00	-0.02	8.02	27.60	3.44
6	-0.07	7.95	4.81	-0.21	0.00	0.00	8.03	26.79	3.34
7	-0.07	7.96	4.80	-0.21	0.00	0.00	8.04	26.25	3.26
8	-0.08	7.94	4.78	-0.21	0.00	0.00	8.03	26.25	3.27
9	-0.05	8.12	6.32	-0.21	0.00	0.01	8.18	27.15	3.32
10	-0.78	1.13	1.11	0.00	0.00	0.89	2.60	27.15	large
11	-0.14	1.54	2.05	0.00	0.00	-1.18	3.23	21.72 ^c	6.72
12	24.66	23.52	2.96	0.75	1.07	-1.42	22.26	30.00	1.35
13	2.87	2.85	0.04	0.00	-0.06	0.04	2.82	27.15	9.63
14	0.61	1.66	-0.07	0.04	-0.09	-0.12	1.77	27.15	large
15	-0.59	1.25	-0.15	0.00	0.05	0.06	1.85	27.15	large

^a See Figure 3.10.3-2 for section locations.

^b Localized bending stresses are secondary and are excluded from evaluation.

^c Allowable stress includes a reduction factor of 0.8 for the closure lid weld.

Table 3.10.3-3 TSC Normal Pressure plus Handling, P + Q, ksi

Section ^a	Component Stresses						S _{int}	S _{allow}	FS
	S _x	S _y	S _z	S _{xy}	S _{yz}	S _{xz}			
1	0.68	12.71	-2.73	-0.02	-0.01	-0.05	15.44	60.00	3.89
2	2.82	-11.18	-19.61	0.00	0.00	-1.19	22.56	60.00	2.66
3	-0.29	-3.60	19.95	0.00	0.04	1.22	23.63	60.00	2.54
4	-0.06	8.18	4.84	-0.21	0.01	0.01	8.25	56.10	6.80
5	-0.07	8.29	4.84	-0.21	0.00	-0.02	8.37	55.20	6.59
6	-0.08	8.33	4.82	-0.21	0.00	0.00	8.42	53.58	6.36
7	-0.08	8.37	4.84	-0.22	0.00	0.00	8.46	52.50	6.21
8	-0.08	8.30	4.84	-0.21	0.00	0.00	8.39	52.50	6.26
9	-0.07	7.92	6.29	0.00	0.00	0.00	7.99	54.30	6.80
10	-0.89	2.51	0.39	0.00	-0.01	1.13	4.06	54.30	large
11	-0.24	2.34	-1.52	0.04	0.01	-0.55	4.06	43.44 ^b	large
12	-41.04	-37.90	-8.45	-1.25	-0.15	-1.51	33.17	60.00	1.81
13	-13.65	-12.13	-3.78	-0.26	0.64	0.28	9.99	54.30	5.44
14	0.06	3.03	-0.40	0.00	0.00	-0.10	3.45	54.30	large
15	-1.13	3.57	-0.13	0.09	-0.01	-0.02	4.70	54.30	large

^a See Figure 3.10.3-2 for section locations.

^b Allowable stress includes a reduction factor of 0.8 for the closure lid weld.

Table 3.10.3-4 TSC Normal Pressure, P_m , ksi

Section ^a	Component Stresses						S_{int}
	S_x	S_y	S_z	S_{xy}	S_{yz}	S_{xz}	
1	-0.10	1.33	3.61	-0.03	0.04	-0.17	3.73
2	0.79	-7.22	-1.16	0.18	-0.01	-0.55	8.17
3	-0.50	-6.93	3.91	0.13	0.02	0.85	11.01
4	-0.03	7.81	3.86	-0.21	0.00	0.00	7.84
5	-0.04	7.81	3.85	-0.21	0.00	0.00	7.86
6	-0.04	7.81	3.85	-0.21	0.00	0.00	7.86
7	-0.05	7.80	3.85	-0.21	0.00	0.00	7.86
8	-0.05	7.80	3.85	-0.21	0.00	0.00	7.86
9	-0.06	7.73	3.85	-0.20	0.00	0.04	7.81
10	-0.40	0.77	0.59	-0.03	0.01	0.27	1.24
11	-0.11	0.95	0.83	-0.03	-0.01	-0.60	1.53
12	0.19	0.23	-0.63	0.00	0.98	-1.13	3.11
13	0.04	0.04	-0.06	0.00	-0.04	0.04	0.15
14	0.31	1.06	-0.09	-0.02	0.00	-0.07	1.16
15	0.09	1.04	0.16	-0.02	-0.01	-0.04	0.97

^a See Figure 3.10.3-2 for section locations.

Table 3.10.3-5 TSC Normal Pressure, $P_m + P_b$, ksi

Section ^a	Component Stresses						S_{int}
	S_x	S_y	S_z	S_{xy}	S_{yz}	S_{xz}	
1	-0.75	-4.52	9.51	0.07	0.02	-0.22	14.03
2	2.37	-11.47	-16.71	0.00	0.00	-0.99	19.19
3	-0.20	-3.23	15.78	0.04	0.03	1.07	19.08
4	-0.06	7.90	3.89	-0.21	0.00	0.01	7.96
5	-0.07	7.90	3.87	-0.21	0.00	-0.02	7.98
6	-0.07	7.90	3.87	-0.21	0.00	0.00	7.98
7	-0.07	7.90	3.87	-0.21	0.00	0.00	7.98
8	-0.08	7.89	3.87	-0.21	0.00	0.00	7.98
9	-0.05	8.19	5.53	0.00	0.00	0.01	8.24
10	-0.75	0.37	-0.33	-0.03	0.02	1.02	2.08
11	0.07	1.40	2.30	-0.04	-0.01	-0.90	2.87
12	19.64	18.71	2.15	0.59	0.79	-1.14	17.91
13	2.24	2.22	0.03	0.00	-0.04	0.04	2.21
14	0.43	1.14	-0.08	-0.02	0.02	-0.05	1.22
15	-0.46	0.84	-0.06	-0.03	-0.01	0.02	1.30

^a See Figure 3.10.3-2 for section locations.

Table 3.10.3-6 TSC Thermal Stresses, Q, ksi

Section ^a	Component Stresses						S _{int}
	S _x	S _y	S _z	S _{xy}	S _{yz}	S _{xz}	
1	-0.05	3.72	0.05	0.00	0.00	0.04	3.79
2	-0.20	2.82	-0.25	-0.08	0.00	-0.01	3.08
3	0.09	1.06	-0.51	0.00	-0.01	-0.03	1.57
4	0.00	-0.27	-0.15	0.01	0.00	0.00	0.27
5	0.00	-0.36	-0.20	0.02	0.00	0.00	0.36
6	0.00	-0.42	-0.21	0.02	0.00	0.00	0.42
7	0.00	-0.43	-0.23	0.02	0.00	0.00	0.43
8	-0.01	-0.44	-0.20	0.02	0.00	0.00	0.43
9	-0.02	-0.57	-0.20	0.03	0.00	-0.01	0.55
10	-0.12	1.37	-0.74	0.00	-0.01	0.24	2.20
11	-0.33	1.63	0.01	0.01	0.00	0.07	1.98
12	-16.87	-14.95	-4.20	-0.50	-1.60	-0.10	13.05
13	-10.85	-9.35	-3.62	-0.26	0.69	0.22	7.38
14	-0.25	1.60	-0.07	0.00	0.00	0.01	1.86
15	-0.49	2.39	0.17	-0.05	0.01	0.02	2.88

^a See Figure 3.10.3-2 for section locations.

Table 3.10.3-7 TSC Off-Normal Pressure plus Handling, P_m , ksi

Section ^a	Component Stresses						S_{int}	S_{allow}	FS
	S_x	S_y	S_z	S_{xy}	S_{yz}	S_{xz}			
1	-0.14	1.84	5.02	-0.05	0.06	-0.21	5.18	22.00	4.25
2	1.07	-10.37	-1.51	-0.26	0.01	-0.76	11.66	22.00	1.89
3	-0.67	-10.75	5.54	-0.21	-0.03	1.16	16.51	22.00	1.33
4	-0.03	9.23	5.48	-0.24	0.00	0.00	9.27	20.57	2.22
5	-0.04	9.23	5.48	-0.24	0.00	0.00	9.28	20.24	2.18
6	-0.05	9.23	5.47	-0.24	0.00	0.00	9.29	19.65	2.11
7	-0.05	9.23	5.46	-0.24	0.00	0.00	9.29	19.25	2.07
8	-0.06	9.22	5.44	-0.24	0.00	0.00	9.29	19.25	2.07
9	-0.08	9.11	5.42	-0.24	0.00	0.04	9.20	19.91	2.16
10	-0.42	1.41	1.20	0.00	0.00	0.11	1.84	19.91	large
11	-0.11	1.32	0.53	-0.01	0.00	-0.96	2.13	15.93 ^b	7.48
12	0.28	0.33	-0.76	0.00	1.44	-1.62	4.47	22.00	4.92
13	0.04	0.04	-0.07	0.00	-0.06	0.06	0.20	19.91	large
14	0.54	1.79	-0.06	0.02	-0.05	-0.14	1.88	19.91	large
15	0.20	1.70	0.11	0.00	0.00	-0.11	1.67	19.91	large

^a See Figure 3.10.3-2 for section locations.

^b Allowable stress includes a reduction factor of 0.8 for the closure lid weld.

Table 3.10.3-8 TSC Off-Normal Pressure plus Handling, $P_m + P_b$, ksi

Section ^a	Component Stresses						S_{int}	S_{allow}	FS
	S_x	S_y	S_z	S_{xy}	S_{yz}	S_{xz}			
1	-1.10	-6.64	13.23	-0.10	-0.03	-0.28	19.88	33.00	1.66
2	3.27	-16.24	-23.02	0.00	0.00	-1.37	26.44	60.00 ^b	2.27
2	3.27	-16.24	-1.51 ^c	0.00	0.00	-1.37	19.87	33.00	1.66
3	-0.28	-5.53	22.31	0.00	0.00	1.47	27.94	33.00	1.18
4	-0.06	9.36	5.52	-0.25	0.00	0.01	9.43	30.86	3.27
5	-0.07	9.38	5.51	-0.25	0.00	-0.03	9.47	30.36	3.21
6	-0.08	9.39	5.51	-0.25	0.00	0.00	9.49	29.47	3.11
7	-0.09	9.39	5.50	-0.25	0.00	0.00	9.49	28.88	3.04
8	-0.09	9.38	5.48	-0.25	0.00	0.00	9.48	28.88	3.05
9	-0.06	9.62	7.34	0.00	0.01	0.01	9.68	29.87	3.09
10	-0.92	1.19	1.05	0.00	0.00	1.08	2.92	29.87	large
11	-0.13	1.79	2.47	0.00	0.00	-1.35	3.75	23.89 ^d	6.37
12	28.23	26.93	3.35	0.86	1.22	-1.62	25.52	33.00	1.29
13	3.27	3.25	0.05	0.00	-0.06	0.05	3.23	29.87	9.25
14	0.68	1.87	-0.09	0.04	-0.09	-0.13	1.99	29.87	large
15	-0.67	1.41	-0.16	0.00	0.05	0.07	2.09	29.87	large

^a See Figure 3.10.3-2 for section locations.

^b Bending stresses are considered secondary, P+Q stress allowable used.

^c Localized bending stresses are secondary and are excluded from evaluation.

^d Allowable stress includes a reduction factor of 0.8 for the closure lid weld.

Table 3.10.3-9 TSC Off-Normal Pressure plus Handling, P + Q, ksi

Section ^a	Component Stresses						S _{int}	S _{allow}	FS
	S _x	S _y	S _z	S _{xy}	S _{yz}	S _{xz}			
1	0.78	14.01	-3.15	-0.02	-0.01	-0.07	17.16	60.00	3.50
2	3.26	-13.26	-22.64	0.00	0.00	-1.37	26.04	60.00	2.30
3	-0.32	-4.19	22.81	0.00	0.04	1.41	27.09	60.00	2.21
4	-0.07	9.61	5.55	-0.25	0.01	0.01	9.69	55.20	5.62
5	-0.08	9.72	5.55	-0.25	0.00	-0.02	9.82	53.58	5.43
6	-0.09	9.77	5.53	-0.25	0.00	0.00	9.87	53.58	5.43
7	-0.09	9.80	5.54	-0.25	0.00	0.00	9.91	52.50	5.30
8	-0.09	9.74	5.55	-0.25	0.00	0.00	9.85	52.50	5.33
9	-0.08	9.41	7.30	0.00	-0.01	0.00	9.49	54.30	5.72
10	-1.03	2.58	0.32	0.00	-0.01	1.31	4.41	54.30	large
11	-0.29	2.43	-1.64	0.04	0.01	-0.61	4.30	43.44 ^b	large
12	-44.54	-41.22	-9.07	-1.36	0.06	-1.71	36.12	60.00	1.66
13	-14.05	-12.53	-3.80	-0.26	0.63	0.29	10.36	54.30	5.24
14	0.43	3.48	-0.16	0.04	-0.09	-0.13	3.66	54.30	large
15	-1.21	3.72	-0.14	0.10	-0.01	-0.01	4.94	54.30	large

^a See Figure 3.10.3-2 for section locations.

^b Allowable stress includes a reduction factor of 0.8 for the closure lid weld.

Table 3.10.3-10 TSC Normal Pressure plus Off-Normal Handling, P_m , ksi

Section ^a	Component Stresses						S_{int}	S_{allow}	FS
	S_x	S_y	S_z	S_{xy}	S_{yz}	S_{xz}			
1	-1.64	1.20	4.54	0.20	0.04	-0.35	6.23	24.75	3.97
2	1.20	-10.15	-1.07	0.26	-0.14	-0.70	11.57	24.75	2.14
3	-0.60	-10.57	5.42	0.01	-0.10	1.06	16.17	24.50	1.52
4	-0.12	7.94	5.63	0.08	0.00	0.00	8.06	22.50	2.79
5	-0.12	7.89	5.63	0.07	0.00	0.00	8.00	22.12	2.77
6	-0.12	7.88	5.59	0.06	0.00	0.00	8.00	21.45	2.68
7	-0.13	7.88	5.57	0.07	0.00	0.00	8.01	21.00	2.62
8	-0.15	7.95	5.45	0.09	0.01	0.00	8.09	21.00	2.60
9	-0.08	7.91	4.90	0.03	-0.08	0.03	7.98	21.75	2.73
10	-6.14	-0.11	0.89	0.66	-0.18	-0.64	7.27	21.75	2.99
11	-4.94	0.30	-0.34	0.75	-0.22	-1.44	6.10	17.40 ^b	2.85
12	0.24	0.32	-0.65	0.00	1.37	-1.51	4.18	24.50	5.86
13	0.02	0.04	-0.06	0.00	-0.06	0.05	0.17	21.75	large
14	-1.58	1.35	-0.21	0.47	0.03	0.07	3.08	21.75	7.06
15	-3.66	0.93	-0.20	0.67	-0.28	-0.27	4.87	21.75	4.47

^a See Figure 3.10.3-2 for section locations.

^b Allowable stress includes a reduction factor of 0.8 for the closure lid weld.

Table 3.10.3-11 TSC Normal Pressure plus Off-Normal Handling, $P_m + P_b$, ksi

Section ^a	Component Stresses						S_{int}	S_{allow}	FS
	S_x	S_y	S_z	S_{xy}	S_{yz}	S_{xz}			
1	-1.04	-6.70	12.44	0.35	0.10	-0.29	19.17	35.40	1.85
2	3.13	-15.72	-1.07 ^b	-0.05	-0.19	-1.29	19.23	35.40	1.84
3	-0.23	-6.17	21.24	-0.14	0.05	1.35	27.49	34.80	1.27
4	-0.14	12.81	7.14	-0.35	0.02	0.01	12.96	31.10	2.40
5	-0.13	12.91	7.18	-0.36	0.00	-0.02	13.06	30.60	2.34
6	-0.13	12.87	7.14	-0.36	0.00	0.00	13.02	29.70	2.28
7	-0.14	12.92	7.13	-0.36	0.00	0.00	13.07	29.10	2.23
8	-0.17	12.75	6.94	-0.35	-0.01	0.00	12.94	29.10	2.25
9	-0.29	9.76	4.16	-0.24	-0.16	0.06	10.06	30.10	2.99
10	-7.43	-1.04	1.17	0.59	-0.18	0.21	8.68	30.10	3.47
11	-5.58	0.24	0.80	0.66	-0.18	-1.51	7.22	24.08 ^c	3.34
12	26.41	25.35	3.25	0.80	1.18	-1.51	23.79	34.80	1.46
13	2.95	3.19	0.05	0.00	-0.06	0.03	3.14	30.10	9.59
14	-1.38	1.63	-0.14	0.52	0.02	0.13	3.20	30.10	9.41
15	-3.47	1.19	-0.12	0.73	-0.20	-0.35	4.95	30.10	6.08

^a See Figure 3.10.3-2 for section locations.

^b Localized bending stresses are secondary and are excluded from evaluation.

^c Allowable stress includes a reduction factor of 0.8 for the closure lid weld.

Table 3.10.3-12 TSC Normal Pressure plus 24-inch Drop, P_m , ksi

Section ^a	Component Stresses						S_{int}	S_{allow}	FS
	S_x	S_y	S_z	S_{xy}	S_{yz}	S_{xz}			
1	-0.11	0.79	0.27	-0.02	0.07	0.37	1.14	47.58	large
2	1.34	-9.26	-8.42	0.24	-0.02	-0.99	10.71	47.58	4.44
3	-0.52	-8.65	-4.81	-0.17	-0.03	0.93	8.33	47.15	5.66
4	-0.03	7.81	-4.26	0.00	0.00	0.00	12.07	44.80	3.71
5	-0.04	7.80	-3.77	-0.20	0.00	0.00	11.58	44.10	3.81
6	-0.04	7.81	-3.33	0.21	0.00	0.00	11.14	42.84	3.85
7	-0.05	7.80	-3.02	0.21	0.00	0.00	10.83	42.00	3.88
8	-0.05	7.80	-2.40	0.21	0.00	0.00	10.21	42.00	4.11
9	-0.05	7.92	-1.81	0.21	0.00	0.05	9.74	43.40	4.46
10	-0.68	-1.09	-2.03	0.00	0.00	1.31	2.95	43.40	large
11	-0.22	0.63	3.05	0.00	0.00	0.63	3.51	34.72 ^b	9.89
12	0.46	0.38	-1.22	-0.01	0.98	-0.95	3.19	47.15	large
13	0.04	0.04	-0.05	0.00	0.02	-0.02	0.10	43.40	large
14	-0.61	-0.65	-0.26	0.00	0.00	0.12	0.44	43.40	large
15	-0.67	-0.56	0.15	0.01	-0.02	0.14	0.87	43.40	large

^a See Figure 3.10.3-2 for section locations.

^b Allowable stress includes a reduction factor of 0.8 for the closure lid weld.

Table 3.10.3-13 TSC Normal Pressure plus 24-inch Drop, $P_m + P_b$, ksi

Section ^a	Component Stresses						S_{int}	S_{allow}	FS
	S_x	S_y	S_z	S_{xy}	S_{yz}	S_{xz}			
1	1.99	7.87	-4.91	0.00	0.00	1.28	13.01	69.80	5.37
2	3.02	-14.27	-8.42 ^b	0.00	0.00	-1.49	17.49	69.80	3.99
3	-0.84	-12.49	-17.20	0.00	-0.01	0.71	16.42	68.60	4.18
4	-0.06	7.90	-4.22	0.21	0.00	0.01	12.13	64.00	5.28
5	-0.06	7.91	-3.75	0.21	0.00	-0.02	11.67	63.75	5.46
6	-0.07	7.91	-3.30	0.21	0.00	0.00	11.22	63.30	5.64
7	-0.07	7.91	-2.99	0.21	0.00	0.00	10.91	63.00	5.77
8	-0.08	7.90	-2.37	-0.21	0.00	0.00	10.28	63.00	6.13
9	-0.08	7.36	-3.87	0.19	0.00	0.06	11.24	63.50	5.65
10	-0.62	-2.86	-7.82	0.00	0.00	1.68	7.95	63.50	7.99
11	-1.59	-0.02	2.52	0.00	0.00	0.86	4.46	50.80 ^c	large
12	17.98	18.23	1.64	0.67	0.76	-0.94	17.24	68.60	3.98
13	0.92	0.92	-0.09	0.00	0.02	-0.02	1.01	63.50	large
14	-0.83	-0.80	-0.46	0.00	0.00	0.17	0.51	63.50	large
15	-1.65	-0.97	-0.29	0.01	-0.02	0.33	1.52	63.50	large

^a See Figure 3.10.3-2 for section locations.

^b Localized bending stresses are secondary and are excluded from evaluation.

^c Allowable stress includes a reduction factor of 0.8 for the closure lid weld.

Table 3.10.3-14 TSC Accident Pressure plus Dead Weight, P_m , ksi

Section ^a	Component Stresses						S_{int}	S_{allow}	FS
	S_x	S_y	S_z	S_{xy}	S_{yz}	S_{xz}			
1	-0.23	3.01	8.15	-0.08	0.09	-0.37	8.42	47.58	5.65
2	1.81	-16.45	-2.76	0.40	-0.01	-1.26	18.61	47.58	2.56
3	-1.13	-15.79	8.74	0.29	0.06	1.93	24.90	47.15	1.89
4	-0.06	17.74	8.63	-0.47	0.00	0.00	17.83	44.80	2.51
5	-0.09	17.74	8.63	-0.47	0.00	0.00	17.85	44.10	2.47
6	-0.10	17.74	8.63	-0.47	0.00	0.00	17.86	42.84	2.40
7	-0.11	17.74	8.64	-0.47	0.00	0.00	17.87	42.00	2.35
8	-0.11	17.73	8.64	-0.47	0.00	0.00	17.87	42.00	2.35
9	-0.15	17.58	8.66	-0.46	0.00	0.08	17.75	43.40	2.45
10	-0.91	1.73	1.29	-0.07	0.02	0.63	2.81	43.40	large
11	-0.26	2.16	1.92	-0.07	-0.02	-1.35	3.47	34.72 ^b	large
12	0.43	0.52	-1.44	-0.01	2.23	-2.57	7.07	47.15	6.67
13	0.08	0.08	-0.13	0.00	-0.10	0.10	0.35	43.40	large
14	0.69	2.39	-0.20	-0.05	0.01	-0.17	2.62	43.40	large
15	0.19	2.35	0.36	-0.06	-0.02	-0.09	2.19	43.40	large

^a See Figure 3.10.3-2 for section locations.

^b Allowable stress includes a reduction factor of 0.8 for the closure lid weld.

Table 3.10.3-15 TSC Accident Pressure plus Dead Weight, $P_m + P_b$, ksi

Section ^a	Component Stresses						S_{int}	S_{allow}	FS
	S_x	S_y	S_z	S_{xy}	S_{yz}	S_{xz}			
1	-1.74	-10.29	21.53	0.15	0.04	-0.50	31.84	69.80	2.19
2	5.41	-26.12	-2.76 ^b	0.00	0.00	-2.26	32.12	69.80	2.17
3	-0.46	-7.35	35.72	0.09	0.07	2.43	43.24	68.60	1.59
4	-0.13	17.95	8.70	-0.47	0.00	0.02	18.10	64.00	3.54
5	-0.15	17.96	8.68	-0.47	0.00	-0.04	18.13	63.75	3.52
6	-0.16	17.95	8.68	-0.47	0.00	0.00	18.14	63.30	3.49
7	-0.17	17.95	8.68	-0.47	0.00	0.00	18.15	63.00	3.47
8	-0.18	17.94	8.69	-0.47	0.00	0.00	18.14	63.00	3.47
9	-0.10	18.62	12.48	0.00	0.00	0.03	18.73	63.50	3.39
10	-1.70	0.77	-0.93	0.00	0.00	2.33	4.73	63.50	large
11	0.17	3.19	5.25	-0.08	-0.03	-2.02	6.49	50.80 ^c	7.83
12	44.60	42.52	4.88	1.35	1.80	-2.58	40.70	68.60	1.69
13	5.04	5.00	0.07	0.01	-0.10	0.10	4.98	63.50	large
14	0.95	2.55	-0.19	-0.05	0.03	-0.12	2.75	63.50	large
15	-1.03	1.90	-0.12	-0.07	-0.02	0.05	2.93	63.50	large

^a See Figure 3.10.3-2 for section locations.

^b Localized bending stresses are secondary and are excluded from evaluation.

^c Allowable stress includes a reduction factor of 0.8 for the closure lid weld.

Table 3.10.3-16 TSC Tip-Over plus Normal Pressure, P_m , ksi

Section ^a	Angle	Component Stresses						S_{int}	S_{allow}	FS
		S_x	S_y	S_z	S_{xy}	S_{yz}	S_{xz}			
1	69	-0.16	1.58	3.91	0.13	0.29	-0.35	4.17	47.58	large
2	69	1.12	-8.58	-2.50	0.16	0.79	-0.72	9.95	47.58	4.78
3	69	-0.55	-8.76	3.00	-0.04	1.22	0.94	12.23	47.15	3.86
4	27	-0.03	8.93	0.26	0.01	3.26	0.00	10.84	44.80	4.13
5	0	-4.82	-12.05	-10.93	12.58	0.33	1.15	26.27	44.10	2.57
6	0	-0.39	8.60	-5.39	-0.10	-0.24	0.06	14.01	42.84	3.06
7	0	-0.32	10.05	-1.64	-0.02	-0.15	0.00	11.69	42.00	3.59
8	0	-0.52	8.21	1.81	0.27	-0.06	0.00	8.75	42.00	4.80
9	33	-1.29	16.48	2.21	1.33	-1.22	0.16	18.09	43.40	2.40
10 ^b	6	-5.49	6.78	-0.91	-2.40	-2.01	-1.82	14.33	43.40	3.03
11 ^c	0 - 6	-23.89	-17.09	-19.05	10.77	-1.77	-8.92	29.05	34.72 ^c	1.20
12	0	0.18	0.23	-0.56	0.00	0.87	-1.04	2.82	47.15	large
13	0	-1.36	-0.23	-0.57	0.12	-0.01	-3.40	6.86	43.40	6.33
14 ^b	6	1.90	-8.88	0.00	5.20	4.00	-2.09	16.65	43.40	2.61
15 ^b	6	0.13	-6.01	-2.29	-0.42	-0.78	0.09	6.36	43.40	6.83

^a See Figure 3.10.3-2 for section locations.

^b Bearing stress evaluation is not required for accident conditions.

^c Stresses are determined by averaging the stresses over the impact region. Allowable stress includes a reduction factor of 0.8 for the closure lid weld.

Table 3.10.3-17 TSC Tip-Over plus Normal Pressure, $P_m + P_b$, ksi

Section ^a	Angle	Component Stresses						S_{int}	S_{allow}	FS
		S_x	S_y	S_z	S_{xy}	S_{yz}	S_{xz}			
1	69	-0.54	-5.28	10.47	0.15	0.51	-0.44	15.81	69.80	4.41
2	66	2.77	-13.66	-2.50 ^b	0.07	0.78	-1.17	16.74	69.80	4.17
3	66	-0.17	-4.90	16.94	-0.06	1.33	1.18	22.09	68.60	3.11
4	27	-0.07	19.54	3.84	0.01	4.15	0.01	20.64	64.00	3.10
5	60	0.68	59.72	41.78	0.02	0.81	0.28	59.06	63.75	1.08
6	60	-0.08	20.79	11.91	-0.01	-0.75	-0.02	20.94	63.30	3.02
7	0	-0.55	18.40	0.89	-0.23	-0.11	0.00	18.96	63.00	3.32
8	0	-0.87	18.35	4.84	0.01	-0.02	0.00	19.22	63.00	3.28
9	30	5.14	55.19	39.08	0.00	-1.26	-1.52	50.22	63.50	1.26
10 ^c	6	-13.17	17.49	7.56	-2.41	2.07	-2.76	31.85	63.50	1.99
11 ^d	0 - 6	-23.93	-16.43	-16.49	11.98	1.54	-13.41	36.44	50.80 ^d	1.39
12	0	18.01	16.62	1.95	0.55	0.71	-1.04	16.40	68.60	4.18
13	0	-4.19	-2.86	-1.41	0.12	0.55	-3.61	7.82	63.50	8.12
14 ^c	6	2.57	-10.04	0.16	5.22	5.18	-2.61	18.87	63.50	3.36
15 ^c	6	8.66	-1.44	0.34	-1.10	0.55	-1.76	10.79	63.50	5.88

^a See Figure 3.10.3-2 for section locations.

^b Localized bending stresses are secondary and are excluded from evaluation.

^c Bearing stress evaluation is not required for accident conditions.

^d Stresses are determined by averaging the stresses over the impact region. Allowable stress includes a reduction factor of 0.8 for the closure lid weld.

3.10.4 Concrete Cask Finite Element Models

3.10.4.1 Pedestal Finite Element Model for Lift Evaluation

An ANSYS finite element model of the concrete cask pedestal (Figure 3.10.4-1) is used to perform the structural evaluation for the lift condition. The model is constructed using SHELL63, LINK8, and CONTAC52 elements. LINK8 elements are used to model the Nelson studs. The model is a quarter-symmetry model. Symmetry boundary conditions are used on the XZ and YZ planes. The pedestal is a welded structure. CONTAC52 gap elements are used to model regions where components are not welded together (stand to pedestal plate, and support rails to stand). The gap elements do not close during the analysis, which maximizes the bending stresses in the support rails and inlet tops; therefore, the analysis is bounding. During a concrete cask top-end lift, the TSC loads the pedestal plate. A pressure load (P_{can}) is used to apply the TSC weight to the pedestal plate.

$$P_{can} = \frac{1.1 \times W_{can}}{A_{ped}} = \frac{1.1 \times 120,000}{4,071} = 32.4 \text{ psi}$$

The load in the pedestal is reacted out by the Nelson studs, which carry the load into the concrete. The tops of the Nelson studs are restrained in all degrees of freedom. An inertia load of 1.1g (Z-direction) is applied to the finite element model for dynamic load factor (DLF). The 1.1g DLF is applied per ANSI/ASME N45.2.15.

3.10.4.2 Concrete Cask Finite Element Model for Thermal Stress Evaluation

A thermal stress evaluation of the concrete cask was performed for normal conditions and off-normal or accident events. A three-dimensional finite element model was created using the ANSYS program. The concrete cask contains 56 periodic radial sections with the 56 vertical rebars. Therefore, the model represents 6.4° ($1/56^{\text{th}}$) of the concrete cask. The model contains only the portion of the concrete cask shell and liner between the top of the lower vents and the lid assembly because the circumferential and vertical rebar are located in this region.

The thermal conduction model is constructed using ANSYS SOLID70 elements for the concrete shell and steel liner. The nodes at the liner/shell interface are coincident and are connected using temperature couples. The model is divided into four sections vertically with 0.1-inch gaps. LINK33 elements are used to connect the four sections to allow for thermal conduction across the gaps. The temperatures vary in the vertical and radial directions. Conservatively, the temperature profile corresponding to the 106°F (off-normal) ambient condition is used for the

normal conditions. The temperature profile for the 133°F ambient condition is used for the accident event. Temperatures are applied to nodes on the inner and outer surfaces of the concrete cask.

The thermal conduction model is modified for the structural evaluation. The SOLID70 elements are replaced with SOLID45 elements. COMBIN14 elements are used between the four vertical sections of the model for the steel liner. CONTAC52 gap elements are used between the liner and concrete shell to permit only compressive loads to be transmitted across the gap. Rebar was modeled into the model using LINK8 elements. LINK8 elements were also modeled across the vertical gaps to represent the vertical rebar; therefore, tensile loads are taken by the rebar. There are 24 vertical rebar on the inner radius and 56 on the outer radius. The properties of the inner vertical rebar are determined by a ratio to represent the $1/56^{\text{th}}$ model (24/56 ratio). The finite element model is shown in Figure 3.10.4-2 and Figure 3.10.4-3. Boundary conditions are shown in Figure 3.10.4-4.

3.10.4.3 Pedestal Finite Element Model for 24-inch Drop Evaluation

Subjecting the concrete cask to a bottom end impact, the TSC produces a force on the base weldment located at the bottom of the cask. The ring above the air inlets is expected to yield. To determine the resulting acceleration of the TSC and deformation of the pedestal, a LS-DYNA analysis is used.

A quarter-symmetry model of the base weldment is shown in Figure 3.10.4-5. The model is constructed using 4-node shell elements. Symmetry boundary conditions are applied along the planes of symmetry (X-Z and Y-Z plane). Rigid mass 8-node solid elements located in the TSC bottom plate represent the loaded TSC. Rigid mass 8-node solid elements located above the air inlet duct top represent the weight of the inner liner shell. The impact plane is represented as a rigid plane. To determine the maximum acceleration and deformations, impact analyses are solved using LS-DYNA program.

The weldment support rails, weldment pedestal plate, air inlet ducts, and the cylindrical stand materials are modeled using the piece-wise linear plasticity model in LS-DYNA. The stress-strain curve used for this analysis was obtained from the Atlas of Stress-Strain Curves and is presented in Figure 3.10.4-6. To ensure that maximum deformations and accelerations are determined, two analyses are performed. One analysis, which uses the upper bound weight of 105 kips, envelops the maximum deformation of the pedestal. The second analysis employs the lower-bound weight of 60 kips to account for maximum acceleration. The details of the model are described as follows.

- All structural components are modeled using shell elements. A layer of solid elements represents the TSC weight.
- The ground base plate of the pedestal is not modeled since the plate is in contact with the impact plane during impact and has no effect on the deformation of the pedestal.
- The gravitational force is aligned with the Z-axis and is acting in the negative Z direction.
- All components of the pedestal are made of ASTM A36 carbon steel.
- The cylindrical shell under the pedestal plate is separated (not welded) from the support rail to allow buckling to occur at a relative lower g-level.
- The loaded TSC is modeled as a rigid body. The density of the TSC is calculated so that the total weight of the TSC model is equal to 105 kips or 60 kips, bounding values for the maximum and minimum TSC loaded weights.
- The concrete cask liner is modeled as a rigid body. The density of the liner is calculated so that the total weight is equal to 16,900 lb, which envelops the weight of the liner shell and the S-shape steel beams attached to the concrete cask liner.
- The column weight of the concrete portion of the concrete cask projected onto the top of an air inlet plate is represented by a uniformly distributed normal pressure acting on the top of the air inlet plate. The weight is only statically applied to the top of the air inlet. Upon impact, since the air inlet is more flexible than the base plate, all of the impact force of the concrete is transmitted to the base plate. The static pressure is always present during the impact.
- The rigid wall is an infinitive rigid plane. The rigid wall featured in LS-DYNA is used to simulate the rigid ground surface on which the concrete cask is supported or dropped.
- The filter frequency used in the LS-DYNA evaluation is determined by performing natural frequency calculations of the various components in the load path of the base weldment. The component with the lowest natural frequency is the cylindrical stand. This calculation results in a natural frequency of 182 Hz. Therefore, a filter frequency of 200 Hz is selected.

Material Property

The pedestal material is A-36 carbon steel. The LS-DYNA material type 24 (Piecewise_Linear_Plasticity) is used. The true stress-strain curve of A-36 is shown in Figure 3.10.4-6.

Initial Condition

The body force applied to the TSC and the pedestal assembly is the 1g acceleration representing the ever-present gravitational force. Body force is a vectored input, depending on the angle of drop. The 1g body force is applied in the -Z direction. Since the 24-inch drop represents the dynamic force input, the initial velocity, V_0 is computed as shown below.

$$V_o = \sqrt{2gH} = \sqrt{2(386.4)(24)} = 136.1 \text{ inch/sec}$$

where:

$$g = 386.4 \text{ inch/sec}^2$$
$$H = 24.0 \text{ inches ----- Drop height}$$

Post-Processing

To obtain output, a node on the TSC tracks the movements of the TSC as it impacts on the top base plate of the pedestal. Since the TSC is modeled as a rigid body, any node on the TSC is sufficient to track the global movements and deceleration of the TSC. The output database contains a time-series of nodal displacement, velocity, and acceleration. The nodal output file is a text file that the post-processor of LS-DYNA can convert into time-history plots and apply to the plotted graphs signal-conditioning operations such as filtering and rescaling. The acceleration of the TSC is obtained directly from the output file and then filtered to eliminate the ripples. The filtered acceleration (in-inch/sec²) is rescaled to units of g (386.4 inch-inch/sec²) value.

3.10.4.4 Concrete Cask Finite Element Model for Tip-Over Evaluation

The concrete cask is designed to hold a TSC during long-term storage conditions and is constructed of a steel liner surrounded by reinforced concrete. The critical locations for measuring accelerations are at the top of the fuel basket and top of the TSC closure lid.

Two half-symmetry finite element models of the concrete cask, concrete pad, and soil subgrade are constructed of solid brick elements using the LS-DYNA program for the cask tip-over evaluation. One model uses a standard sized pad, and the other model uses an oversized pad. The difference between the two models reflects the segments in the concrete pad. The finite element models are shown in Figure 3.10.4-7.

Material Properties

The mechanical properties used in the analyses are described in the following sections. The densities of each part are calculated to account for the total weight of nonstructural components that are not modeled as part of the finite element model.

Concrete:

The concrete is represented as a homogeneous isotropic material. The effect of the reinforcing steel is ignored. The concrete for the cask and the pad are modeled as LS-DYNA material 16

(Mat_Pseudo_Tensor), which represents a concrete constitutive model in LS-DYNA. This material model requires an equation-of-state represented in LS-DYNA as EOS_Tabulated_Compaction. The LS-DYNA input for the cask concrete is shown below.

$$\begin{aligned}
 f'_c &= 4,000 \text{ psi} \text{----- Compressive Strength} \\
 \rho_c &= 148 \text{ pcf} = 0.0002217 \text{ lb-sec}^2/\text{in}^4 \text{----- Density} \\
 \nu_c &= 0.22 \text{----- Poisson's Ratio} \\
 E_c &= 33\rho_c^{1.5} \sqrt{f'_c} = 3.758 \times 10^6 \text{ psi} \text{----- Modulus of Elasticity} \\
 G_c &= \frac{E_c}{2(1+\nu_c)} = 1.540 \times 10^6 \text{ psi} \text{----- Shear Modulus} \\
 K_c &= \frac{E_c}{3(1-2\nu_c)} = 2.237 \times 10^6 \text{ psi} \text{----- Bulk Modulus} \\
 \epsilon_v &= \frac{f'_c}{K_c} = 0.001788 \text{----- Volumetric Strain}
 \end{aligned}$$

Using the same formulae presented above, the required input data for the pad concrete is shown below.

f'_c (psi)	ρ_c (lb/ft ³)	E_c (psi)	G_c (psi)	K_c (psi)	ϵ_v
5,000	160	4.723×10^6	1.936×10^6	2.811×10^6	0.001779

Soil:

An elastic model with the following properties is used to represent the subgrade soil material of the site.

$$\begin{aligned}
 \rho &= 100 \text{ pcf} \text{----- Density} \\
 \nu_s &= 0.45 \text{----- Poisson's Ratio} \\
 E &= 30,000 \text{ psi} \text{----- Modulus of Elasticity}
 \end{aligned}$$

Steel Inner Liner:

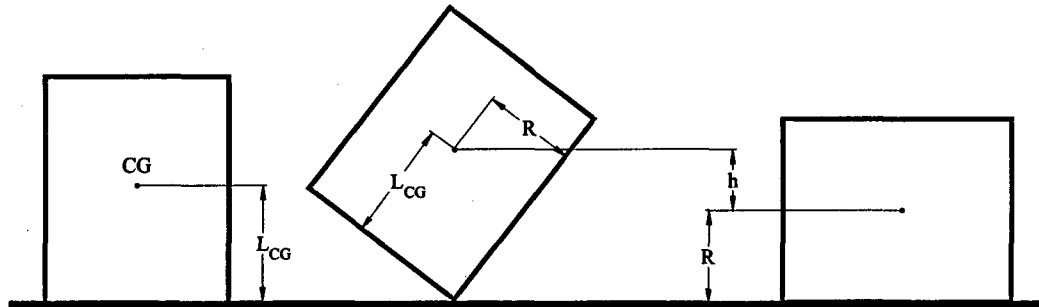
The steel liner is represented by a rigid material model with the following properties.

$$\begin{aligned}
 \nu &= 0.31 \text{----- Poisson's Ratio} \\
 E &= 29 \times 10^6 \text{ psi} \text{----- Modulus of Elasticity}
 \end{aligned}$$

Boundary Conditions

Automatic_Surface_To_Surface contact conditions are employed between the concrete cask and the pad, between the pad and soil, and between the cask steel liner and concrete. Symmetry boundary conditions are applied to all parts at the plane of symmetry (see Figure 3.10.4-7). The vertical displacements at the bottom of the soil subgrade and horizontal displacements for the three vertical boundaries of the soil are restrained.

Tip-over is simulated by applying an initial angular velocity, ω , to the entire concrete cask. The angular velocity value is determined by the conservation of energy about the center of gravity, as the concrete cask rotates from end to corner to side orientations as shown in the figure below.



To ensure accuracy, the LS-DYNA output kinetic energies are compared to actual calculated potential energy. Equating the potential to the kinetic energy during tip-over is as follows.

$$mgh = \frac{I\omega^2}{2}$$

where:

- $\omega = 1.527 \text{ rad/sec}$ ----- Angular velocity for concrete cask
- $m = 785.6 \text{ lb}_m$ ----- Total mass of the concrete cask
- $g = 386.4 \text{ inch/sec}^2$ ----- Acceleration due to gravity
- $h = \sqrt{R^2 + L_{CG}^2} - R$ ----- Height change of the concrete cask mass center
- I ----- Total mass moment of inertia (lb-inch^2) of the concrete cask about the pivot point (automatically calculated by LS-DYNA)
- $R = 68 \text{ inches}$ ----- Outside radius of concrete cask

The potential energy due to the height change of the concrete cask's mass center during tip-over is bounded by the kinetic energy of $2.0 \times 10^7 \text{ inch-lb}$.

Load Cases

Bounding load cases are used to evaluate the loaded concrete cask during tip-over conditions. Two concrete pad and subsoil combinations are considered to bound all possible storage configurations: the standard pad configuration and oversized pad configuration. The standard pad represents typical storage pad properties and boundary conditions. The oversized pad is used as a sensitivity study to determine the effect of increased foundation size on accelerations.

The dimensions of the standard concrete pad are 30 ft (length) × 30 ft (width) with subsoil measuring 35 ft (length) × 35 ft (width). The dimensions of the oversized concrete pad are 60 ft (length) × 30 ft (width) with subsoil measuring 70 ft (length) × 35 ft (width).

With the exception of pad size, the standard and oversized pads use identical parameters and boundary conditions. The mesh density and element aspect ration of the oversized pad is maintained from the standard model.

Figure 3.10.4-1 Concrete Cask Pedestal Finite Element Model for Lift Evaluation

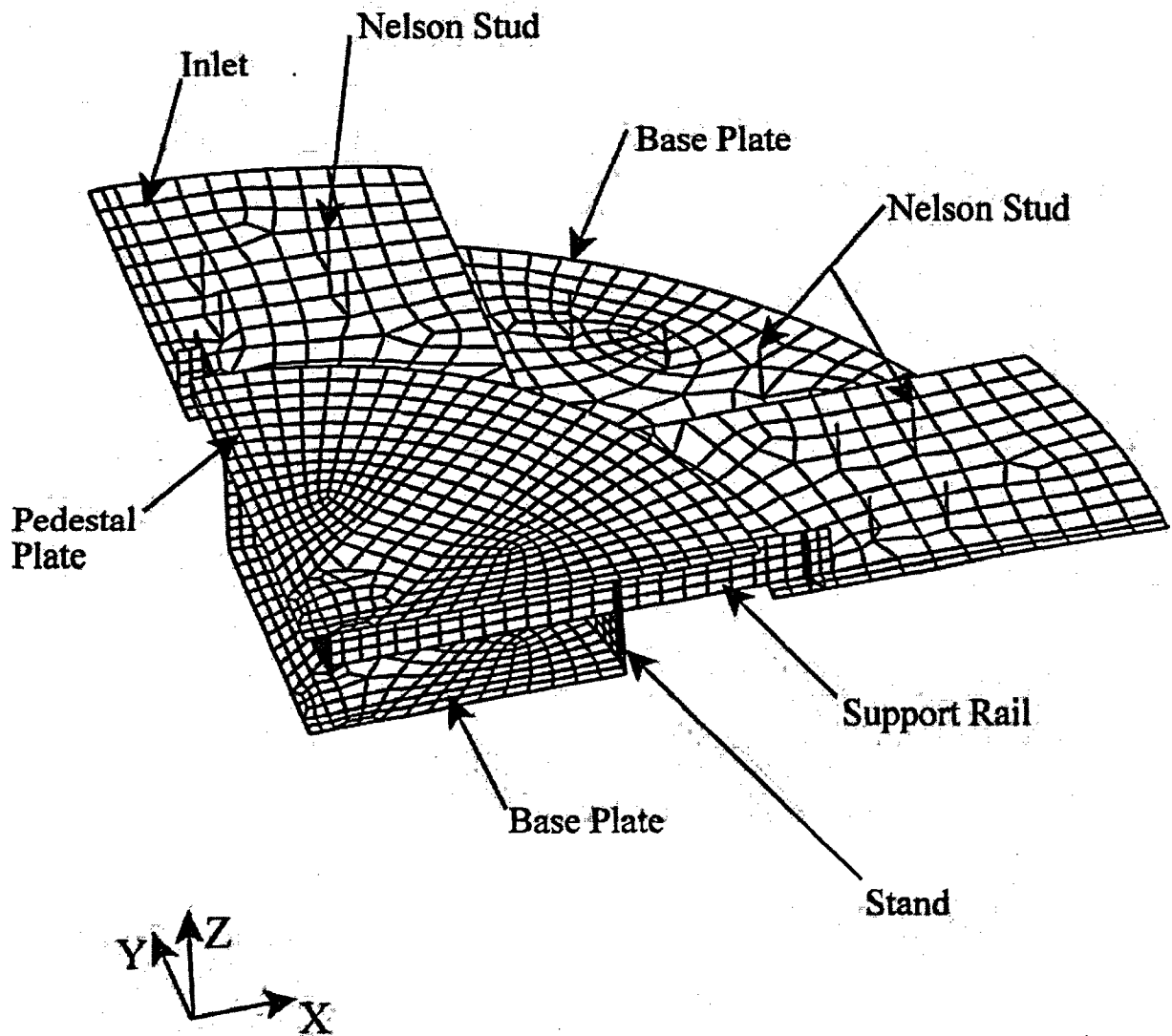


Figure 3.10.4-2 Concrete Cask Finite Element Model for Thermal Stress Evaluation

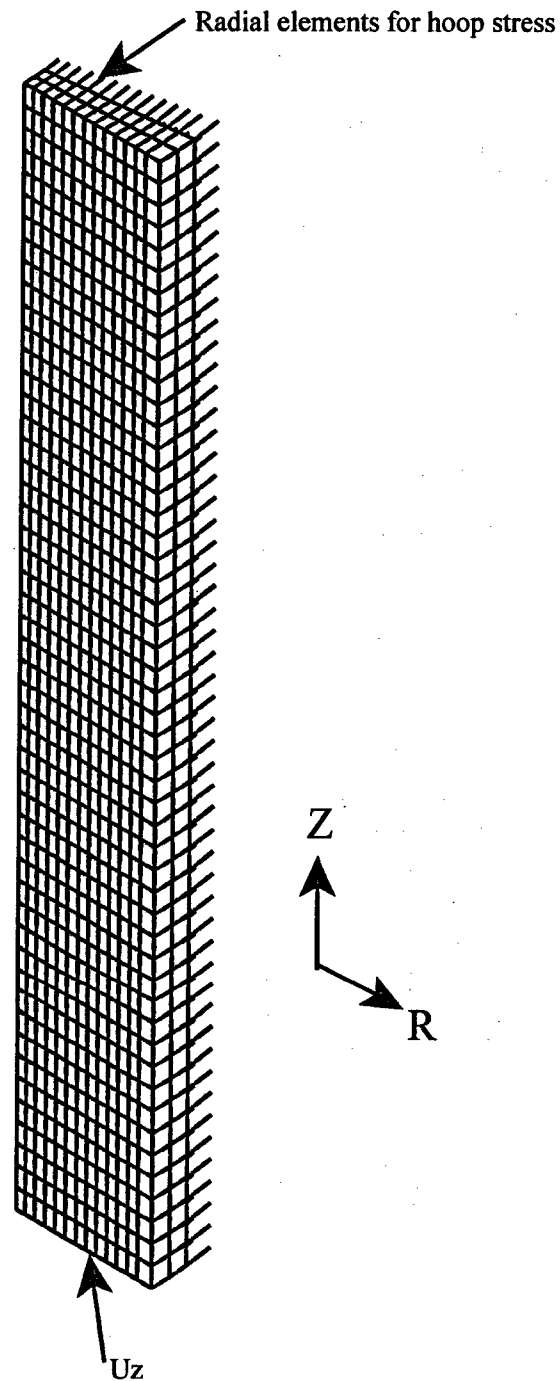


Figure 3.10.4-3 Concrete Cask Model – Elements for Rebar

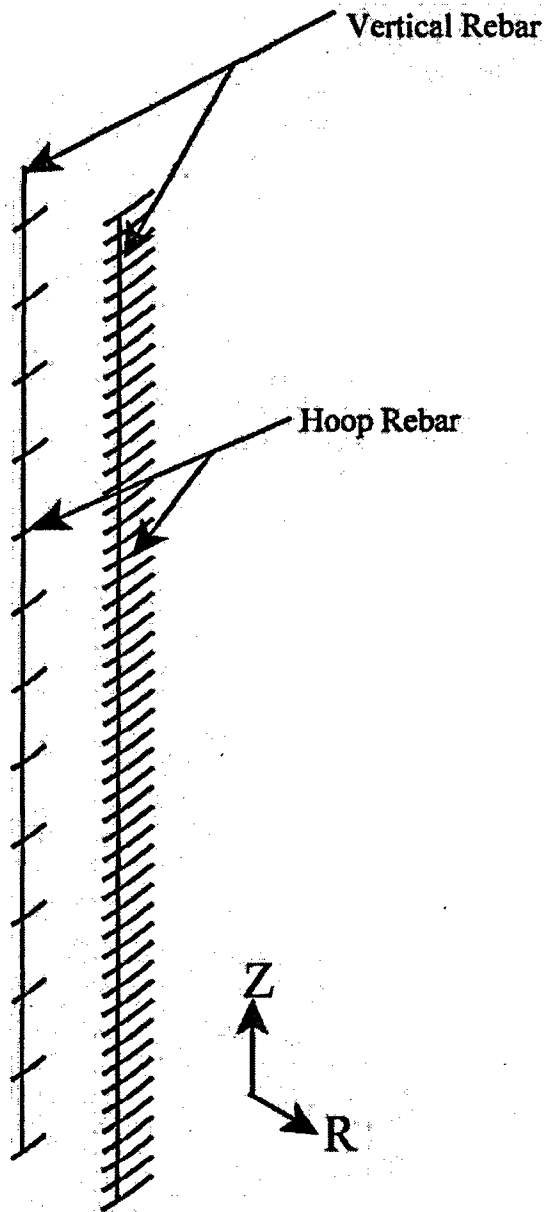


Figure 3.10.4-4 Concrete Cask Model Boundary Conditions

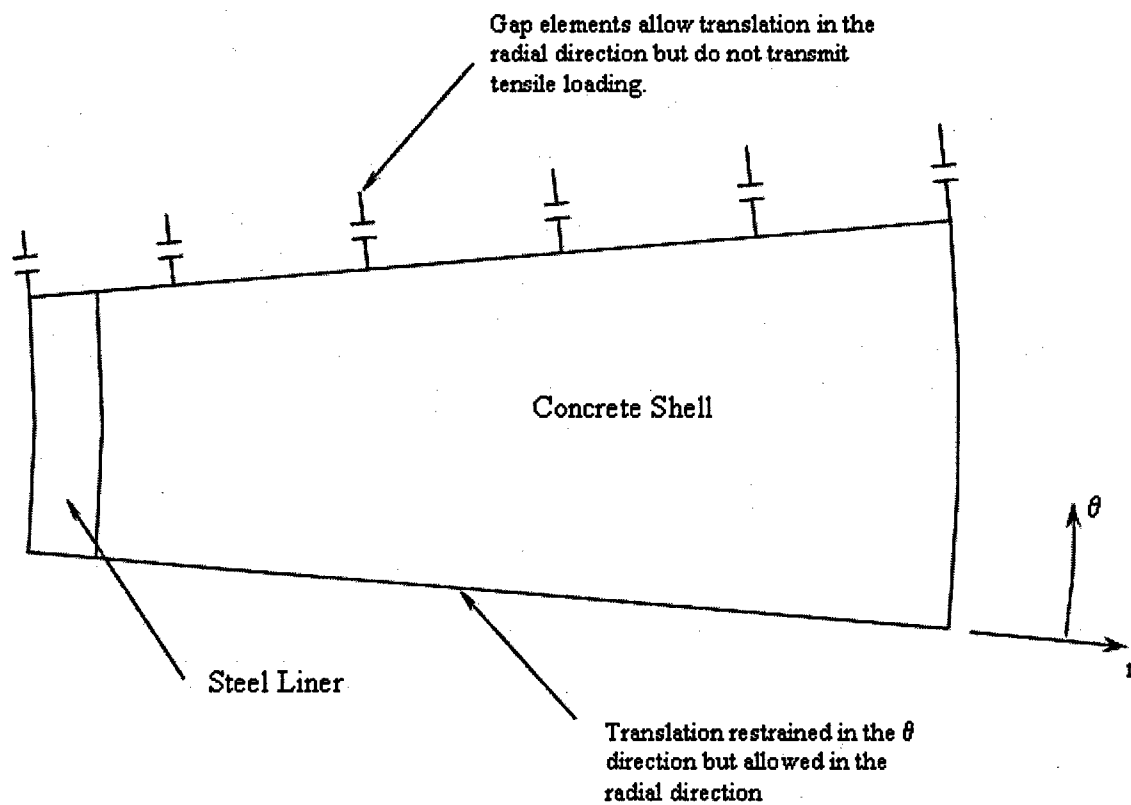


Figure 3.10.4-5 Concrete Cask Pedestal Finite Element Model for 24-inch Drop Evaluation

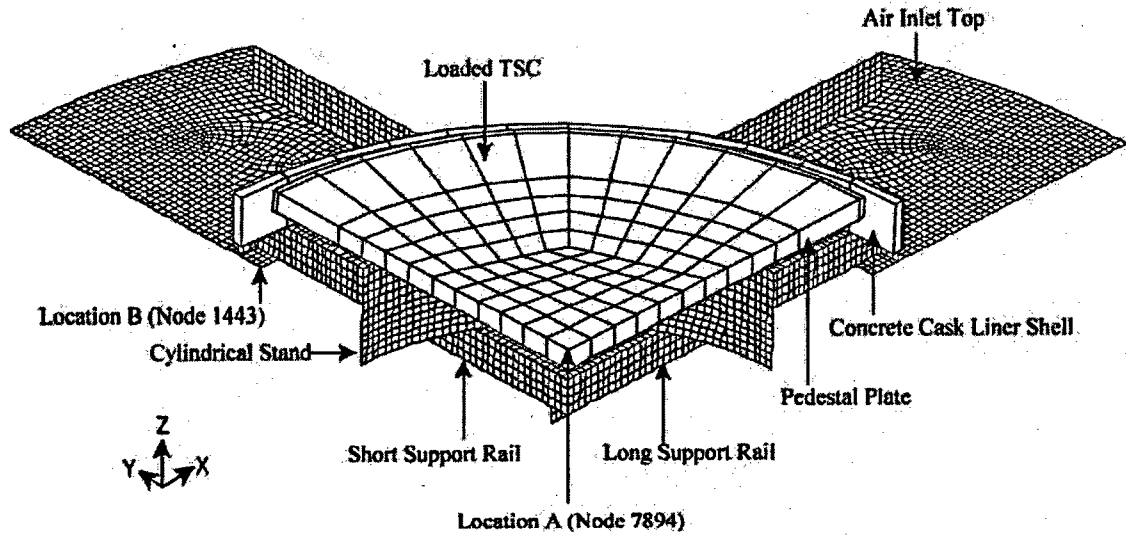


Figure 3.10.4-6 Stress-Strain Curve for A36 Carbon Steel

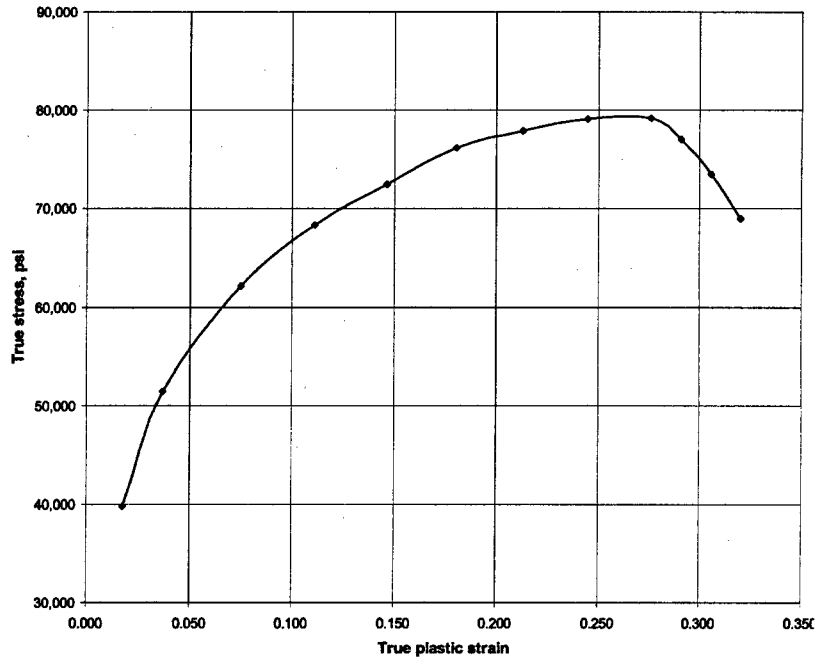
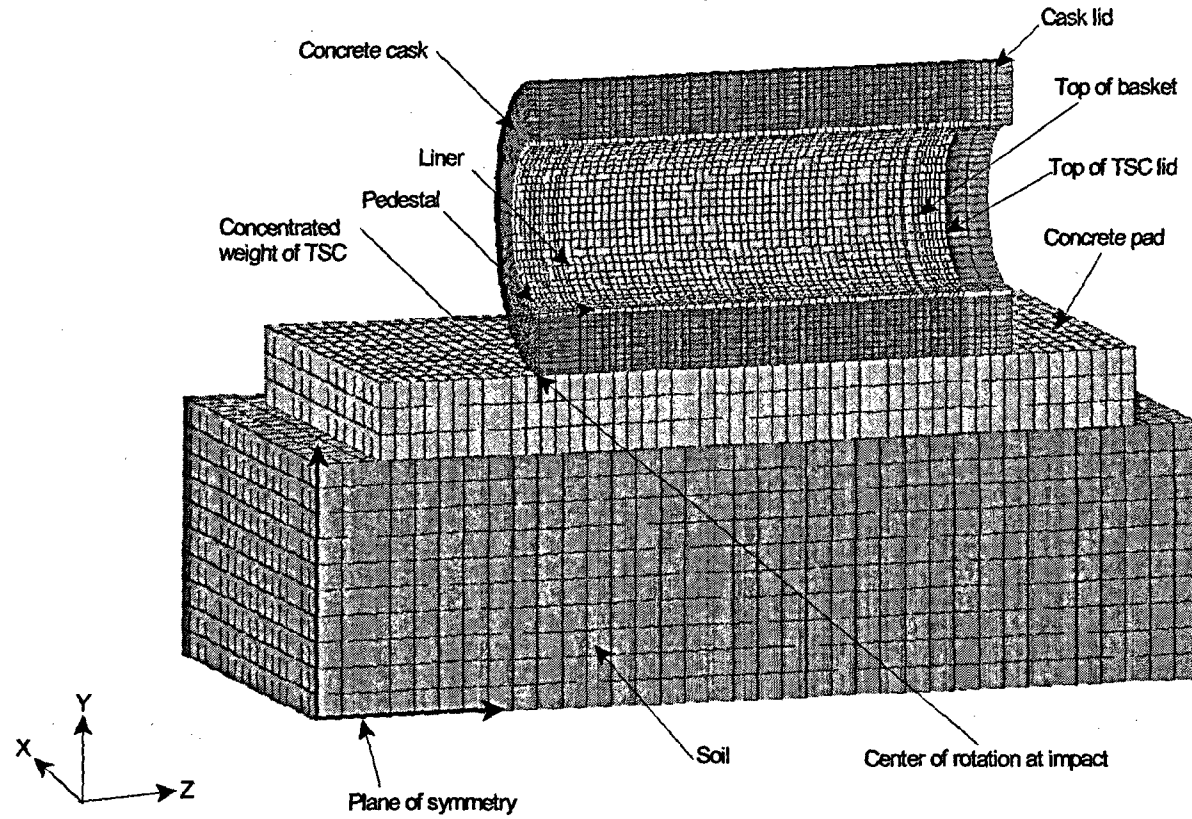
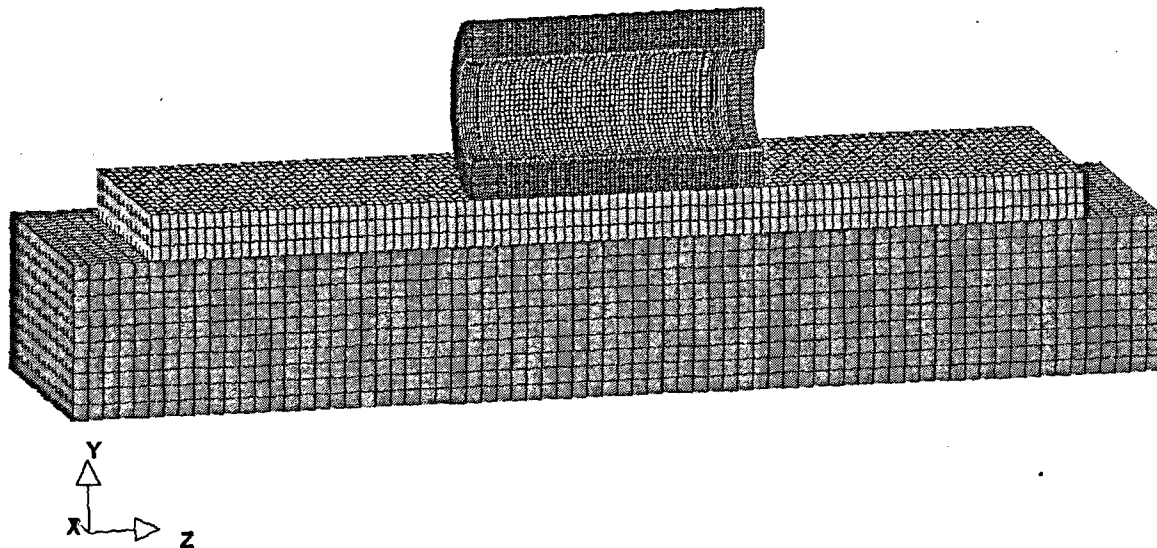


Figure 3.10.4-7 Finite Element Models for Tip-Over Evaluation

Standard Pad Model



Oversized Pad Model



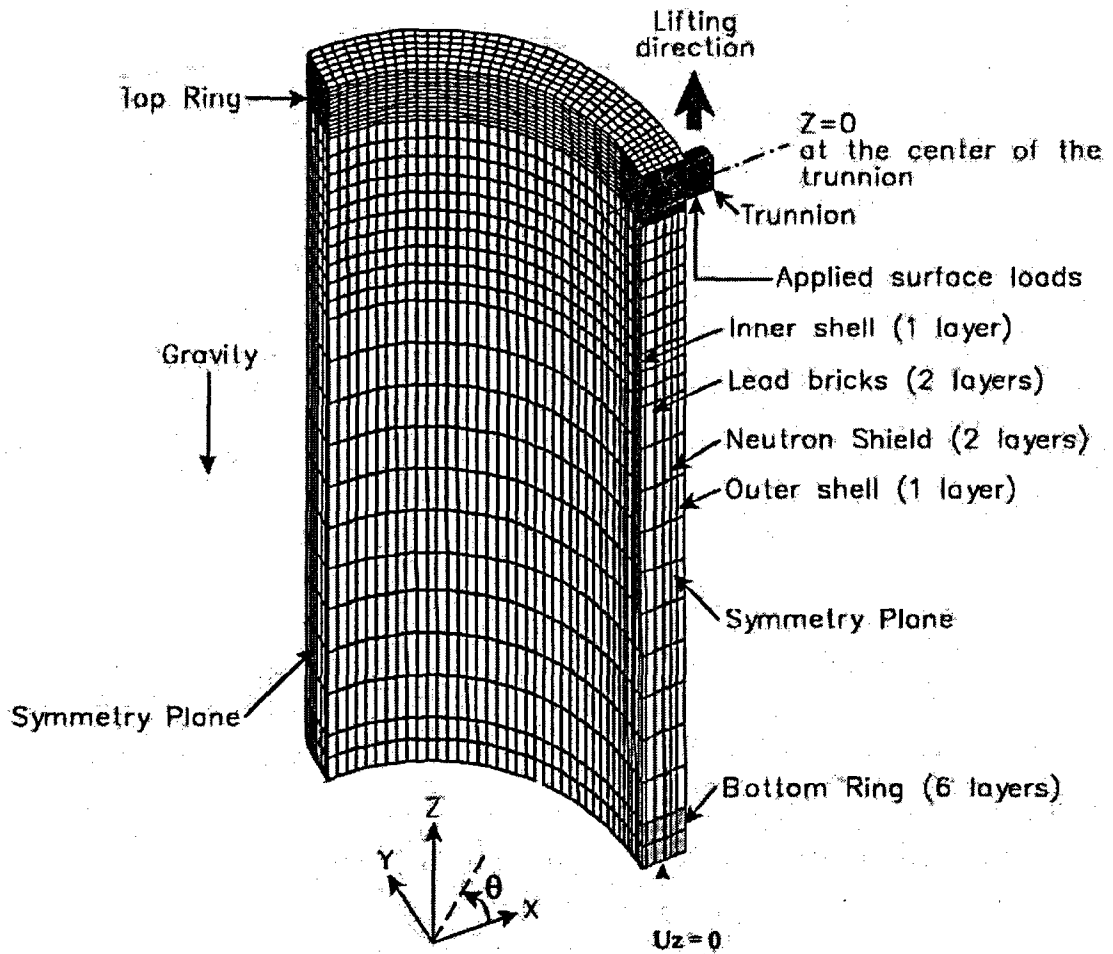
3.10.5 Transfer Cask Finite Element Model

The top section of the transfer cask is a solid ring made of carbon steel. A pair of trunnions, 9 inches in diameter, are mounted 180° apart on this ring. The middle section of the transfer cask is comprised of a steel inner shell, a lead layer, a neutron shield layer, and a steel outer shell. The bottom section is a solid ring made of carbon steel. A pair of rails is welded to the bottom of the solid forging. A pair of steel doors is inserted in the rails. The overall height of the transfer cask is 198.0 inches. The overall diameter of the cask is 88.0 inches. The maximum loaded weight of the transfer cask is 230,000 pounds.

A three-dimensional finite element model is used to evaluate the lifting of a fully loaded MAGNASTOR transfer cask. Because of symmetry, only one-quarter of the transfer cask is modeled, as shown in Figure 3.10.5-1. The model includes the trunnions, the top ring at the trunnion region, the inner and outer shells, the bottom, and the lead and the neutron shield between the inner and outer shells. ANSYS SOLID45 elements (8-node brick element) are used to model the transfer cask. The trunnions are partial penetration welded to the top ring. CONTAC52 elements are used to model the interface between the trunnion and the top ring. The groove welds attaching the trunnion to the top ring are represented by coupled nodes between the two components.

The total weight of the heaviest loaded transfer cask is less than 115 tons. A conservative load of 120 tons, plus a 10% dynamic load factor, is used in the model. The load used in the quarter-symmetry model is $(240,000 \times 1.1)/4 = 66,000$ pounds. The load is applied upward at the trunnion as a "surface pressure load" whose location is determined by the lifting yoke dimensions. The magnitude of the surface pressure load is calculated so that the total upward force is equal to the load of 66,000 pounds. The model is restrained along two planes of symmetry with symmetry boundary conditions. Vertical restraints are applied to the bottom of the model to resist the force applied to the trunnion.

Figure 3.10.5-1 Finite Element Model for the Transfer Cask



3.10.6 Basket Stability Evaluation for Concrete Cask Tip-Over Accident Condition

This section describes the LS-DYNA model and the analyses confirming the stability of the MAGNASTOR fuel basket for the hypothetical concrete cask tip-over accident.

The geometric stability of the basket ensures that the fuel tubes remain in their initial configuration during and after the tip-over accident. Confirmation that the basket does not buckle during the tip-over accident is addressed in Sections 3.7.2.1.2 and 3.7.2.2.2. Sections 3.5 through 3.7 also demonstrate that there are no other loads or stress-based failures that can contribute to instability in the MAGNASTOR basket design.

In this section, the geometric stability evaluation for the fuel basket is based on as-built conditions that may lead to fuel tube movement during the tip-over accident, resulting in an alteration of the initial basket configuration.

In the geometric stability evaluation of the MAGNASTOR fuel basket, only the BWR basket is considered since the 45 tubes in the basket exhibit a greater degree of response to dimensional variations than the 21 tubes in the PWR basket. The larger number of tubes in the BWR basket represents the bounding conditions that could challenge the geometric stability of the basket.

During the tip-over accident, lateral loading is applied to the fuel basket. The accelerations experienced by the fuel basket are computed in Section 3.7.3.7, and the accelerations at the top of the basket are shown in Figure 3.7-6. Since the cask is rotating about its base, the accelerations applied to the basket monotonically decrease towards the base of the cask. Since the lateral loading can be applied in an arbitrary angular direction, certain angular orientations of the basket may use an additional half-symmetry model as shown in Figure 3.10.6-1 and Figure 3.10.6-2 for the 0° and 45° basket orientations, respectively. For other arbitrary basket orientations, a full model is required, as shown in Figure 3.10.6-3 for the 22.5° basket orientation.

The most significant condition affecting the stability of the fuel basket is gaps between adjacent fuel tubes. Specifically, those fuel tubes that are not physically attached to the side weldment or corner weldment are identified as most susceptible to instability issues. The gaps between the fuel tubes may be developed due to a lack of straightness of the tubes and/or dimensional tolerance due to fabrication. This gap is defined in Figure 3.10.6-4, and values of 0.005 inch, 0.015 inch, 0.03 inch and a maximum value of 0.069 inch are considered for different fuel basket orientations. In performing these analyses, the similarity of results has indicated that it was not required that all gap sizes and pin modeling conditions be evaluated for all basket orientations.

This gap is implemented in the finite element model by first generating all of the fuel tubes using nominal dimensions and then reducing the outer dimensional width of the interior tubes (those tubes that are not attached to a weldment) by the value of the gap of interest while maintaining:

- 1) the thickness of the fuel tube wall,
- 2) the radius of the socket and pin, and
- 3) the initial center positioning of the fuel tube.

Use of this approach results in the initial position of the fuel tube, in the transient evaluation, being suspended without contact between the individual tubes. While this is analytically possible, the occurrence of such gaps during fabrication is not physically possible. The assembly process, horizontal stacking, will result in minimal gaps that would generally occur along the length of the fuel tubes between points of contact. Additionally, the fuel basket design provides connector pin assemblies at the top and bottom ends of the basket that develop an assembly verification of tube-to-tube interface and act as restraints against any arbitrary motion of the interior tubes. Analyses performed neglecting the connector pin effect further maximize the condition of instability, since there are no other attachments between the interior fuel tubes to restrain them from arbitrary motion.

Model Description

The models shown in Figure 3.10.6-1 through Figure 3.10.6-3 are mainly comprised of brick elements representing the fuel tubes, the BWR fuel assembly, the pins, the support weldments, the canister and the concrete cask.

The support weldment is represented by shell elements and the shell elements are modeled along the centerline of the weldment. Since LS-DYNA takes into account the thickness of the shell element during the transient evaluation, the model must have a gap incorporated between the shell and the solid elements corresponding to a minimum value of the half-thickness of the shell element. To model the bosses and the bolts connecting the weldment to the fuel tubes, constraints are applied to nodes at the location of the bosses and bolts. For the locations corresponding to bolts, the X and Y displacements of the node on the weldment and the node on the fuel tube are made equal throughout the transient analysis. For the locations corresponding to the boss, a constraint is applied which only prevents a relative sliding motion between the fuel tube and the weldment. At these locations, the weldment is not restricted from moving normal to the fuel tube surface.

Some analyses have the pins (other than those for the connector pin assembly) that are welded to the fuel tubes prior to the assembly of the fuel tubes to form the basket. These welds prevent

independent arbitrary motion of the pins and more appropriately represent the actual tube-to-tube interface. For those analyses containing this weld, two neighboring nodes on the pin and fuel tubes are constrained for displacements in the lateral direction of the pin.

The model employed in the evaluation is a periodic model, which implies that the end effect of the connector pin assembly is to be neglected. There are analyses (Cases 5 and 7) where the effect of the connector pin assembly at the end of the basket was incorporated by modeling a linear spring between the flats of two adjacent fuel tubes. The stiffness of this spring was computed by treating the fuel tube as a simply supported beam in which the restraints at the end of the fuel tube correspond to the connector pin assembly. The stiffness at the midspan between the connector pin assemblies results in the minimum value and is bounded by the effective stiffness at the other interior pin locations. Since the fuel tube cross-section is symmetric about two orthogonal axes, the cross-sectional moment of inertia of the fuel tube is invariant with respect to basket orientation.

The finite element model also contains the concrete cask, which is represented by elastic brick elements with a thickness of 3.75 inches. The purpose of these elements is to impose the accelerations on the canister and basket computed in Section 3.7.3.7.

Material Properties

The mechanical properties used in the analyses are described in the following sections.

Carbon Steel Fuel Tubes and Weldments:

The fuel tubes and the corner and end weldments are represented by a piecewise linear plasticity model with the following elastic properties.

Fuel tubes at 700°F (SA537, Class 1, carbon steel)

Yield strength = 32.3 ksi

Ultimate strength = 68.4 ksi

Ultimate strain = 21%

$\nu = 0.31$ ----- Poisson's Ratio

$E = 25.5 \times 10^6$ psi ----- Modulus of Elasticity

The density corresponding to the fuel tubes was adjusted to account for the neutron absorber material

Side and corner weldments at 500°F (SA537, Class 1, carbon steel)

Yield strength = 35.4 ksi

Ultimate strength = 68.4 ksi

Ultimate strain = 21%

$\nu = 0.31$ ----- Poisson's Ratio

$E = 27.3 \times 10^6$ psi ----- Modulus of Elasticity

Canister Shell (SA240, Type 304/304L stainless steel)

The canister shell is represented by inelastic material with the following properties at 500°F.

Yield strength = 19.4 ksi

Ultimate strength = 63.4 ksi

$\nu = 0.31$ ----- Poisson's Ratio

$E = 25.8 \times 10^6$ psi ----- Modulus of Elasticity

Steel Inner Liner (A36 carbon steel)

The steel liner is represented by inelastic material with the following properties at 500°F.

Yield strength = 29.3 ksi

Ultimate strength = 58.0 ksi

$\nu = 0.31$ ----- Poisson's Ratio

$E = 27.3 \times 10^6$ psi ----- Modulus of Elasticity

Fuel Assembly

The element representing the fuel assembly were modeled with the following inelastic properties

Yield strength = 1 ksi

$\nu = 0.49$ ----- Poisson's Ratio

$E = 1 \times 10^5$ psi ----- Modulus of Elasticity

The density for the fuel assembly corresponds to the design weight of the BWR fuel assembly.

Boundary Conditions

Automatic surface-to-surface contact conditions are employed between the pins and the fuel tubes, the end and corner weldments, the basket and the canister, and the canister and the concrete cask. Symmetry boundary conditions are applied to all parts at the plane of symmetry (see Figure 3.10.6-1, typical). The axial displacements were restrained on both axial faces of the model. The initial condition of all nodes in the model was the velocity of 283 in/sec, which

corresponds to the top of the fuel basket due to angular velocity occurring during the tip-over. The angular velocity is computed in Section 3.10.4.4.

To represent the accelerations applied to the basket during the tip-over, the acceleration time history shown in Figure 3.7-6 was applied to the nodes of the concrete cask elements.

A uniform body force was applied to simulate gravity.

Load Cases

Table 3.10.6-1 lists the cases evaluated using the model and load conditions described in this section. The variation in the cases includes the maximum range for the gap. The different conditions for the pin being welded to the fuel tube, as well as the incorporation of the effect of the connector pin assembly, were also included in some of the transient analyses.

Post-Processing

The primary output of these analyses is the resulting motion and final position of the fuel tubes.

0° Basket Orientation

The motion of two pins and adjacent fuel tubes is shown in Figure 3.10.6-5 for Case 2. The plot of the pins depicts the initial separation of the fuel tubes; but as the impact continues, the fuel tubes contact (as shown in the plot associated with the time of 0.0225 seconds) and load the adjacent tubes via the pin and socket design. The results also display that all basket gaps close during the impact, including the fuel tubes attached to the weldments, indicating deflections that allow the exterior fuel tubes to move with the interior fuel tubes and maintain contact. The plots of the deformed configuration at the different times confirm that the interface between the pins and the fuel tubes is correctly functioning. No out-of-phase motion was observed for either Case 1 or Case 2. The results for Case 1 are expected to be similar to Case 2, since the angular orientation is the same. This confirms that the fuel tube size for the 0° angle orientation has a minimal effect on the basket response. Since the developed tube and the fuel tube correspond to different dimensional widths, the gaps between the fuel and the adjacent surface are also different. Since the basket and fuel nodes have the same initial velocity, the time at which the elements of the fuel will impact the nearest surface will also be different, which would maximize the opportunity for out-of-phase motion for the different fuel tubes. The absence of out-of-phase motion is consistent, however, with the initial conditions and the applied accelerations. While the acceleration time history is not monotonic, the fuel tube momentum monotonically decreases until the basket is nearly at rest. After impact, the fuel tubes remain in contact except for those tubes adjacent to those that are attached to the side and corner support weldments. Since a gap

was incorporated into the model around each fuel tube to artificially, and conservatively, include fabrication tolerances, the gravitational force moved the fuel tubes to their lowest position, while the fuel tubes attached to the weldment returned to their original position. The result is a large gap between the interior fuel tubes and the exterior fuel tubes at the upper part of the basket (opposite of the impact direction). This gap is artificial since the initial condition gap cannot exist during fabrication.

Independent of the artificial conservative boundary, the results of the use of a uniform 0.069-inch gap show that the basket is stable during the 0° impact, thus indicating that the factor of safety for instability is larger than 2 because the largest allowable fabrication tolerance gap is 0.031 inch (1/32).

22.5° Basket Orientation

For the 22.5° basket orientation, the entire basket was required to be modeled, and in this case, no credit was taken for the pins welded to the fuel tubes or the effect of the connector pin assembly. Figure 3.10.6-6 shows various stages of the motion of the pin and socket for an interior fuel tube and for a fuel tube attached to the corner weldment. Once the basket begins to experience deceleration, the artificial 0.069-inch gaps begin to close. Similar to the response for the 0° orientation, the deflection of the weldments permits all gaps to close. Following the interior fuel tubes coming to rest, the rebound of the weldments again results in large gaps occurring in the model for the top-most interior fuel tubes. This gap is also artificial since the initial condition gap cannot exist during fabrication.

The results of the use of a uniform 0.069-inch gap show that the basket is stable during the 22.5° impact, thus indicating that the factor of safety for instability is larger than 2 because the largest allowable fabrication tolerance gap is 0.031 inch (1/32).

45° Basket Orientation

For the 45° basket orientation, a half-symmetry model of the cross-section was used in the evaluation. Whereas the 0° basket orientation results in the maximum loading conditions for the buckling evaluation, the 45° basket orientation results in the maximum distortion of the fuel tube cross-section. Four cases were evaluated as shown in Table 3.10.6-1.

Figure 3.10.6-7 and Figure 3.10.6-8 show the pin near the top of the fuel basket for times of 0.0225 and 0.043 seconds for all four cases at the 45° orientation. The four sets of plots confirm that regardless of the gap or the pin conditions, the gaps between the adjacent tubes are closed. The presence of the effect of the connector pin assembly does reduce the size of the vertical gaps

occurring between the adjacent fuel tubes in the basket. As with the 0° orientation, out-of-phase loading of the fuel tubes was not observed.

Use of a 0.069-inch gap in Case 7, which shows the basket is stable during the impact, confirms that the factor of safety for instability is larger than 2 because the largest allowable fabrication tolerance gap is 0.031 inch (1/32).

Summary

In this section, a description of a transient evaluation of the BWR fuel basket has been provided. Three basket orientations have been examined for the tip-over conditions that are considered to bound other possible orientations. The minimum and maximum fuel tube distortion corresponds to the 0° and 45° orientations, respectively. The closure of the modeled gaps between fuel tubes occurred for all orientations, and no alteration of the positioning of the fuel tubes was observed. The maximum gap, artificially imposed, was 0.069 inch and demonstrates that a factor of safety greater than 2 exists for basket instability during a concrete cask tip-over accident. This significant safety factor is consistent with the fact that out-of-phase loading does not occur during the deceleration of the basket.

Figure 3.10.6-1 Finite Element Model for the 0° Fuel Basket Orientation for a Concrete Cask Tip-Over Accident

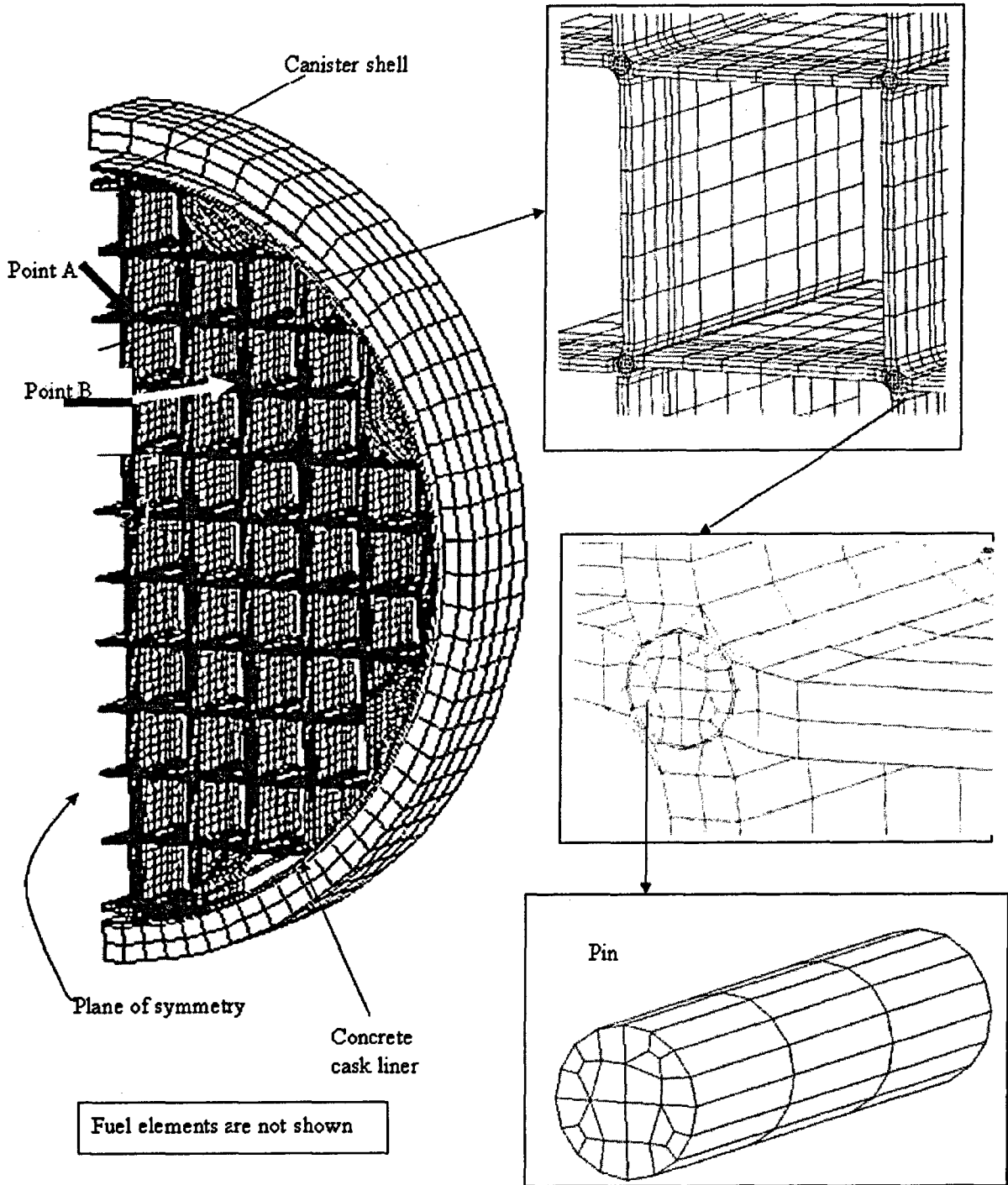


Figure 3.10.6-2 Finite Element Model for the 45° Fuel Basket Orientation for a Concrete Cask Tip-Over Accident

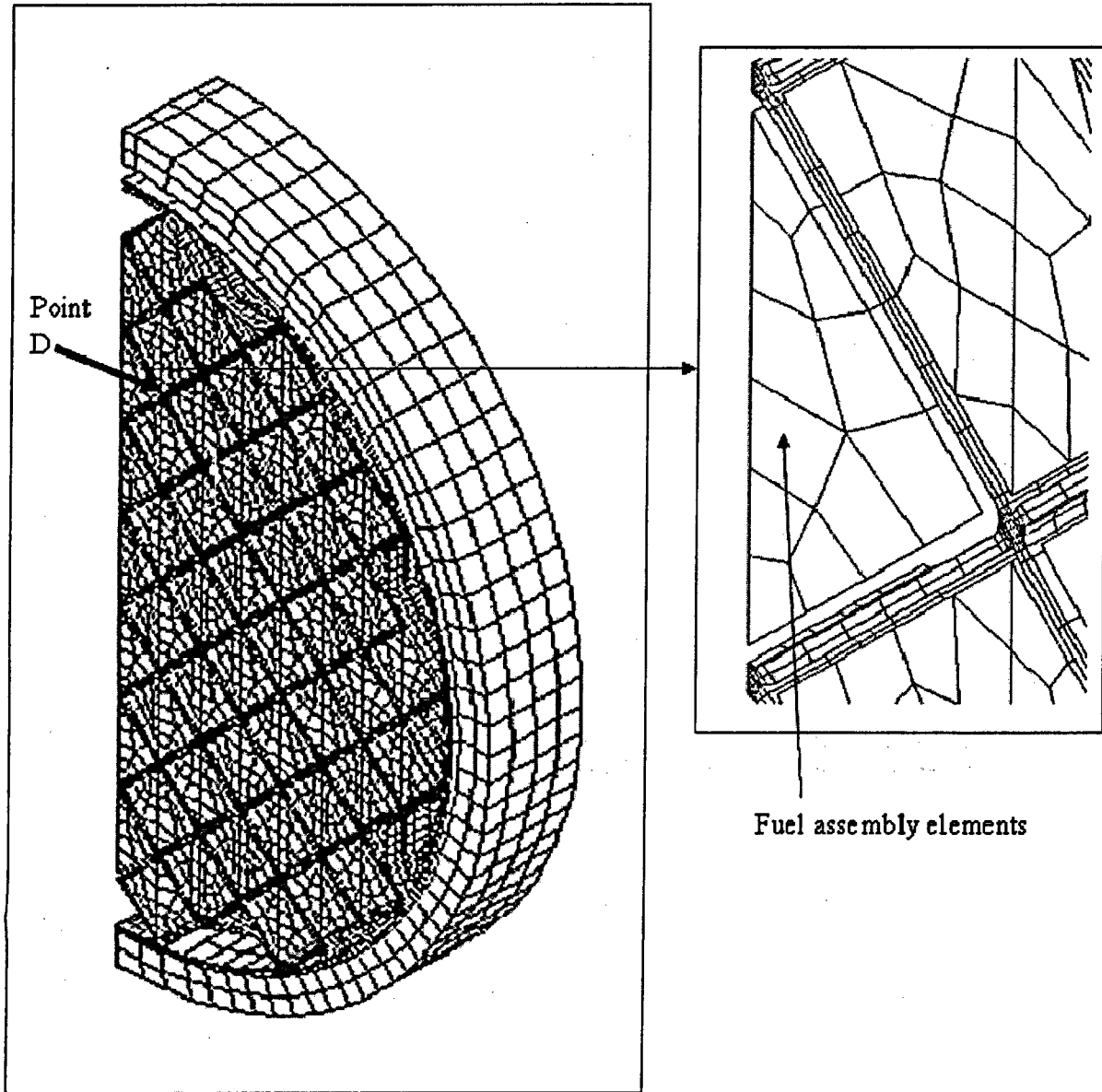


Figure 3.10.6-3 Finite Element Model for the 22.5° Fuel Basket Orientation for a Concrete Cask Tip-Over Accident

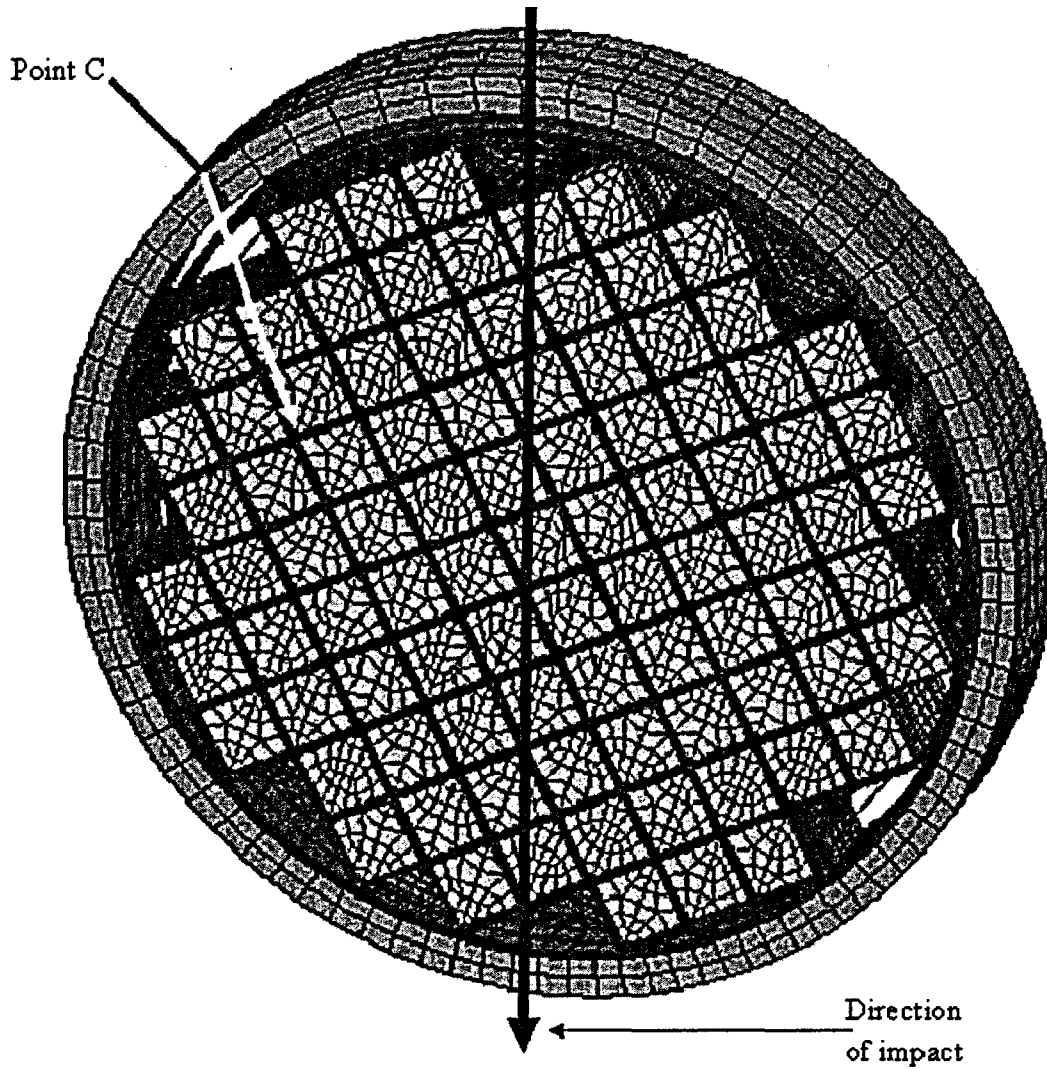


Figure 3.10.6-4 Definition of Tube Reduction for Fuel Basket Stability Evaluation

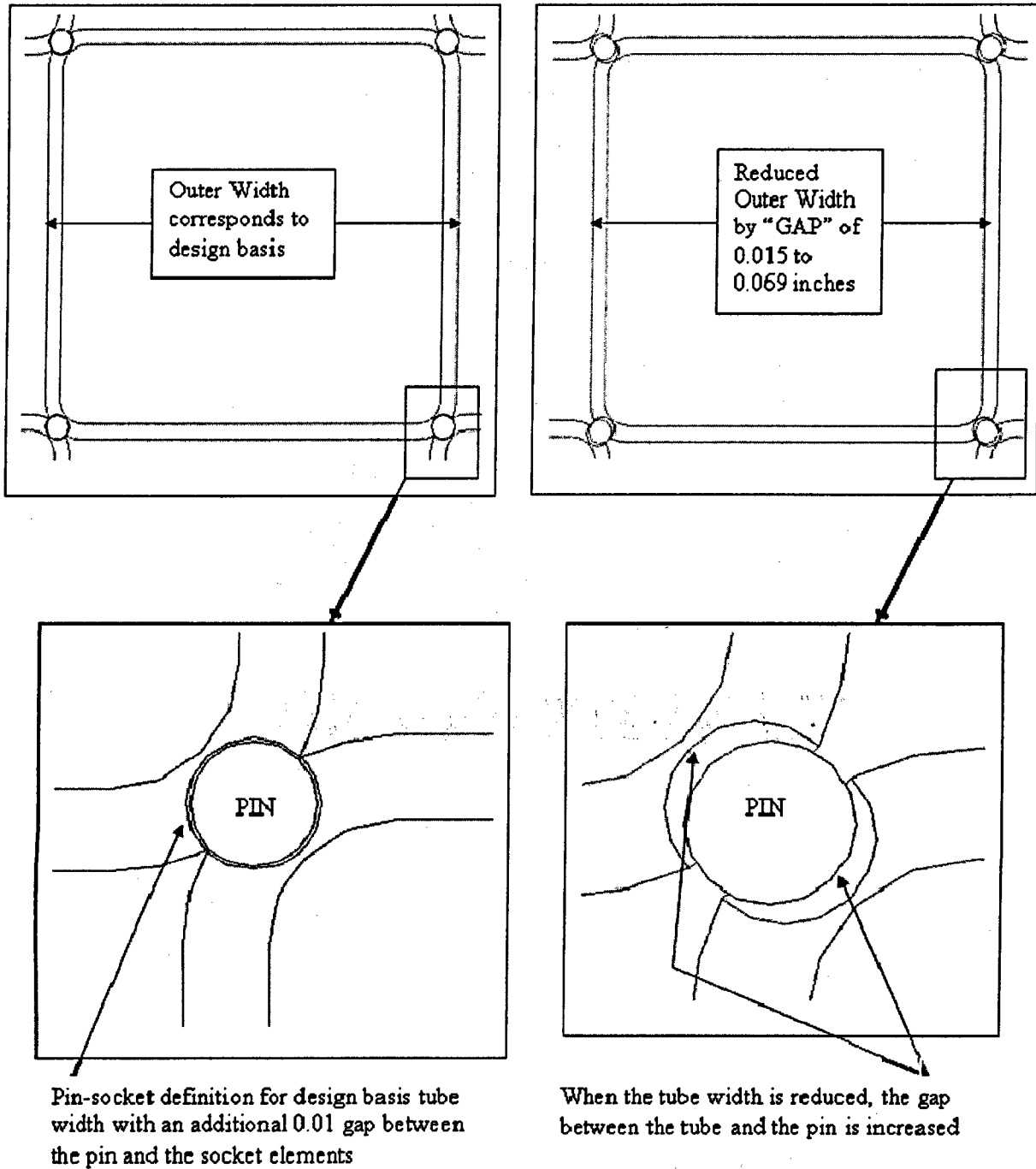
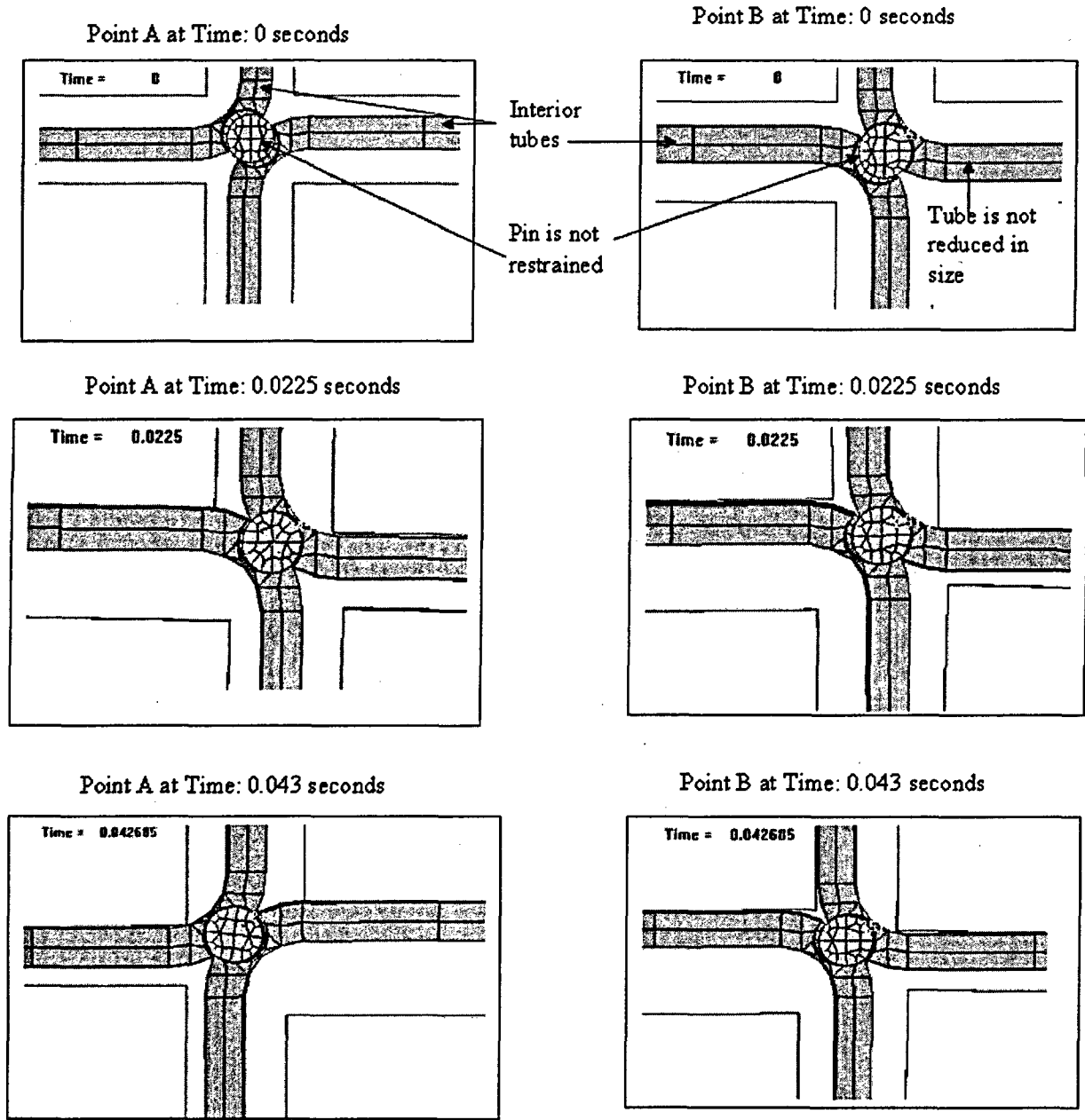
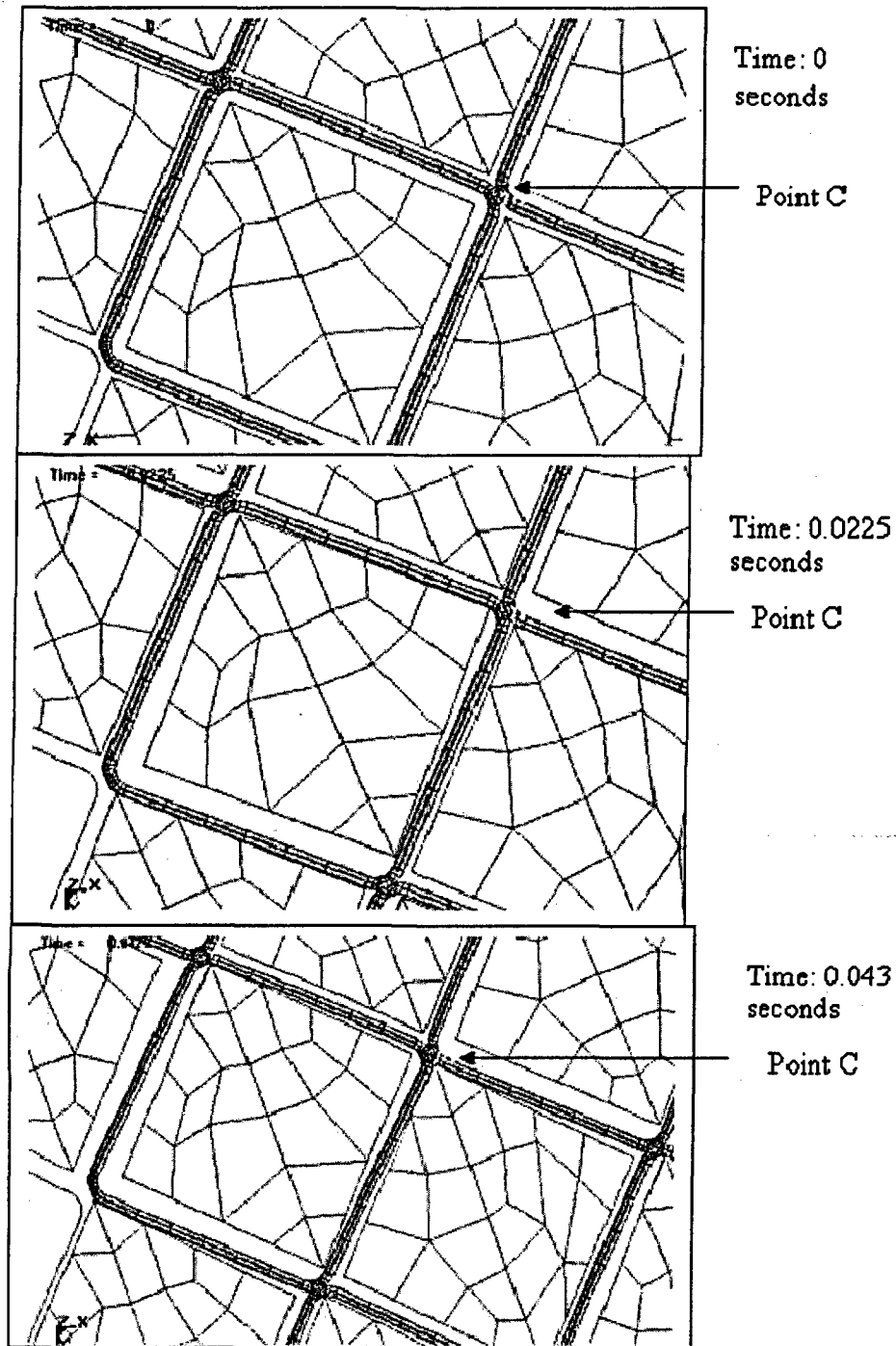


Figure 3.10.6-5 Motion of Fuel Tubes for the 0° Fuel Basket Orientation (Case 2)



Note: Points A and B are defined in Figure 3.10.6-1.

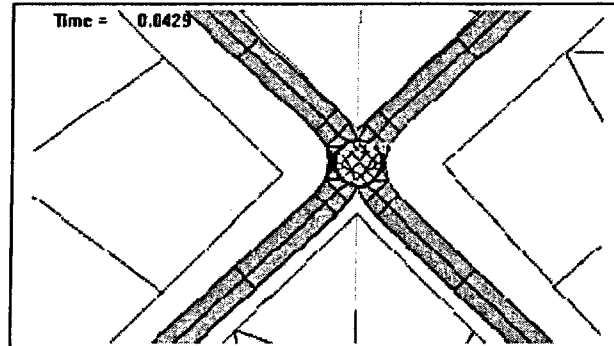
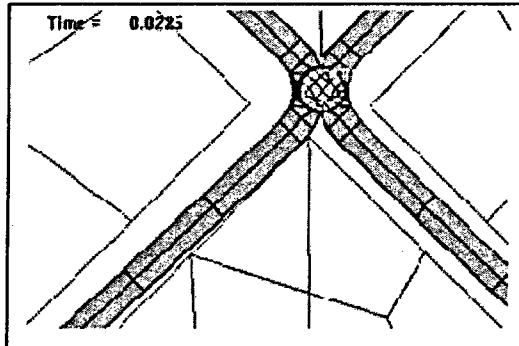
Figure 3.10.6-6 Motion of Fuel Tubes for the 22.5° Fuel Basket Orientation (Case 3)



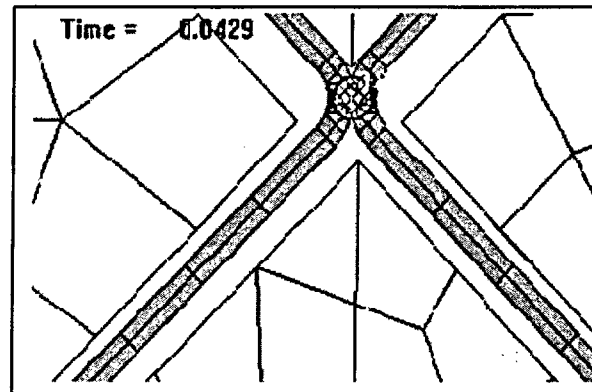
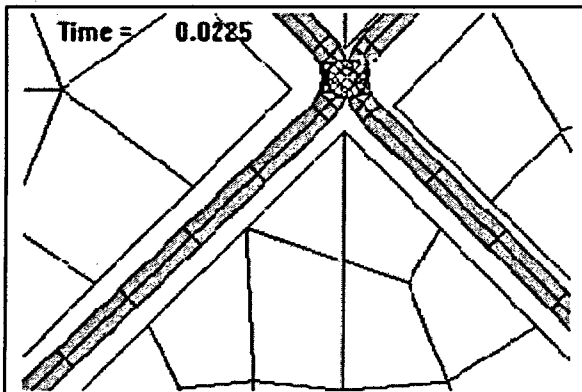
Note: Point C is identified in Figure 3.10.6-3.

**Figure 3.10.6-7 Motion of Fuel Tubes for the 45° Fuel Basket Orientation
(Case 4/Case 5)**

Case 4 Results at Point D at Time 0.0225 seconds and 0.043 seconds



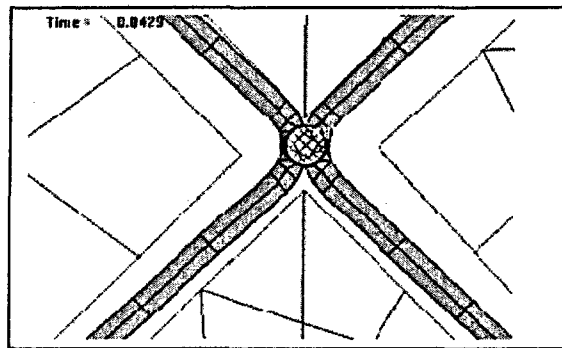
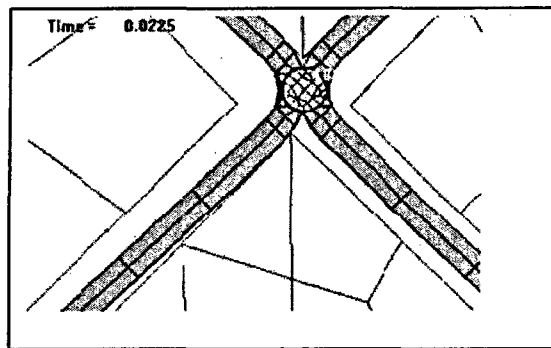
Case 5 Results at Point D at Time 0.0225 seconds and 0.043 seconds



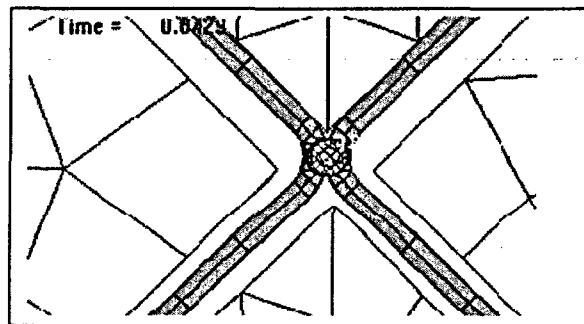
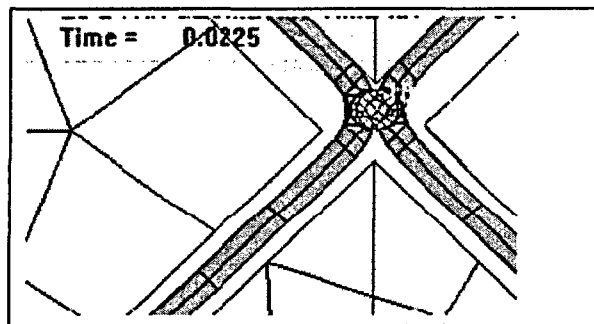
Note: Point D is identified in Figure 3.10.6-2.

**Figure 3.10.6-8 Motion of Fuel Tubes for the 45° Fuel Basket Orientation
(Case 6/Case 7)**

Case 6 Results at Point D at Time 0.0225 seconds and 0.043 seconds



Case 7 Results at Point D at Time 0.0225 seconds and 0.043 seconds



Note: Point D is identified in Figure 3.10.6-2.

Table 3.10.6-1 Load Cases Evaluated for Fuel Basket Stability

Case	Basket Orientation	Gap between basket tubes (inch)	Pins welded to the basket tube	Connector pin Assembly spring Included
1	0	0.005	No	No
2	0	0.069	No	No
3	22.5	0.069	No	Yes
4	45	0.005	No	No
5	45	0.015	Yes	Yes
6	45	0.030	Yes	No
7	45	0.069	Yes	Yes

3.10.7 Fuel Tube Plastic Analysis for Concrete Cask Tip-Over Accident Condition

This section describes the LS-DYNA models for the fuel tubes in the PWR and BWR fuel baskets and the analyses to evaluate any possible permanent deformation of the fuel tubes for the hypothetical concrete cask tip-over accident.

Model Description

As shown in Figure 3.10.7-1, a three-dimensional half-symmetry model is constructed to represent a half cross-section of a PWR fuel tube using the LS-DYNA program. The model for the BWR fuel tube is similar to that for the PWR fuel tube. The model contains a cross section of the fuel tube and a rigid block through which the displacement is applied to the top of the fuel tube.

Material Properties

Piecewise linear plastic properties corresponding to 700°F are used for the carbon steel fuel tubes.

Boundary Conditions

Automatic surface-to-surface contact conditions are employed between the block imposing the displacement and the top of the fuel tube. The motion at the bottom of the fuel tube is limited by the definition of a rigid plane. Symmetry boundary conditions are applied to the plane of symmetry (see Figure 3.10.7-1, typical). The vertical displacement of the block is specified as a triangular shaped time history with the maximum displacement of 0.294 inch for the PWR fuel tube and 0.225 inch for the BWR fuel tube. The displacement for the PWR tube corresponds to the maximum diagonal displacements of the fuel tubes for the tip over condition as evaluated in Section 3.7.2.1.2. For the BWR configuration, the displacement corresponds to the BWR evaluation using LS-DYNA in Section 3.10.6. The duration of the motion is 0.045 seconds which reflects the duration of the impact in the tip-over accident. The analysis is continued until a time of 0.060 seconds to obtain the final deformed shape of the fuel tube.

Post-processing

The permanent deformation of the fuel tubes is determined by computing the difference in the vertical displacements of Point A and Point B (Figure 3.10.7-1) in the final deformed shape. The

maximum permanent diagonal displacement of the fuel tubes is computed to be 0.008 inch and 0.018 inch for the PWR and BWR fuel tubes, respectively.

Figure 3.10.7-1 Typical Finite Element Model for the Basket Fuel Tube Displacement

